

**Geochemical Origins of Travertine limestones  
in the Lake Edward Basin, Albertine Rift,  
DRC – UGANDA.**

**Master of Science (Research) Thesis of University of Dublin  
Trinity College**

**2020**

**Sylvain Mangoni Kezir**

**DECLARATION**

*I, Sylvain Mangoni Kezir, declare that this thesis is entirely my own work, except where duly acknowledged in the text. It has never been submitted as an exercise for any degree at this or any other University and henceforth owns the copyrights.*

*I agree to deposit this thesis in the University's open access institutional repository or allow the library to do so on my behalf, subject to the Irish Copyright Legislation and Trinity College Library conditions of use and acknowledgement.*

*Signed: Sylvain Mangoni Kezir*

*Date:*

-----

-----

-

## ABSTRACT

From 2007 to 2014, geological field surveys have been undertaken within the East African Rift System where hot spring Travertine and limestones have been discovered, precipitated at active, or palaeo-spring sites around the margins of the Lake Edward, Lake George and Lake Albert basins.

These Travertines are often outcropping over deep-seated rift-bounding faults, linking their origin to meso- and hydro-thermal groundwater flux along fault planes. For this groundwater to attain the necessary high concentration of bicarbonate to potentially precipitate the calcite found in spring pools at the surface, the requirement is that this ground water must have percolated through a substantial carbonate bedrock unit at depth, typically a regional sedimentary limestone. However, the Lake Albert and Lake Edward - Lake George rift basins are infilled by fluvial, deltaic and lacustrine siliciclastic sediments, such as sandstones, claystones and conglomerates. No limestone beds have been documented so far in Albertine rift-fill sediments, either at the surface in outcrop, or at subsurface level in well penetration.

Thin caliche paleosols are probably present in rift-fill sediments exposed around the margins of the lake, but these are only poorly developed carbonate concretionary horizons and have not developed into full, laterally continuous calcretes. Thus the presence of these Travertine outcrops, and more specifically, the origin of their bicarbonate, remains enigmatic. Considering the groundwater carbonate chemistry required to precipitate these Travertines, and the complete absence of any fluvial or lacustrine limestone beds in the Lake Albert and Lakes Edward – George rift-fill stratigraphy, the big question remains about how and why these unexpected Travertine limestones have been formed?

The present Master of Science degree by research titled “Geochemical Origins of Travertines in the Lake Edward Basin, Albertine Graben, DRC/ Uganda”, succeeded to understand through the reversible reaction  $\text{Ca}^{2+} + 2\text{HCO}_3^- = \text{CaCO}_3 + \text{CO}_2 + \text{H}_2\text{O}$ , the source of the Bicarbonate by which carbonates, and therefore Travertine, are precipitated respectively in cold and hot springs very localized in lines along many Eastern Africa rifts bounding faults.

This geochemical origin inquiry has actually found evident answers by running from 2013 to 2018 three series of ICP-MS analyses on Rare Earth Element (& Yttrium) concentrations in a suite of 50 Travertines samples collected within the EARS.

Carbon  $\delta^{13}$ /Oxygen  $\delta^{18}$  stables isotopes analyses on selected Travertine samples revealed the surface fractionation processes within the hot spring pools at the surface, because they are mostly affected from  $\text{CO}_2$  outgassing as the water bubbles to the surface. Strontium isotope ratios low values ( $\sim 0.703$ ) suggested hydrothermal carbonatite origin while the marine sediment and the continental weathering origin has been easily recorded by their intermediate and high values ( $\sim 0.708$  and  $\sim 0.711$ ). (Wierzbowski, 2013) The Travertine respective REE concentrations MUQ normalized values gave the evidence to have derived their bicarbonate from one of three carbonate sources at depth:

- Igneous Carbonatites, either present at depth as buried carbonatite lavas, or as intrusives
- Marine Limestone, which suggests that it is part of a pre-Tertiary rift unit; likely to be either a failed Karoo-Mesozoic rift package, or part of the ‘basement’ Proterozoic (possibly Neoproterozoic ‘Schisto-Calcaire’)
- ‘half-way house’ mixture between these two end-members.

## SUMMARY

This thesis presents the possible geochemical origins of unpredicted Travertine recently discovered in outcrops in a series of lined localized cold springs in the Lake Edward Basin, DRC-Uganda.

The study area forms a part of the East African Rift System with a classical rift valley successions mainly fluvial and lacustrine deposits.

The East African Rift System (EARS) can be considered as a unique succession of graben basins linked by intracontinental transforms and segmented by transfer zones and accommodation zones. This could also be described like a lithospheric scale structure, characterized by uplift of hot asthenospheric elongate diapirs across the upper mantle, responsible for shoulder uplifts. This forms a kind of intracontinental ridge system of several hundreds of kilometres wide and several thousands of kilometres long, which is quite equivalent to the oceanic ridge system.

It clearly appears that the inscribed continental graben valleys and basins are organized over a major failure, related in the crust to a main border fault and low angle detachment fault, inducing asymmetric roll-over structure, eventually accompanied by smaller normal faulting and tilted blocks.

It seems to appear like external tensional stresses have caused the continent to split along lines of pre-existing lithospheric weaknesses marked by old tectonic patterns that focus the extensional strain.

Considering its size, structure and occurrence of oceanic lithosphere, the EARS could easily be taken as a model of the beginning of oceanic opening inside a continent.

This opening propagates normally on the whole from north to south— including local nucleation's of lithospheric faults—due to SE-ward relative divergent drifting of a not yet well individualized plate.

The EARS history is strongly linked by the role of plume impacts. This plume phenomenon which had occurred approximately at around 30 Ma, was in Lake Tana region (Ethiopia). His main action was weakening the lithosphere and preparing the first rifting along a Pan-African suture zone bordering the future Afar region. This rift propagated afterward along the suture zone, activation of low angle detachment fault reworking former opposing faults belonging to the double verging ancient belt associated to structure.

When supposing the plume has migrated southward, or other plumes emplaced, preparing other nucleations of failure along former suture or transform zones, the actual rift system propagated and is still developing southwards towards the Lake Edward basin.

Much about the geological history of the Lake Edward basin remains unknown. There is a lack of any useable age dates, either absolute or from biostratigraphy so other methods must be created to attempt to constrain unit deposition, including linking litho- and chrono-facies with glacial/interglacial episodes. Rapid lateral facies changes present in onshore sediments and the fact that all sediments are either lacustrine or fluvial mean that chrono-stratigraphic units must be used instead of more traditional 'formations' and at much higher resolution. Poor exposures across much of the vast area, and only one exploration well in the entire

basin make for a sparse data set which must be overcome to be able to explore successfully for hydrocarbons.

The Lake Edward basin geologic informations recorded so far by this thesis can be summarized as below:

- The presence of the numerous oil seeps observed in the Edward basin surface may indicate that organic rich Carbonate source rocks are present in subsurface;
- The organic rich clays observed outcropping in surface are suggesting that they were generated from source rocks deposited in a lacustrine environment and dominated by Type 1 algal Kerogen; (Nicholas, 2009)
- The organic rich black shales observed outcropping in surface are suggesting that they were generated from source rocks deposited in a more saline lacustrine environment;
- The weathering of basement rocks along the escarpment and rift flanks of the Albertine Graben, their subsequent transportation and deposition of their weathered products into the Graben could yield good reservoir quality sediments identifiable from their outcrop in the field;
- Sandstones in Edward basin outcrops help to define prior to the drilling the porosity trend of the potential reservoir which exact porosity % will be measured in the shallow cores;
- The aerial observation of modern rivers meanderings may be resulting from the palaeo depositional environment of sediments fill in the basin;(Nicholas, 2017)
- Many field observations of faults scarps, unconformities and difference of successive elevations in the surface are supposed to be correlate with Dip reversals against faults and fault and fault-on-fault traps structures which could be confirmed by seismic data acquired throughout the whole basin;
- Clay's samples collected in the field, once analysed for mineral contents, may help to understand the protective skills of a potential regional seal covering sands reservoirs in place.
- Mysterious Travertine with great oolites cavities found in outcrop with live Oil stains in Ugandan side and without proven live Oil stains in DR Congo side, may suggest a Cenozoic carbonate reservoir with a wonderful porosity network, if these Travertine could be confirmed in a potential exploration well; (SOCO, 2010)

This present thesis is focussed only on the research of the geochemical origins of these mysterious Travertine inside the classical siliclastic sediment fill of the EARS.

After its abstract, summary, dedication and acknowledgement, this thesis will present the whole work in the first Chapter: Introduction, hypothesis, aims and objectives.

The summary of all the books, articles, journal and previous published thesis consulted and referenced has been put together in the second Chapter: Literature Review.

The third Chapter is treating about the methodology and techniques used to achieve this thesis objectives

The fourth Chapter is detailing the three series of field trips from 2007 to 2009 in Uganda side, in 2010 and in 2014 in the DRC side of the Lake Edward basin, while the Chapter Five illustrates the Travertine petrography work. Chapter Six presents all results which argued the scientific discussions and geologic venues noted in Chapter Seven. This thesis is ending by some conclusions and petroleum implications in Chapter Eight.

## DEDICATION

*My daughter, Alliancia!*

*My beloved MingoDias!*

*Vital, Esther, Patrick, Lydia, Guyguy, Junior and Gloria!*

*Joëlle, Ariel, Christelle, Gaëlle, Gracia, Ethan, Splendeur and Estelle,.....!*

*Miguel lanzaroti, Dr Susan, Andy, Trish, Eddy, Louis Fitzgerald,*

*All Dundalk Community Center,*

*All my Africa fellows,*

*Wherever you are, whatever you are doing, whenever you may (or not) read this page,*

*May you find here my sincere gratitude for all your encouragements and trust on me.*

*May this scientific work make each of and all around you more proud of your son, brother,  
uncle, father, love, friend, best friend,...I am and will always be for you.*

*I will never ever forgot anyone of all your support and trust on me.*

*Thank you again,*

Sylvain.

## ACKNOWLEDGEMENT

I would like to extend my sincere gratitude to the Government of my country Democratic Republic of Congo (DRC), the Ministry of Hydrocarbons and SOCO Exploration-Production Ltd for the sponsorship of this research degree.

I am very grateful for their support from the beginning to the end. My heartfelt thanks are going to Serge Lescaut, Steeve Creswell, Jose Sangwa, Jean Muganza, Joseph Pilipili, Georges Byeragi Safari, Karin Barrios, Adrian Woods, Adina Lupu, Georgetta Tufis, Thierry Mulumba, Sir Katoto Christian, Jean-Pierre Akemba, and my inspiratory Pr.Dr. Vincent Kanda Nkula.

Special thanks go to my supervisor Dr. Christopher J. Nicholas for introducing and guiding me so well throughout this entire work from the very long field investigation season, samples preparation, laboratory analysis, results interpretation and discussions to this present thesis write-up. I am so grateful for all his encouragement, constructive criticism and critical reading of this manuscript from the beginning to its end. Because of the collaborative nature of this Msc Research, the Figures I.1, II.1, II.2, II.3, II.4, II.5, II.28, II.29, II.32, II.33, VI.1, VI.7, VI.8, VI.9, VI.10, VI.11, VI.12, VI.13, VI.14, VI.15, VI.16, VIII.1, VIII.2 and field notes have been provided by Dr. Christopher J. Nicholas who personally participated to all the field trips.

I also extend my thanks to Jean Dyer and Mike Babehuck for their active participation to the first ICP-MS analysis in 2013, to Finbarr Mc Teirnan for his very contributive participation to my field trip in 2014, and finally to Cora Mc Kenna for her kind patience and guidance during the laboratory work on ICP-MS analyses on all my samples at the Unit 7 of Expertise lab center from 2016 to 2018.

My heartfelt thanks go to all the staff of Department of Geology at Trinity College, University of Dublin for the guidance and support throughout the entire research degree most especially for all the taught thoughts, seminar, conferences I did attend. In this regard, I would like to thank Dr. Robbie Goodhue, Dr. Balz Kambeer and Dr Dave Chew.

I would like to extend my appreciation to the technicians Frank, Noel and Maura for all the precious help and kind assistance during the samples preparation steps and their guidance when the going seemed to be very hard.

My profound gratitude to my fellow postgraduate students: Joel, Kareer, Almahdi, Maurice for making me feel comfortable all the times.

To Africa, my beloved country Democratic Republic of Congo, my family and all my friends spreaded all over the world, you deserve this work.

## TABLE OF CONTENTS

ABSTRACT.....	3
SUMMARY.....	4
ACKNOWLEDGEMENT.....	7
CHAPTER ONE: INTRODUCTION, AIMS AND OBJECTIVES.....	15
I.1- INTRODUCTION.....	15
I.2- HYPOTHESIS.....	17
I.3- AIM AND OBJECTIVES.....	18
CHAPTER TWO: LITTERATURE REVIEW.....	20
II.1- MODERN LIMNOLOGY.....	21
II.2- BASIN STRUCTURE.....	21
II-3 RUWENZORI MOUNTAINS.....	26
II.4 ASSOCIATED VOLCANICS.....	27
II.5- SEDIMENT FILL.....	29
II.6- PRE-RIFT BASEMENT.....	33
II.7- PETROLEUM POTENTIAL OF THE ALBERTINE GRABEN.....	33
II.7.1- SOURCE ROCKS AND OIL SEEPAGES.....	33
II.7.2- RESERVOIR ROCKS.....	34
II.7.3- TRAPS AND SEALS.....	34
II.8- PREVIOUS PUBLISHED USE OF ICP-MS FOR CARBONATE DISCRIMINATION.....	34
CHAPTER THREE: METHODOLOGY.....	39
III.1- FIELD TRIPS:.....	39
III.2- TRAVERTINE PETROGRAPHY.....	47
III.2.1- THIN SECTION PREPARATION.....	47
III.2.2- MICROSCOPY.....	51
III.3- OXYGENE AND CARBONE STABLE ISOTOPES ANALYSIS:.....	52
III.3.1- CARBONE STABLE ISOTOPE ANALYSIS:.....	52
III.3.2- OXYGEN STABLE ISOTOPE ANALYSIS:.....	53
III.4- STRONTIUM ISOTOPES RATIO ANALYSIS.....	54
III.5- GAS CHROMATOGRAPHY MASS SPECTROMETRY (GC-MS).....	55
III.6. INDUCTIVELY COUPLED PLASMA – MASS SPECTROMETRY (ICP-MS) ANALYSIS.....	56
III.6.1- SAMPLE INITIAL PREPARATION FROM SOLID TO POWDER STAGE.....	58
III.6.2- SAMPLE SPECIAL PREPARATION FROM POWDER TO SOLUTION STAGE.....	60
III.6.2.3 - FINAL DILUTION.....	66
III.6.3- ICP-MS ANALYSIS ON SAMPLES IN SOLUTION.....	66
III.6.4- ICP-MS RESULTS INTERPRETATION.....	71



CHAPTER FOUR: FIELD TRIPS.....	75
IV.1- HISTORY OF ALBERTINE RIFT FIELD WORKS .....	75
IV.2- EA1, EA4A & EA4B (UGANDA) FIELD WORK .....	76
IV.3- BLOCK FIVE (DR CONGO) 2010 FIELD WORK .....	82
IV.4- BLOCK FIVE (DR CONGO) 2014 FIELD WORK .....	84
IV.4.1- GEOLOGIC ENVIRONMENT AND FIELD DESCRIPTIONS OF TRAVERTINE SAMPLES COLLECTED IN BLOC V IN 2014 .....	85
IV.4.2- OVERVIEW OF BLOCK V OTHERS CARBONATES OUTCROPS.....	94
IV.4.3- STRUCTURE, HEAT & FLUID FLOW.....	100
IV.4.3.1- REGIONAL STRUCTURE .....	100
IV.4.3.2- HEAT AND FLUID FLOW .....	104
CHAPTER FIVE: EARS TRAVERTINE PETROGRAPHY .....	108
V.1- TRAVERTINE SAMPLES FROM 2007 TO 2010 FIELD TRIPS.....	108
V.2- PCK LIMESTONES SAMPLES .....	112
V.3- TRAVERTINE SAMPLES FROM 2014 FIELD TRIP .....	112
V.4- MANDAWA BASIN LIMESTONES SAMPLES.....	115
CHAPTER SIX: GEOCHEMISTRY RESULTS .....	117
VI.1- ISOTOPE RATIO MASS SPECTROMETRY (IRMS) .....	117
VI.1.1- CARBON (PDB) VERSUS OXYGEN (SMOW) STABLE ISOTOPES.....	118
VI.1.2- CARBON (PDB) VERSUS OXYGEN (PDB) STABLE ISOTOPES .....	118
VI.1.3- CARBON (PDB) VERSUS TRAVERTINE PRECIPITATION TEMPERATURE.....	119
VI.2- STRONTIUM ISOTOPE RATIO ANALYSIS.....	120
VI.3- GC-GCMS ANALYSIS .....	121
VI.3.1- GCMS RESULTS FOR (LES 18) SAMPLE .....	123
VI.3.2 – GC-GCMS RESULTS FOR LYEMBUMUZA (LE25) SAMPLE .....	123
VI.3.3 – GC-GCMS RESULTS FOR LYEMBUMUZA (LE25) SAMPLE .....	124
VI.3.4- CG RESULTS FOR MUHOKIYA SAMPLE (LE 27).....	124
VI.3.5- CGMS RESULTS FOR MUHOKIYA SAMPLE (LE 27).....	125
VI.3.6- SUMMARY OF THE GC-GMS RESULTS .....	125
VI.4- INDUCTIVELY COUPLED PLASMA MASS SPECTROMETRY (ICP-MS).....	126
VI.4.1 - ICP-MS RESULTS OF 2013 EXPERIMENT .....	126
VI.4.2 - ICP-MS RESULTS OF 2016 EXPERIMENT .....	131
VI.4.3 - ICP-MS RESULTS OF 2018 EXPERIMENT .....	151
CHAPTER 7: RESULTS DISCUSSIONS .....	169
VII.1 – FIELD TRIP RESULTS.....	169
VII.2 – MICROSCOPY OBSERVATION RESULTS .....	173
VII.3 – STABLE CARBON AND OXYGEN ISOTOPE RESULTS .....	177

VII.4 – STRONTIUM ISOTOPE RATIO RESULTS.....	180
VII.5– GC-GCMS RESULTS.....	181
VII.6– ICP-MS RESULTS INTERPRETATION.....	183
CHAPTER 8: CONCLUSIONS.....	228
REFERENCES.....	238

## LIST OF TABLES

<i>Table 1: 20 End members Samples from the 2013 experiment run again in 2016</i>	70
<i>Table 2: Travertine Samples collected in Uganda, 2007 -2009</i>	76
<i>Table 3: Travertine samples collected in DR Congo, 2014</i>	86
<i>Table 4: MUQ values of PCK samples obtained in 2016</i>	147
<i>Table 5: Marine limestone criteria check box for the PCK samples</i>	148
<i>Table 6 Marine limestone criteria check box for 2014 Bloc V Samples</i>	151
<i>Table 7 Marine limestone criteria check box for the Mandawa samples</i>	159

## LIST OF ENCLOSURES IN MEMORY STICK

1. Literature review (Chapter 2): articles, revues, books...pdf versions.
2. 2013 ICP-MS results of Travertine samples collected from 2007 to 2010.
3. 2016 ICP-MS results of 2007 to 2010 and PCK samples for method confirmation.
4. 2018 ICP-MS results of Travertine samples collected in 2014 and Mandawa Samples.

## LIST OF APPENDICES

1. Samples preparation lab notes
2. ICP-MS Results REE tables
3. Field notes

## TABLE OF FIGURES

### Chapter One

Figure I.1:	Travertine locations in the Eastern Africa Rift basins (Nicholas, 2016)	15
Figure I.2:	Lithology log of the Waki-B1 in the Albert Basin (Karp et al., 2012).	16
Figure I.3:	Lithology log of the Ngaji-1 well in the Edward Basin (Dominion Ltd)	17

### Chapter Two

Figure II.1:	Southern Eduard Basin Cross section (Lærdal et al., 2002)	22
Figure II.2:	Gravimetric Map of the Bloc V, DRC.(SOCO, 2010)	23
Figure II.3:	Main boundary faults in the Eduard basin (Lærdal et al., 2002)	24
Figure II.4:	Tectonic map of the Ruwenzori region (Ring, 2008)	25
Figure II.5:	Photographs illustrating the topography of the Ruwenzori mountain	26
Figure II.6:	Map of equatorial part of the EARS (Rosenthal et al., 2009)	27
Figure II.7:	Location of the major volcanic fields in SW Uganda (Eby et al., 2009)	28
Figure II.8:	Typical sedimentation sequence in Rift Lake	29
Figure II.9	Typical alluvial fan structure and depositional environments in EA4B	31
Figure II.10:	Effect of tectonics and climate have on sedimentation.	32

### Chapter Three

Figure III.1:	Nyakakoma Base camp, SOCO 2014	40
Figure III.2:	Geologist accommodation unit, SOCO 2014	41
Figure III.3:	Ablution facilities and water tanks, SOCO 2014	41
Figure III.4:	Kitchen, mess facilities and radio room, SOCO 2014	41
Figure III.5:	Geologist's tent and office, SOCO 2014	42
Figure III.6:	Shelves and Samples boxes, SOCO 2014	42
Figure III.7:	Helicopter in its landing zone, SOCO 2014	43
Figure III.8:	Field equipments, SOCO 2014	43
Figure III.9:	Field Maps (SOCO, 2014)	44
Figure III. 10	Field Observations (SOCO, 2014)	45
Figure III.11:	Spectral Gamma Ray field recording and record sheet (Avalonia,2014)	46
Figure III.12	Samples collection (SOCO, 2014)	47
Figure III.13:	Travertine thin sections (TCD,2018) (Hill, 2007) (Hill, 2007) (Hill, 2007) (Hill, 2007) (Hill, 2007)	50
Figure III.14:	Nikon LV 100 optical Microscope (CMA, 2018)	51
Figure III.15:	Typical diagram of an IRMS (lab notes sketch)	52
Figure III.16:	Phanerozoic Climate change graph. (Veizer et al., 2000)	54
Figure III.17:	Variation of $^{87}\text{Sr}/^{86}\text{Sr}$ ratio of the Phanerozoic sea waters.	55
Figure III.18:	Periodic table of the elements obtained by ICP- OES and MS analysis.	57
Figure III.19:	Microscopic observation &, Drilling of Travertine textures	58
Figure III.20:	Travertine Slices sample preparation by Sylvain K. &J. D	59
Figure III.21:	Drilling process trough visible textures, structures and/or fabrics	59
Figure III.22:	Drilling tool used in 2013	59
Figure III.23:	Different sizes of the drill bits used	59
Figure III.24:	Example of the drilling residual powder of a visible textures	60
Figure III.25:	Small tubes for textures, structures and/or fabrics	60
Figure III.26:	Electronic scale used to weight the Travertine samples powder ICP-MS	63
Figure III.27:	weighting of the Travertine samples powder	64
Figure III.28:	Geometry the ICP-MS quadrupole + sample holder	67
Figure III.29:	Quadrupole Model ICAP-Q ICP-MS, (TCD, unit 7)	67
Figure III.30:	Approximate detection capabilities ELAN 6000/6100 quadrupole	69

Figure III.31	: Sample V20 final ICP-MS results	72
Figure III.32:	characteristic REE+Y patterns in depositional environment	73

#### **Chapter Four**

Figure IV.1:	Travertine location Field Maps (Nicholas, 2009)	77
Figure IV.2:	Travertine collected samples (Nicholas, 2009)	81
Figure IV.3:	Travertine collected samples (Nicholas, 2009)	81
Figure IV.4:	Travertine collected samples (Nicholas, 2009)	81
Figure IV.5:	Travertine collected samples (Nicholas, 2009)	82
Figure IV.6:	Travertine collected samples (SOCO, 2010)	83
Figure IV.7:	Travertine collected samples (SOCO, 2010)	83
Figure IV.8:	Travertine collected samples (SOCO, 2010)	83
Figure IV.9:	V2 collection at Biruma Quarry (SOCO, 2010)	84
Figure IV.10:	Block V Field Map (SOCO, 2010)	84
Figure IV.11:	Travertine collected samples (SOCO, 2014)	86
Figure IV.12:	Travertine collected samples (SOCO, 2014)	87
Figure IV.13:	Travertine collected samples (SOCO, 2014)	87
Figure IV.14:	Travertine collected samples (SOCO, 2014)	88
Figure IV.15:	Travertine collected samples (SOCO, 2014)	89
Figure IV.16:	Bing 2018 Aerial view of the Eduard basin Travertine occurrences.	91
Figure IV.17:	Bing 2018 Aerial view of the ZOI	92
Figure IV.18:	Geologic considerations of the ZOI. Samples & Hot Springs observed.	92
Figure IV.19:	©Bing 2018 Aerial view of the Biruma Quarry	93
Figure IV.20:	Geologic considerations of the Biruma Quarry. Samples collected	93
Figure IV.21:	Vitshumbi fault scarp looking north at log section BVγ-10.	94
Figure IV.22:	Road cutting along the side of the Ruindi river valley	96
Figure IV.23:	Calcitised reed impression in Lithofacies 'a' at log section	97
Figure IV.24:	Pustulous textured microbial mat in Lithofacies	97
Figure IV.25:	Cross-bedding in Lithofacies in Ruindi river valley.	98
Figure IV.26:	Marl rip-up clasts in Lithofacies 'in Ruindi river valley.	98
Figure IV.27:	Gamma Ray response of the Vitshumbi fault scarp.	99
Figure IV.28:	Structural map of onshore Block V. Major rift faults.	101
Figure IV.29	a,b Bloc V sketch cross section	102
Figure IV.29	c,d: Bloc V sketch cross section	103
Figure IV.30:	Measuring the temperature of hot spring in the Rutshuru River.	104
Figure IV.31:	Graph showing spring temperatures at each locality	105
Figure IV.32:	Completed Geologic Map of the Southern Lake Edward Basin	106
Figure IV.33:	Completed chrono & stratigraphy of the Southern Lake Edward Basin	107

#### **Chapter Five**

Figure V.1:	2007-2010 Travertine thin sections observations.	108
Figure V.2:	PCK carbonate layered Slice.	112

#### **Chapter Six**

Figure VI.1:	Travertine samples locations in the Lake Edward basin.	117
Figure VI.2:	Edward Lake basin carbon (PDB) versus oxygen (SMOW) stable isotopes	118
Figure VI.3:	Edward Lake basin carbon (PDB) versus oxygen (PDB) stable isotopes	119
Figure VI.4:	Edward Lake basin carbon (PDB) stable isotopes versus site temperature	119
Figure VI.5:	$^{87}\text{Sr}/^{86}\text{Sr}$ ratio variation of Phanerozoic seawater.	120
Figure VI.6:	$^{87}\text{Sr}/^{86}\text{Sr}$ ratio variation of Phanerozoic seawater.	120
Figure VI.7:	$^{87}\text{Sr}/^{86}\text{Sr}$ ratio curve for the Proterozoic.	121

Figure VI.8 :	<i>Oil slicks collected in the Lake Edward</i>	121
Figure VI.9:	<i>Sterile lyophilic cloths for Oil slick collection</i>	122
Figure VI.10:	<i>GC–MS–extracted ion profiles of steranes in Lake Edward oil sample</i>	122
Figure VI.11:	<i>GC–MS–extracted biomarker distribution from sample LES 18.</i>	123
Figure VI.12:	<i>GC results sample LE 25 from Lyemubuza quarry</i>	123
Figure VI.13:	<i>GCMS results sample LE 25 from Lyemubuza quarry</i>	124
Figure VI.14:	<i>GC results sample LE 27 from Muhokiya quarry</i>	124
Figure VI.15:	<i>GCMS results sample LE 27 from Muhokiya quarry</i>	125
Figure VI.16:	<i>Plots of C27 – C29 distributions Edward slicks &amp; Lyemubuza + Muhokya</i>	125
Figure VI.17:	<i>Block V Travertine REE signatures by ICP-MS in 2013</i>	126
Figure VI.18:	<i>Carbonatites signature plotted alongside Fort Portal &amp; Freshwater</i>	127
Figure VI.19:	<i>Carbonatites correlation coefficient with Fort Portal Carbonatites.</i>	128
Figure VI.20:	<i>Travertine signature plotted alongside Marine lst &amp; Devonian Reef Lst.</i>	129
Figure VI.21:	<i>Marine limestones Travertine correlation coefficient with Devonian Reef</i>	129
Figure VI.22:	<i>Marine limestones Travertine correlation coefficient with Devonian Reef</i>	129
Figure VI.23:	<i>2013 Travertines Hybrid signature.</i>	130
Figure VI.24:	<i>LE 32 Correlation coefficient with Fort Portal</i>	130
Figure VI.25:	<i>LE 32 Marine limestones Check Box</i>	131
Figure VI.26:	<i>ICP-MS 2016: All signatures</i>	131
Figure VI.27:	<i>ICP-MS 2016: Carbonatites signatures alongside Fort portal Lava</i>	132
Figure VI.28:	<i>2007- 2010 Block V Carbonatites correlation coefficient with Fort Portal</i>	133
Figure VI.29:	<i>Carbonatites signatures Comparison of the 2013 – 2016 ICP-MS</i>	136
Figure VI.30:	<i>Block V Travertine Marine limestone signatures by ICP-MS in 2016</i>	137
Figure VI.31:	<i>Block V Marine limestone Correlation Coefficient</i>	138
Figure VI.32:	<i>Marine Limestones signatures Comparison of the 2013 – 2016 ICP-MS</i>	146
Figure VI.33:	<i>PCK Samples REE fresh water signature,</i>	148
Figure VI.34:	<i>PCK &amp; LE 26 REE +Y</i>	149
Figure VI.35:	<i>PCK &amp; LE 26 Correlation Coefficient</i>	150
Figure VI.36:	<i>ICP-MS, 2018: All signatures</i>	151
Figure VI.37:	<i>ICP-MS, 2018: Carbonatites signatures</i>	152
Figure VI.38:	<i>Bloc V signatures correlation coefficient with Fort Portal #3</i>	152
Figure VI.39:	<i>All Marine Limestones REE signatures detected by ICP-MS</i>	153
Figure VI.40:	<i>All Marine Limestones Correlation coefficient with Devonian Reef</i>	154
Figure VI.41:	<i>Bloc V 2014 Marine Limestones signatures</i>	155
Figure VI.42:	<i>Bloc V Marine Limestones Correlation coefficient with Devonian Reef</i>	156
Figure VI.43:	<i>All Marine Limestones and published REE signatures</i>	157
Figure VI.44:	<i>2013 Marine Limestones R<sup>2</sup> with published carbonates REE</i>	158
Figure VI.45:	<i>2016 Marine Limestones R<sup>2</sup> with published carbonates REE</i>	159
Figure VI.46:	<i>2018 Marine Limestones R<sup>2</sup> with published carbonates REE</i>	160
Figure VI.47:	<i>Mandawa Basin &amp; LE 26 REE +Y patterns</i>	162
Figure VI.48:	<i>Mandawa Basin &amp; LE 26 correlation coefficient</i>	163
Figure VI.49:	<i>Mandawa Basin &amp; Bloc V REE +Y patterns</i>	164
Figure VI.50:	<i>Mandawa Basin &amp; Bloc V Correlation Coefficient</i>	165
Figure VI.51:	<i>Bloc V 2014 Travertine Hybrid signatures by ICP-MS 2018</i>	166
Figure VI.52:	<i>Bloc V 2014 Hybrid and Marine Limestones signatures by ICP-MS 2018</i>	166
Figure VI.53:	<i>Bloc V 2014 Hybrid Correlation coefficient with Devonian Reef</i>	167
Figure VI.54:	<i>Bloc V 2014 Hybrid Correlation coefficient with Fort Portal Carbonatites</i>	167

### **Chapter Seven**

<i>Figure VII.1: Travertine ICP-MS results Map of Albertine Rift basin</i>	225
<i>Figure VII.2: Travertine ICP-MS results Vs Carbon and Oxygen stable isotopes results.</i>	226

### **Chapter Eight**

<i>Figure VIII.1 Schematical hypothetical cross section of Bloc V, (Nicholas, 2013)</i>	232
<i>Figure VIII.2 Travertine geochemical origin localisation in the Albertine Graben</i>	236

## **LIST OF ABBREVIATIONS**

1. ICP-MS: Inducted coupled Plasma Mass Spectrometry
2. REE: Rare Earth Element
3. FP: Fort Portal
4. EARS: Eastern Africa Rift System
5. SSTs: Sandstones
6. LBF: Lubero Border Fault
7. KF: Kichwamba Fault
8. KKK-FZ: Kazinga-Kiruruma-Kikarara Fault Zone
9. PEPD: Petroleum Exploration production Department ( Uganda)
10. MIS : Marine Isotope Stage
11. GC: Gas Chromatography
12. GCMS: Gas Chromatography Mass Spectrometry
13. IRMS : Isotope Ratio Mass Spectrometry
14. CMA: Centre for Microscopy Analysis
15. MUQ: Mud of Queensland
16. ZOI: Zone of Interest

# CHAPTER ONE: INTRODUCTION, AIMS AND OBJECTIVES

## I.1- INTRODUCTION

The multi-million dollar Oil exploration industry in the Albertine Rift Valley of East Africa is currently based entirely on the premise that there is only one rifting process happened in the region, this is the active East African Rift System (EARS). The basic assumptions being that the source rock for the oil and the reservoir sands that hold it in their traps, are all within this rift, which is no older than Miocene, approximately 10 million years.(Nicholas et al., 2016)

During series of geological field surveys conducted in the EARS from 2007 to present, live Oil have been discovered in Travertine limestones cavities at Lyemumbuza (Uganda) hot springs, precipitated as well as many others similar springs at active, or palaeo-, spring sites around the margins of the Lake Edward, Lake George and Lake Albert basins (Figure I.1).

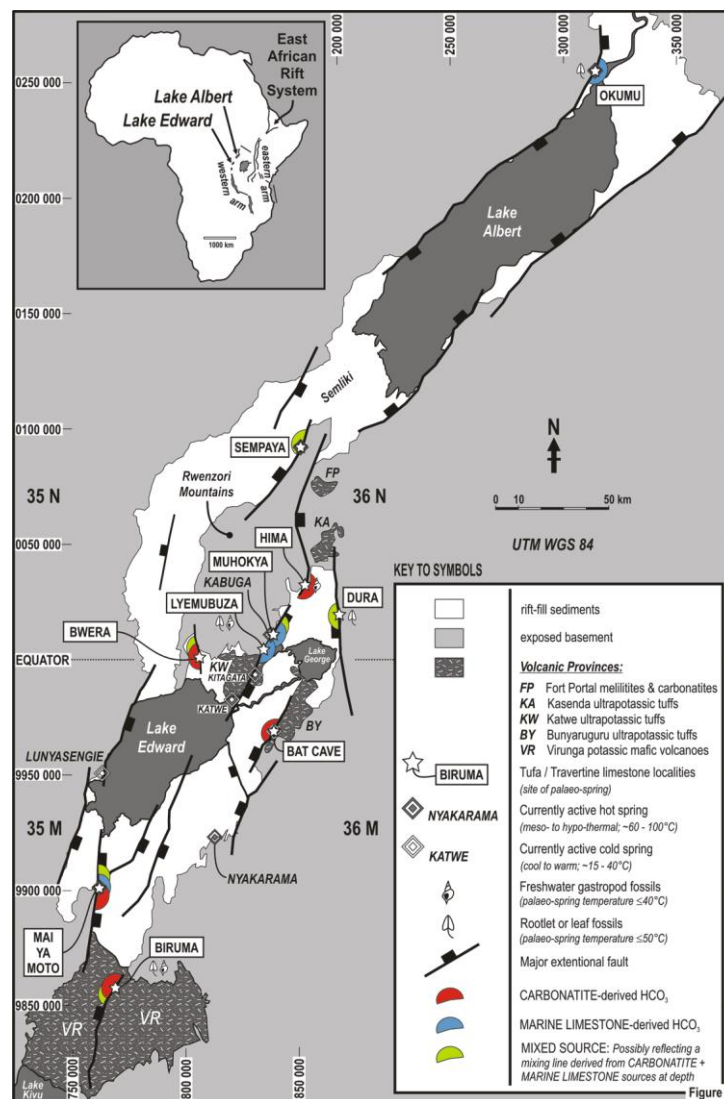


Figure I.1: Travertine locations in the Eastern Africa Rift basins (Nicholas, 2016)

These Travertine limestones are much localised and they are always situated over deep-seated rift-bounding faults, linking their origin to meso- and hydro-thermal groundwater flux along fault planes. For the groundwater to attain the high concentration of bicarbonate necessary to potentially precipitate calcite in a spring pool at the surface, the requirement is that it must have percolated through a substantial carbonate bedrock unit at depth, typically a regional sedimentary limestone. However, as shown in the Figures I.2 and I.3 below (Karp et al., 2012) and (Nicholas, 2009) both Lake Albert and Lake Edward rift basins are infilled by fluvial, deltaic and lacustrine siliciclastic sediments, such as sandstones, claystones and conglomerates.

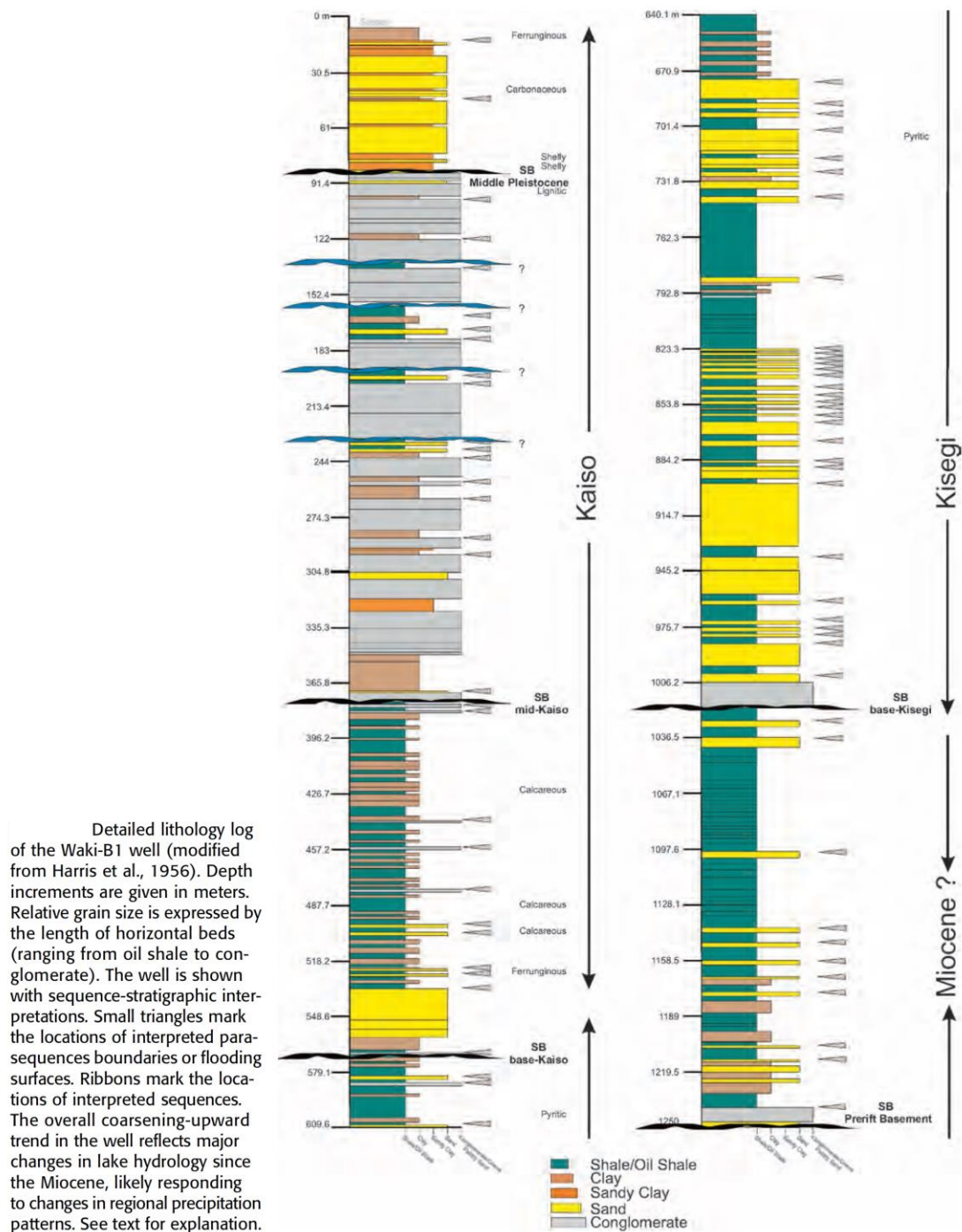


Figure I.2: Lithology log of the Waki-B1 in the Albert Basin (Karp et al., 2012)



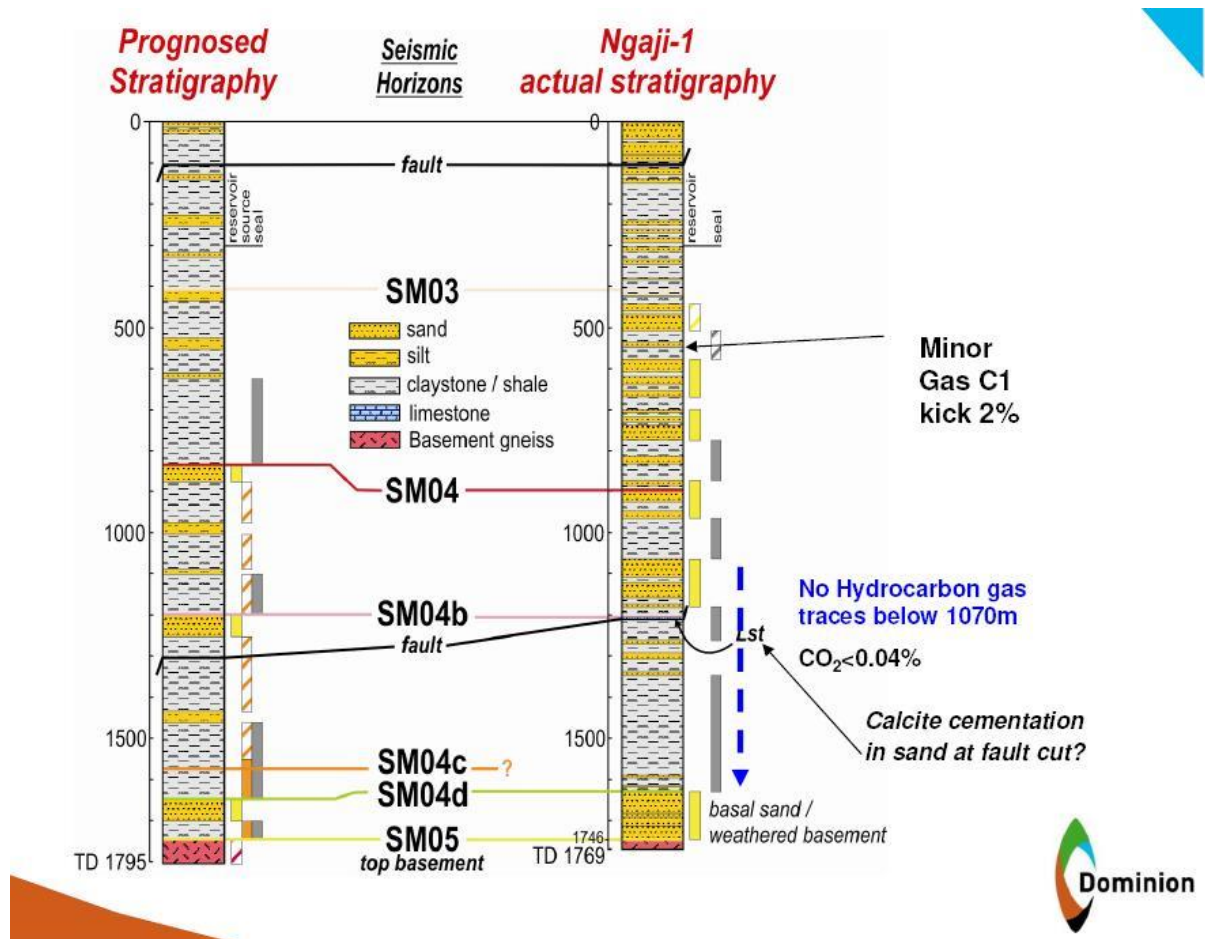


Figure I.3: Lithology log of the Ngaji-1 well in the Edward Basin (courtesy of Dominion ltd)

No limestone beds are known in Albertine rift-fill sediments, either at the surface in outcrop, or subsurface in well penetration. In Lake Albert, thin caliche paleosols are present in rift-fill sediments exposed around the margins of the lake, but these are only poorly developed carbonate concretionary horizons and have not developed into full, laterally continuous calcretes. Thus the presence of these Travertine limestones, and more specifically, the origin of their bicarbonate, remains enigmatic. Given the groundwater chemistry required to precipitate Travertine limestones, and the complete absence of any fluvial or lacustrine limestone beds in the Lake Albert and Lakes Edward rift-fill stratigraphy, it begs the question as to how and why the more or less relatively common Travertine occurrences have been formed.

### I.2- HYPOTHESIS (problem to solve or questions to answer)

Rift fill sediments in the Albertine Graben are all siliclastics except for much localised patches of Travertine limestones precipitates which are very common in the Lake Edward and Lake Albert basins of the East African Rift System. Rift-fill sediments are usually entirely composed of siliclastics and so, precipitation of the limestones is something of a mystery and could be linked to hydrothermal fluids passing up the major faults which bound the rift graben.

All this poses some questions which has a direct consequence for both the Geology understanding and Oil Exploration industry in the region:

### **How and why did these Travertine limestones form?**

#### **What is the source of their originating carbonate?**

There would seem to be only 2 possible sources to be scientifically confirmed or not for the bicarbonate needed to precipitate the limestones:

- If the bicarbonate comes from Carbonatites, then igneous intrusive sills must be common at depth throughout the rift.
- If the bicarbonate comes from a marine limestone at depth there may be a pre-tertiary rift beneath the Cenozoic rift.

Extremely rare carbonatite lavas are exposed nearby and this raises the possibility that carbonatite magmas at depth might be the source of bicarbonate. Conversely, it has been hypothesised that older, pre-rift Cretaceous sediments may underlie the current Tertiary rift. **Could marine limestones in these have yielded carbonate to the hot fluids passing up faults?**

### I.3- AIM AND OBJECTIVES:

The principal aim of the present MSc study is to give the scientific answer to the three (3) above geochemistry questions which will play a major role in understanding the geologic evolution of the Albertine sedimentary basin.

The main objective of this study is to understand through the reversible reaction  $\text{Ca}^{2+} + 2\text{HCO}_3^- = \text{CaCO}_3 + \text{CO}_2 + \text{H}_2\text{O}$ , the geochemical source of the Bicarbonate by which carbonates in Travertine, are precipitated in hot springs very localized in straight lines along many Eastern Africa rifts bounding faults.

As specific objectives, this work will:

1. Undertake detailed field trips in the Albertine Rift and use the maximum of the field informations collected to understand and describe the geologic environment of these Travertine outcrops;
2. Describe and Collect properly the maximum Travertine samples from their originate field environment in order to make petrographic observations and geochemical analysis;
3. Make petrographic observations and describe the slabs and/or thin section using the latest Nikon microscope benefits;
4. Compare previous geochemistry results obtained from Carbon and Oxygen stable isotopes and Strontium isotope ratio run on selected Travertine samples;
5. Run ICP-MS on selected Travertine samples to determine the REE elemental concentrations in order to scientifically well discriminate the both end members: igneous Carbonatites intrusions/ volcanics and sedimentary marine Carbonates.
6. Discuss about all field trips, petrography and geochemistry results and publish any new scientific contribution to the best knowledge of the EARS geology.

## Chapter 1 Conclusion:

*The present Msc. Research study aims to solve the geologic question about:*

- *the possible presence of a pre-tertiary rift marine limestone beneath the Cenozoic classical Eastern Africa Rift System by using the geochemistry to investigate the undocumented Travertines field evidences.*
- *the source of Carbonate found in these localized Travertines deposits mainly outcropping along both East and West Rift bounding faults through which the carbonated groundwaters are emerging in surface (hot and cold springs).*

*The next Chapter, named the Literature review:*

- *has been sourced from either the existing publications available in the public domain or Oil exploration reports obtained by the courtesy of SOCO Exploration Production DRC and its Partner Dominion Ltd.*
- *summarizes the revised Eastern Africa Rift System publications in regards to the geologic knowledge about the Travertines and other limestones found in outcrops within the Albert-Edward basins.*
- *allows the reader of the present Msc research to be aware of the actual level of geological knowledge of the Eastern Africa Rift System in order to better assess its scientific contribution to the Albert-Edward Basins geological knowledge.*
- *updates the reader with some of the previous, documented and successful uses of ICP-MS to detect the marine limestones REE signatures patterns and their respective correlation coefficients with published carbonates REE (Fort Portal, Devonian Reef, Sea Waters...)*

## CHAPTER TWO: LITTERATURE REVIEW

The Eastern Africa Rift System is an active continental rift zone in East Africa which consists of two main branches, the Eastern and Western Rift valleys. The Western branch of the EARS extends southwards from Sudan through Lakes Albert, George, Edward, Kivu, Tanganyika, Rukwa and Nyasa to the Urema Graben of Mozambique. Three sectors are recognised within the Western branch; northern, central and southern. The northern sector or Albertine Rift Valley comprises the three lakes of Albert, George, and Edward with the national border between Uganda and DRC passing along the centre of the valley. The Albertine Rift is structurally segmented into a series of asymmetric graben depocentres, or domains, each separated by NW-SE or W-E trending Accommodation Zones (Rubondo, 2005). For the purposes of petroleum exploration, each of the rift basins has been subdivided into blocks, like for instance Block V on the DRC side of Lake Edward, or 'Exploration Areas' (EA), and EA4A and EA4B on the Ugandan side. The Ruwenzori Mountains also separate Lake Albert from Lakes Edward and Georges.

Mandawa Basin located in coastal Tanzania, is geologically considered as a result of tensional forces related to the Gondwana break-up and the opening of the Indian Ocean. This Basin seems to have been created by transgressive and regressive phases which have led to deposition of various sedimentary sequences from Late Triassic to recent age. These sedimentary sequences have been deposited in different depositional environments, from alluvial fans proximal to source area to deep marine, distal environments. The sedimentary sequences display various mineralogical and textural compositions and heavy mineral contents. (Nerbråten, 2014). Samples from Mandawa basin have been used in this Msc to be referred as Marine limestone origin proxy.

Lake Edward basin, the case study of this MSc research project, consists of an asymmetric half-graben structure with major controlling faults bounding the western edge of the lake, filled with inter-bedded sands and clays, as is typical of continental rift basins. Both climate and tectonics have affected the sedimentation in the Lake Edward basin, periods of active or quiet tectonics have occurred in the past, as have glacial and/or interglacial periods of significant climate change, these have all caused fluctuations in the lake level and in the sedimentation style and its architecture over time.

Field mapping of the onshore part of the basin in Exploration Area 4B (EA4B) has shown that several sedimentary fan systems extend from the basin flanks NW towards the lake (Nicholas, 2009). More recently, a detailed map and working stratigraphic framework of EA4B has been established (Nicholas et al., 2016). Security issues in Block V on the DRC side of the basin prevented any field work from being undertaken until 2010 when a brief field reconnaissance was carried out by SOCO International plc. followed by a thorough field survey of Block V in July and August of 2014. This MSc. project had incorporated all these field works into it to form the basis of the first complete appraisal of the sedimentology, stratigraphy and structure, and petroleum geology of the entire Lake Edward basin.

## II.1- MODERN LIMNOLOGY

Lake Edward is the smallest one of the Great Rift Lakes of the East African Rift System and has a maximum depth of 117m (Beuning and Russell, 2004),(Russell and Johnson, 2005),(Russell et al., 2003) to 120m (Lærdal et al., 2002). Lake Edward drains to Lake Albert northwards via the Semliki channel (Russell and Johnson, 2005; (Lærdal et al., 2002) and Lake George to the northeast drains into Lake Edward via the Kazinga channel. The water level in Lake Edward, like most of the great rift lakes, is highly sensitive to rainfall due to the highly variable monsoonal rainfall pattern in the region of East Africa (Beuning and Russell, 2004). The lake is permanently anoxic below 80m depth and periodically anoxic below 40m depth, and it is considered a eutrophic system (Russell et al., 2003).

Palynological and sedimentary proxies indicate sub-millennial-scale events related to changes in riverine discharge and runoff in the Edward basin. These variability in runoff, and hence precipitation, could be attributed to Holocene variability in Indian or Atlantic Ocean SSTs or to shifts in the relative contribution of Indian and Atlantic moisture sources to the western Rift of equatorial Africa. (Beuning and Russell, 2004).

Sediments of the Edward Lake contain like the most of EARS lakes, a unique and sensitive record of past climate change. This unique and sensitive record is in part a consequence of hydrological balance that are dominated by evaporation rather than outflow that in turn influences the biological, geological, and chemical processes in the lake basins. (Beuning and Russell, 2004).

## II.2- BASIN STRUCTURE

The East African rift system comprises a unique succession of graben basins linked and segmented by intracontinental transform, transfer and accommodation zones. (Chorowicz, 2005).

The most characteristic features in the EARS are mainly narrow elongate zones of thinned continental lithosphere related to asthenospheric intrusions in the upper mantle. A part of the EARS structure could be observed on the surface by thermal uplift of the rift shoulders.

The Albertine graben valleys and basins have been in place over a major failure in the lithospheric mantle, and in the crust comprise a major border fault, linked in depth to a low angle detachment fault, inducing asymmetric roll-over pattern, eventually accompanied by smaller normal faulting and tilted blocks. (Chorowicz, 2005).

The Lake Edward basin is an extensional asymmetric half-graben basin (Fig.II.1: (Lærdal et al., 2002), with the major controlling fault bounding the western edge of the lake in the DRC (Nicholas et al., 2016) and an estimated sediment fill of up to 4 km (Upcott et al., 1996); (Byakagaba, 1997).

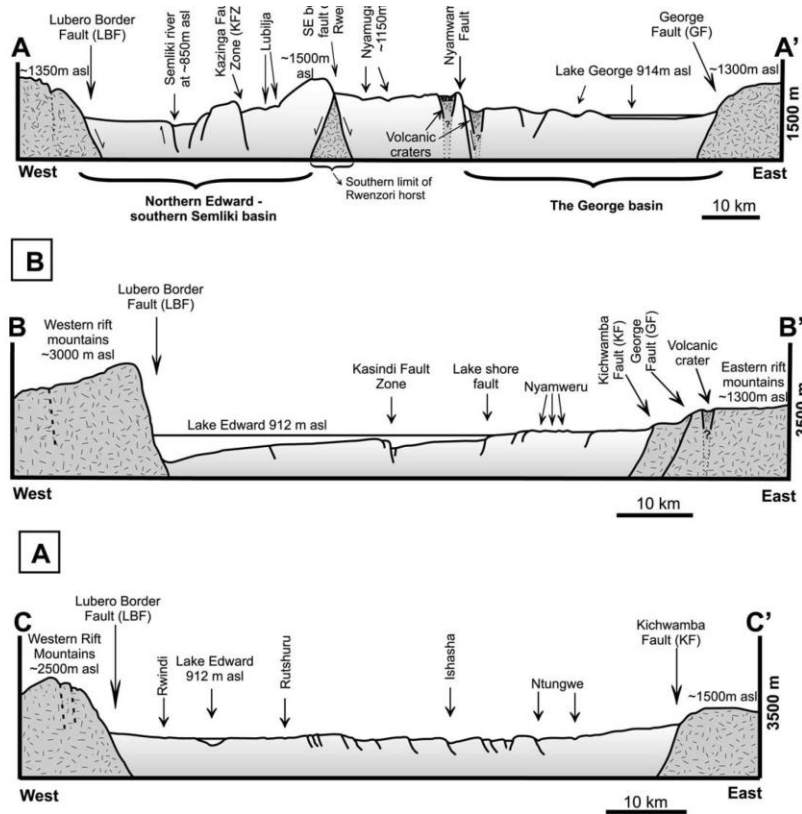


Fig. Cross-section through the southern Edvard basin. (B) Cross-section through the central Edvard basin. (C) Cross-section through the northern Edvard-George basin. See Fig. 5 for location of the transect lines. (Throw on the KFZ (B) is exaggerated relative to the vertical scale of the figures. Fault scarp is ~12 m on the lake floor.)

Figure II.1 :Southern Eduard Basin Cross section (Lærdal et al., 2002)

This asymmetric graben or asymmetric half-graben structure has been confirmed by Seismic sections combined with Airmag and magnetic data showing clearly that the Lake Edward basin has a major controlling fault bounding the western edge of the lake in the DRC. (Nicholas et al., 2016).

These successions of half-graben basins structures are generally bordered on the two sides by high relief, comprising almost continuous parallel mountain lines and plateaus, and sometimes volcanic massifs. Other uplifted areas in the region are due to belts, which may be recent (Atlas, Zagros belts) or ancient (Karoo belt), or to intracontinental hotspots (Hoggar, Tibesti plateaus).(Chorowicz, 2005).

The asymmetric nature of the basin can be seen in gravity survey images with the axis located close to the western bounding fault in Figure II.2: (SOCO, 2010).

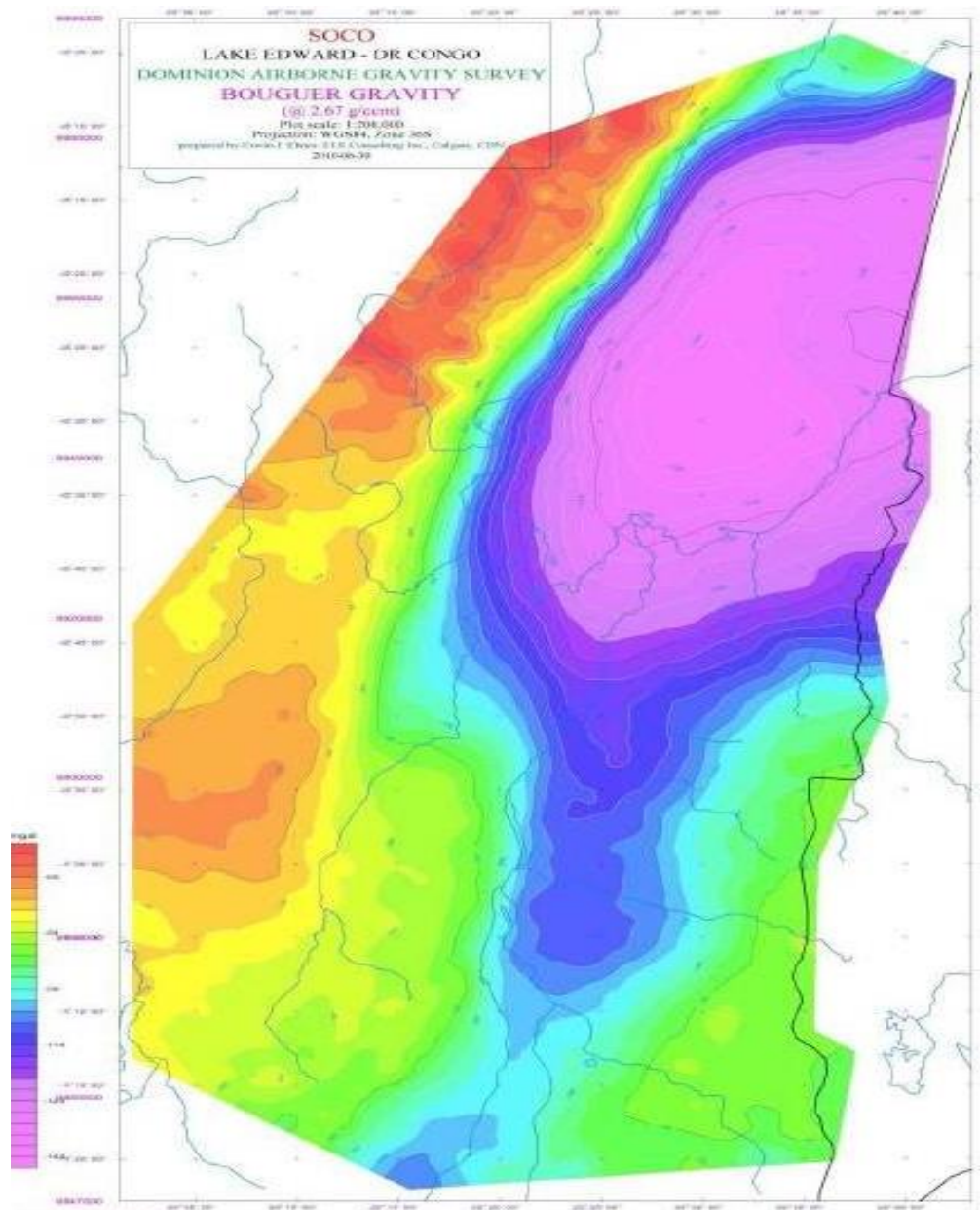


Figure II.2 : Gravimetric Map of the Bloc V, DRC.(SOCO, 2010)

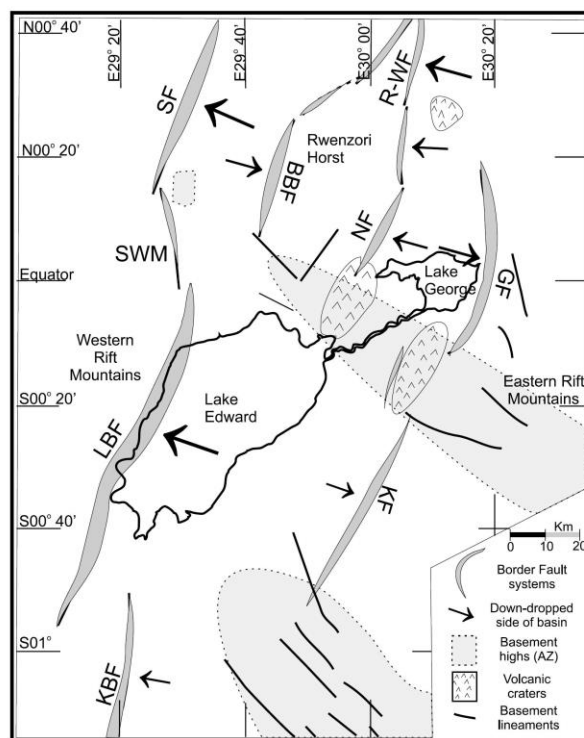
The main boundary fault to the West of the basin is the Lubero Border Fault (LBF), and the main boundary fault to the East is the Kichwamba Fault (KF) (Figure II.3 :(Lærdal et al., 2002). The throw on the LBF estimated to be a maximum of 7km decreasing in a southerly direction. The Figure II.3: (Laerdal et al., 2002) below shows the decrease in

the difference between the cross sections from North to South (Upcott et al., 1996; Laerdal et al., 2002).

Nicholas (2009, 2016) outlines the structure of exploration area EA4B to the SE of Lake Edward. A 15km wide NE-SW trending Kazinga-Kiruruma-Kikarara Fault Zone (KKK-FZ) is exposed across the centre of EA4B, the Kiruruma and Kikarara faults trend towards each other and are thought to have a relay ramp between them which is exploited by rivers for drainage and so are thought to be the same fault (Nicholas, 2009; Nicholas et al., 2016).

When cross sections and seismic traces are correlated, it can be seen that a network of ESE dipping normal faults compartmentalise the basin. Extensional movement along the KKK-FZ has created a sub-basin known as the Bwambara Trough which trends NE-SW along the SE rift margin.

The oldest unit in the Bwambara Trough sediment fill (Kisenyi Formation) contains a bed of reworked tuffs at the top of the section, interpreted as originating from the nearby Bunyaraguru tuffs. This would date the beginning of subsidence of the Bwambara Trough to before the eruption of the Bunyaraguru tuffs estimated to within the last 84,000 yrs (Boven et al., 1998); Nicholas et al., 2016). More recent raised 'pod' structures formed on the footwall crest where curved antithetic faults are seen to join up with the main fault scarp suggest that the neotectonic phase in onshore EA4B is compressional or transpressional.



Map showing the location of the main boundary faults in the area. Arrows point towards down-thrown side of the basin. Shaded areas, with a roughly NW-SE orientation, correspond to basement highs (high relief AZs). Volcanic areas and basement lineaments show some correlation to these areas. Modified from McConnell (1972); Reynolds (1984); Ebinger (1989a) and Upcott et al. (1996).

Figure II.3: Main boundary faults in the Eduard basin (Lærdal et al., 2002)



The accommodation zone separating the Lake Edward basin and the Lake Albert basin consists of two small extensional basins; the Semliki basin and the Lake George basin, which are separated by the Ruwenzori Mountains (Ring, 2008). A general view of the area is shown in Figure II.4 : (Ring, 2008).

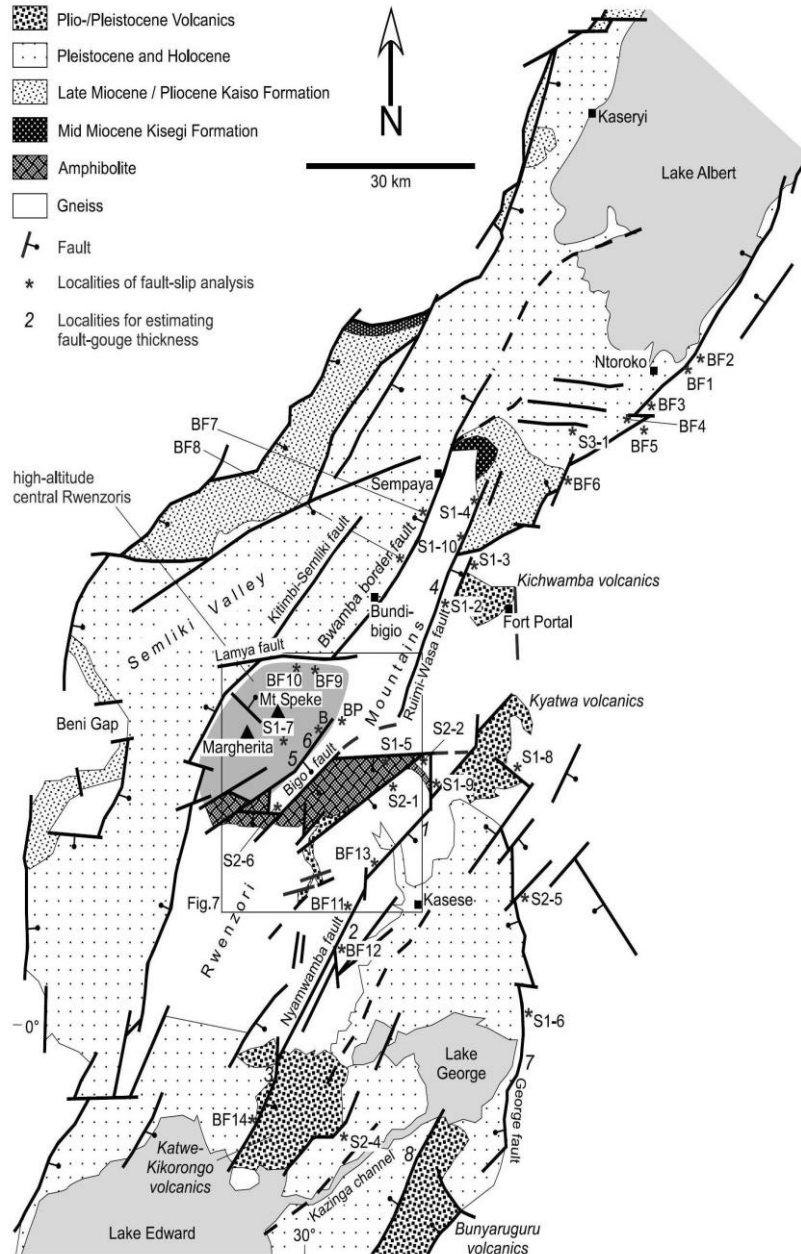
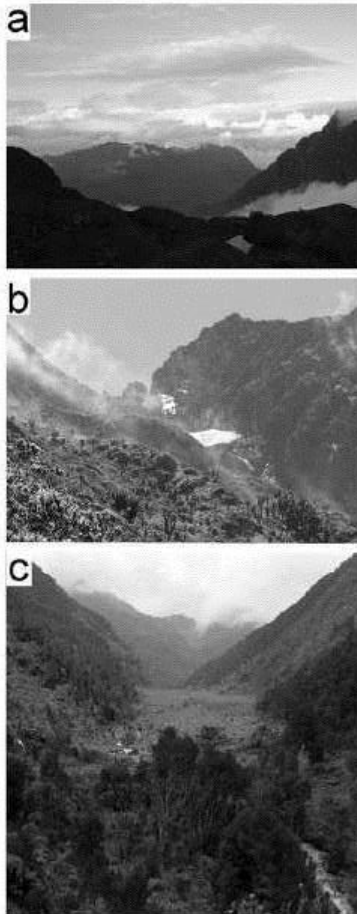


**Figure 5.** Detailed tectonic map of the Rwenzori region with locations of stations where fault-slip data have been obtained. The youngest volcanic rocks occur between Lake Edward and Fort Portal and are associated with young faulting (i.e. Nyamwamba fault); these volcanics in part obscure major rift faults. NNW of Fort Portal a NNE-striking fault cuts through young alluvial fan deposits. Box marks area of map shown in Figure 7; gray-shaded area marks region of high elevation in central Rwenzoris.

*Figure II.4 :Tectonic map of the Ruwenzori region (Ring, 2008)*

## II-3 RUWENZORI MOUNTAINS

The Ruwenzori Mountains are a 5 km high block of Precambrian metamorphic basement with peaks of amphibolite (Bauer et al., 2010) bounded by two major faults (Ring, 2008; Bauer et al., 2010). It is the only uplifted basement block in Africa which is glaciated and has deeply incised glacial valleys (Figure II.4: Ring, 2008) and so is an extreme expression of rift mountain-uplift (Ring, 2008).



Photographs illustrating the pronounced topography in the central Rwenzori Mountains. The name Rwenzori comes from “rwe nzururu” meaning place of snow in Swahili. (a) The Portal Peaks are 3911 m high; note that the Portal Peaks are surrounded by deeply incised valleys. (b) The rugged topography of the Mt. Speke massif. (c) The Bigo valley; the floor of the deeply incised valley is about 3,800 m high and infilled with raised bog, to the left (N) is Mt. Speke (4,890 m) and to the right (S) is Mt. Edward (4,843 m); the image gives a qualitative impression that glaciers are very efficient erosive agents and that glacial (and fluvial) erosion produced considerable relief.

Figure II.5 : (Lærdal et al., 2002)

The Lake George basin sits directly to the East of the Ruwenzori Mountains bounded to the West by the Nyamwamba Fault (NF), the Ruimi-Wasi Fault (R-WF) further to the North and to the East by the George Fault (GF) (Figure II.3 : (Lærdal et al., 2002)) which forms a 400m high fault scarp (Upcott et al., 1996). Lake George has an average depth of 2.4m but this varies due to wet/dry seasonal changes (Viner & Smith, 1973) to a maximum of around 3m, the lake is around 25km wide (E-W) and 20km long (N-S). Most of the water flow comes from the run off from the Ruwenzori Mountains (Viner and Smith, 1973) forming large alluvial fans prograding away from the mountains to the East (Lærdal et al., 2002).

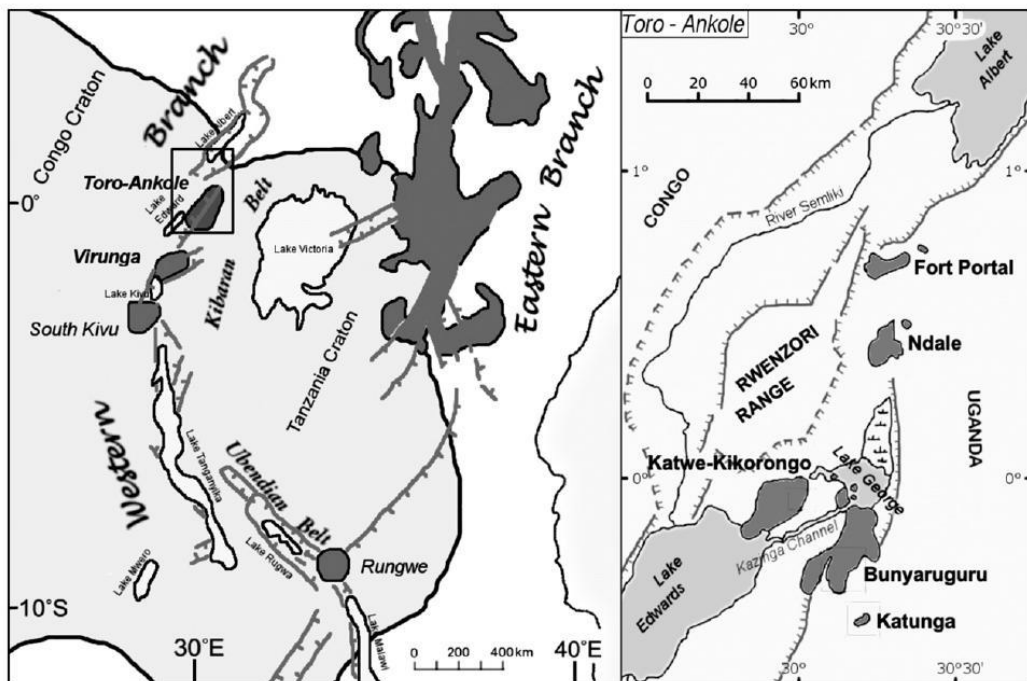
It is the most seismically active area in Uganda with most earthquakes concentrated around border faults and volcanic zones (Lærdal et al., 2002) indicating that these faults are still active. The faults in the mountain range consist of both N-NNE striking normal faults, almost parallel to border faults (Ring, 2008) and local reverse faults and strike slip faults which traverse the range trending broadly E-W ((Lærdal et al., 2002); Ring, 2008; (Koehn et al., 2008)) such as the Buganda Toro Fault (Lærdal et al., 2002). These E-W trending faults appear to reactivate the foliation and shear zones in the basement rock (Ring, 2008). The onset of uplift of the Ruwenzori's ranges from 2.3Ma (Ring, 2008) to 10Ma (Bauer et al., 2010) and is thought to have been caused by Rift Induced delamination of the lithosphere and subsequent isostatic rebound of the mantle between the two rift segments (Wallner and Schmelting, 2010). The Semliki valley (or Semliki basin) (Figure II.5) borders the Rwenzori Mountains to the West, its Eastern border fault is the Bwamba Border Fault (BBF) and it is bordered to the West by the Semliki Fault (SF) (Figure II.3 : (Lærdal et al., 2002).

The Lake George basin sits directly to the East of the Ruwenzori Mountains bounded to the West by the Nyamwamba Fault (NF), the Ruimi-Wasi Fault

Sedimentary strata are thought to be around 1.5km thick within the basin (Upcott et al., 1996) consisting of lacustrine, alluvial and fluvial sediments thought to be Pliocene-Pleistocene in age and tilted in a Westerly direction ((Ebinger, 1989);(Lærdal et al., 2002)). The area between the Lake Edward basin and the Lake George basin is thought to be a high relief accommodation zone associated with the Toro Ankole volcanic province.

#### II.4 ASSOCIATED VOLCANICS

The volcanic province closest to the Lake Edward basin is the Toro-Ankole volcanic field, located to the East of the Rwenzori Mountains (Figure II.6 : (Rosenthal et al., 2009)) related to the accommodation zone separating the Lake Edward and Lake George basins (Lærdal et al., 2002).



Simplified map of the equatorial part of the East African Rift (left; modified after Tappe et al., 2003) and the distribution of the volcanic fields within the Toro-Ankole province of the western branch, lying E and SE of the Rwenzori Mountains (right; modified after Holmes, 1950). Dark shading indicates extent of volcanic rocks, light shading indicates lakes. The shaded region (left) is the continuous Congo-Tanzanian craton.

Figure II.6: Map of equatorial part of the EARS (Rosenthal et al., 2009)

It consists predominantly of kamafugites (strongly silica-undersaturated potassic lavas), often in the form of tuffs, lapilli tuffs or tuff breccias (Musisi, 1991) of varying compositions (Kampunzu et al., 1998) and carbonatite (over 50% carbonate minerals) tuffs. Carbonatites in the Toro-Ankole field occur in Fort Portal (and Kasakere). The Fort Portal carbonatites are dated to 6,000 to 4,000 yr BP by  $C^{14}$  dating (Eby et al., 2009). These volcanics are the youngest and most northerly situated volcanics on the western arm of the East African Rift System (Rosenthal et al., 2009). They are dated to have erupted no earlier than 50 ka BP (Boven et al., 1998), and this 50 ka period coincides with renewed Quaternary volcanism in the Virunga and South Kivu volcanic provinces and a tectonically active period in the region (Lærdal et al., 2002).

The Virunga volcanoes trend approximately W-E and occur on the high relief accommodation zone between the Edward and Kivu basins (Ebinger, 1989); (Lærdal et al., 2002). The province has been subjected to two major eruption periods; the first occurred during the Miocene, ca.11 Ma, and consisted of basaltic lavas, the second consists of potassic lavas, began in the Pliocene and is ongoing today ((Bellon and Pouclet, 1980); Ebinger, 1989; Kampunzu et al., 1998). The Virunga fault separates the field into two segments (Figure II.7 : Eby et al., 2009) with only the Western segment exhibiting active volcanism (Platz et al., 2004).

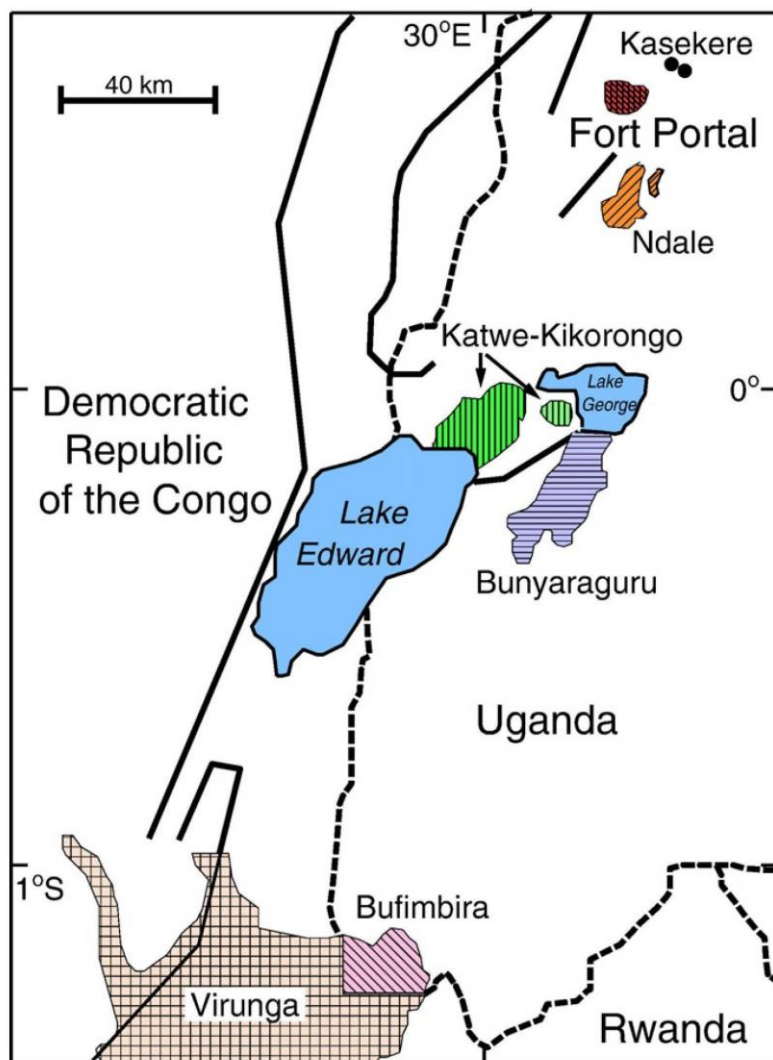


**Fig.** ations of the major volcanic fields in the southwest Uganda portion of the western branch of the East African rift system. Fort Portal and Kasekere – calciocarbonatites; Ndale, Katwe-Kikorongo, and Bunyaraguru – kamafugites; Bufimbira (part of the larger Virunga field) – potassic mafic-felsic flows and pyroclastics.

*Figure II.7: Location of the major volcanic fields in the SW Uganda (Eby et al., 2009)*

## II.5- SEDIMENT FILL

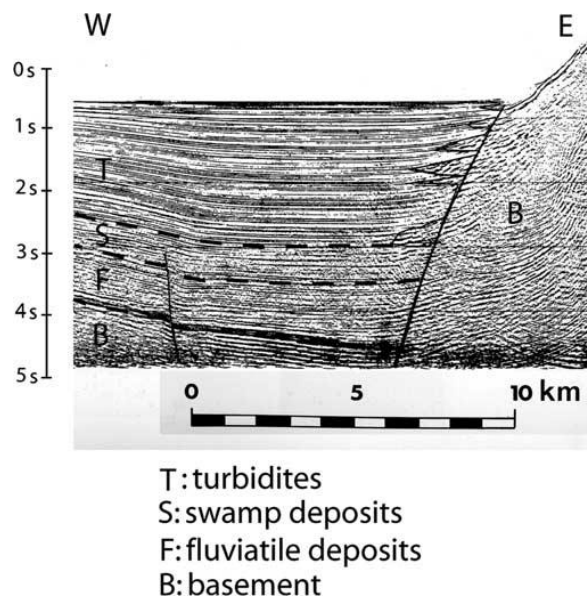
The sedimentation patterns in the EAR system are controlled by structures, with strong influence of climatic environments and occurrence of great lakes ((Crossley, 1984); (Le Fournier et al., 1985); (Tiercelin et al., 1992); (Frostick and Reid, 1990); (Lambiase and Bosworth, 1995).

Detritic sediments accumulate at piedmont of Lake Edward basin major border faults, forming alluvial cones, alluvial and delta systems, down slope fan deltas and deep fan deltas.

There is sometimes development of littoral platforms with fan deltas, prograding deltas, underflows from canyons, carbonate deposits, stromatolites. (Chorowicz, 2005).

Organic sediments are preserved in deep and sometimes shallow basins. Evaporitic sediments are under semi-arid climate, in shallow basins. Metallogenic deposits are related to hydrothermalism along major border faults ((Tiercelin et al., 1992);(Chorowicz, 1990).

Sedimentation in EARS could be considered like a combination of organic and detrital deposits in shallow lakes. The first sediments resting on the basement are sand-dominated fluviatile deposits (F in Figure II.8). They are followed by clay and silt deposits with high organic content corresponding to swamp environment (S in Figure II.8). In late stage of rifting, sedimentation changes and is characterized by thick deposits of deep lacustrine detrital sequences forming turbidites. (Chorowicz, 2005).



B: basement; F: sand-dominated fluviatile deposits; S: clay and silt deposits with high organic content, corresponding to swamp environment; T: turbidites

*Figure II.8: Typical sedimentation sequence in Rift Lake as seen from seismic Profile (Project PROBE)(Versfelt and Rosendahl, 1989)*

The oldest rift-fill sediments of the Albert – Edward basin are considered to be of Late Miocene age and contemporaneous with the onset of volcanic activity. Age dates of between 8 Ma to 12 Ma are proposed for the earliest lacustrine sediments (Hopwood and Lepersonne, 1953 cited by (Doornkamp and Temple, 1966); Ebinger, 1989a; (Pickford et al., 1993).

Thin, Neogene and younger formations have been recognised by Ugandan PEPD in the Ugandan side of Lake Edward basin and they include: Kazinga Formation, Kankoko Formation, Channel Formation, Ishasha Formation, Kiruruma Formation, Mweya Formation, Kikorongo Formation, Nchwera Formation and Rwenshama Formation. (Tumushabe, 2012).

Many studies before the year 2000 have identified stratigraphic units that were very difficult to correlate and lacked formal boundaries and defining facies characteristics. The mapped units; clays, sands and conglomerates were thought to date from the mid-Miocene onwards when they were dated by Pickford et al (1993). The Mid-Miocene date comes from bivalve and mollusc species found in association with mammalian species which are dated to Miocene in age in other East African locations. Other areas along the Albertine rift in Uganda also yielded Miocene ages, such as Karugamania, Nyamavi, and Sinda-Mohari, as a result of these fossil assemblage analysis (Pickford et al., 1993).

The problem is that these biostratigraphical constraints relied on the correlation between gastropod and mammalian fossil assemblages in Lake Edward with those found amongst dated tuffs in Ethiopia, and there is no way of proving that these fauna arose simultaneously in both locations. More recent Palynological analysis of onshore samples from EA4B produced a younger age of Pleistocene to Holocene (~20,000 yrs B.P. to the present day) and subsequent analysis of palynomorphs from the entire Ngaji-1 well, a 4.5km deep exploration well drilled by Dominion in EA4B and the only one in the basin, only extended this estimate to the Pliocene to present day (SOCO, 2010). The well showed interbedded sands and clays consistent with a fluvial-lacustrine depositional environment as seen onshore. The nature of large scale fluvial dominated deposits of this type means that facies are likely to vary significantly both laterally and distally down dip from the sediment source and this is proven when they are mapped (Nicholas et al, 2016).

Onshore EA4B has been mapped and a working stratigraphy established with five rift fill sediment formations (Nicholas et al, 2016).

The oldest *Kisenyi Formation* consists of low energy, distal fluvial flood basin plain and marginal lacustrine deposits and an abrupt change to a coarse, immature sedimentary fill to the south-east suggests that extensional movement has created a sub-basin known as the *Bwambara formation* trough which has been infilled with sediment shed directly from the exposed basement to the south-east. The Bwambara trough contains three recognisable units. The *Kayonza Formation* is a fluvial unit with well developed channel conglomerates and thick clay intervals which were deposited drainage ponded during the initial subsidence of the trough. The *Kihiki formation* is characterised by low energy

fluvial sediments and occasional swamp hardground horizons with freshwater gastropods. To the NE of the Nyamirama high, the main area of subsidence accumulated the Bwambara Formation which is composed of thick comparatively structureless, dominantly coarse sands grits and conglomerates representing the immature relatively rapid sub basin fill in the trough (Nicholas et al, 2015). The youngest unit is the *Kikyere Formation*. It can be recognised only in sporadic exposures and is composed of swamp clays which are formed or are currently forming typically along the hanging walls of faults scarps due to the present day interglacial wet phase which East Africa is experiencing, equivalent to Marine Isotope Stage (MIS) 1 (Nicholas et al, 2016).

No dateable tuff deposits in any exposed or drilled sediments, or further indication from palynology make age constraints on stratigraphic units extremely difficult. Recognising arid intervals, wet phases, and their correlation with an oscillating East African climate during glacial/interglacial episodes in the litho-facies and chrono-facies of onshore Lake Edward may be the key to establishing a working stratigraphy for the basin.

According to Chris J. Nicholas, the spatial distribution of depositional environments of each sediments fill in EA4B and/or Bloc V (Lake Edward basin) are described as shown in the conceptual cartoon of typical alluvial structure below in Figure II.9 :

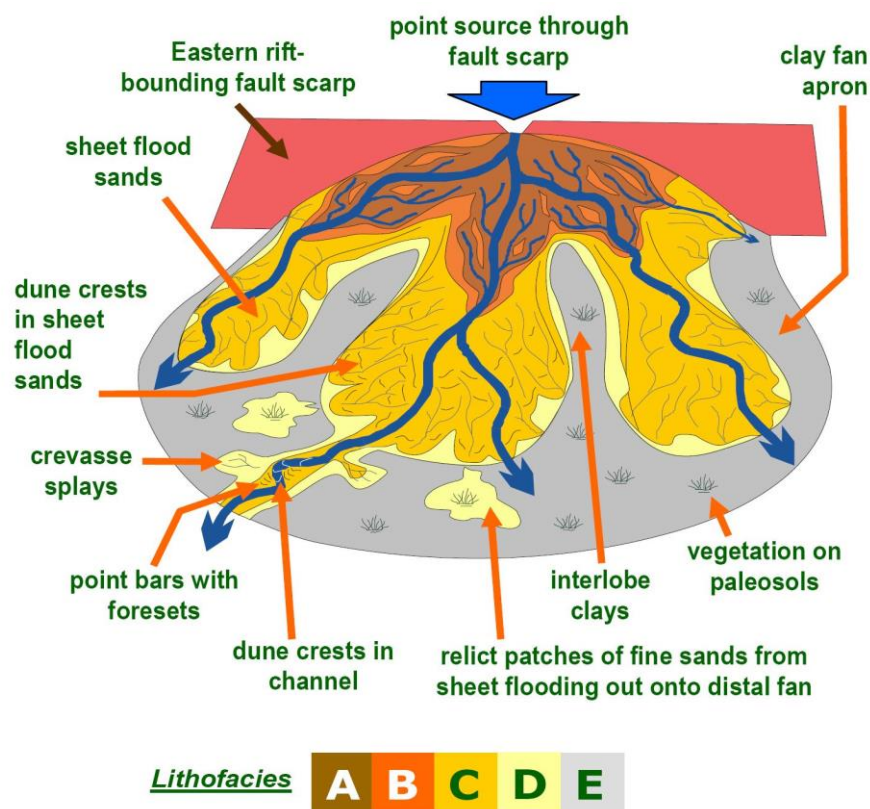


Fig. Conceptual cartoon of typical alluvial fan structure and spatial distribution of depositional environments in EA4B.

Figure II.9: Typical alluvial fan structure and spatial distribution of depositional environments in EA4B (Nicholas et al., 2016)

Climate and tectonics both had major effects on the sedimentation with the Lake Edward basin so an attempt was made to reconcile these two effects over the history of the basin by creating a Coupled Climate-Tectonic Model to determine the effect both climate and tectonic mechanisms could have on lake water volume and accommodation space over sub-millennial timescales (Tumushabe, 2012). There are several processes that effect the climate on both short and long term timescales such as rainfall controlled by the two wet/dry seasons each year, Milankovitch cycles from which processional minima cause equatorial wet episodes, and longer term effects such as glacial episodes and processional cycles in the order of thousands of years. Tectonic effects would include the uplift of the Ruwenzori Mountains and the uplift of the East African Rift System as a whole which has contributed to the drying out of Africa (Tumushabe, 2012). Climate and tectonics are in operation separately but both affect sedimentation within the basin. Figure II.10 : (Nicholas et al., 2016) shows a model developed to analyse the effect both tectonics and climate have on sedimentation. At any one time the sedimentation in the Lake Edward basin would sit between the end members, the model can predict when source or reservoir for example would be deposited in the basin if the climatic and tectonic conditions for that time period were known.

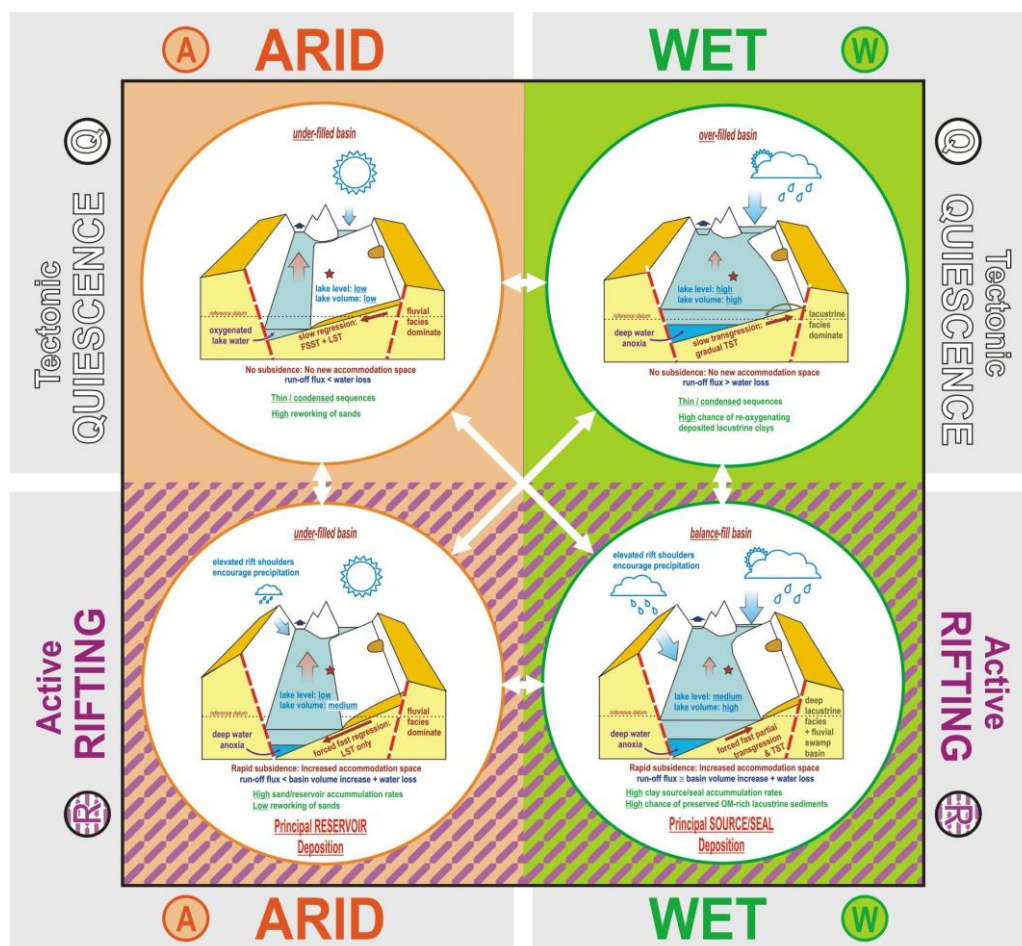


Figure II.10: Effect of tectonics and climate have on sedimentation. (Nicholas et al., 2016)



## II.6- PRE-RIFT BASEMENT

The Precambrian Basement in the area around Lakes Edward and George is composed of a variety of metasediments, mafic intrusives and acid gneisses. The Mbarara 1:250 000 sheet subdivides the Precambrian units of the region into Basement Complex, Toro System and Karagwe – Ankolean System (Geological Survey of Uganda, 1961) cited by (Hepworth and Macdonald, 1966).

PEPD reports do not use these divisions and instead subdivide on the basis of metamorphic facies (Byakagaba, 1997). Metasediments include irregularly-bedded silver white and reddish-brown phyllites and phyllitic shales, in some localities overlain by quartzites (Byakagaba, 1997). The quartzites are micaceous or at times schistose and ferruginous, ranging in colour from white to grey-brown. They are also found in association with metamorphosed cherts. Biotite-, quartz-, amphibole- and mica-schists are present in the region, indicative of a higher grade of metamorphism than the phyllites and quartzites. They apparently grade at times into gneisses or can be found interbedded with gneisses at some localities (Byakagaba, 1997). The gneisses themselves display a foliation parallel with the main regional structural trend. Although dominated by quartz and feldspar, they (gneisses) also contain accessory minerals of hornblende, biotite, tourmaline and muscovite. There are occasional pods of schists enclosed within the gneisses (Byakagaba, 1997). Mafic intrusions are also present in the Lake Edward – George basins. These consist of massive, little altered, dark green, porphyritic diorites and dolerites – gabbros (composed of plagioclase, augite, amphiboles, olivine, siderite, quartz and magnetite) which can be seen intruding the gneisses, quartzites and schists. However, they have not so far been observed to cross-cut the Neogene and younger rift fill sediments (Byakagaba, 1997). Thus, both their precise age and subgroup extent remain unclear at present.

## II.7- PETROLEUM POTENTIAL OF THE ALBERTINE GRABEN

According to Rubondo (2005) the Albertine Graben has good source and reservoir rocks, traps and seals.

### II.7.1- SOURCE ROCKS AND OIL SEEPAGES

There are over five confirmed substantial oil seepages in the Albertine Graben and these include two live oil seeps on the Victoria Nile near Paraa, two seeps at Kibuku in the Semliki basin and the Kibiro seepages on the shores of Lake Albert. The presence of these oil seeps indicates that organic rich source rocks are present.

Rubondo, 2005 reports that geochemical analysis of oils from these seepages indicates that they were generated from source rocks deposited in a lacustrine environment and dominated by Type 1 algal kerogen. There are differences between oils from the Paraa and Kibiro seeps and that of Kibuku in that the later depicts origins from source rocks deposited in a more saline lacustrine environment and with more contribution of higher land plants to the source rocks. This variation is important because it points the presence of at least two origins for oil in the graben (Rubondo, 2005).

### II.7.2- RESERVOIR ROCKS

Basement rocks along the escarpment and rift flanks of the Albertine Graben comprise mostly gneisses, granitic gneisses and quartzites. The weathering of these rocks, the subsequent transportation and deposition of their weathered products into the Graben could yield good reservoir quality sediments. Coarse clastics constitute much of the sedimentary formations outcropping in the Graben especially in the Kisegi and Kaisotonya river valleys of the Semliki basin (Rubondo, 2005).

Sandstones with good reservoir quality are present as porosities of over 30% have been measured in the shallow cores recovered from the Kibiro area. Porosities of up to 22% have also been measured in aeolian and fluvial channel deposits outcropping at Kibuku in the Semliki Basin (Rubondo, 2005).

Live Oil have been found and confirmed in cavities of Travertine in Lyemumbuza quarry in Uganda, suggesting a potential carbonate reservoir in the Edward lake basin. (Nicholas, 2009)

### II.7.3- TRAPS AND SEALS

Structural styles in the Graben are dominated by down-to-the basement block faulting which plays a major role in the formation of hydrocarbon traps. Dip reversals against faults and fault and fault-on-fault traps are present. A large number of small tilted fault blocks, apparent rollovers as well as anticlinal features associated with a fault block rotation were identified from the seismic data acquired in the Semliki Basin (Rubondo, 2005).

Relatively rapid facies changes common in terrestrial alluvial fan, deltaic and lacustrine sediments provide the potential for stratigraphic traps with or without structural components. Unconformities in the sedimentary section also provide for stratigraphic, combined stratigraphic and structural traps.

The more than 30m thick clay bed mapped on top of the good reservoir quality sandstone in the Kisegi area of the Semliki Basin is a potential regional seal (Rubondo, 2005).

### II.8- PREVIOUS PUBLISHED USE OF ICP-MS FOR CARBONATE DISCRIMINATION

Absolute geochemistry sourcing methods such as the ICP-MS uses isotope dilution techniques to provide the full suite of the REE range as well as other trace elements in very low detection limits, yielding precise and accurate data to present REE at ppb concentration levels. The geochemical sourcing of the EARS travertines, which is the primary objective of this MSc research, is focussed on any possible discrimination evidence between different carbonates structures, textures and/or fabrics visible in each analysed sample.

The REE are extremely advantageous geochemical proxies because the changes in their atomic structure across any carbonate sample vary predictably and in much smaller increments than any other group of elements (Lawrence and Kamber, 2006).

The analysis of REE in hydrogenous sediments (such those observed in EARS) has significantly increased in scope with the application of Inductively Coupled Plasma

Mass Spectrometry (ICP-MS), as exemplified by the landmark publications of Bau and others (Bau and Dulski, 1996; Möller and Bau, 1993; Bau and Möller, 1993).

The geochemical study of REE distribution spans decades and results obtained have answered many crucial biogeochemical questions such the carbonates' origin in travertines (Goldberg et al., 1963; Elderfield, 1988; Piepgras and Jacobsen, 1992; Sholkovitz, 1992, 1995; Sholkovitz et al., 1992; Zhang and Nozaki, 1996; Lerche and Nozaki, 1998; Runnalls and Coleman, 2003; Wyndham et al., 2004).

Byrne and Sholkovitz (1996; p. 529) suggest that the dependence of concentration and slope of REE pattern is chiefly controlled by surface reactions where pH is a variable parameter in establishing the absolute and relative lanthanide abundance.

Undeniably, REE traces found in Carbonates samples can, as per Elderfield's (1982) suggestion, be employed as tracers of geochemical processes in sea waters (Elderfield and Greaves, 1982; De Baar et al., 1985). More recently, the REE concentrations of terrestrial waters such as groundwaters and lakes have been examined as potential tracers of processes affecting their geochemical evolution (Banner et al., 1989; Smedley, 1991; Fee et al., 1992).

For this Msc correlations purposes, the following published use of ICP-MS for tracing back the carbonate sourcing have been considered:

- The Quaternary Fort Portal carbonates and Katwe Kikorongo carbonatitic lapilli-tuffs (4–6 m thick) samples have been analysed by Eby et al., 2009 and their geochemistry results provided referenced ppm values of La, Ce, Nd, Sm, Eu, Gd, Tb, Tm, Yb, Lu, and Y. (Eby et al., 2009)
- A. Bellanca has studied the REE distribution through the Albian-Cenomanian interval of a stratigraphic succession (Cismon section, Scaglia Variegata Formation, Venetian Prealps) consisting of rhythmically alternating carbonate-rich and carbonate-poor strata which are the sedimentary expression of systematic variations of surface fertility and bottom-water redox conditions in the depositional basin. (Bellanca et al., 1997)
- Rare earth element and yttrium (REE+Y) concentrations were determined in 49 Late Devonian reefal carbonates from the Lennard Shelf, Canning Basin, Western Australia. REE+Y normalized patterns of the Late Devonian samples display features consistent with the geochemistry of well-oxygenated, shallow seawater. (Balz et al., 2004)
- The purpose of the Corkeron et al., 2012 research was to test if trace element (primarily REE+Y) geochemistry could be used to determine if the sampled Neoproterozoic fine-grained stromatolites were the products of:(1) trapping and binding of ambient particulate sediment, or, (2)in situ precipitation of carbonate minerals. (Corkeron et al., 2012)

This MSc research study followed step-by-step the same procedures used by Balz Kamber (2004) who basically used ICP-MS and MUQ datas normalization to understand the carbonates' origin and involvement in the REE signal in the Achaean microbial carbonate and to document information on ocean redox and biogenicity. Balz Kamber (2004)

The carbonate samples have been entirely dissolved into 2% HNO<sub>3</sub> solution and the results obtained from the ICP-MS experiments on them revealed a scaled look at the carbonate chemistry in both major and trace REE. Field and laboratory blanks were prepared for each batch of samples and reference material were treated as unknown. Two separate digestions of U.S.G.S. dolerite W-2 were used as calibration standards and two other U.S.G.S. basalt reference materials BIR-1 and BHVO-2 were analysed as unknowns. Comprehensive illustration of REE spectral signature patterns opens a discussion of the EARS travertine samples' overall shape with quantitative expression of anomalies. REE anomalies are calculated as REEn/REEn\* where REEn\* is the expected normalised concentration when interpolated from an appropriate combination of near neighbours (Lawrence and Kamber, 2006).

Values > 1 indicate a positive anomaly and values < 1 indicate a negative anomaly. We use the Prn/Ybn ratio as a general descriptor of the slope of the pattern, with values > 1 indicating light enrichment and values < 1 indicating heavy enrichment (neither Pr nor Yb behave anomalously thus are suitable representative elements) (Lawrence and Kamber, 2006).

Middle REE enrichments, similar to those described by Shiller (submitted), can be evaluated with Prn/Tbn and Tbn/Ybn. Anomaly calculations in aquatic REE are complex than in solid geological materials such as in our EARS travertine samples.

The principal satisfying requirement for calculating anomalies recorded in this Msc research was that the near neighbours used in the calculation do not show any anomalous behaviour themselves (Lawrence and Kamber, 2006). For instance, for the calculation of La\* anomalies, we cannot use Ce as the oxidation from Ce<sup>3+</sup> to Ce<sup>4+</sup> as it often leads to an under abundance of Ce.

La anomalies were calculated using the nearest available non-anomalous REE Prn and Ndn. Similarly, Ce\* was also calculated from Prn and Nd due to the possible overabundance of lanthanides (Lawrence and Kamber, 2006). The extent of La, Gd and Lu anomalies is expected to be small but well beyond analytical uncertainty.

Calculating anomalies with the Lawrence and Kamber (2006) method is assuming that the difference in concentration between neighbouring pairs is constant. Thereafter, graphically, the REE+Y spectral signature pattern will behave linearly in the region of the near neighbours on a linear-linear plot (Lawrence and Kamber, 2006). The majority of the REE speciation studies supporting this assumption have been conducted using seawater or other natural waters of moderate to high pH and less work has been focused on acidic waters.

The ICP-MS analysis run on freshwater samples reveal that lanthanide anomalies are relatively small compared to that of seawater in which it averages 2.62 (an average of MUQ-normalised values calculated from data published by Zhang and Nozaki (1996; 1998) (Zhang and Nozaki, 1998; Alibo and Nozaki, 1999; Nozaki and Alibo 2003; Nozaki et al., 1999).

Referring to Gadnium anomalies, previous studies have documented an anthropogenic origin for Gadnium anomalies (Bau and Dulski, 1996; Nozaki et al., 2000b), but there is no reason to suspect and no evidence to support an artificial Gd source in the EARS travertine samples.

Thermodynamic calculations performed by Akagi and Masuda (1998) indicate that Cerium oxidation is favoured under normal aquatic conditions, but comprehensive understanding of the weathering reactions of carbonate source bedrock and the subsequent transport of REEs appears critical to resolving the nature of freshwater carbonatites or marine limestone Cerium behaviour.

Lawrence and Kamber (2006) calculated Ce anomaly as a linear extrapolation between La and Nd (the closest available elements from isotope dilution methods), an approach that is naturally biased towards a substantially negative Ce anomaly due to the possible overabundance of La. The previously reported pH dependence of the negative Ce anomaly is in fact due to a pH dependence of the undetected La anomaly.

This requires further investigation with complete REE datasets (Lawrence and Kamber, 2006).

Negative Cerium anomalies represent a marine REE feature, but they are also commonly observed in river waters (Sholkovitz, 1995; Byrne and Sholkovitz, 1996).

According to Lawrence (2006) a negative cerium anomaly is developed in limestones due to differing mobility of Ce compared to other REE (Pinares-Patiño et al., 2003). This implies that this negative Ce anomaly is also a geochemical source with enough potential for providing the carbonate provenance information. Lawrence (2006) also suggested that the Ce anomaly is related to weathering, inorganic aquatic processes or biological mediation (Lawrence and Kamber, 2006). Cerium oxidation and precipitation is widely accepted as the mechanism for generating a negative Ce anomaly (Moffett, 1990; Alibo and Nozaki, 1999; Bau, 1999). Therefore, it is expected that the Ce anomaly should deepen with distance downstream, but this is clearly not the case in the EARS travertine samples analysed in our MSc research study.

One of the main features characterising the marine REE spectral signature patterns is the strong positive lanthanide anomaly (Bau and Dulski, 1996; Zhang and Nozaki, 1996; Shields and Webb, 2004). The explanation of this above-mentioned relative lanthanide abundance as presented by Lawrence and Kamber (2006) is that the removal of LREE expresses a positive lanthanide anomaly even before reaching the estuarine trap or when reaching the surface cooling depth. Lawrence and Kamber (2006) also indicate that this behaviour might be related to the electronic structure of the  $\text{La}_{3+}$  ion which has a noble gas configuration.

Additionally, Kamber published in 2004 the following key criterias for recognizing a REE+Y marine limestone signature :

- $\text{Pr}_n / \text{Ybn} \ll 1$  Praseodymium / Ytterbium ratio
- $\text{Y}/\text{Ho} > 40$  Yttrium / Holmium ratio
- $\text{La}/\text{La}^* > 1.1$  Lanthanum anomaly
- $\text{Gd}/\text{Gd}^* > 1.1$  Gadolinium anomaly
- $\text{Ce}/\text{Ce}^* < 0.8$  Cerium anomaly

Where:

- $\text{La}/\text{La}^* = \text{La} / ((\text{Pr}^* / (\text{Pr}/\text{Nd})^2))$
- $\text{Gd}/\text{Gd}^* = \text{Gd} / ((\text{Tb}^* / (\text{Tb}/\text{Dy})))$
- $\text{Ce}/\text{Ce}^* = \text{Ce} / ((\text{Pr}^* / (\text{Pr}/\text{Nd})))$

## Chapter 2 Conclusion:

- *The starting point of this Msc. Research Study was the detailed review of all the Eastern Africa Rift System existing publications available in the public domain in terms of Modern limnology, Basin structure, associated metamorphic (Ruwenzori Mountains), associated volcanics (Fort Portal), Sediment fill, Pre-rift basement and the petroleum potential of the Albertine Graben.*
- *None of those previous studies mentioned the Travertines outcropping in hot springs or the possible pre-tertiary marine limestone under beneath the classical siliclastic Eastern Africa Rift System*
- *Details of previous published uses of geochemical data to discriminate and trace back the bicarbonate sources of Travertines have been reviewed and updated.*
- *The geochemistry analysis procedure to reach the objectives of the present Msc Research follows the published Balz Kamber (2014) ICP-MS experiment where Rare Earth Element + Y signals, particularly in combination with radiogenic isotopes (e.g. Pb and Sr; Kamber & Webb 2001; Bolhar et al. 2002), have been useful to discriminate the Archaean microbial carbonates depositional environments between stromatolites that formed in lacustrine, restricted marine and open marine depositional settings.*
- *Furthermore, the cited literature review helped us to use the initial set of geologic data package and the geochemistry analysis methods for planning and adjusting good samples field description and collection, and good petrography to select the ideal textures, structures or fabrics to drill through and carefully prepare input solutions.*

## *The next Chapter, entitled Methodology:*

- *Describes the details of the methods and analytical procedures chosen to reach out the aims and objectives of this research paper.*
- *Allows the reader of this Msc Research to acknowledge the high confidence level in the efficiency of the opted methods and analytical procedures in terms of reducing risks of errors and samples contaminations in the lab.*

## CHAPTER THREE: METHODOLOGY

The aims and objectives of this MSc. Research will be achieved by following the below methodology:

1. Undertake series of field trips in the Lake Edward basin to describe the geologic environment , to log the reference cliffs , to record Spectral gamma ray responses and finally to collect Travertine samples for Petrography and geochemical analysis;
2. Undertake the Petrography analysis of Travertine samples in slabs and/or thin section stained in alizarin and /or observed in Cathodoluminescence if required. This just means to execute a serie of Carbonate microscopic observations through the most recent version of Nikon optical microscope (available in TCD) on a suite of selected Travertine limestones slabs and alizarin stained thin section and Cathodoluminescence petrography of microstructural fabrics in deformed limestones to point out the fossils shoreline units, their petrographic composition (Ooids, Peloids, bioclasts), and structure / texture ( fibrous, grained cement, porous, crystalline phases) may reflect times of partial, or modest platform flooding
3. Discuss in detail the Carbon and Oxygen stables isotopes analysis run in 2013 on the Block V 2010 field work Travertine collected samples ;
4. Discuss in detail the Strontium isotope ratio analysis run in 2013 on the Block V 2010 field work Travertine collected samples;
5. Run a serie of ICP-MS analysis on a suite of samples from Travertine limestones collected from around the margins of Lake Albert and Lake Edward for their whole rock and rare earth element (REE) concentrations, Carbon and Oxygen stable isotope and Sr isotope ratios, in an attempt to discern how limestones lie at depth within the rift, and their geochemical origin.
6. Interpret the final output results to provide key evidence about the interaction between deep structure, groundwater flux, geochemistry, and ultimately the geologic evolution and timing of rifting within these two Lake Albert and Edward basins.

### III.1- FIELD TRIPS:

As an investigation method, field trips are a key aspect for the best understanding of the geologic environment where Travertine samples have been collected. They provided to this MSc research project the required back-up for any of the further analysis in laboratory.

The main benefit of these field trips was that they allowed a better visual understanding of: (1) the architecture of units; (2) multi-stage deformation during subduction/exhumation; (3) the geodynamic significance of continental basement juxtaposition with syn- to post-rift sediments.

The main objectives and steps of these field trips in each locality visited were:

- Identification of key stratigraphic units and their subsequent geological mapping across the region,
- Structural mapping across the region with a synthesis of structural style,
- Field observations,
- Rocks and mineral macroscopic descriptions,
- Limestone field tests,
- Spectral gamma ray acquisition,
- Field discussion,
- Sampling and packing for the shipment to laboratory.

The field trip logistic and equipments here below listed and shortly described have been provided by Oil companies and/or government (Uganda/DRC) for the best technical organization. They are here just for illustration to give an idea of how the field trips as a method of this MSc research project have been organized and how they did help to achieve their objectives efficiently.

#### 1. The base camp : (SOCO,2014)

The ideal Base camp of these field trips we need to illustrate in this work is the Nyakakoma Base camp (DRC) provide by SOCO International Plc in 2014. (Figure III.1 to III.9). It was put in place originally in order to support the accommodation of the crew of seismic operations in the Edward Lake but its duration stay was extended to welcome the geologist's team. It was made of easily dismantled several tents (respecting the environment) around an oil generator for power supply. Water supply and waste management were perfectly organized.



*Figure III.1: Nyakakoma Base camp, SOCO 2014*





*Figure III.2: Geologist accommodation unit, SOCO 2014*



*Figure III.3: Ablution facilities and water tanks, SOCO 2014*



*Figure III.4: Kitchen, mess facilities and radio room, SOCO 2014*

The Nyakakoma Base Camp had got a special tent which was used as the Geologist office where A0 geologic and operations Maps were displayed, shelves have been put in place for the storage of samples daily collected before their final packing for shipment, samples bags and samples big boxes were available for the same purpose.

The Geologist's office in the Nyakakoma Base camp was fully provided with Wi-Fi laptop connected, printers, scanners, and all required extension cables.



*Figure III.5: Geologist's tent and office, SOCO 2014*



*Figure III.6: Shelves and Samples boxes, SOCO 2014*

2. The Helicopter: (SOCO, 2014)



*Figure III.7: Helicopter in its landing zone, SOCO 2014*

To facilitate the daily movement of geologists, their equipments, and their security teams in the field, and helicopter has been provided. The different helicopter landing zones were chosen accordingly to the geologic objective in the area. The helicopter landed to the cleared zone the closest possible to the outcrop or cliff interesting the field trip geologist team.

The field equipments

1. **Structural map,**
2. **GPS,**
3. **Hand auger,**
4. **Hand held spectral gamma ray**
5. **Hammers**
6. **Topographic sheets**
7. **Sample bags**
8. **Compass**
9. **Cameras**
10. **Hand lens**
11. **Binoculars**
12. **Bags, Field notes, rain coats....**



*Figure III.8: Field equipments, SOCO 2014*

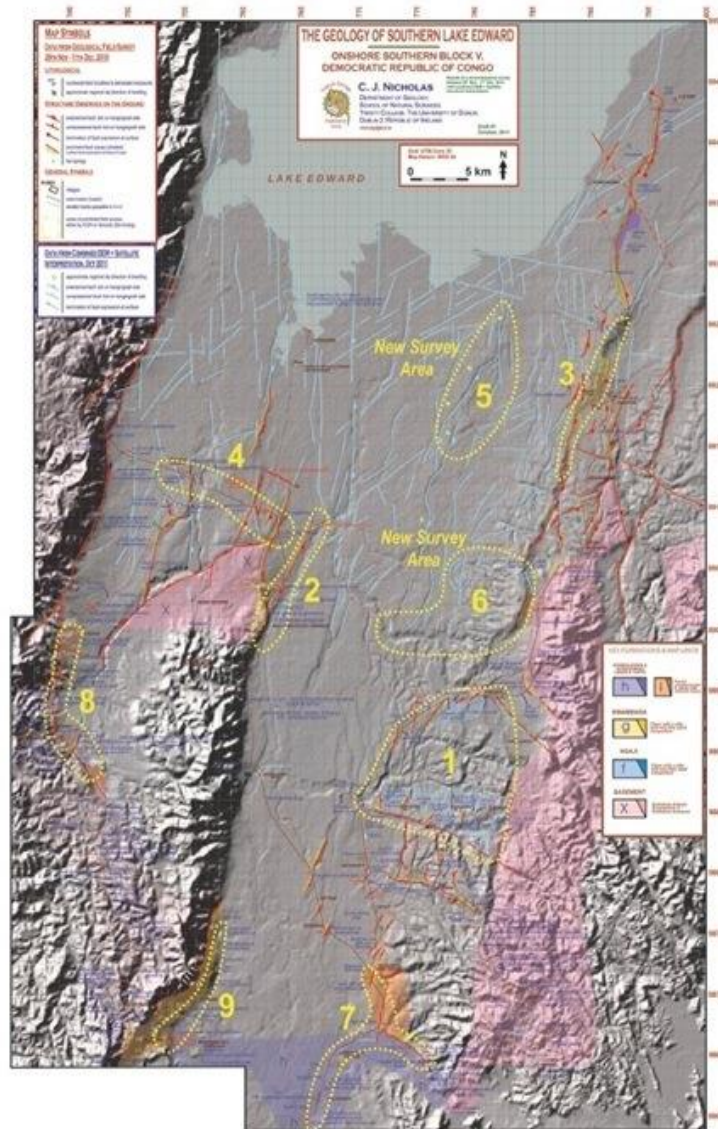
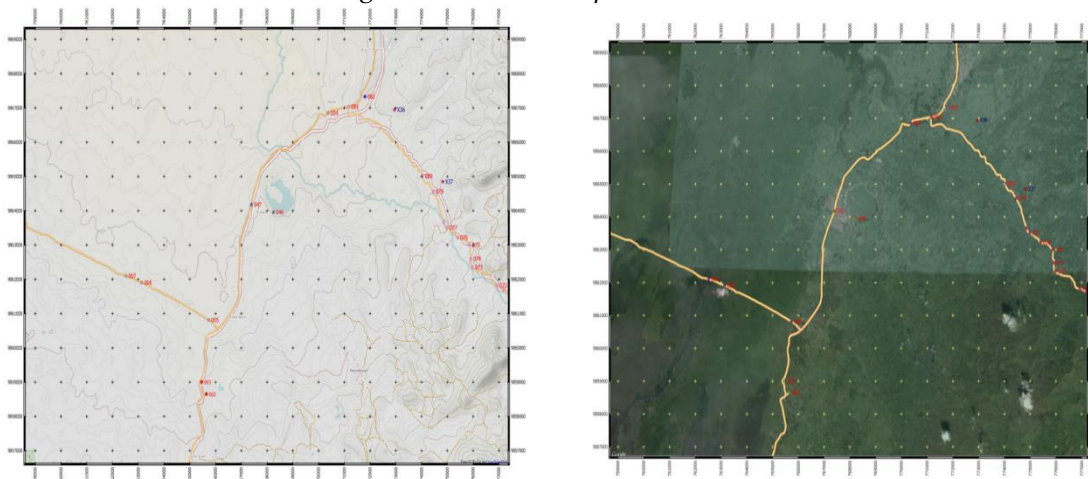


Figure III.9: Field Maps (SOCO, 2014)



SRTM (Shuttle Radar Topographic Mission) and Landsat Satellite images of the region of interest at 1:50,000 have been provided to each geologist to fill his observations with coloured pencils.

3. Geologists activities in front of an outcrop

A. Observation from far firstly and from closer view



Figure III. 10 a, b, c, d, e Field Observations (SOCO, 2014)

B. Field Macroscopic description ( human eyes)



C. Field Microscopic observation ( Hand lens)

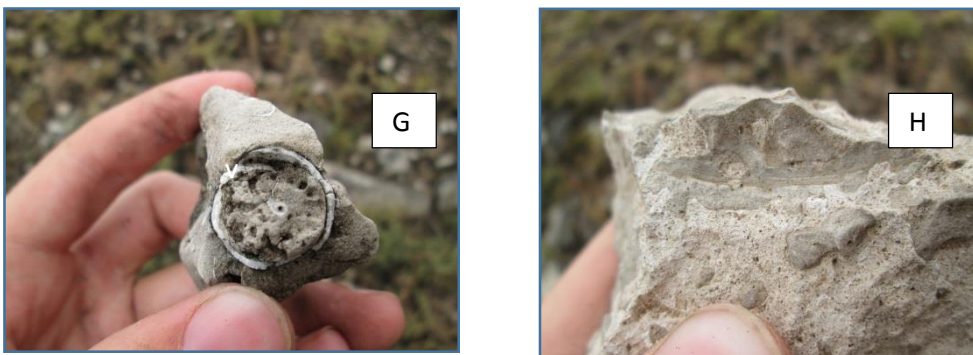


Figure III.10 e, f, g, h: Field Observations (SOCO, 2014)

### D. Spectral Gamma Ray recording and logging sheet filling

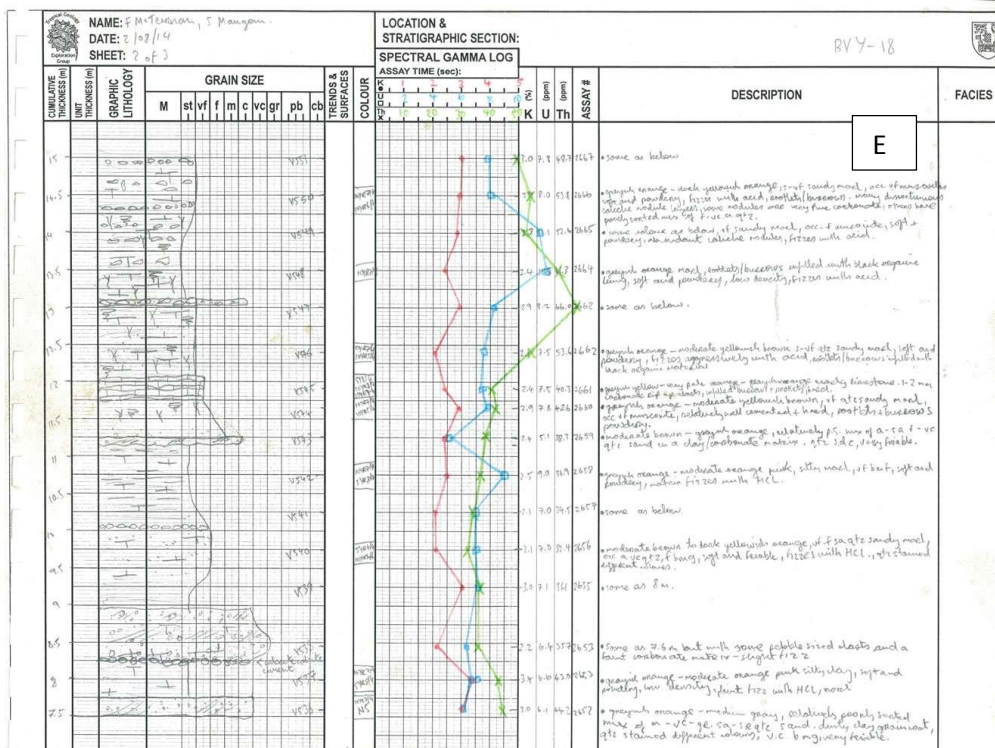
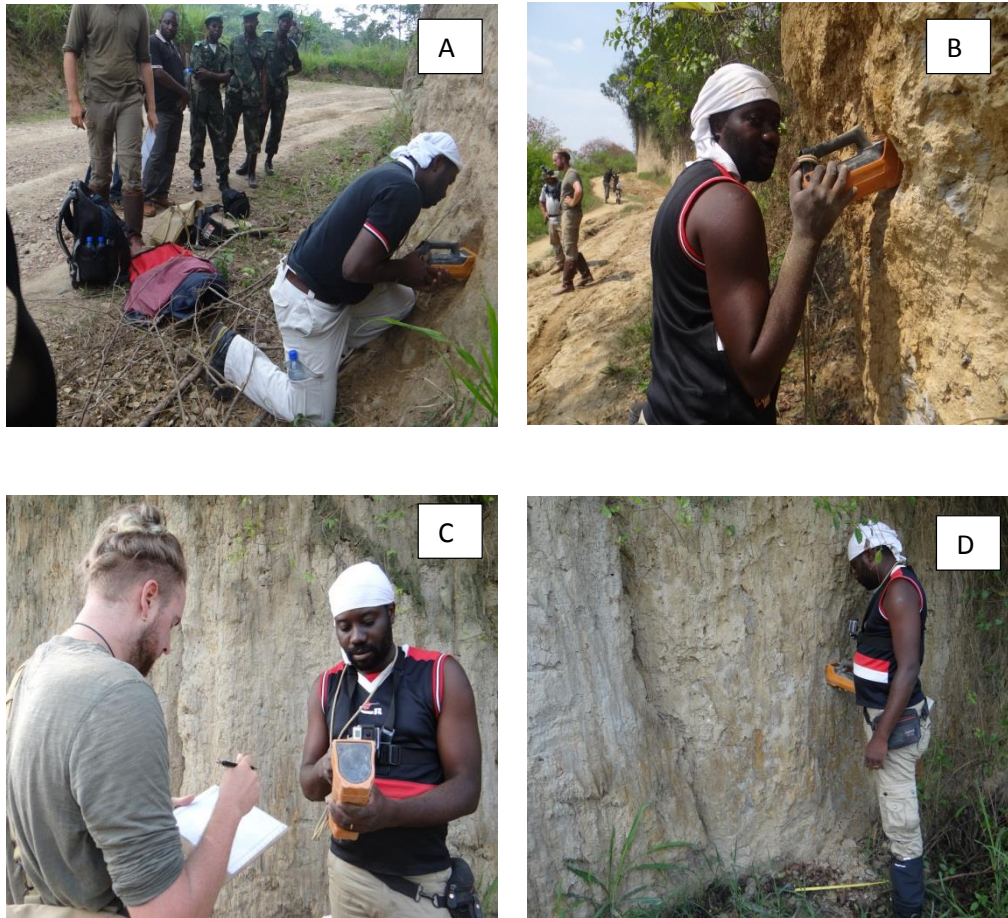


Figure III.11 a, b, c, d, and e: Spectral Gamma Ray field recording and record sheet (Avalonia, 2014)

## E. Sample collection and packing



Figure III.12 a, b : Samples collection (SOCO, 2014)

### III.2- TRAVERTINE PETROGRAPHY:

In order to achieve the objectives of this MSc. Research, the Travertine samples collected in the field should be prepared for laboratories analysis among them the Inducted Coupled Plasma Mass Spectrometry (ICP-MS) to detect Rare Earth Elements (REE) in any of each visible textures, structures and /or fabrics.

The Carbonates Petrography have been the perfect method to think about after these series of field trips to get closer with these mysterious Travertine collected in the Eastern Africa Rift basins. Techniques for Examining Carbonate Rocks in Sawing and Polishing (slabs) have been used as well as the necessary basic procedure for limestones observation and description.

This method has been done entirely in the museum Building technician's lab and in the ICRAAG facilities in the Trinity College, the University of Dublin.

The successive steps for the Travertine observation and description could be described as below:

- Cut a slab (3-5 cm square and a few mm thick) across or through any visible bedding, structure, texture and/or fabrics.
- Polish one side.
- Etch with weak acid.
- If required, use light mineral oil for fine observation.
- Study the slap under binocular scope with reflected light.

#### III.2.1- THIN SECTION PREPARATION

Samples have been cutted in the technician's lab using a small bench mounted cutter machine perfectly used for cutting small specimens, trimming, larger slabs, small slices, This tool have also been used to remove any kind of bulk in samples already mounted for thins section preparation.

The cutting discs size used for each Travertine sample varied between 120 mm to 250 mm according to the need of sample microscope observation. They were provisions of grinding wheel discs made available for replacing any broken cutting disc during operation, but this case never happened.

Thin Sections preparation process which mainly aimed to grind slightly thicker than 30 microns (for deeper colour contrast under plane light), was done following the basic principles of geological thin section preparation.

This very important process has been done according to the minimum standard requirements of carbonate study as below described (Allman, 1972):

- Cut or break the original specimen to produce a slice or chip.
- Grind one surface for the slice or chip on successively finer grades of abrasive to produce a flat, satin polished surface;
- Mount the chip, prepared surface downwards, on to a microscope glass slide;
- Grind the exposed surface of the chip so that it is parallel to the first face using, as before, successively finer grades of abrasive;
- When the chip is reduced to a thickness of 30 microns, as determined by observation through a microscope. Clean the section and cement a cover glass over it for protection;
- Clean again to remove surplus mounting medium and finally label.
- The section is then ready for study.

Each of this above stages is in fact made up several operations and every operation has associated dangers which if neglected may cause the destruction of the section.

Staining techniques for geological purposes is one of the methods based on selectivity of certain dyes. The term selectivity describes the ability of a dye or staining reagent to colour only a specific material, mineral or fossil, even in the presence of other similar materials. (Allman, 1972).

The selective property of this staining method on carbonates minerals is not only aiming to the simple differentiation of Calcite and Dolomite, but also the sophisticated methods devised by Friedman and later modified and extended by Warne, which allow the identification of some carbonates different types of minerals. (Allman, 1972).

The staining of Travertine samples collected during series of field trips in the EARS basins has been done following the Rodgers method of Calcite discrimination on the surface of limestones blocks.

Many staining solutions, once made up, oxidise very quickly regardless of how many specimens have been processed. Provisions of solutions have been made available for the case of quick oxidation during the process, however this case never happened during the staining process of this MSc research.

The staining of Travertine specimens of this MSc Research have been done according to the Friedman's method (1959) who devised the staining procedure suitable only for hand specimens, polished surfaces and chips of carbonate rocks which allow a very positive identification for Calcite, aragonite, dolomite, magnesite, high magnesium calcite, gypsum and anhydrite. (Allman, 1972)



According to Friedman (1959), the following solutions should be made up as stock solution:

- Pre-stain etching bath.
- General solution Alizarin red S. + 30% sodium hydroxide.
- Alizarin red S. + 5% sodium hydroxide.
- Titan yellow (dolomite staining solution)
- Trypan blue (magnesite staining solution)
- Harris's haematoxylin (specific for calcite)
- Feigl's solution (specific for aragonite)

Only the following solutions have been made for the case of this present study:

1. Solution A : Pre-stain etching bath

10% Hydrochloric acid solution:

Add 100ml. HCl (36% fuming) to circa 500ml water and top up the solution with water to give a final volume of 1000ml.

2. Solution B: General solution Alizarin red S. + 30% sodium hydroxide

Alizarin red S.	1g
0.2% hydrochloric acid (cold)	1000 ml
Add 2ml. HCl (36% fuming) to circa	500 ml water and top up the solution
with water to give a final volume of 1000ml.	

The steps and procedure below described have been followed (Allman, 1972):

1. Prepare the limestone sample by cutting and grinding flat one face;
2. Polish the surface using first 3F, then F600 and finally F800 grade Carborundum;
3. Ensure the surface is washed clean with soft brush and a Teepol solution and then dry it.
4. Immerse the specimen in the Alizarin red S. + 30% sodium hydroxide solution. (Do not allow the polished surface to contact with the bottom of the tank. This tank should have a close fitting lid to minimise evaporation. Before the next step, it is advisable to dip the specimen in distilled water once or twice although the pale green stain is very delicate at this stage.
5. Without washing and drying the specimen, immerse it in the ammonium hydroxide solution for about 30 seconds.
6. Wash the specimen and gently polish the surface with a soft cloth to remove any extra precipitate. The alizarin red S. Stain will be fixed and should not be damaged.

The colour formed on the calcite mineral varies from a pale (as in Figure III.13 below) to deep pink to Brown. This stain is very selective even in fine grained specimens. If calcite fossils are present in the specimen, this method will render them clearly visible more specifically if the reflected light is used.

The peel technique which can reveal a great deal of information or petrographic details not visible by the examination of the specimen itself, has been used as a thin section complementary method. All the 2014's Travertine samples have been peeled before their microscopic observations.

This old used technique consists in applying to a prepared surface on a specimen a thin coating or layer of suitable material in a solvent. The layer is allowed to harden and is then peeled from the specimen. So, the peel can have either a thin layer of the actual specimen which has been removed from the surface of the specimen adhering to the peel, or there will be impressed on one surface of the peel a very low relief pattern corresponding to the texture, structure of fabric of the specimen.

Very useful for the microscopic study of carbonaceous, calcareous, and siliceous fossils as coal balls and corals, this technique is specifically used to record the non-porous replicas structures.

Cellulose acetate sheets or films like Clarifoil or Kodatrace produce excellence peels of specimens which are non-porous and without holes in their surface and where it is possible to obtain only flat surface on the specimen.

The acetate sheet technique is very fast and cheap method to produce peels of very high quality with acetone as solvent. The others advantages of this peeling method are:

- Peels are excellent for high magnification work where crystals of a few microns need to be distinguished;
- Peels make good photographs;
- Peels can be used with transmitted light through any type of microscope ;
- No colour contrast;
- Few mineral identification

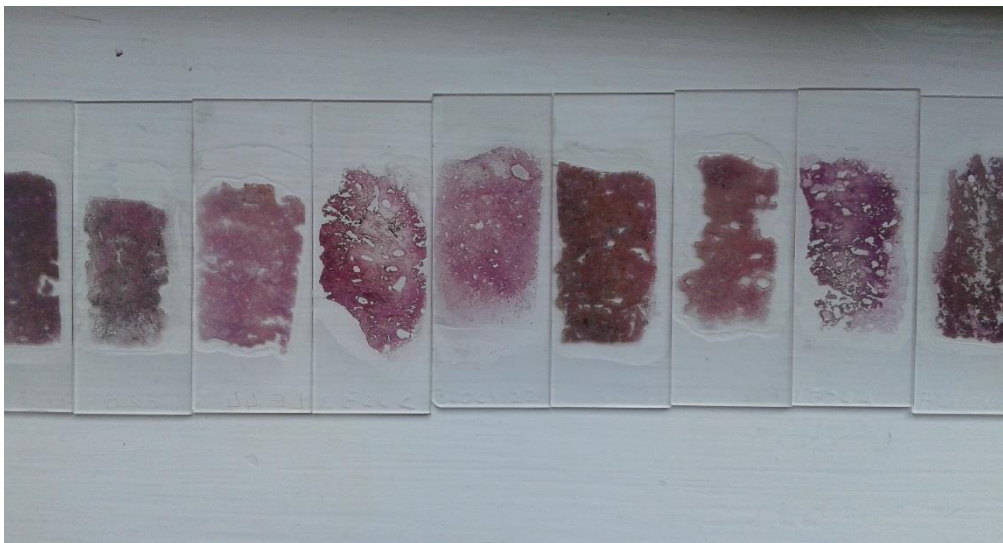


Figure III.13 : Travertine thin sections (Sylvain ,TCD,2018)(Hill,

### III.2.2- MICROSCOPY

Microscopic observation is the most effective way of knowing the mineralogical, the structures, textures, fabrics and other constituents (like fossils) of the carbonate rocks.

For the Travertine study of the present MSc Research project , thin sections were prepared and studied under microscope, following the procedure of Folk (1959).

The volumetric analysis of different constituents had done with the help of manual counting technique, for the petrographical classification of Travertine limestone. The textural study had carried out for Dunham's classification (Dunham 1962).

The petrographic study from thin sections was prepared to identify and decipher the nature of different constituents, textures, structures and fabrics of the Travertine specimens exactly at the location where the samples have been drilled for ICP-MS analyses purposes.

Thin sections made from Travertine samples were observed with parallel and crossed Nicol prisms of the Nikon LV100 optical microscope offers 2.5, 10, 20, 50, and 100x magnification. Integrated image capture software provides many options for processing as shown in the Figure III.14 below:



*Figure III.14: Nikon LV 100 optical Microscope (CMA, 2018)*

### III.3- OXYGENE AND CARBONE STABLE ISOTOPES ANALYSIS:

In 2013, the Isotope ratio mass spectrometry (IRMS) was used by Sylvain and Jean to measure the isotopic ratios of carbon and oxygen. The IRMS equipment scheme illustrated in the Figure III.15 below, have been available in TCD to perform O and C stable isotope analysis as the ICP-MS complementary tool. Actually under repair works, this IRMS equipment was not available during the present MSc Research short time. So, only the first EARS field trips season Travertine samples have been run, and their results presented and discussed further down this thesis.

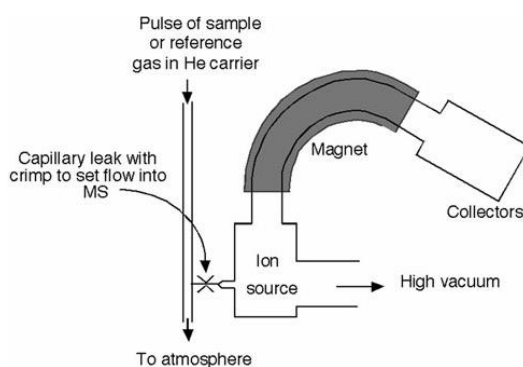


Figure III.15: Typical diagram of an IRMS (lab notes sketch)

#### III.3.1- CARBONE STABLE ISOTOPE ANALYSIS:

Knowledge of the variations in the relative abundance of the stable (non-radioactive) isotopes of Carbon and Oxygen in any geologic material may furnish a powerful tool for the evaluation of the various geochemical and biochemical cycles through which this material has passed during very long time because of its geochemical and biochemical importance and also because of the relative ease of the laboratory technique required.(Craig, 1953)

$^{12}\text{C}$  and  $^{13}\text{C}$  are the stable isotope ratio (noted  $\delta^{13}\text{C}$ ) which were measured in the standard established Pee Dee Belemnite (PDB) based on a Cretaceous marine fossil, *Belemnitella Americana*, which was from the Pee Dee Formation in South Carolina. This material had an anomalously high  $^{13}\text{C}:^{12}\text{C}$  ratio of 0.0112372 (Lynch-Stieglitz et al., 1995).

The variations in  $^{13}\text{C}/^{12}\text{C}$  ratio  $\delta^{13}\text{C}$  in limestones may be attributed to the following factors:

- (1) variations in the calcium carbonate parts of organic debris incorporated in the rock, probably due in part to a vital effect of the organism,
- (2) variations in precipitated carbonate due to photosynthesis of marine plants,
- (3) possible equilibration with organically derived carbon dioxide, and
- (4) Degree of attainment of isotopic equilibrium during precipitation.

The rate of precipitation of carbonate can affect the isotopic composition, and the oolitic character of these formations would indicate that both represent rapid precipitation.

However, the fossiliferous character of the geologic formation appears to be a quite reasonable explanation of the isotopic difference.

The carbonates show a range of isotopic composition greater than that of any other group but the graphites, the range of  $\delta$  being about 24 ‰. However the marine limestones shows a range of only 5.7 ‰. (Lynch-Stieglitz et al., 1995)

In the case of the present study:

- Magmatic carbon in a carbonate would be expected to have a  $\delta^{13}\text{C}$  between -7 and -10 ‰ relative to PDB belemnite.
- Marine carbon in a carbonate would be expected to have a  $\delta^{13}\text{C}$  between -2 and +2 ‰ relative to PDB belemnite.

Therefore, higher  $\delta^{13}\text{C}$  in marine fossils is indicative of an increase in the abundance of vegetation. (Craig, 1953).

The Carbon stable isotope ratio analysis  $\delta^{13}\text{C}$  has been done on the EARS samples in 2013 using TCD facilities and equipments by Sylvain K. Mangoni and Jean Dyer and the results are shown and discussed further in this thesis.

### III.3.2- OXYGEN STABLE ISOTOPE ANALYSIS:

The presence of preserved physical characteristics of the past that stand in in a Travertine sample for direct meteorological measurements purposes are enabling scientists to reconstruct the climatic conditions over a longer fraction of the Earth's history. (Hays and Grossman, 1991)

Measurements of the ratio of oxygen-18 to oxygen-16 have been done by Sylvain K.M and Jean Dwyer in 2013 using TCD facilities to analyse some EARS Travertine samples and interpret their palaeoclimate changes. The calculated ratio of the masses of each Oxygen stable isotope present in the Travertine sample is then compared to a standard, which can yield information about the temperature at which the sample was formed. The microorganism most frequently referenced as standard is *foraminifera* from Standard Mean Ocean Water (SMOW).

A higher abundance of  $^{18}\text{O}$  in calcite is indicative of colder water temperatures, since the lighter isotopes are all stored in the glacial ice and the lower abundance of  $^{18}\text{O}$  in the calcite (Travertine samples) indicates the warmer temperatures. (Hays and Grossman, 1991)

The Figure III.16 below shows the long-term evolution of oxygen isotope ratios during the Phanerozoic eon as measured in fossils, reported by Veizer et al. (2000). Such ratios reflect both the local temperature at the site of deposition and global climate changes associated with the extent of permanent continental glaciation. As such, relative changes in oxygen isotope ratios can be interpreted as rough changes in climate. Quantitative conversion between these data and direct temperature changes is a complicated process subject to many systematic uncertainties, however it is estimated that each 1 part per thousand change in  $\delta^{18}\text{O}$  represents roughly a 1.5-2 °C change in tropical sea surface temperatures (Veizer et al., 2000).

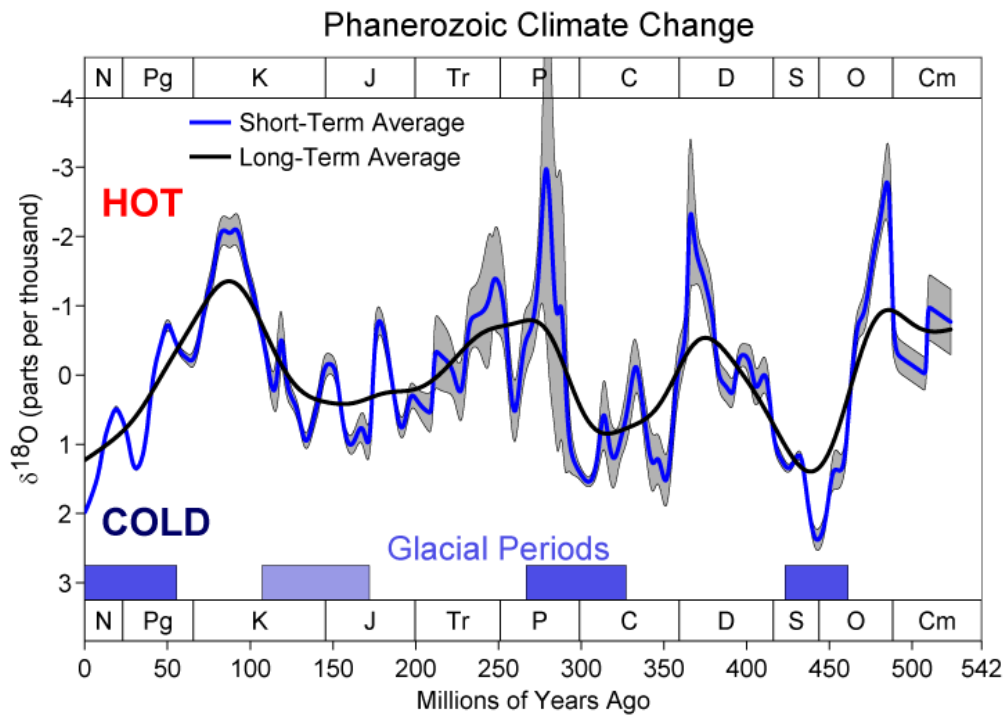


Figure III.16: Phanerozoic Climate change graph. (Veizer et al., 2000)

#### III.4- STRONTIUM ISOTOPES RATIO ANALYSIS

Strontium isotope ratio of ancient sea waters may be reconstructed from well-preserved authigenic carbonate minerals and used for dating marine sediments. (Wierzbowski, 2013)

Because of a change in the Strontium isotope ratio between sea- and freshwaters it can also be employed for the determination of paleosalinities or the reconstruction of diagenetic processes of marine limestones.

Measurements of the  $^{87}\text{Sr}/^{86}\text{Sr}$  have been done in 2013 by Sylvain and Jean Dwyer using TCD facilities to analyse and interpret some EARS Travertine samples palaeo origins.

The modern sea water  $^{87}\text{Sr}/^{86}\text{Sr}$  ratio is 0.709175. The sea water Strontium isotope composition has changed through the geologic history of the Earth owing to changing inputs of Strontium.

Three major input sources influence the Strontium isotope composition of the sea water (Wierzbowski, 2013) :

- Strontium of low  $^{87}\text{Sr}/^{86}\text{Sr}$  ratio around 0.703 is derived from hydrothermal circulation at mid-ocean ridges;
- Strontium of intermediate  $^{87}\text{Sr}/^{86}\text{Sr}$  ratio around 0.708 originates from submarine dissolution and recrystallization of carbonates sediments;
- Strontium of high  $^{87}\text{Sr}/^{86}\text{Sr}$  ratio around 0.711 is derived from continental weathering.

The temporal sea water Strontium isotope curve here below in Figure III.17 is characterized by several maxima and minima which shows the change in Strontium inputs. This Figure suggests that two deepest minima occurred in the Late Permian and at the Middle-Late Jurassic transition and an almost continuous increase of the sea water  $^{87}\text{Sr}/^{86}\text{Sr}$  ratio has occurred since the Late cretaceous.

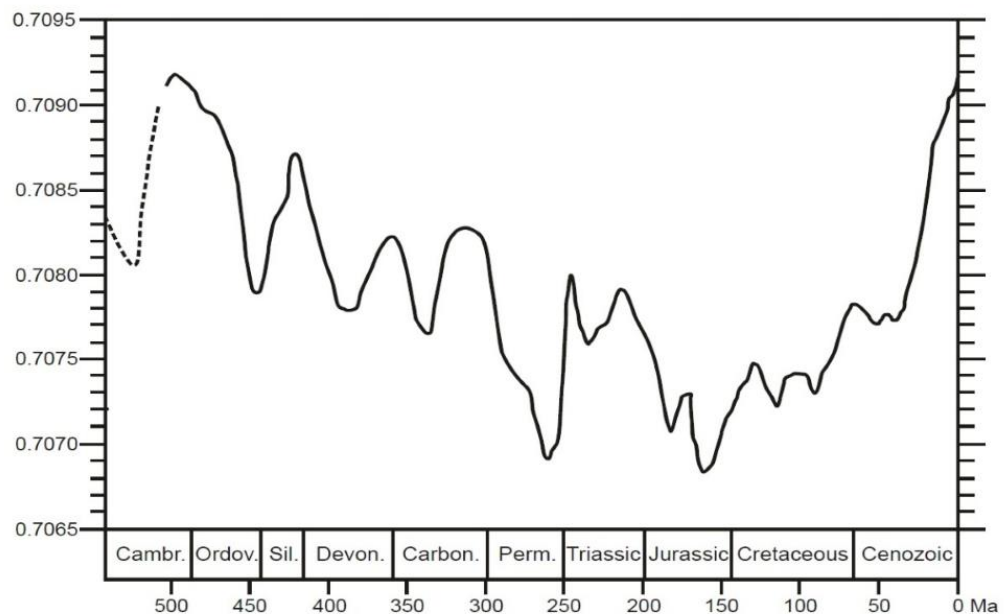


Figure III.17 : Variation of  $^{87}\text{Sr}/^{86}\text{Sr}$  ratio of the Phanerozoic sea waters.(Wierzbowski, 2013)

### III.5- GAS CHROMATOGRAPHY MASS SPECTROMETRY (GC-MS)

GC-MS has been carried out in 2008 at the LGC laboratory in London ([www.lgcstandards.com](http://www.lgcstandards.com)) by means of an HP 5890-II series GC connected to a mass selective detector (MSD) 5970 (Hewlett-Packard, Palo Alto, CA). The system control and the data acquisition have been executed by an HP 59970 ChemStation (Hewlett-Packard). The GC-MS was operated in selected ion monitoring (SIM) mode, which allowed for the study of the ions that were selective for the previously mentioned compounds with respect to the identification goals. A quartz capillary column (25-m  $\times$  0.32-mm  $\times$  0.52- $\mu\text{m}$  film Ultra-2) was used. The GC operation conditions were as follow: carrier gas, helium (1.4 mL/min); and injector and detector temperature, 300°C. The temperature program was 0 min at 90°C, then ramped to 270°C at 6°C/min, and held for 30 min at 270°C. The injected quantity was 1  $\mu\text{L}$  of 2% volume solution in tetra chloromethane of the Oil slick sample.(Pavlova and Papazova, 2003)

The GC-MS method which may be able to separate the hydrocarbons molecule types according to their weight, therefore size, and their petrochemical affinity to the column used, has been used for performing qualitative and quantitative analysis on two (2)

Lyemubuza oolithes samples found in outcrop with evident black staining resembling to crude oil in them.

Broad range of petrochemicals, fuels and hydrocarbon mixtures, including gasoline, kerosene, naphthenic acids, diesel fuel various oil types, transformer oil, biodiesel, wax and broad range of geochemical samples (including waxes up to  $C_{74}H_{150}$ ) can be analysed by this GC- GCMS method of analysis that measures the peaks in relation to one another.

In this method, the tallest peak is assigned 100% of the value, and the other peaks being assigned proportionate values.

The unique aim of the GC-GCMS analysis in this present MSc Research, is to determine the chemical composition and properties of these evident black staining.

In other terms, this method will suggest the natural (live oil) origin or artificial (Oil distilled products) of these black staining compound discovered in outcrop in Lyemubuza quarry in Uganda.

### III-6. INDUCTIVELY COUPLED PLASMA – MASS SPECTROMETRY (ICP-MS) ANALYSIS

Rare earth elements (REE) in geological materials provide important information about the formation and the geochemical processes that rocks undergo. Therefore, there is a constant necessity for accurate data and reliable and fast analytical methods. However, the low concentrations of these elements typically found in rocks require quantification by sufficiently sensitive techniques, such as Inductively Coupled Plasma Mass Spectrometry (ICP-MS). (Mastandrea et al., 2010)

In order to trace the geochemical origin of Travertine limestones samples collected during the long field season (from 2007 to 2010, in 2014 and 2017) in the Albertine Graben of the East African Rift, the main and unique method we used was the Inductively Coupled Plasma Mass Spectrometry (ICP-MS) which behave in the same time as a method, a technique and as well as also an instrument.

The present MSc. Research project is trying to use the previously demonstrated power of ICP-MS as a tool in petrogenetic studies, mineral tracing, and geologic story by showing that ICP-MS is able to perform a quantitative trace metal analysis with the lowest detection limits (part per trillion %) for the greatest level of productivity by measuring the isotopic composition of any sample except these containing the Mendeleev periodic table elements which don't have isotopes and also H, C, N, O, F, He, and Ne. The Figure III.18 below shows the range of chemical elements detected only by ICP-MS, ICP-OES only and both ICP methods.



Hydrogen 1 H 1.006																	Helium 2 He 4.0026						
Lithium 3 Li 6.94	Beryllium 4 Be 9.0122																	Boron 5 B 10.81	Carbon 6 C 12.011	Nitrogen 7 N 14.007	Oxygen 8 O 15.999	Fluorine 9 F 18.998	Neon 10 Ne 20.180
Sodium 11 Na 22.990	Magnesium 12 Mg 24.305																	Aluminum 13 Al 26.982	Silica 14 Si 28.085	Phosphorus 15 P 30.974	Sulphur 16 S 32.06	Chlorine 17 Cl 35.45	Argon 18 Ar 39.948
Potassium 19 K 39.098	Calcium 20 Ca 40.078(4)	Scandium 21 Sc 44.956	Titanium 22 Ti 47.867	Vanadium 23 V 50.942	Chromium 24 Cr 51.996	Manganese 25 Mn 54.938	Iron 26 Fe 55.845(2)	Cobalt 27 Co 58.933	Nickel 28 Ni 58.693	Copper 29 Cu 63.546(3)	Zinc 30 Zn 65.38(2)	Gallium 31 Ga 69.723	Germanium 32 Ge 72.63	Arsenic 33 As 74.922	Selenium 34 Se 78.96(3)	Bromine 35 Br 79.904	Krypton 36 Kr 83.798(2)						
Rubidium 37 Rb 85.468	Strontium 38 Sr 87.62	Yttrium 39 Y 88.906	Zirconium 40 Zr 91.224(2)	Niobium 41 Nb 92.906(3)	Molybdenum 42 Mo 95.94(2)	Technetium 43 Tc [97.91]	Ruthenium 44 Ru 101.07(2)	Rhodium 45 Rh 102.91	Palladium 46 Pd 106.42	Silver 47 Ag 107.87	Cadmium 48 Cd 112.41	Indium 49 In 114.82	Tin 50 Sn 118.71	Antimony 51 Sb 121.76	Tellurium 52 Te 127.60(3)	Iodine 53 I 126.90	Xenon 54 Xe 131.29						
Cesium 55 Cs 132.91	Barium 56 Ba 137.33	* Lu 57-70 147.07	Hafnium 72 Hf 178.49(2)	Tantalum 73 Ta 180.95	Tungsten 74 W 183.84	Rhenium 75 Re 186.21	Osmium 76 Os 190.23(2)	Iridium 77 Ir 192.22	Platinum 78 Pt 195.08	Gold 79 Au 196.97	Mercury 80 Hg 200.59	Thallium 81 Tl 204.38	Lead 82 Pb 207.2	Bismuth 83 Bi 208.98	Polonium 84 Po [209]	Astatine 85 At [209.99]	Radon 86 Rn [222.02]						
Francium 87 Fr [223.02]	Radium 88 Ra [226.03]	** Lr 89-102 [262.11]	Rutherfordium 104 Rf [261.10]	Dubnium 105 Db [268.10]	Seaborgium 106 Sg [269.10]	Bohrium 107 Bh [270.10]	Hassium 108 Hs [277.10]	Mt 109 [276.10]	Darmstadtium 110 Ds [281.10]	Roentgenium 111 Rg [280.10]	Copernicium 112 Cn [285.10]	Uun 113 [284.10]	Flerovium 114 Fl [289.10]	Uup 115 [288.10]	Livermorium 116 Lv [293]	Ununseptium 117 Uus [294]	Ununoctium 118 Uuo [294]						

*Lanthanides	Lanthanum 57 La 138.91	Cerium 58 Ce 140.12	Praseodymium 59 Pr 140.91	Neodymium 60 Nd 144.24	Promethium 61 Pm [144.91]	Samarium 62 Sm 150.36(2)	Europium 63 Eu 151.96	Gadolinium 64 Gd 157.25(3)	Terbium 65 Tb 158.93	Dysprosium 66 Dy 162.50	Holmium 67 Ho 164.93	Erbium 68 Er 167.26	Thulium 69 Tm 168.93	Ytterbium 70 Yb 173.05
** Actinides	Actinium 89 Ac [227.03]	Thorium 90 Th 232.04	Protactinium 91 Pa 231.04	Uranium 92 U 238.03	Neptunium 93 Np [237.05]	Plutonium 94 Pu [244.06]	Americium 95 Am [243.06]	Curium 96 Cm [247.07]	Berkelium 97 Bk [247.07]	Californium 98 Cf [251.08]	Einsteinium 99 Es [252.08]	Fermium 100 Fm [257.10]	Mendelevium 101 Md [258.10]	Nobelium 102 No [259.10]

ICP MS ONLY    ICP OES ONLY    ICP OES & MS    S - Regarded as semi-quantitative by ICP analysis

Figure III.18: Periodic table of the elements highlighting those obtained by ICP- OES and MS analysis. (McCabe, 2015)

The main reasons ICP-MS technique has been chosen for the geochemical tracing origin of Travertine samples from the Albertine Graben in the East African Rift is because (Wolf, 2005):

- ICP-MS has many chemical elements detection advantages over other elemental analysis techniques such as atomic absorption, optical emission spectrometry (ICP-OES) and ICP Atomic Emission Spectroscopy (ICP-AES)
- ICP-MS is so far the mostly appropriate pre concentration methods used for his low detection limits on Rare Earth Elements (REEs) in the limestones or any Carbonate rock samples.
- ICP-MS seems to be likely the most appropriate or the only possible method so far, which can provide the analysis of all REEs with high sensitivity and acceptable precision with the lowest limit of detection.
- ICP-MS superior detection capabilities, particularly for the rare-earth elements (REE).

This method has been used three times for this MS research purposes:

- In 2013 for the Travertine samples collected in EARS from 2007 to 2010;
- In 2016 on the same previous Travertine samples to check the result reproducing ability of the ICP-MS Method;
- In 2018 on the 2014 Travertine samples collected in Block V.

During this initial experiment in 2013, the ICP-MS analysis has been done according to the following steps:

- 1st step: Sample initial preparation from solid rock stage to powder stage;
- 2nd step: Sample special preparation from powder to solution stage before ICP-MS analysis;
- 3rd step: ICP-MS analysis on samples in solution;
- 4rd step: Results interpretation.

### III.6.1- SAMPLE INITIAL PREPARATION FROM SOLID TO POWDER STAGE

During the field sample collection, only fresh and non-weathered samples have been chosen. These samples have been collected from the most massive portion of the outcrop after chipping out the top weathered layers. (At least) 0.5-1 kg of the rock sample was collected for the ICP-MS analysis purpose from each location. To avoid any cross contamination, the samples were reduced to centimetre size (2-5 cm) on the outcrop itself by sledge hammer and packed in cloth bags.

For the best result to obtain through geochemistry, the representative Travertine samples from each location have been checked through hand specimen and thin section observation.

The initial sample preparation for ICP-MS analysis consisted in breaking Travertine rock samples collected in the field in small pieces then cutted in slabs representing in each of them, the maximum amount of their characterized fabrics, textures and/or structures.

Each Slab of Travertine samples has been observed in the macroscopic size and any of their eyes level visible texture or structure has been correctly outlined and described. Any confusing texture or structure in the slab suggested a deeper observation in the microscopic level to well outline them for drilling purposes.

The Figure III.19 below is showing an example of microscopic observation and description in the lab notebook of the confusing structure and texture in the Travertine slab.



*Figure III.19: Microscopic observation and texture/structure description, Drilling of Travertine rock samples by Sylvain K.M. & J. Dwyer in 2013*

Each piece of Travertine slab has been cutted according to their visible textures /structures or fabrics in slices of 0.5 cm thick each then, washed with deionized water for cleaning of any extra material which may have adhered to the samples and finally dried in the ambient air. The Figure III.20 below is showing the Travertine 0.5 cm thick slices cutted as they've been washed and dried in 2013.



*Figure III.20: Travertine Slices sample preparation, cutted, washed and dried by Sylvain K. M and Jean Dwyer in 2013*

After their washing and drying, all the cutted slabs have been drilled in their two sides according to any visible textures, structures or fabrics.

The drilling process have been done accordingly to the thickness size of the visible textures, structures or fabrics outlined in the sample which has also determined the size of the drill bit used for the drilling.

The small drill bit (Bosh Silver concrete drill bit 5x35 mm) was used to drill through the small thickness size of textures, structures and/or fabrics seen in the sample while the bigger one (Bosh Silver concrete drill bit 25x85 mm) was used for greater thickness sizes. The Figures III.21, III.22 and III.23 below show respectively the drilling process through visible textures, structures and/or fabrics present in the sample, the drilling tool and all different sizes of the drill bit.

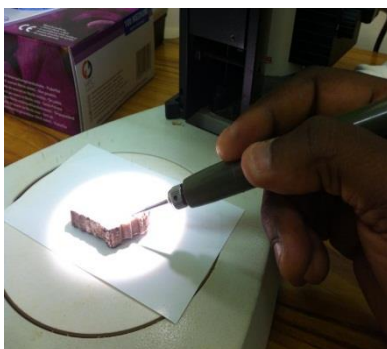


*Figure III.21: Drilling process trough visible textures, structures and/or fabrics present in the sample.*



*Figure III.22: Drilling tool used in 2013*

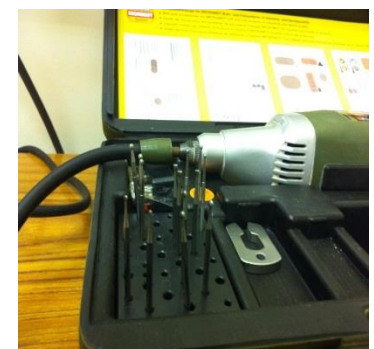


*Figure III.23: Different sizes of the drill bits used for different thickness size of textures, structures and/or fabrics present in the sample.*

Each visible textures, structures and /or fabrics found in each rock sample has been drilled through and their respective residual powders shown in Figure III.24 below have been described in the lab notebook and stored in small tubes illustrated in Figure III.25 below.



*Figure III.24: Example of the drilling residual powder of a visible textures, structures and/or fabrics present in the sample.*



*Figure III.25: Small tubes for textures, structures and/or fabrics powder storage*

8 to 13 milligrams of the residual powders (grain size around between 45  $\mu\text{m}$  and 53  $\mu\text{m}$ ) from drilled Travertine textures, structures and or fabrics have been diluted and put in  $\text{HNO}_3$  solution before they become ready for ICP-MS analysis.

The details of the next following steps: sample dilution, solution, ICP-analysis and results interpretation are available in both Jean Dwyer and Mike Babechuk lab notebook and ICP-MS analysis report TCD, 2013.

### III.6.2- SAMPLE SPECIAL PREPARATION FROM POWDER TO SOLUTION STAGE

Before running the ICP-MS, routine lab procedures for this trace element analysis were performed in a clean lab environment. Nitric acid used for cleaning and digestion was prepared from in-house triply distilled stock diluted with Milli-Q (18 $\Omega$ ) water. Aliquots of sample powder were weighed ( $1 \pm 0.01$  mg) and transferred into acid-leached, polypropylene micro-centrifuge tubes. The sample powders were digested by adding 2 mL of 5%  $\text{HNO}_3$ .

For analysis, an aliquot of the 5%  $\text{HNO}_3$  was diluted gravimetrically to a 2%  $\text{HNO}_3$  solution containing an internal standard mixture ( $^6\text{Li}$ , Rh, Re, Bi,  $^{235}\text{U}$ ). Solutions were analysed with an iCAP-Q ICP-MS equipment which was tuned for optimal sensitivity across the full analyte range (Li to U). This experiment was done at Unit 7 in the Expertise lab center of Trinity College Dublin.

Samples were injected into the nebuliser from a 1.5 mL Teflon loop at a stable rate of 250 $\mu$  Lmin<sup>-1</sup> over an interval of 6 minutes using an ESI microFAST system.

Experiment design followed a method adapted from (Eggins et al., 1997) where batches of 20-25 unknowns were bracketed with repeated measurement of a monitor sample for external drift correction and preceded by blanks and calibration and quality control standards.

Calibration of sample unknowns was performed using multiple digestions of USGS standard W-2 diluted between 20,000 and 80,000 with the preferred values reported elsewhere (Babechuk et al., 2010).

This technique, appropriate for minerals easily dissolved in diluted HNO<sub>3</sub> (e.g., carbonate, apatite) is advantageous in permitting detection of very low-level concentrations with negligible blank contribution by avoiding the use of large quantities of concentrated acids.

This is evident by the total procedural rare earth element blanks: Y (0.2 ppt), La (2 ppt), Ce (4 ppt), Pr (0.4 ppt), Nd (1.5 ppt), Sm (0.2 ppt), Eu to Lu (<0.1 ppt). Error in the accuracy of the final concentration is generated primarily by the available precision of the balances used for weighing the ultra-low masses of sample powder, yet robust normalised REE+Y patterns and element ratios were generated from samples even at the lowest signal intensity.

#### III.6.2.1- LAB EQUIPMENT CLEANING

The cleaning of the lab equipments is an obligatory process before the beginning in of any type of analysis. Depending on the chemicals that are on the equipment and how the equipment is going to be used, cleaning protocols differ drastically. A good rule of thumb followed was to overclean instead of underclean, but always we did ensure that any cleaning chemicals would not interfere with future experiments using the equipment.

This cleaning process has been done twice during each of our ICP-MS analysis. Firstly, when the lab is being set up for the experiment and during the last task to do before to conclude the experiment.

It's never been done in between every batch of Travertine samples as the contamination risk has been reduced the more possible and more precautions has been taken during each Travertine sample manipulation.

The lab internal environment, the tools, the equipments and all others lab items involved in the Travertine samples ICP-MS experiment have been carefully and totally cleaned in acid by Michael Babechuk in 2013 and Cora in 2016 and 2018, enough to avoid any kind of contamination before, during and after the samples preparation for and during each of our ICP-MS analysis.

The first task done before this present MSc Research ICP-MS experiment was only the cleaning of the lab work station and all items involved in our analysis, not the whole lab. This washing work took 14 days approx. and consisted in successive and repeated operations aiming to wash and rinse 3 times with Milli-Q ultra-pure water, then dry all the lab items to be used in the fume hood and wrap them with a transparent plastic sheet (parafilm paper) in order to avoid any dust to come down in and contaminate them.

All the items used for the samples preparation and ICP-MS analysis have been taken out from the Unit 7 Expertise Center lab warehouse, clearly identified by labels as well inventoried in a register book and get ready for their cleaning process before their use.

The required items for the samples preparation and ICP-MS analysis which have been ordered and got delivered from the TCD usual provider of geochemical analysis items, were cleaned again three times, even if they've never been used and they're new delivery from the geochemical items provider.

The cleaning steps followed were:

- Clean the involved items (glass items like beakers, tubes...) thoroughly with soap and water for basic cleaning. We may needed to use sometimes a wire brush to remove some residue.
- Rinse with purified Milli-Q ultra-pure water to ensure that all soap residue is removed.
- Rinse in the case, the lab Polypropylene items, with boiled purified water to remove any evident caked-on material like solidified agar or other gelatine-like products.
- Rinse in the case, with acetone to remove traces of organic materials including soap residue.
- Rinse in the case, with ethanol to sterilize any lab equipment that must have all bacteria and other microorganisms removed before use.
- Dry in the fume hood the necessary time to get the lab equipment completely dried and ready for use.
- Wrap the items grouped in a parafilm paper and store them for the next use.

All the lab items used for samples preparation and ICP-MS analysis were in Polypropylene which is the best plastic material used so far because it produces the lowest amount of blanks and the native properties of polypropylene make the compound strong and resistant against many chemical solvents, acids and bases.

Here down are some others advantages of the Polypropylene which made us think of it a suitable choice for our ICP-MS analysis:

1. Polypropylene is readily available and relatively inexpensive.
2. Polypropylene has high flexural strength due to its semi-crystalline nature.
3. Polypropylene has a relatively slippery surface.
4. Polypropylene is very resistant to absorbing moisture.
5. Polypropylene has good chemical resistance over a wide range of bases and acids.
6. Polypropylene possesses good fatigue resistance.
7. Polypropylene has good impact strength.
8. Polypropylene is a good electrical insulator.

For each of batch containing 20 Travertine samples (plus standards and blanks included) to be prepared and analysed, the lab items were:

- +/- 50 test tubes (13 ml) with their cap seals (lid);
- +/- 150 microtubes (2ml) with incorporated lids;
- +/- 250 pipettes (up to 1 ml)

### III.6.2.2 – ACID DIGESTION

#### A- Weighing the stock tubes:

Before their weighing, all the test tubes (13ml) have been firstly labelled. A new ID (lab ID) was necessary to make the difference between the field ID and the lab ID of the samples analysed.

The label SMK followed by 3 digits (SMK=Sylvain Mangoni Kezir) was chosen. The first batch of 20 samples have been labelled from SMK 001 to SMK 020.

The blank procedural which was used has been labelled as SMK blank 1 and the limestone standard prepared has been labelled as SMK LTD 1.

#### B- Weighing the sample powder :

The samples powders were stored in their initial microtubes from the drilling operation of the field samples slices cutted according to their original textures and fabrics. Before to weight them, they have been transferred with many cares from their microtubes (which were their drilling storage during the previous operation on samples) to their test tubes (which will be their lab storage for the next operations on samples).

The electronic weight scale illustrated in the Figure III.26 a&b here below, was used and set up to minimise the error to +/- 0.01.

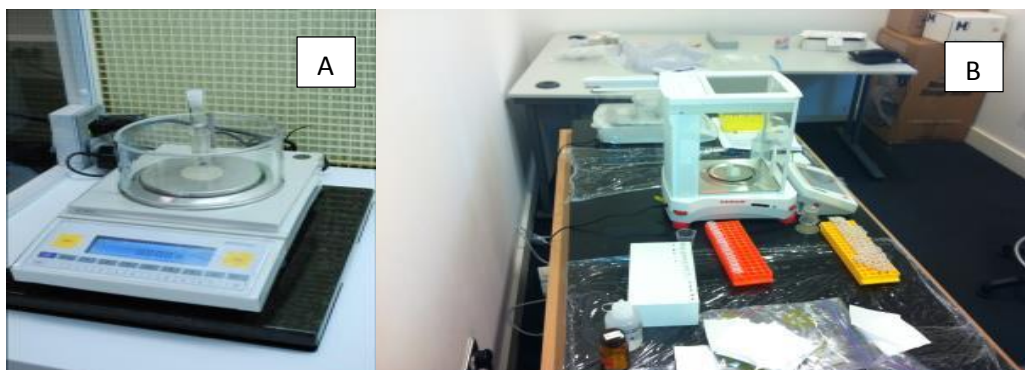


*Figure III.26: Electronic scale used to weight the Travertine samples powder analysed by ICP-MS.*

0.6 to 0.9 mg of sample powder have required for the ICP-MS analysis but the better was to have more available sample than to lack. If any powder were spilt away during the transfer operation, then the action to take was to clean properly the lab environment with a tissue and purified Milli-Q water with a piece of lab absorbent paper then change the glove before processing next.

We note that two scales have been used to weight the required amount of sample powder.

The steps here below have been carefully followed to weight the Travertine samples powder drilled from each fabric, textures and /or structures (Figure III.27 below):

- Place an empty stock tube in the first scale and note its initial weight;
- Tare the first scale;
- By using tweezers cleaned in ethanol Fold in half and Put a 5cm x5cm coated paper in the second scale; then note the weight
- Tare the second scale;
- Open the drilled sample microtube lid and carefully tipping its bottom and reverse around 0.6 mg of the sample powder onto the coated paper;
- Tap gently the bottom of the microtube and stop when the sufficed quantity of powder value is reached in the scale screen;
- Note the weight of the coated paper + sample powder;
- Roll up the coated paper and carefully tipping the sufficed weighted powder into new stock tube; close the lid and note the weight of Stock tube+sample powder.
- Place the stock tubes containing around 0.6 to 0.9 mg of sample powder in a rack Tupperware box for acid digestion which is the next step.



Figure III.27: weighting of the Travertine samples powder analysed by ICP-MS  
by Sylvain KM. and jean D., 2013

#### C- Acid digestion:

The next step for the ICP-MS sample preparation is the “Acid digestion”. This step is best to be done close to the time of running the samples in the ICP-MS machine. So, less risk of contamination leech out of the plastic tubes.

As per rule, acid digestion procedures are employed for the determination of chemical elements in solids subsequent to sampling and mechanical samples preparation in order to completely transfer the analytes into solutions so that can be introduced into the determination step of ICP-MS in a “liquid form”.

The goal of every digestion process is therefore the complete solution of the analytes (samples powder) and the complete decomposition of the solids (matrix) while carefully avoiding loss or contamination of the analyte.

#### Goals:

- Make the samples powder (analytes) completely in acid solution for digest purposes;
- Get the complete decomposition of the matrix;
- Avoiding as possible analytes losses and/or contamination;
- Reduction of handling and process times.



In this context, wet chemical digestion can/will utilize various minerals acids (eg. HCl, HNO<sub>3</sub>, HF, H<sub>2</sub>SO<sub>4</sub>, etc...)

During the samples preparation of this present ICP-MS experimentation, the HNO<sub>3</sub> acid was utilized.

Regarding the sensitivity of the actual stage of the process, firm instructions have been given by the Lab responsible who showed herself the right way to do things with the blanks, the standard and then samples SMK 001, SMK002, SMK003. Then the lab responsible supervises me doing the same for the samples SMK 004, SMK 005, SMK 006 before she felt confident of my work technique and let me go ahead with the all remaining samples.

#### D- Adding 0.1 ml of HNO<sub>3</sub> @ 10%:

All the HNO<sub>3</sub> acid couldn't be put in the samples tubes in one time for digestion because of their strong potential feezing reaction with Carbonates samples. If all the 10% HNO<sub>3</sub> stronger acid was initially put in Carbonates samples, the feezing reaction would be completely out of control.

The best way to operate was then suggested to add the acid gradually in different times with short break of time between successive acid adding.

Firstly, the sample digestion carefully started by the 5% less concentrated acid HNO<sub>3</sub> to allow that all the possible reaction to be done with safety then, the stronger HNO<sub>3</sub> 10 % acid concentration was used to complete the sample digestion with safer carbonates predictable reaction.

Leaving all the stock tubes overnight with lid loose allowed to any possible feezing HNO<sub>3</sub> acid reaction to be slowly done. The next morning, all the stock tubes were found without any feezing.

After the passage of all the samples test tubes in the fume hood overnight, they have been totally degased and absolutely out of feezing reactions. 5% HNO<sub>3</sub> reacts with CaCO<sub>3</sub> release CO<sub>2</sub> with slow feezing reaction and deposit of residue.

The majority of Travertine samples have been found with "No obvious residue" but some of them have been found with either small or large amount of residue from impurities from surrounding rocks. The colour of these residues varies from dark brown-light brown- light grey-dark grey.

Due to the time restrictions, these residues weren't run for X-Rays Diffraction (XRD) even if a full training on radiological protection and some preliminary XRD theory and practical exercises have been done under the supervision of Dr. Robbie Goodhue.

### III.6.2.3 - FINAL DILUTION

Due to the small diameters of the orifices in the sampler and skimmer cones of the instrument, ICP-MS may have some limitations regarding the amount of total dissolved solids present in the solution samples.

Generally, it is recommended that solution samples have no more than 0.2% total dissolved solids (TDS) for best instrument performance and stability.

If samples with very high TDS levels were run, the orifices in the cones would eventually become blocked, causing decreased sensitivity and detection capability and requiring the system to be shut down for maintenance.

This is why many sample types, including digested soil and rock samples have been very well diluted before running on the ICP-MS.

The Travertine limestones samples have strictly respected all the technical requirements before to be analysed in the ICP-MS. Firstly, they have been diluted once again from the digested solution to a new solution with the right concentration for more trustable results obtained by ICP-MS.

### III.6.3- ICP-MS ANALYSIS ON SAMPLES IN SOLUTION

The technique described by Ruth E. Wolf recommend that the sample to be analysed is typically introduced into the ICP plasma as an aerosol, either by aspirating a liquid or dissolved solid sample into a nebulizer or using a laser to directly convert solid samples into an aerosol (colloid of fine solid particles or liquid droplets, in air or another gas. Eg: fog, forest exudates and geyser steam which are natural or haze, dust, particulate air pollutants and smoke which are artificial). (Wolf, 2005)

Once the Travertine samples in aerosol form have been introduced into the ICP torch, they are completely desolvated and the elements in the aerosol are converted first into gaseous atoms and then ionized towards the end of the plasma.

Once all the elements in the sample are converted into ions, they are then brought into the mass spectrometer via the interface cones.

The interface region in the ICP-MS transmits the ions traveling in the argon sample stream at atmospheric pressure (1-2 torr) into the low pressure region of the mass spectrometer ( $<1 \times 10^{-5}$  torr). (Note that the 1 torr is an atmospheric unit which equals 0.00131579 atm.)

This is done through the intermediate vacuum region created by the two interface cones, the sampler and the skimmer. The sampler and skimmer cones are metal disks with a small hole (~1mm diameter) in the center.

The purpose of these cones is to sample the center portion of the ion beam coming from the ICP torch. A shadow stop or similar device blocks the photons coming from the ICP torch, which is also an intense light source.

The ions coming from the ICP source are then focused by the electrostatic lenses in the system. Remember, the ions coming from the system are always positively charged, so the electrostatic lens, which also has a positive charge, serves to collimate the ion beam and focus it into the entrance aperture or slit of the mass spectrometer.

The ICP-MS equipment used on this MSc research Travertine samples was a Quadrupole Model ICAP-Q ICP-MS manufactured by ThermoScientific combined with a sample holder Model MVX 7200 manufactured by Teledynicetac. The Figure III.28 and III.29 illustrate the ICP-MS quadrupole geometry and equipment used.

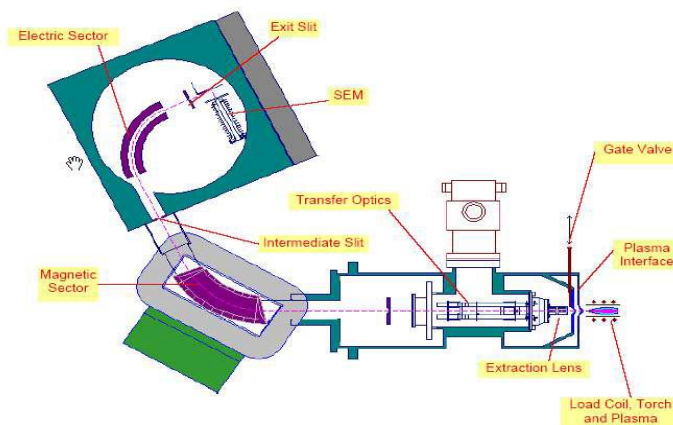


Figure III.28: Geometry the ICP-MS quadrupole (Wolf, 2005) (Courtesy of Thermo Finnegan, San Jose, CA.)



Figure III.29: Quadrupole Model ICAP-Q ICP-MS, (TCD, unit 7)

In any analytical chemistry process, the Instrumental Detection Limit (IDL) which is also called the lowest limit of detection (LOD), is the lowest quantity of a substance that can be distinguished from the absence of that substance (a blank value) within a stated confidence limit. The detection limit is estimated from the mean of the blank, the standard deviation of the blank and some confidence factor.

Another consideration that affects the detection limit is the accuracy of the model used to predict concentration from the raw analytical signal. (Wolf, 2005) .

For the case of this present study, IDL of each element to be detected have been calculated as 3 times the standard deviation of a blank measurement and represent the best possible detection capability of the instrument.

The Figure III.30 below, used by Ruth E. Wolf with the courtesy of PerkinElmer, Inc. shows the approximate detection capabilities of the ELAN 6000/6100 quadrupole ICP-MS which expresses the elements traditionally determined by ICP-MS and their approximate Instrumental Detection Limit (IDL).

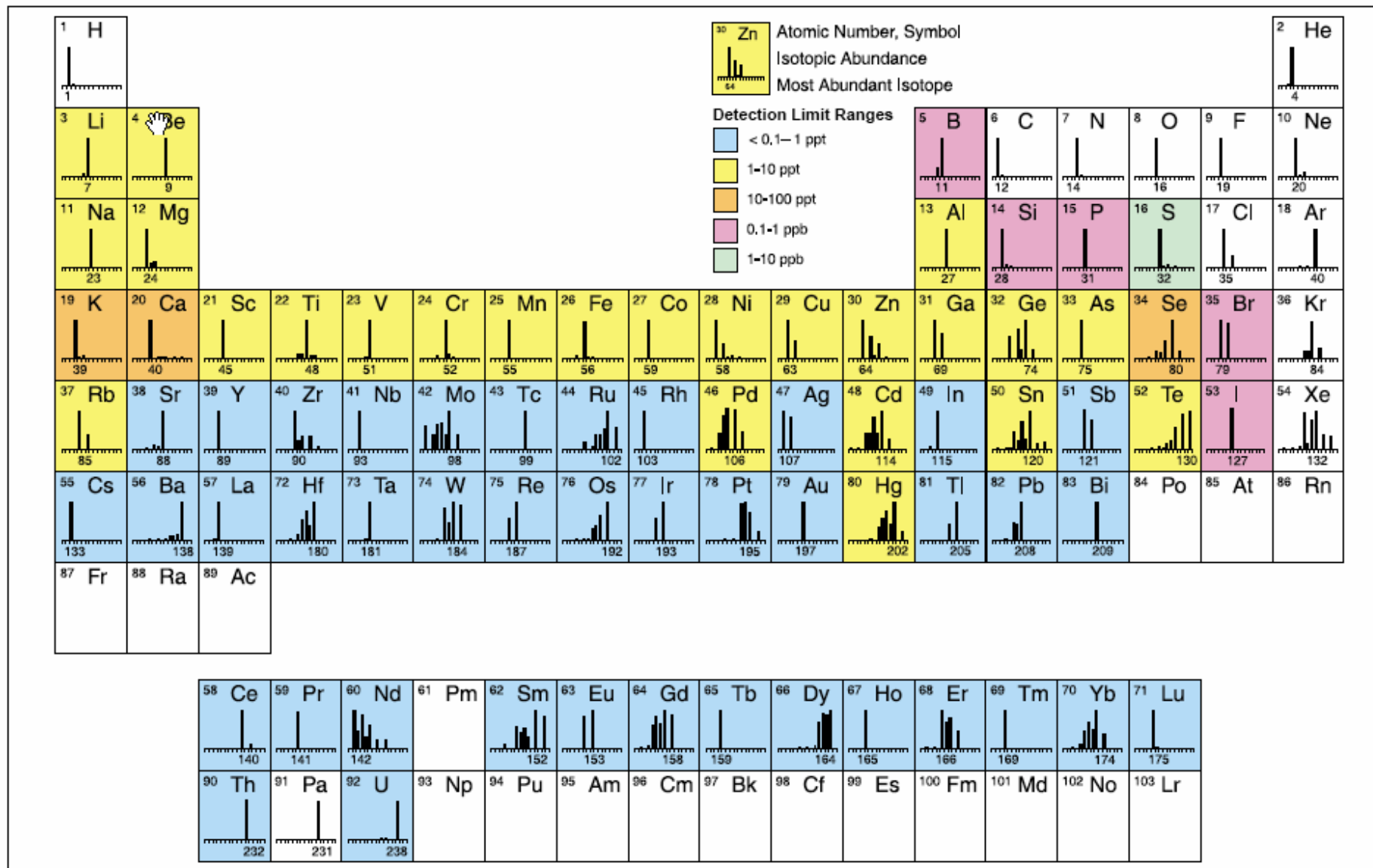


Figure III.30 : Approximate detection capabilities of the ELAN 6000/6100 quadrupole ICP-MS. (Wolf, 2005)(Courtesy of PerkinElmer, Inc.)

Due to the fact that the ICP-MS analysis in 2013 didn't detected the Europium element in the Travertine samples from 2007 to 2010 field trips, the ICP-MS method needed to be fully checked and confirmed trustable by its ability to reproduce at anytime and anywhere else the same results on the same samples whoever would be the lab operator. Before to run the ICP-MS analysis of Travertine collected in 2014 and 2017 in the Graben Albertine of the Eastern African Graben, it was necessary to reproduce the same experiment on the main end member's samples in order to fully trust this method used the first time on our Travertine samples in 2013.

From July to September 2016, ICP-MS lab analysis were done on the same Travertine samples collected during the 2007-2010 field trips in the Albertine Graben which were already analysed at the TCD Enterprise Centre Unit 7 (in 2013 by Jean Dwyer and Mike Babechuk). This aimed to compare the obtained results in both 2013 and 2016 experiments and confirm or not the confidence with the ICP-MS method by its ability to reproduce the same results on the same samples whoever (Cora McKenna and Sylvain M.K in 2016-2018) would be the lab operator.

The Travertine samples proposed to double check the ICP-MS experiment in 2016 have been collected during 2007 to 2010 field's works in ten (10) palaeo-spring sites in the Albertine Graben, East African Rift system where no previous literatures have mentioned their presence so far. However, the ICP-MS experiment results obtained in 2013 revealed the both end members Carbonatites lavas (hot origin) signature and marine limestone (cold origin).

The Twenty (20) Travertine samples presented in the table 1 below were drilled exactly from the same drilling sites drilled in 2013 and run in 2016. All these 20 samples re-drilled ( with a powder weight of around 8 to 10 mg each) for the second time in 2016 have been labelled with the same label used in 2013 added with slash two (/2) new label to make the difference and to show that they have been drilled for the second time.

<b>Carbonatites signature in 2013</b>		<b>Marine limestones signature in 2013</b>	
1	V2b/2	1	P12b/2
2	V20a/2	2	LE24a/2
3	V20b/2	3	LE24b/2
4	V22a/2	4	LE26a/2
5	LE44a/2	5	LE26b/2
6	LE44b/2	6	LE28a/2
7	LE41a/2	7	LE28d/2
8	LE41b/2	8	V19a/2
		9	PCK a/1
		10	PCK b/1
		11	PCK c/1
		12	PCK d/1

Table 1: the 20 End members Samples from the 2013 experiment run again in 2016

The Procokin PCK limestone sample has been collected in a quarry in the western side of DR Congo where literature universally recognized the presence of stromatolite fossils which suggest a fresh water depositional environment or origin. It represents actually the closest limestone outcrop found in DR Congo.

The ICP-MS analysis of the four (4) PCK limestone samples during 2016 experiment aims to confirm by ICP-MS method and instrument the fresh water origin of these stromatolite neighbouring samples which would later be used as matching correlation tool or comparator for / with any other previously known fresh water limestone REE signature or isotopic fingerprint sample to increase again our confidence in the ICP-MS methods ability to trace back the origin of carbonates

The sample forms and photos in Appendix I, are describing the details of the drilling operation highlighting the sample texture/fabric description, the weight of the empty tube, the weight of the tube with sample, the drill bit size, the powder colour after drilling, and remarks during the Travertine slabs drilling.

#### III.6.4- ICP-MS RESULTS INTERPRETATION

Considering the work done by Kamber in 2014, The REE + Y, particularly in combination with some of radiogenic isotopes (e.g. Pb and Sr), are useful to discriminate between stromatolites that formed in lacustrine, restricted marine and open marine depositional settings, and in exceptional cases it is also possible to infer relative water depth or proximity to hydrothermal fluid sources in a sequence of microbial carbonates (Kamber et al., 2014).

However, in order to eliminate the Oddo-Harkins effect which is the presence of obsolete concentrations values in data of some odd-even REE naturally occurring differently in nature, a normalization process of restructuring the Excel database REE results in accordance with a standard has been done prior to averaging in order to reduce data redundancy and improve data integrity.

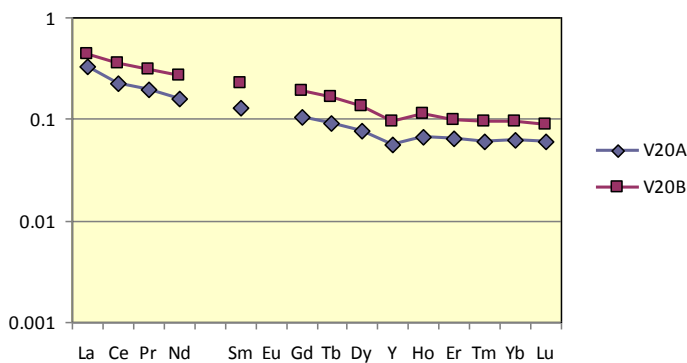
Following exactly the Kamber method for carbonates depositional environment and their respective geochemical origin discrimination used in TCD in 2014, all the ICP-MS concentrations values obtained during this MSc work have been normalized to the standard of 'Mudstone of Queensland (MuQ)': i.e. 'typical' upper crustal siliciclastics. (Kamber et al., 2014)

The Tables in Appendix 2 show the original results (Trace elements data in ppb and normalized in MuQ) of all the three above ICP-MS experiments which were run with a very low detection limits yielding to precise and accurate data for REE and Y elements present in the sample at ppb concentration levels.

Carbonatites limestones REE signatures or “hot” isotopic fingerprints are satisfying the following criteria:(Kamber et al., 2014)

- ✚ Light and heavy REE enriched
- ✚ High Li, Rb, Cs, and Ti concentration
- ✚ Perfect correlation matching with Fort Portal Carbonatites (universally recognized in the literature with Carbonatites fingerprint) with a correlation coefficient above or equal to 0.95 which express the measure that determined the degree to which these samples above are associated with the Fort Portal Carbonatites lavas origin.

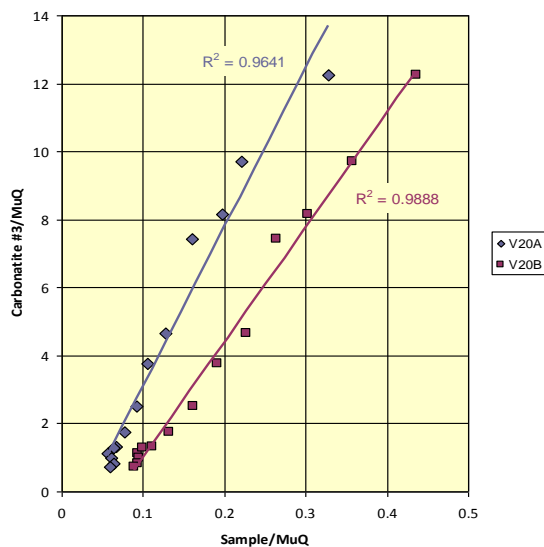
This simply means that the correlation coefficient is a statistical measure of the strength of a linear relationship between paired data (eg in this case Fort Portal Carbonatite data with EAB and /or Block V carbonatite datas). This correlation coefficient can range from -1 to +1, with -1 indicating a perfect negative correlation, +1 indicating a perfect positive correlation, and 0 indicating no correlation at all. The sample V20 ICP-MS result interpretation in the Figure III.31 below is taken as an example:



MUQ values from the Original Excel file (enclosed in CD1) raw datas plotted in an exponential Excel chart, as per Kamber experiment results presentation.

V20A: Fabric: dark grey crystal  
V20B: Replica from the other side of the slice

The REE normalized concentration chart shows signature curves almost matching between them with the published Carbonatites fingerprint curve of Fort Portal, Uganda.



Individual V20A and V20B samples from each slide did not matched with marine limestone criteria, then have been plotted in an Excel chart against Fort Portal Carbonatite #3: their Correlation Coefficient  $R^2 = > 0.95023$

The Correlation Coefficient is never null and his graph can't be starting by the origin 0 because neither the large range (1 to +15) of published MUQ Fort Portal “lavas” Concentrations (Stoppa and Schiazza, 2013) nor the small range (0 to + 0.5) of MUQ Travertine deposited in Albertine Rift carbonate outcrop in hot springs by thermal less carbonated fluids, has null value.



Marine limestones REE signatures or “cold” isotopic fingerprints had satisfied the following anomalies :(Kamber et al., 2014)

- ✚ Gd anomalies
- ✚ Ce anomalies
- ✚ La anomalies

Additionally, the following key criterias for recognizing a REE+Y marine limestone signature have been applied:(Kamber et al., 2014)

- ✚ (Prn / Ybn <<1 Praseodymium / Ytterbium ratio
- ✚ Y/Ho > 40 Yttrium / Holmium ratio
- ✚ La/La\* > 1.1 Lanthanum anomaly
- ✚ Gd/Gd\* > 1.1 Gadolinium anomaly
- ✚ Ce/Ce\* < 0.8 Cerium anomaly

Where:

- $La/La^* = La / ((Pr^* / (Pr/Nd))^2)$
- $Gd/Gd^* = Gd / ((Tb^* / (Tb/Dy)))$
- $Ce/Ce^* = Ce / (Pr^* / (Pr/Nd))$

The reference graph below in Figure III.32 which show the characteristic REE+Y patterns in shallow seawater, freshwater sediments, marine limestones and rift Carbonatites, is used in this work as a comparison tool. Their MUQ values from the existing literatures extend in a large range from  $10^{-3}$  and  $10^1$  as per Kamber experiment graphs.

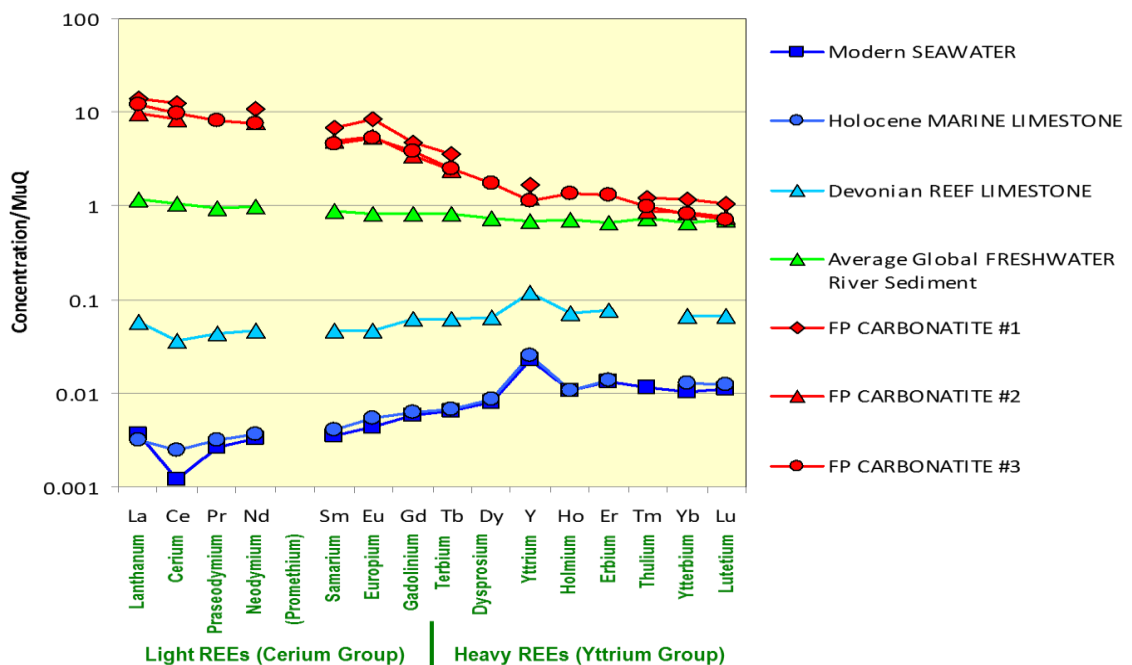


Figure III.32 : characteristic REE+Y patterns in shallow seawater, freshwater sediments, marine limestones and rift Carbonatites (Stoppa and Schiazza, 2013) .(Nicholas, 2009)

### Chapter 3 Conclusion:

*To reach the objectives of this work, our methodology followed the following steps:*

- 1. Travertines field investigation, description and sampling as above detailed in terms of logistic, equipments, field environment and geologist field activities.*
- 2. Travertines petrography investigation: thin section preparation, microscopic observation using the latest technology to identify and describe the ideal structures, textures and/or fabrics containing carbonates mineral or cement for geochemistry analysis purposes.*
- 3. Oxygen and Carbon stable isotope as well as Strontium isotopes analyses and Gas Chromatography Mass Spectrometry to evaluate the various geochemical and biochemical cycles they passed through during their geologic process of deposit.*
- 4. Travertines palaeoclimate changes implications referring to SNOW and PDB values, and their depositional environments datation attempt referring to the Sr isotope ratio.*
- 5. ICP-MS experiments on Carbonates diluted solutions for low detection of Rare Earth Element concentration in ppm, then normalized in MUQ as per Balz Kamber experiment in 2014.*
- 6. REE spectral signatures correlation with the closest know signatures of Carbonatites (Fort portal, Uganda), marine limestones (Mandawa basin, Tanzania), mesoic karoo and Neoprotozoic Schisto-calcaire (Stromatholites).*

*The next Chapter, titled Field Trips, highlights the different seasons of Travertines field investigations, description and sampling. The Travertines depositional environments have been documented by their field evidences using updated field data recording tools, methods and procedures all provided by Dr Chris Nicholas who participated personally in all the Travertines field investigations.*

## CHAPTER FOUR: FIELD TRIPS

This Chapter is treating essentially about all the field trips carried out around the region of the Travertine occurrences in the Albertine Rift. It describes both the Travertine samples collected and the geologic environment of the Hot springs generating these Travertine, coupled in some localities with the temperature records and the spectral gamma response.

Each of these field trips has been sponsored either by Government or Oil companies who provided all logistic and work plans needed for the well organization of the field work during these campaigns. The field trips treated in this present chapter have been supervised by Dr Chris Nicholas assisted by a mixed team made of geologists coming from either TCD postgrads students or respective Governments and Oil companies sponsoring. This Field trips Chapter presents the previous field trips history and then each of the most recent field trips summary highlighting their respective outputs in terms of field informations collected and incorporated to the general understanding of the Travertine presence in the Edward Lake basin.

### IV.1- HISTORY OF ALBERTINE RIFT FIELD WORKS

Initial mapping in the Edward Lake region was for the first time undertaken by the Geological Survey of Uganda in the late 1950's, mainly to identify mineral resources in the Proterozoic basement (Geological Survey of Uganda, 1961).(Rubondo, 2005)

Although the Late Pleistocene -Holocene Katwe and Bunyaruguru volcanics were identified, the remaining rift-fill sediments were left undifferentiated. However, some lineations on aerial photographs were recognised as potential faults trending NE-SW across the onshore area.(Rubondo, 2005)

Academic research in conjunction with some preliminary mapping and a prior gravity survey by the Petroleum Exploration and Production Department PEPD) of the Ministry of Energy and Minerals Development, Uganda between 1960 and 2000 in the Lake Edward - Lake George region identified up to approximately thirteen informal formations in various litho- and chrono-stratigraphic schemes.(Rubondo, 2005)

These were typically assigned an approximately age range of Late Miocene to Holocene. However, without clear field identification and definition of formational bounding surfaces, lateral geologic correlation of these units were still difficult.

Field mapping of the onshore part of the basin in Exploration Area 4 (EA4A) carried out in 2007 has shown that several sedimentary fan systems extend from the basin flanks NW towards the lake (Nicholas, 2009) and more recently from 2009 to 2011 a detailed field map and working stratigraphic framework of EA4B has been established (Nicholas et al, 2015).

Security issues in Block V on the DRC side of the Lake Edward basin prevented any field work from being undertaken until 2010 when a brief field recognisance and later a proper field campaign in 2014 were carried out by SOCO International plc.

#### IV.2- EA1, EA4A & EA4B (UGANDA) FIELD WORK

The geological survey of the Oil Blocks EA1, EA4A and EA4B in the Ugandan side of the Albertine Basin was undertaken by Chris Nicholas, PEPD and Dominion Petroleum Ltd as below:

- *Chris Nicholas (Chief Geologist, Dominion Petroleum),*
- *Dozith Abeinomugisha (Senior Geologist, PEPD),*
- *Catherine Amusugut (Geologist, PEPD),*
- *Tonny Sserubiri (Geologist, PEPD),*
- *Lauben Twinomujuni (Postgraduate Student, Makerere Univeristy, Kampala).*
- *Wilson Tumisabe (Geologist, PEPD and Postgraduate student TCD).*

Travertine samples have been found in outcrops whilst the team was trying to drive towards Kasese locality to look for evidences of exposed Ruwenzori border fault across Ugandan oil blocks EA1 and EA4A. Many lime works and quarries were visited along the road and gave enough interesting Travertine samples which have been firstly described in the field then collected and shipped to TCD for the petrography and geochemical analysis treated in this present study. Many active and not active hot springs surrounding the Travertine outcrops have been documented as possible generating factor.

The Table 2 below presents the Travertine samples described and collected, their respective origin localities as well as their related Oil exploration block geographic coordinates (UTM 36S).

Exploration Block	Locality	X	Y	Z	Travertine Samples
EA1	Okumu,	313104	252027	670 m	P12,
EA4A	Dura	325823	0025483	767 m	LE 32
EA1	Hima	185823	0031483	967 m	LE 37, 38
EA1	Bwera,	806239	0001981	647 m	LE 41, and 42
EA4A	Lyemubuza	833417	0000617	974 m	LES 18, LE 19, and LE 20, LE26, LE 24,
EA4A	Muhokiya	171989	0011737	949 m	LE 27 and LE 28
EA4B	Bat Cave	177790	9966892	683 m	LE 44

*Table 2: Travertine Samples collected in Uganda, 2007 -2009.*

The Figure IV.1 below gives the location of the above limestones quarries and lime works in the Ugandan Oil block EA4A.

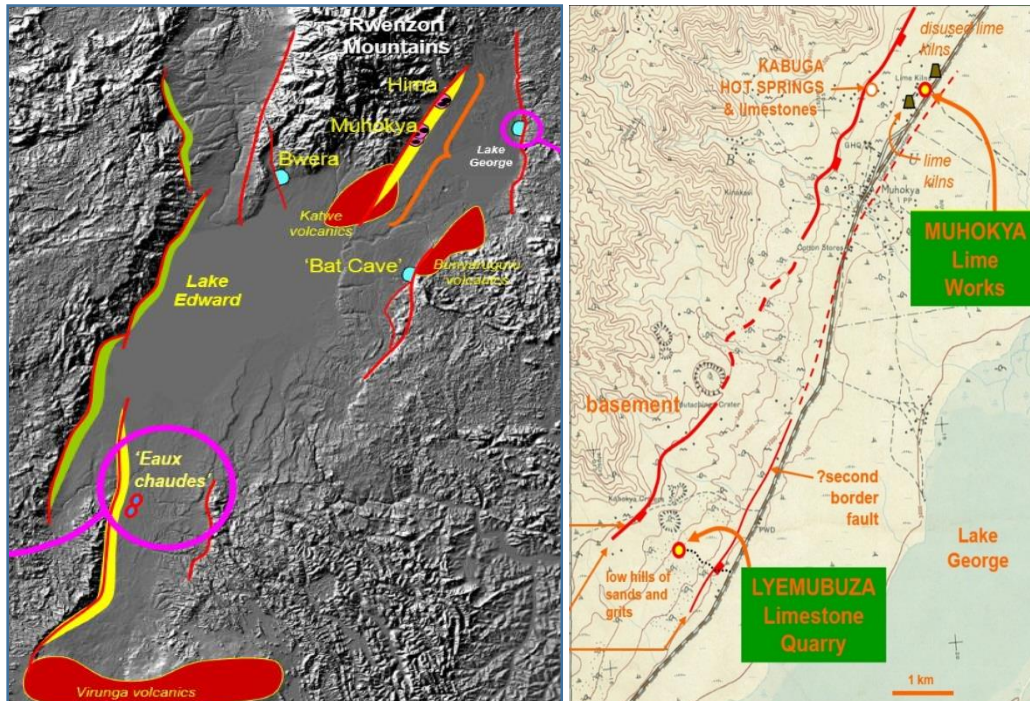


Figure IV.1: Travertine location Field Maps (Nicholas, 2009)

Travertine samples collected in Lyemubuza quarry have been found with Oil stain in cavities and two grabs of samples (LE 19 and LE 20) have been collected one of which (LE 20) appeared to have bitumen(?) Oil residue lighting into its cavities (?) at Lyemubuza quarry

The samples LES 15, 18, 20, 25 and LE 27 have been carefully collected, shipped in LGC Standards laboratory in London and analysed by GC-GCMS in 2008 and their results are presented with the courtesy of Dominion Petroleum Ltd in the Results chapter further in the present thesis.

The remaining samples have also been carefully collected, shipped in Ireland observed with the Nikon latest microscope available in the Centre of Microscopy Analyses (CMA) and analysed by ICP-MS in the Unit 7 Expertise Center of the Trinity College, the University of Dublin in 2013 and their results are also treated in the Results further in the present thesis.

GEOLOGICAL ENVIRONMENT AND FIELD DESCRIPTIONS OF UGANDAN  
TRAVERTINE SAMPLES  
(Chris Nicholas field notes)

**1. Sample P12**

- Geological environment: Okumu and Avoca Hot Springs.

Moderately warm to hot but not too hot to touch located in a NE rift fault intersection with a younger NW active trending fault. No major stream flowing through gorge and the spring appears to be genuinely along the main rift fault.

No obvious strong H<sub>2</sub>S smell. Dispersed Carbonatites caliche throughout.

- Field description: P12

- Travertine with fossil tubes and visible rootlets;
- Small blocks of basement caught up in these fossil tubes;
- Few fossil leaves;
- Apparent black relicts in cavities.
- Feezing with HCl acid.

**2. Samples LE 32, 37 and LE 38**

- Geological environment: Hima cement works mine.

Located just downstream north of a river bank flowing through the Ruwenzori border fault.

- Field description: LE 32, 37, and LE 38

- Very porous light brown limestones;
- Vugs visible presence dispersed in all sample;
- Feezing with HCl acid.

**3. Samples LE 41 and LE 42**

- Geological environment: Bwera Hot springs.

Travertine exposed the East bank of a bounding and NW-SW trending fault against which the Hot springs have developed.

Difficult to see how far they go deep into the hill or whether they are superficial covering. Excellent outcrop of paleostalactites.

- Field description: LE 41 & LE 42
  - Light brown limestones;
  - Visible different layers spreaded in the whole sample;
  - Feezing with HCl acid.

#### 4. Oil slicks LES 15 and LES 18

- Geological environment:

Oil scum floating round Lake Margin at the SW side where “hot springs” are marked onshore Lyemubuza. Seems like an Oil seep underground conduit.
- Field description: LES 15 and LES 18
  - Black algal scum floating on the lake shore;

#### 5. Sample LE 20

- Geological environment: Kasese towards Ruwenzori border fault.

Travertine exposed around 92 m above the current level of Lake George which is not far away suggesting an uplift of limestones along the Ruwenzori border fault.

Difficult to see how far they go deep into the hill or whether they are superficial covering.
- Field description: LE 20
  - Travertine with big cavities seeming to have bitumen residue lining the cavities and/or some black ore mineral growth.
  - Feezing with HCl acid.

## 6. Samples LE 24, LE 26, LE 27 and LE 28

- Geological environment:

Calcite formed in an inverted fairly impressive cliff appearing like a rotational uplift on top of a normal fault block. No evidence of continuous limestone bands.

- Field description: LE 26, LE 27 and LE 28

- Travertine with primary porosity seeming to have black organic rich fill to their primary porosity.
- Feezing with HCl acid.

## 7. Sample LE 44

- Geological environment: Bat cave

Low tufts roofed cave apparently with Travertine in its walls. The underground river system with potholes has produced the cave through the thin tufts. Many pools flowing down west on uphill seeming to be springs bubbling along a geological junction looking like a border fault where thermal waters come up along the junction between impermeable basement and whatever sediments on top.

- Field description: LE 44

- Stalagmites? Composed of several columnar fabrics layers where the crystals with intercrystalline voids elongated perpendicular to the substrate.
- Moderately porous fine-medium crystalline Carbonate.
- Feezing with HCl acid.

The Figures IV.2 *a,b* and IV.3*a,b* below show the geologic environment of LE 20 and LE24, 26, 27,28 samples collected from Lyemubuza quarry while the Figure IV.4 *a,b* and IV.5 *a,b* are showing the geologic environment of LE 41 and LE 42 samples collections respectively from Bwera and Hima localities.



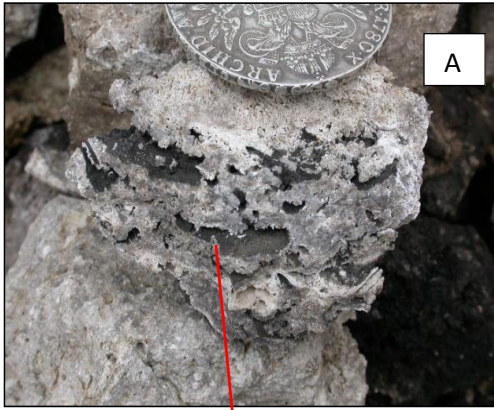


Figure IV.2a: LE 20 (Nicholas, 2009)



Figure IV.3a: LE 27 and 28 (Nicholas, 2009)



Figure IV.2b: Lyemubuza Quarry (Nicholas, 2009)



Figure IV. 3b: Muhokiya Quarry (Nicholas, 2009)

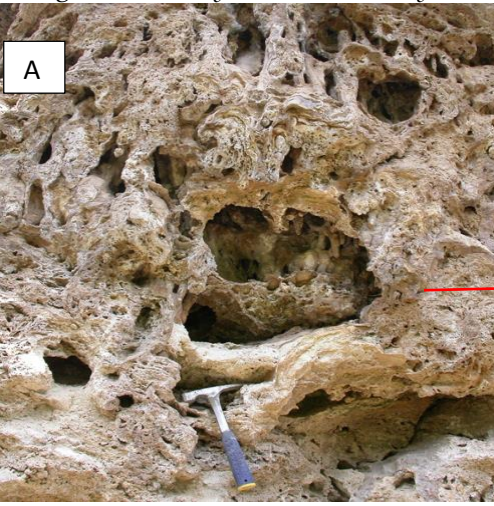


Figure IV.4 a: LE 41 (Nicholas, 2009)

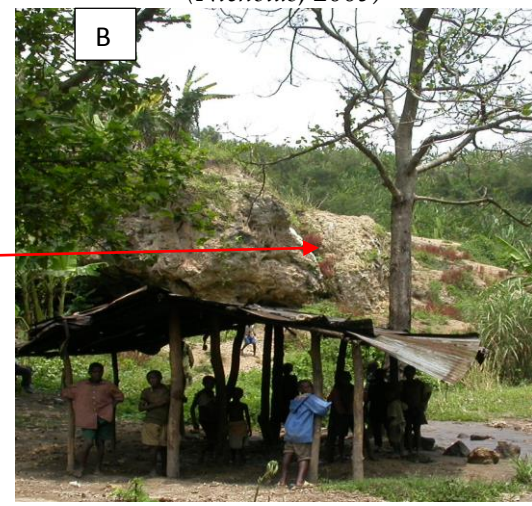


Figure IV.4 b: Bwera locality (Nicholas, 2009)

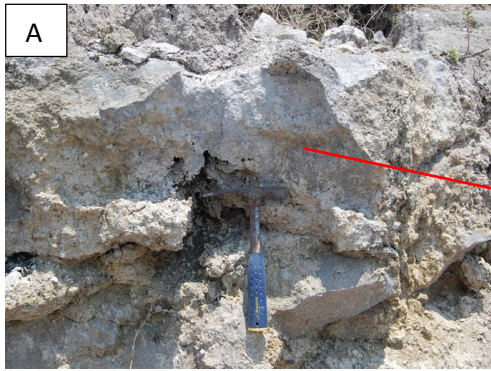


Figure IV.5a: LE 42 (Nicholas, 2009)



Figure IV.5 b: Hima Quarry (Nicholas, 2009)

### IV.3- BLOCK FIVE (DR CONGO) 2010 FIELD WORK

The first geological field survey of Bloc V, the Congolese side of the Edward Lake Basin was undertaken by SOCO International Plc between November and December 2010.

The field team comprised the following people:

- Chris Nicholas (Trinity College, University of Dublin),
- **Sylvain K. Mangoni** (Geologist, SOCO DRC),
- Bichou Ndanze ( Driver, SOCO DRC),
- Jumbo Binji ( Security Officer, DRC army)
- Military escort.

This geological field survey was timed in part to coincide with the safe periods of the volatile security situation of the onshore of the Congolese side of the Edward Lake basin, the block V owned and operated by SOCO International Plc. This enabled the field team to use temporarily cleared itinerary to enter in safer areas. The Block V contains more than 70% of the area of the Virunga National Park itself a much protected world heritage owning. This much protected area status restricted the geologic work as the access to the National Park was subject of many authorizations and long administrative processes. No authorization have been granted.

An initial set of Travertine samples were collected in the field, correctly packed and shipped to Trinity College Dublin (TCD) for microscopy and geochemical analyses (ICP-MS) to augment field datas in order to identify if there were any mineralogical or geochemical differences between these samples structures/textures/ fabrics that might indicate the geochemical origin of the carbonates generating these Travertine.

The following Travertine samples have been collected for the purpose of geochemical analysis treated in this present study: V2 in Biruma (Southern East), V19, V20, V21, V22 in Mayi Ya Moto (West).

The field photos illustrated in figure IV.6, IV.7, IV.8 and IV.9 below shows the field environment of V2 and V19, V20, V21, V22 samples collected respectively from Biruma and Mayi ya Moto.

GEOLOGICAL ENVIRONMENT AND FIELD DESCRIPTIONS OF DR CONGO  
TRAVERTINE SAMPLES

V2: Light Brown very crumble limestone with vugs porosity and visible rootlets branches and plant tubes;

V19, V20, V21, and V22: Black stained lining in white vugs spreaded Travertine.

Note:

Due to security issues, the number of localities to visit and field time restrictions per locality, we didn't have time to describe the geological environment and collected samples. No gamma ray has been recorded, the tool was not available. Mayi ya Moto locality has been targeted as main visit for the next field trip under better security conditions.



Figure IV.6: Sample V2 Biruma (SOCO, 2010)



Figure IV.7: Sample V20 Mayi ya Moto (SOCO, 2010)

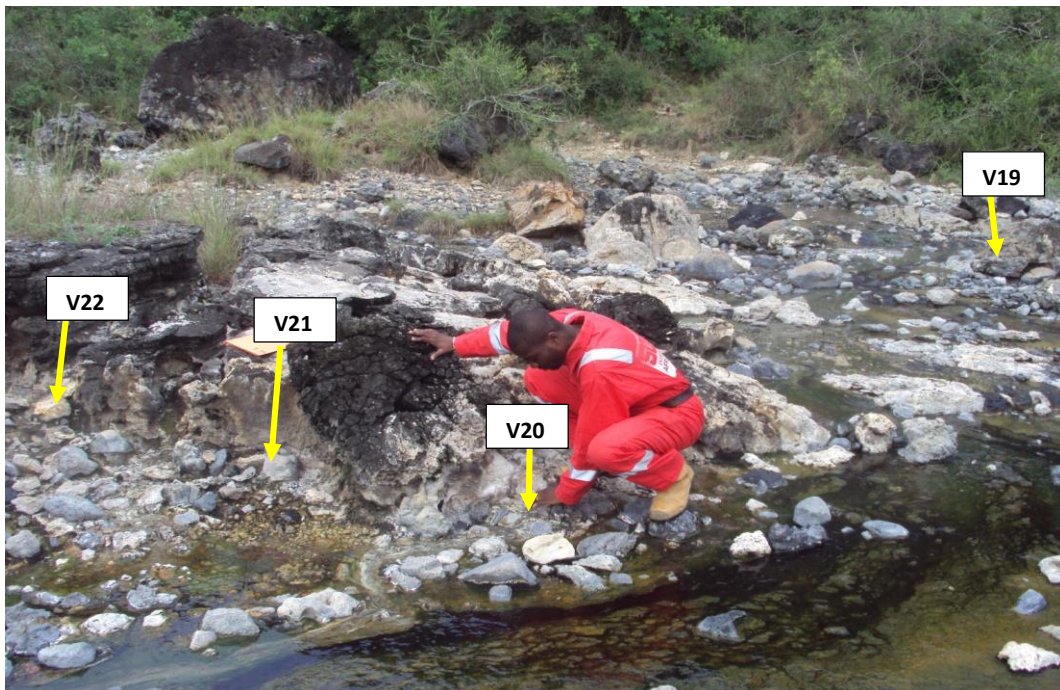


Figure IV.8: Sample V19, 20, 21 & 22 @ Mayi ya Moto (SOCO, 2010)



Figure IV.9: V2 collection at Biruma Quarry (SOCO, 2010)

#### IV.4- BLOCK FIVE (DR CONGO) 2014 FIELD WORK

The second geological field survey of Bloc V, the Congolese side of the Edward Lake Basin was undertaken by SOCO International Plc. between May and August 2014. Figure IV.10 shows in red line the limits of Block V in the Lake Edward basin.

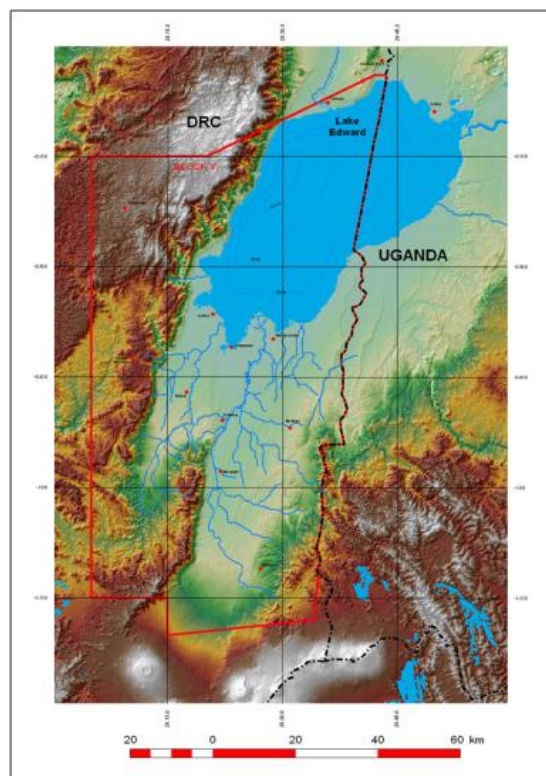


Figure IV.10: Block V Field Map (SOCO, 2010)

The field team assigned to this field trip comprised the following people:

- Chris Nicholas (Trinity College, University of Dublin),
- **Sylvain K. Mangoni** (Geologist, SOCO DRC),
- Finbaar Mc Teirran (Postgraduate student, Trinity College, University of Dublin)
- Peter Kock (Field Security Officer)
- Steve (Helicopter pilot)
- Bichou (driver)
- Military escort.

This geological field survey which was a bit longer than the previous, was timed in part to coincide with the access grant to the Virunga national park, the improvement of security situation of the whole Block V and the seismic acquisition operations in the offshore of the Congolese side of the Edward Lake basin as part of the block V owned and operated by SOCO International Plc. This enabled the field team to use temporarily cleared itinerary to enter in safer areas, SOCO base camp in Nyakakoma village and efficient field logistic support including the use of a Helicopter for survey flights with possibility of landing anywhere, the base camp of seismic operations, vehicles 4x4 wheels, radio tracking devices, etc .

In order to better understand the Travertine occurrences in the region, an investigation of others surrounding Carbonates outcrops have been done in the purpose of overview their spatial extend correlation in the regional level.

The main targets of this new field trip in Block V were:

- Revisit the 2010 Travertine localities ( Mayi ya Moto and Biruma) and visit new other limestones localities (Katanda Terraces and Vitshumbi unit),
- Detailed geological description of Travertine exposures (numbered as field localities), and recognition of a set of lithofacies associations,
- Sedimentology logs of reference cliffs along main hot springs faults.
- Spectral Gamma Ray recording at specific intervals from the base to the top of these cliffs,
- Travertine samples collections at each location of the Spectral Gamma ray recording,

#### IV.4.1- GEOLOGIC ENVIRONMENT AND FIELD DESCRIPTIONS OF TRAVERTINE SAMPLES COLLECTED IN BLOC V IN 2014

(Sylvain's field notes)

The two sites (Mayi ya Moto and Biruma) visited in 2010 have been revisited in 2014 and two new sites (Katanda terrace with black shining stuffs and Vitshumbi carbonate unit) have been added to the itinerary during this field trip.

The Table 3 below presents the Travertine samples described and collected, their respective origin localities as well as their related Oil exploration block geographic coordinates (UTM 35M).

Exploration Block	Locality	X	Y	Z	Travertine Samples
Block V	Mayi Ya Moto	313104	252027	670 m	V149, V150, V153
Block V	Katanda	185823	0031483	967 m	V159,V161b,V162a,V163b, V164
Block V	Vitshumbi	806239	0001981	647 m	V338,V344,V352,V356
Block V	Biruma	833417	0000617	974 m	V363, V364, V385

Table 3: Travertine samples collected in DR Congo, 2014

Their geologic environment and samples field descriptions and their photos can be see here below:

The Travertine in and around Mai ya Moto (Figures IV.11 to IV.13) had very high TOTAL GR values, whereas the deposits in Biruma have very depleted KUTH values. It is mainly composed of clean white limestones with dense reed and rootlet beds where the carbonate has encrusted vegetation which probably grew in an extensive shallow pool fed by carbonate rich hot springs.

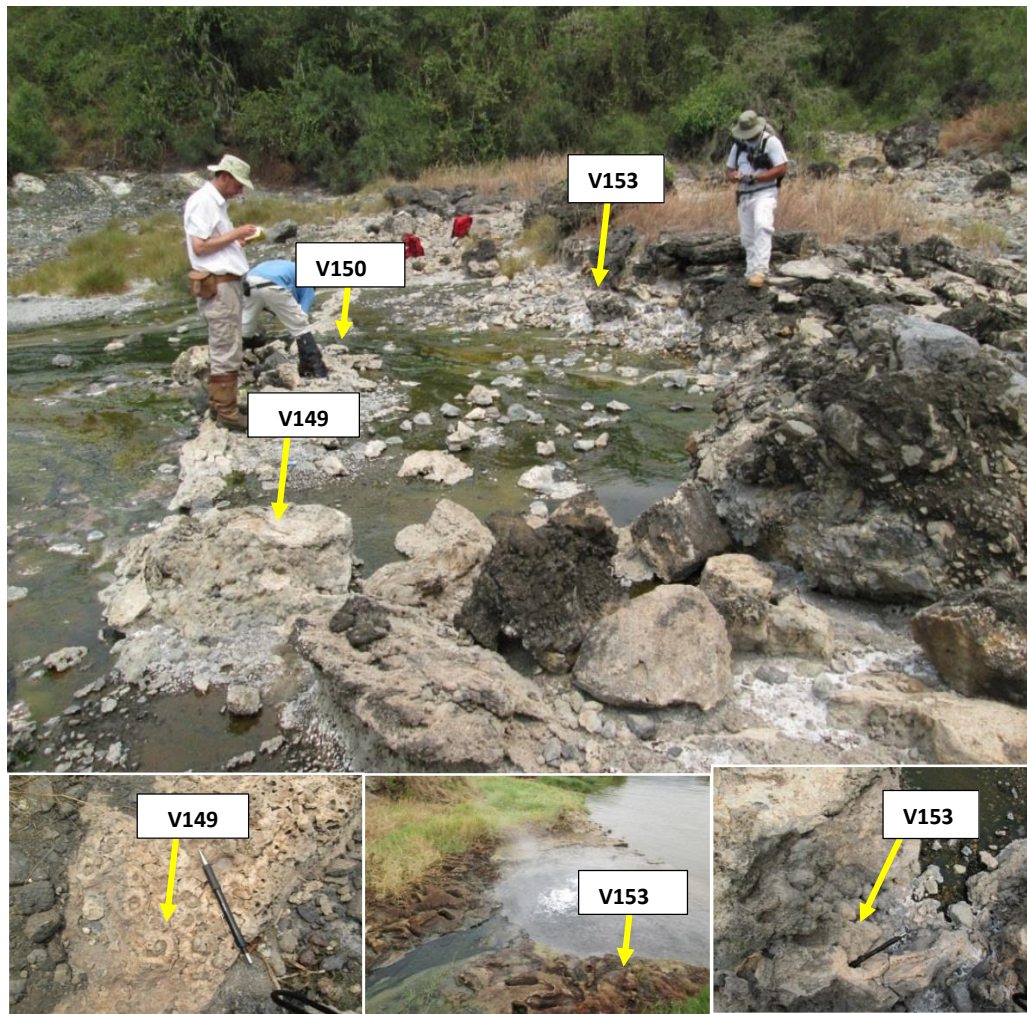


Figure IV.11: Sample V149, V150 and V153 @ Mayi ya Moto (2014)

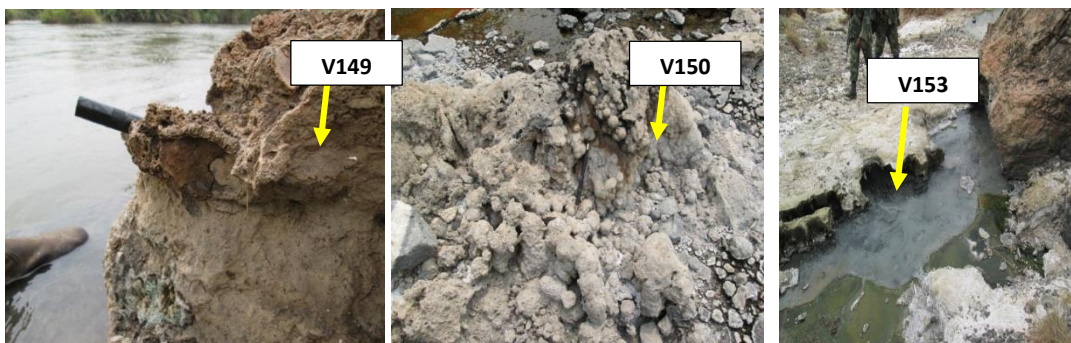


Figure IV.12: Sample V149, V150 and V153 @ *Mayi ya Moto* (2014)  
 At Katanda, a large active hot spring was located at the main western bounding fault's surface expression, with several palaeo-springs forming 'terraces' at intervals up the fault scarp.

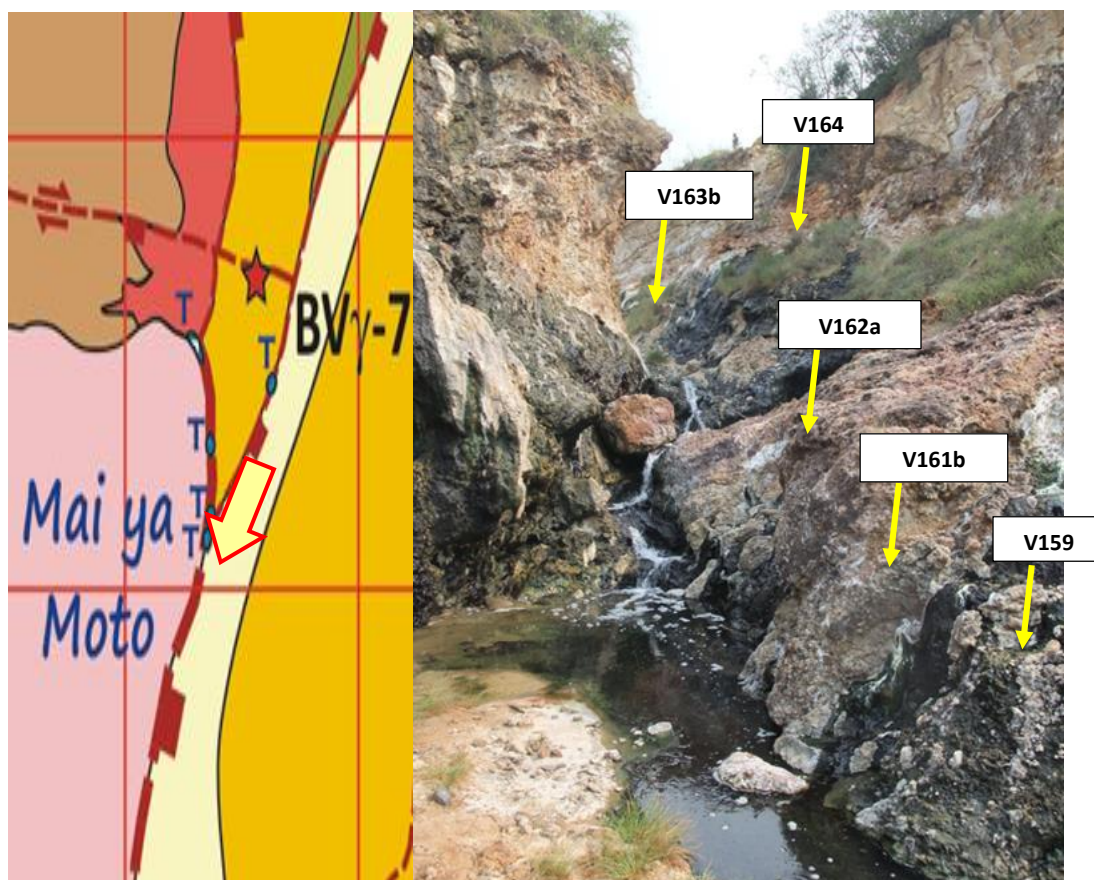


Figure IV.13: Gorge (*Katanda*) with extensive Travertine limestones covering and hot spring pools linked by streams. Samples collected for ICP-MS

These palaeo-springs may have been abandoned as movement on the fault shunted them upwards, away from the fault plane up which the fluids are fluxing. Samples V159, V161b, V162a, V163b and V164 have been collected for ICP-MS analyses.

Active hot springs were also found further north-east away from the main fault up a north-north-east – south-south-west fault on the banks of the Rutshuru River. This along with structural mapping suggests that the springs are situated around the triangular intersection of 3 major rift faults, and not solely associated with the main western bounding fault.

Another 1-2km<sup>2</sup> Travertine limestone outlier in Biruma was revisited on this trip. Here the limestones are apparently underlain by older basaltic volcanics and are at least 50m thick and are quarried by the locals to form lime for construction.

The Travertine in and around Mai ya Moto had very high TOTAL GR values, whereas the deposits in Biruma have very depleted KUTh values. It is mainly composed of clean white limestones with dense reed and rootlet beds where the carbonate has encrusted vegetation (Figure IV.14) which probably grew in an extensive shallow pool fed by carbonate rich hot springs.

Samples V338, V 344, V 352, V 356, V363, V 364, and V 385 have been collected for ICP-MS analyses.

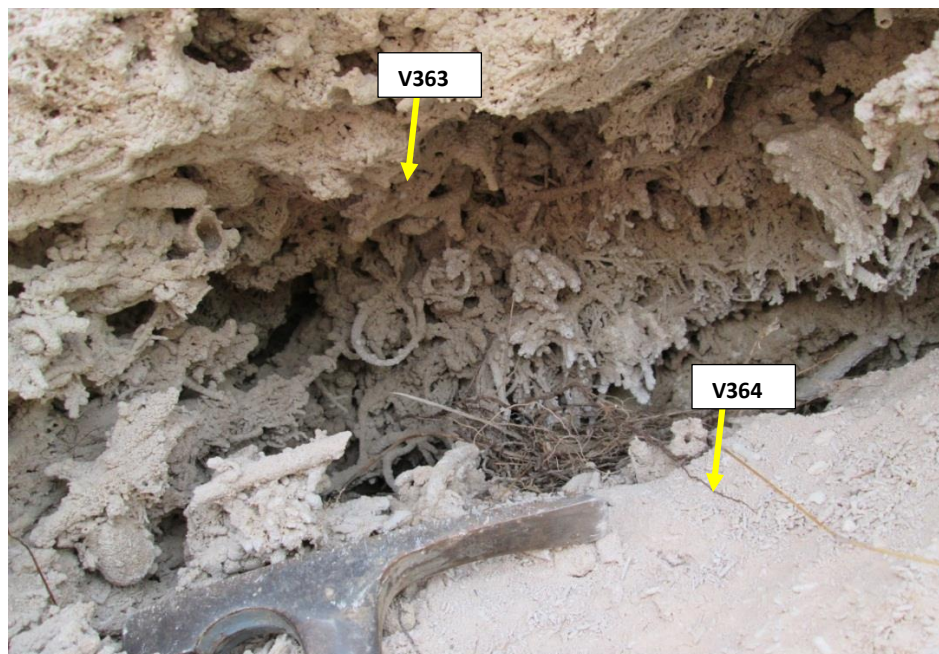


*Figure IV.14: White carbonate encrusts reeds and rootlets at Biruma.*



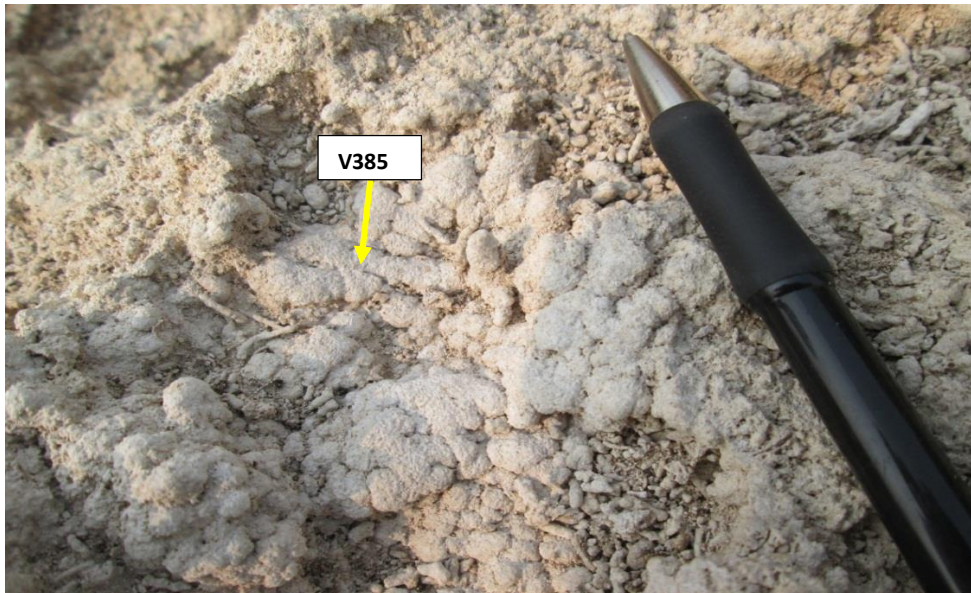


Figure IV.15: Pustulose texture, similar to that seen at the mouth of active springs, precipitated close to where the spring would have emerged.

GEOLOGICAL ENVIRONMENT AND FIELD DESCRIPTIONS OF DR CONGO  
TRAVERTINE SAMPLES 2014

I. Mayi ya Moto hot springs (Revisited)

**Coordinates:**

761398  
9900789  
@ 605 m

**Geologic environment**

Bubbling Hot springs lined just below an active fault evidence in the Eastern flank of the Eduard basin. Algal hot waters are flowing in small streams.

3 Patches of Travertine outcrops have been observed:

- Patch dipping 80/036 where the closest Hot spring temperature = 93°C
- Patch dipping 63/028 where the closest Hot spring temperature = 96°C
- Patch dipping 42014 where the closest Hot spring temperature = 93° C

**Gamma ray values:**

K= 0.9 % U= 66.8 ppm Th = 12.7 ppm (assay 2265)

**Samples description**

**V149:** single block. Light brown fibrous Travertine with Breccia gap and cavities.

**V150:** Microbially laminated white Travertine with fibrous layers.

**V153:** Travertine with chimney structure that provides ventilation for hot flue gases or smoke from underground processes, then cooled at surface in ambient temperature.

II. **Katanda gorge** (New locality)

**Coordinates:**

761494  
9902714  
@ 685 m

**Geologic environment**

Incised valley trending 320° NW at first glance from the helicopter (aerial view below in Figure IV.17) appeared to have relict Oil seep. In the ground, it is a linear Hot springs locality with algae growing up the steep sides.

A network of hematite veins sheets through the rift-fill sediment here and there. The Travertine are dragging the steep valley sides.

The hot water stream turn back on itself further to the NW and it is following the steeply dipping and curving basement edge, rather than linear rift-fault.

**Gamma ray values:**

K= 3.6 % U= 410.8 ppm Th = 11.8 ppm (assay # 2266) upstream

K= 1.4 % U= 309.2 ppm Th = 57.5 ppm (assay 2267) downstream

The GR values in general, Th and U values in particular appears to decrease downstream away from main stream full of cyanobacteria evidence suggesting increasing oxygenation downstream.

**Samples description:** (Upstream towards downstream)

<b>Travertine</b>	<b>Elevation</b>	<b>Sample</b>	<b>Field description</b>
Terrace #4	995 m	V162 a and b	Hematite stained Travertine crumbled
Terrace #3	985 m	V163 a and b	Hematite stained Travertine crumbled
Terrace #2	976 m	V159 ,V161	Hematite stained Travertine crumbled
Terrace #1	962 m	V164	Hematite stained Travertine crumbled

III. **Mabenga hot springs** ( New locality)

**Coordinates:**

761774  
9900764  
@ 687m

**Geologic environment**

Small pool of 4 bubbling springs at eastern river bank.

Temperatures 84.7°C , 75.2 °C, 82.2 °C, 75.7°C . Presence of white salt crusts and small chimneys with maximal temperatures of 90 °C.

**Gamma ray values:**

K= 1.0 % U= 200.9 ppm Th = 25.1 ppm (assay # 2268) upstream

**Samples description:**

Sample	Field description
V 344	Travertine with inputs of plants and tree rootlets
V352&356	Travertine with inputs of plants and tree rootlets
V363&364	Vertical zoned Travertine including gas holes around large cavities
V385	Vertical zoned Travertine including gas holes around large cavities

**IV. Vitshumbi fault scarp** ( New locality)

**Coordinates:**

763580

9903605

@ 689 m

**Geologic environment**

Boiling springs on west side bank of Rutshuru River bubbling along a length of around 40 m in a series of pools as the main river.

**AERIAL VIEW (BLING SATELLITE IMAGE) AND GROUND CONSIDERATIONS OF EXPLORED SITES IN BLOC V.**

(Figures IV.16 to IV.20)

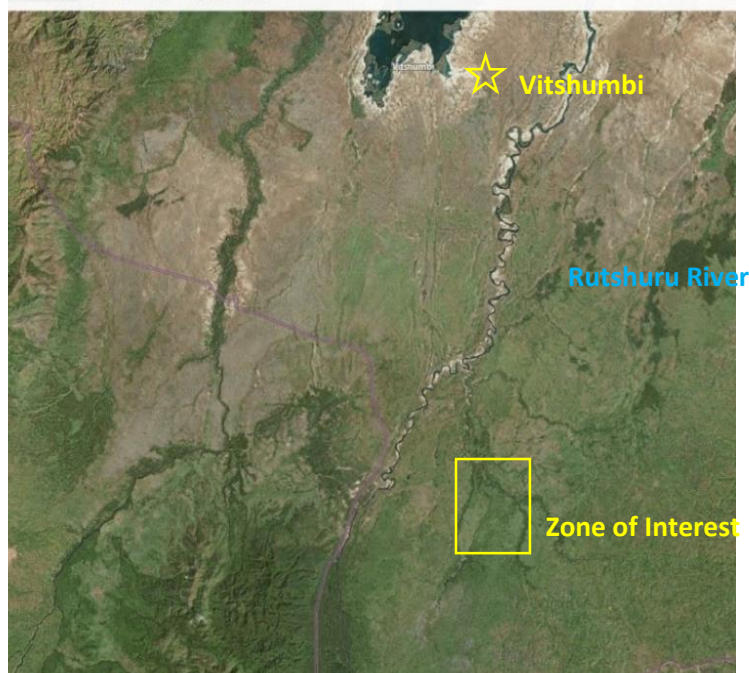


Figure IV.16: ©Bing 2018 Aerial view of the Eduard basin Travertine occurrences. Zone of interest. 1cm = 5 Km

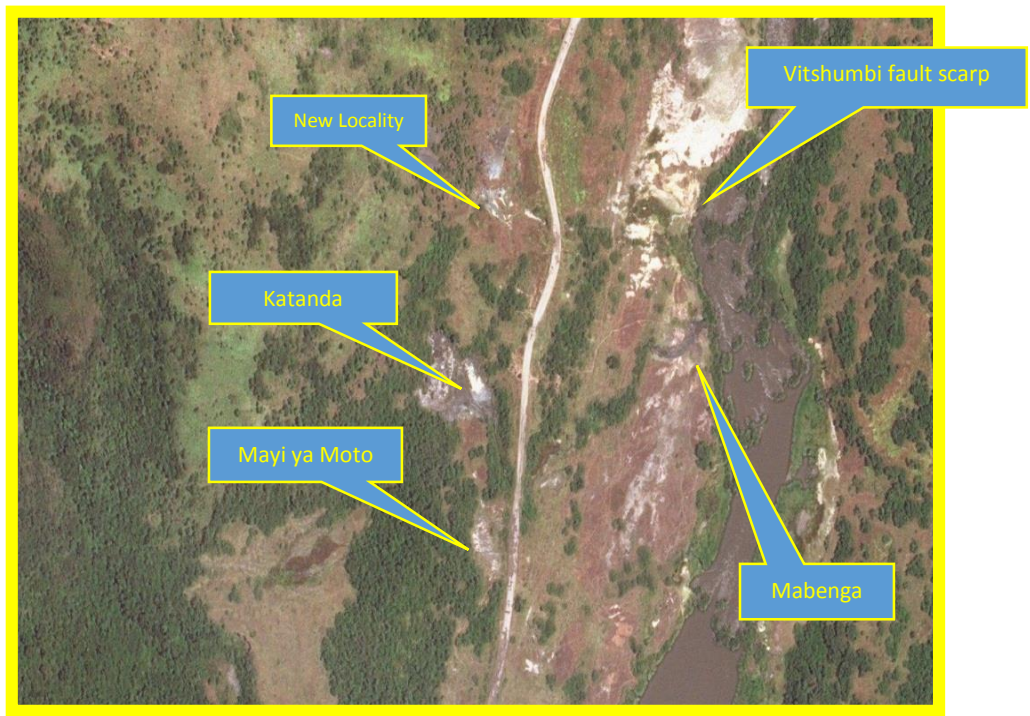


Figure IV.17: ©Bing 2018 Aerial view of the ZOI ~5 Km<sup>2</sup>. Visited Sites

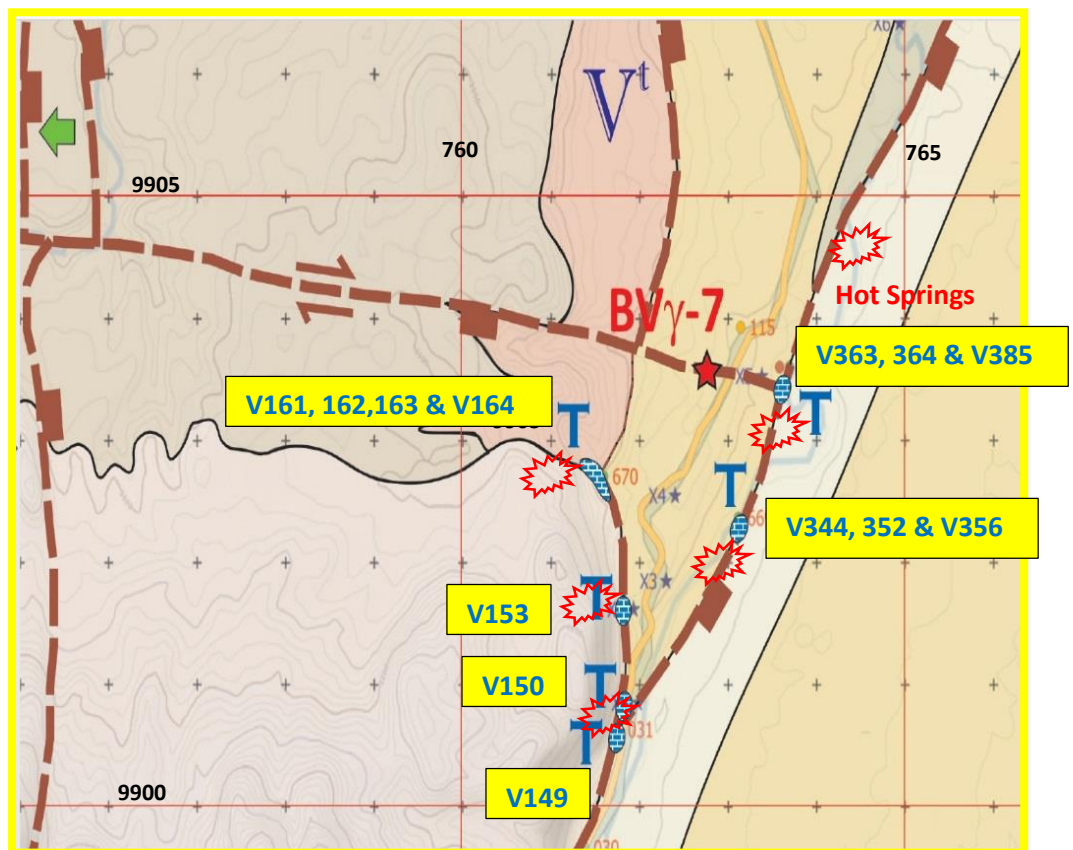


Figure IV.18: Geologic considerations of the ZOI. Travertine samples collected. Hot Springs observed.



Figure IV.19: ©Bing 2018 Aerial view of the Biruma Quarry

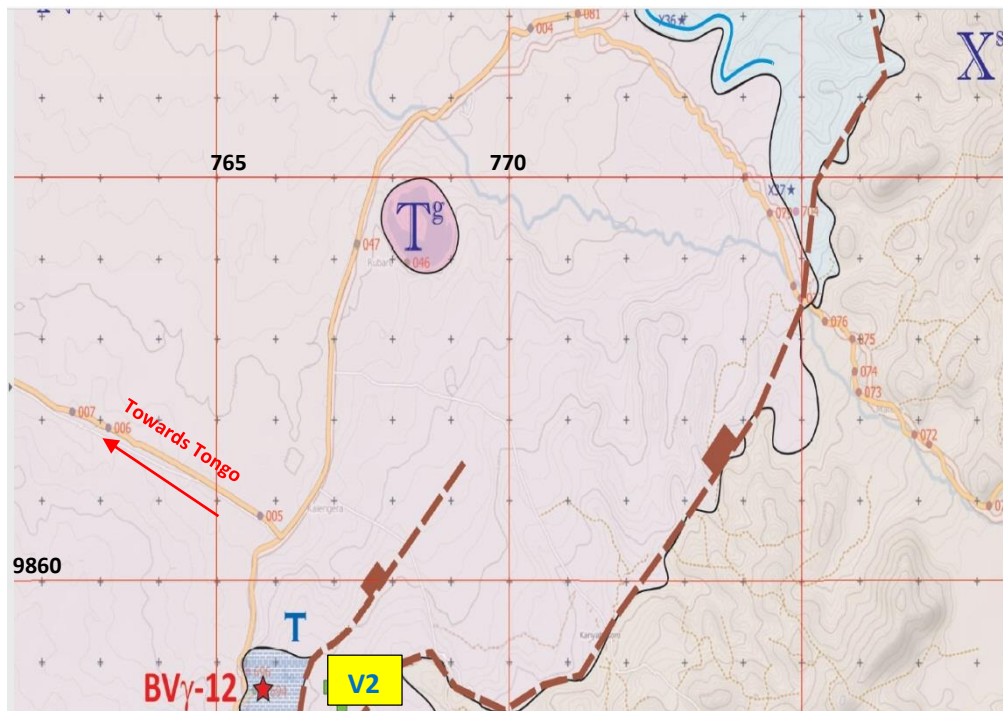


Figure IV.20: Geologic considerations of the Biruma Quarry. Travertine samples collected

#### IV.4.2- OVERVIEW OF BLOCK V OTHERS CARBONATES OUTCROPS

The only others carbonates outcrops encountered during the field trip in the Block V were located in the Vitshumbi Unit. This unit is described and its spectral Gamma response are presented below:

##### A.1 Lithofacies and Stratigraphic Definition

South of Lake Edward inland from its marshy margins are the mostly flat, sparsely vegetated grasslands. Exposures can be seen in the scarps of north-south and northeast-southwest trending faults South-south-west of the Village of Vitshumbi (Figure IV.21) which lies on the southern-most tip of the lake a well exposed scarp with prominent bedding stood out from the helicopter. The fault was followed north and south where its surface expression could be seen dying out in either direction so, the thickest and most well exposed point along the scarp was chosen for logging as time constraints related to permissions to work in the area meant the fault could not be explored further on foot.

The lack of vegetation made landing on the footwall dip-slope easy, and the lowest most in-situ exposure at the base of the scarp was found on foot. Standing on the top of the scarp looking east a smaller west-facing antithetic fault could be seen in the distance creating a miniature graben. This small valley runs north-south up to the western side of Vitshumbi village, and so its name was used to refer to the characteristic stratigraphic unit exposed here [UTM 761080 9915289; Locality CJN 263].



Figure IV.21: Vitshumbi fault scarp looking north at log section BV $\gamma$ -10.

Further exploration later in the field trip added more informations to the Vitshumbi unit knowledge. A further exposure of this formation was scouted out east of the village of Kirima in the southern and highest part of the Ruindi sub-basin in a deeply incised river valley through which the Ruindi River flows.

The helicopter was landed in the village football field, much to the excitement of the locals, and then military vehicles were then taken to the river valley.

A dirty road handily shown below in Figure IV.22 cut into the sediments in the tall banks of the river runs from a bridge across the river to the top of the valley exposing, and allowing easy access to, approximately 20m of rift-fill sediments [UTM 745239 9890867; Locality C/JN 095]. (Figure IV.22 below)

Security in the area allowed for only one days logging of this locality, but the ease of access to the exposure meant it was completed.

Both sections were defined as part of the Vitshumbi Formation due to having very similar lithofacies, the presence of abundant carbonate which fizzed readily in the presence of dilute HCL, their high Total GR (from 160-500 API) and very high U and Th concentrations earning them the name 'hot limestones'.

The fact that the better developed hard limestones of this unit weather proud and are easily visible even in small fault scarps, and that anything similar to this unit has not been seen elsewhere in the basin, suggests that the rest of this unit must lie deeper, buried under youger rift-fill sediments.



*Figure IV.22: Road cutting along the side of the Ruindi river valley to the east of Kirima village at log BVγ-18.*

These two sections were logged in detail and consist of marls and marly limestones with 5 main lithofacies: (Figures IV.23 to IV.26)

- a) Light brown marly limestone with fine to medium sub-angular quartz, well rounded coarse quartz grains, abundant fine to medium sub-angular black mineral grains, hard crumbly calcitised plant material at small and large scale, rootlet/burrow systems and occasional shell fragments.
- b) Pale reddish brown marl, poorly sorted mix of very fine, fine and medium sub-angular quartz stained different colours, fine to medium sub-angular black mineral grains.
  - b') As for b) but with a coarser quartz grain size making it more crumbly.
- c) Light brown dominantly fine sandy limestone, quartz grains stained different colours, admixture of fine to medium sub-angular quartz, fine black mineral grains, hard calcretes layers with desiccation cracks and pustulous microbial mat texture.
- d) Greyish orange to moderate orange pink silt to very fine quartz sandy marl, very fine black mineral flecks, powdery and friable, rootlet/burrow system sometimes still with black organic carbon lining cavities, discontinuous caliche nodule layers.
- e) Greyish orange to medium grey relatively poorly sorted mix of medium to very coarse sized sub-angular to sub-rounded quartz grains, powdery clay grain coat, cross-bedding on 40cm scale, very coarse black mineral grains, quartz stained different colours, very friable, layers of marl rip-up clasts.



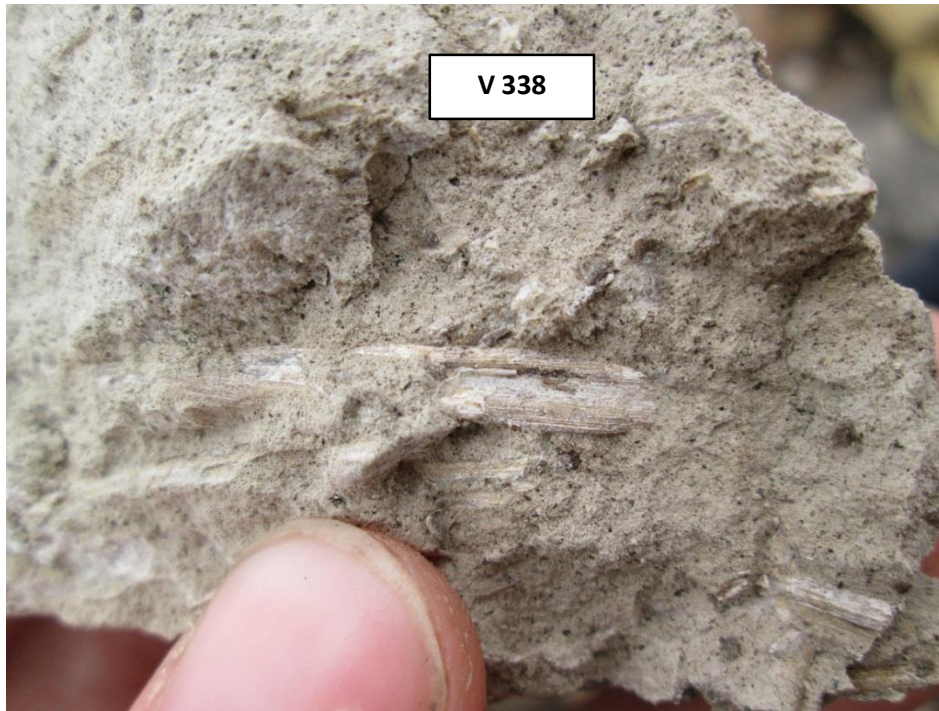


Figure IV.23: Calcitised reed impression in Lithofacies 'a' at log section BV $\gamma$ -10. (V338)

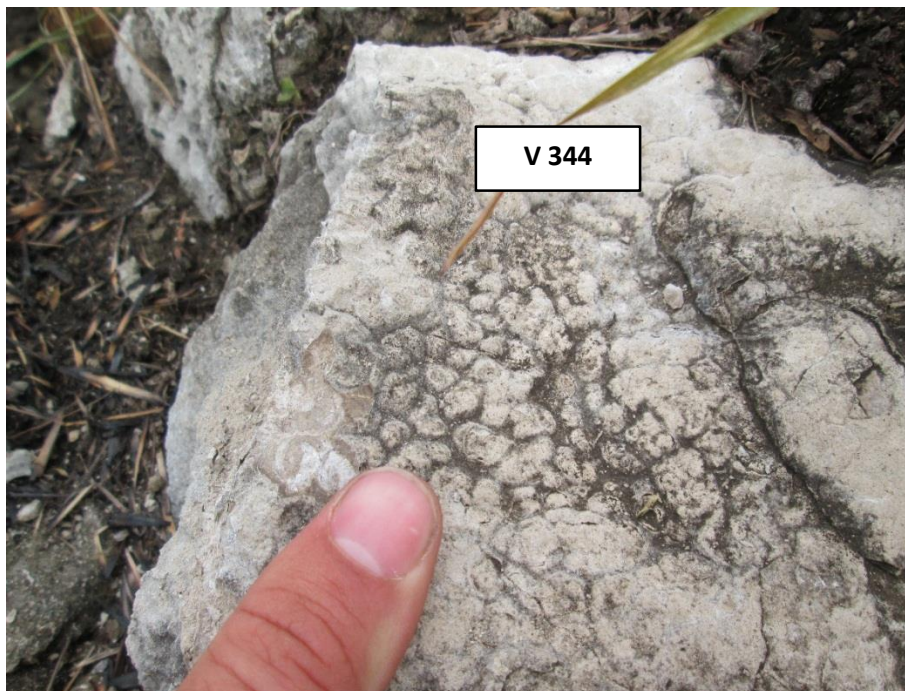
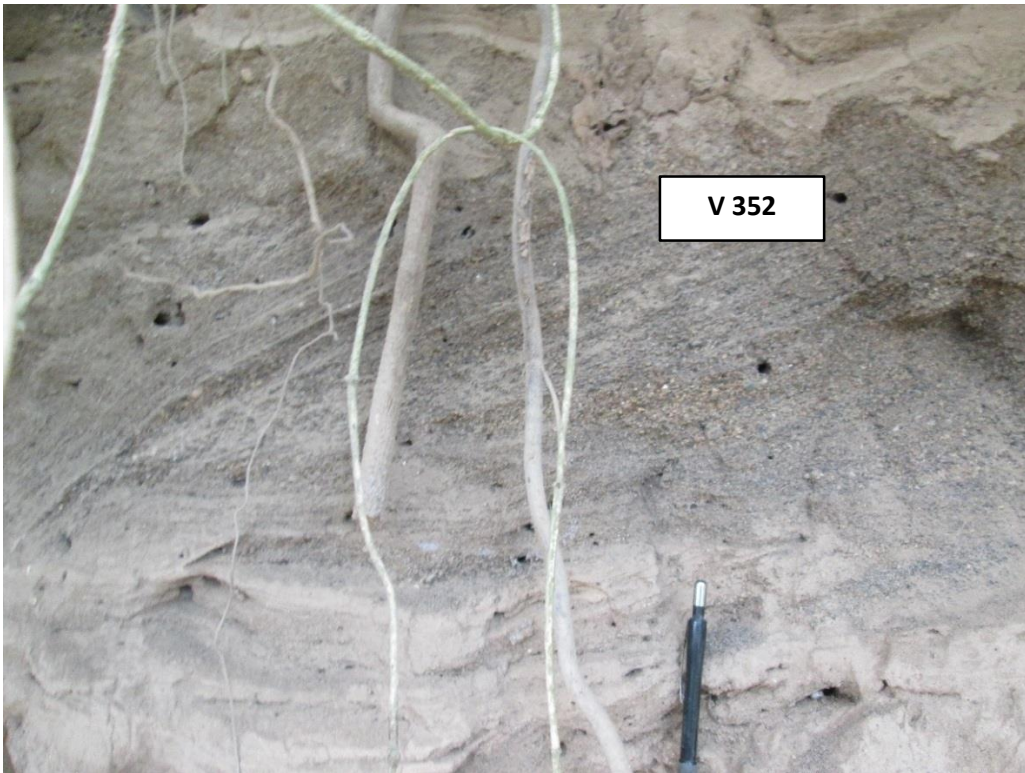


Figure IV.24: Pustulous textured microbial mat in Lithofacies 'b' at log BV $\gamma$ -10. (V344)



*Figure IV.25 Cross-bedding in Lithofacies 'e' at log BVγ-18 in Ruindi river valley.  
(V352)*



*Figure IV.26: Marl rip-up clasts in Lithofacies 'e' at log BVγ-18 in Ruindi river valley.  
(V356)*

A.2 Spectral Gamma Response

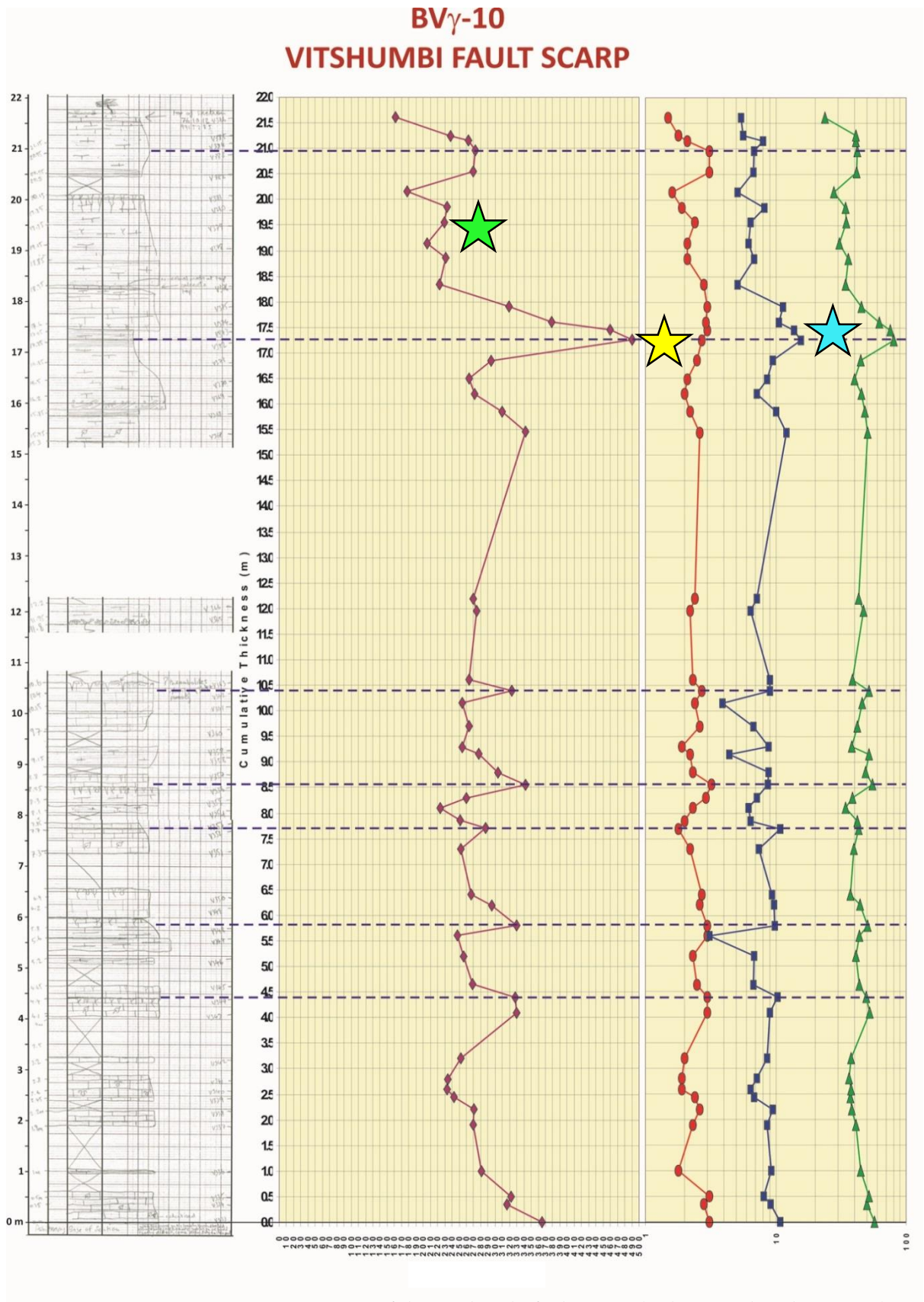


Figure IV.27: Gamma Ray response of the Vitshumbi fault scarp. (Sylvain and Finbaar 2014)

BV $\gamma$ -10: Vitshumbi Unit

- Total Gamma from 160-500 API, higher than any other unit so far discovered in the basin.
- Blue Star: K, U, Th all peak together in 1.5m-2m cycles.
- Peaks are usually associated with hard calcretes tops with associated desiccation cracks and microbial mats.
- Yellow Star: Marked spike in Total GR, U and Th in finer laminated silty marl.
- Green Star: Total GR clearly falls towards top of the section.

The high gamma response (Figure IV.27 above) suggests that these carbonates are being precipitated from reducing, U and Th rich waters, possibly related to water percolating up the main rift-bounding fault which still feed active hot springs today.

#### IV.4.3- STRUCTURE, HEAT & FLUID FLOW

As the hot springs and Travertine outcrops are located along margin faults, a structural study and heat flow research was necessary to understand in the field.

##### IV.4.3.1- REGIONAL STRUCTURE

A series of aerial surveys were flown systematically across Block V. By hovering directly above the fault's surface expression, an accurate GPS coordinate could be obtained allowing faults to be mapped onto topographic base maps during the flight. This produced a structural map showing all major rift faults in the region.

Some faults were easily recognised by the presence of major fault scarps with beds rotated to dip into the cliff, however, in areas with little or no exposure faults were identified using a number of observations, for instance:

- Markedly asymmetric hills with raised, angular or rounded footwall crests immediately above a scarp slope,
- The presence of marked scarps which are not obviously due to river incision,
- Low-angled, uniform dip slopes forming obvious benches in the topography,
- Clear elevation differences between hills separated by scarps and across valleys (lowering the helicopter down into valleys until level with the ridges at the top and looking side to side with the long axis parallel to the long axis of the valley made any difference in height extremely apparent.)
- Hanging wall lakes or swamp areas at the base of fault scarps.

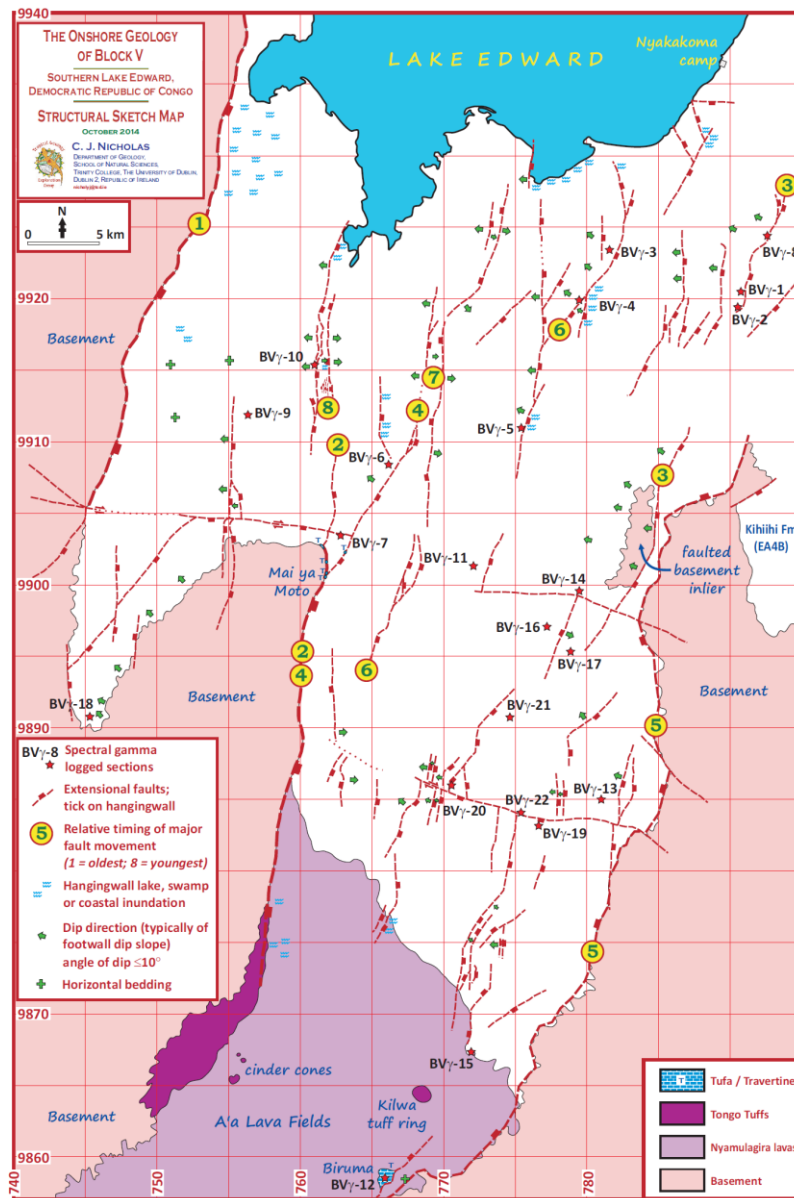


Figure IV.28: Structural map of onshore Block V showing all major rift faults.

The series of field sketches below in figure IV.29 a, b, c, d (SOCO, 2010) illustrates the cross section (not in scale) of the Block V structural configuration evidences from field observations.

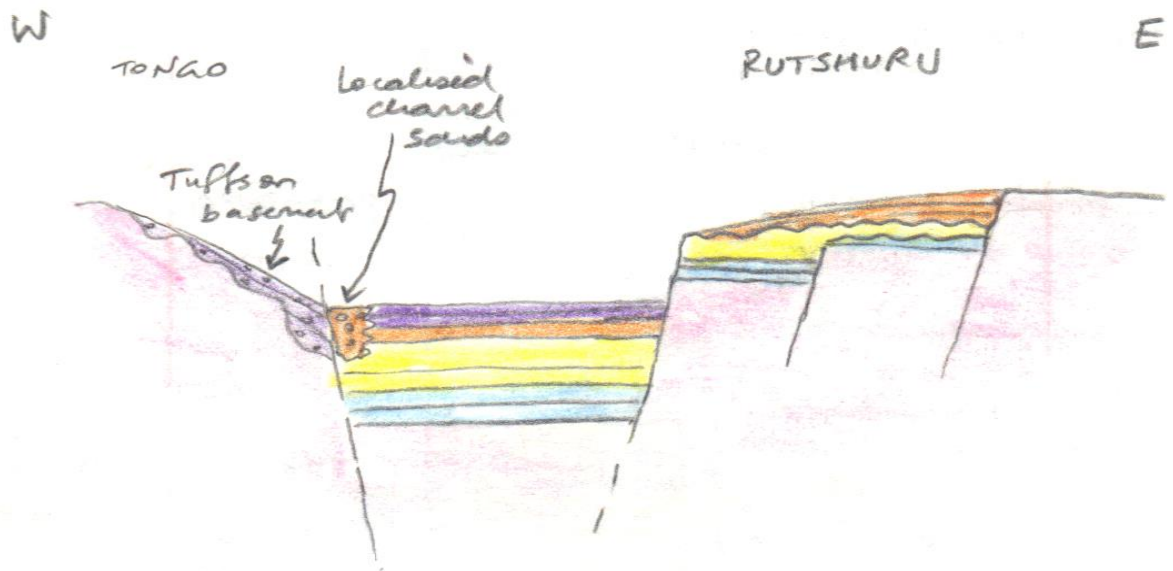


Figure IV.29 a: not to scale Bloc V sketch cross section (Nicholas, 2009)

The Block V 2010 field trip observations helped to understand the generalized explanation of the propagation Rift and development of sequences on the flanks. The figures 52 b, c and d below from field sketch suggest that the propagation of active faults seems to be confined to the central axis and as extension product, the older faults tend to move away from the axis and become less active or inactive.

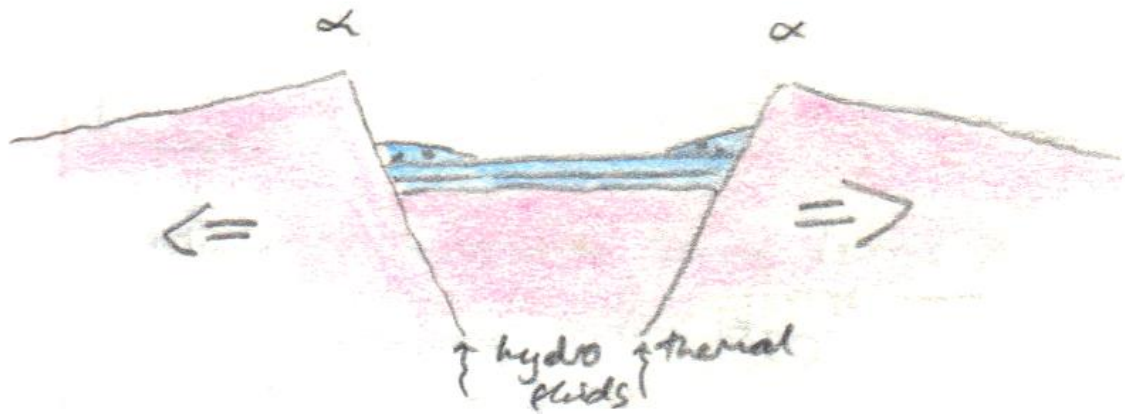


Figure IV.29 b: not to scale Bloc V sketch cross section (Nicholas, 2009)

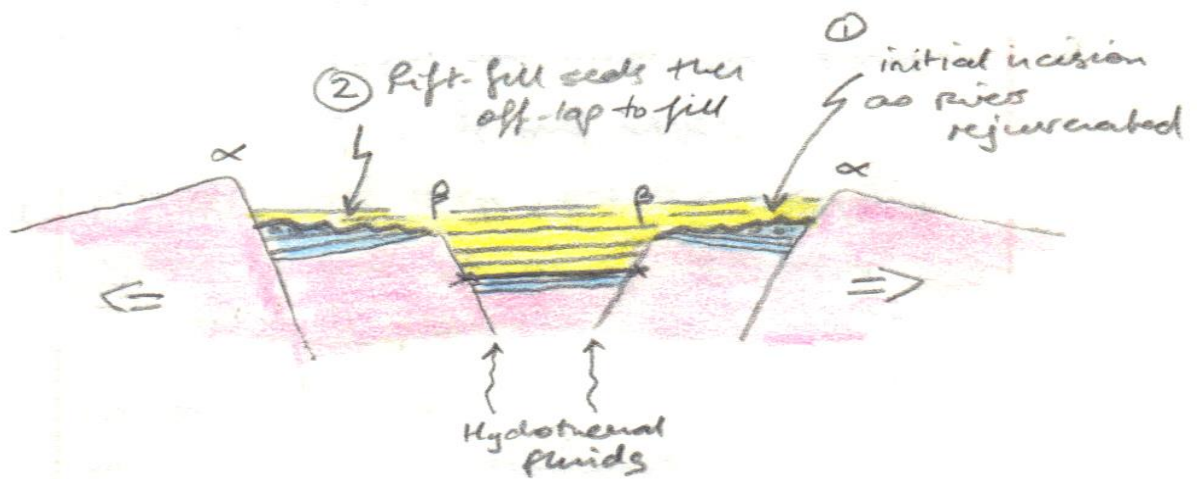


Figure IV.29 c: not to scale Bloc V sketch cross section (Nicholas, 2009)

The structural configuration evidences from field observations reveal that Carbonates Hot water or “hydrothermal fluids” pass through a nearby fractures rocks (active, less active or inactive faults) and possible porous spaces within the rock, altering its own originate chemical composition This chemical alteration can be the result of “adding, removing, or the redistribution of the chemical components as for instance the Calcite content”.

Many locations along margin faults field evidences show hot water bubbles up through the surface of the earth. The related field observations suggest and confirm that each of their resulting Hot springs is produced by the emergence of geothermal heated groundwater that rises carbonates minerals from the Earth's crust.

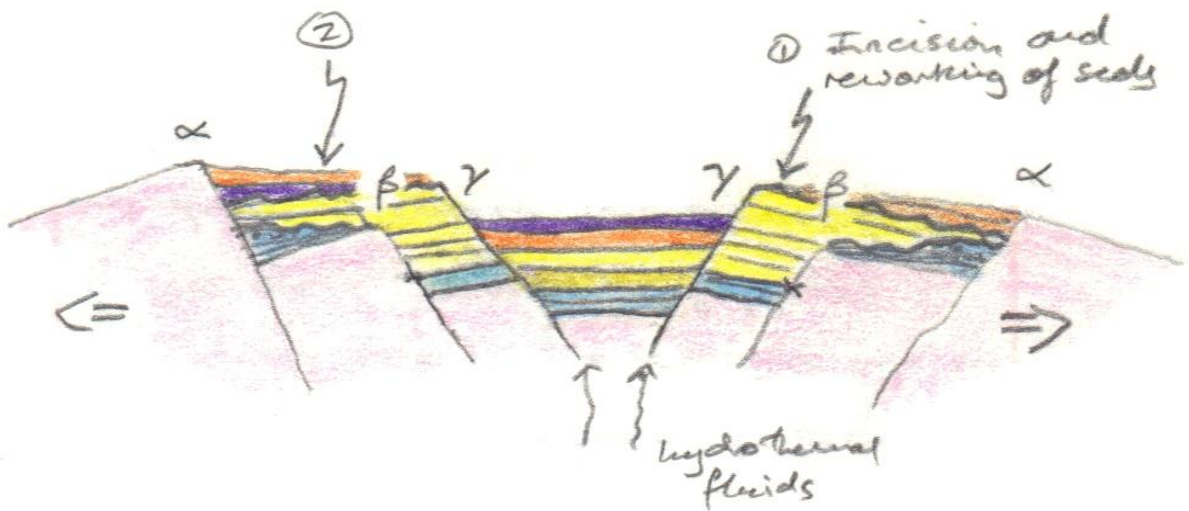


Figure IV.29 d: not to scale Bloc V sketch cross section (Nicholas, 2009)

#### IV.4.3.2- HEAT AND FLUID FLOW

Hot springs are known at Mai ya Moto, and in 2010 associated palaeo-spring Travertine limestones were documented at Mai ya Moto and further to the south at Biruma.

On this trip several more hot springs and limestones at a further 5 localities were documented, all within 2-5km of Mai ya Moto.

Mai ya Moto itself is a small rocky opening in the bush across which several streams of steaming, foul smelling water slide, spewed from small bubbling springs dotted around the perimeter. Heat loving slimes of yellow, green and black thrive in the flows close to the boiling springs and form long gloopy trails that wiggle in the fast moving water.

These cyanobacteria and/or algae growing at hot spring mouths appear to actively scavenge uranium and thorium, giving them very high TOTAL GR values, with U & Th concentrations falling away over a few metres distance from the spring mouth.

Large black patches of algae were spotted from the air on a rock face just north of Mai ya Moto. Investigation on foot discovered extensive Travertine limestones precipitated along either side of an incised gorge which appeared to follow the basement margin around the nose of the basement spur. Several hot spring sites were present in a series of terraced pools connected by streams.

The Figure IV. 30 and IV.31 below illustrate one of the Hot springs temperature recording in the west bank of the Rutshuru River and the graph of the all temperatures recorded around the zone of interest.



*Figure IV.30: Measuring the temperature of a hot spring on the east bank of the Rutshuru River.*



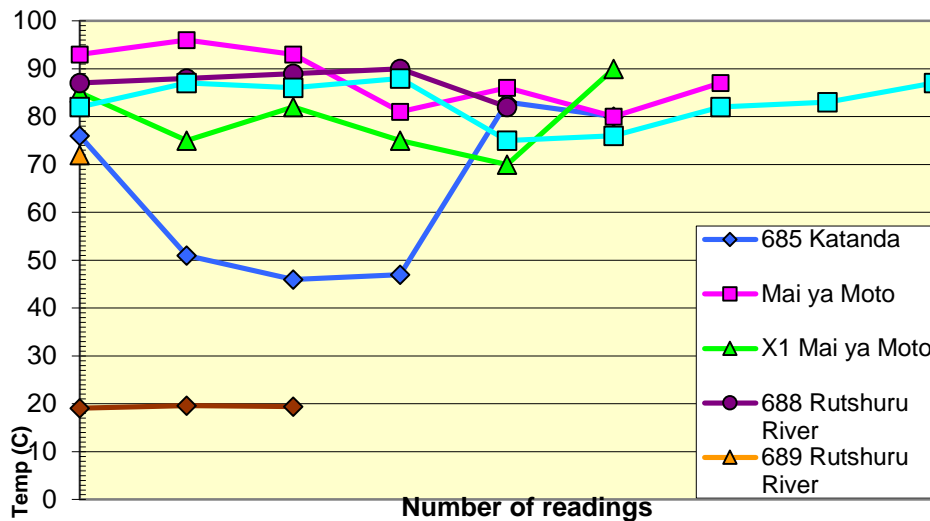


Figure IV.31: Graph showing spring temperatures at each locality. Temperatures were often above 80 degrees where it hasn't been lowered by passing through a pool of water at the surface. Spring water temperatures were recorded with a digital infrared thermometer.

#### Chapter 4 Conclusion

Further to the samples collection for laboratory analysis, the outputs of the 2007 to 2014 series of Travertines field investigation are:

- Perfect geologic correlations made between outcrops from both sides of the Albertine Rift basin: for instance, the Bwambara formation in EA4B block in Uganda shows many petrographic similarities with Rutshuru formation in Block V in DRC; the same is for the Kihihi and Kayonza formations in EA4B in Uganda which show many field evidences of common deposit timing with Fuko and Ruindi formations in Block V in DRC. The Kisenyi and Ngaji formations in EA4B suggest approximately some petrographic similarities and common geologic timing of deposit with Kasoso and Kigunda units in Bloc V. The half graben structures from where hydrothermal fluids flow up to the surface along bounding faults are still producing mainly the same Travertine facies on both sides of the DRC and Uganda borders.
- The most updated geologic map across all the Lake Edward onshore basin. The figure IV.32 below is showing the whole view of the completed geologic map of the Southern Lake Edward basin summarizing all the updated field informations collected from 2007 to 2014.

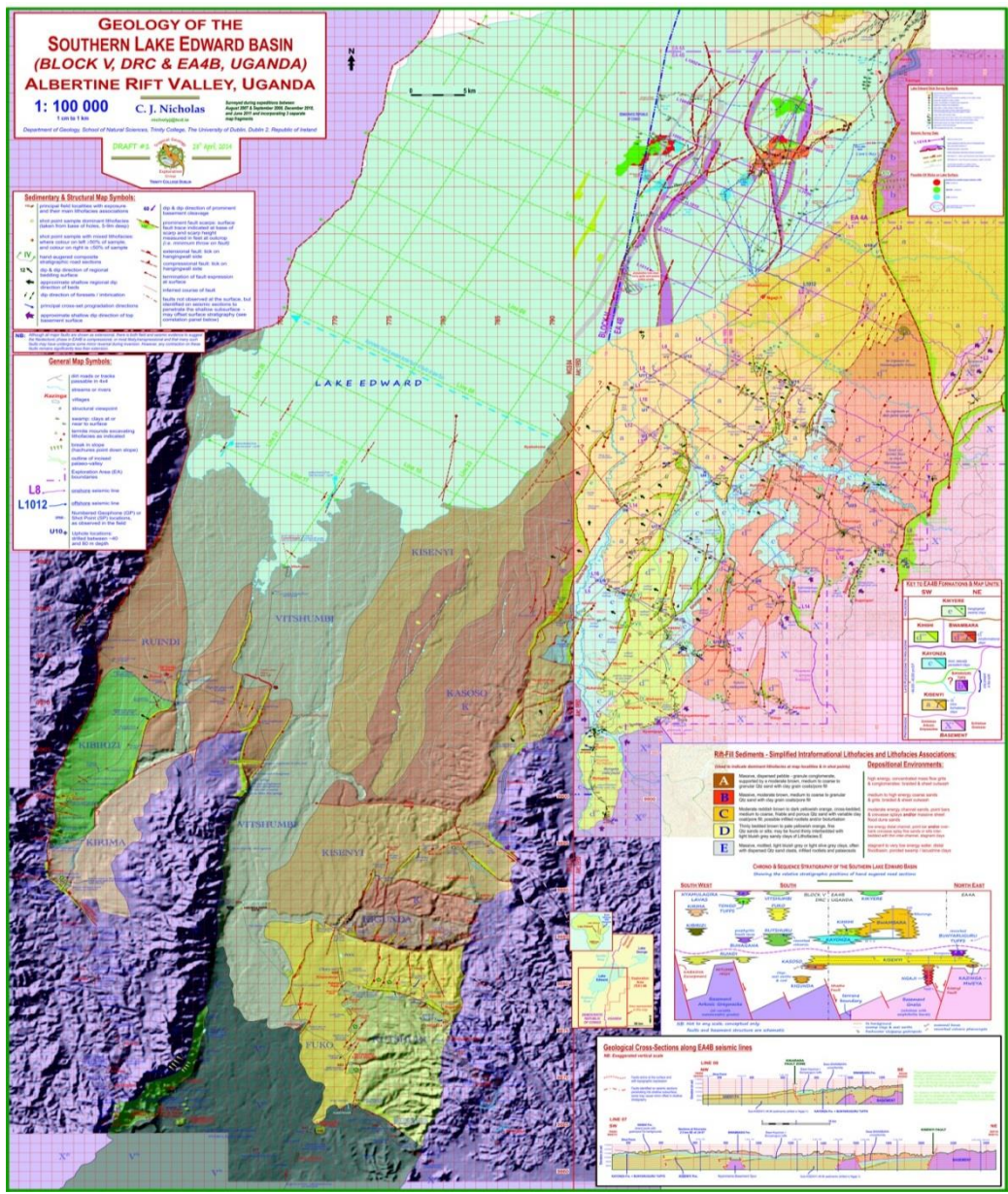


Figure IV.32: Completed Geologic Map of the Southern Lake Edward Basin

- The possible working chronostratigraphic framework across southern the Lake Edward basin. As shown in the Figure IV.33 here below, the chrono and sequence stratigraphy of the southern Edward lake basin attempt from field trips informations made the geologic correlation between Block V (DRC) and EA4B (Uganda).

### CHRONO- & SEQUENCE STRATIGRAPHY OF THE SOUTHERN LAKE EDWARD BASIN

Showing the relative stratigraphic positions of hand augered road sections

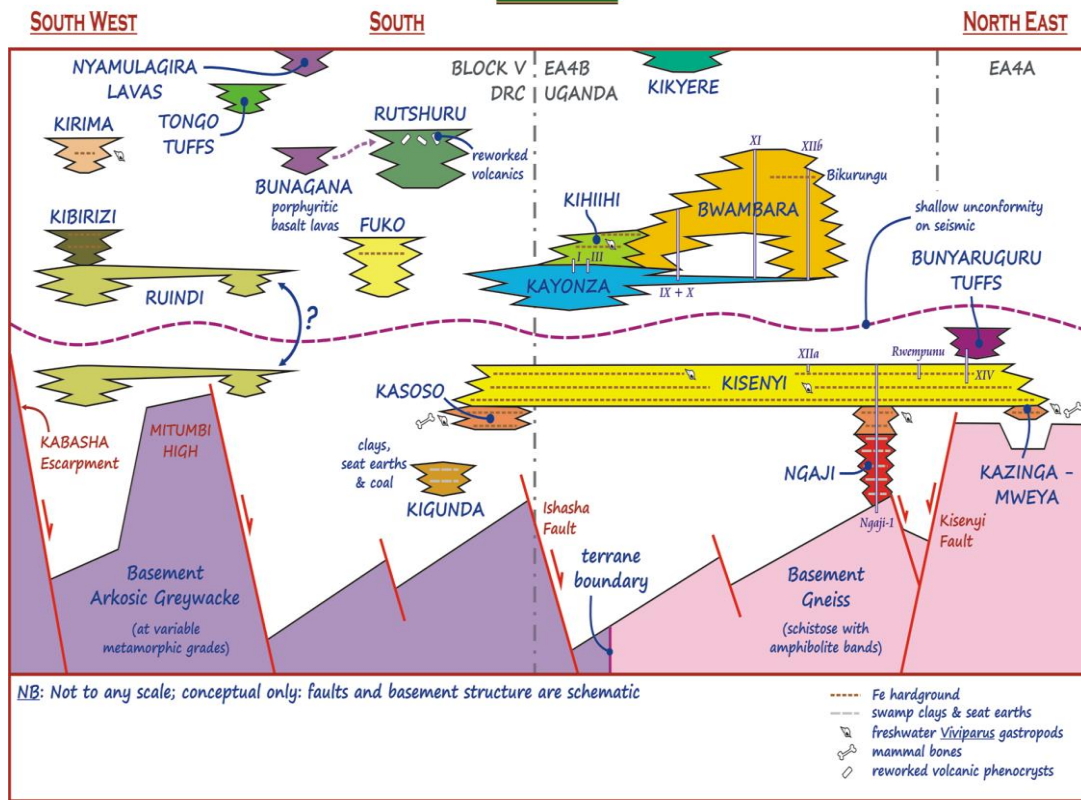


Figure IV.33: Completed chrono and sequence stratigraphy of the Southern Lake Edward Basin

The next Chapter, entitled *Travertines Petrography*, is essentially based on the collected Travertines field samples thin sections microscopic observation.

It gives the reader a good idea about the respective textures, structures and/or fabrics from each Travertines field samples ideally selected for REE detection by ICP-MS.

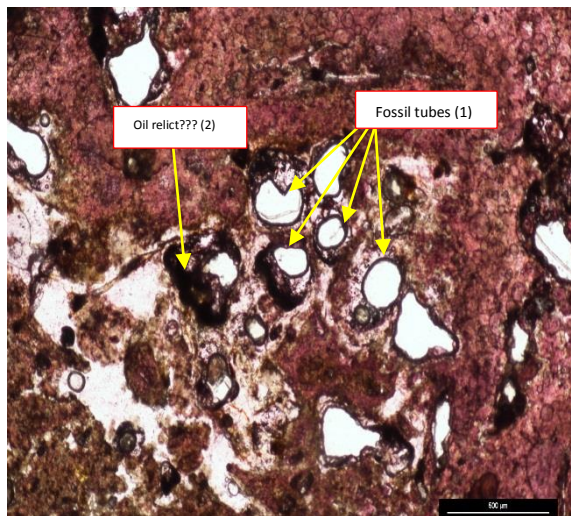
All the figures exposed in the Chapter below show the location drilling of each Travertine sample in classical thin section size and scale as observable in any microscope.

## CHAPTER FIVE: EARS TRAVERTINE PETROGRAPHY

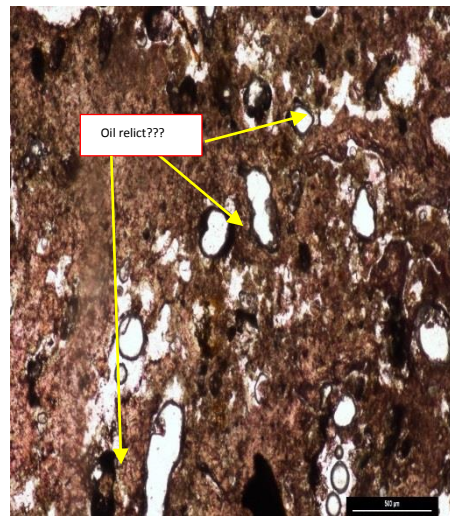
This Chapter presents the photographs of Travertine thin sections taken with the Nikon LV100 optical microscope in the Centre of Microscopy analysis (CMA). The Travertine slabs have been polished in thin sections through the fabrics, textures and structures drilled for ICP-MS. The respective microscopy descriptions and interpretations of each carbonate fabric, texture or structure are further discussed below in the discussion chapter.

### V.1- TRAVERTINE SAMPLES FROM 2007 TO 2010 FIELD TRIPS

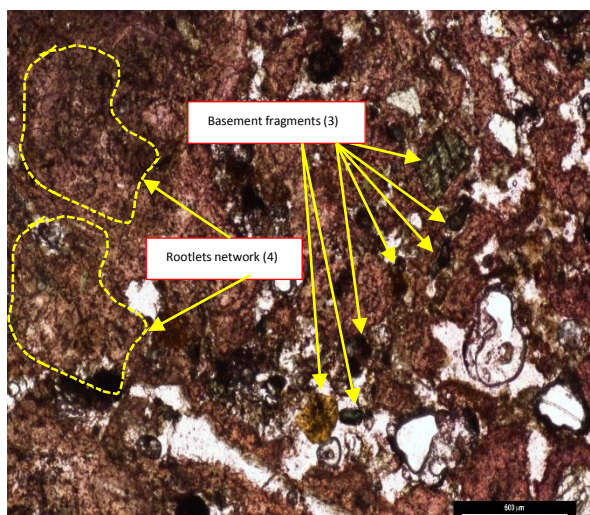
*(Figure V.1: 2007-2010 Travertine thin sections observations)*



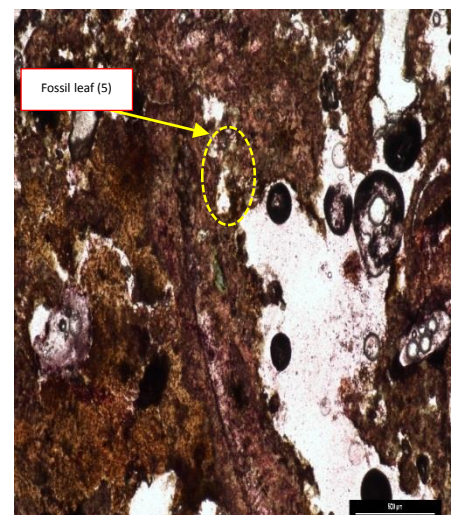
**P12 a**



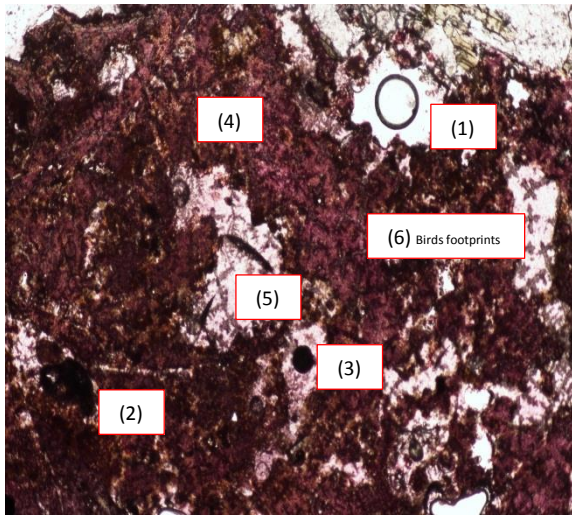
**P12 b**



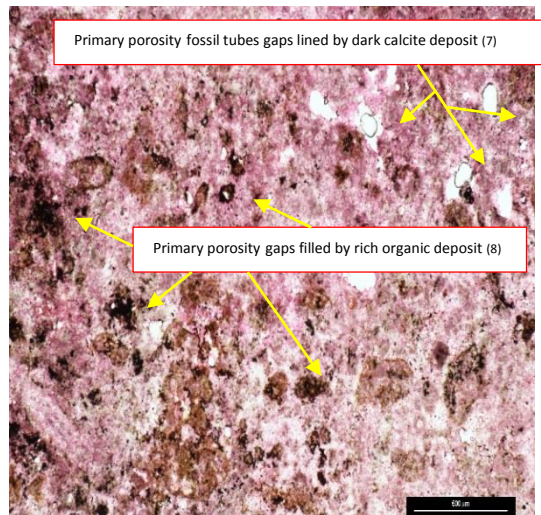
**P12 c**



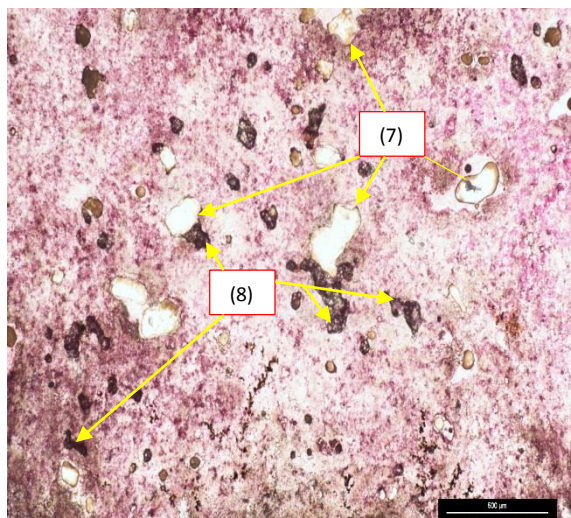
**P12 d**



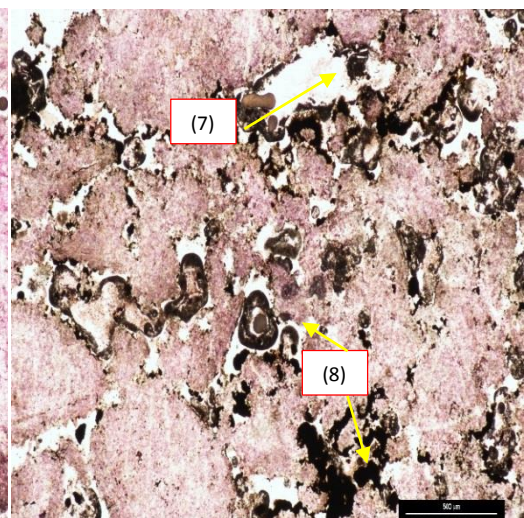
P12 e



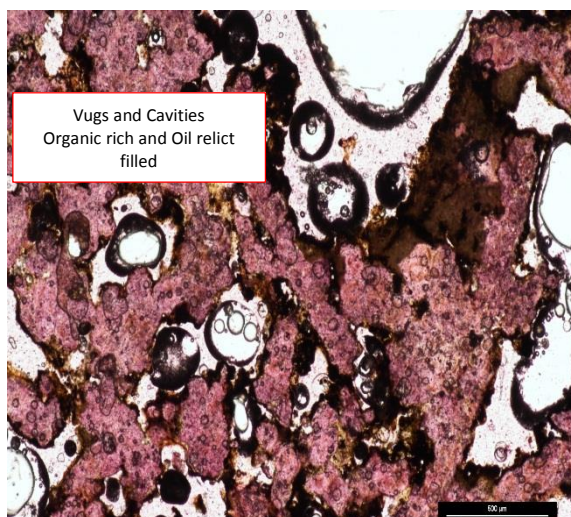
LE 24



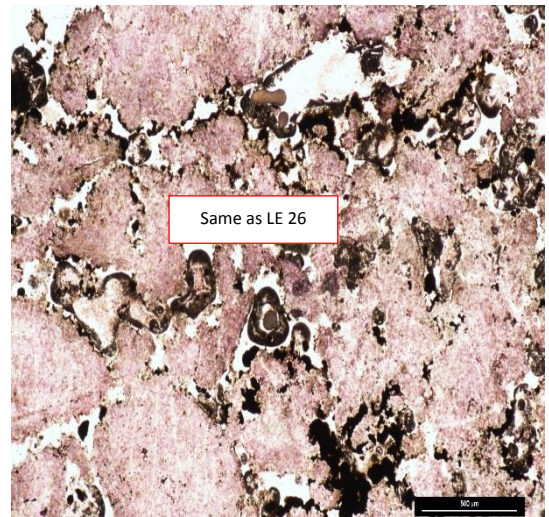
LE 24 a



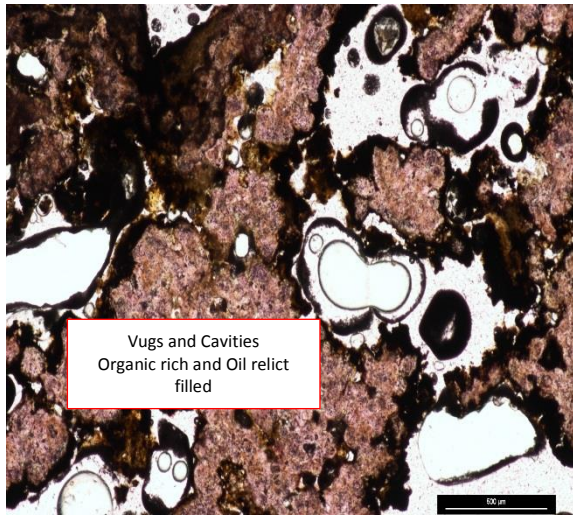
LE 26



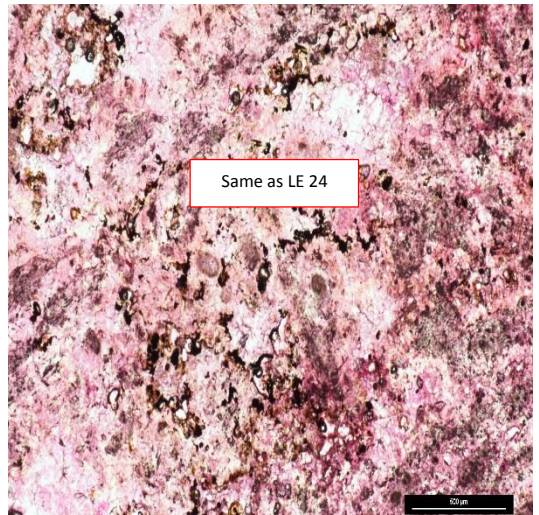
LE 27 a



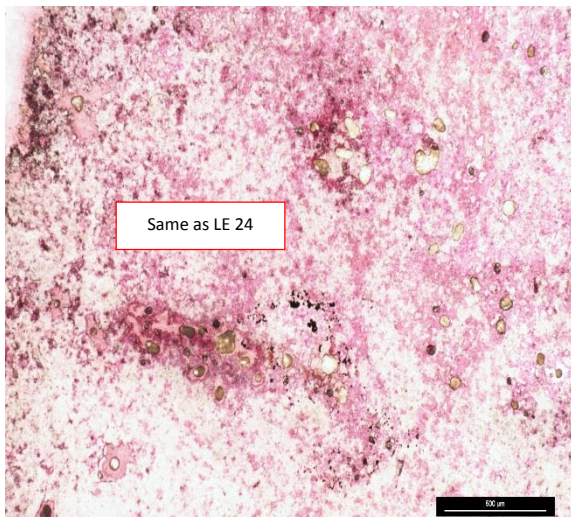
LE 27 b



LE 27 c



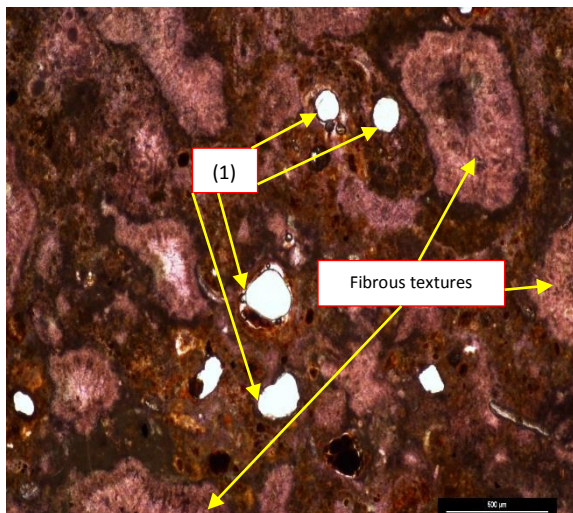
LE 28 a



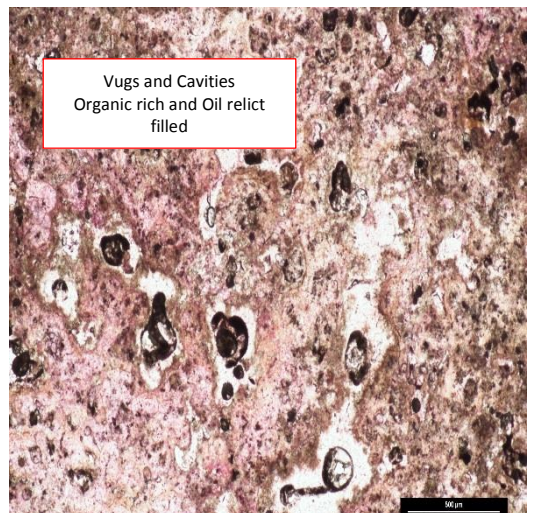
LE 28 b



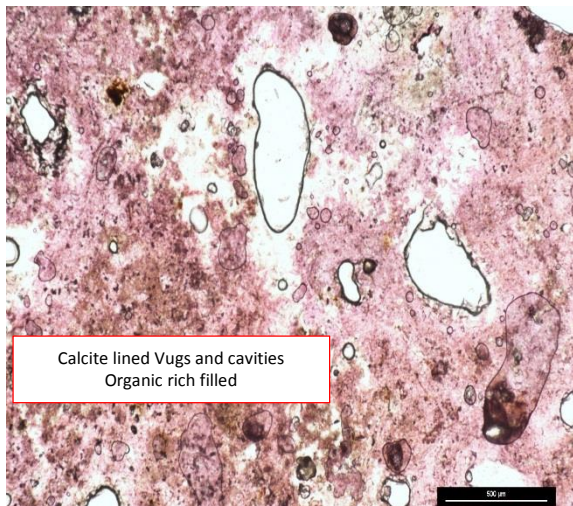
LE 37



LE 38



LE 41



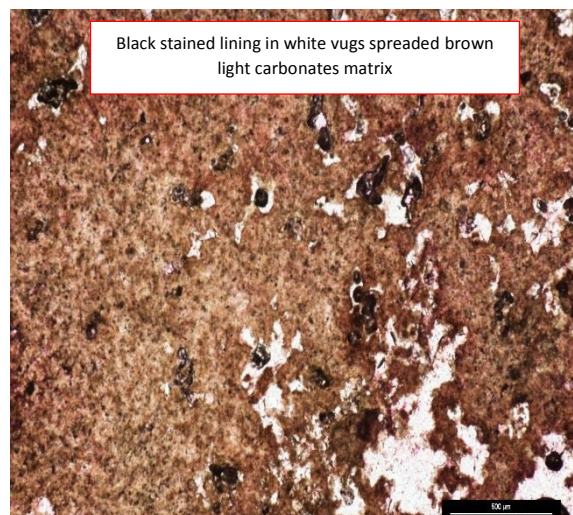
LE 42



LE 44



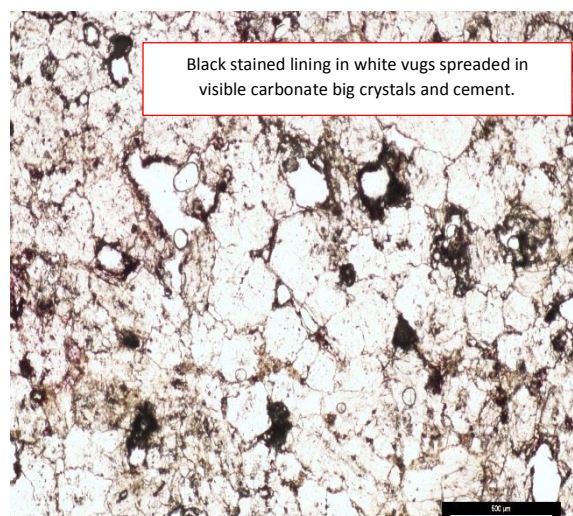
V2



V19



V20



V22

V.2- PCK LIMESTONES SAMPLES

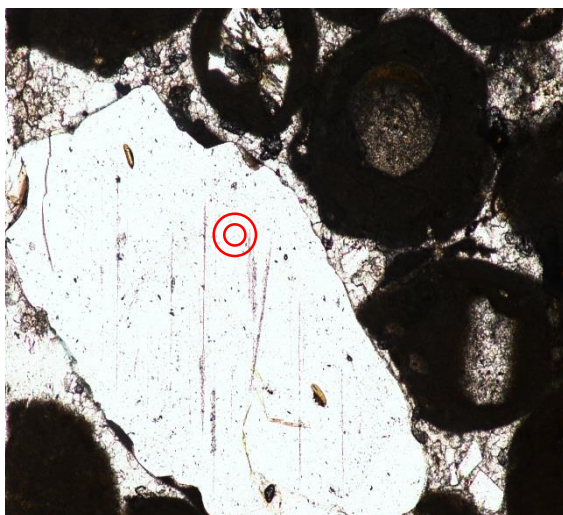


*Figure V.2: PCK carbonate layered Slice.*

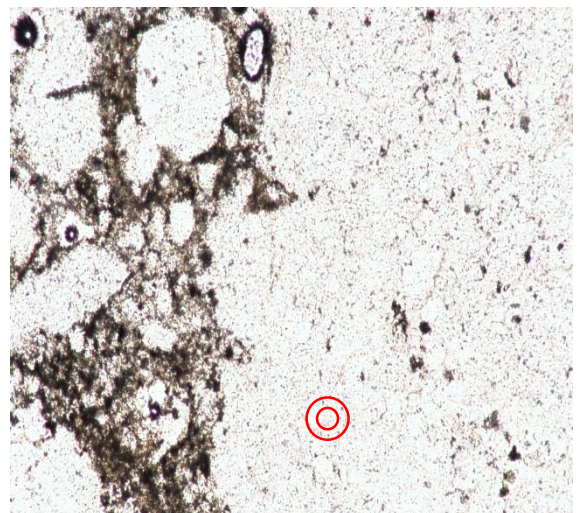
V.3- TRAVERTINE SAMPLES FROM 2014 FIELD TRIP

*Same graphic scale as above thin sections*

⊙ *Drilling location anyway into Calcite mineral and cement*

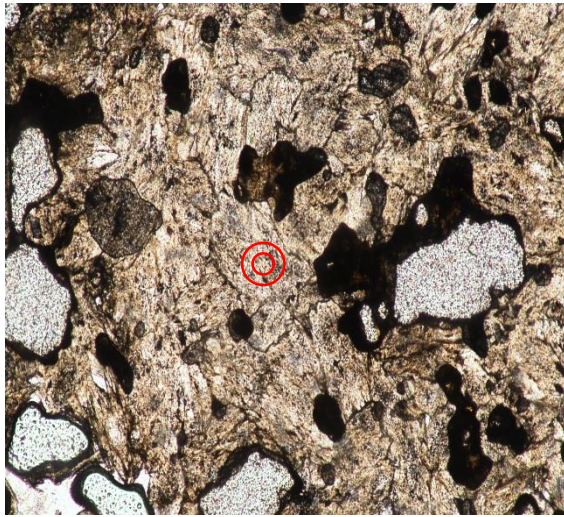


BV 125

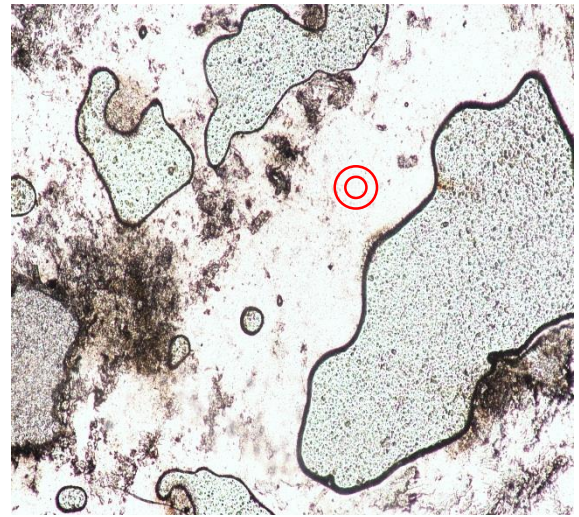


BV 149a





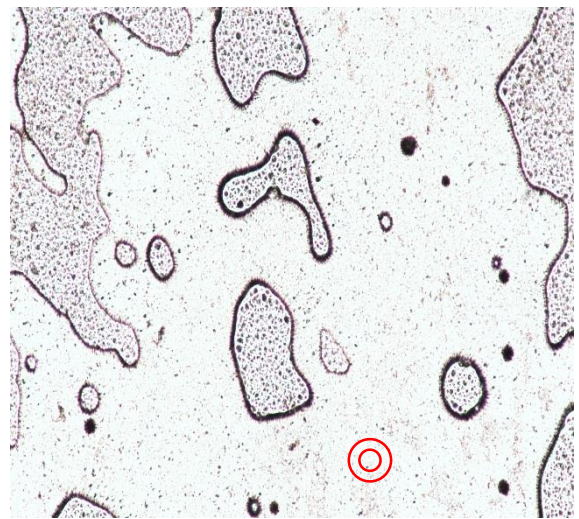
BV 150



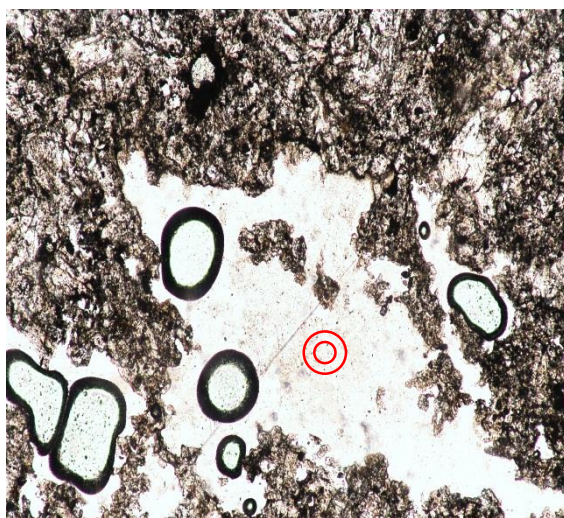
BV 153



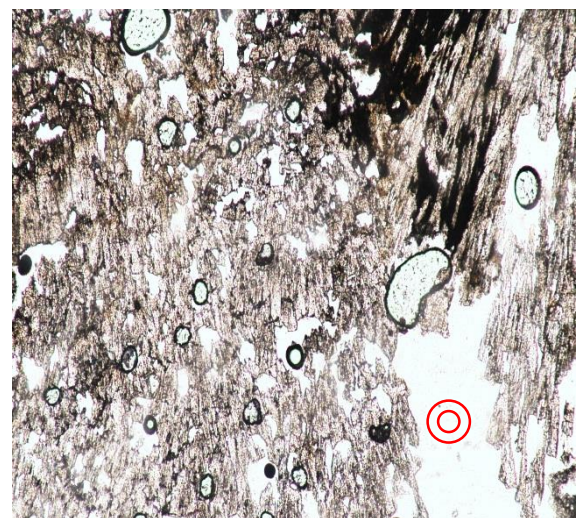
BV 159



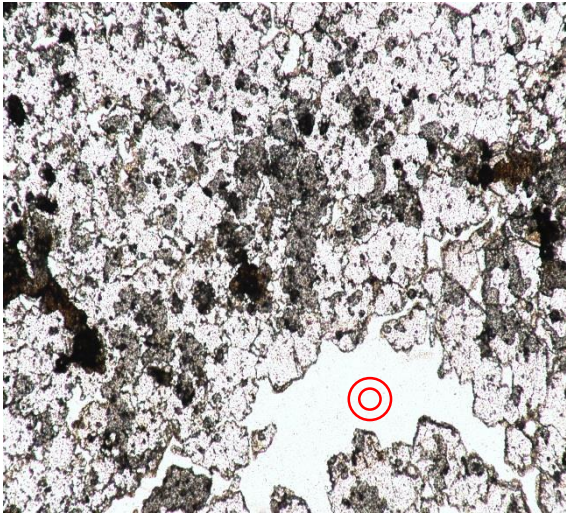
BV 161b



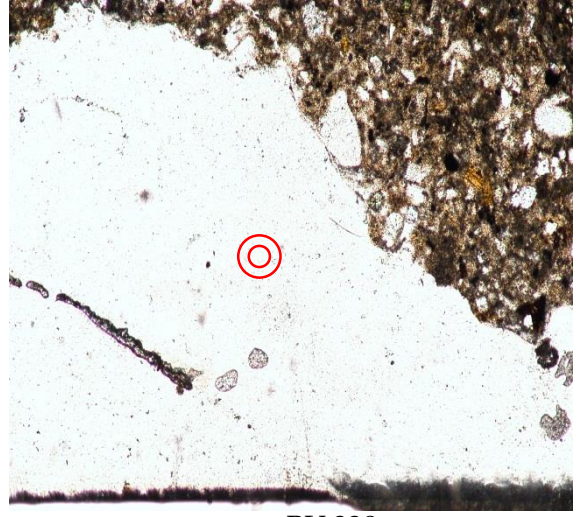
BV 162a



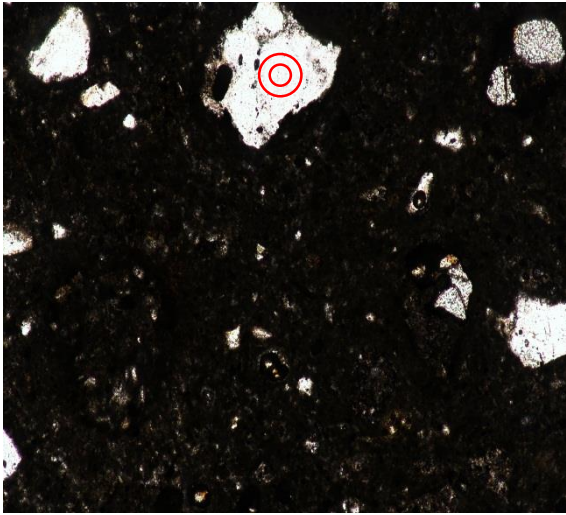
BV 163b



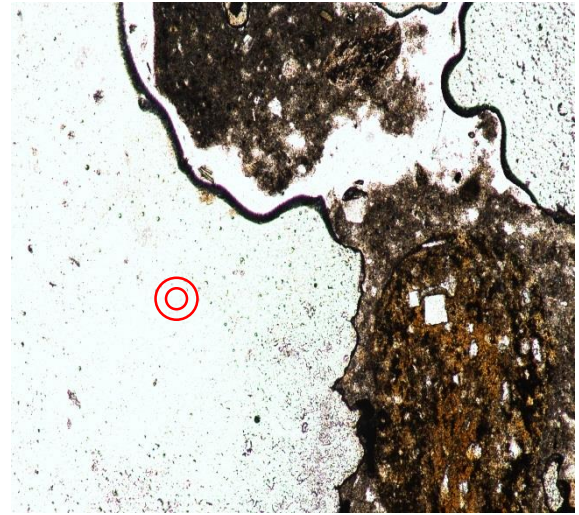
BV 164



BV 338



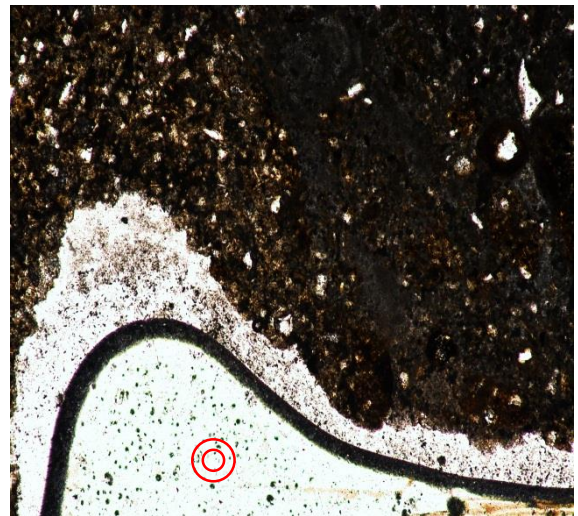
BV 352



BV 356



BV 363



BV 385

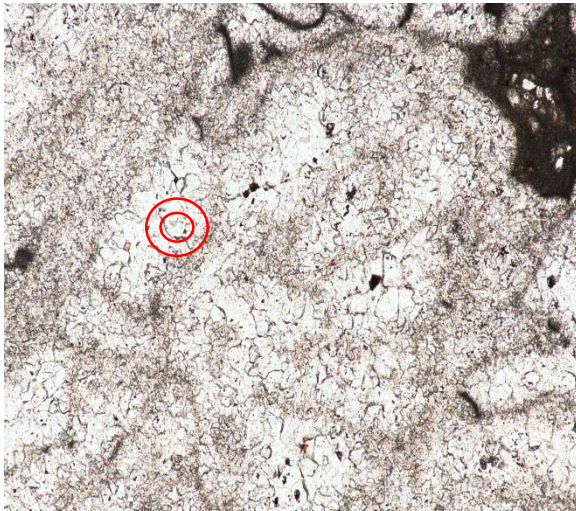
V.4- MANDAWA BASIN LIMESTONES SAMPLES



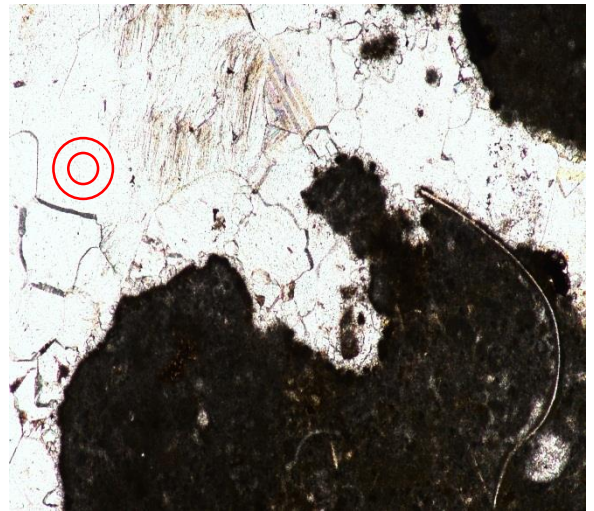
MDW 42



MDW 43



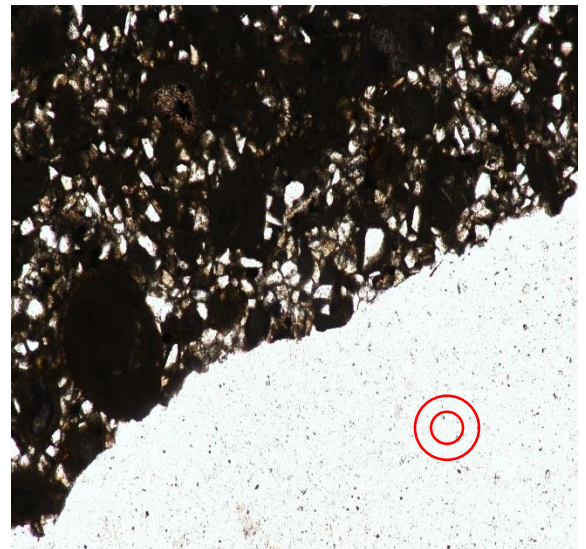
MDW 74



MDW 162



MDW 276



MDW 277

## Chapter 5 Conclusion

*In order to reach out the answer of this present Msc research question about the geochemistry origin of the Bicarbonate found in the EARS Travertines samples, their petrography investigation contributed as below:*

- *The Carbonates textures, structures and/or fabrics observed in the microscope are matching with the Travertines field description and their geological environment location in the Eastern Africa Rift System.*
- *For ICP-MS analysis purposes, the ideal Travertines textures, structures and or fabrics have been identified and their drilling zone opted.*
- *Microscopic structures, textures and/or fabrics are showing the depositional story of successive carbonates layers which should be individually drilled for geochemistry analysis purposes.*

*The next Chapter, titled Geochemistry Results, exposes all the chemical outputs obtained from all samples analysed throughout the present Msc research work. The final results from analysed samples were presented according to their respective location and the timing of the geochemical analysis undertaken.*

## CHAPTER SIX: GEOCHEMISTRY RESULTS

### VI.1- ISOTOPE RATIO MASS SPECTROMETRY (IRMS)

The Travertine samples run for IRMS analysis in 2013 were collected along the Edward Lake basin margin fault in Uganda (Lyemubuzza, Muhokya, Dura, Hima, Bwera, Bat Cave, Okumu and Sempaya) and DRC (Biruma). The Mayi ya Moto Travertine were collected along the Western margin fault in DRC side. Figure VI.1 below:

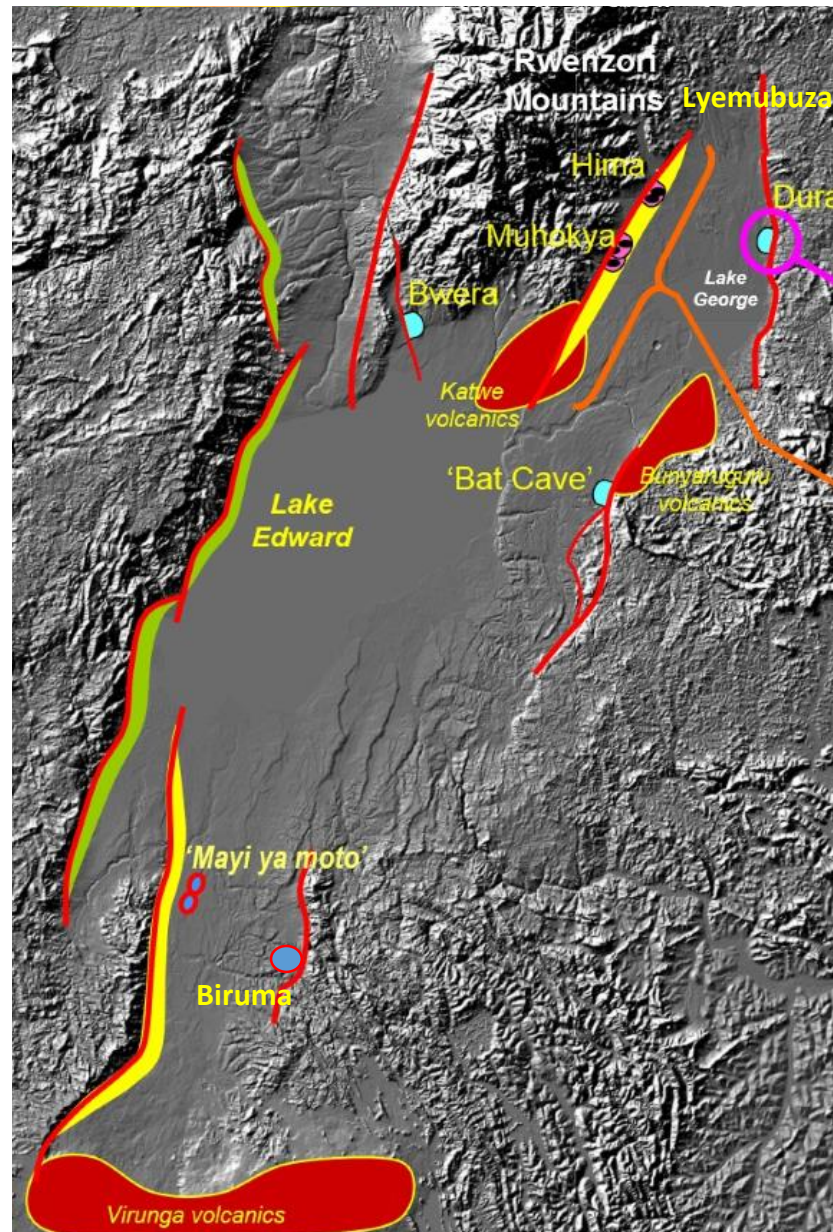


Figure VI.1: Travertine samples locations in the Lake Edward basin.(Nicholas et al., 2016)

### VI.1.1- CARBON (PDB) VERSUS OXYGEN (SMOW) STABLE ISOTOPES

According to (Lynch-Stieglitz et al., 1995) :

- Magmatic carbon in a carbonate would be expected to have a  $\delta^{13}\text{C}$  between  $-7$  and  $-10$  ‰ relative to PDB belemnite.
- Marine carbon in a carbonate would be expected to have a  $\delta^{13}\text{C}$  between  $-2$  and  $+2$  ‰ relative to PDB belemnite.

A higher abundance of  $\delta^{18}\text{O}$  in calcite is indicative of colder water temperatures, since the lighter isotopes are all stored in the glacial ice and the lower abundance of  $^{18}\text{O}$  in the calcite (Travertine samples) indicates the warmer temperatures. (Hays and Grossman, 1991)

The graph illustrated in the Figure VI.2 below, presents the C and O stable isotopes ratio of the Edward basin Travertine samples analysed by IRMS in 2013:

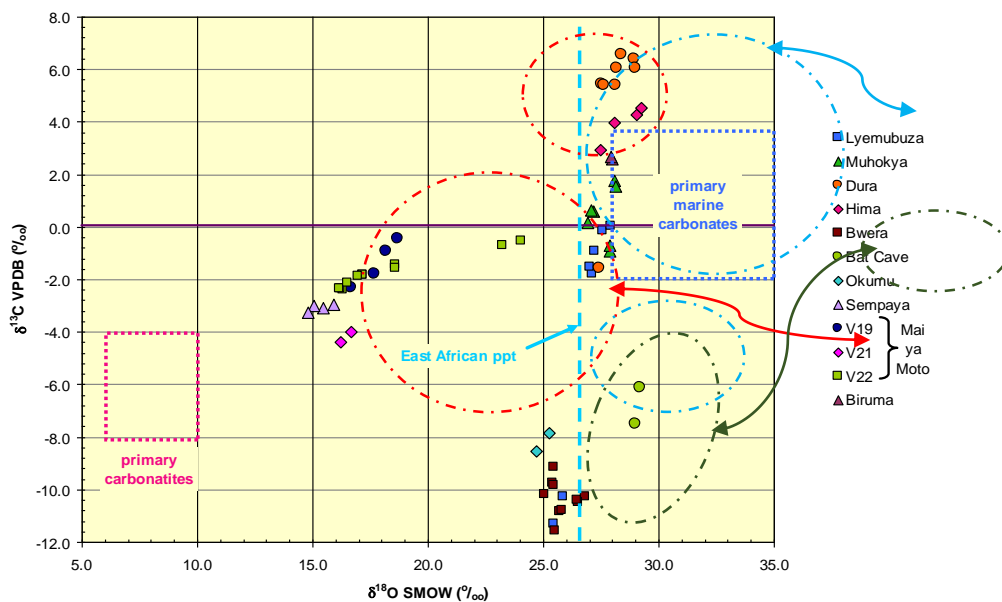


Figure VI.2: Edward Lake basin carbon (PDB) versus oxygen (SMOW) stable isotopes

### VI.1.2- CARBON (PDB) VERSUS OXYGEN (PDB) STABLE ISOTOPES

According to (Lynch-Stieglitz et al., 1995) :

- Magmatic carbon in a carbonate would be expected to have a  $\delta^{13}\text{C}$  between  $-7$  and  $-10$  ‰ relative to PDB belemnite.
- Marine carbon in a carbonate would be expected to have a  $\delta^{13}\text{C}$  between  $-2$  and  $+2$  ‰ relative to PDB belemnite.

A higher values of both  $\delta^{13}\text{C}$  (PDB) and  $\delta^{18}\text{O}$  (PDB) in calcite is indicative of  $\text{CO}_2$  outgassing evaporation, since the  $^{16}\text{O}$  and  $^{13}\text{C}$  isotopes are all removed and the lower values of both  $\delta^{13}\text{C}$  and  $\delta^{18}\text{O}$  in calcite (Travertine samples) indicates a zone of  $\text{CO}_2$  contribution.

The graph illustrated in the Figure VI.3 below, presents the C and O stable isotopes ratio of the Edward basin Travertine samples analysed by IRMS in 2013

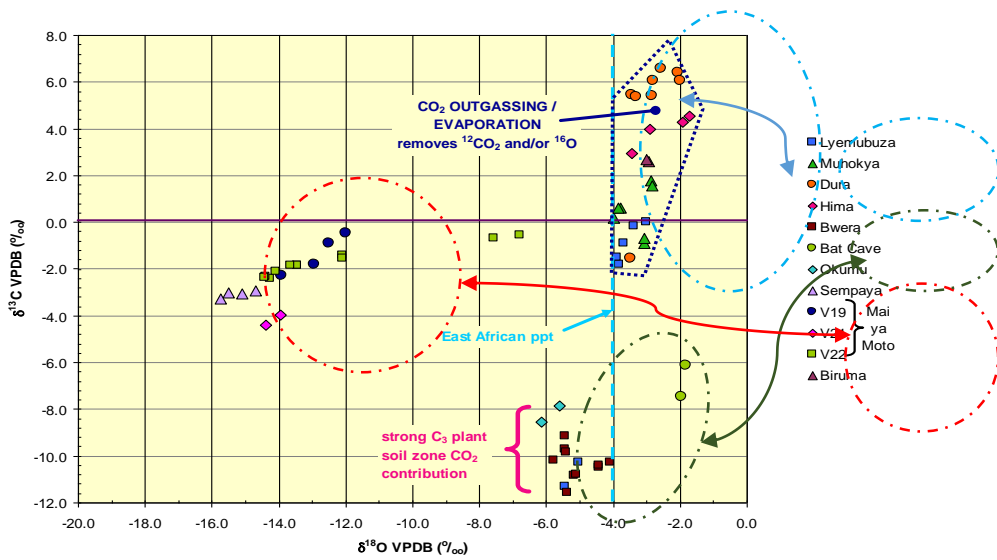


Figure VI.3: Edward Lake basin carbon (PDB) versus oxygen (PDB) stable isotopes

### VI.1.3- CARBON (PDB) VERSUS TRAVERTINE PRECIPITATION TEMPERATURE

According to (Lynch-Stieglitz et al., 1995) :

- Magmatic carbon in a carbonate would be expected to have a  $\delta^{13}\text{C}$  between  $-7$  and  $-10$  ‰ relative to PDB belemnite.
- Marine carbon in a carbonate would be expected to have a  $\delta^{13}\text{C}$  between  $-2$  and  $+2$  ‰ relative to PDB belemnite.

The graph illustrated in the Figure VI.4 below, presents the C (PDB) stable isotopes ratio of the Edward basin Tufa/ Travertine samples analysed by IRMS in 2013.

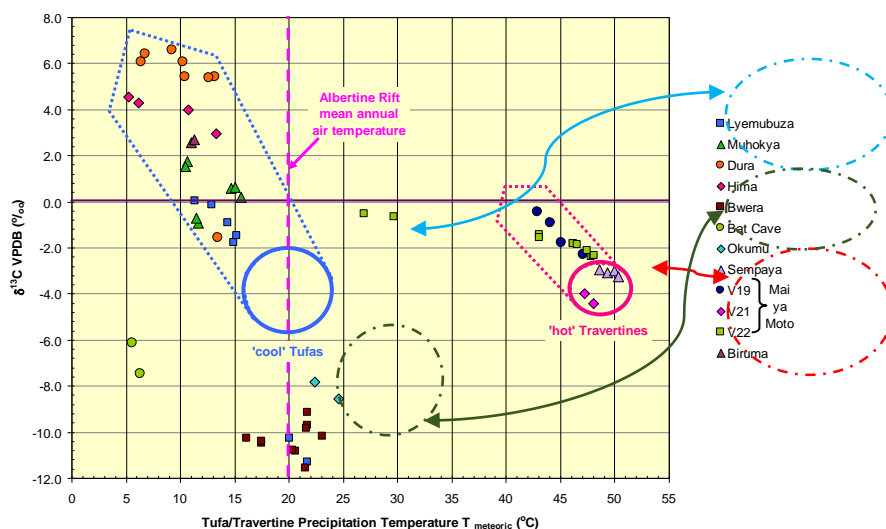


Figure VI.4 Edward Lake basin carbon (PDB) stable isotopes versus site temperature

## VI.2- STRONTIUM ISOTOPE RATIO ANALYSIS

Based on the following assumptions that three major input sources influence the Strontium isotope composition of the sea and ground water (Wierzbowski, 2013) :

- Strontium of low  $^{87}\text{Sr}/^{86}\text{Sr}$  ratio around 0.703 is derived from hydrothermal circulation at mid-ocean ridges and volcanic zones;
- Strontium of intermediate  $^{87}\text{Sr}/^{86}\text{Sr}$  ratio between 0.707 and 0.709 originates from submarine dissolution and recrystallization of carbonates sediments.
- Strontium of high  $^{87}\text{Sr}/^{86}\text{Sr}$  ratio around 0.711 is derived from continental weathering;

The analysis results of Travertine samples shown in the table below suggest a very high range of strontium isotope ratios from 0.7068069 to 0.7482648.

However, Only 2 values (LE 41 from Bwera and LE42 from Dura) are within the range expected for marine carbonates. These two values have been plotted in both the Burke and Wierzbowski Phanerozoic  $^{87}\text{Sr}/^{86}\text{Sr}$  ratio variation graphs below: (Figure VI.5 and VI.6)

Sample	LE24 A	LE26 A	LE27 A	LE28 A	LE41 A	LE42B	LE37 A	LE38 A	V20B
$^{87}\text{Sr}/^{86}\text{Sr}$	0.7482	0.7487	0.7380	0.7388	0.7071	0.7068	0.7152	0.7153	0.7457
Sr	64	56	57	00	20	06	75	47	00

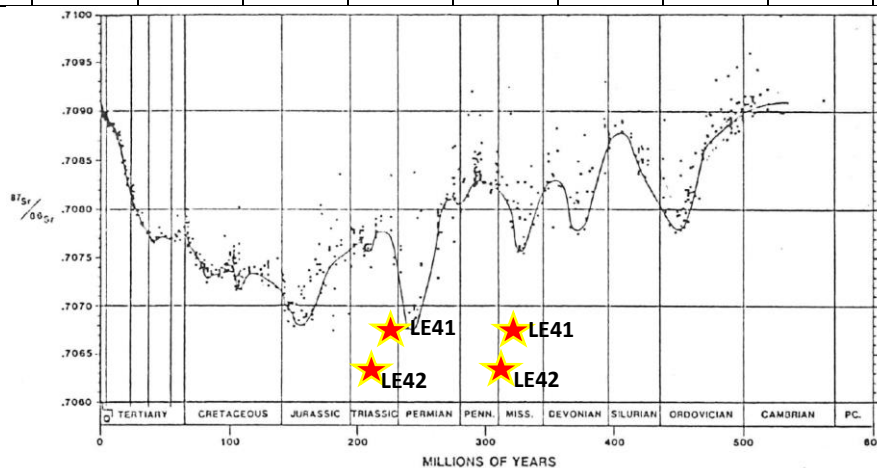


Figure VI.5  $^{87}\text{Sr}/^{86}\text{Sr}$  ratio variation of Phanerozoic seawater. (Burke et al., 1982)

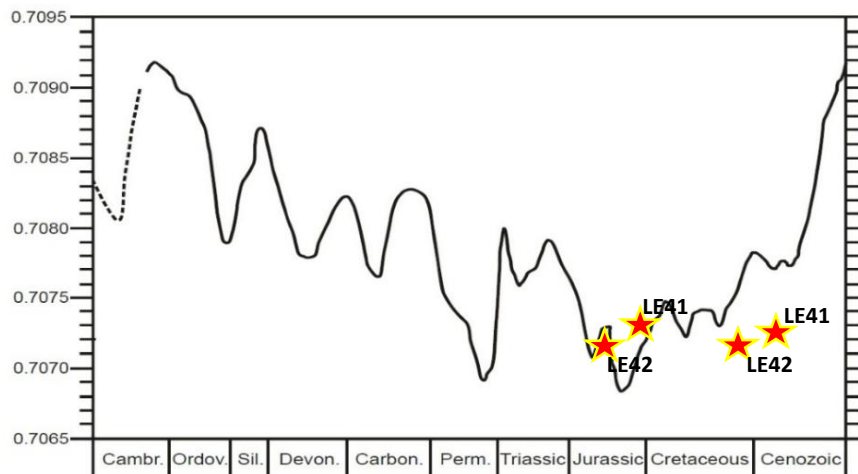


Figure VI.6:  $^{87}\text{Sr}/^{86}\text{Sr}$  ratio variation of Phanerozoic seawater. (Wierzbowski, 2013)



The plotting of these 2 samples in the below Phanerozoic graphs suggest their possibly Late Jurassic or Late Permian age or possibly late Neoproterozoic as their plotting in the Sr seawater isotope curve here below in Figure VI.7 for the Late Neoproterozoic and Cambrian (Nicholas, 2009):

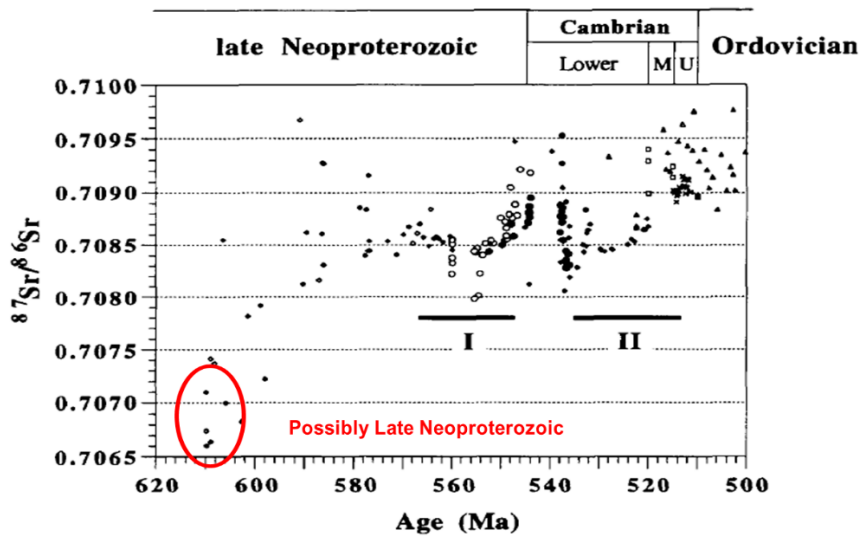


Figure VI.7:  $^{87}\text{Sr}/^{86}\text{Sr}$  ratio curve for the Proterozoic. (Nicholas, 2009)

### VI.3- GC-GCMS ANALYSIS

The crude oil identification of the black staining in Lyemubuza (Uganda) Travertine is accomplished on the bases of a quantitative comparison between their respective ion chromatograms and biomarkers distribution with the famous Oil slick samples LES 15 and LES 18 collected from the Lake Edward during the slick survey conducted from 28<sup>th</sup> August to 1<sup>st</sup> September 2008.(Nicholas, 2009)

The slicks presenting the form of long trails of white 'foam' (Figure VI.8 below) were investigated by GC-GCMS by the motivation of many various unconfirmed satellite and aerial reports of possible oil slicks out on the Lake Edward.



Figure VI.8 : Oil slicks collected in the Lake Edward.(Nicholas, 2009)

Sampling of these possible oil slicks was undertaken using special, sterile lyophilic cloths which absorb low concentrations of dispersed oil into the fabric.

As shown in the Figure VI.9 below, the sterile lyophilic cloths were attached to metal clips and secured on the end of a telescopic pole.



Figure VI.9 : Sterile lyophilic cloths for Oil slick collection.(Nicholas, 2009)

GC / GCMS analyses which were then performed on the Lake Edward Oil slick samples have confirmed the mature hydrocarbons signature illustrated in the (X, Y) graph below (Figure VI.10) where:

- X axis indicates the retention times of the respective n-alkanes in the mass spectrograms;
- Y axis indicates the ions abundance number and % in the sample.

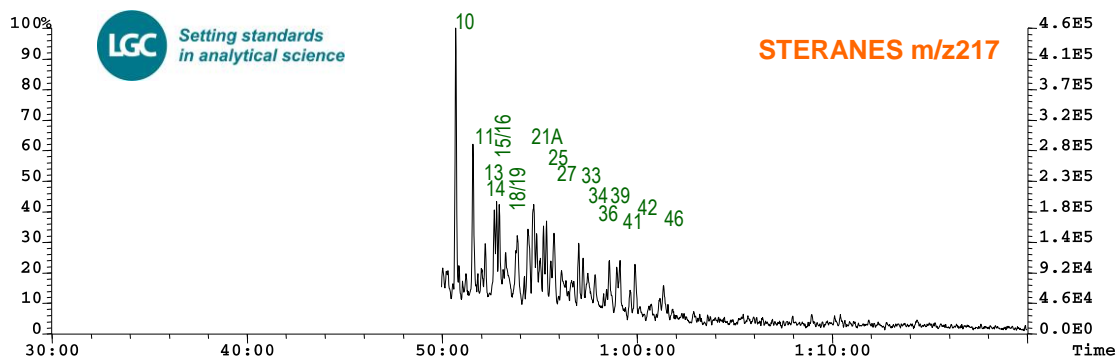


Figure VI.10 : GC–MS–extracted ion profiles of norhopanes, hopanes, methyl hopanes, steranes, and monoaromatic steranes in Lake Edward oil sample (LES 15).(Nicholas, 2009)

The figure here above indicates the peaks distribution of n-alkanes, isoprenoids, polycyclic aromatic hydrocarbons and their alkyl-homologues, and biomarker compounds (hopanes and steranes) which were used as bench marks for certain  $C_n$  interval fixation in the Oil slick collected in Lake Edward in 2008.

According to the results above illustrated, the Lake Edward slick is proven to be a live crude Oil and could be used for reference comparison with the Lyemubuza black staining in Travertine cavities.

### VI.3.1- GCMS RESULTS FOR (LES 18) SAMPLE

The GCMS results on the oil slick Sample LES 18 are presented in the graphs below:

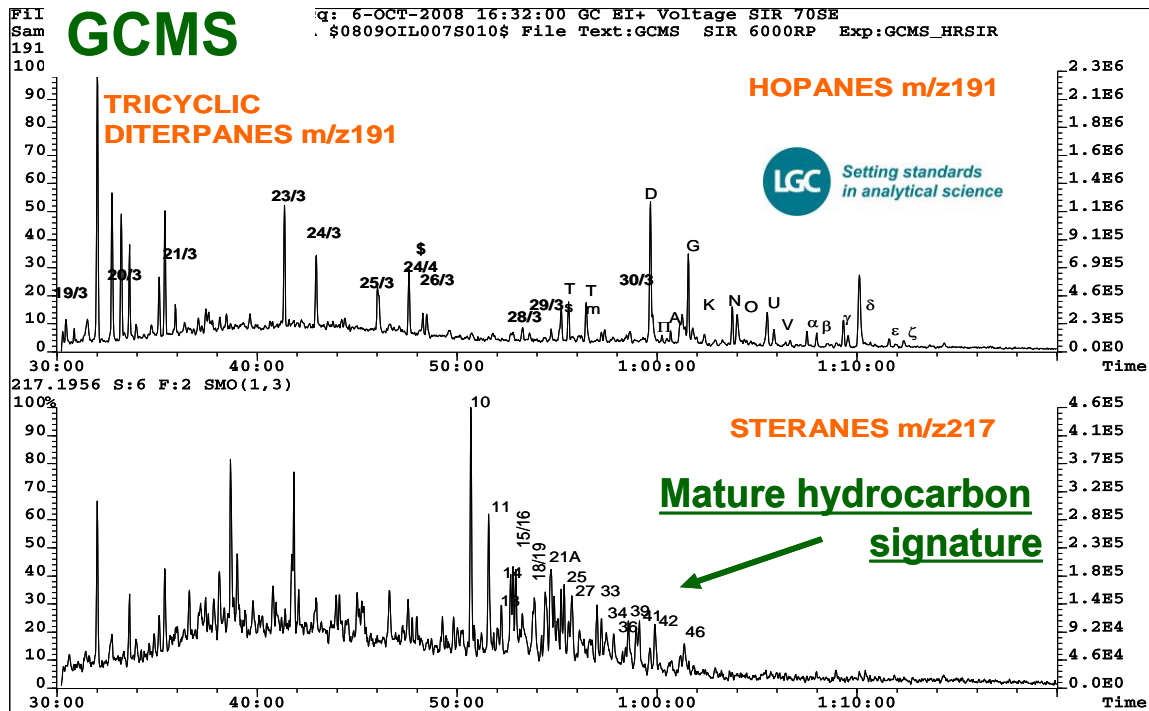


Figure VI.11: GC-MS-extracted biomarker distribution from sample LES 18. (Nicholas, 2009)

According to Chris Nicholas, The biomarker distribution from sample LES 18 indicates a marine shale source mixed with a waxier, lacustrine component.(Nicholas, 2009)

### VI.3.2 – GC-GCMS RESULTS FOR LYEMBUMUZA (LE25) SAMPLE

The GC results on the Sample LE 25 are presented in the graph below:

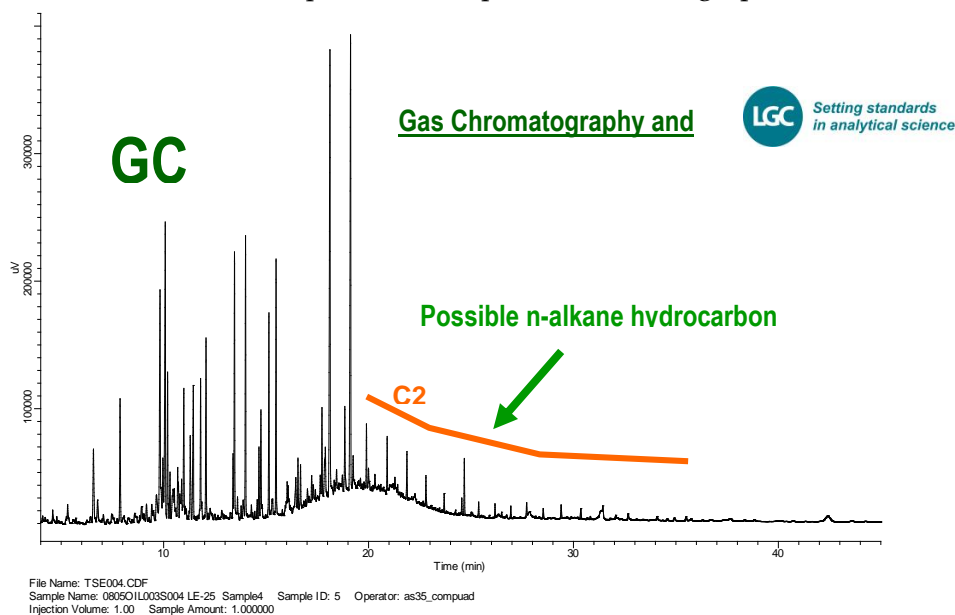


Figure VI.12 : GC results sample LE 25 from Lyemubuza quarry.(Nicholas, 2009)

### VI.3.3 – GC-GCMS RESULTS FOR LYEMBUMUZA (LE25) SAMPLE

The GCMS results on the Sample LE 25 are presented in the graph below:

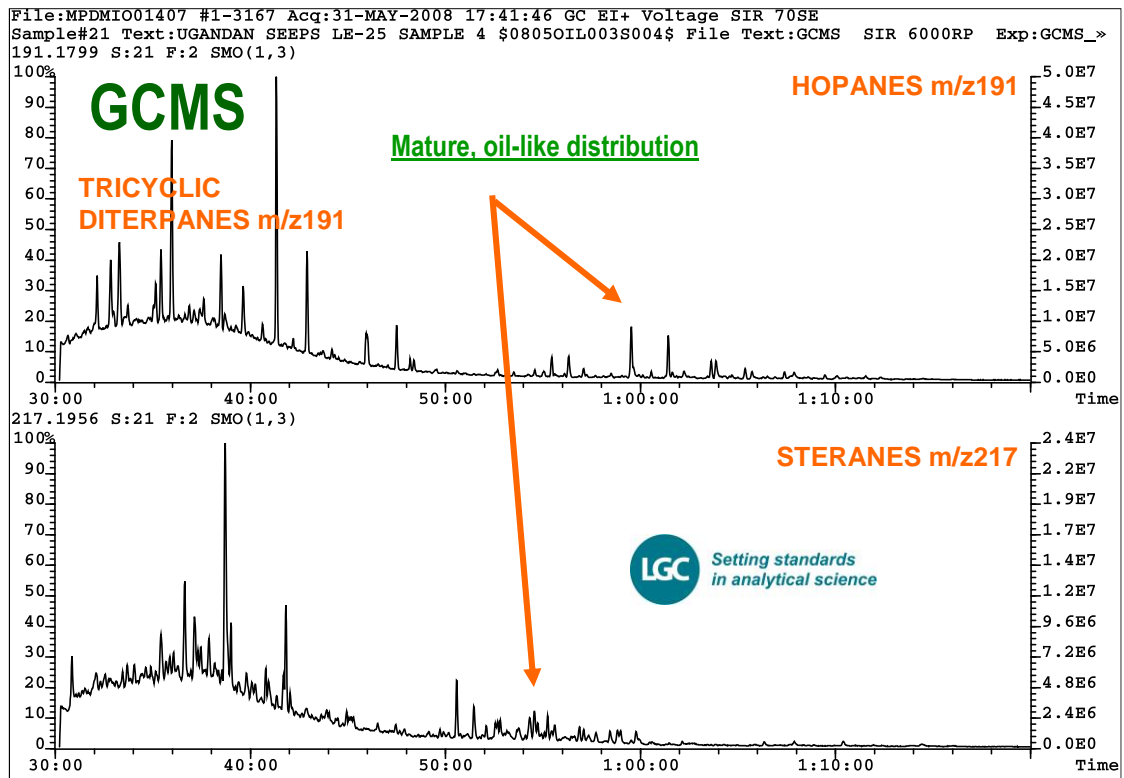


Figure VI.13 : GCMS results sample LE 25 from Lyemubuza quarry. (Nicholas, 2009)

### VI.3.4- CG RESULTS FOR MUHOKIYA SAMPLE (LE 27)

The GC results on the Sample LE 27 are presented in the graph below:

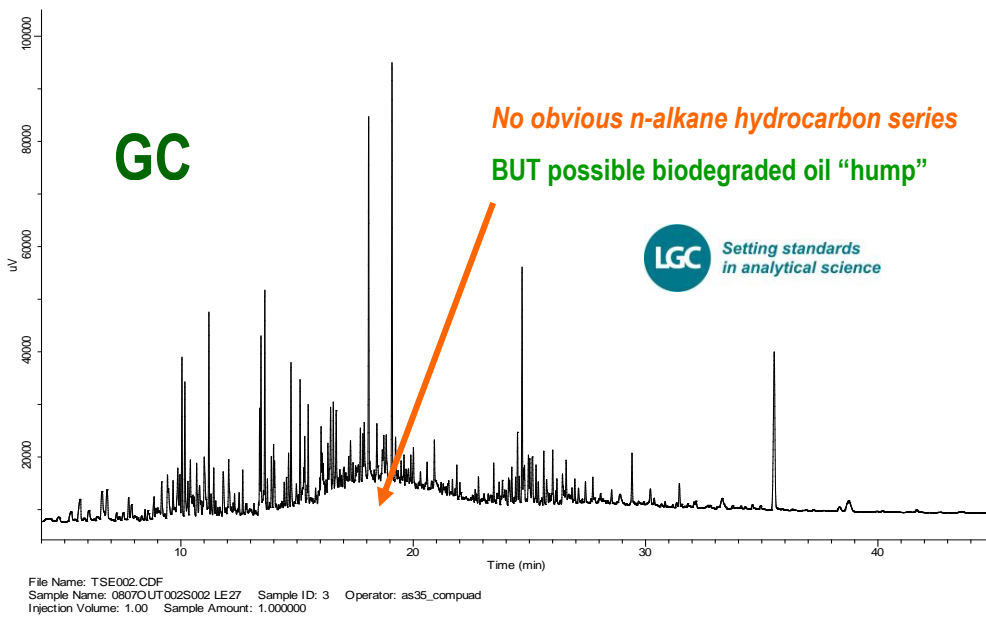


Figure VI.14 GC results sample LE 27 from Muhokiya quarry. (Nicholas, 2009))

VI.3.5- CGMS RESULTS FOR MUHOKIYA SAMPLE (LE 27)

The GCMS results on the Sample LE 27 are presented in the graph below:

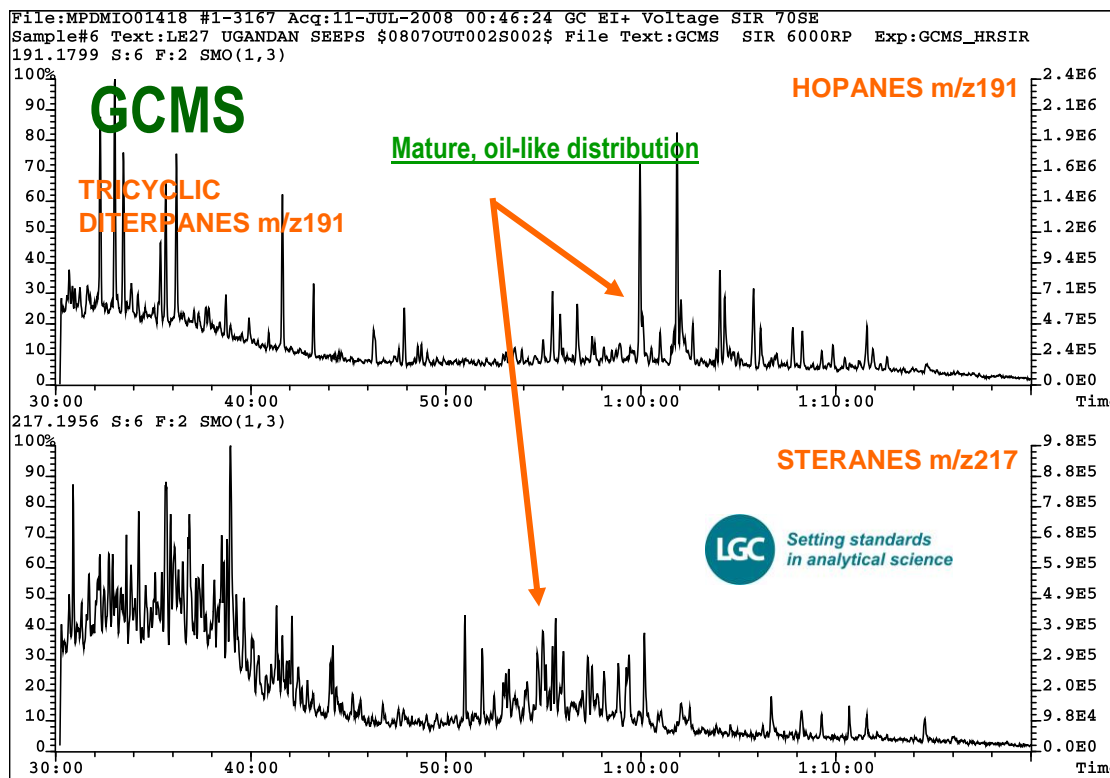


Figure VI.15 : GCMS results sample LE 27 from Muhokiya quarry.(Nicholas, 2009)

VI.3.6- SUMMARY OF THE GC-GMS RESULTS

The GC-GCMS results obtained in 2008 by LGC Standards from the EA4A onshore Oil stains found in oolites of Tufa/Travertine samples have been compared to those of the Edward Lake slicks. Their summary has been plotted in the triangular graph below in Figure VI.16 illustrating the AAA Steranes Distribution of Ugandan seeps and slicks.

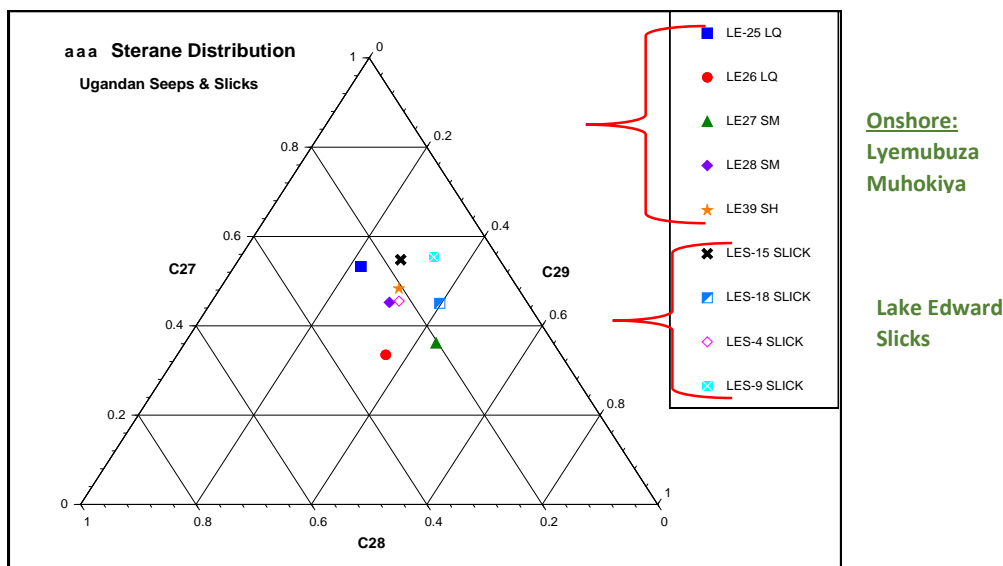


Figure VI.16 : Plots of C27 – C29, aaa and abb Steranes distributions from Lake Edward slicks and the Lyemubuza + Muhokiya limestones.(Nicholas, 2009)

#### VI.4- INDUCTIVELY COUPLED PLASMA MASS SPECTROMETRY (ICP-MS)

Inductively Coupled Plasma Mass Spectrometry (ICP-MS) results illustrate the measure of the low detection of Rare earth elements (REE) concentrations including the lanthanide series elements (La, Ce, Pr, Nd, Pm, Sm, Eu, Gd, Tb, Dy, Ho, Er, Tm, Yb, and Lu) plus Sc and Y).

ICP-MS method which is the main experiment used to reach the objectives of this present MSc research, has been done three times for Carbonates geochemical origins purposes:

- In **2013** by Jean Dwyer, Sylvain K. Mangoni and Michael Babechuk using the 2007 to 2010 Travertine samples collected in Albertine Rift basin;
- In **2016** by Sylvain K.M and Cora mc Kenna using the end members samples of the previous experiment and the PCK limestone sample to confirm the ICP-MS results reproducing ability regardless to the time and human resources (after 3 years and with different human resources team);
- In **2018**, after method confirmation by Sylvain and Cora using the 2014 Travertine samples collected in Block V;

##### VI.4.1 - ICP-MS RESULTS OF 2013 EXPERIMENT

The ICP-MS results of the 2013 experiment have produced the elements concentrations in ppb and normalized in MUQ as per Kamber experiment method. These values are presented in the tables in appendix 2 and their original excel files (ICP\_MS2013.xls) enclosed to this thesis in memory stick.

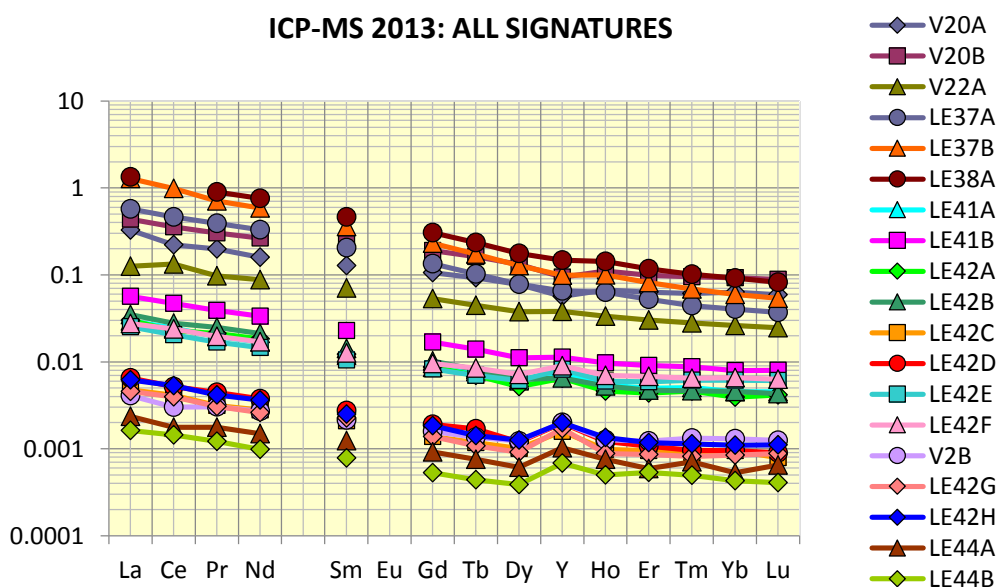


Figure VI.17: 2007- 2010 Block V Travertine REE signatures by ICP-MS in 2013

VI.4.1.1- 2013 TRAVERTINE WITH CARBONATITES SIGNATURES

Samples (fabrics, textures, structure and/or their replica) correlating with Fort Portal Carbonatite #3 (Stoppa and Schiazza, 2013) with a Correlation Coefficient of  $R^2 > 0.95$ , are shown plotted alongside all Fort Portal Carbonatites & Freshwater Sediments in the Figure VI.18 below:

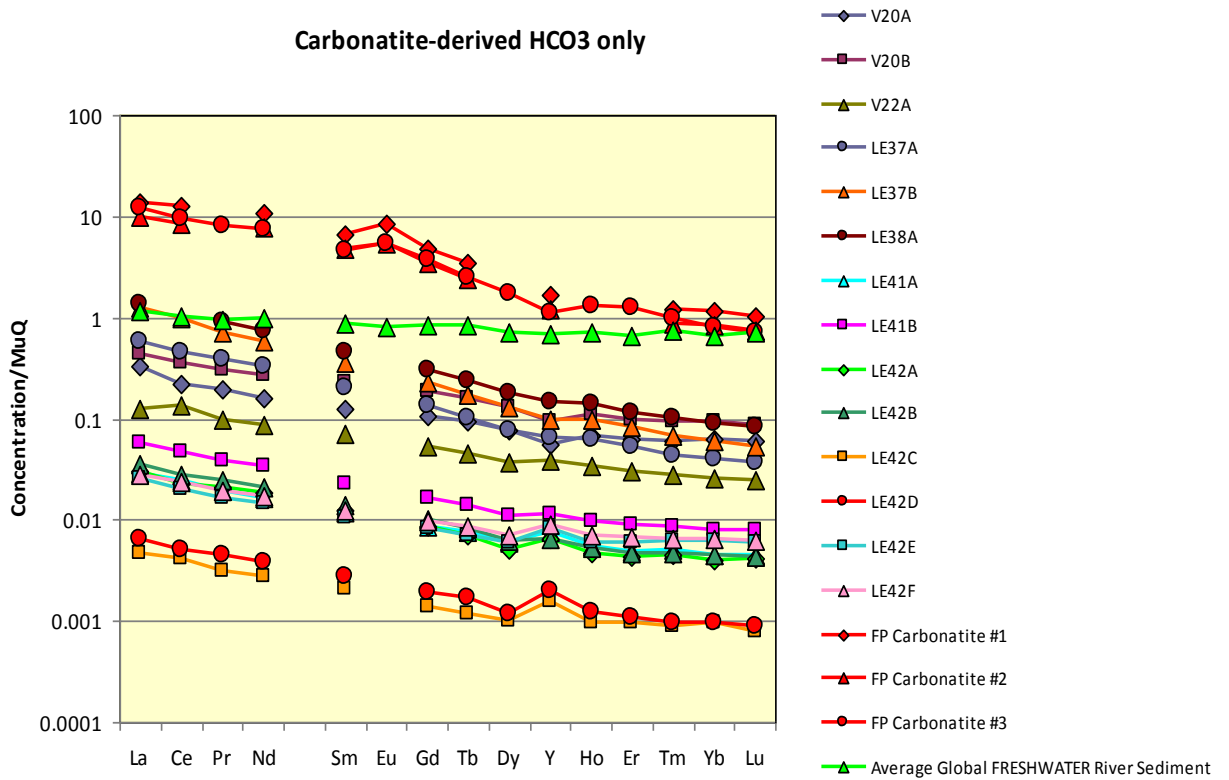


Figure VI.18: ICP-MS Carbonatites Travertine signature shown plotted alongside all Fort Portal Carbonatites & Freshwater Sediments.

Samples (fabrics, textures, structure and/or their replica) correlating with Fort Portal Carbonatite #3 (Stoppa and Schiazza, 2013) with a Correlation Coefficient of  $R^2 > 0.95$ , are shown plotted alongside all Fort Portal Carbonatites in the Figure VI.19 below:

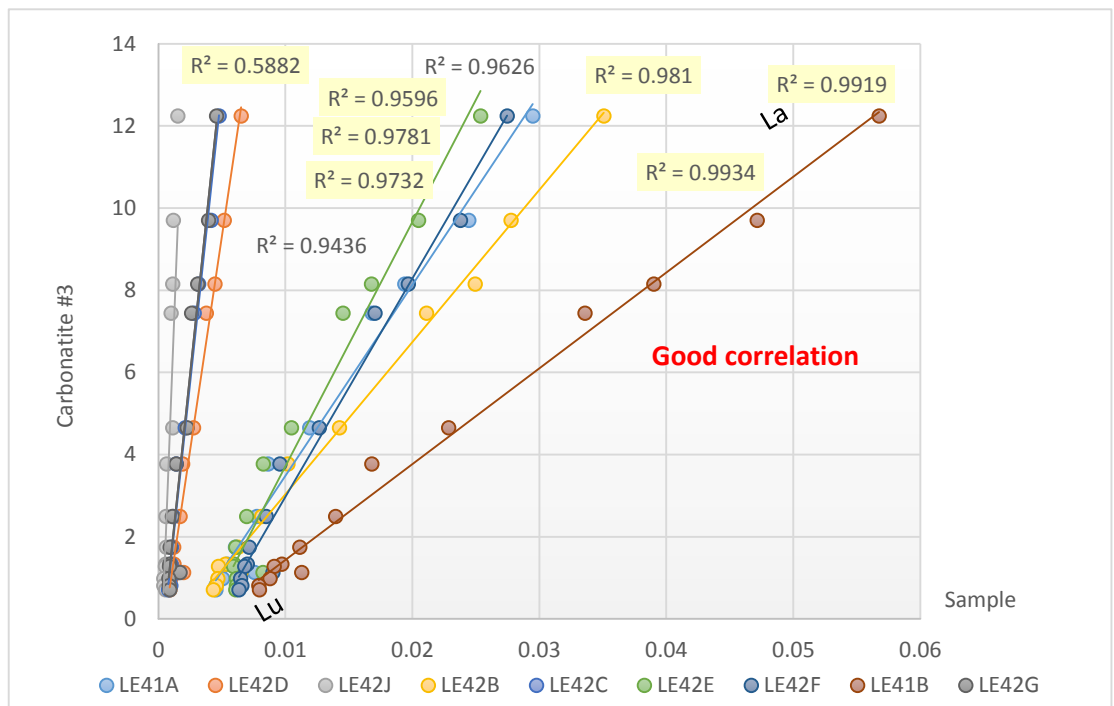


Figure VI. 19: Chart of Carbonatites Travertine correlation coefficient with Fort Portal Carbonatites.

VI.4.1.2- 2013 TRAVERTINE WITH MARINE LIMESTONE SIGNATURES

Samples (fabrics, textures, structure and/or their replica) satisfying all the 5 geochemical main criteria of Marine limestones involvement (Kamber et al., 2014), are shown plotted with modern Seawater, Holocene Marine Limestones and Devonian Reef Limestones in the Figure VI.20 below :

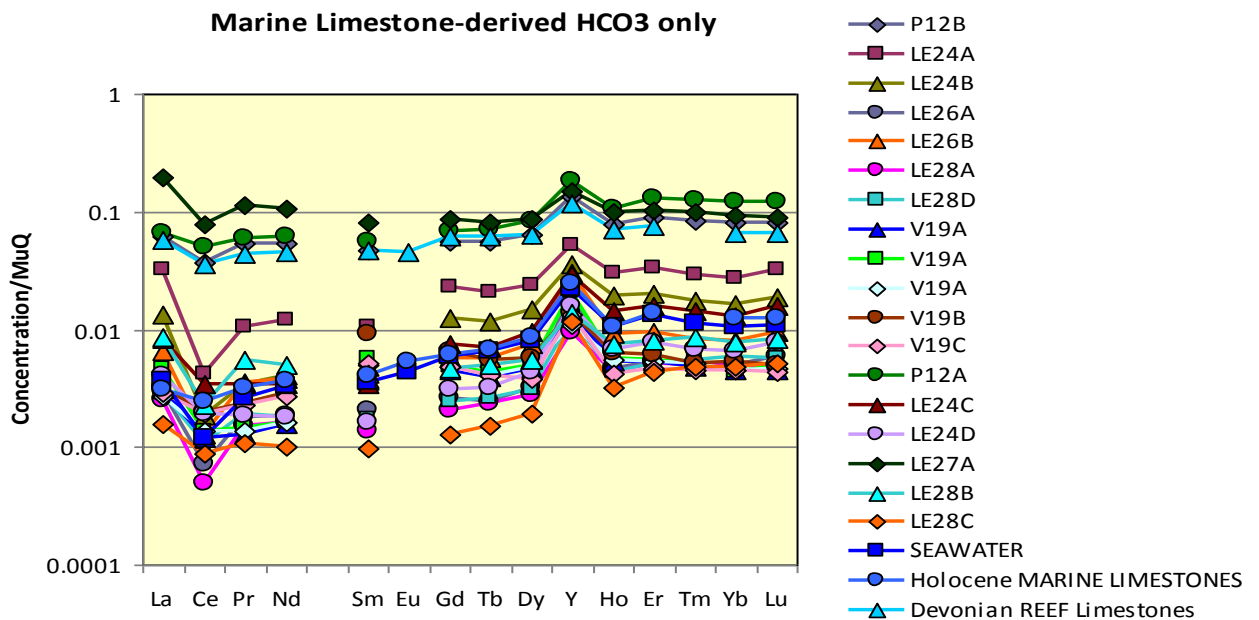


Figure VI.20: ICP-MS Marine limestones Travertine signature shown plotted alongside Holocene Marine Limestones and Devonian Reef Limestones & Seawater Sediments.



Samples (fabrics, textures, structure and/or their replica) from Ugandan side correlating with Devonian Reef limestones (Stoppa and Schiazza, 2013) with a Correlation Coefficient of  $R^2 > 0.80$ , are shown plotted alongside modern Seawater, Holocene Marine Limestones and Devonian Reef Limestones in the Figure VI.21 below:

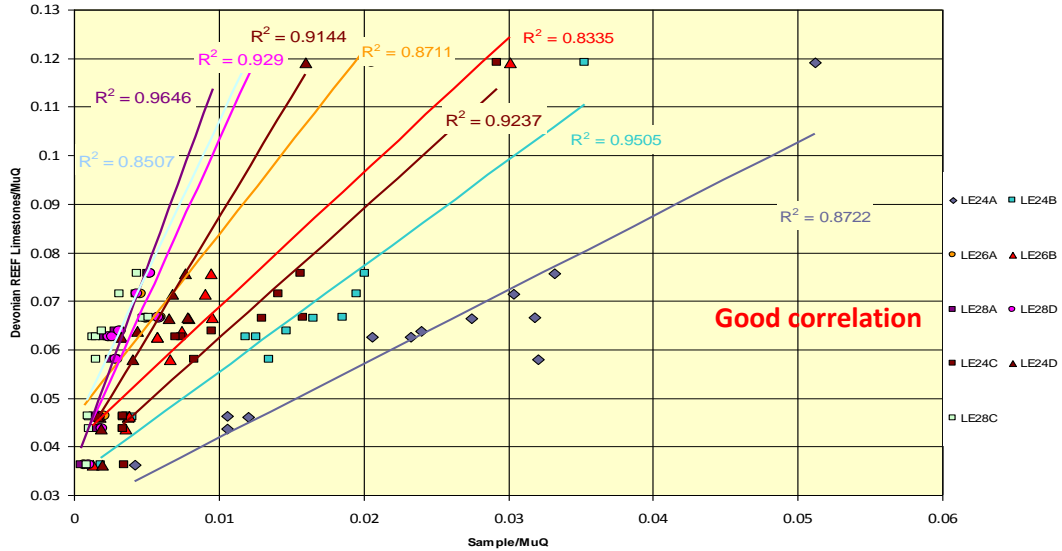


Figure VI.21: Chart of Marine limestones Travertine correlation coefficient with Devonian Reef limestones.(Stoppa and Schiazza, 2013). Ugandan side of Albertine Rift basin

Samples (fabrics, textures, structure and/or their replica) from DRC side correlating with Devonian Reef limestones (Stoppa and Schiazza, 2013) with a Correlation Coefficient of  $R^2 > 0.80$ , are shown plotted alongside modern Seawater, Holocene Marine Limestones and Devonian Reef Limestones in the Figure VI.22 below:

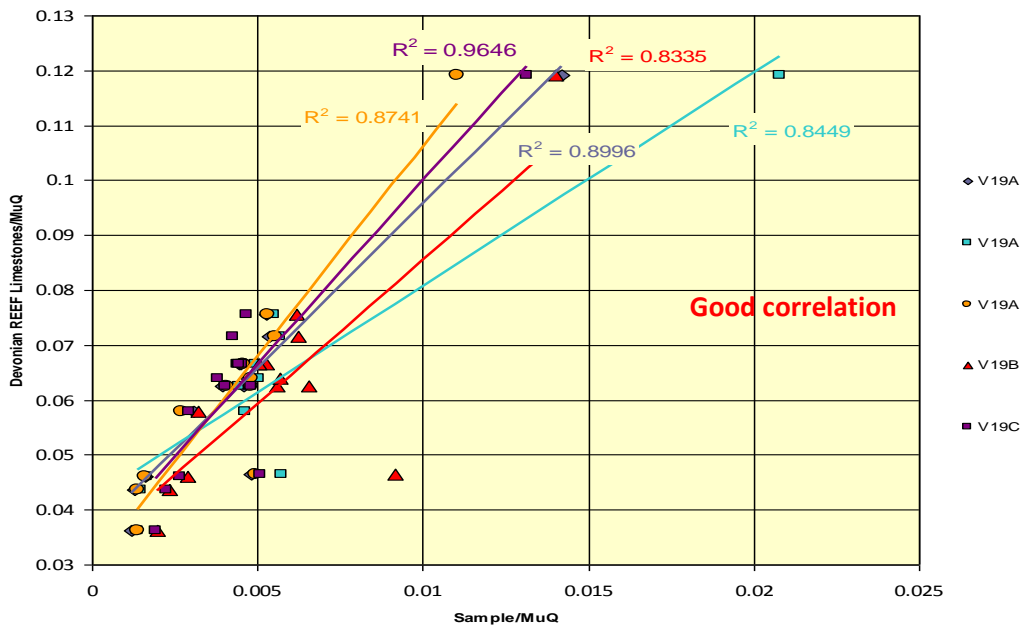


Figure VI.22 : Chart of Marine limestones Travertine correlation coefficient with Devonian Reef limestones.(Stoppa and Schiazza, 2013). DRCongo side of Albertine Rift basin

VI.4.1.3- 2013 TRAVERTINE WITH HYBRIDE SIGNATURES

During the 2013 experiment, some samples like those LE 32 collected in Dura Uganda / EA4A have given different results from either Carbonatites or Marine limestones signatures.

The sample LE 32 was drilled through the visible textures, structures and fabrics and analysed gave spectral signatures in Figure VI.23 below showing a decreasing the light rare earths

Lanthanum, cerium, praseodymium, neodymium, promethium, and samarium and an increasing the "heavy rare earths "Yttrium, europium, gadolinium, terbium, dysprosium, holmium, erbium, thulium, ytterbium, and lutetium.

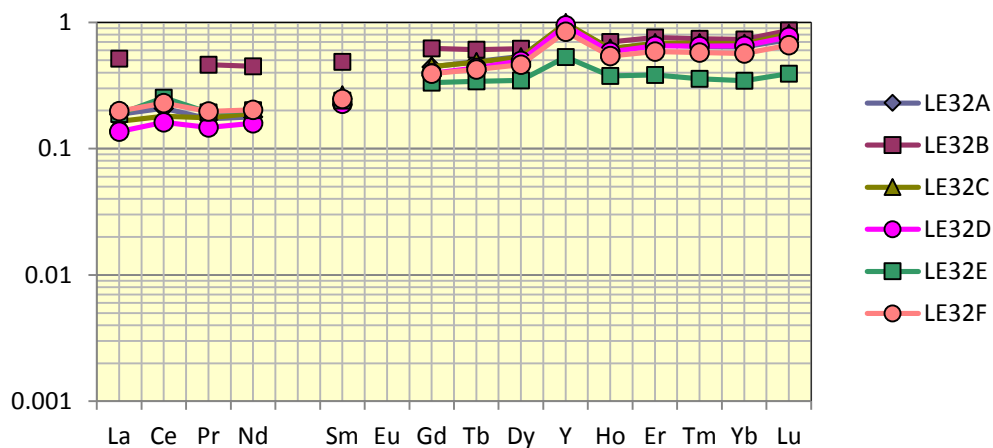


Figure VI.23: 2013 Travertines Hybrid signature.

REE values obtained for each structure, texture or fabric by ICP-MS and normalized in MUQ neither satisfy the Marine limestones criterias as per Balz Kamber approach nor the Correlation coefficient with Fort Portal Carbonatites. The Figures VI.24 and VI.25 below give respectively an overview of the LE 32 sample Correlation coefficient with Fort Portal and Marine limestone check box.

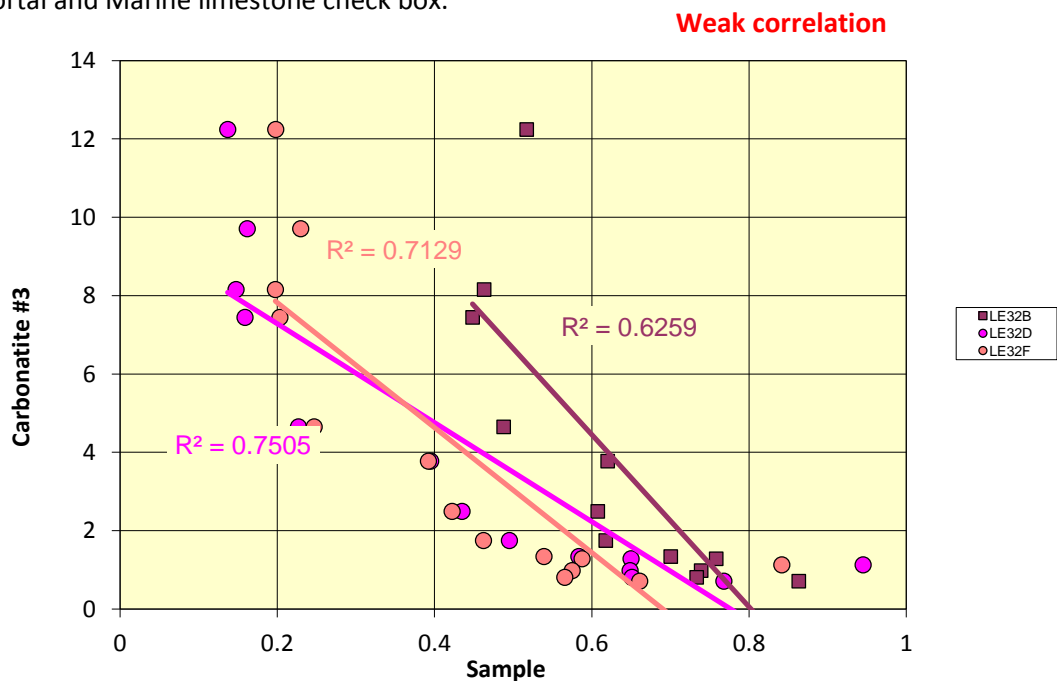


Figure VI.24: LE 32 Correlation coefficient with Fort Portal

Weak correlation

	LE32A	LE32B	LE32C	LE32D	LE32E	LE32F
Key criteria for Marine Limestones	$Pr_n/Yb_n \ll 1$	✓	✓	✓	✓	✓
	$Y/Ho > 40$	✓	✗	✓	✓	✗
	$La/La^* > 1.1$	✓	✗	✓	✗	✗
	$Gd/Gd^* > 1.1$	✗	✗	✗	✗	✗
	$Ce/Ce^* < 0.8$	✗	✓	✗	✗	✗

Figure VI.25: LE 32 Marine limestones Criteria Check Box

#### VI.4.2 - ICP-MS RESULTS OF 2016 EXPERIMENT

The 2016 ICP-MS experiment aimed to repeat exactly the 2013 experiment per Balz Kamber ideas, confirm the results reproducible ability and use the method on the last batch from 2014 samples with more confidence.

For unexpected spectral interferences on europium from may be  $[BaO]^+$ , the 2013 experiment didn't afford to detect it properly by the way of sensitive measurement of  $Eu^{2+}$  ions. The europium has been properly detected during the 2016 experiment.

One of the main purpose of the 2016 ICP-MS experiment was to redo the 2013 experiment with both Carbonatites and Marine limestones end members Travertine samples, including Europium measurement in the final results.

All the signatures detected from 18 field samples during the 2016 ICP-MS experiment are represented in the logarithmic scale of 10 in the Figure VI.26 below:

### ICP-MS 2016: ALL SIGNATURES

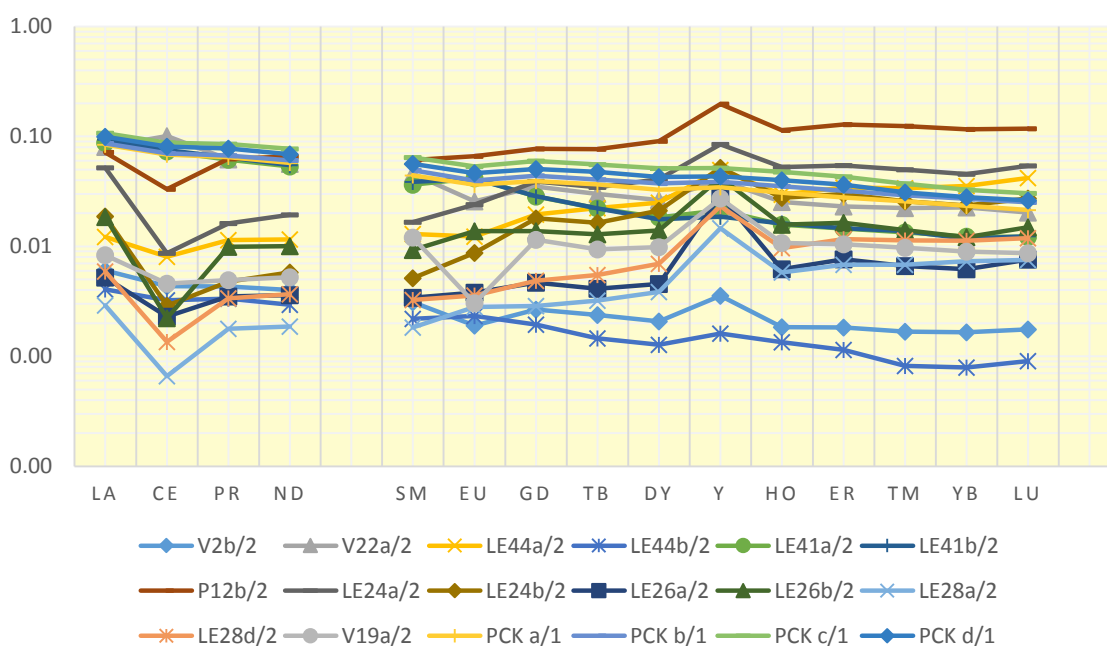


Figure VI.26: ICP-MS 2016: All spectral signatures

VI.4.2.1- 2016 TRAVERTINE WITH CARBONATITES SIGNATURES

The results from the 2007-2010 field samples of the rift end members found with Carbonatites signatures during the 2016 ICP-MS experiment are presented in Fig VI.27 below alongside with Fort Portal Carbonatites lavas.

**ICP-MS 2016: CARBONATITES SIGNATURES**

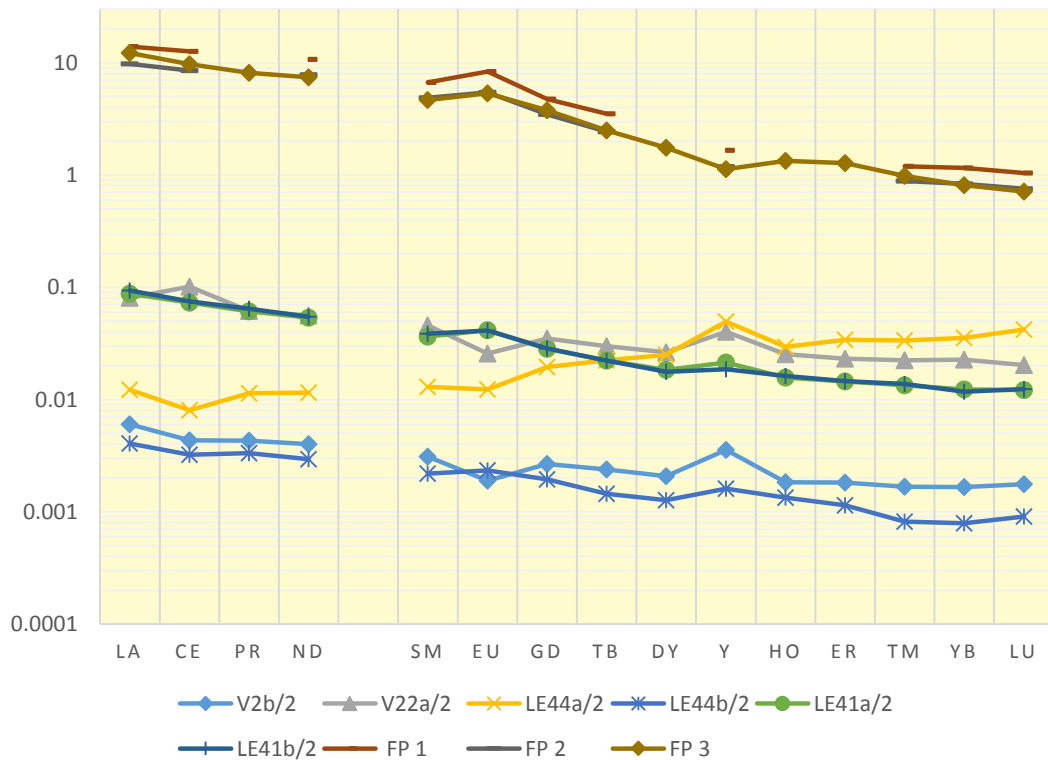


Figure VI.27: ICP-MS 2016: Carbonatites signatures alongside Fort portal Lava #1,#2 & #3

Samples (fabrics, textures, structure and/or their replica) correlating with Fort Portal Carbonatite #3 (Stoppa and Schiazza, 2013) with a Correlation Coefficient of  $R^2 > 0.75$ , are shown plotted alongside Fort Portal Carbonatites lavas in the Figure VI.28 below:

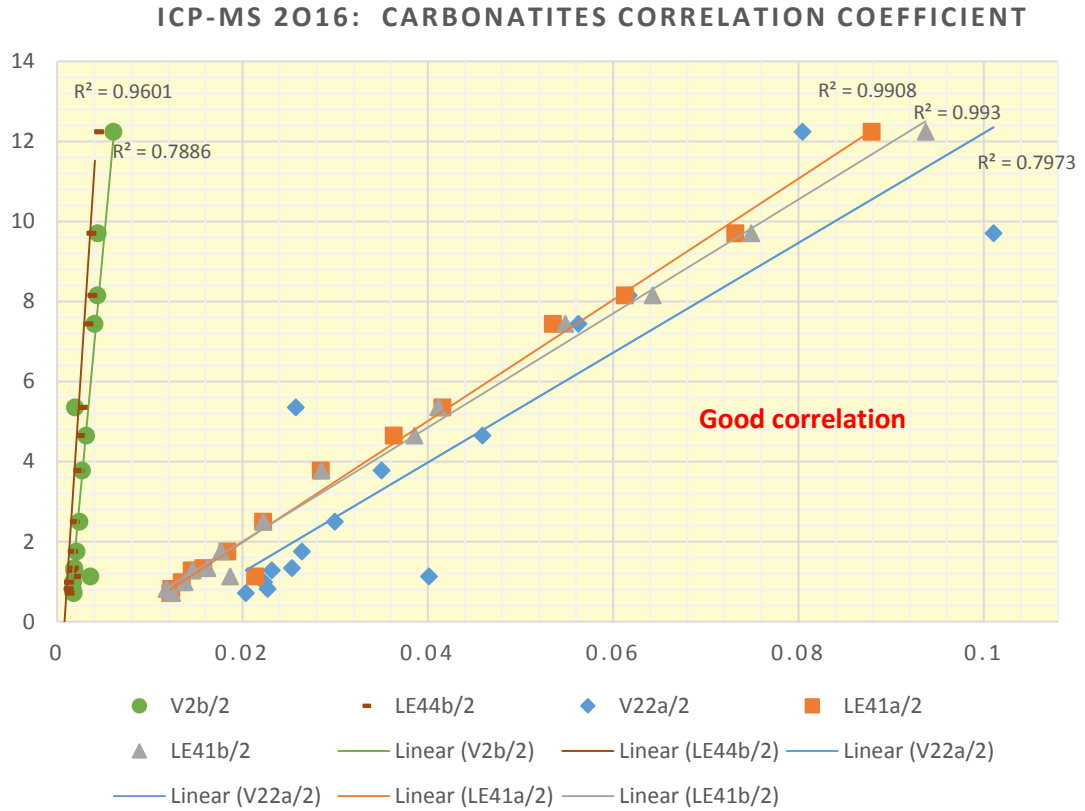
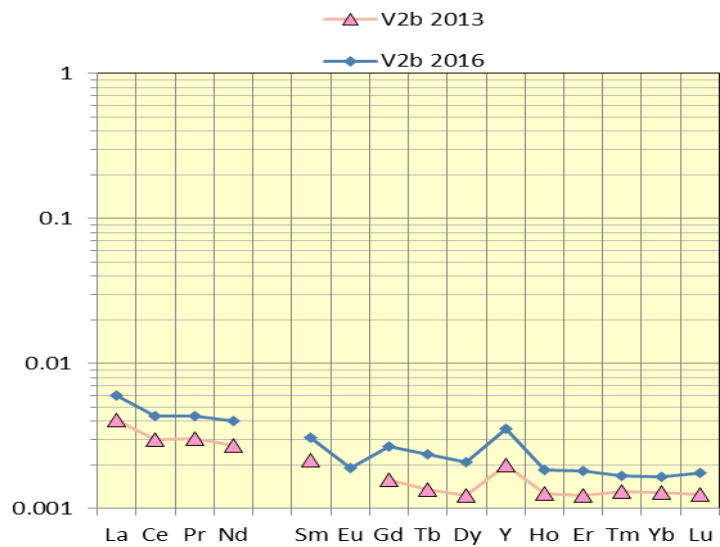


Figure VI.28 : 2007- 2010 Block V Carbonatites correlation coefficient with Fort Portal #3

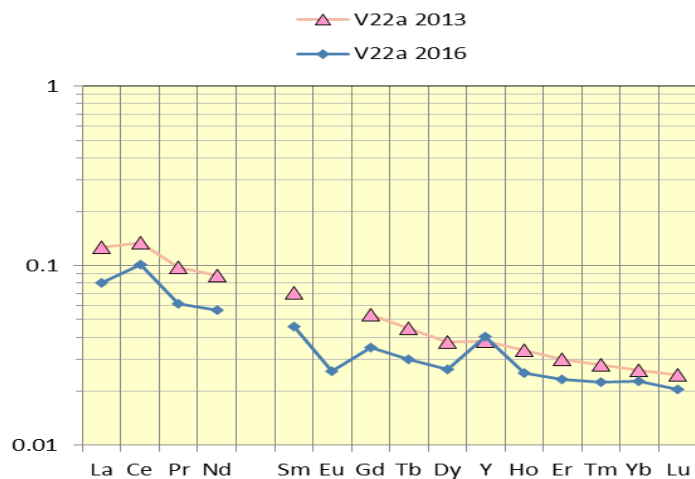
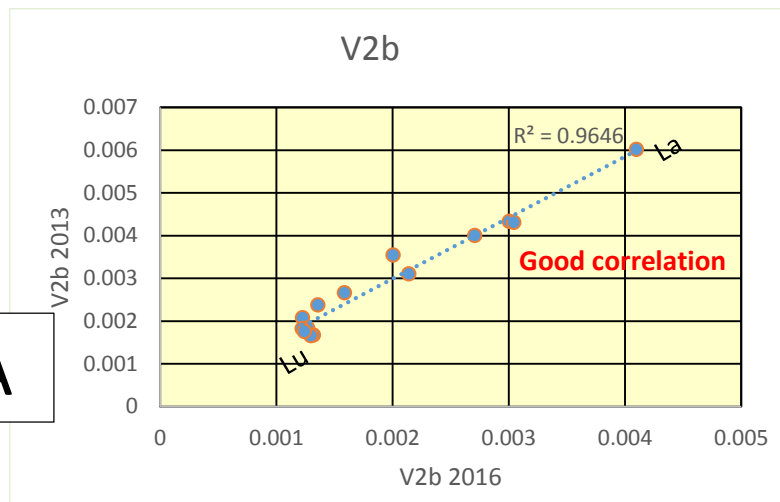
These results which have been made from the respective 2013 and 2016 MUQ raw datas in the table 2 of the appendix 2, are presented in form of comparative Charts. Each of these following Charts in Figure VI.29 below are showing comparisons of 2013 and 2016 REE concentrations spectral signatures and their respective positive correlation coefficient with the Fort Portal Carbonatite lava flow.

The 2016 Travertine Samples (fabrics, textures, structure and/or their replica) correlating with the 2013 Carbonatites rift end members samples with a Correlation Coefficient of  $R^2 > 0.85$ , are shown plotted alongside in the graphs below which each of them, illustrates results comparisons of both above 2013 and 2016 experiments.

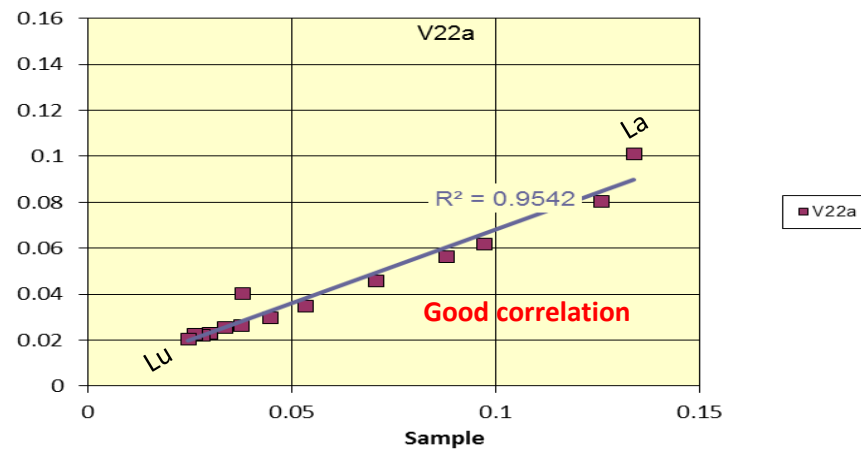
### Carbonatites Results Comparison of the 2013 – 2016 ICP-MS experiments

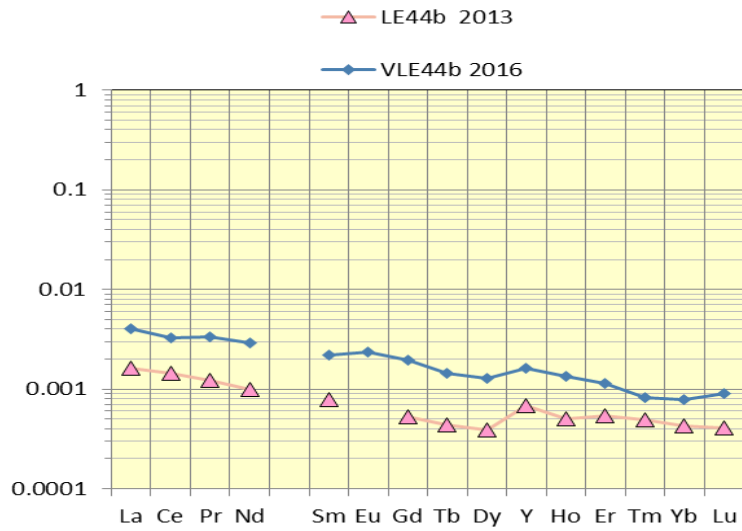


A

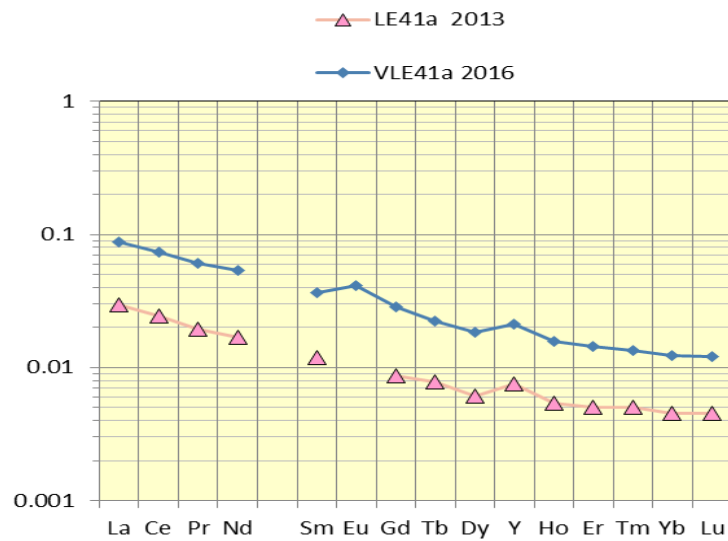
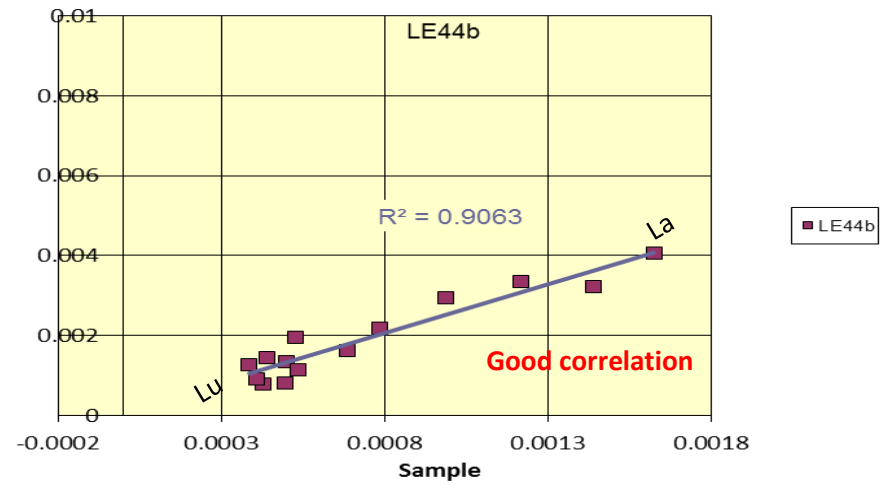


B

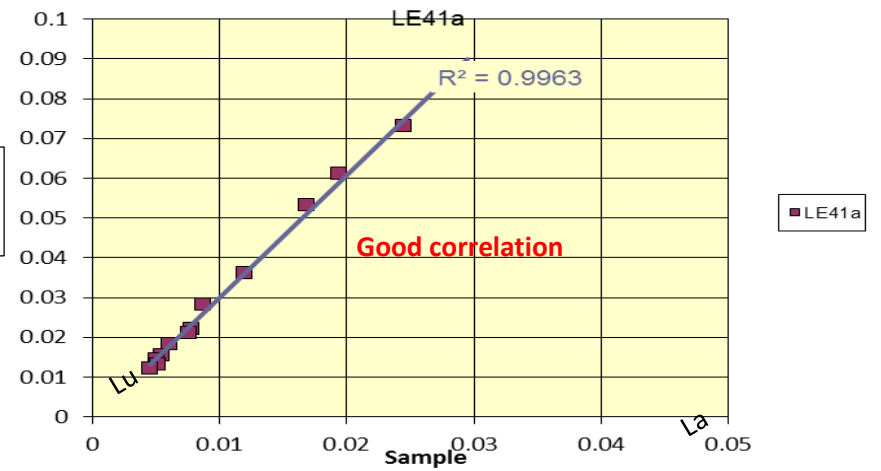


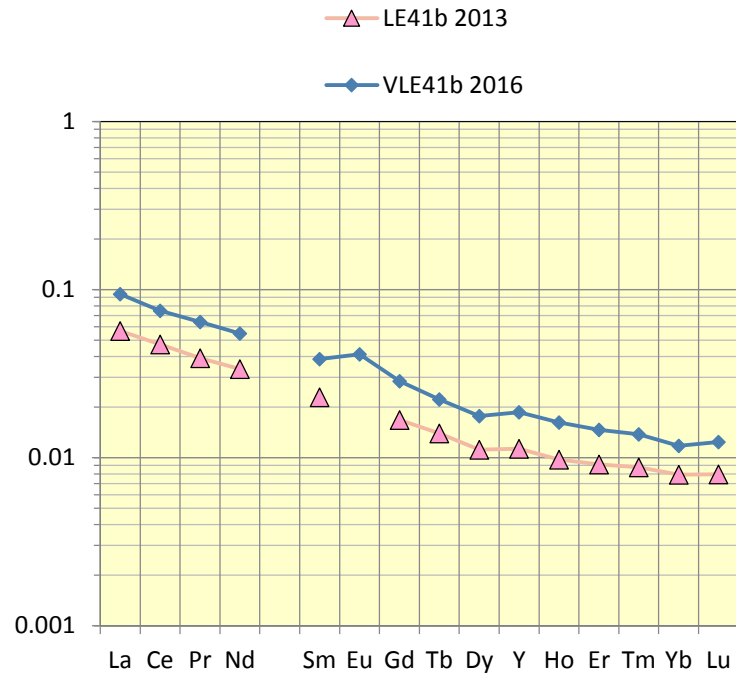


C



D





E

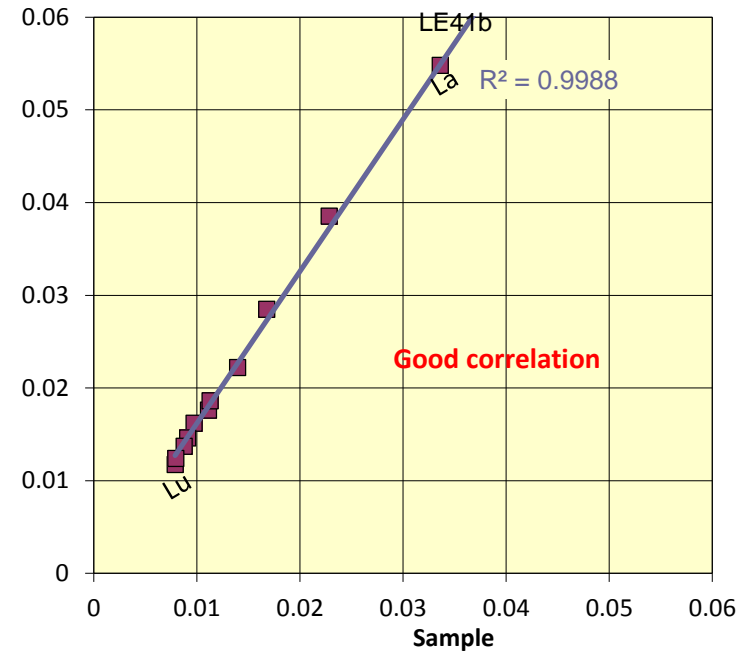


Figure VI.29 a, b, c, d, and e: Carbonatites signatures Comparison of the 2013 – 2016 ICP-MS experiments.



VI.4.2.2- 2016 TRAVERTINE WITH MARINE LIMESTONES SIGNATURES

From the analyzed sediment samples, it can be deduced that the Procokin samples have confirmed their known fresh waters origin as well as the 2013 marine limestones signatures have been close to the 2016 signatures with enough confidence. The Figures VI.27 and VI.28 below, show respectively the 2016 all marine limestones signatures alongside fresh waters, sea waters, Holocene marine, Devonian reef and their correlation coefficient

These results which have been made from the respective 2013 and 2016 MUQ raw datas in the table 3 of the appendix 2, are presented in form of comparative Charts. Each of these below Charts in Figure VI. 30 are showing together both 2013 and 2016 experiment REE concentrations spectral signatures and in Figure VI.31 their respective correlation coefficient  $R^2 > 0.80$ .

### ICP-MS 2016: MARINE LIMESTONE SIGNATURES

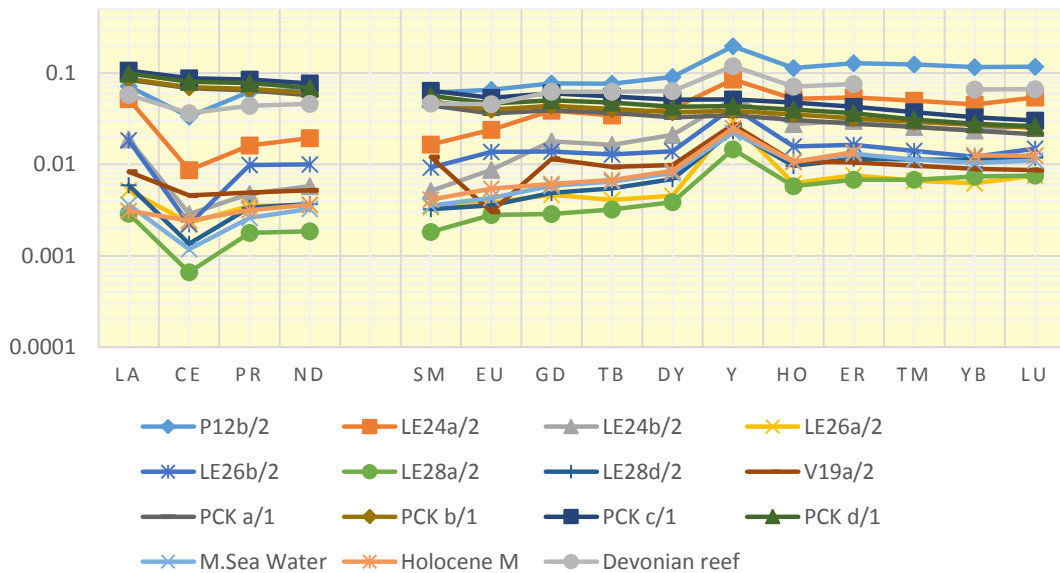


Figure VI.30: 2007- 2010 Block V Travertine Marine limestone signatures by ICP-MS in 2016

### ICP-MS 2016: MARINE LIMESTONE CORRELATION COEFFICIENT

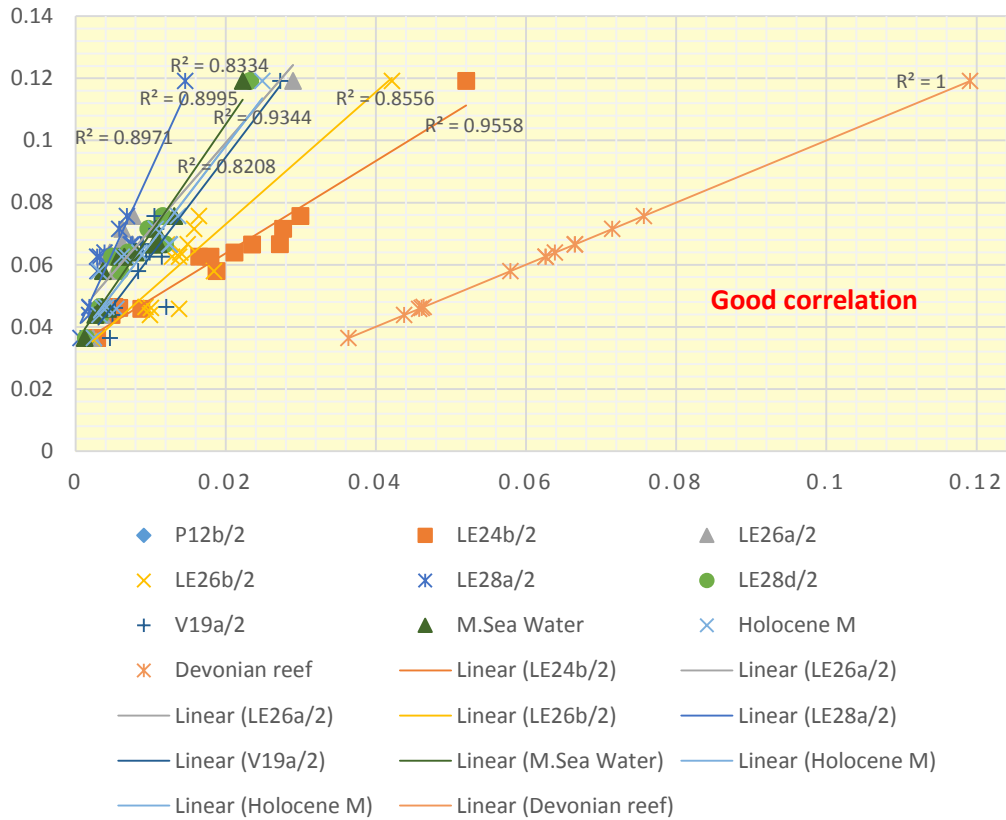
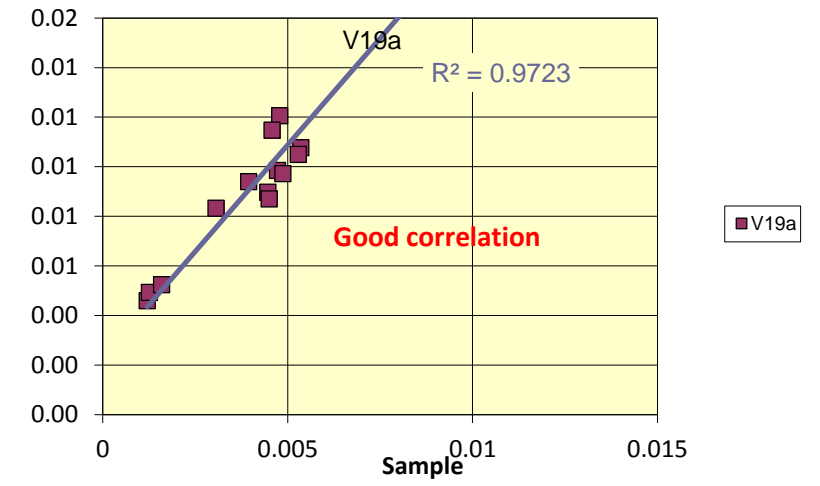
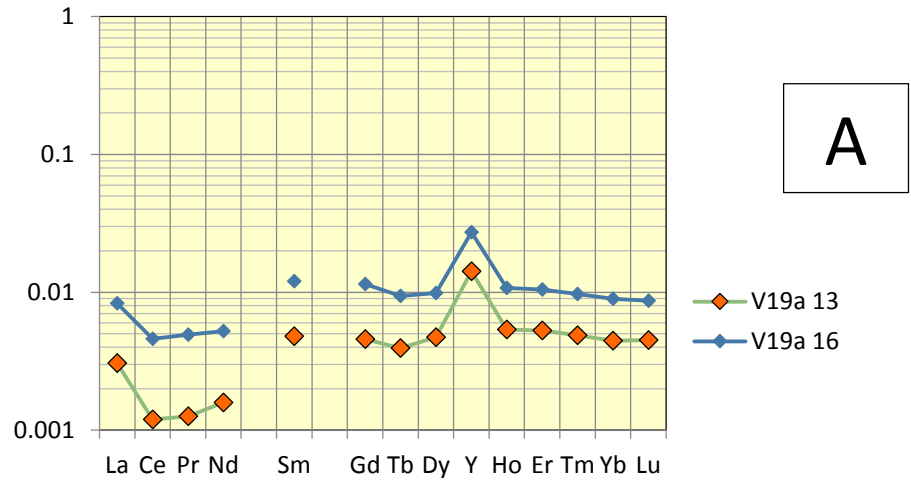


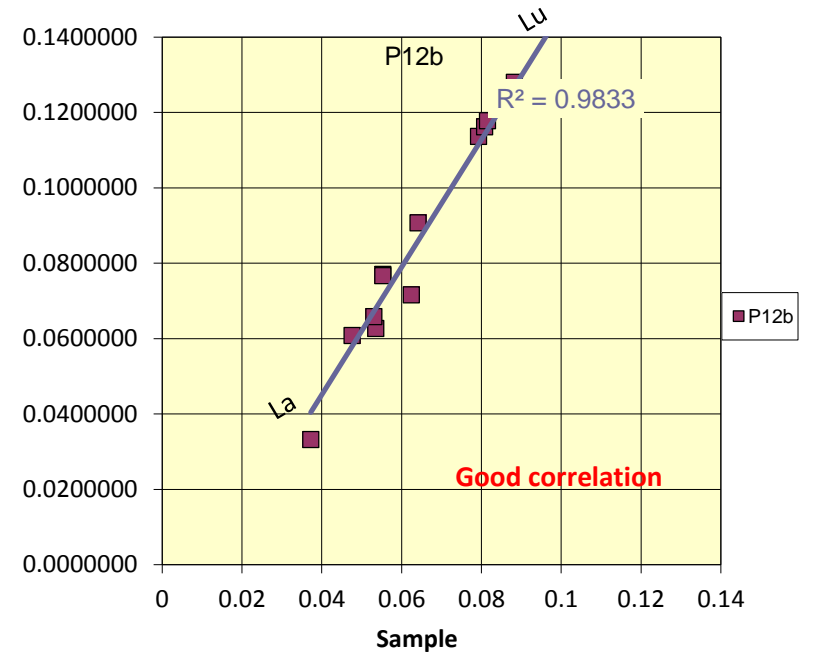
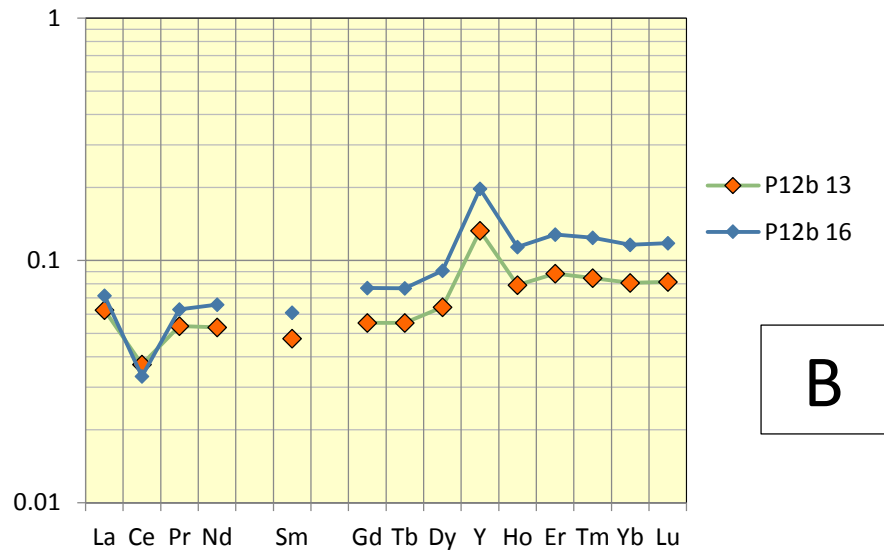
Figure VI.31: 2007- 2010 Block V Marine limestone Correlation Coefficient

The 2016 Travertine Samples (fabrics, textures, structure and/or their replica) correlating with the 2013 marine limestones end members samples with a Correlation Coefficient of  $R^2 > 0.85$ , are shown plotted alongside in the Figures below which illustrate results comparisons of both above experiments.

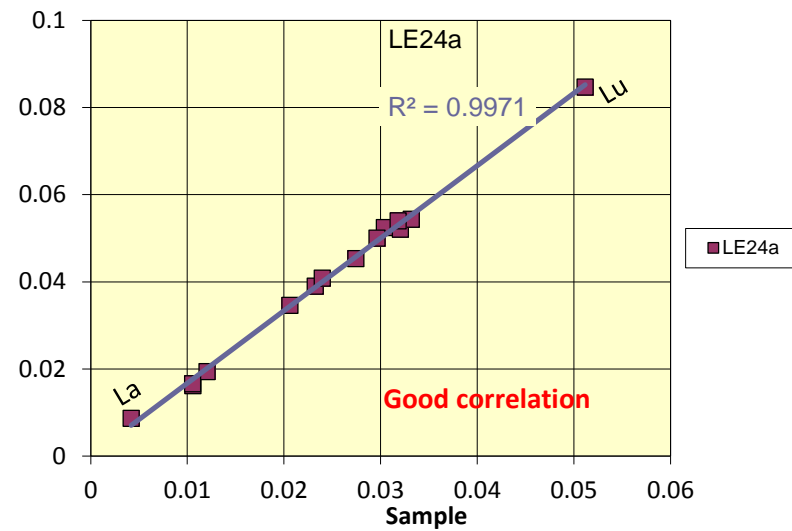
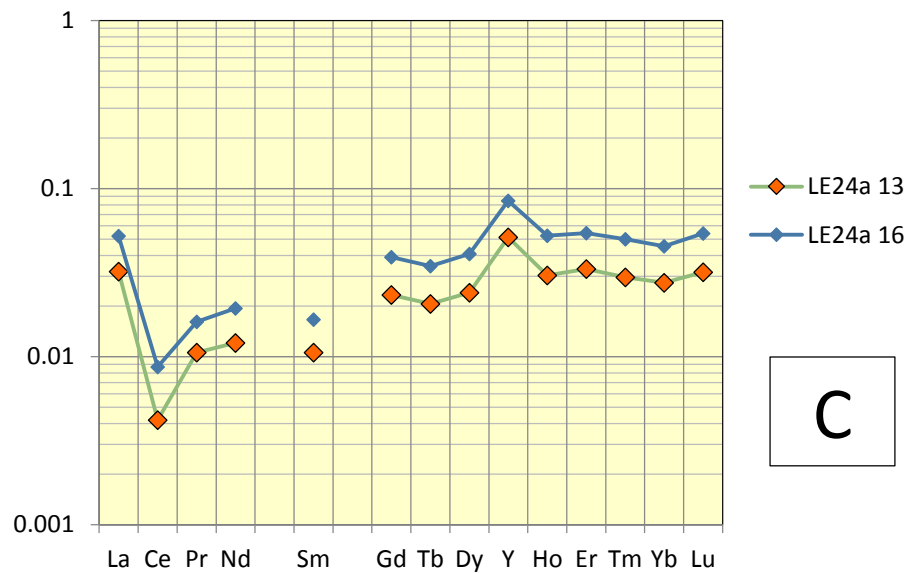
**Marine limestones Results Comparison of the 2013 – 2016 ICP-MS experiments**



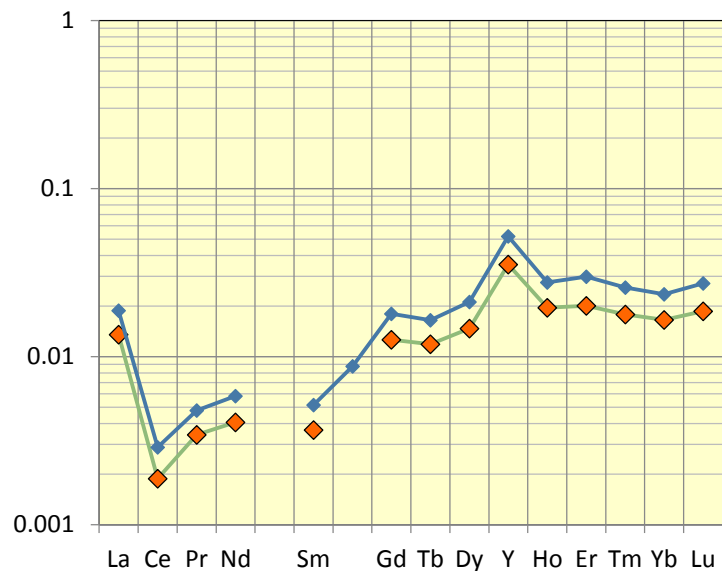
		V19_2013	V19_2016	CRITERIA
>>40	Y/Ho	2.647209	2.528275378	No
>1.1	La/La*	3.862916	1.905987731	Yes
<0.8	Ce/Ce*	1.196555	0.988580433	No
>1.1	Gd/Gd*	1.390965	1.281446498	Yes
<<1	Prn/Ybn	0.282225	0.549309056	Yes



		P12b_2013	P12b_2016	CRITERIA
>>40	Y/Ho	1.676789	1.736822864	No
>1.1	La/La*	1.144282	1.2565824	Yes
<0.8	Ce/Ce*	0.688419	0.555940519	Yes
>1.1	Gd/Gd*	1.159656	1.187210291	Yes
<<1	Prn/Ybn	0.662329	0.539920851	Yes

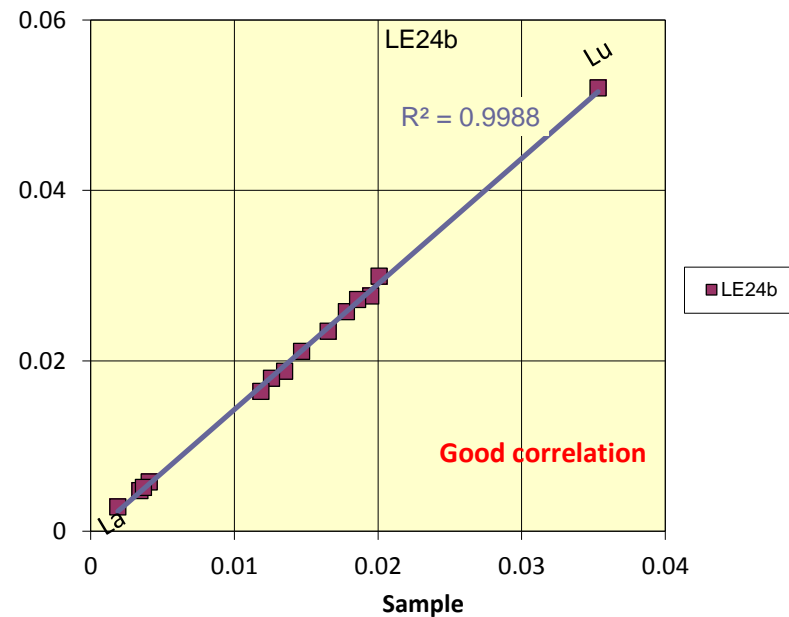


		LE24a_2013	LE24a_2016	CRITERIA
>>40	Y/Ho	1.684022	1.61376769	No
>1.1	La/La*	3.930147	4.655112628	Yes
<0.8	Ce/Ce*	0.450244	0.647059055	Yes
>1.1	Gd/Gd*	1.312061	1.332444626	Yes
<<1	Prn/Ern	0.318632	0.296964028	Yes
>1.1	Prn/Ybn	0.385356	0.355994184	Yes

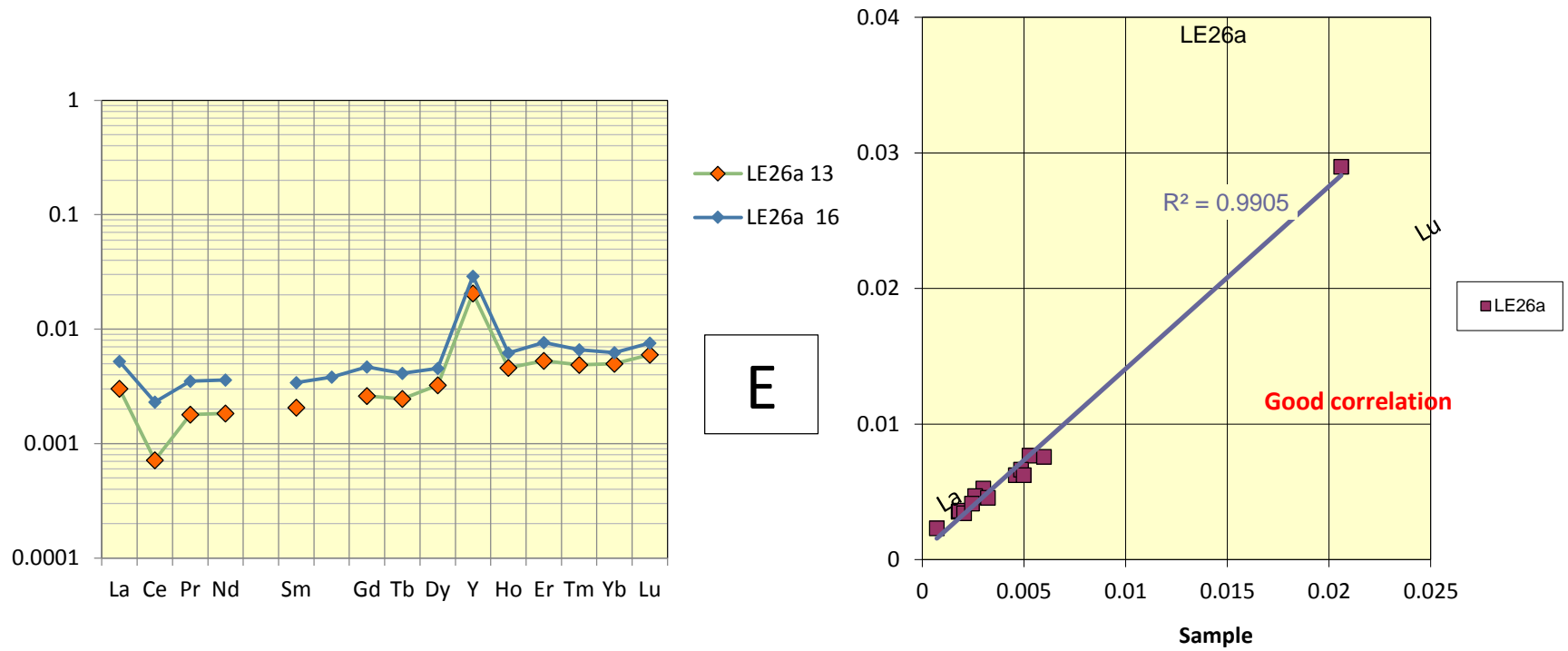


◆ LE24b 13  
◆ LE24b 16

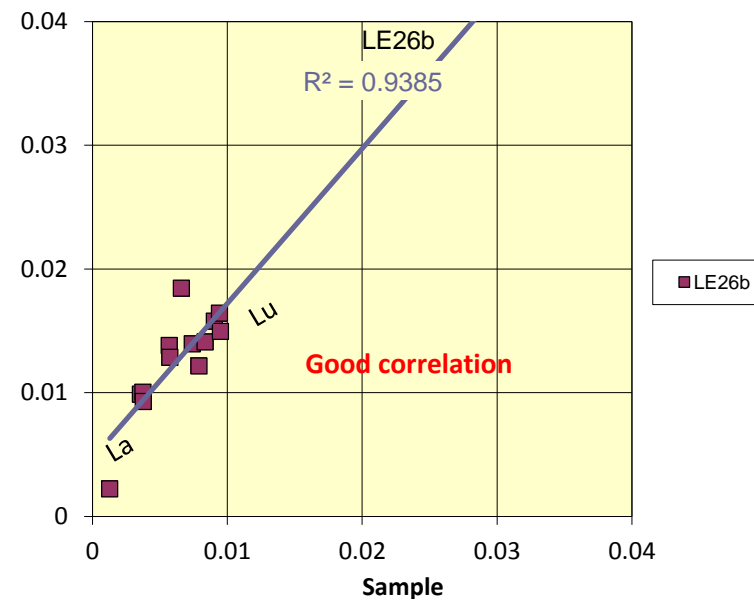
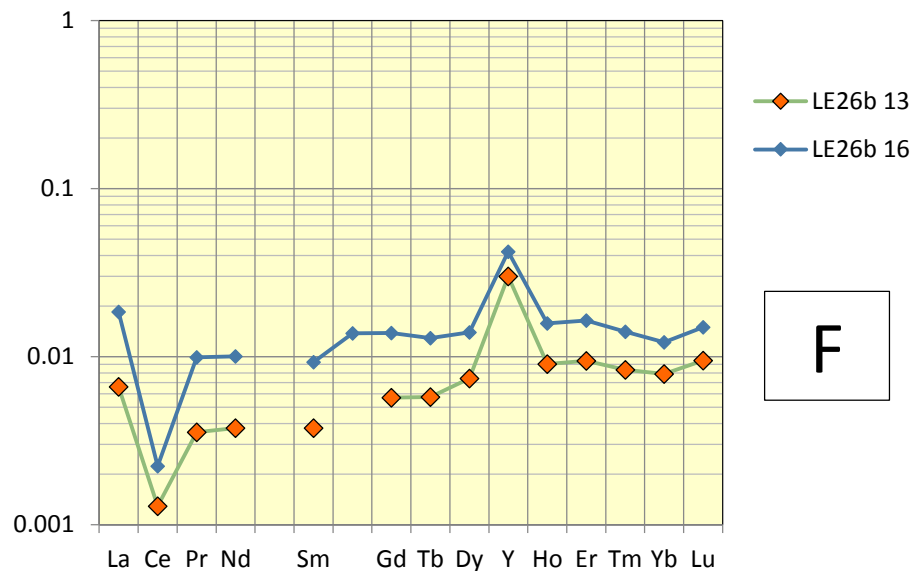
D



		LE24b_2013	LE24b_2016	CRITERIA
>>40	Y/Ho	1.810488	1.882843	No
>1.1	La/La*	5.588996	5.850131	Yes
<0.8	Ce/Ce*	0.653983	0.736502	Yes
>1.1	Gd/Gd*	1.31779	1.403539	Yes
<<1	Prn/Ern	0.170343	0.159299	Yes
>1.1	Prn/Ybn	0.20682	0.202891	Yes

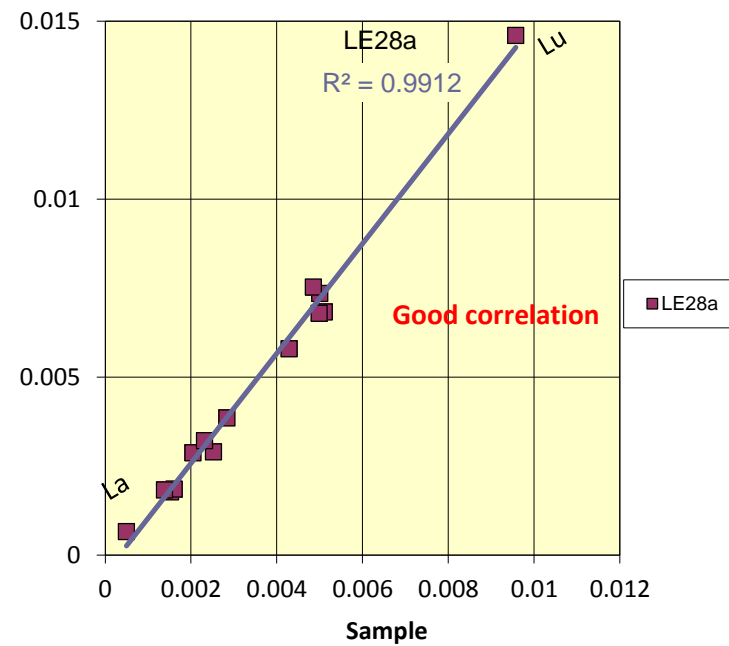
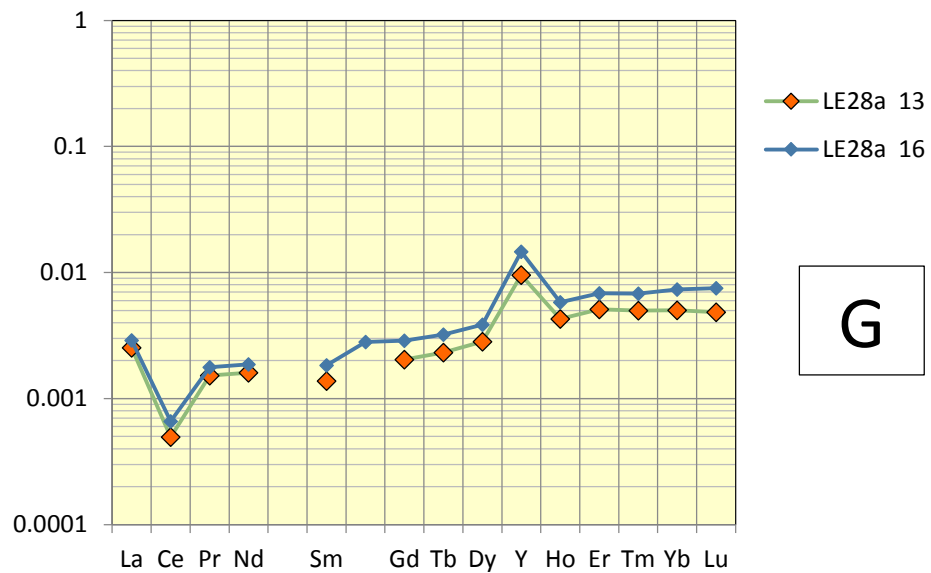


		LE26a_2013	LE26a_2016	CRITERIA
>>40	Y/Ho	4.466672	4.66481185	No
>1.1	La/La*	1.754767	1.55708473	yes
<0.8	Ce/Ce*	0.407432	0.66997316	yes
>1.1	Gd/Gd*	1.405288	1.25855032	yes
<<1	Prn/Ern	0.339981	0.45935575	yes
>1.1	Prn/Ybn	0.359746	0.56559113	yes

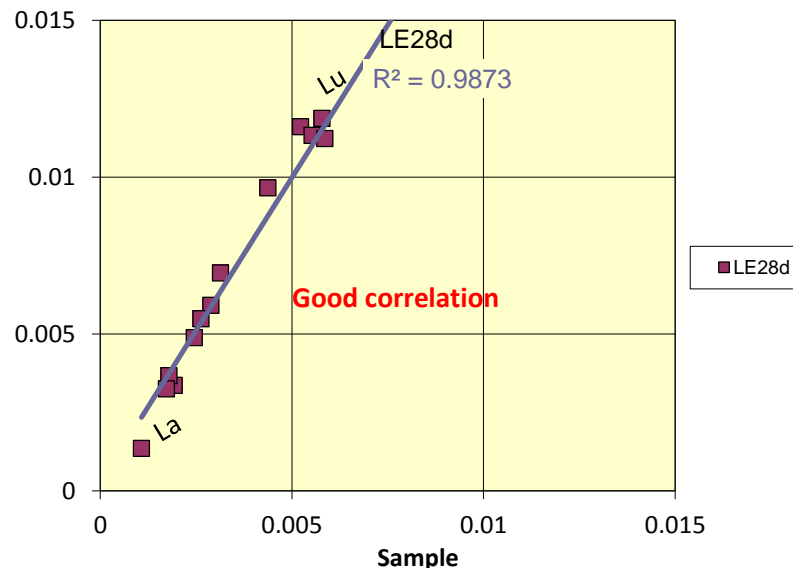
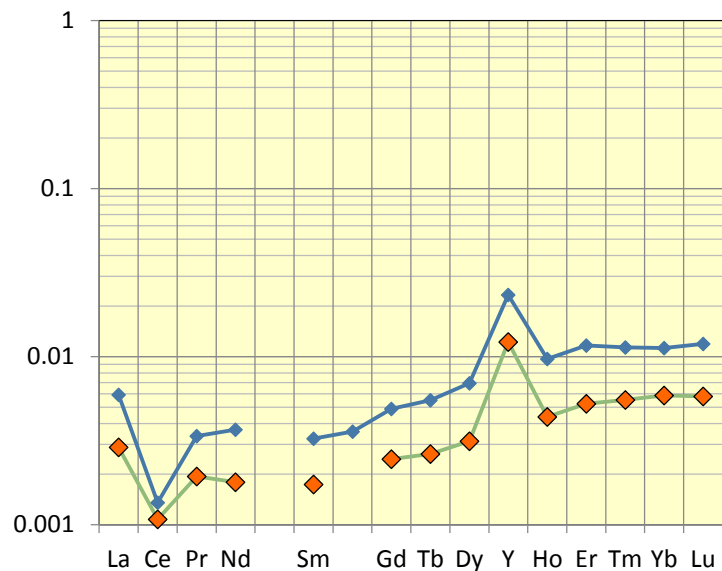


		LE26b_2013	LE26b_2016	CRITERIA
>>40	Y/Ho	3.3276	2.671762452	No
>1.1	La/La*	2.069303	1.922907527	Yes
<0.8	Ce/Ce*	0.382303	0.228412875	Yes
>1.1	Gd/Gd*	1.277765	1.162146847	yes
<<1	Prn/Ern	0.377323	0.602416007	yes
>1.1	Prn/Ybn	0.450106	0.813763021	Yes





		LE28a_2013	LE28a_2016	CRITERIA
>>40	Y/Ho	2.233285	2.519508897	No
>1.1	La/La*	1.834335	1.793265394	yes
<0.8	Ce/Ce*	0.340781	0.389999676	yes
>1.1	Gd/Gd*	1.077712	1.069167803	No
<<1	Prn/Ern	0.298544	0.260256782	yes
>1.1	Prn/Ybn	0.304755	0.241748024	Yes



		LE28d_2013	LE28d_2016	CRITERIA
>>40	Y/Ho	2.799444	2.40548692	No
>1.1	La/La*	1.284375	2.09905312	Yes
<0.8	Ce/Ce*	0.515165	0.43903494	Yes
>1.1	Gd/Gd*	1.11428	1.12480308	Yes
<<1	Prn/Ern	0.369575	0.28947432	Yes
>1.1	Prn/Ybn	0.329835	0.29935288	Yes

Figure VI.32a, b, c, d,e,f,g,and h: Marine Limestones signatures Comparison of the 2013 – 2016 ICP-MS experiments.

#### VI.4.2.3- PROCOKIN LIMESTONES

The Procokin PCK limestone sample has been collected in a quarry in the western side of DR Congo where existing literature (detailed in Chapter II) universally recognized the presence of stromatolite fossils which clearly suggest a fresh water depositional environment as origin.

The geochemical analysis of the four (4) PCK limestone samples in 2016 confirmed by ICP-MS method and available instrument the fresh water limestone origin of this stromatolite sample which was supposed to be used as matching correlation tool or geochemistry comparator factor with any other limestone REE signature from East African Rift System samples as the Fort Portal Carbonatites and Devonian Reef marine limestones are used through this whole study as geochemistry referring tool.

The table 4 below, shows the MUQ values of the PCK samples obtained in 2016 ICP-MS experiments :

	PCK 1	PCK2	PCK3	PCK4
La	0.084436	0.086158	0.106982	0.099262
Ce	0.068209	0.070235	0.087565	0.08063
Pr	0.064645	0.067175	0.085331	0.077553
Nd	0.05749	0.060468	0.07718	0.068976
Sm	0.044346	0.049172	0.064215	0.05625
Eu	0.036293	0.039803	0.053516	0.046363
Gd	0.039151	0.043947	0.059906	0.050472
Tb	0.036626	0.040586	0.055485	0.047495
Dy	0.032784	0.037301	0.051138	0.042699
Y	0.034505	0.038587	0.051523	0.043391
Ho	0.030738	0.035303	0.047705	0.039852
Er	0.027923	0.031958	0.042997	0.036439
Tm	0.025765	0.029275	0.037255	0.030941
Yb	0.023452	0.027068	0.032708	0.027966
Lu	0.02149	0.025224	0.030388	0.026143

Table 4: MUQ values of PCK samples obtained by ICP-MS in 2016

The table 5 below which help to check the marine origin criterias, suggest that the PCK samples are effectively limestones, however, they are not from Marine origin.

		PCK 1	PCK 2	PCK 3	PCK 4	CRITERIA
	Y/Ho	1.122578755	1.093018229	1.080030426	1.088788393	No
>>40	La/La*	1.032997327	1.039261044	1.025661941	1.012462442	No
>1.1	Ce/Ce*	0.93834339	0.941160431	0.928161005	0.924690281	No
<0.8	Gd/Gd*	0.956806242	0.99515329	0.995081664	0.955379132	No
<<1	Prn/Ern	2.315143088	2.10194569	1.984578098	2.128291981	No
>1.1	Prn/Ybn	2.756461791	2.481738751	2.60889605	2.773108949	No

Table 5: Marine limestone criteria check box for the PCK samples

The Figure VI.33 below, shows the fresh water limestones spectral signature obtain by ICP-MS for all the 4 layered structures drilled within the PCK sample.

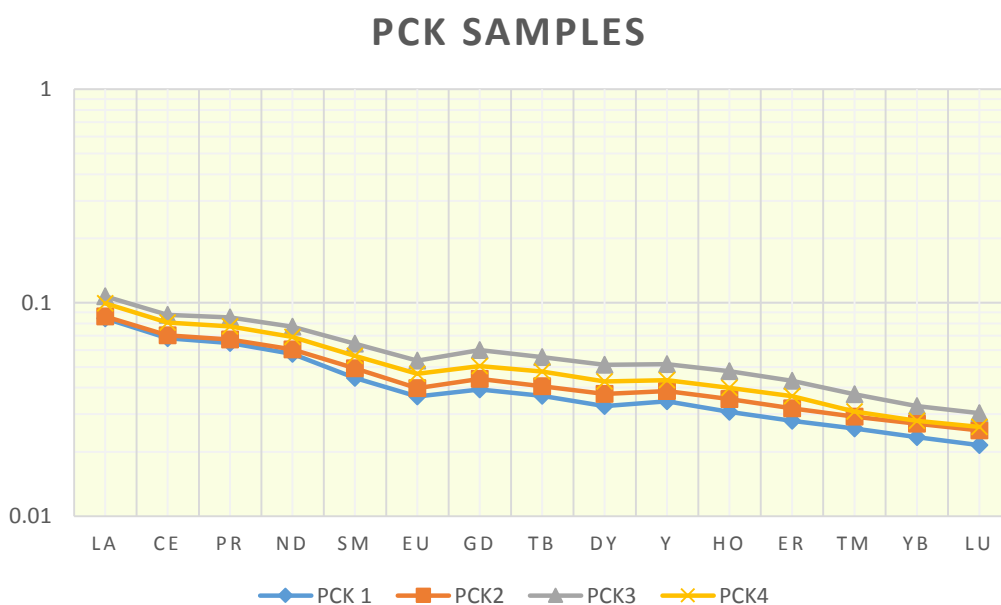


Figure VI.33: PCK Samples REE fresh water signature, ICP-MS, 2016

The fresh waters PCK Samples are one of the first limestone DRC occurrence documented so far. Comparing the Travertine limestones geochemistry found in Albertine Graben to these closest documented limestone found so far within DRC territory, would be ideal to guess their origin link. However, as shown in the figures VI.34 and VI.34 below, they are not good enough to be used for the case of this present study as a matching correlate or a comparator tool because they are not from Marine origin as those collected in East African Rift basin.

So, the need to find another comparator limestone rock sample which can be found in outcrop nearby the Albertine Graben pushed to run ICP-MS on Mandawa Basin limestones.

PROCOKIN & LYEMUBUZA REE+Y PATTERNS

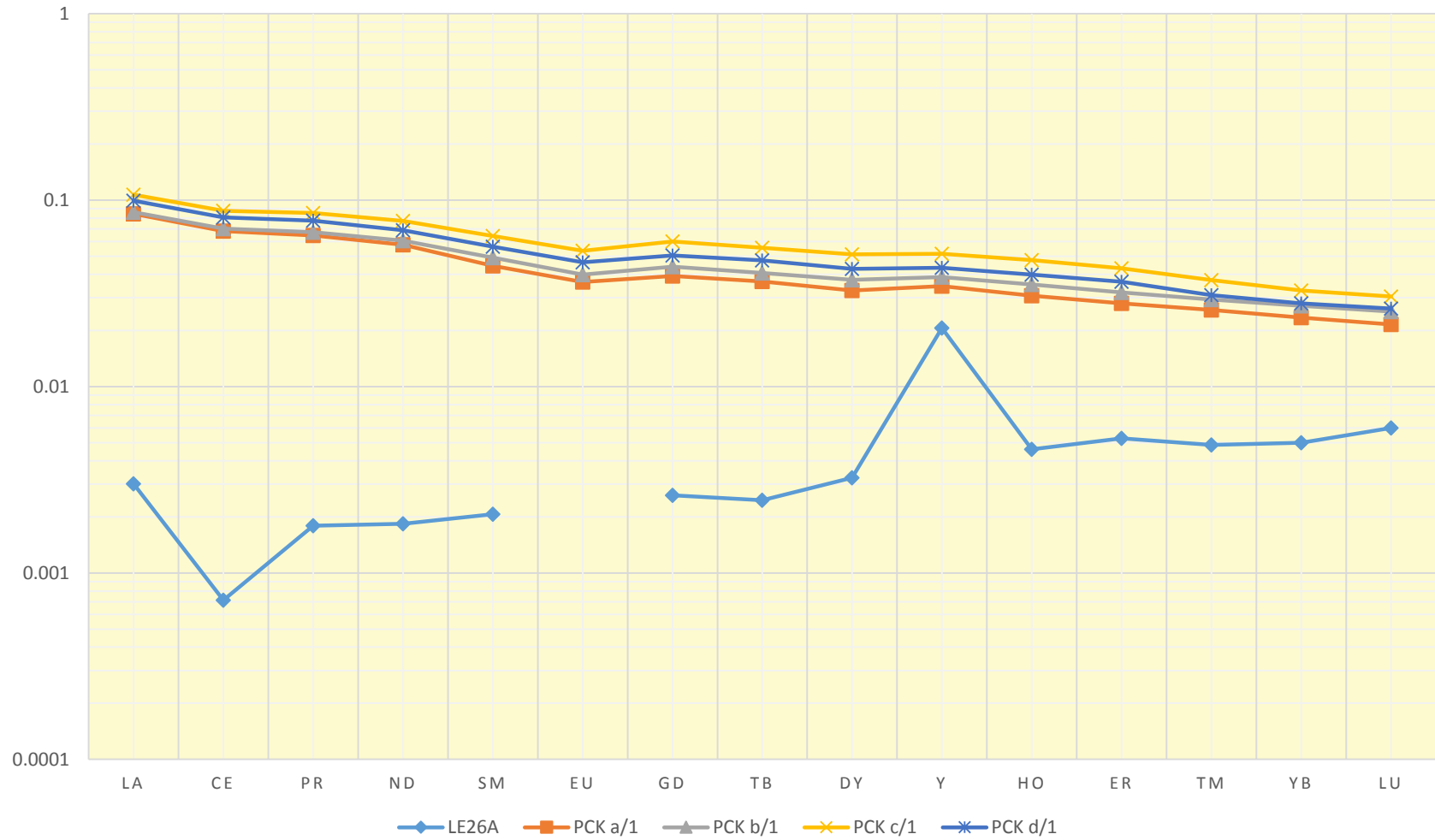


Figure VI.34: PCK & LE 26 REE +Y Patterns by ICP-MS

### PROCOKIN & LYEMUBUZA CORRELATION COEFFICIENT

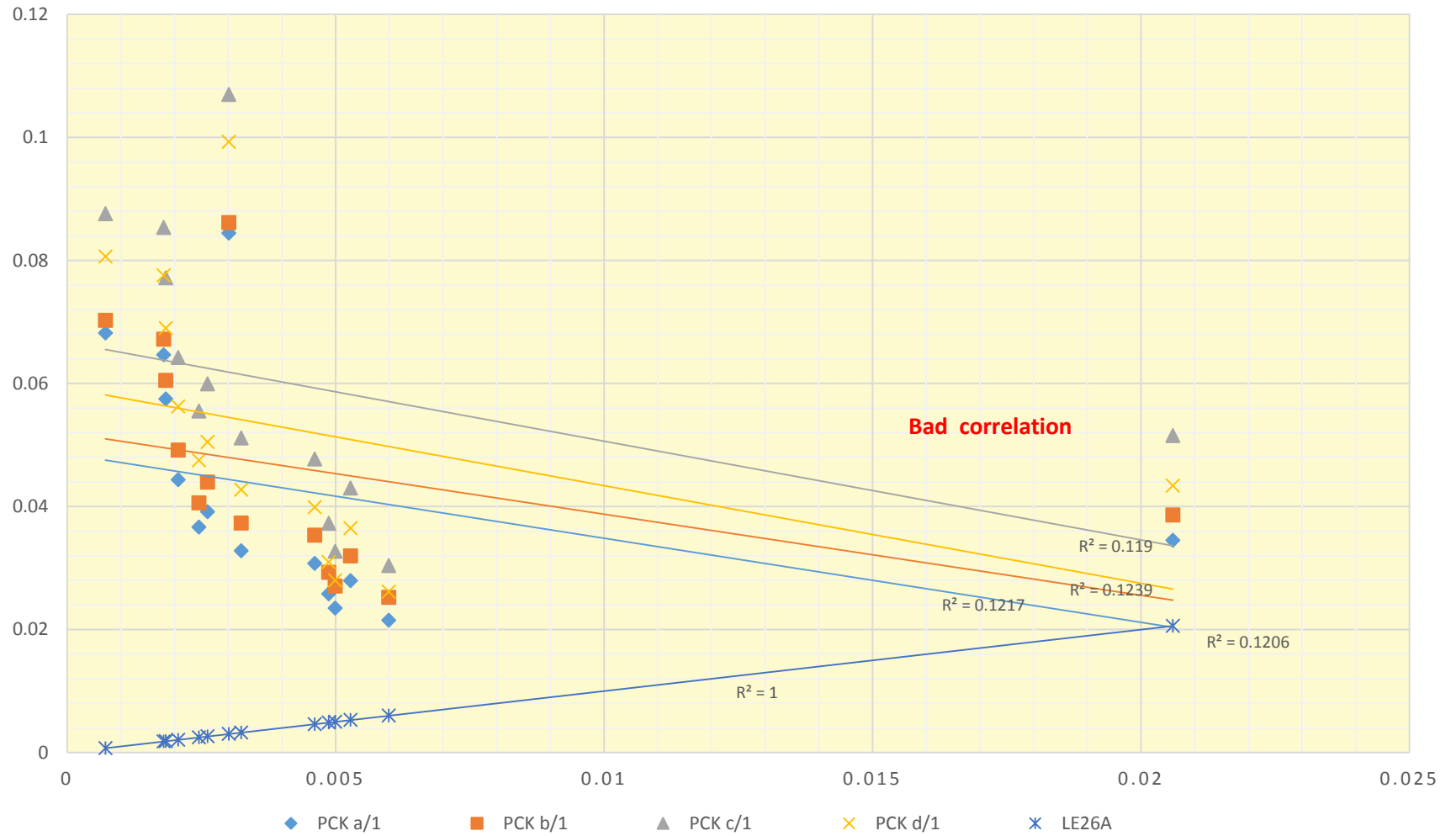


Figure VI.35 : PCK & LE 26 Coefficient Correlation

### ICP-MS 2018 : ALL SIGNATURES

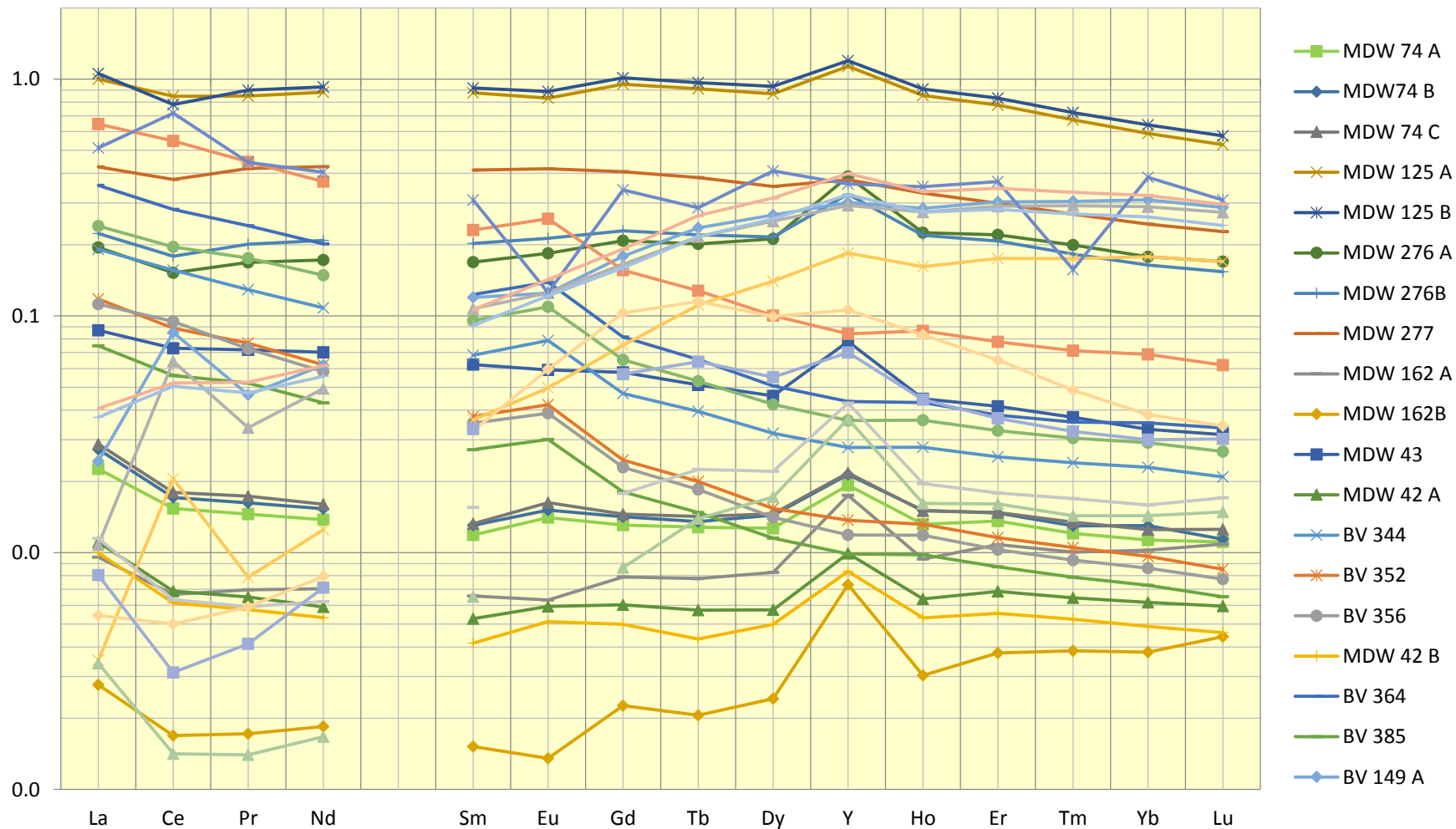


Figure VI.36: ICP-MS, 2018: All spectral signatures

VI.4.3.1- 2018 TRAVERTINE WITH CARBONATITES SIGNATURES

The results from the 2014 field samples found with Carbonatites signatures during the 2018 ICP-MS experiment are presented in Fig VI.35 below alongside with Fort Portal Carbonatites lavas as well as are lower illustrated in Fig. VI.36 their correlation coefficient  $R^2 > 0.95$  to the Fort Portal Carbonatites samples.

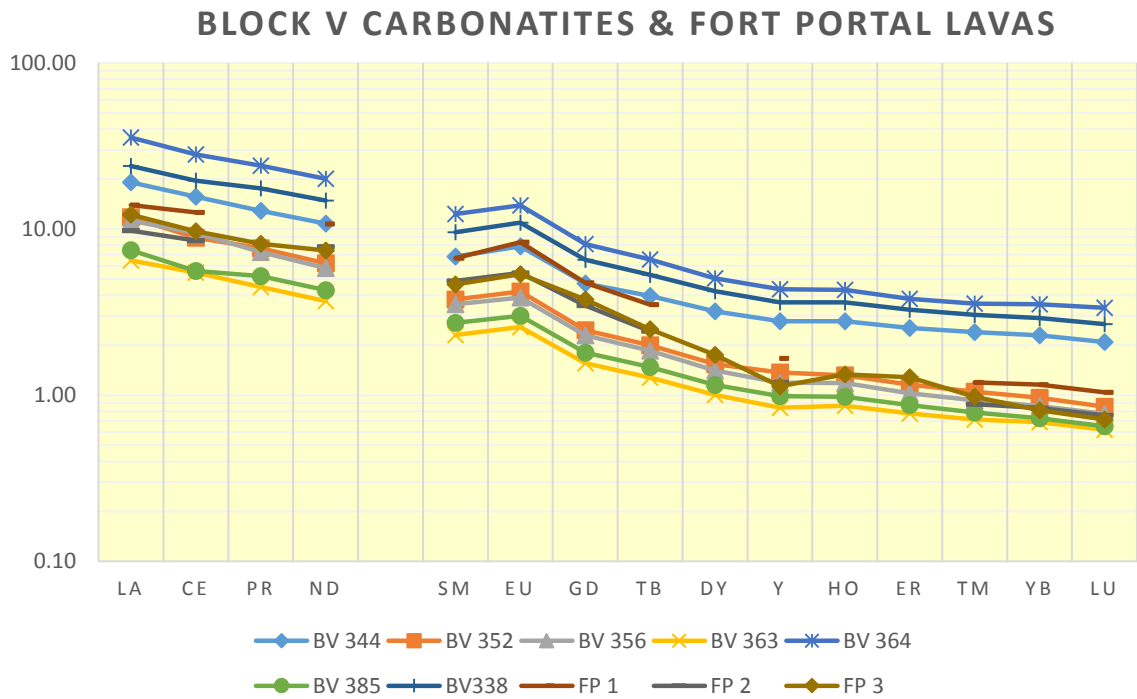


Figure VI.37: ICP-MS, 2018: Carbonatites signatures

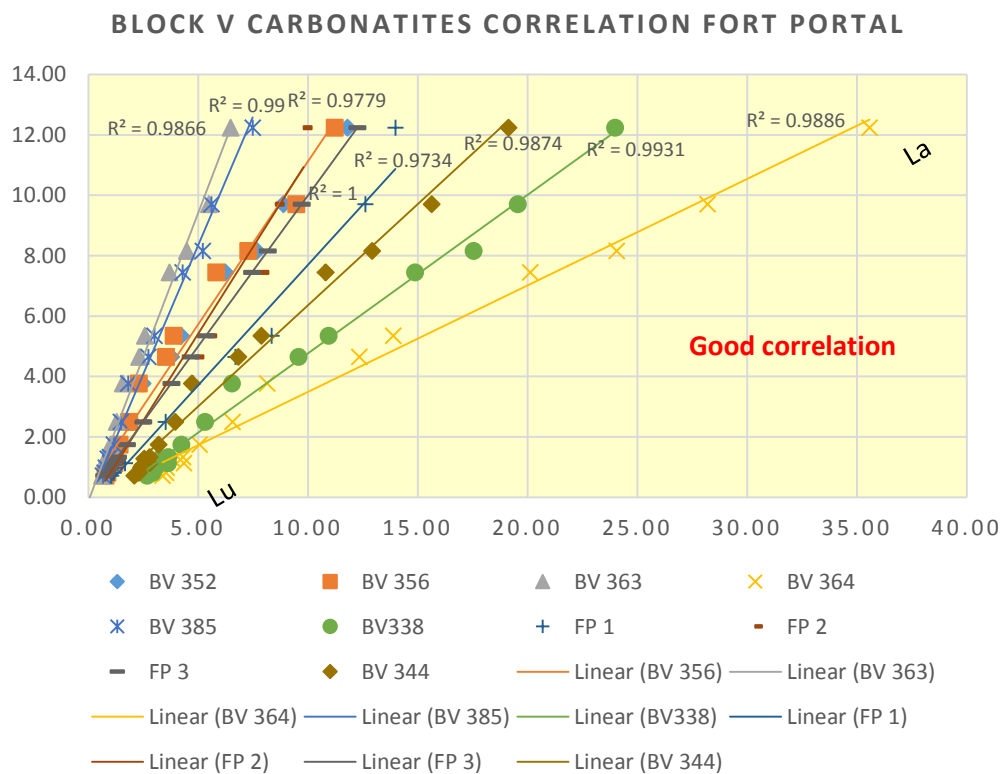


Figure VI.38: Bloc V Carbonatites signatures correlation coefficient with Fort Portal #3



VI.4.3.2- 2018 TRAVERTINE WITH MARINE LIMESTONES SIGNATURES

The 2018 Travertine Samples (fabrics, textures, structure and/or their replica) correlating with the known marine limestones (Mandawa Basin Tanzania, Holocene Marine, Modern Sea water, Devonian reef) with a Correlation Coefficient of  $R^2 > 0.75$ , are shown plotted alongside in the Figures below which illustrate comparisons of results experiments.

Additionally, a check box table of the Kamber’s paper Marine limestones key criteria has been set up for each Travertine with marine limestones spectral signature.

The table 7 below which help to check the marine origin criterias, suggest that some ones 2014 Bloc V field samples drilled regarding their textures, structures or fabrics have more Marine signatures involvement origin and some others don’t.

		BV 161 B		BV 162 A		BV 163 A		BV 164	
>1.1	La/La*	2.154878	YES	1.660919	YES	5.823986	YES	3.464977	YES
<0.8	Ce/Ce*	1.185219	NO	1.529005	NO	2.257441	NO	1.438689	NO
>1.1	Gd/Gd*	0.778326	NO	0.771417	NO	0.761166	NO	0.765242	NO
<< 1	Prn/Ybn	0.371749	YES	0.154034	YES	0.137344	YES	0.097544	YES
>40	Y/Ho	2.191354	NO	1.274174	NO	1.57862	NO	2.275306	NO

Table 6: Marine limestone criteria check box for the 2014 Bloc V field samples

All these samples have satisfied only two (2)) of the marine limestones criteria). These results which have been made from the 2018 MUQ raw, are presented in the

**BLOCK V (2018) & KNOWN MARINE LIMESTONE**

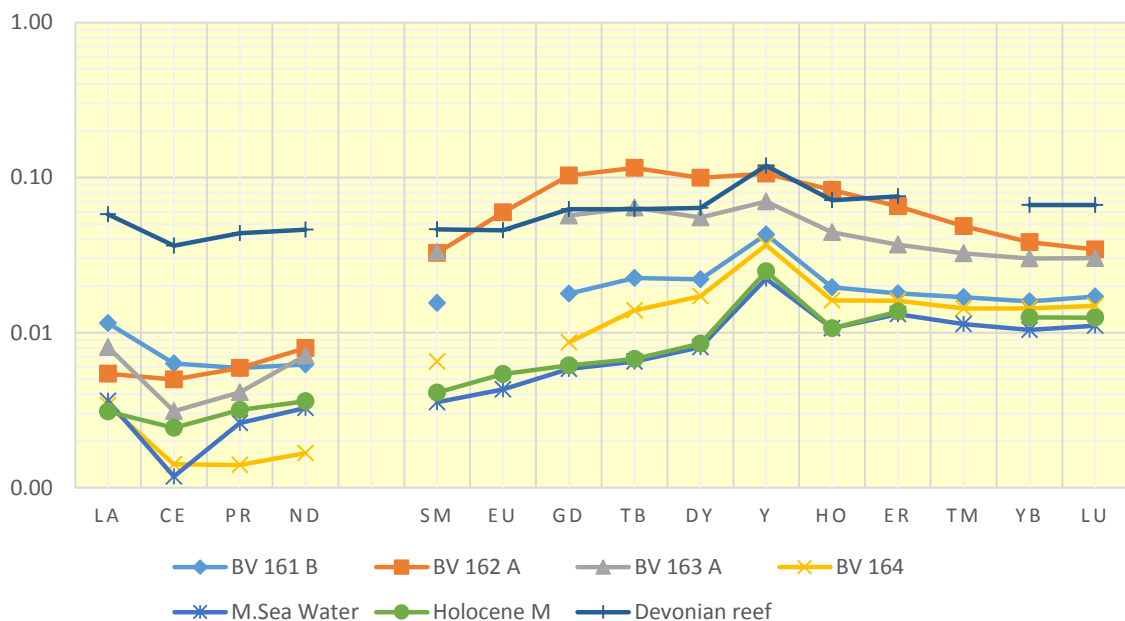


Figure VI.39: Bloc V 2014 Marine Limestones signatures by ICP-MS 2018

The Bloc V 2014 Travertine field Samples (fabrics, textures, structure and/or their replica) correlating with the known marine limestones (Mandawa Basin Tanzania, Holocene Marine, Modern Sea water, Devonian reef) with a Correlation Coefficient of  $R^2 > 0.85$ , are shown plotted alongside in the Figure VI.38 below:

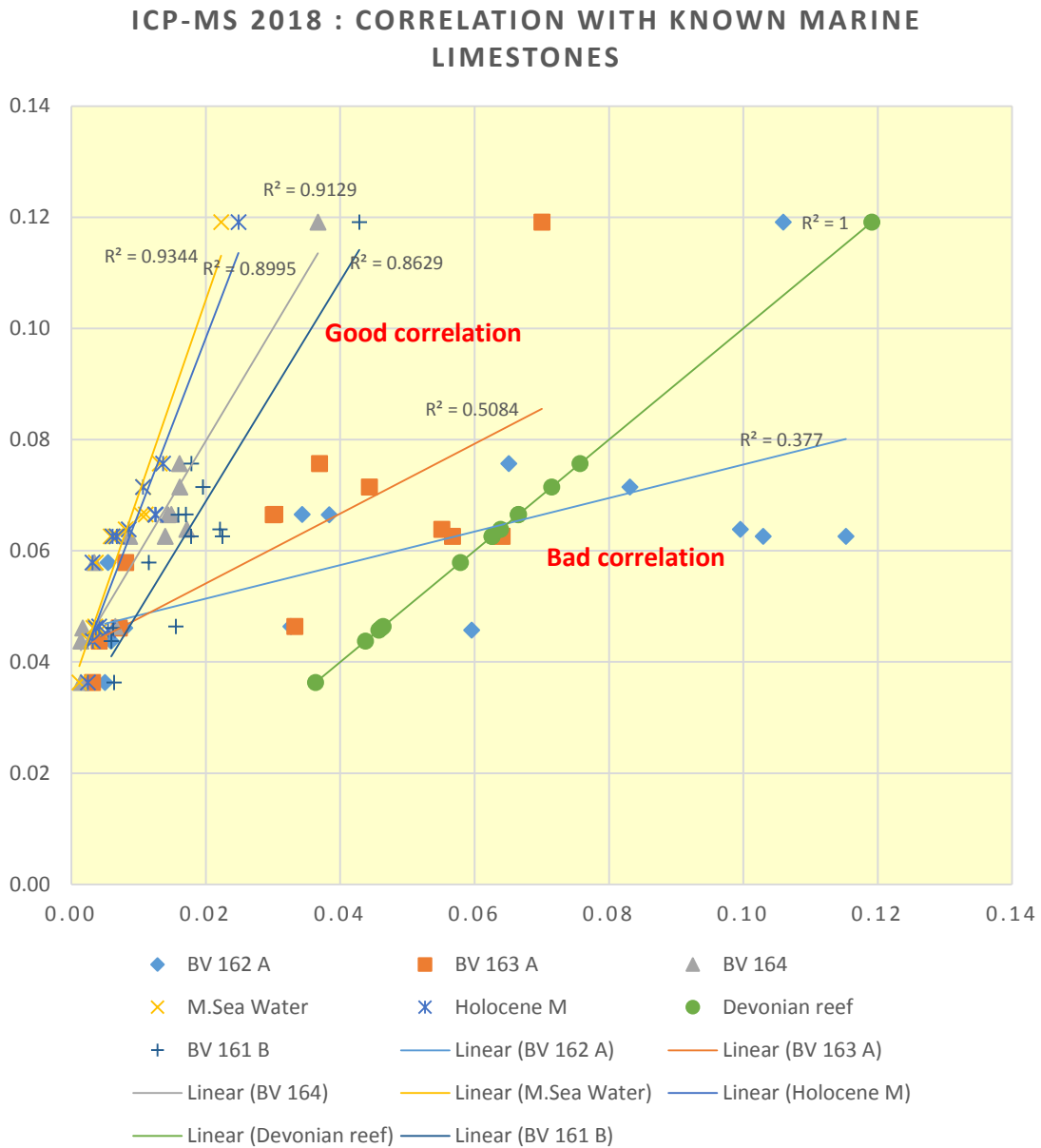


Figure VI.40: Bloc V 2014 Marine Limestones Correlation coefficient with Devonian Reef

This above graph shows clearly that samples BV 161 and 164 have marine limestones signatures correlating with Devonian Reef while clearly it's discriminating the samples BV 162 and BV 163 collected in the field few meters around in the same gorge (Katanda)

The ICP-MS results of the 2018 experiment have produced the elements concentrations in ppb and normalized in MUQ as per Kamber experiment method. These values are presented in the tables in appendix 2 and their original excel files enclosed to this thesis in a memory stick.

The Figures VI.39 to VI.44 below show the REE pattern graph of all Msc. ICP-MS marine limestones signatures and their respective correlation coefficient  $R^2 > 0.80$  with Devonian reef.

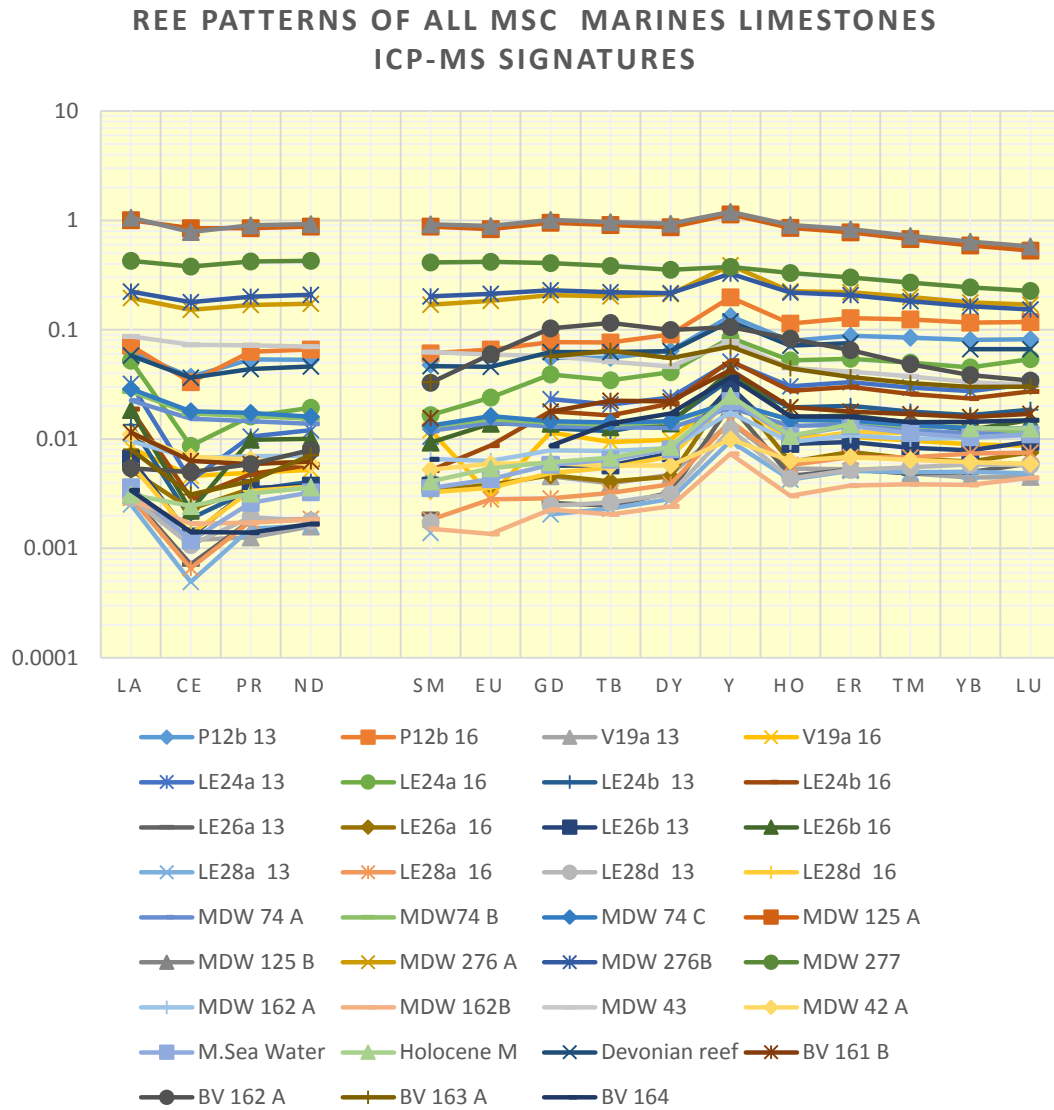


Figure VI.41: REE patterns of all Marine Limestones signatures detected by ICP-MS from 2013 to 2018

### ALL MSC MARINE LIMESTONES CORRELATION COEFFICIENT

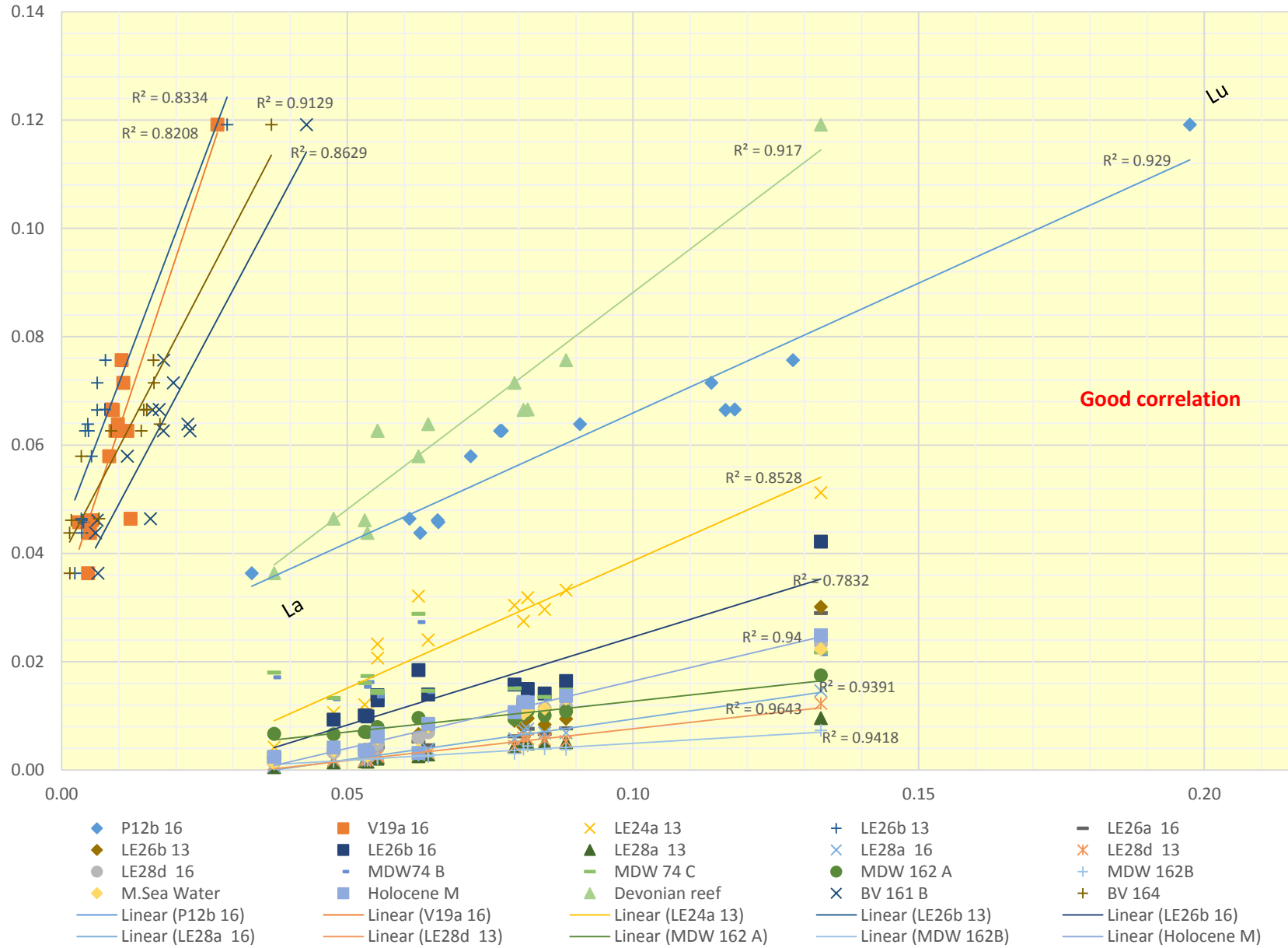


Figure VI.42: All Marine Limestones Correlation coefficient with Devonian Reef

### REE PATTERNS OF ALL MSC MARINE & PUBLISHED LIMESTONES ICP-MS SIGNATURE

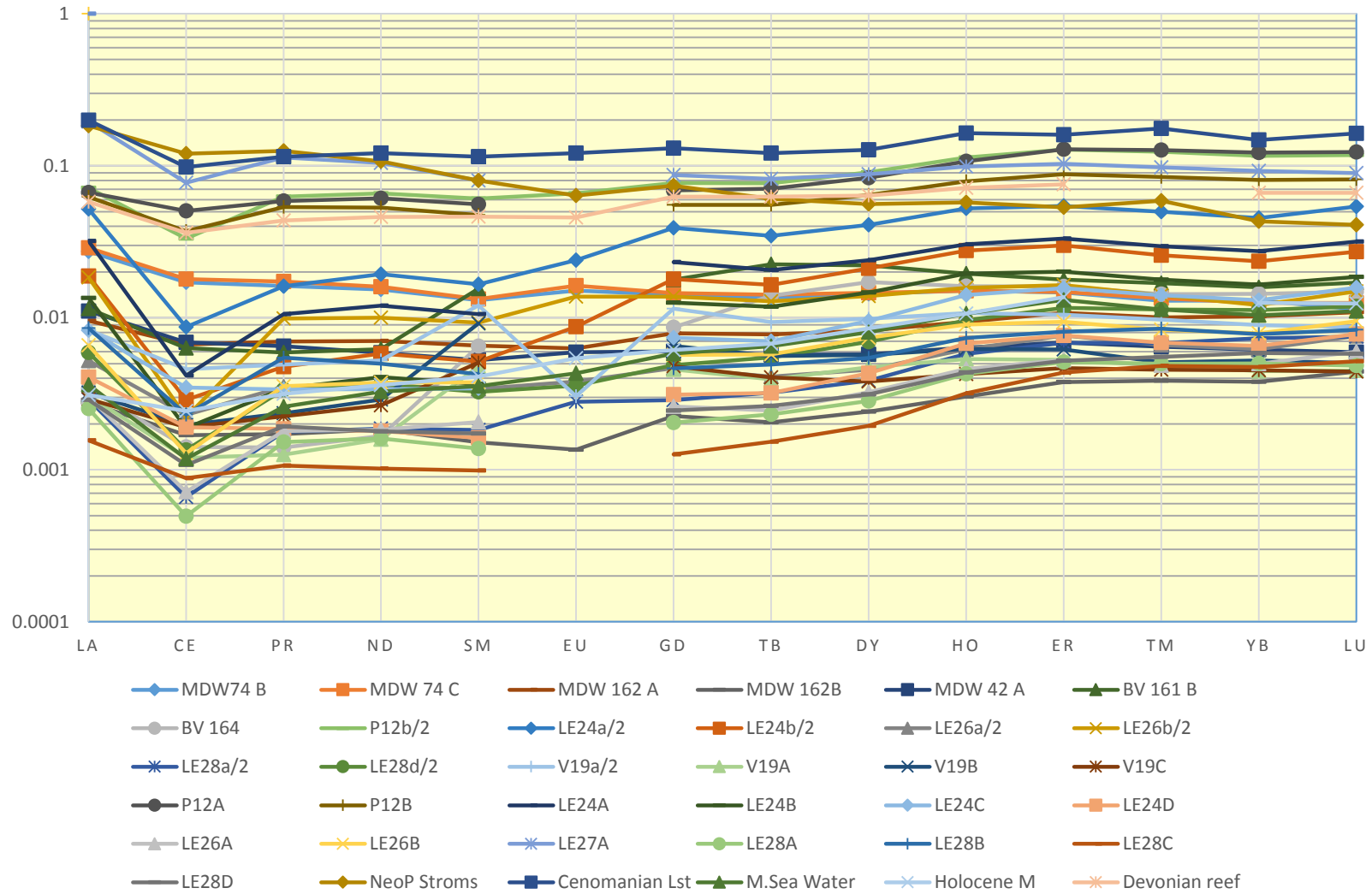


Figure VI.43: REE patterns of all Marine Limestones signatures detected by ICP-MS from 2013 to 2018 & published marine limestones

## CORRELATION COEFFICIENT OF 2013 MARINE LIMESTONES EXPERIMENTS, CENOMANIAN LIMESTONES AND NEOPROTEROZOIC STROMATOLITHES WITH DEVONIAN REEF

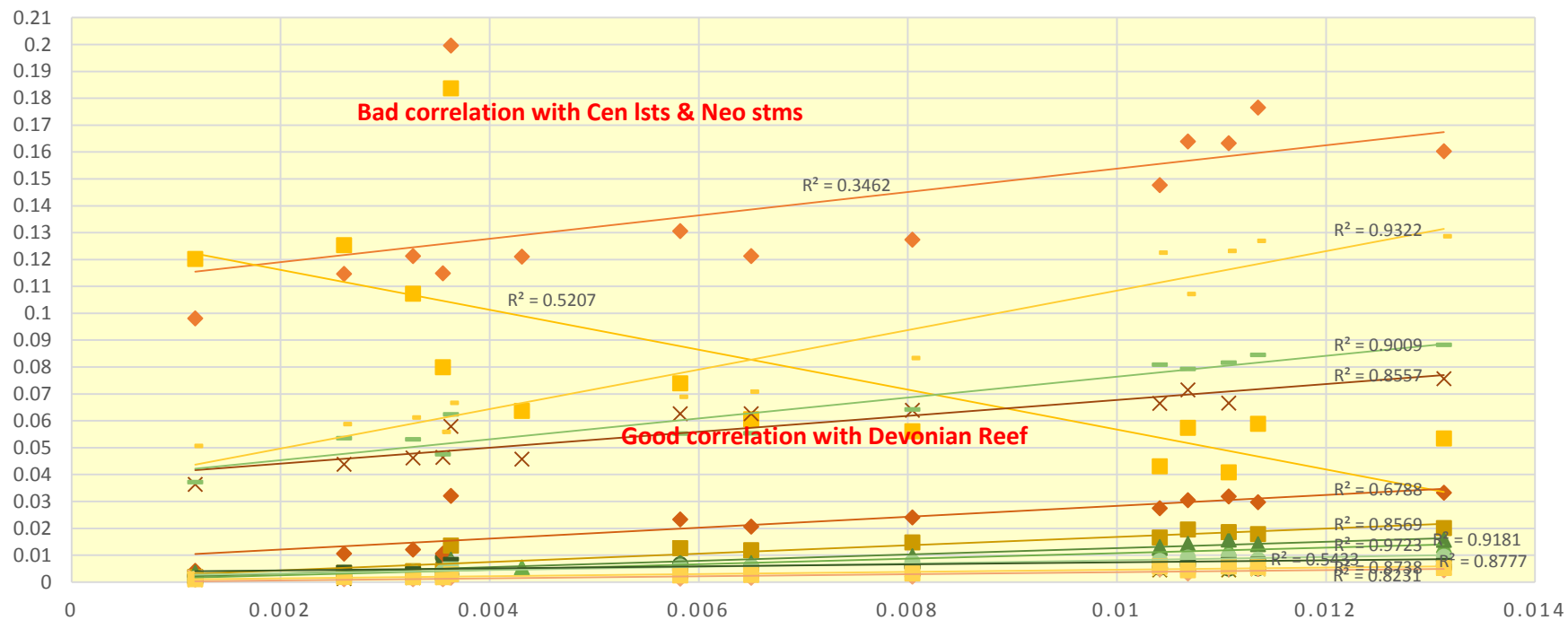
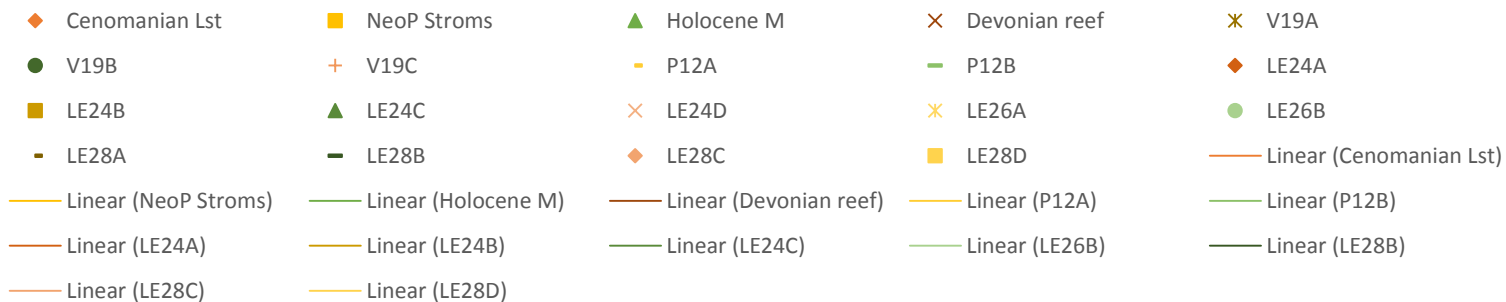


Figure VI.44: Correlation coefficient of 2013 marine's limestones experiments, Cenomanian limestones and Neoproterozoic stromatolites with Devonian reef.

## CORRELATION COEFFICIENT OF 2016 MARINE LIMESTONES EXPERIMENTS, CENOMANIAN LIMESTONES AND NEOPROTEROZOIC STROMATOLITHES WITH DEVONIAN REEF

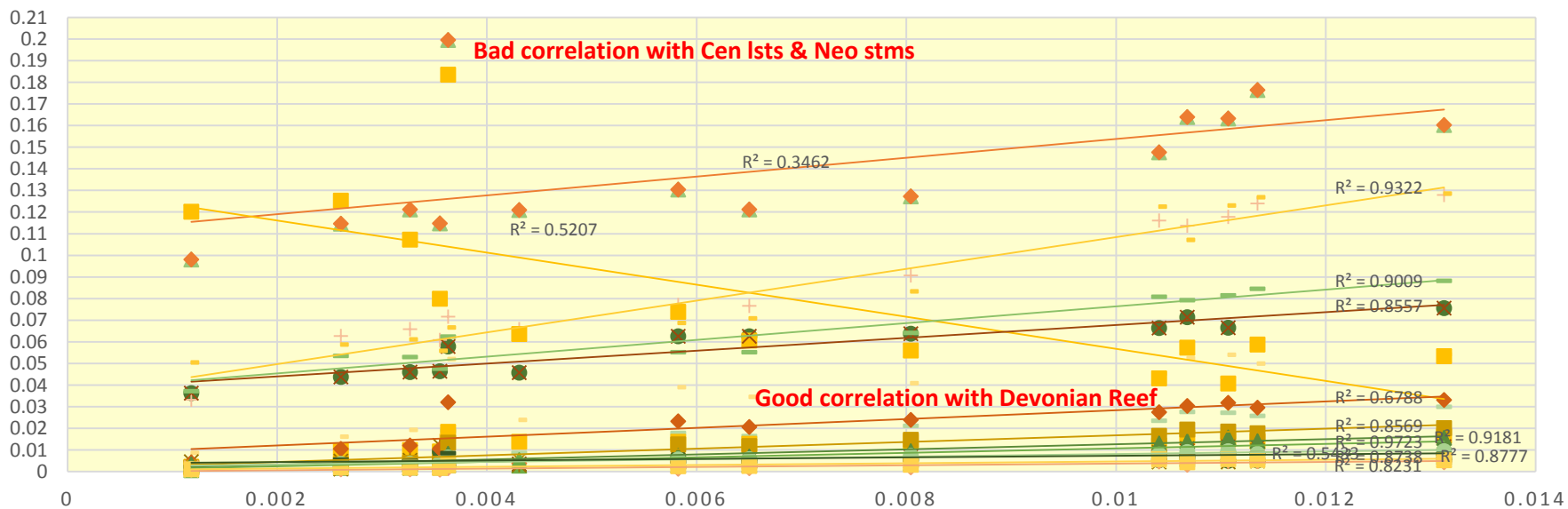
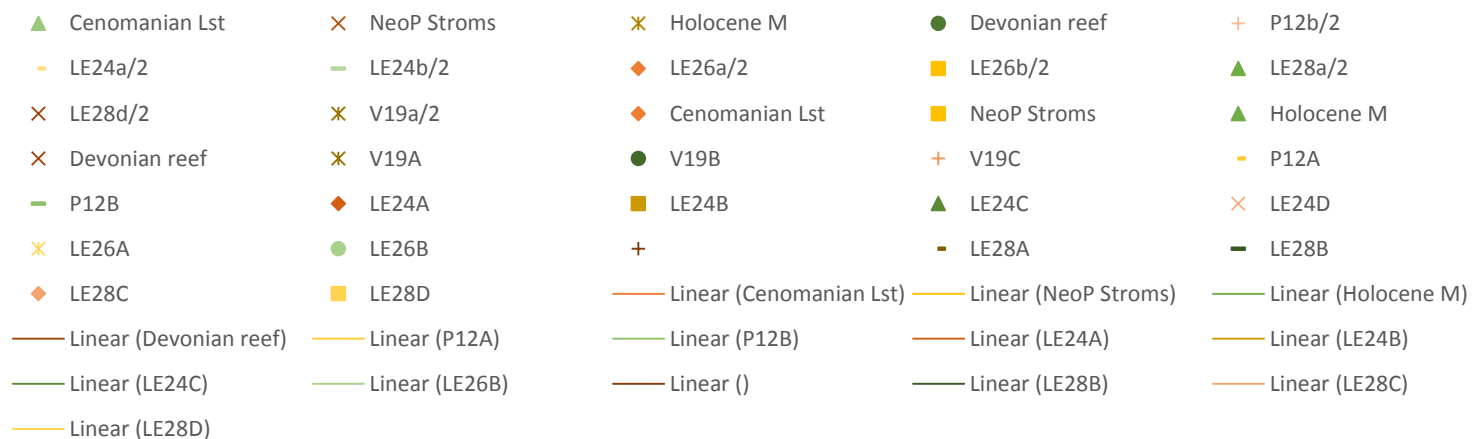


Figure VI.45 Correlation coefficient of 2016 marine's limestones experiments, Cenomanian limestones and Neoproterozoic stromatolites with Devonian reef.

## CORRELATION COEFFICIENT OF 2018 MARINE LIMESTONES EXPERIMENTS, CENOMANIAN LIMESTONES AND NEOPROTEROZOIC STROMATOLITHES WITH DEVONIAN REEF

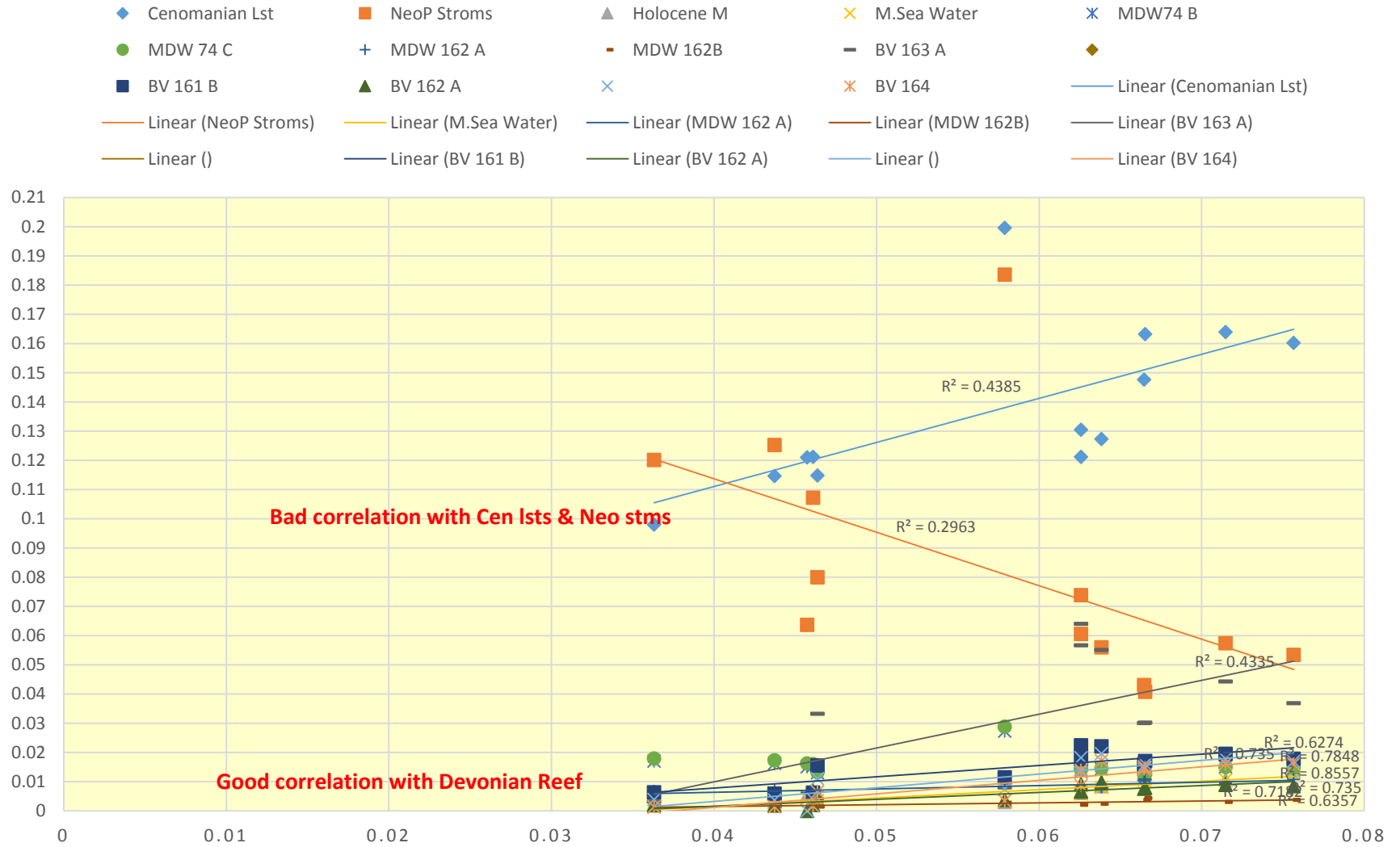


Figure VI.46: Correlation coefficient of 2016 marine's limestones experiments, Cenomanian limestones and Neoproterozoic stromatolites with Devonian reef.



VI.4.3.2. A- MANDAWA BASIN

12 Samples collected from the Mandawa basin have been drilled anyway regardless any structures textures / fabrics. Their resulted MUQ values are presented in the enclosed ICP\_MS 2018 Excel file.

The table 6 below which help to check the marine origin criterias, suggest that some ones Mandawa samples drilled anywhere regardless their textures, structures or fabrics have more Marine signatures involvement origin and some others don't.

		MDW 74 A	MDW74 B	MDW 74 C	MDW 125 A	
<b>Y/Ho</b>	>40	1.464249325	1.417060269	1.44541142	1.328873324	NO
<b>La/La*</b>	>1.1	1.390040154	1.502736134	1.426742804	1.262298878	YES
<b>Ce/Ce*</b>	<0.8	1.185218824	0.940697888	0.889180228	1.067263955	NO
<b>Gd/Gd*</b>	>1.1	1.007091911	1.11449575	1.05275512	0.997297002	YES
<b>Prn/Ern</b>	<< 1	1.068561526	1.10490484	1.171038765	1.09286449	NO

		MDW 162B	MDW 43	MDW 42 A	MDW 125 B	
<b>Y/Ho</b>	>40	2.41541563	1.74105218	1.556907429	1.317345028	NO
<b>La/La*</b>	>1.1	1.858908106	1.151967364	1.401107236	1.251236675	YES
<b>Ce/Ce*</b>	<0.8	1.136103665	0.968169275	0.870740649	0.924284767	YES
<b>Gd/Gd*</b>	>1.1	1.295522052	1.013696268	1.053472317	1.009120174	YES
<b>Prn/Ern</b>	<< 1	0.455385923	1.732430997	0.94878573	1.081120978	YES

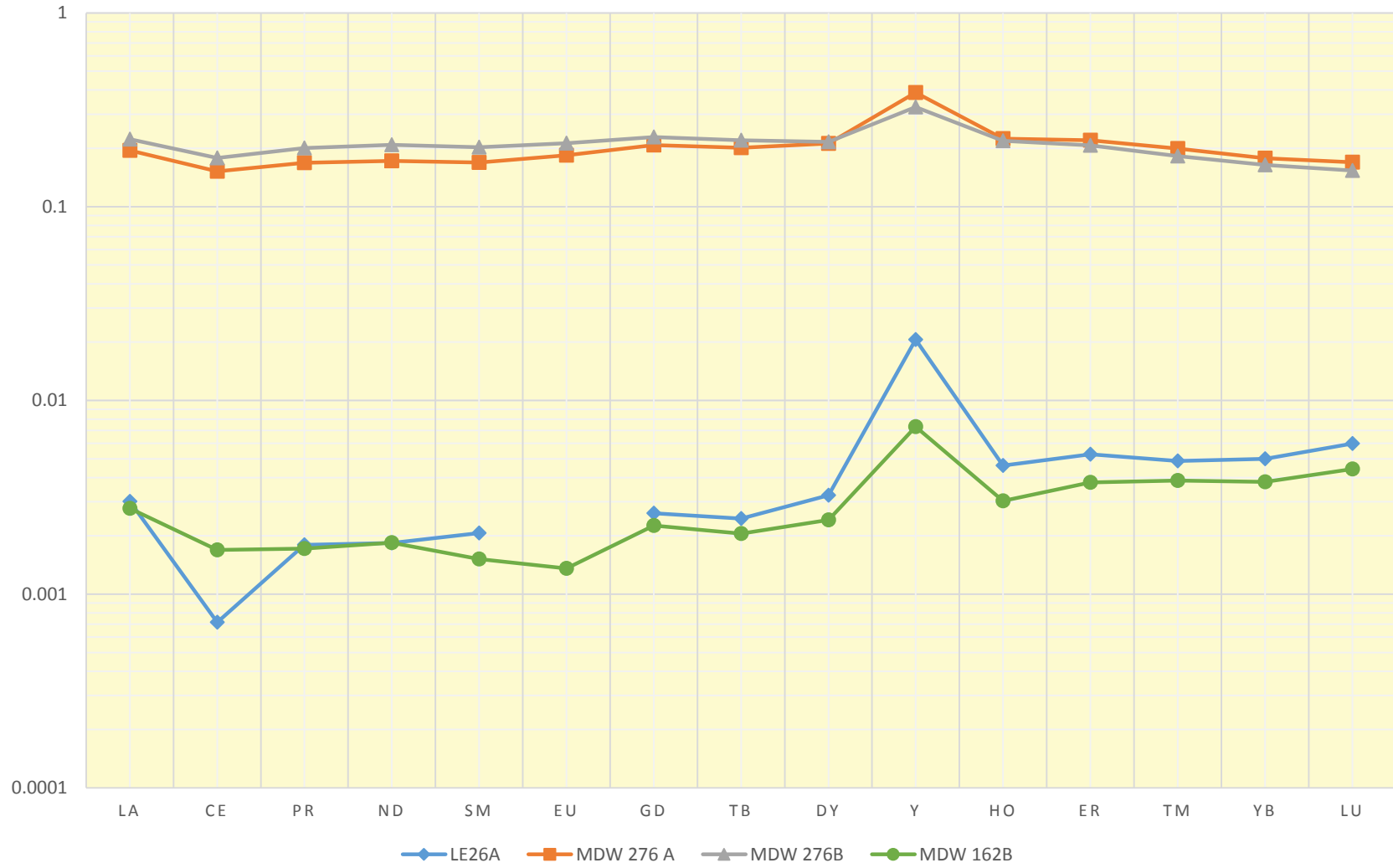
		MDW 276 A	MDW 276B	MDW 277	MDW 162 A	
<b>Y/Ho</b>	>40	1.725870939	1.49369084	1.13811642	1.856451681	NO
<b>La/La*</b>	>1.1	1.213272103	1.19539257	1.05197194	1.401416525	YES
<b>Ce/Ce*</b>	<0.8	0.94734948	0.95618783	0.93056389	0.975616616	NO
<b>Gd/Gd*</b>	>1.1	1.085927382	1.01730623	0.97258153	1.078965793	YES

Table 7: Marine limestone criteria check box for the Mandawa samples

Seven (7) in blue from 12 samples have satisfied at least three (3) of the marine limestones criteria) while five (5) in red haven't. These results which have been made from the 2018 MUQ raw, are presented in form of comparative Charts enclosed to this Msc in an Excel file. The Mandawa samples shows a clearly marine limestone origin as confirmed in the existing literature.

Both Lyemubuza and Bloc V Travertine Samples (fabrics, textures, structure and/or their replica) REE values correlating with the known marine limestones Mandawa Basin Tanzania with a Correlation Coefficient of  $R^2 > 0.75$  are shown plotted alongside in the Figures VI. 45, VI.46, VI.47 and VI.48 below:

### MANDAWA BASIN & LYEMUBUZA REE+Y PATTERNS



*Figure VI.47: Mandawa Basin & LE 26 REE+Y Patterns*

## MANDAWA BASIN & LYEMUBUZA CORRELATION COEFFICIENT

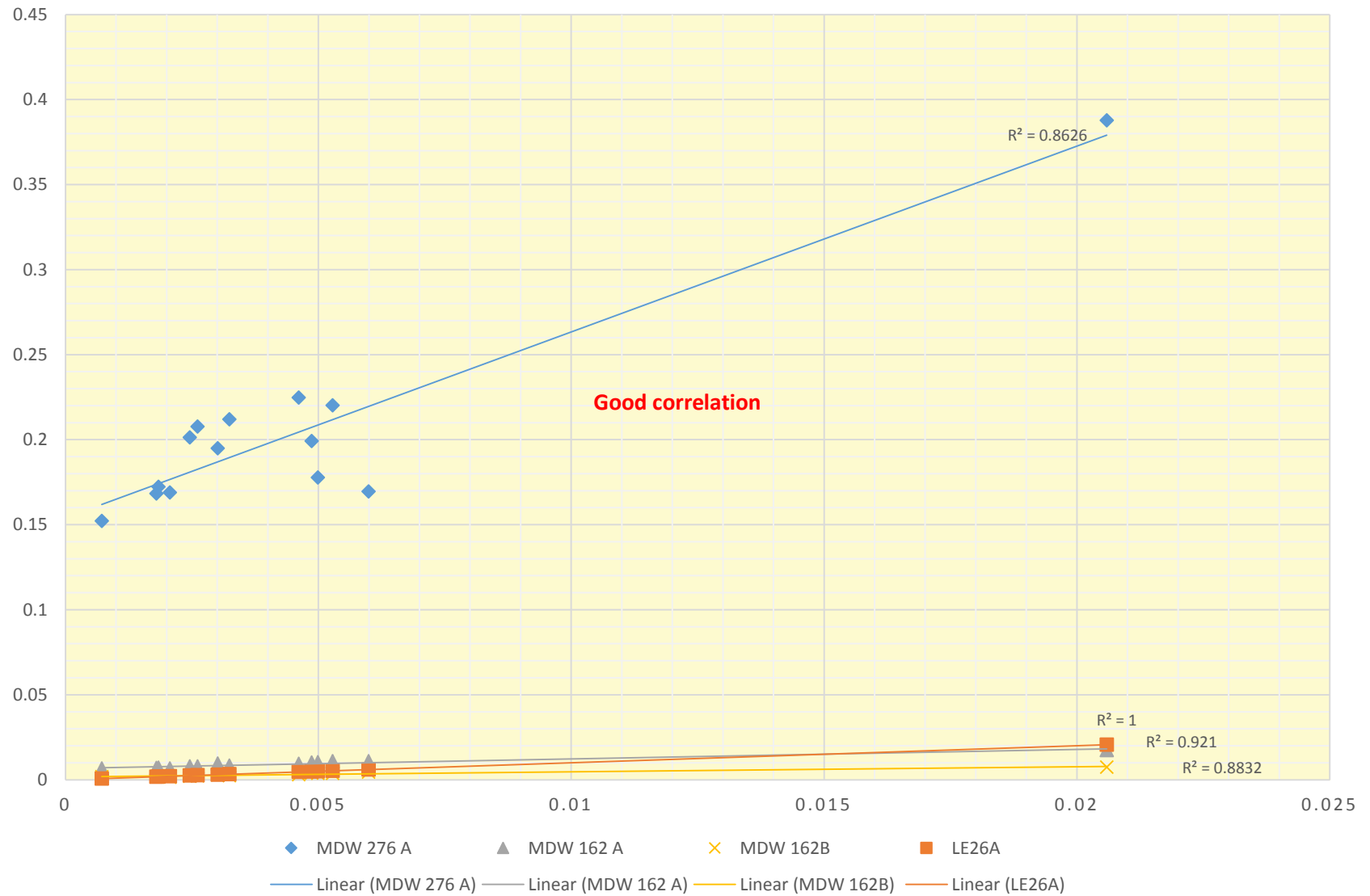


*Figure VI.48: Mandawa Basin & LE 26 correlation coefficient*

### MANDAWA BASIN AND BLOC V REE + Y PATTERNS

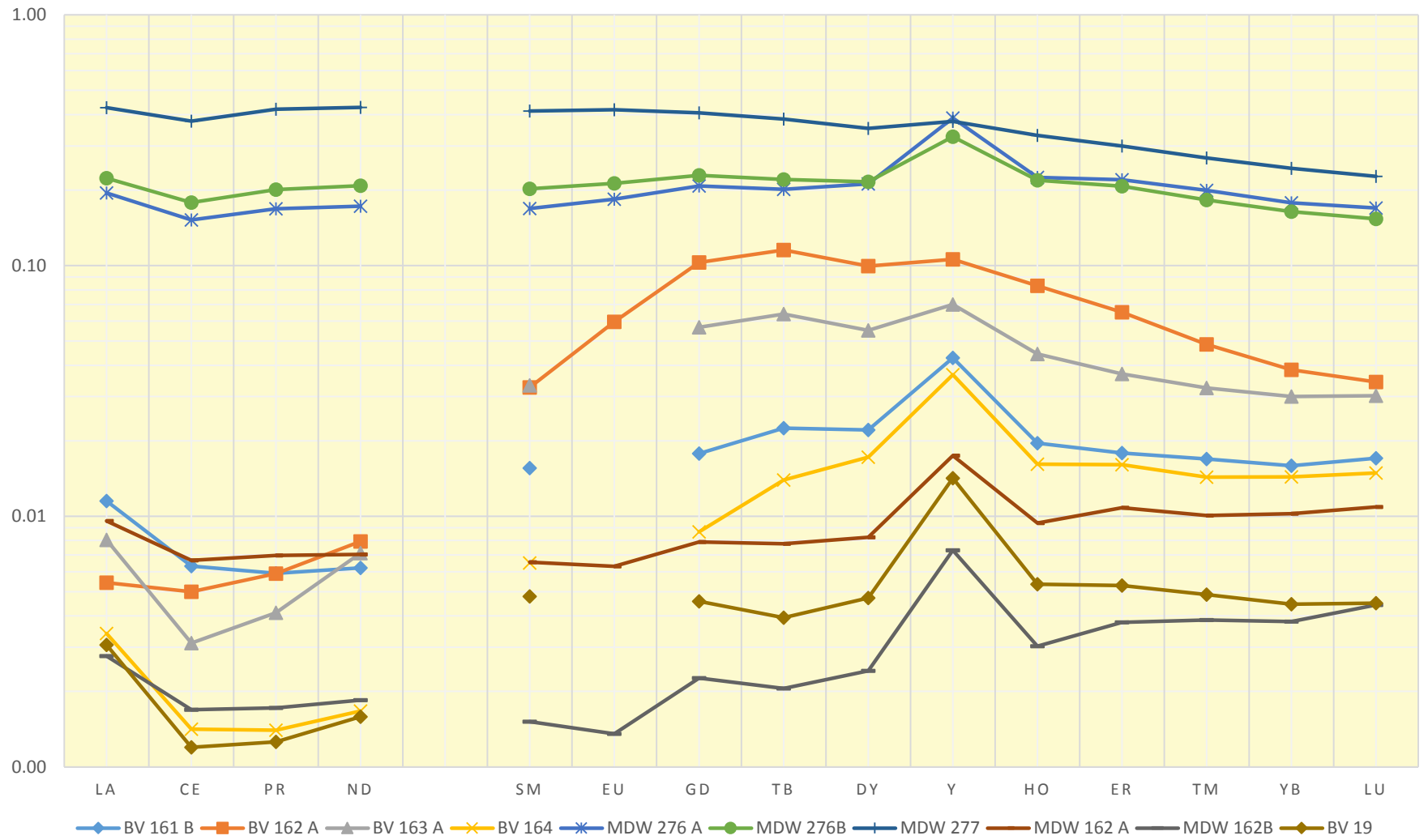


Figure VI.49 : Mandawa Basin & Bloc V REE+Y Patterns

## CORRELATION COEFFICIENT OF MANDAWA BASINS AND BLOC V

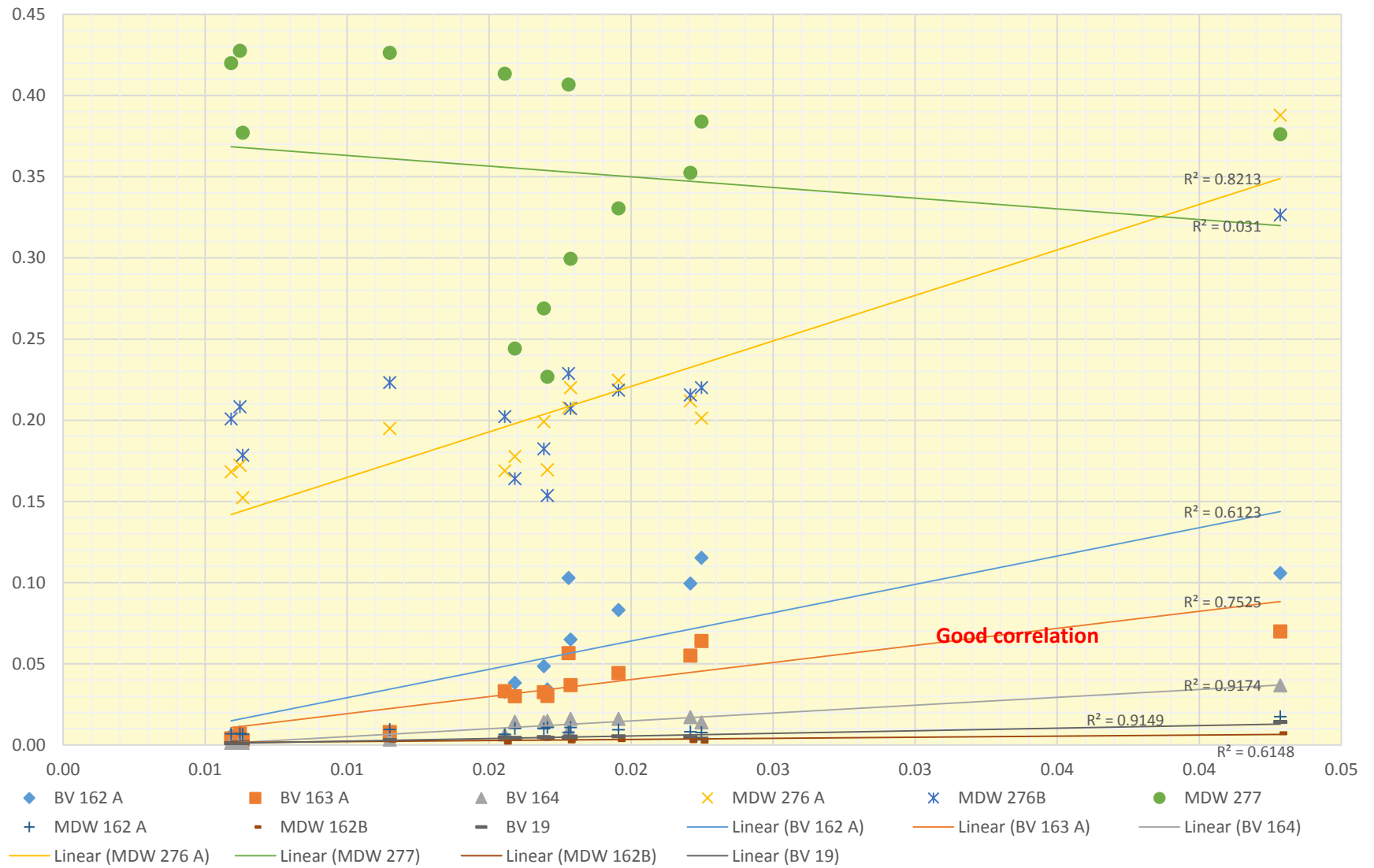


Figure VI.50 : Mandawa Basin & Bloc V Correlation Coefficient

VI.4.3.3- 2018 TRAVERTINE WITH HYBRIDE LIMESTONES SIGNATURES

Samples BV 149,150 and 159 have given different results far from either Carbonatites or Marine limestones signatures. They gave spectral signatures in Figure VI.43 below showing a decreasing the light rare earths Lanthanum, cerium, praseodymium, neodymium, promethium, and samarium and an increasing the "heavy rare earths" Yttrium, europium, gadolinium, terbium, dysprosium, holmium, erbium, thulium, ytterbium, and lutetium. Respective correlation with Marine limestones and Fort Portal are presented in Figures VI.47, 48, 49 and VI.50 below

**ICP-MS 2018: HYBRID SIGNATURES**

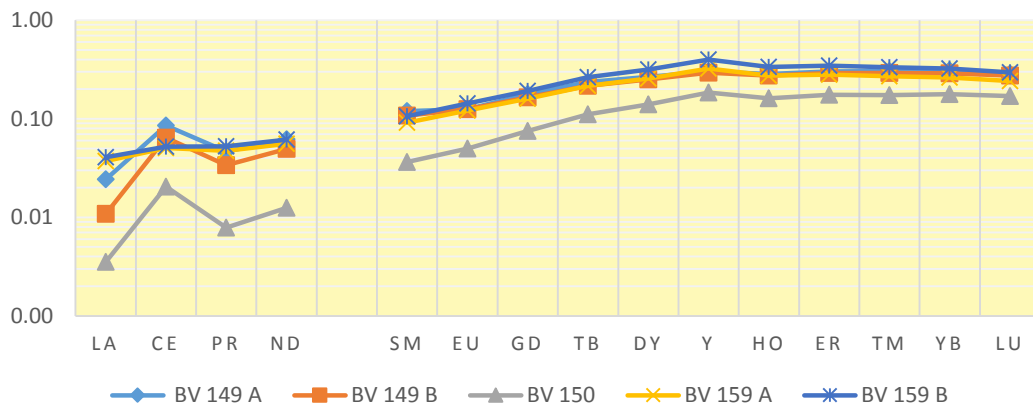


Figure VI.51 : Bloc V 2014 Travertine Hybrid signatures by ICP-MS 2018

**ICP-MS 2018 MARINE & HYBRIDE SIGNATURES**

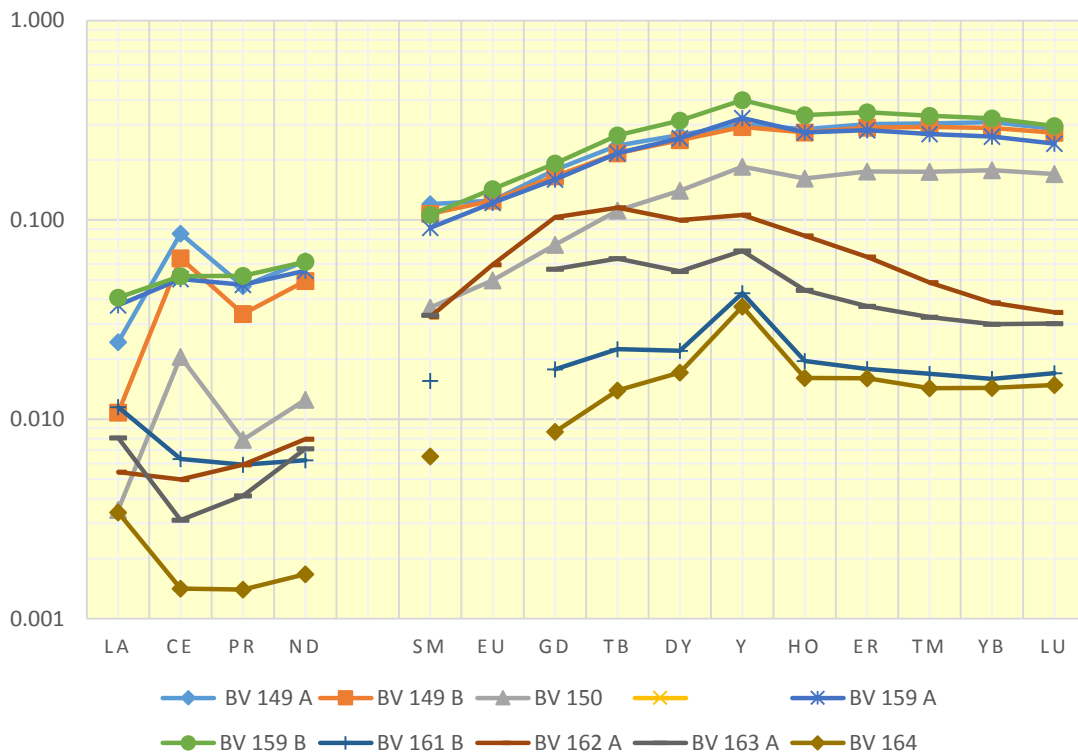


Figure VI.52 : Bloc V 2014 Hybrid and Marine Limestones signatures by ICP-MS 2018

### HYBRID SAMPLES CORRELATION WITH DEVONIAN REEF

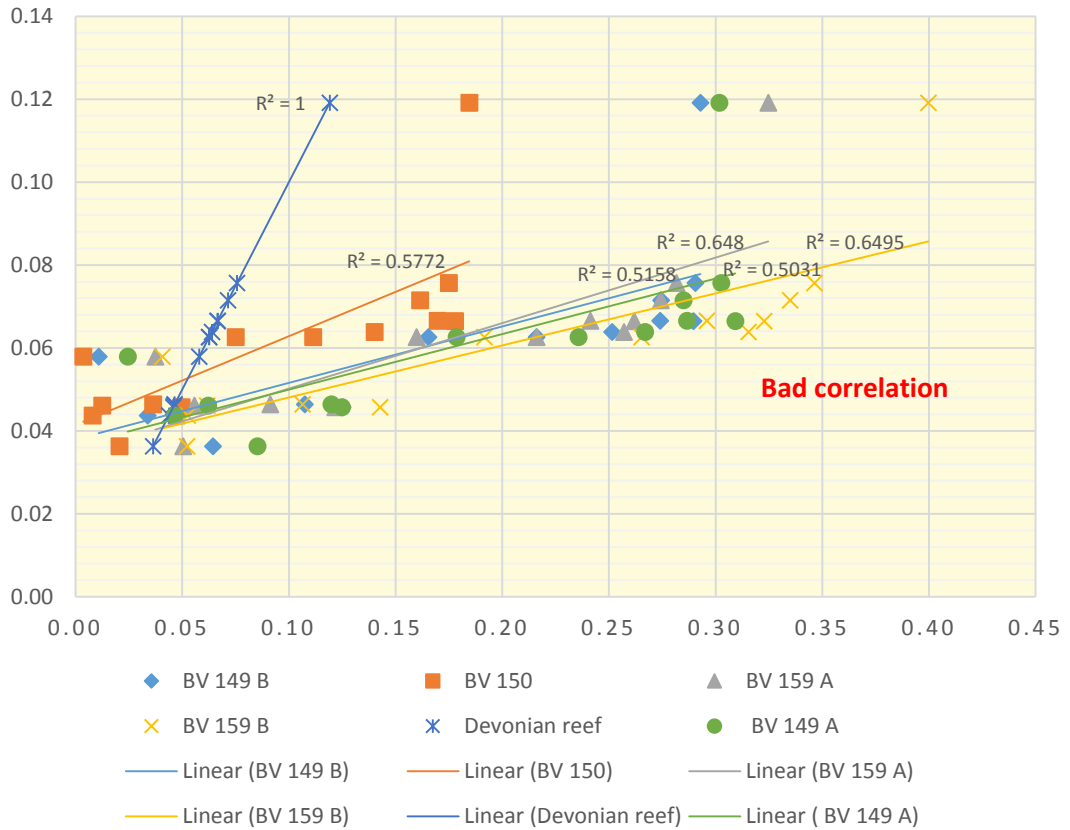


Figure VI.53 Bloc V 2014 Hybrid Correlation coefficient with Devonian Reef

### HYBRID SAMPLES CORRELATION WITH FORT PORTAL

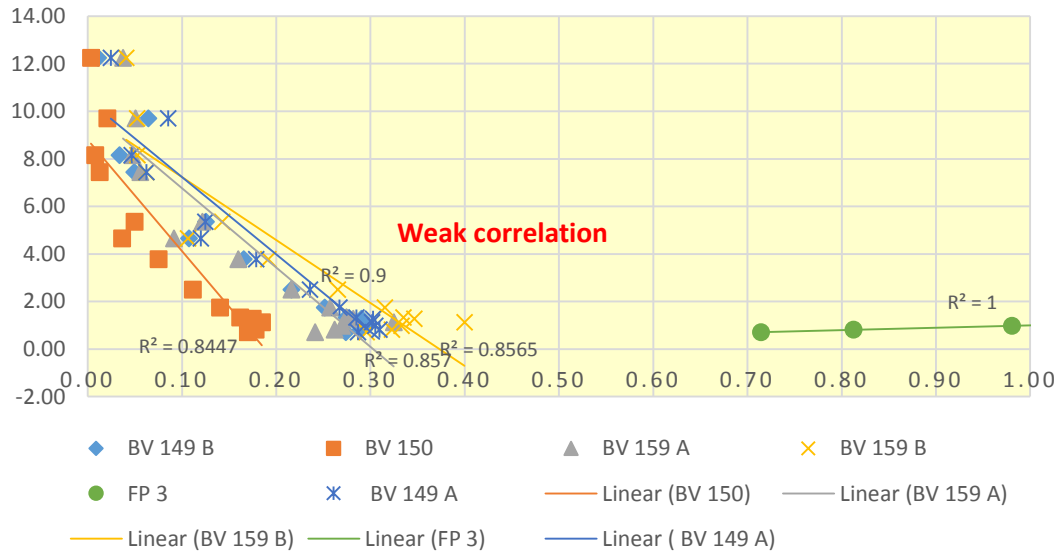


Figure VI.54 : Bloc V 2014 Hybrid Correlation coefficient with Fort Portal Carbonatites #3

## Chapter 6 Conclusion

*The geochemistry analysis results obtained by the research methodology have been presented in tables, graphs and figures as below:*

- *The stable Carbon (PDB) and Oxygen (SNOW) signatures and Strontium isotopic ratio in order to define respectively the level of isomerism and aromatisation of their carbonates biomarkers and their palaeoclimate.*
- *Edward Lake offshore Oil slicks samples analysed by Gas Chromatography Mass Spectrometry and which results have been compared with the onshore Oil stains found in Travertines cavities described and collected in Lyemubuza and Muhokiya quarries located in Edward Lake onshore in Uganda. These results comparison suggested these offshore Oil slicks and onshore Oil stains origin as from a marine shale source with a waxier, lacustrine component.*
- *Around 50 Travertines samples described and collected throughout the Eastern Africa Rift System went through the ICP-MS experiments which processed well for all samples.*
- *The ICP-MS process gave in output the REE+Y concentrations in ppb normalised in MUQ as per Balz Kamber similar experiments in 2014.*
- *The EARS ICP-MS results presented REE spectral signatures graphs per their respective geochemical origin and correlation coefficient charts with Fort Portal lavas for Carbonatites signature and with Devonian reef limestones for marine signature.*
- *EARS Travertines marines' limestones correlations with Cenomanian limestones referring to the Mesozoic Karoo and Neoproterozoic stromatolites associated to the west Congo schisto-Calcaire have been done in order to discriminate definitively the marine source of their bicarbonate.*

*The next Chapter, named Results discussion, shows how our Msc research study used these above geochemistry results to solve the geologic answer of the possible carbonate origin of these Travertines samples in the siliclastic classical Eastern Africa Rift System.*

*This Chapter relates to the reader our personal thoughts and interpretations on the obtained geochemistry results based on scientific facts that we noted all along the previous sections of this present Msc research study.*



## CHAPTER 7: RESULTS DISCUSSIONS

### VII.1 – FIELD TRIP RESULTS

The field trip outputs are the starting point of this MSc research study's discussions and interpretations. Different travertine lithofacies and/or lithofacies associations have been observed in the field and documented in Chapter IV. Each of these field observations have opened the way to many venues for further discussions and interpretations with respect to the Eastern African Rift System (EARS), our MSc research study's zone of interest.

The classical depositional framework of the Eastern African Rift System is generally dominated by clastic sediments among which fluvial and lacustrine environments have been the most commonly observed, documented and collected in the field during the recent geologic campaigns undertaken in the Eastern African Rift basin.

The above described (fluvial/lacustrine) deposit field evidences have confirmed their respective lithologies known from the existing literature, varying from conglomerates through sandstones to mudstones, cherts, oil shales and coals (Selley, 1982).

The distribution, orientation and internal geometry of these fluvial/deltaic deposits are controlled by many factors including climate, water discharge, sediment load, river mouth processes, waves, tides, currents, winds and the tectonics and geometry of the receiving basin (Selley, 1978).

Fluvial sediments are randomly located in the entire Eastern African Rift System. They are mostly dominated by sandstones, conglomerates, siltstones and interbedded sandstones. Lacustrine package outcrops were also clearly identified in many locations in the field. They are composed of siltstones, clay stones and thin clay layers in interbedded sandstones.

Moreover, many travertines occurrences have been found outcropping in the field, often associated with a biotype of flowing waters with high calcium content. The development of such carbonates might result from low-Mg calcite precipitation by cyanophytes, prokaryotes, eukaryotes, diatoms, bryophytes, tracheophytes and other bacteria (Pentecost, 2005).

During exceptionally rainy seasons, floodplain inundation promoted the seasonal growth of diverse environments ranging from fluvio-lacustrine basins to hydrothermal settings in which the above-mentioned travertine carbonates have been found biologically precipitated. They represent a particular continental carbonate facies providing an important source of geological data through their natural gamma radiations (GR) which were used in this MSc research field trip's discussion to provide evidence for carbonates' hydrological and physico-chemical deposit conditions.

The natural gamma radiations in sedimentary rocks are almost entirely attributable to Potassium and isotopes from the Uranium and Thorium families. Some carbonate rocks outcropping in the **Vitshumbi** formation (see point IV.4.2 in Field trip Chapter) showed high concentration of U, Th, and K visible in Figure IV.27 on page 99.

According to Adams and Weaver (1958), the Th/U ratio has proven to be useful in the recognition of geochemical facies.

This ratio can be used as a good indicator of sedimentary processes specifically in the determination of their geochemical facies.

The Th/U ratios in most sedimentary rocks range from less than 0.02 to more than 21. Ratios in many oxidised continental deposits are above 7, whereas most marine deposits have ratios much below 7. Therefore, the Th/U ratio varies with sedimentary processing and depositional environment. A cyclothem and several other sedimentary sequences illustrate the use of this ratio to distinguish environments and processes (Adams and Weaver, 1958).

The radiations recorded in the Vitshumbi unit (BV $\gamma$ -10 page 99) reveal that the total GR varies from 160–500 API, which is higher than in any other carbonate unit discovered so far in the EARS basin. The Vitshumbi unit's recorded values suggest calcrite tops with associated desiccation cracks and microbial mats. A marked spike in the total GR, U and Th amounts are noticed in finer laminated silty marl. However, the total GR seems clearly depleted towards top of the section composed of sandy limestones with calcitised fragments. The high gamma response (Figure IV.27 page 99) suggests that these Vitshumbi carbonates with high U, K, Th pics are being precipitated from reducing U and Th rich waters. These U and Th reductions are due to the groundwater percolating up the main rift-bounding faults which are still feeding active cyanobacteria in hot springs today. These cyanobacteria and algae growing at hot spring mouths appear to actively scavenge U and Th by giving to them very high total GR values, and the U and Th concentrations fall away over a few metres' distance from the spring mouth.

From the gamma rays recorded in-depth during the drilling in Kansas, USA, Macfarlane (1989) suggests that the Th/K log defines the Cretaceous/Permian sharp boundary and, along with the Th/U log, they emphasise the contrast between marine Upper Cretaceous rocks of the Greenhorn depositional cycle and nonmarine to transitional rocks of the Lower Cretaceous. The long-term cyclic pattern of the Th/U log is an excellent indicator of a broad transgression/regression observed during the Greenhorn cycle on an open marine shelf. However, extreme fluctuations of Th/U in the Lower Cretaceous rocks suggest a high degree of short-term environmental variability (Macfarlane et al., 1989).

This short-term environmental variability has been shown to be applicable in areas with speleothem uraniferous groundwaters and low levels of natural lead (Richards et al., 1998). Indeed, during speleothem deposition, Uranium in solution in the percolating drip waters is co-precipitated into the calcite crystal lattice. Moreover, Thorium concentrations in the drip water and the deposited calcite are negligible, resulting in extreme fractionation between the parent and intermediate nuclides. Their Calcite deposition time is determined by U–Th dating from the ingrowth or decay of intermediate nuclides.

The U, Th, K gamma Ray values recorded in either the carbonates on the EARS travertines, calcitised reeds or pustulous textured microbial mat outcrops are all documented in detail by this MSc study's Chapter Four. They have been used as available geological instrument based on the idea that the determination of the relative Thorium and Uranium distribution in the speleothems found in **Bat cave** carbonate sediments (Sample LE 44 page 80, page 111) might be treated as a function of the depositional environment.

This means that the Th/U ratio could serve as atmospheric oxygen indicator and thereby provide more knowledge of the oxygen content of the palaeo atmosphere during these carbonates' deposition.

Speleothems and spring-deposited travertines over the last 160000 years have been climatically controlled largely by a combination of temperature and aridity effects (Baker et al., 1993). Speleothems observed in LE 44 thin sections (page 111) could be used as major palaeoclimate and palaeoenvironmental data archives because of their oxygen and carbon isotopic variation records which are supposed to rely on a trustable chronological framework with U-series dating. These isotopic signals help to efficiently interpret the isotopic fractionation conditions during calcite precipitation. The context of speleothem formation is somehow linked to Th and U isotopes.

$^{230}\text{Th}/^{234}\text{U}$  isotope analysis of the speleothems found in the Bat cave carbonates has not been conducted in this MSc research because the suitable speleothems' identification for dating by Th/U analytical methods required further assessment of the degree of detrital thorium contamination (Moseley et al., 2013). Financial restrictions for the lab analysis did not allow further laboratory assessment. However, some interpretations described below have been made only regarding the K, U, and Th values recorded during the DRC field trip in 2014.

The gamma ray recorded for the travertines found in **Mayi ya Moto** (Samples V149, V150, V153 pages 89 and 112–113) provided the following mean values for  $\text{K} = 0.9\%$   $\text{U} = 66.8\text{ ppm}$   $\text{Th} = 12.7\text{ ppm}$  and deduced a ratio  $\text{Th}/\text{U} = 0.190$ , confirming the presence of speleothems in these carbonates. Moseley et al. (2013) found the same Th/U ratio value for the speleothems discovered in limestone caves in the Gunung Mulu national Park, Sarawak, Malaysia.

In **Katanda** (Samples V159, V161, V162, V163 and V164 pages 90 and 113) the following values were recorded:

- $\text{K} = 3.6\%$   $\text{U} = 410.8\text{ ppm}$   $\text{Th} = 11.8\text{ ppm}$  (assay #2266) upstream
- $\text{K} = 1.4\%$   $\text{U} = 309.2\text{ ppm}$   $\text{Th} = 57.5\text{ ppm}$  (assay #2267) downstream

In this locality, the GR, Th and U values appear to decrease downstream away from main stream abundant with cyanobacteria evidence. These decreasing Th and U values suggest increasing oxygenation downstream.

In **Biruma** (Samples V338, V 344, V 352, V 356, V363, V 364, and V 385 pages 91 and 114), the GR values  $\text{K} = 1.0\%$   $\text{U} = 200.9\text{ ppm}$   $\text{Th} = 25.1\text{ ppm}$  suggest that the carbonate deposits present substantially depleted the K, U, Th values. These deposits are mainly composed of clean white limestones with dense reed and rootlet beds because the carbonate has encrusted vegetation (samples V363 and 364 Figure IV.14 page 88) which probably grew in an extensive shallow pool fed by carbonate rich palaeo hot springs.

To summarise, the EARS travertines analysed in this research study show typical morphology and chemistry reflecting both formation conditions and the effects of post-diagenesis weathering processes. Their geological investigation in the field outcrops have been convenient for understanding their palaeo environments. Their carbonates dissolve in acidic waters but do not dissolve at equal rates; the process is dependent on joints and fractures in the potential carbonate bedrock as well as on porosity (Trudgill, 1985).

According to Williams (2004) such limestones could be formed from back-reef lagoonal environments (Williams et al., 2004); (Vinson, 1962).

Other studies suggest these limestones to be composed of shallow water sediments from the Jurassic to the Tertiary periods (Hartshorne, 1989).

Pentecost (2005) indicates that some calcite content minerals entered into the travertines as erosion or weathering products derived from the carbonate bedrock.

Most of these weathering products are water borne and the carbonate minerals enter in their structure through animal activity (Pentecost, 2005). A suggestive example is bats living in caves in the visited Bat Cave locality in Uganda where numerous phosphate minerals originating from the bat guano and bone beds are known from their association with cave travertine (Hill et al., 1997).

All the EARS travertines have been investigated, described and properly collected at a specific localised number of active and palaeo-spring sites around the margins of the Eastern Africa Rift System. These EARS travertines' occurrence is linked to the presence of hot springs and these are linearly situated along both the Eastern and the Western major rift-bounding faults where there is significant fluid flux from depth. Their fluid temperature field records show a range of high temperature around the aligned, bounding fault hot springs although the collected travertines have been found outcropping in surrounding cold areas.

The bicarbonate source of these EARS travertines is strongly linked to the significant geothermal fluid flux from depth flowing to the surface in hot springs which as quaternary volcanoes, fumaroles, boiling pools, hot and steaming grounds, geysers and sulphur deposits are manifesting the occurrences of geothermal activity within the EARS. However, geochemistry results clearly indicate a marine limestone involvement in some of the analysed carbonates samples. Active hot springs or inactive palaeo hot springs as well as the geothermal activity in the East African Rift System seem intricately connected to the occurrence of palaeo volcanoes located within the axis of the rifts. Documented examples of these geologic configuration are found on either side of the rift valley in the Fort Portal region in the north east and in Nyragongo Nyamulagira region in the south west. The EARS travertines have been observed in the field situated along deep-seated, rift-bounding faults. The discussion was still open, linking their origin to groundwater flux along these faults. This MSc research study terminated the mentioned discussion and confirms the geological fact that the carbonatite lavas' spectral signature is relatively close to the Fort Portal lavas in Uganda's side and from both Nyragongo and Nyamulagira in the DRC side. However, the clear marine signature found in localised hot springs definitely suggests the presence of a pre-tertiary carbonate bedrock underneath the EARS Cenozoic basin. The field evidence of these identical travertine outcrops observed in both Eastern (Uganda) and Western (DRC Bloc V) major rift-bounding faults have actually proved the geothermal flux involvement in the EARS carbonate precipitation on surface. Moreover, the geochemistry results opened the discussion regarding these travertine layers' thickness variation, which are possibly laterally impersistent and of limited subaerial extent. The travertine samples with marine limestones' spectral signatures, found on both sides of the EARS aligned along the western and the eastern bounding faults, lead to presume to have geothermal waters pure Calcite contamination from a Devonian carbonate bedrock from depth. This supports the geologic considerations about the possible presence of a marine limestone bedrock unit beneath the classical known siliclastic deposit in the Eastern African Cenozoic rifting.

A fissure ridge can be defined as a Travertine fault trace fissure-ridge, adding a helpful example for studying the relationship between faulting and travertine deposition (Brogi and Capezzuoli, 2009). Based on Brogi and Capezzuoli's (2009) studies, the idea of the presence of travertine fissure-ridges within the EARS bounding fault is not negligible.

Some possible fissure-ridge developments along the trace of a normal fault with small displacement were found located in the margin of EARS basins.

Brogi and Capezzuoli (2009) point out that these fissure ridges are often formed from supersaturated hot waters (39.9°C) flowing from thermal springs aligned along the trace of the normal fault, dissecting limestones not older than Late Pleistocene ( $24 \pm 3$  ka). They indicate also that hot fluids flowing up from cones are located at the extremities of the ridge exactly where the travertine is deposited. More possible fissure-ridge evidences are still being researched and if found, they would entirely diversify the depositional morphology in the Eastern Africa Rift System because they will always appear in the field formed around the area in which hot spring waters emerge along a joint, extensional fracture or fault on an elevation.

The fissure-ridge sedimentation style described above suggests that it could have resulted from seasonal higher and lower water table levels that allow temporary pools to form with organic matter and low Ph, favouring the EARS travertines formation.

All these travertines field considerations are not sufficient to determine the origin of the bicarbonates which constitute the EARS travertines samples. They need to be sustained by the following microscopy inputs and furthermore by geochemical analysis to assist this MSc study in the EARS travertines' possible palaeoclimate reconstruction.

Combining the existing literature reviewed in Chapter Two and field results obtained in Chapter Four, it was advantageous to use microscopic observation prior to geochemistry analysis to document the petrography of each travertine texture, structures and/or fabrics followed by drilling through each of them and running the ICP-MS process. In other terms, the microscopic section below highlights the strong link between each petrographic observation of textures, structures and/or fabrics and their respective ICP-MS results. This means that each of the observed EARS travertine textures, structures and/or fabrics' respective REE+Y ppb values and spectral signatures would be correlated as per the Balz Kamber method (Kamber et al., 2014) with the universally recognised Fort Portal Carbonatite lavas or Devonian reef and Mandawa basin marine limestones.

## VII.2 – MICROSCOPY OBSERVATION RESULTS

The microfacies analysis of EARS travertines' thin sections was performed, where applicable, with Alizarin red stain to efficiently distinguish the calcite from the dolomite. The microscopic observations were complemented with field-documented data including determination of the HCl acid freezing reaction.

The EARS travertines' thin-section observations indicate a progressive development of successive carbonate layers which occurred during the deposit and culminated in parallel and subsequent layering. In a later stage of subaerial exposure, calcification occurred, overlapping the original facies. Around the beginning of the Tertiary, a marine transgression favoured this EARS calcification overlapping process involving a sea level rise. Due to this palaeo sea level changes and climatic factors, these carbonate sediments were seen superimposed lacustrine or in intertidal to subtidal horizons, diagenetically altered, thereby presenting a complicated REE+Y facies pattern.

Spring limestones precipitate at several temperatures and this can be observed under the microscope in different fabrics, textures and structures in association with plant rootlets, tubes and leaf prints. The main carbonate fabrics, structures and textures observed microscopically are fibrous, crystalline, speleothems and porous.

Therefore, fine structures of calcite crystal lattice were examined but the existence of fossils were not clearly observed in the EARS travertines.

The microscopic observations of the above structures, textures and/or fabrics suggest that these travertines are commonly formed in clear, warm, near-surface and shallow marine waters in environments such as deltas and/or estuaries. They appear similar to organic sedimentary filling formed by the precipitation of calcium carbonate from lake or ocean water accumulation of shell, coral, algal, and faecal debris. The chief mineral component of our EARS travertines is calcite which is mostly composed of a heterogeneous aggregation of fine, medium and coarse grains mixed with white and striped calcite veins. This particular structure is due to further carbonation of fine grains of limestone.

The observed constituents of Eastern Africa Rift travertines, as visible under a microscope, have been categorised as follows:

#### 1. Terrigenous constituents

These are the materials derived from outside the basin of deposition, through the process of weathering, erosion and transportation, as sediments to the depositional site. They were also named detrital travertines by Casanova (1994) in his attempts to trace back the EARS palaeo drainage patterns. The observed terrigenous materials in the P12 thin section (on page 105) are colourless, anhedral quartz grains from the basement and show wavy extinction under crossed nicols.

#### 2. Allochemical constituents

The Allochemical constituents or 'Allochems' are the dominant constituents and are those materials which are formed within the basin of deposition by chemical and bio-chemical precipitation but are organised into discrete aggregated bodies and have mostly suffered some degree of transportation (Folk, 1959). The allochemical constituents observed in this study are categorised as follows:

- i. Intraclasts, including early carbonate sediment fragments, that have been eroded or by biochemical activity from the adjoining areas of the sea bottom and redeposited to form new sedimentary rock (Folk, 1959), leaving spaces between them and yielding the primary porosity of samples V 162 on page 113 and samples LE 24, LE26, LE27 and LE28 on page 109.

- ii. Ooids are spherical or sub-spherical accretionary bodies, less than 2mm in diameter, and thin section oolites often show concentric structures. Its nucleus might be composed of a carbonate but different from carbonate in colour and texture. No ooids evidence was found in thin sections. However, the concentric layers observed in samples P12 on page 108 and samples LE 26 and LE 27 on page 109 are not confirmed as ooids but are merely root traces and plant tubes filled with sparry calcites.
- iii. Fossils are the broken and unbroken skeleton and trace of carbonate secreting organisms as one of the major constituents of these three limestone members, no fossil evidence was found in the EARS travertines thin sections.
- iv. Pellets are the homogeneous aggregate of microcrystalline calcites and small spherical-to elliptical-shaped bodies and are devoid of any internal structure. They are distinguished from oolites by their lack of radial or concentric structures, from fossils by their lack of internal structures and from intraclasts by their uniformity of size and shape. They have been observed in samples V2 on page 111 and the LE 24, 26, 27 and 28 thin sections on pages 109.

### 3. Orthochemical constituents

Orthochemical constituents are those precipitated in the basin of deposition or within the rock itself. They show little or no evidence of significant transportation. The following have been observed in most of the travertine thin sections observed:

- Microcrystalline calcite matrix (micrite): Sample V125 on page 112
- Sparry calcite (spar): Samples V161 on page and 113, V338, V356, V385 on page 114

### 4. Fabric and micro-texture

The study of Travertine fabrics and microstructures is applicable because it specifies the chemical activity and mode of occurrences within the EARS carbonate sediments. The main fabrics and microstructures found in the EARS Travertines are grouped as follows:

- i. Strained calcite crystal lattices have been observed as turbid, showing undulose extinction. The strained calcite crystals in the EARS travertine thin section samples V149 on page 115 and V164 on page 116 seem to be formed by the diagenetic neomorphism of microcrystalline calcite matrix under stress, i.e. the product of tectonic effect on neomorphic sparry calcite grains.
- ii. Veins observed in sample V2 on page 111 are usually composed of microspar and sparry calcite and vary in shape from straight to irregular with uniform thickness throughout the thin section. These calcitised veins are the rootlet traces and tube plant fingerprints, testifying delta or estuary vegetation presence during the depositional time.
- iii. Microstylolites observed in samples V150 and V163 on page 113 are commonly intergranular and mark contacts between adjacent structures.

## 5. Depositional structures:

A sedimentary structure is deemed a primary depositional feature of sediment that is large enough to be seen by the naked eye (Selley, 2000) and is distinguished from the fabric which has microscopic structural features of sediment. The EARS travertine sedimentary structures observed are arbitrarily divided into the following:

- i. Primary (physical) classes: Primary structures are those generated in sediment during or shortly after deposition. They result mainly from the physical processes e.g., cross bedding and slumps. They were observed in samples V352 on page 114, MDW 42, 43, 74, 162, 276 and MDW 277 on page 115.
- ii. Secondary (chemical) classes: Secondary sedimentary structures are those that are formed sometime after sedimentation i.e., they are post-depositional microstructures. They essentially result from chemical processes such as those which lead to the diagenetic formation of concretions, microbial mats and/or speleothems (Selley, 2000). They were observed in samples V 153 on page 113 and LE 44 on page 111.

The PCK limestone sample from West DR Congo (see page 109) categorised in the above-mentioned secondary class presents some alternately grey and white layered mounds, columns and sheet-like sedimentary rocks. Their original formation designates a progressive growth of overlapping layers of cyanobacteria activity photosynthesizing microbe in the shallow shelf such as lakes, fresh waters rivers, and even soils.

Stromatolites, known as one of the earliest fossil evidence of life on Earth, have been observed in the Procokin quarry in a visible layer containing calcium carbonate precipitated over the growing mat of bacterial filaments. Assuming that photosynthesis in the cyanobacteria depletes the carbon dioxide in the surrounding water, it is clear that the carbonate precipitation in PCK Samples was most abundant during the Late Proterozoic, about 3.8 billion years ago. The PCK limestone samples' petrography analysis suggests that they were formed in shallow fresh water because cyanobacteria use water, carbon dioxide and sunlight to create their food and expel oxygen.

However, the petrography analysis of Mandawa carbonate sediments reveals that they display enough similarities under the microscope with EARS Travertines samples P12, LE 24, LE 26, LE 28 and V 19 found with marine limestones' spectral signature. Microscopic analysis has been used as a tool for reconstructing the provenance of the marine limestone sedimentary sequence. The Mandawa samples' carbonate mineral assemblages in the Tanzanian Basin seem to be influenced by several different processes such as transport, weathering and diagenesis, which can alter the original composition such that they might no longer reflect the true composition of their source area. More petrographic studies are required to identify these microscopic similarities.



### VII.3 – STABLE CARBON AND OXYGEN ISOTOPE RESULTS

The use of carbon and oxygen's stable isotopes on terrestrial carbonate deposits as recorders of climatic and environmental change through the present MSc research study was inspired by the fact that carbonates, including travertines, contain regional climatic and environmental signals (Andrews et al., 1994).

Numerous recent studies (Chafetz et al., 1991; Merz, 1992; Andrews et al., 1994) suggest that the interpretation of carbon and oxygen's stable isotopic compositions obtained from the Eastern African Rift travertines' isotope ratio mass spectrometry (IRMS) analysis are based on certain assumptions about the conditions of carbonate precipitation. These assumptions are summarised below.

The oxygen-stable IRMS assumptions specify that the possible relationship between  $\delta_{18}\text{O}$  of meteoric water precipitation and temperature is developed by the condensation of water vapour as a direct consequence of cooling. Further condensation of a given air mass occurs at lower temperatures which is isotopically lighter than previously formed phases, proving the hidden link between temperature and rainout effects. Therefore, temperature changes might be responsible for much of the 1% variability of our results even if we are unable to obtain evident respective contributions from source and rainout effects. Oxygen isotope ratios in the calcites are close to equilibrium with mean  $\delta_{18}\text{O}$  in rainfall at average annual water temperatures, while carbon isotope variations reflect carbon inputs from soil, aquifer rock dissolution and equilibration with atmospheric  $\text{CO}_2$  (Andrews et al., 1994).

However, Atkinson et al. (1987) indicates that the dependence of  $\delta_{18}\text{O}$  on temperature is not linear, and at some values around 8 to 10°C this dependence is suitable for most English Holocene sites; in this case, 1% change in  $\delta\text{w}$  corresponds to about a 2°Cmax change in air temperature (Yurtsever, 1975).

Moreover, Pazdur similarly (1988) suggests that oxygen-derived isotopes might be efficiently used to determine the palaeotemperatures from Tufas and Travertines and constrain their palaeoenvironmental and palaeoclimatic reconstructions.

According to Lawler (1987), the observed changes in the oxygen isotopic composition of travertine-precipitating waters ( $\delta\text{w}$ ) would be controlled by variation in rainfall composition which feed the groundwater and ultimately surface river water.

The results presented in section VI.1.1, Figure VI.2 page 118, indicate that travertine samples collected in Bwera (samples LE41 and LE42), Bat cave (Sample LE44) and OKUMU (Sample P12a and P12b) present values from -7 to -10‰ of PDB Belemnite and high abundance of  $\delta_{18}\text{O}$  between 25 and 29.

The stable isotope results for the travertine samples collected in Lyemubuza (Samples L24 and LE26), Muhokiya (LE 28 and LE27), Dura (Sample LE32) and Hima (Samples LE37 and LE38) show values from -2 to +7 ‰ relative to PDB Belemnite and the same high abundance of  $\delta_{18}\text{O}$  between 25 and 29. Interpreting the results shown in Figure VI.2 in page 118, it is noted that higher  $\delta\text{w}$  values in carbonates correspond to lower temperatures (colder climate during Pleistocene glaciation) therefore the lower  $\delta\text{w}$  values in carbonate samples refers to higher temperatures (warmer climate during Holocene interglacial) (Yurtsever, 1975; Siegenthaler, 1979; Rozanski et al., 1993).

The IRMS results plotted in Figure VI.3 on page 119 reveal that the travertine samples collected from the localities of Lyemubuza, Muhokiya, Dura and Hima (Uganda) have higher  $\delta w$  values in carbonates between 27 and 30 corresponding to lower temperatures of marine carbonate deposition conditions. These results also indicate that the travertine samples collected from the localities of Sempaya (Uganda), Mayi ya Moto and Biruma (DRC) have lower  $\delta w$  values in carbonates between 15 and 23 corresponding to higher temperatures of carbonatite deposition conditions. Figure VI.3 also confirms that the travertine samples collected from localities of Bwera, Bat cave and Okumu (Uganda) have medium  $\delta w$  values in carbonates between 23 and 27 corresponding to a mixture of both the above deposition conditions. At a given latitude, a number of mechanisms are known to cause variations in  $\delta w$ , including variation in the source of an air mass (e.g., Heathcote and Lloyd, 1986; Lawler, 1987), temperature of the air mass (Yurtsever, 1975), successive precipitation ('rainout' or 'amount') effects (Dansgaard, 1964) and altitude effects (Gat, 1980).

This implies that, for a given geographic locality, some of these effects will be either constant (e.g., altitude effects) or will fluctuate on short term (<seasonal) timescales, e.g., rainout effects. Temperature effects have been seen to vary over seasonal (Siegenthaler, 1979) or longer timescales (Rozanski et al., 1993) and this is most clearly seen in polar continental regions (Lawrence and White, 1991).

In temperate regions, the temperature effect is more difficult to resolve from the rainout effects in historical proxy records (Lawrence and White, 1991). Air mass source effects might also vary over longer timescales (Mckenzie and Hollander, 1993) although there is relatively little evidence available to demonstrate the significance of this effect in equatorial regions at any EARS given site.

Regarding the carbon stable Isotope Ratio Mass Spectrometry assumptions, they indicate that the depositional environment of the EARS travertines could be well understood and documented using  $^{14}\text{C}$  and biostratigraphy (Andrews et al., 1994). However, it can be argued that smooth  $^{18}\text{O}$  variations in the travertines as well in the Tufa calcite are caused by changes in the isotopic composition of regional rainfall which in turn were caused primarily by changes in air temperature (palaeoclimate).

Generally, lower  $^{13}\text{C}$  values for calcite correspond to higher  $^{18}\text{O}$  values, suggesting a stronger component of soil-derived carbon during warmer climatic phases.

This assumption implies that variations in carbon isotope geochemistry can be related to environmental changes which affected the carbonate precipitating waters.

Kinetic isotope effects are insignificant, except at spring heads (TURI, 1986), as observed in most of the EARS travertine sites discussed in this research study.

The stable carbon and oxygen isotopic signatures obtained from IRMS analysis on selected EARS travertine samples reflect surface fractionation processes within the hot or cold spring pools at the surface. They are affected mostly by the  $\text{CO}_2$  outgassing as the water bubbles to the surface. This field evidence suggests that the  $\text{CaCO}_3$  precipitation is differently distributed within the EARS travertine depositional environment. In some locations, this precipitation was not sufficiently effective to complete the calcification process at this end.

Therefore, it is interpreted that the EARS travertine calcites precipitate within a range of precipitation rates when dissolved CO<sub>2</sub> held under pressure underground outgasses upon reaching the surface at a spring, pushing the reversible reaction to the right (CO<sub>2</sub> is present in groundwaters by dissociation of biogenic methane at depth etc.).

Plotting the EARS travertine IRMS result data in C-O isotopic chart in Figure VI.2 on page 118 and VI.3 in page 119, it is evident that in general, lower  $\delta_{13}\text{C}$  values correspond to higher  $\delta_{18}\text{O}$  values. This implies that EARS warmer climatic phases were characterised by a stronger component of isotopically light, soil-derived carbon. This climate-soil relationship is plausible as warmer climatic phases might be related to more active plant growth, soil-activity and higher soil CO<sub>2</sub>, (Buyanovsky and Wagner, 1983).

The IRMS analysis conducted in this MSc research study on EARS travertine samples reveals that the values of <sup>13</sup>C and <sup>18</sup>O respectively vary between -6.47 to -15.10 ‰ and 20 to 30 ‰. Regarding the <sup>18</sup>O ‰, SMOW and <sup>13</sup>C ‰ PDB values, intersect with each other. Therefore, it can be concluded that an isotopic clumping supports the venue that the travertines have precipitated in different depositional conditions and hybrid environments. The resultant <sup>13</sup>C were found unexpectedly low enough in the EARS travertine lithofacies to characterise either pools or stagnant water conditions.

According to Lynch-Stieglitz (1995), the 20 to 30 ‰ PDB value range found in these aforementioned travertines localities could be interpreted as evidence of marine carbon involvement (Lynch-Stieglitz et al., 1995); this is generally supposed to occur in colder temperatures due to the high abundance of  $\delta_{18}\text{O}$  as the majority of the lighter oxygen isotopes are stored in the glacial ice as suggested by Hays and Grossman (1991). Andrews et al. (1994) indicate that climatic warming corresponding to wetter conditions caused more effective flushing of soil-carbon into groundwater and river systems. They are appropriate as independent palaeoclimate indicators for the EARS travertine samples.

Based on the aforementioned C/O isotope ratio considerations and IRMS results presented in Chapter Six, Figure VI.4 on page 119 reveals the three travertine palaeo environments according to the chart comparing  $\delta_{13}\text{C}$  PDB with palaeo temperature:

- i. Closer to primary marine limestones in *Lyemubuza*, *Muhokiya*, *Duma* and *Hira* localities in Uganda where carbon dioxide outgassing evaporation removes C and O isotopes;
- ii. Approximately primary carbonatite lavas in *Mayi ya Moto* and *Biruma* localities in DRC;
- iii. Hybrid results mixing both the above palaeo environments in *Bat Cave*, *Okumu* and *Bwera* localities in Uganda where strong carbon plant soil zone a CO<sub>2</sub> contribution.

The same figure also suggests that the palaeo environment temperature of EARS carbonates is divided in two main groups of cold marine limestones (e.g. tufa, travertines) and hot carbonatite (e.g. travertines) and clearly a kind of intermediate mixed group considered like the hybrid one.

#### VII.4 – STRONTIUM ISOTOPE RATIO RESULTS

Discovered by Adair Crawford in 1790, strontium is beneficial for this MSc research study because carbonate minerals generally contain relative constant abundance of incorporated  $^{87}\text{Sr}$  in many carbonate crystal lattices.

Strontium is also a mobile element during carbonate weathering and dissolution (Vaniman and Chipera, 1996). A positive correlation between Sr and REE reflects the epigenetic influence of meteoric waters moving over the bedrock (Tlig and M'Rabet, 1985).

Considering the fact that continental weathering and oceanic hydrothermal processes are potentially able to deliver  $^{87}\text{Sr}/^{86}\text{Sr}$  to seawater, our perspective is that some global tectonic activity which would control the relative proportions of the wide variation of  $^{87}\text{Sr}/^{86}\text{Sr}$  in seawater through geologic time. Seawater  $^{87}\text{Sr}/^{86}\text{Sr}$  is related to a major erosion of ancient limestones which reflect earlier seawater O and C isotopic compositions (Dickson et al., 1990). Furthermore, the strontium isotopic ratio contained in marine limestones and dolomites, has its isotopic composition that depends on the age of the rocks, reflecting the temporal variations in oceanic  $^{87}\text{Sr}/^{86}\text{Sr}$ . Considering the actual equatorial climate in the EARS, a consideration could be made on early meteoric diagenesis where the  $^{87}\text{Sr}/^{86}\text{Sr}$  signature of calcite precipitated during stabilisation of aragonite and magnesian calcite might generally be inherited from the previous phase of metastable carbonate phase.

This very high Sr content of marine carbonates is relative to the levels of Sr usually seen in dilute fresh meteoric waters (Banner et al., 1989).

The relative abundances of  $^{87}\text{Sr}$  in the Eastern Africa Rift travertine samples are expressed as the ratio  $^{87}\text{Sr}/^{86}\text{Sr}$  and are presented in Figures VI.5 on page 120, VI.6 on page 120 and VI.7 on page 121. The charts of  $^{87}\text{Sr}/^{86}\text{Sr}$  secular variation for the Phanerozoic sea waters from Burke et al., (1982), Wierzbowski, (2013) and Nicholas, (2009) in Figures VI.5 on page 120 and VI.6 on page 120 are sufficiently detailed to permit the use of strontium isotope ratios in high-resolution stratigraphy and chronology. Strontium isotope ratios of selected EARS travertine samples with a strong marine limestone or carbonatite REE+Y signature showed a very high range of strontium isotope ratios from 0.7068069 to 0.7482648.

However, only 2 values LE 41 and LE 42 (a, b) are within the range expected for marine carbonate dating from Jurassic to Permian. These are from Bwera and Dura at the northern end of Lake Edward. Sr isotope ratios within the seawater carbonate range might be Late Neoproterozoic, Late Permian or Late Jurassic in age.

Most of the remaining travertine samples exhibit a very high radiogenic strontium value, suggesting crustal contamination from Rubidium, but there is no correlation between Rb concentration and Sr isotope ratios. This could explain how the  $^{87}\text{Sr}/^{86}\text{Sr}$  of marine carbonate samples might differ from the value of seawater at the time of its deposition; thus, their difference value can be attributed to diagenetic alteration by either younger seawater or nonmarine fluids.

## VII.5– GC-GCMS RESULTS

Both gas chromatography (GC) and mass spectrometry (MS) yield better detailed geochemistry results by their conjoint use. GC can effectively separate volatile and semi-volatile compounds with acceptable resolution but unfortunately cannot identify them. MS might be able to provide detailed structural information on most compounds such that they can be exactly identified but unfortunately it cannot separate them. Therefore, the combination of the two techniques is preferably suggested for the geochemistry results' efficiency, targeting the study of biomarkers (Strandberg et al., 2001).

This suggests that very sensitive methods of analysis employing gas chromatography-mass spectrometry (GC-MS) are absolutely necessary for the biomarkers' scientific recording.

Biomarkers consist of complex organic molecules from chemical structures which could stay largely unchanged during the diagenesis and oil generation processes. This chemical property allows these biomarkers to get traced back to their original molecules in living organisms.

This suggests that generally, biomarkers are proven to be able to retain the majority of the original carbon skeleton from the initial organisms. Biomarkers are also called molecular fossils because of their possible structural similarities to diagenetic alteration of natural products from living organisms. This is why these structural similarities have been called, in some previous works, "molecular fossils". Biomarkers are also considered a group of parcels, mainly hydrocarbons, often found in oils, rock extracts, recent sediment extracts and soil extracts. Biomarkers are considered minor components of a crude oil or rock extract. According to Wheaterford (2018), some biomarkers are prolific in many organisms while others are only found in specific types of organisms and hence these can be used as markers of source input. Additionally, some biomarkers do not appear until their parent organism has evolved, and therefore, the presence of these compounds are used as an age diagnostic marker. Similarly, some biomarker structures are more stable in certain depositional environments than others and hence their abundance can be used to infer depositional environments. Moreover, subtle chemical transformation from one chemical structure into another can occur due to thermal stress and, hence, the ratio of these biomarkers can be used as a maturity marker. When oil samples are available and their potential source rocks are known, biomarkers can be used to make oil source rock correlations.

However, if source rocks samples are neither available nor known, the biomarker distribution in oil can be used to infer characteristics of the source rock that generated the oil without examining the source rock itself.

Specifically, biomarkers obtained by GC-GCMS from an oily sample can reveal the relative amount of oil-prone vs. gas-prone organic matter in the source kerogen, the age of the source rock, the environment of deposition as marine, lacustrine, fluvio-deltaic or hyper saline, the lithology of the source rock (carbonate vs. shale) and the thermal maturity of the source rock during generation (Peters and Moldowan, 1993).

The main reason to use Dominion Ltd.'s GC-GCMS analysis results in this MSc research study is to explore the constituents of biomarkers from the Edward Lake oil slicks and compare them with the black-lined substance found in cavities in the EARS travertines collected and documented in the Lyemubuza quarry in EA4A in Uganda. There are significant parameters of biomarkers which makes them important to study in this MSc research work, for instance, the use of biomarkers in oil to assess source thermal maturity as a function of source rock maturity is indicative of source rock organic matter input and depositional conditions. Consequently, a variety of biomarker parameters have been identified that are applicable for characterising the source rock maturity simply from the analysis of the migrated oil (e.g., Peters and Moldowan, 1993).

These above-mentioned maturity parameters are appropriate to explain the processes that occur during source rock maturation such as cracking (large molecules break into smaller molecules), isomerisation (changes in the 3-dimensional arrangements of atoms in molecules.) and finally aromatisation (formation of aromatic rings by loss of hydrogen from naphthenes). In order to better access the EARS travertine source rocks by interpreting the biomarker results presented and described in section VI.3 page 121, the following aspects have been considered. The relationship between a biomarker and the source maturity is a function of heating rate, source lithofacies and source organic facies (kerogen type). From the GC-GCMS results obtained through this research study, we note that the maturity (i.e., vitrinite reflectance equivalent) is linked to specific values from biomarker parameters showing few (negligible) changes from offshore oil slicks in the Edward basin to onshore Lyemubuza carbonate outcrops. This reveals the non-linear relationship between a biomarker maturity indicator and source rock maturity. Observing the local increase of maturity indicators in some locations within the Edward Lake basin close to the Kigunda locality in the South West of Edward Lake where Black shales were found flaming smokes in the surface, it is proven that many biomarkers within the EARS might reach terminal values, in others words, the stage of "overmaturity". Moldowan et al. (1992) argue that the concentrations of biomarkers in petroleum decrease with thermal maturity. Despite these limitations, biomarkers as indicators of source maturity are extremely convenient. Moreover, biomarker maturity parameters are used to determine if the API gravity of biodegraded oil was or not prior to biodegradation. This is possible by collecting a suite of non-degraded oils from the same petroleum system as the degraded oils. Using the non-degraded oils, the geochemist develops a correlation or "transform" between a biomarker maturity parameter and API gravity. Moldowan et al. (1992) provide an excellent example of this approach in which they determine the original gravity of degraded Adriatic oils. The same biomarker parameter is then measured on degraded oil, and its original gravity is determined using the transform developed from the non-degraded oil suite. This MSc research study used the GC-GCMS analysis to correlate their respective biomarkers' behaviour in detail. The most effective biomarkers studied in this work are those based on GC-GCMS analysis (Hopanes m/z 191, Tricyclic Diteranes m/z 191 and Steranes m/z) of compounds that are highly resistant to biodegradation such as the n-alkane hydrocarbon series from sample LES 18 presented in figure VI.11 on page 123.

The Dominion Ltd. GC/GCMS analyses demonstrate that duplicate samples from Lyemubuza Quarry and Muhokya Lime Works, localities ~10km apart, contain the same mature oil biomarkers. This correlating fact suggests the lateral extension of a possible limestone extended cavity layer containing the same migrating pre-peak oil. The different levels of isomerism and aromatisation observed in the biomarker compounds of traces of a relict, biodegraded oil, lining the cavities of the travertine samples collected at Lyemubuza Quarry and Muhokya Lime Works along the Ruwenzori border fault, suggest early (pre-peak) oil generation. The obtained results of the GC/GCMS analyses indicate that this is pre-peak oil apparently generated from a marine shale source rock and migrated into these very porous EARS travertines. This is interpreted as the source rock type that would typically generate oils such that the relict biomarker distributions seen in these samples are from the marine shales source. Not only do the Lake Edward slick samples show a mature hydrocarbon signature but the polycyclic ring biomarkers are strikingly similar – particularly the 4-ring steranes – to the relict oil extracted from the travertines documented at Muhokya. Figure VI.16 on page 125 presents plots of C27 – C29, AAA and ABB sterane distributions from the Lake Edward slicks and the Muhokya limestones which reveals that the data are homogenous and cluster together. This is the scientific evidence that the GC/GCMS analysis run by Dominion Ltd. proved that the relict oil preserved in the travertine cavities at Lyemubuza and the one leaking to the surface on Lake Edward are from the same marine shale source rock.

#### VII.6– ICP-MS RESULTS INTERPRETATION

The main reason to use rare earth element detection with ICP-MS analysis for the EARS travertine samples collected from each of the geological sites being investigated through the present MSc research study is linked to its great advantage to identify and distinguish at very low level all the inherited carbonate material from a potential local limestone rock at depth. On this basis Allwood et al., (2009) and Allwood and Goodacre, (2010) infer that the very low detection limits of modern ICP-MS instruments allows the analysis of full REE + Y patterns for samples smaller than 100 µg.

The REE concentrations found in EARS travertines samples which were selected because of their potential importance in carbonate minerals were obtained in the full suite of trace elements detected by the ICP-MS method which has proven a very low detection limit by providing precise and accurate output data for elements (Sc, Y, La, Ce, Pr, Nd, Pm, Sm, Eu, Gd, Tb, Dy, Ho, Er, Tm, Yb and Lu) present in the sample at ppb concentration levels.

However, results for Be, K, Ti, As, and Sb are not reported because they were below the instrument's detection limits. As the REE are considered reliable indicators of the chemical evolution of waters flowing through carbonates (Vaniman and Chipera, 1996), their concentrations in each EARS travertine's respective textures, structures and/or fabrics were relevant to analyse in the purpose of understanding the geochemical origin of the bicarbonate contained in the EARS travertine samples and determine the geological environment for their time of deposition.

The objective of this present section (ICP-MS result discussion) is firstly to examine and interpret the geochemical footprints obtained from the EARS travertine samples to determine their intra-sample and inter-site variability.

Secondly, is to compare their spectral signature trends to those obtained either for Fort Portal carbonatite lava samples in Uganda or Devonian Reef fresh waters and Mandawa marine limestones in Tanzania which are both universally recognised and studies on them have been published in the actual literature like their respective spectral signatures references.

This section summarises the geochemical findings and scientific contributions obtained from the use of ICP-MS method on carbonates for the detection of lowest EARS travertine REE spectral signatures. The ICP-MS analyses conducted in our MSc research study performed well, yielding both significant positive and negative correlation results. The respective ICP-MS spectral signatures detected on each EARS travertine analysed sample purposed to correlate them with either Fort Portal or Devonian Reef reference spectral signatures. The acceptable threshold of the positive correlation coefficient used for this MSc experiment ranged from  $1.00 \geq R_2 \geq 0.96$ . Any correlation coefficient value under 0.90 was considered a negative correlation. The results of this MSc research study confirmed that ICP-MS is one of the most appropriate methods which helps to understand the geochemical origins of carbonates found in travertines and other limestones found in outcrop whenever can arrive in the laboratory after their field collection. As the EARS samples collected from 2007 to 2011 analysed in 2016 gave the same results with those obtained from the same samples after their 2013 analysis, this method proved its results reproducing whenever, whatever the lab operator, wherever the experiments were done.

The ICP-MS results presented in (the previous) Chapter 6 demonstrated the following geologic evidences:

The Procokin limestone samples drilled through their visible textures, structures or fabrics presented typical spectral signatures which confirmed their stromatolites and microbial mat structures and their geochemical fresh water origin as universally recognised in the existing literature (Casanova, 1994). Some of the Mandawa (Tanzania) limestones drilled regardless of their visible textures, structures or fabrics presented typical spectral signatures which confirmed their geochemical marine limestone origin also universally recognised in the existing publications (Nerbråten, 2014).

Both Procokin and Mandawa ICP-MS analysis performed well in this MSc laboratory work. The respective results confirmed the spectral signature evidence for Procokin fresh water and Mandawa marine limestones. The respective analysis allowed the discovery of the closer fresh water and marine limestones outcropping in and around the Albertine Graben Rift to compare their spectral signature patterns as well as their correlation coefficient.

The EARS travertine geochemistry results obtained using ICP-MS analysis varies according to deposition conditions and post-diagenesis processes affecting their chemistry.

Some selected EARS travertines samples analysed through this present MSc research study show negative Cerium anomalies with an average value of approximately 0.86.

This value means that there is no correlation between the extents of Cerium anomaly or between the concentrations of Mn and Ce (considering that variations in catchment geology would probably mask such kind of correlation).



Referring to Cerium anomaly ( $Ce/Ce^*$ ) and total REE abundance ( $\Sigma REE$ ) preserved in our EARS travertines, three possible depositional environments could be suggested: spreading ridge proximal, ocean-basin floor and continental margin. These three (3) depositional environments which are based on Cerium anomalies provide a potential tool for tectonic and stratigraphic reconstructions which are subdivided as follows:

Extremely low Ce anomalies ( $Ce/Ce^*=0.29$ ) found in some EARS travertines with marine limestone spectral signature reveal that they were deposited near the spreading ridge under the influence of metalliferous activity. Less extreme Ce anomalies ( $Ce/Ce^* \sim 0.55$ ) correspond to an ocean-basin floor deposit, and the deposit from continental margin regimes corresponds to slight anomalies ( $Ce/Ce^* \sim 0.90$  to  $1.30$ ).

Calculation of the Gd anomaly (relative to MUQ) for the ultra-filtered depth profiles presented by Alibo and Nozaki (1999) yields the same range for EARS travertine samples from 1.02 in the surface waters to a maximum of 1.32 in the intermediate carbonate geothermal water with an average of 1.13. Some of the freshwater PCK samples have shown the same comparably Gadnium large anomalies.

The Y/Ho ratio found in the EARS travertine samples is variable. It ranges from 1.015 to 5.8025 (average of 3.0467) which is different from the average upper continental crust, and chondrite value of 26 to 39 indicates significant fractionation (Kamber et al., 2005a). This clearly indicates less fractionation. According to Kamber et al., (2005), the Y/Ho ratio of the marine limestone criteria is required to be more or less higher than 40. However, many marine limestones universally recognised in the existing literature do not fill this  $Y/Ho \geq 40$  criteria.

In a carbonate sample, the level of Y/Ho ratio is either an anthropogenic feature or a fractionation feature. This assumption suggests that the EARS travertine samples presenting low Y/Ho ratio (average 3.4) reflect a non-anthropogenic source while elevated Y/Ho is a feature of marine phosphate deposits, which are a major source of phosphate fertilisers (Hu et al., 1998).

There is a surprisingly high level of coherence in the EARS REE spectral signature obtained by ICP-MS analysis. This described coherence further enhanced the reliability of the results discussed in the following paragraphs.

Considering the comparisons of all the REE spectral signature patterns including La, Gd, Y and Ho, it is clearly evident that a strong linear correlation is noticed between respective EARS individual REE concentrations with either carbonatite spectral signatures or marine limestones ones, with high correlation coefficients ( $R_2 > 0.96$ ) (Lawrence and Kamber, 2006).

This strong correlation between the REEs spectral signature indicates that no significant fractionation occurs between the respective REE spectral signatures within the same EARS travertine sample structures, textures or fabrics despite the significant change they show in their respective concentrations (Lawrence and Kamber, 2006).

This is clearly visible where the REE+Y MUQ normalised data in combination with radiogenic isotopes e.g. Pb and Sr are applicable to discriminate between carbonates that formed in lacustrine, restricted marine and open marine depositional settings (Kamber and Webb, 2001; Bolhar et al., 2002). In exceptional cases, it is also possible to infer relative water depth or proximity to hydrothermal fluid sources in a sequence of microbial carbonates (Kamber et al., 2014).

REE concentrations are altered by dolomitization as well as other epigenetic weathering processes, but the exact relationship between them is still unclear (Bolhar et al., 2002; Nothdurft et al., 2004).

Ji and Gao, (2004) indicate that the weathering of dolomites causes the uneven transport of REE which is strongly dependent on the climatic weathering conditions and the stability of the REE-carrying rock. This is why microscopic observations were necessary prior to the geochemistry analysis to avoid these above-mentioned unclear dolomitization issues. This petrographically guided micro-sampling allowed the removal of micro-samples from each crystal lattice in a portion of limestone rock less affected by later overprint (Kamber et al., 2004).

This crystal lattice structure inside the calcite mineral is highly robust and can absorb a variety of divalent metal cations, in addition to Mg and Sr, without becoming disordered (Ford and Williams, 1989). According to Reeder (1996), this mode of sharing cations of varying sizes is favoured by the calcite lattice because its corner sharing structure can take in ions larger or smaller than calcium. Other metals commonly adsorb onto the calcite crystal surface rather than being incorporated into the calcite crystal lattice. However, the elements that substitute directly into the Ca site in the lattice are the most common minor components.

Moreover, Wolf et al. (1967) note that many epigenetic factors involved in such recrystallization processes causes the leaching and migration of trace and minor elements.

The behaviour of minor and trace REE found either in the calcite crystal lattice or as inclusions in the EARS travertines themselves are important for distinguishing the spectral signature between different travertine textures, structures and /or fabrics because their respective REE geochemistry results document different geologic formations and epigenetic conditions. This means that the spectral signature differences shown in the trace and minor elements' composition of carbonates at the EARS sites are effectively demonstrated by their respective REE concentrations. This demonstration is not only by characterising their spatial geochemical variations at their respective field sites but also by distinguishing spectral signature discrimination between their different textures, structures and /or fabrics.

Based on the visible structures, textures and or fabric result discriminations, the ICP-MS experiments conducted through this MSc research study suggest that the results within each single travertine sample seems very similar.

However, the experiments done in this MSc research reveal that the EARS travertine samples from the same field location do not have completely identical ICP-MS results. This implies that their respective spectral signature patterns are not identical irrespective of the fact that they have been collected around the same hot springs where degassing waters bubbles are visible. This could be explained by the fact that fractionation processes at the surface are continually changing the REE initial distribution in each EARS travertine structure, texture and fabric.

Additionally, some geochemical data obtained through statistical interpretations allowed to draw appropriate comparisons between both EARS travertine samples' internal sets and their respective site locations. Consequently, the ICP-MS results obtained from each of the travertine samples analysed suggest the geologic evidences of a questionable carbonate bedrock chemistry across the EARS.

Regarding geothermal waters-rock interactions, Hodder (1991) suggests that rainwater that percolates down major faults and fractures is retained in suitably porous and permeable rocks. This rainwater can be heated by molten rocks at great depths in the crust.

Rather dilute brines are formed as a result of fluids and gases from the molten rocks being mixed with the rainwater and also because of reactions that occur between the water and the rocks at these high temperatures (~250°C) and pressures (~12 bar) (Hodder et al., 1991).

Knowing that carbonate rocks generally dissolve slowly in water, most of their dissolution reactions occur more readily at higher temperatures, and if we assume that the water-rock interaction liberates ionic species which can produce a metal-saturated liquid as well as calcite-saturated water passing through carbonates rocks, it is understood that the rising water to the surface cools itself slowly. Therefore, silica and other carbonate minerals are precipitated. Hodder et al. (1991) also contend that this might help "cap" the aquifer and prolong the geothermal system's existence. This implies that underground water that does reach the surface through faults and fractures will cool further and produce sinter mounds and terraces that are typical around geysers and hot springs.

Several chemical reactions occur within geothermal waters. These are mostly associated with interactions between the geothermal water and the rock of the chambers in which it is located (Hodder et al., 1991). The rock of the chambers in which the geothermal waters are located have clear carbonate characteristics as suggested by ICP-MS results obtained through geochemistry analysis. It is clearly noted that many other reactions occurred and these typically involved sulphur, calcium and/or metal cations.

EARS rock-water interactions involving calcium carbonates are more frequent because of the geothermal waters that have moved away from the aquifer are likely to have lower temperatures derived from silica concentrations than higher temperatures derived from concentrations of Na, K and Ca (Hodder et al., 1991).

Any hydrating layer of water containing trace metals, adsorbed onto the calcite surface, initially interacts with partially unsatisfied charges of the Ca and CO<sub>3</sub> ions which might result in a hydrolysed layer on the mineral surface that can become incorporated into the structure upon recrystallization (Lakshtanov and Stipp, 2007).

Geothermal waters in EARS are often associated with active (or recently active) areas of volcanic activity.

Moreover, several lined springs in the most significant EARS sites have been associated with tectonics activities rather than magmatism (e.g. rift bounding faulting process).

However, weathering and karstification processes caused due to the exposure of underlying carbonate strata are adding some variability in the composition, density and porosity of the carbonate bedrock (Trudgill, 1985).

As interpreted from the obtained ICP-MS spectral signatures of REE concentrations, each of the EARS travertine samples have been weathered by geothermal waters and have been washed in formations since their deposition time. This should more or less confirm Trudgill's (1985) assumption on weathering and karstification processes. Therefore, it is noted that groundwaters can obtain REE signatures from the rocks or aquifer material with which they interact (Lawrence and Kamber, 2006).

Consequently, Choppin et al. (1986), Wood (1990) and Lee and Byrne (1992) demonstrated with models, the importance of speciation and complexation of the REEs with various ligands in controlling their dissolved concentrations.

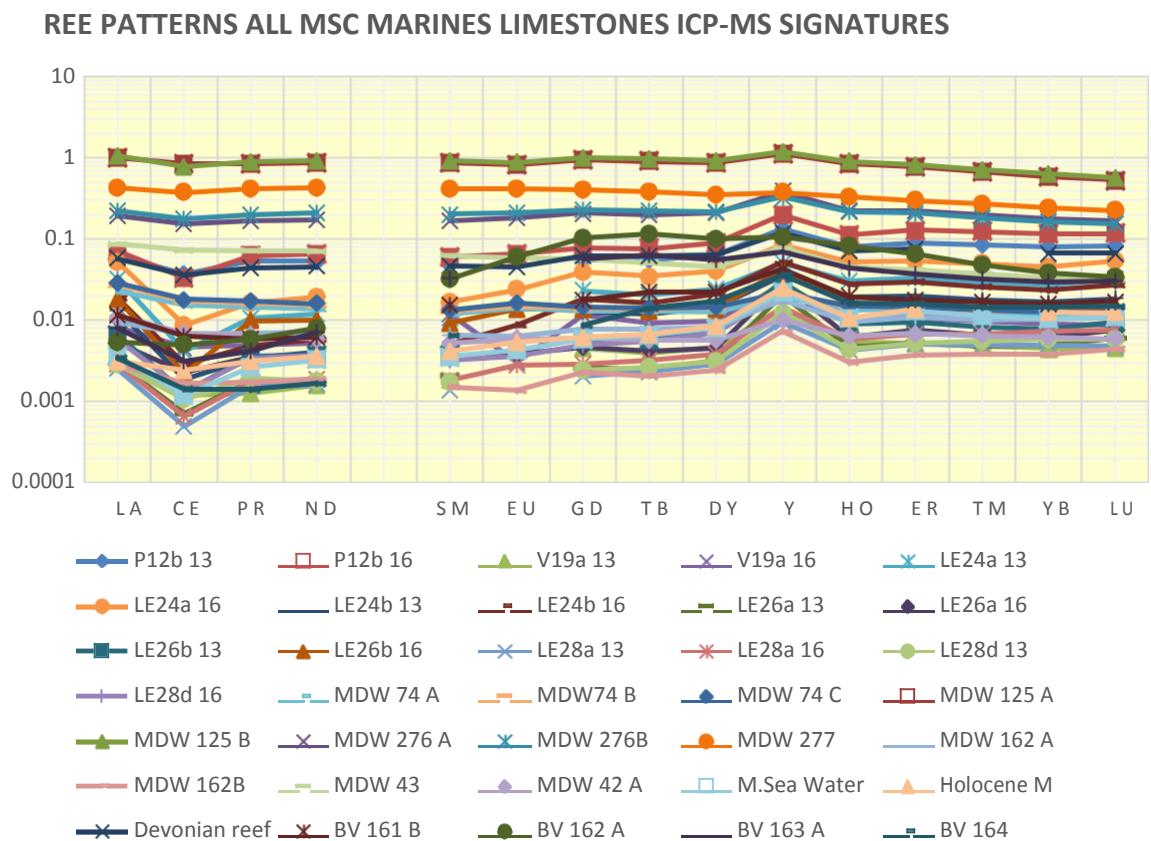
From the present MSc research study geochemical results and its key findings that emerge from the REE+Y data obtained by ICP-MS experiments the following three types of sample can be recognised:

- Samples which have derived their HCO<sub>3</sub> from a carbonatite source are only as observed in samples V20, V22, LE37, LE38, LE41 and LE42 in Figure VI.18 on page 127 and Figure VI.19 on page 128 and samples BV 344, BV 352, BV356, BV 363, BV 364 and BV 385 in Figures VI.35 and VI.36 on page 150.
- Samples which have derived their HCO<sub>3</sub> from a marine limestone source are only as observed in samples P12, LE 24, LE 26, LE 28 and V19 in Figure VI.20 on page 129 and Figure VI.21 on page 129 and samples BV 161, BV 162, BV 163, BV 164, MDW 42, MDW 43, MDW 74, MDW 125, MDW 276 and MDW 277 in Figure VI.37 on page 151 and Figure VI.38 on page 152.
- Samples which have a mixed source, possibly mixture of carbonatite-marine limestone are as observed in samples LE32 in Figures VI.23 and VI.24 on page 130 and samples BV 149, BV 150 and BV 159 in Figures VI.47-VI.48 on page 161 and VI.49-VI.50 on page 162.

The source of bicarbonates is more of predictable, expected geochemical origin because the EARS region is very closely surrounded by active and inactive volcanoes such as Nyragongo, Nyamulagira and Ruwenzori. The mixed source of bicarbonates is more confusing but explicable by the surface CO<sub>2</sub> degassing where carbonates minerals from different origins are mixed in a kind of messy bubbling visible activity.

However, the marine limestone source clearly discriminated by the ICP-MS results is the most important finding of the present MSc research study because this unexpected geochemical origin represents a significant discovery for the best understanding of the geologic wonder about the potential presence of a pre-tertiary (Cenozoic) carbonate basin underneath the Albertine Rift. This MSc research has discovered that there is definitely a Devonian marine limestone beneath the Cenozoic EARS although not all Balz K marines' limestone criteria were met. Indeed, Mandawa (Tanzania) limestones did not meet all these criteria, however, they are recognised from the literature to belong to the marine limestone family.

Figure VI.37 on page 151 and here below reproduced shows the graph of all EARS travertine samples analysed using ICP-MS the results of which confirmed the marine limestone signature patterns. This logarithmic graph of REE concentrations in their carbonates mineral reveal that all the EARS travertine samples analysed in this MSc research, presenting marine limestones' spectral signatures patterns, corresponds to the Devonian Reef's spectral signatures referencing the marine limestones. This means that there is clearly a marine limestone source of bicarbonate found in some of the EARS travertines.

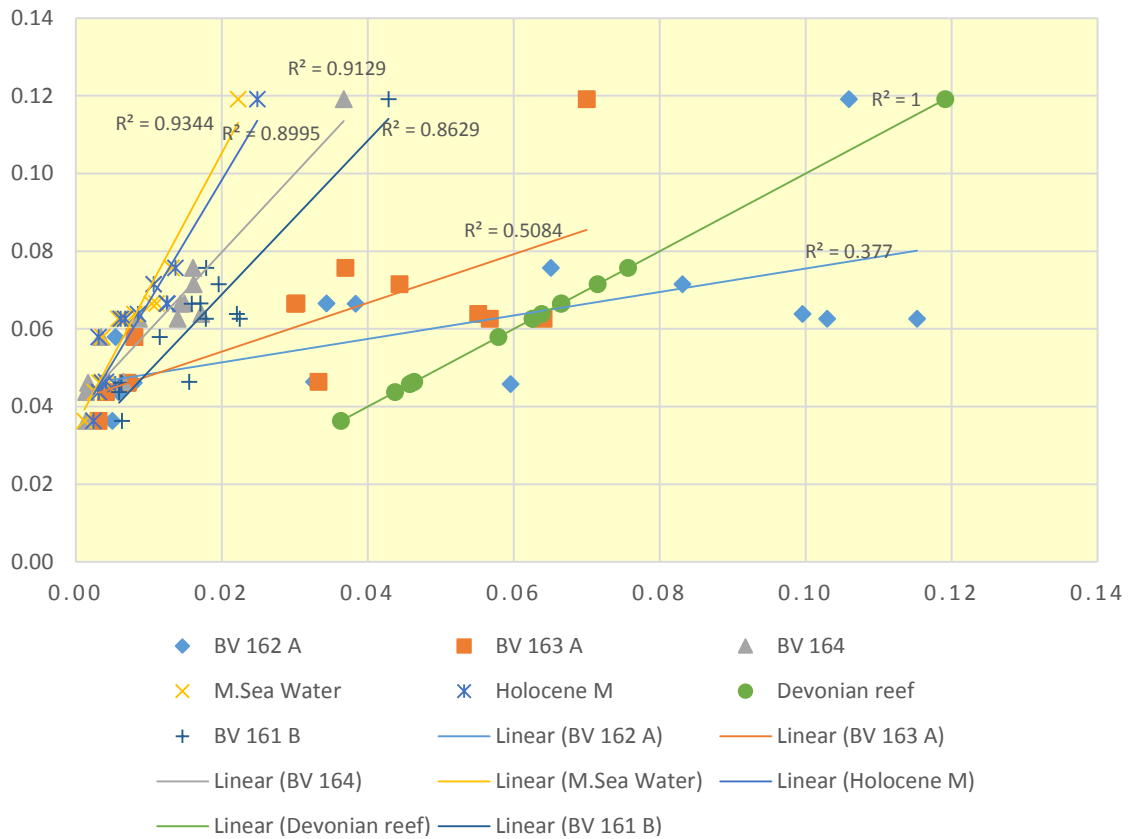


Indeed, from the general overview of the graph, it is evident that Cerium anomalies are marked by a depletion in the spectral signature pattern and Y/Ho ratios are marked by an uplift in the referenced spectral signatures of Devonian Reef, Holocene Marine and marine sea water. This graph also suggests that the selected EARS travertine spectral signatures correspond to the marine limestones in different levels of alteration and field location. This is visible in this graph by the logarithmic different value of Y-axis. Some of these selected EARS travertine samples have satisfied, 80% that is four of the five Balz (2004) criteria. This definitely confirms the presence of marine limestones in the EARS.

Figure VI.38 on page 152 and here below reproduced shows the chart of all EARS travertine samples analysed by ICP-MS the results of which confirmed their respective correlation coefficient  $R^2 > 0.80$  with Devonian reef.

This logarithmic graph of REE concentrations in their carbonates mineral reveal that all the EARS travertine samples analysed in this MSc research, presenting marines limestones REE MUQ values by ICP-MS, corresponds to the Devonian Reef's correlation coefficient referencing the marine limestones.

### ICP-MS 2018 : CORRELATION WITH KNOWN MARINE LIMESTONES



Indeed, from the general overview of this graph, it is evident that the EARS travertines found with marine limestone spectral signature have a positive correlation coefficient  $R_2 \geq 0.80$  with the referenced Devonian Reef. This graph also suggests that the selected EARS travertine spectral signatures correspond to the marine limestones in different levels of alteration and field location with a correlation coefficient variation of  $R_2$  values in the range  $1 \geq R_2 \geq 0.80$ . Some of these selected EARS travertine samples have satisfied with 80% that is four of the five Balz (2004) criteria. This definitely confirms the presence of marine limestones in the EARS.

The 3 charts in Figure VI.42 in page 156, Figure VI.43 in page 157 and Figure VI.44 in page 158 reveal respectively the correlation coefficient of 2013, 2016 and 2018 ICP-MS experiments Marine limestones with published Cenomanian limestones, Neoproterozoic stromatolites with Devonian reef.

All the EARS Travertines samples found with marine limestones REE signatures correlate to:

- Devonian Reef REE signatures (Balz et al., 2004) with a correlation coefficient  $R^2 \geq 0.80$
- Cenomanian Limestones (Bellanca et al. 1997) with a correlation coefficient  $R^2 = 0.3462$
- Neoproterozoic Stromatolites (Corkeron et al. 2012) with a correlation coefficient  $R^2 = 0.5207$

This definitively provide the geologic sourcing of the bicarbonate marine limestones found in the EARS Travertines samples as regrouped in the tables below.

#### II.6.1- BLOC EA41 AND EA4 UGANDA FIELD TRIP, 2007-2009 / ICP-MS 2013

Eleven travertine samples collected in Uganda from 2007 to 2009 show their 2013 ICP-MS results grouped as follows:

<b>CARBONATITES</b>	<b>MIXTURE</b>	<b>MARINE LIMESTONE</b>
LE 44	LE 27	LE 24, LE 26
LE 41	LE 32	LE 28
LE 42	LE 37, LE 38	P12

#### VII.6.2- BLOC V, DRCONGO FIELD TRIP, 2010 / ICP-MS 2013

5 Travertines samples collected in DRC in 2010 show their 2013 ICP-MS results grouped as below:

<b>CARBONATITES</b>	<b>MIXTURE</b>	<b>MARINE LIMESTONE</b>
V2	V 21	V 19
V 20	V 22	

#### VII.6.3- METHOD CONFIRMATION / ICP-MS 2016

16 Travertines samples analysed in 2013 and run again in 2016 show their ICP-MS results grouped as below:

<b>CARBONATITES</b>	<b>MIXTURE</b>	<b>MARINE LIMESTONE</b>
V2b, V20a, V20b	-	P12b,
V22a	-	V19a
LE44a, LE44b	-	LE24a,LE24b, LE26a,LE26b
LE41a, LE41b	-	LE28a,LE28b

#### VII.6.4- BLOC V, DRCONGO, FIELD TRIP 2014 / ICP-MS 2018

13 Travertines samples collected in DRC in 2014 show their 2018 ICP-MS results grouped as below:

CARBONATITES	MIXTURE	MARINE LIMESTONE
BV 338	BV 149	BV 161
BV 352	BV 150	BV 164
BV 356	BV 153	
BV 363	BV 159	
BV 364	BV162	
BV 385	BV 163	

The 46 EARS Travertines samples analysed by this research study using ICP-MS, as above grouped in tables by their geochemistry results from their respective geochemical origin spectral signature, their respective field location, field trip period and their respective ICP-MS analysis calendar, are summarized below with a general view on each Travertine field location and a combination of geologic and geochemistry informations collected by this Msc Research study.

Each of the posters below which group the 46 above Travertines samples regarding their respective field localities, is composed of the Field location of the sample collection in the top left, the sample ID and locality in the top center, the geologic sample and environment description in the top right.

These below posters contain also the thin section microscopic image of each sample and the summary of the geochemistry results obtained in laboratory.

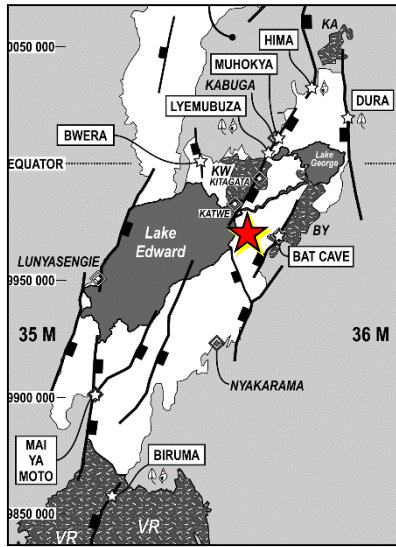
The geochemistry obtained in laboratory by ICP-MS as per our methodology steps, are presented in the below posters in forms of comparative charts showing the spectral signatures of their respective REE obtained values in logarithmic scale from 0 to 10, their respective correlation coefficient charts with Fort Portal for Carbonatites REE and Devonian Reef and Mandawa Basin for Marines limestones as well for hybrid signature. Additionally to the Marine limestones typical signature spectral recognized by the Cerium depletion and Y high pic, the Balz Kamber (2014) Marine limestones criteria check table is associated to each EARS Travertines samples found with Marine limestones and these Key criterias matching are then evaluated and defined as well as are done all the correlation coefficient.

The geological and geochemistry informations gathered together in the below posters are so useful for the better understanding of the palaeo environment of each of the EARS Travertines analysed through this present research study.

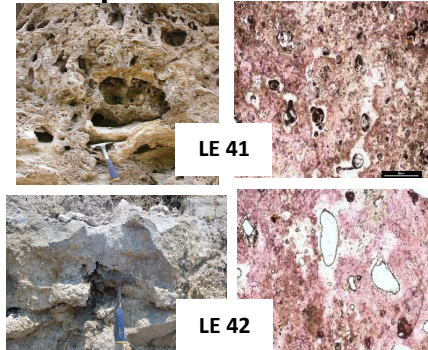
For the best overview of the geochemical origin of EARS travertines, all the samples analysed by ICP-MS in the present MSc research study have been grouped in the following posters according to their exploration basins' field trip period and their respective ICP-MS analysis year. These posters summarise the EARS travertines' geochemical origin field configuration, each sample's petrography and respective ICP-MS results. They also show their respective field samples photos, field environment photo and thin section microscopic photo graphically scaled 1cm to 500  $\mu$ m.







# BWERA Northern Lake Edward, EA4A, Uganda Samples LE41 & LE42



## Samples LE 41 and LE 42

Geological environment: Bwera Hot springs.

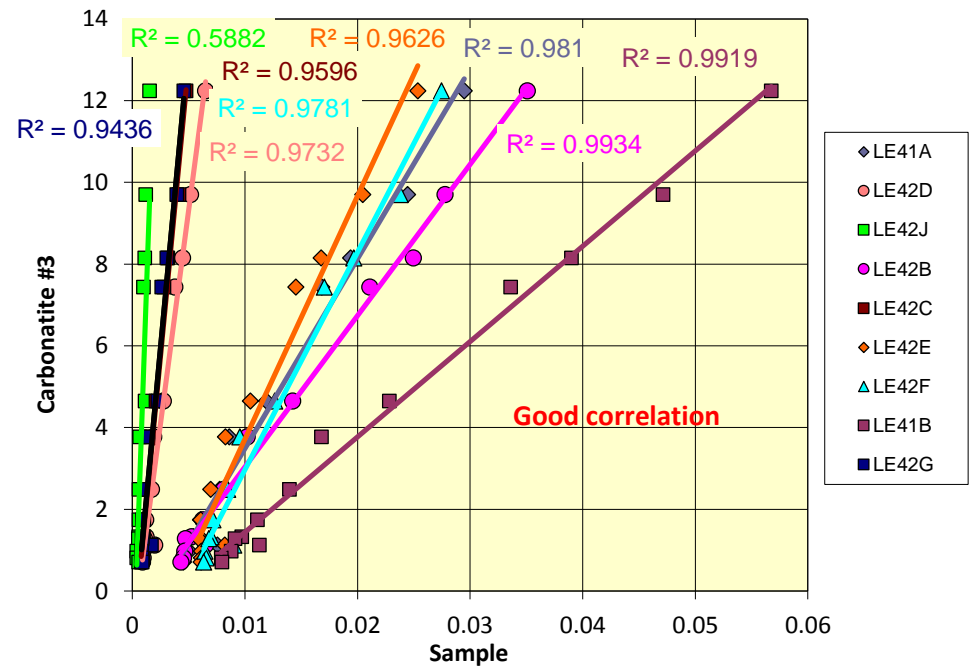
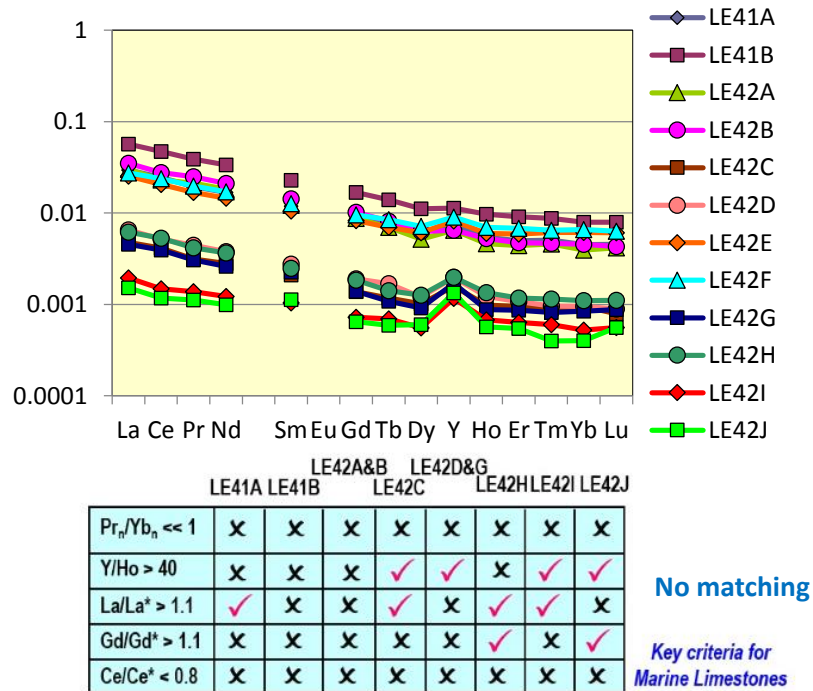
Travertine exposed the East bank of a bounding and NW-SW trending fault against which the Hot springs have developed.

Difficult to see how far they go deep into the hill or whether they are superficial covering. Excellent outcrop of paleostalactites.

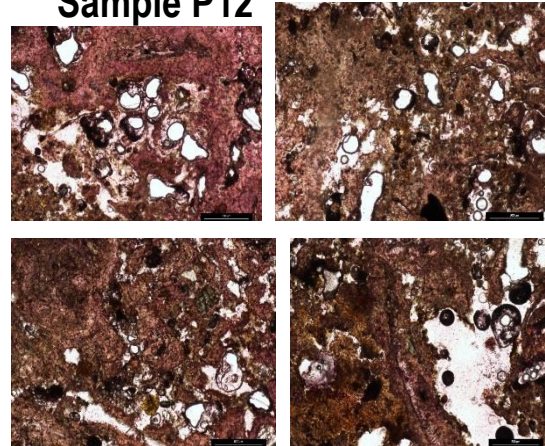
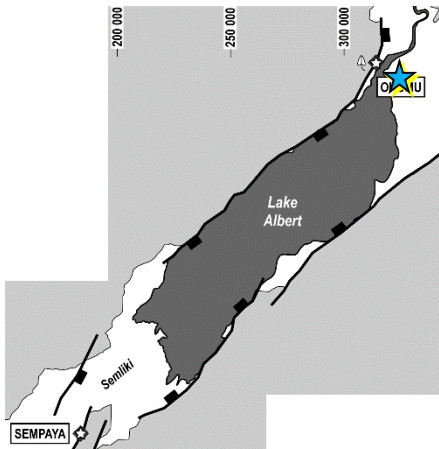
Field description:

LE 41: Light brown limestones; visible vacuoles. High porosity. Possible Veins Network; Freezing with HCl acid.

LE 42: Freezing with HCl acid. Carbonate grains and cement. Visible different layers spreaded in the whole sample



**OKUMU (HOT SPRINGS)**  
**North-western Lake Albert,**  
**EA1, Uganda**  
**Sample P12**

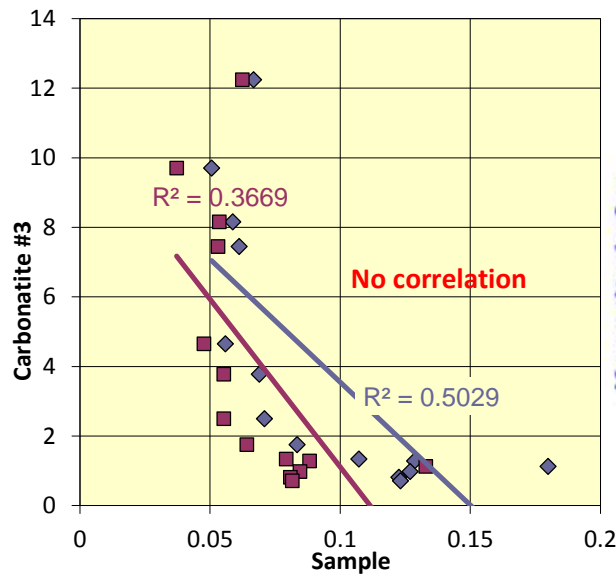


**Sample P12**

Geological environment: Okumu and Avoca Hot Springs. Moderately warm to hot but not too hot to touch located in a NE rift fault intersection with a younger NW active trending fault. No major stream flowing through gorge and the spring appears to be genuinely along the main rift fault. No obvious strong H<sub>2</sub>S smell. Dispersed Carbonatites caliche throughout.

Field description: P12

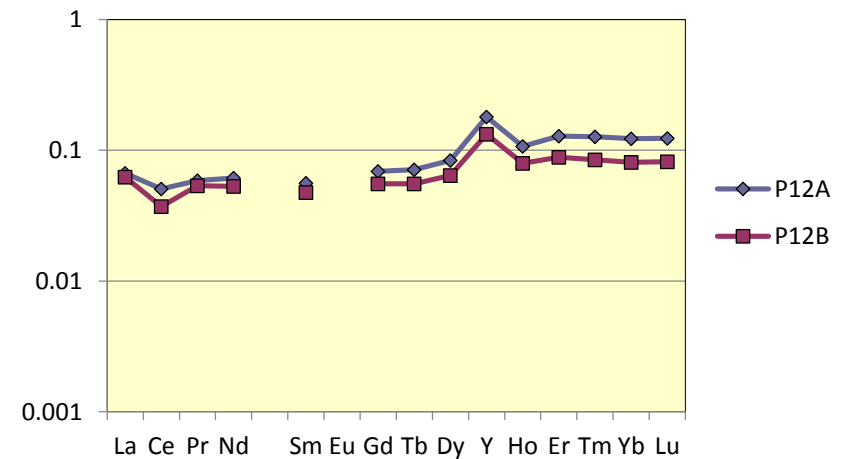
Travertine with fossil tubes and visible rootlets;  
 Small blocks of basement caught up in these fossil tubes;  
 Few fossil leaves;  
 Apparent black relicts in cavities.  
 Feezing with HCl acid.



Matching P12A P12B

$Pr_n/Yb_n << 1$	✓	✓
$Y/Ho > 40$	✓	✓
$La/La^* > 1.1$	✓	✓
$Gd/Gd^* > 1.1$	✓	✓
$Ce/Ce^* < 0.8$	✗	✓

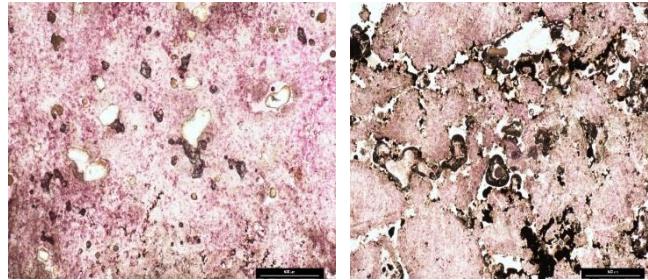
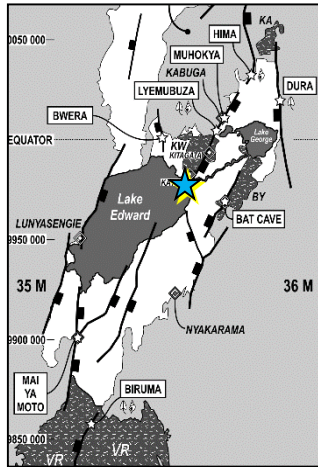
Key criteria for Marine Limestones



# LYEMUBUZA

## Western Lake George, EA4A, Uganda

### Samples LE24 & LE26



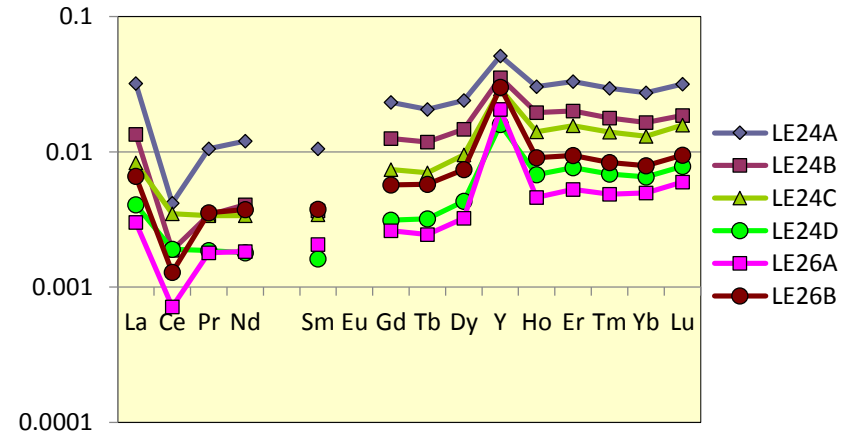
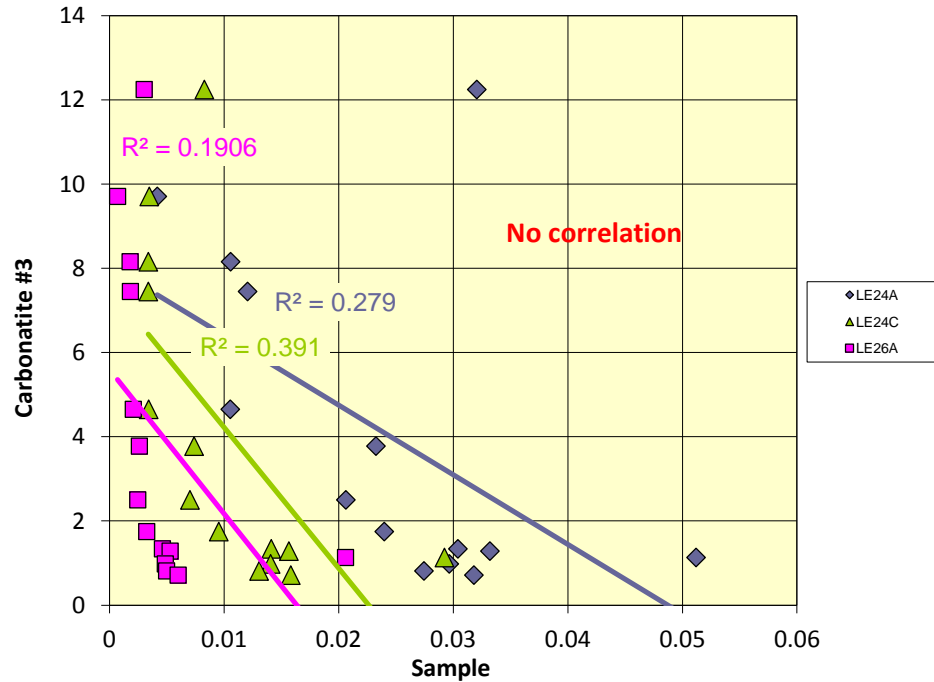
### Samples LE 24, and LE 26.

#### Geological environment:

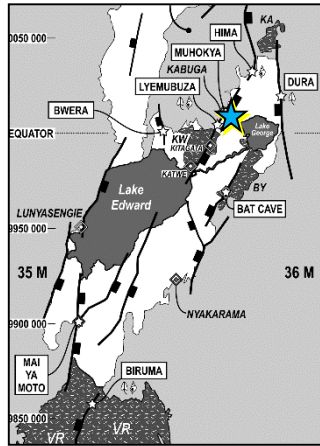
Calcite formed in an inverted fairly impressive cliff appearing like a rotational uplift on top of a normal fault block. No evidence of continuous limestone bands.

#### Field description: LE 24 and LE 26

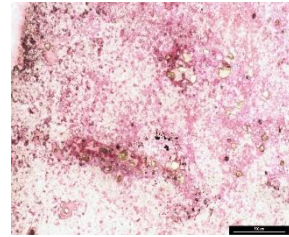
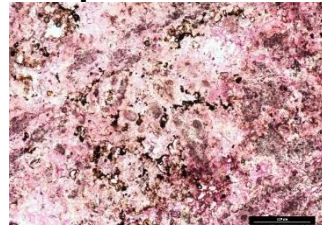
Travertine with primary porosity seeming to have black organic rich fill to their primary porosity. Feezing with HCl acid.



Matching	LE24A	LE24B	LE24C	LE24D	LE26A	LE26B
$Pr_n/Yb_n << 1$	✓	✓	✓	✓	✓	✓
$Y/Ho > 40$	✓	✓	✓	✓	✓	✓
$La/La^* > 1.1$	✓	✓	✓	✓	✓	✓
$Gd/Gd^* > 1.1$	✓	✓	✓	✓	✓	✓
$Ce/Ce^* < 0.8$	✓	✓	✗	✗	✓	✓



**MUHOKYA**  
**Western Lake George,**  
**EA4A, Uganda**  
**Sample LE28**



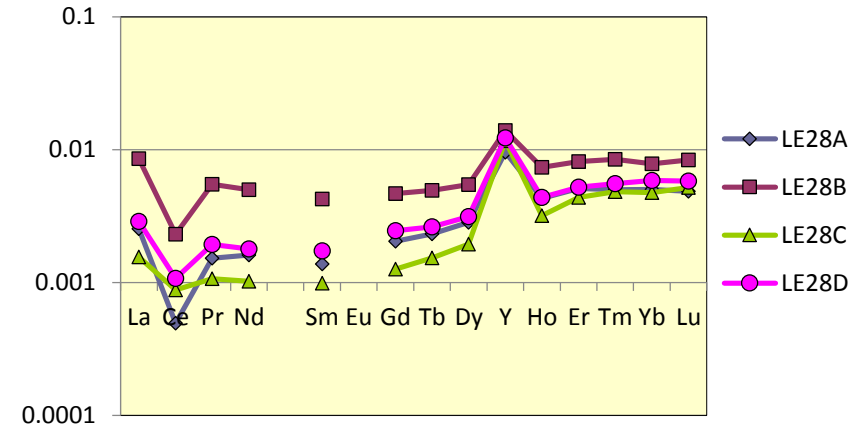
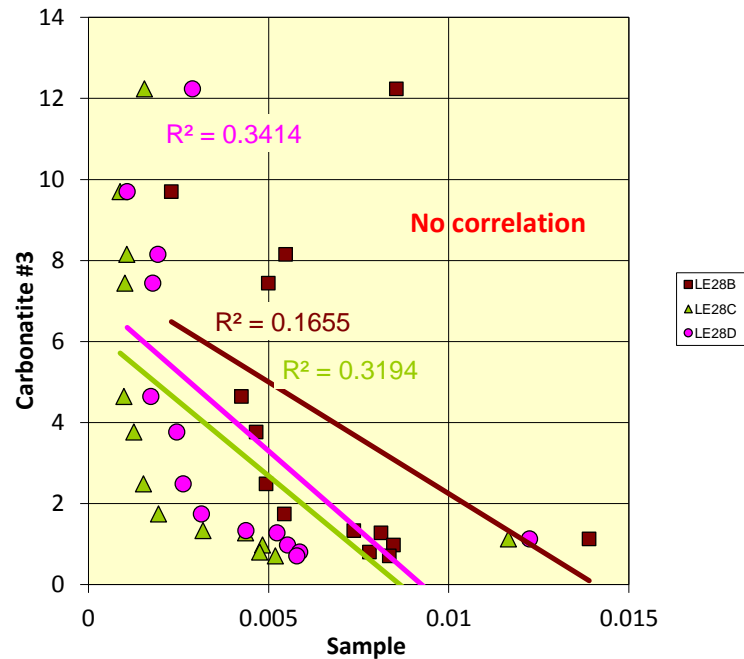
**Samples LE 28**

Geological environment:

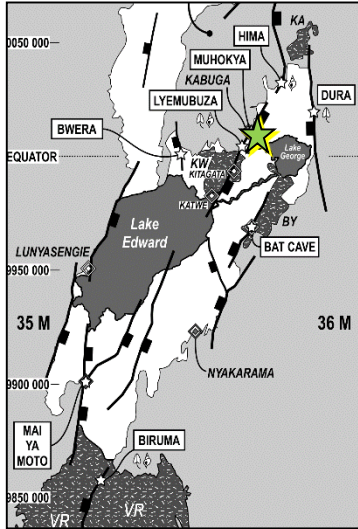
Calcite formed in an inverted fairly impressive cliff appearing like a rotational uplift on top of a normal fault block. No evidence of continuous limestone bands.

Field description: LE 28

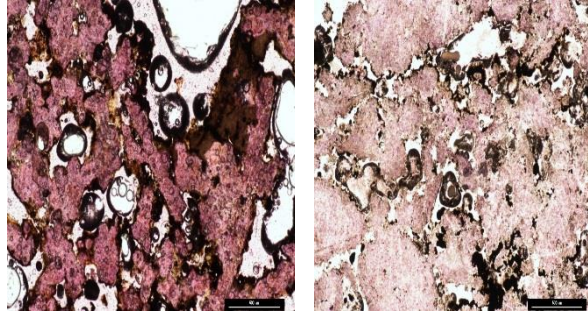
Travertine with primary porosity seeming to have black organic rich fill to their primary porosity. Feezing with HCl acid.



Matching	LE28A	LE28B	LE28C	LE28D
$Pr_n/Yb_n \ll 1$	✓	✓	✓	✓
$Y/Ho > 40$	✓	✓	✓	✓
$La/La^* > 1.1$	✓	✓	✓	✓
$Gd/Gd^* > 1.1$	✓	✓	✓	✓
$Ce/Ce^* < 0.8$	✓	✗	✗	✓



**MUHOKYA**  
**Western Lake George,**  
**EA4A, Uganda**  
**Sample LE27**



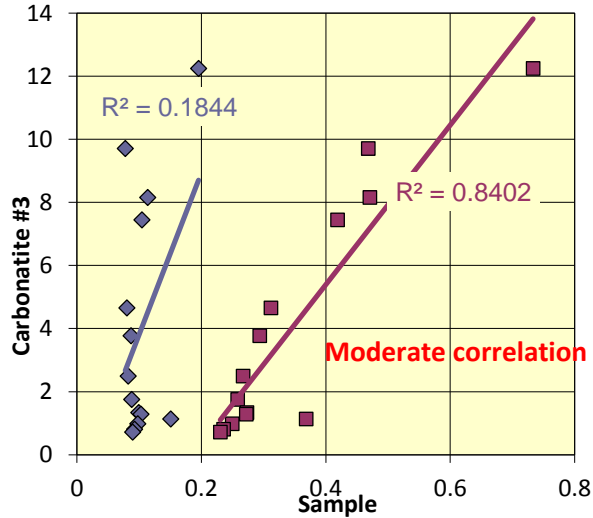
**Samples LE 27**

Geological environment:

Calcite formed in an inverted fairly impressive cliff appearing like a rotational uplift on top of a normal fault block. No evidence of continuous limestone bands.

Field description: LE 27

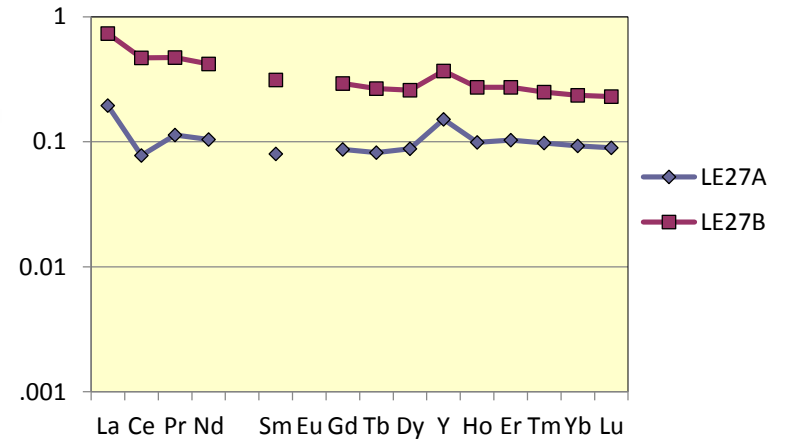
Travertine with primary porosity seeming to have black organic rich fill to their primary porosity. Feezing with HCl acid.

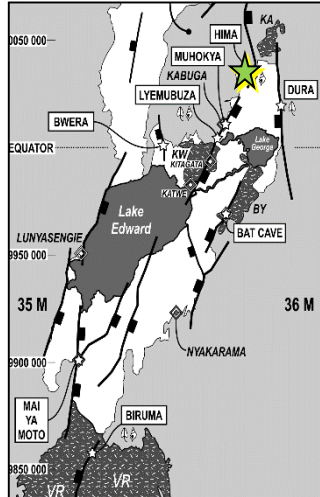


Key criteria for Marine Limestones

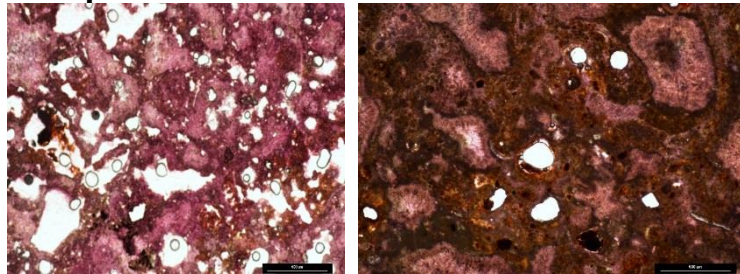
	LE27A	LE27B
$Pr_n/Yb_n \ll 1$	X	X
$Y/Ho > 40$	✓	X
$La/La^* > 1.1$	✓	✓
$Gd/Gd^* > 1.1$	✓	X
$Ce/Ce^* < 0.8$	✓	X

Moderately Matching

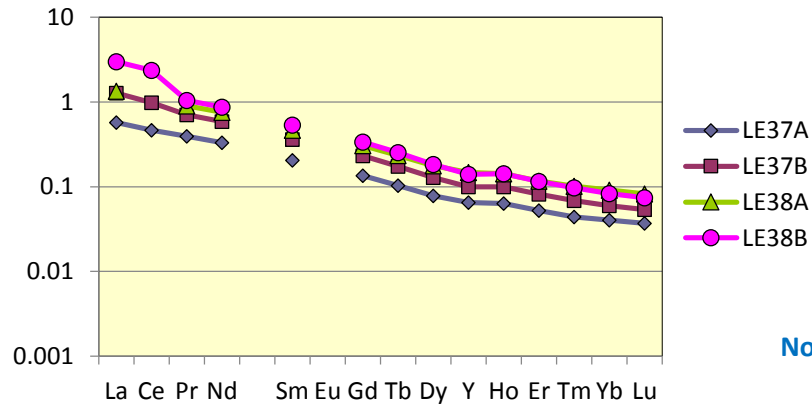




**HIMA CEMENT QUARRIES**  
**Western Lake George,**  
**EA4A, Uganda**  
**Samples LE37 & LE38**



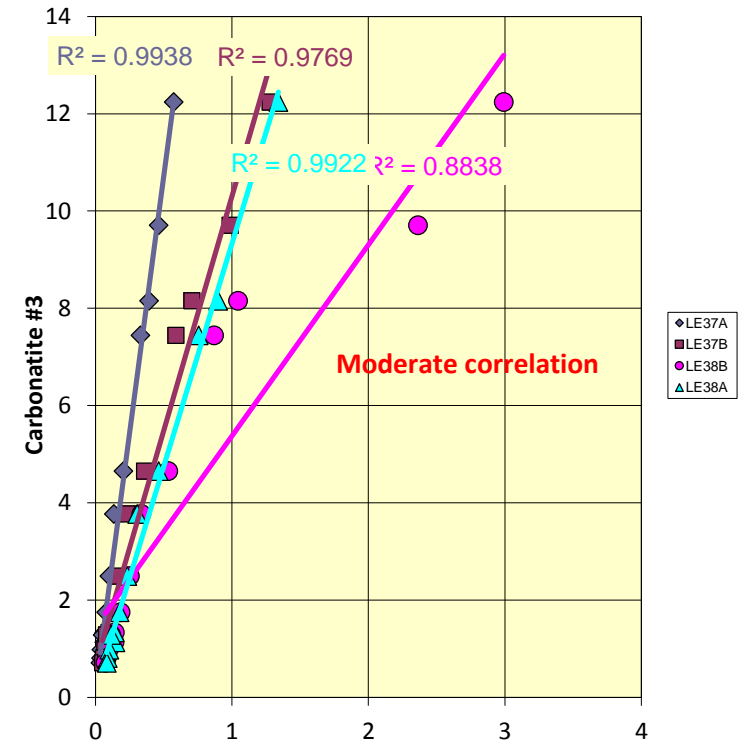
**Samples LE 37 and LE 38**  
Geological environment: Hima cement works mine.  
 Located just downstream north of a river bank flowing through the Ruwenzori border fault.  
Field description: 37, and LE 38  
 Very porous light brown limestones;  
 Vugs visible presence dispersed in all sample;  
 Feezing with HCl acid.

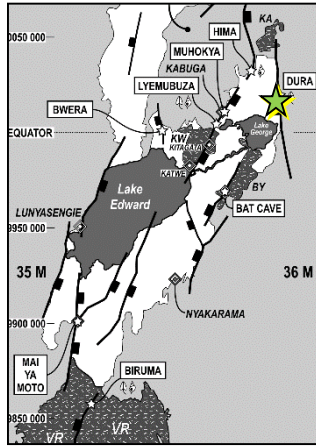


No matching

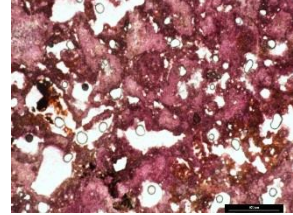
Key criteria for Marine Limestones

	LE37A	LE37B	LE38A	LE38B
$Pr_n/Yb_n \ll 1$	X	X	X	X
$Y/Ho > 40$	X	X	X	X
$La/La^* > 1.1$	X	✓	X	✓
$Gd/Gd^* > 1.1$	X	X	X	X
$Ce/Ce^* < 0.8$	X	X	✓	X





**DURA**  
**Eastern Lake George,**  
**EA4A, Uganda**  
**Sample LE32**

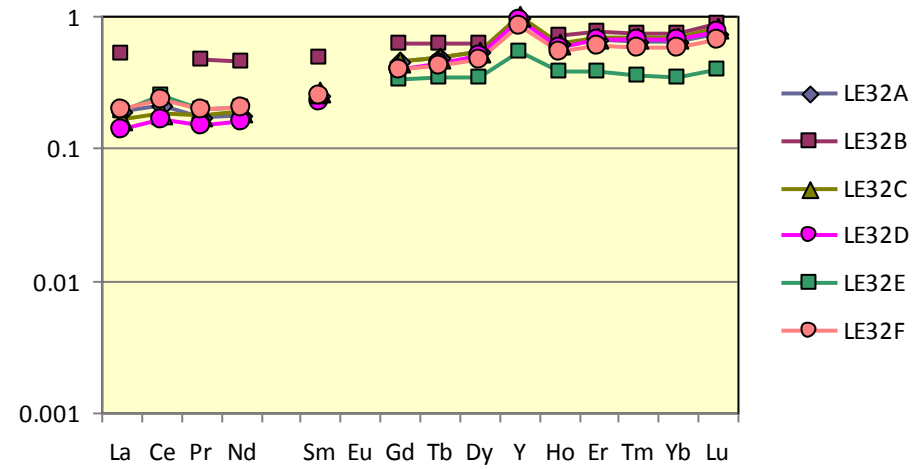
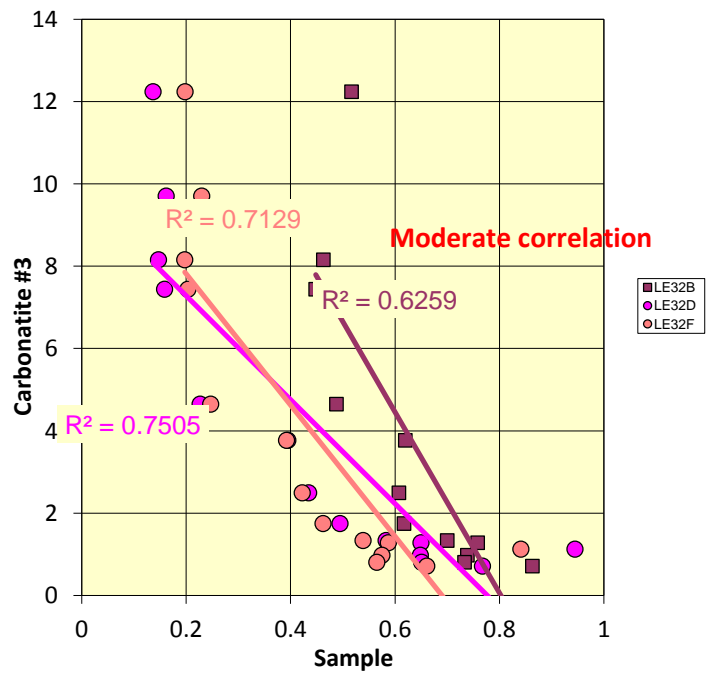


**Samples LE 32**

Geological environment: Dura cement Works mine.  
 Located just downstream north of a river bank flowing through the Ruwenzori border fault.

**Field description:** LE 32, 37, and LE 38

Very porous light brown limestones;  
 Vugs visible presence dispersed in all sample;  
 Feezing with HCl acid.



Moderately matching LE32A LE32B LE32C LE32D LE32E LE32F

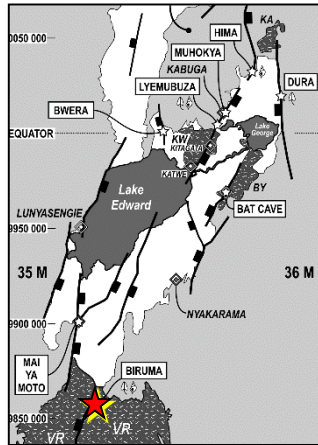
Key criteria for Marine Limestones	Pr <sub>n</sub> /Yb <sub>n</sub> << 1	✓	✓	✓	✓	✓	✓
	Y/Ho > 40	✓	✗	✓	✓	✗	✓
	La/La* > 1.1	✓	✗	✓	✗	✗	✗
	Gd/Gd* > 1.1	✗	✗	✗	✗	✗	✗
	Ce/Ce* < 0.8	✗	✓	✗	✗	✗	✗



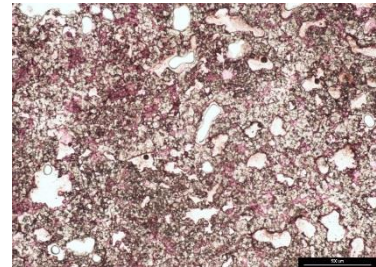
The result here above provides some evidence of geochemistry origin for different Carbonates outcropping in the Ugandan side of Albert Graben, EARS. They have demonstrated that:

- Samples LE 44A & B, drilled respectively through its white and dark layers, gave a typical Carbonatites signature with high pics of light REE (lanthanide) and Yttrium concentrations which are characterizing apatite's Carbonatites associations with very good correlation coefficient  $R^2 > 0.90$  with Fort Portal sample #3. No Marine limestones criteria matching. These basic findings are consistent with this research objectives showing that there is involvement of Carbonatites emerging from depth to the subsurface through groundwaters;
- LE 41 & LE 42, drilled through vacuoles, grains or cement, gave also a typical Carbonatites signature with also high pics of light REE (lanthanide) and Yttrium concentrations which are characterizing apatite's Carbonatites associations with a very good correlation coefficient  $R^2 > 0.94$  with FP #3. Very few marine (negligible) limestones criteria matching not enough to conclude a marine limestone involvement. This fact clearly implies the involvement of Carbonatites groundwaters depositing Carbonatites in around an evident hot spring;
- P12, drilled through carbonates fill tubes avoiding rootlets, fossil leaves, small basement blocs caught up in these fossil tubes and black relics in the cavities, the P12 ICP-MS results revealed a Marine limestones spectral signatures interesting facts. Negative correlation coefficient  $R^2 = 0.36$  with FP#3 has been scientifically established while a matching has been found with the Marine Limestones Balz procedure criteria with Ce anomalies ( $Ce/Ce^* \sim 0.55$ ) suggesting palaeo ocean-basin floor setting. This result demonstrates the first clear evidence of underneath Marine limestone deposit involvement for the origin of the carbonates in this Travertine outcrop;
- LE 24, LE 26 and LE 28, have been drilled as above through visible carbonates textures, structures or fabrics avoiding any black organic rich fill to their primary porosity, these samples ICP-MS results revealed a Marine limestones spectral signatures interesting facts. No correlation with FP#3 has been scientifically established while a matching has been found with the Marine Limestones Balz paper procedure criteria with Ce anomalies ( $Ce/Ce^* \sim 0.55$ ) suggesting palaeo ocean-basin floor setting. This result demonstrates further evidence of underneath Marine limestone deposit involvement for the origin of these carbonates;
- LE 27, 32, 37 and 38, have been drilled as above through visible carbonates textures, structures or fabrics avoiding any black organic rich fill to their primary porosity, these samples ICP-MS results revealed a kind of weird

spectral signatures different from typical Carbonatites or Marine limestones. Negative to Moderate correlation with FP#3 and No to moderately matching with Balz paper criteria. These results demonstrate that a kind of hybrid (intermediate) source of carbonates does exist within the Rift basin. This hybrid source seems to be a mixture of Carbonatites and Marine limestones sources.



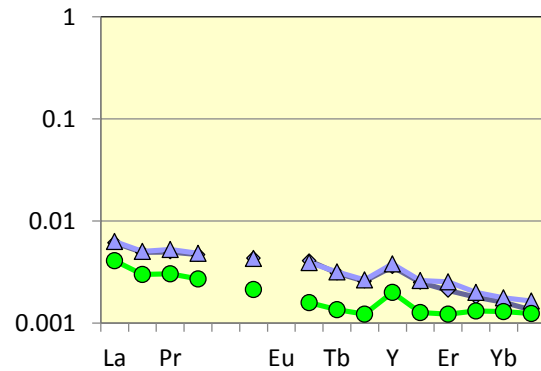
**BIRUMA**  
**Southern Lake Edward,**  
**Block V, DRC**  
**Sample V2**



**Samples V2:**

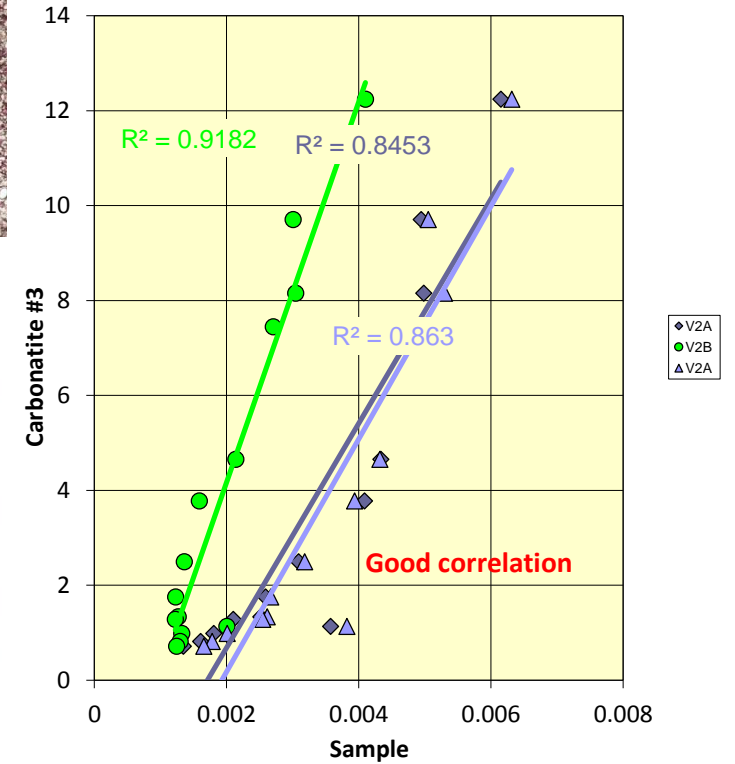
Light Brown very crumble limestone with vugs porosity and visible rootlets branches and plant tubes;

For security reasons and safety, field time was restricted for more field detailed description.

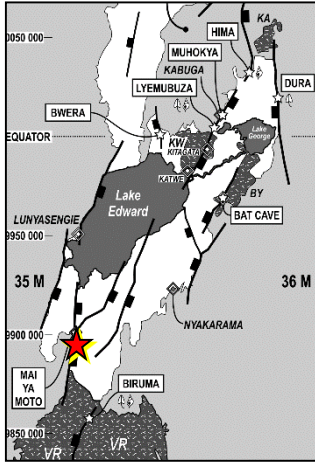


**Key criteria for Marine Limestones**

	No matching	V2A	V2A	V2B
$Pr_n/Yb_n << 1$		X	X	X
$Y/Ho > 40$		X	X	✓
$La/La^* > 1.1$		✓	X	X
$Gd/Gd^* > 1.1$		✓	X	X
$Ce/Ce^* < 0.8$		X	X	X



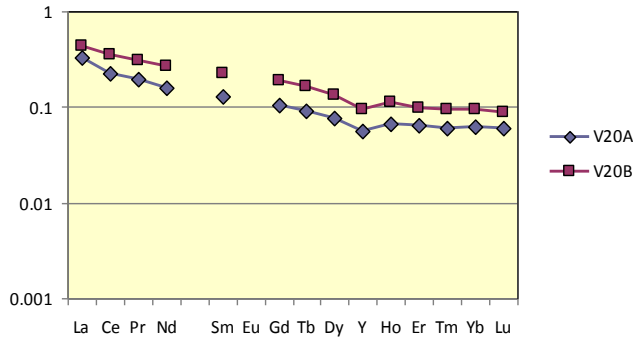
# MAI YA MOTO (HOT SPRINGS) Southern Lake Edward, Block V, DRC Sample V20



## Samples V20:

Black stained lining in white vugs spreaded Travertine.

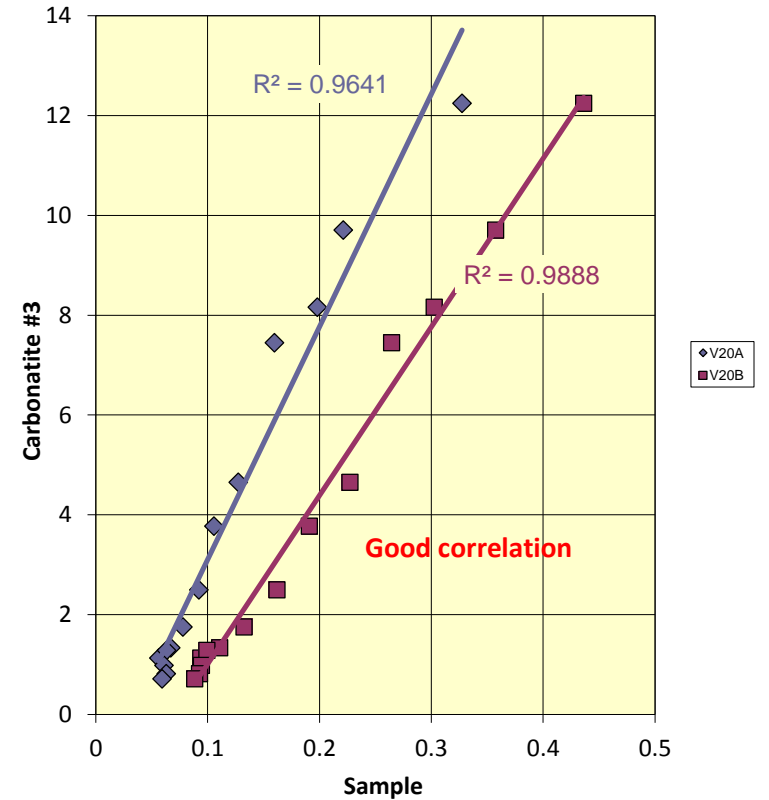
For security reasons and safety, field time was restricted for more field detailed description.



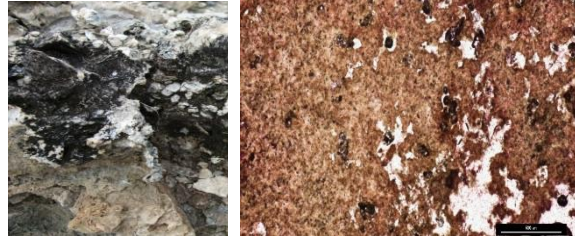
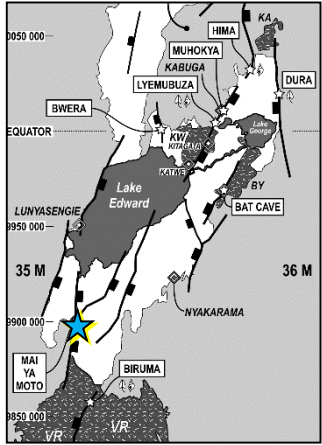
No matching V20A V20B

*Key criteria for Marine Limestones*

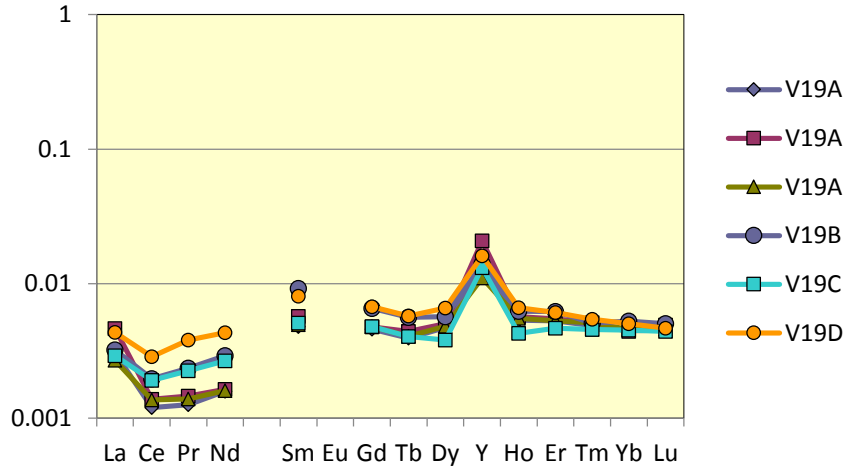
$Pr_n/Yb_n \ll 1$	X	X
$Y/Ho > 40$	X	X
$La/La^* > 1.1$	X	✓
$Gd/Gd^* > 1.1$	X	X
$Ce/Ce^* < 0.8$	X	X



# MAI YA MOTO (HOT SPRINGS) Southern Lake Edward, Block V, DRC Sample V19



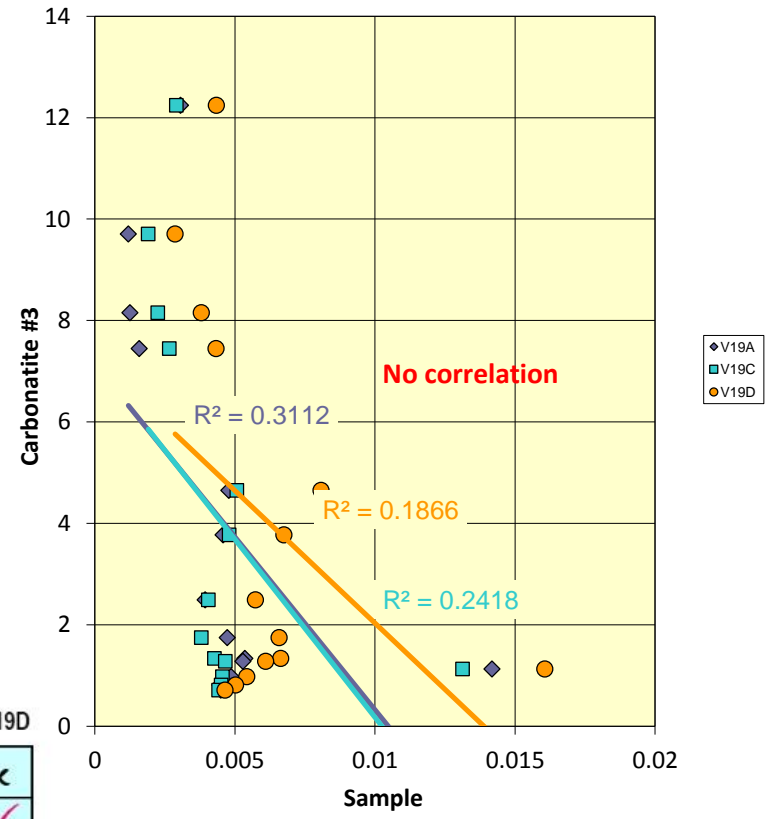
**Samples V19:**  
Black stained lining in white vugs spreaded Travertine.  
For security reasons and safety, field time was restricted for more field detailed description.



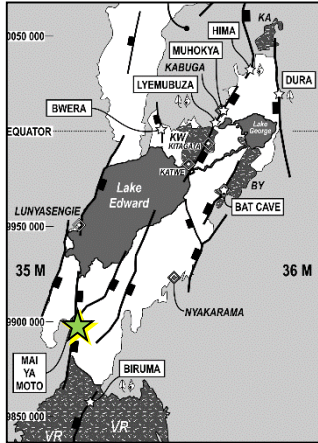
**Matching** V19A V19A V19A V19B V19C V19D

*Key criteria for Marine Limestones*

$Pr_n/Yb_n << 1$	✓	✓	✓	✓	✓	✗
$Y/Ho > 40$	✓	✓	✓	✓	✓	✓
$La/La^* > 1.1$	✓	✓	✓	✓	✓	✓
$Gd/Gd^* > 1.1$	✓	✓	✓	✓	✓	✓
$Ce/Ce^* < 0.8$	✗	✗	✗	✗	✗	✗



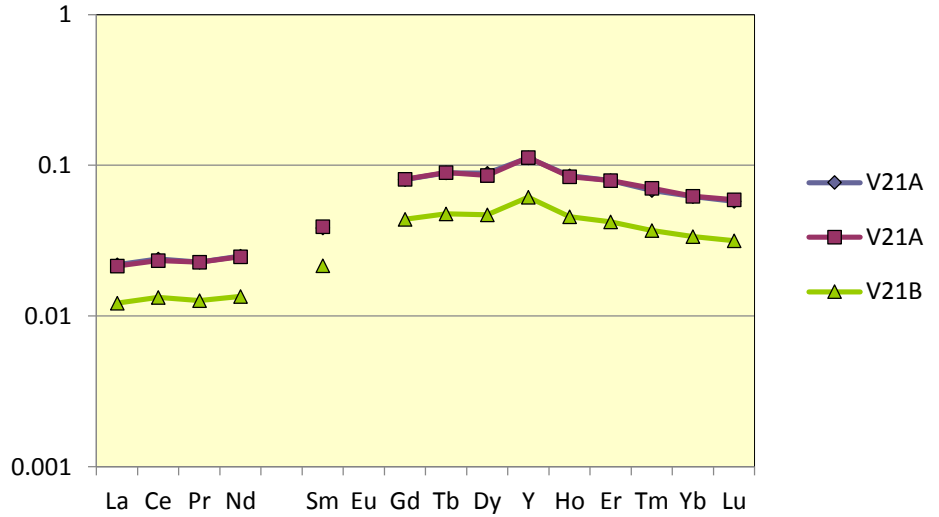
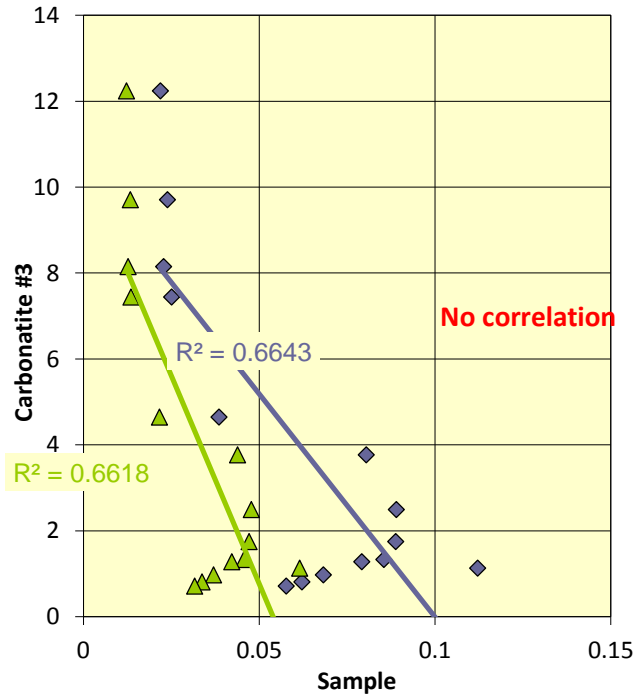
**MAI YA MOTO (HOT SPRINGS)**  
**Southern Lake Edward, Block V,**  
**DRC**  
**Sample V21**



**Samples V21:**

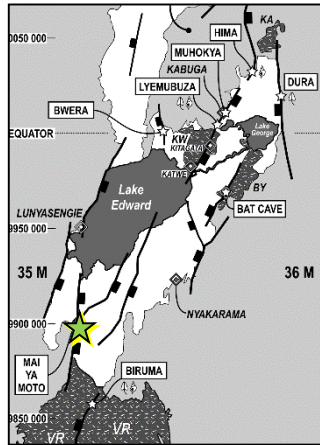
Black stained lining in white vugs spreaded Travertine.

For security reasons and safety, field time was restricted for more field detailed description.



No matching

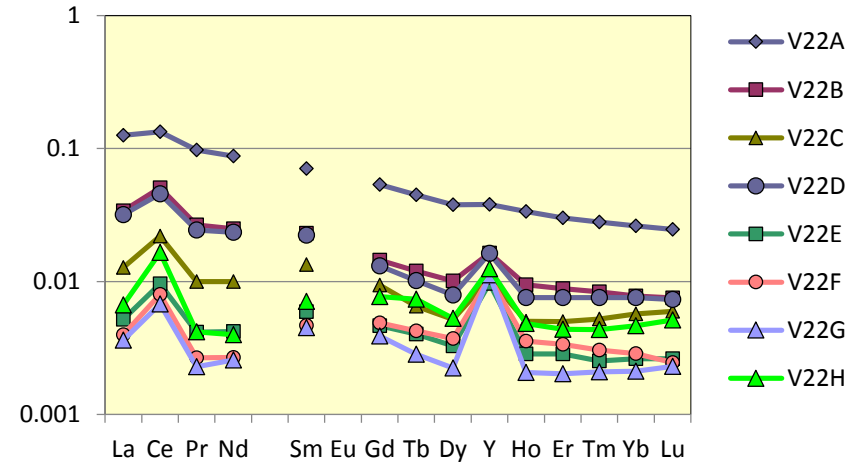
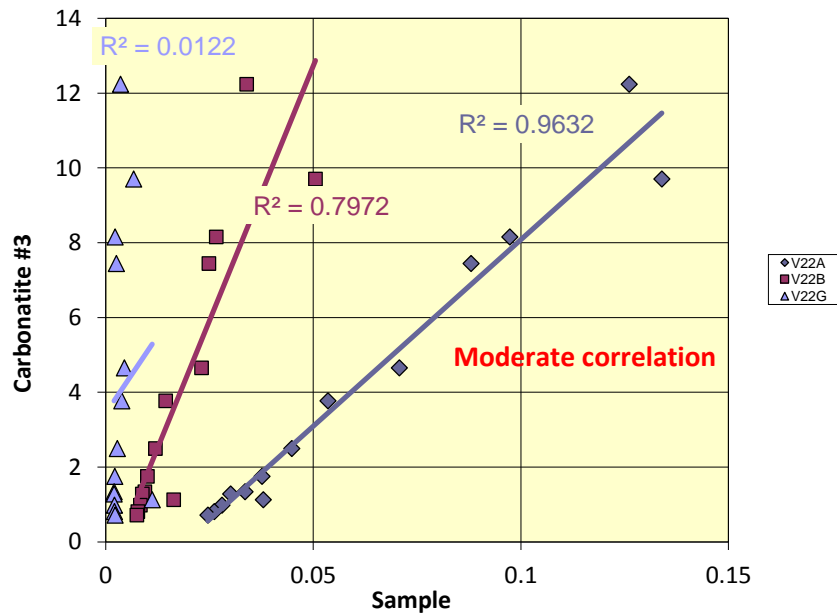
	V21A	V21A	V21B
<i>Key criteria for Marine Limestones</i>			
$Pr_n/Yb_n \ll 1$	✓	✓	✓
$Y/Ho > 40$	✗	✗	✗
$La/La^* > 1.1$	✓	✓	✓
$Gd/Gd^* > 1.1$	✗	✗	✗
$Ce/Ce^* < 0.8$	✗	✗	✗



## MAI YA MOTO (HOT SPRINGS) Southern Lake Edward, Block V, DRC Sample V22



**Samples V22:**  
Black stained lining in white vugs spreaded Travertine.  
For security reasons and safety, field time was restricted for more field detailed description.



Moderately matching

	V22A	V22B	V22C	V22D	V22E	V22F	V22G	V22H
$Pr_n/Yb_n << 1$	X	X	X	X	X	X	X	X
$Y/Ho > 40$	X	✓	✓	✓	✓	✓	✓	✓
$La/La^* > 1.1$	X	✓	✓	✓	✓	✓	✓	✓
$Gd/Gd^* > 1.1$	X	X	✓	X	X	X	X	X
$Ce/Ce^* < 0.8$	X	X	X	X	X	X	X	X

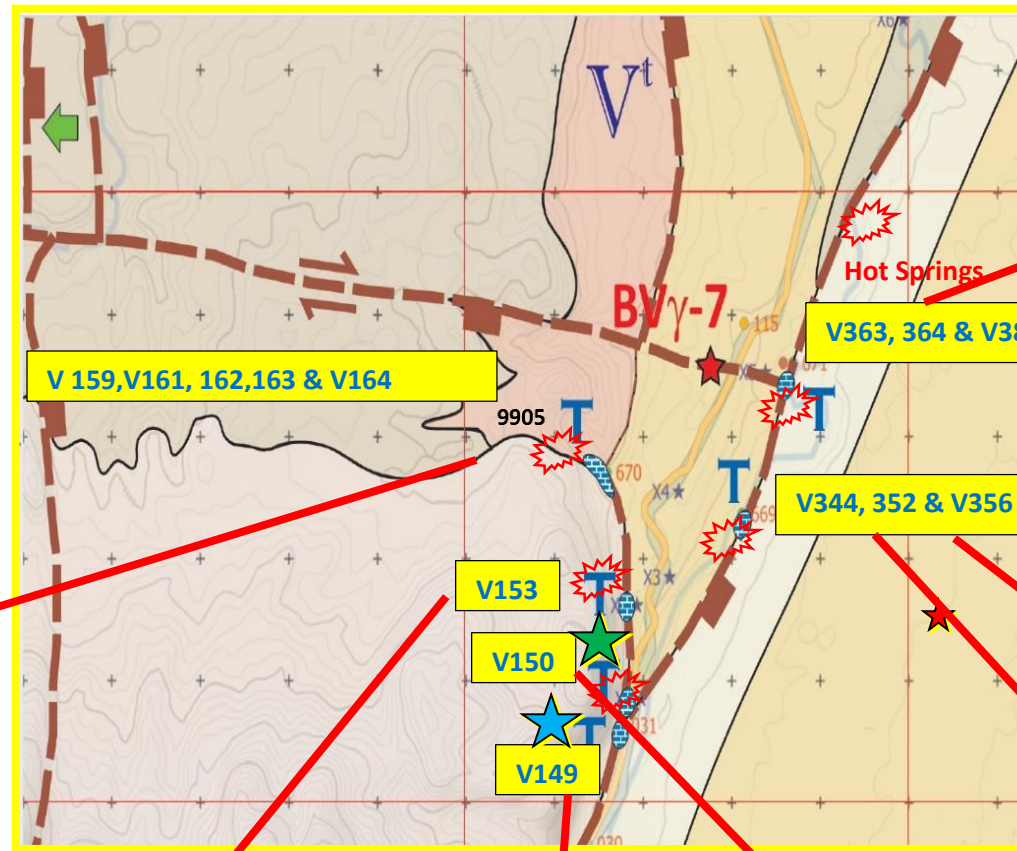
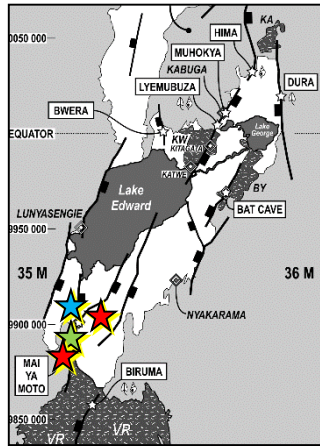
The result here above provides some evidence of geochemistry origin for different Carbonates outcropping in the DR Congo side of Albert Graben, EARS. They have demonstrated that:

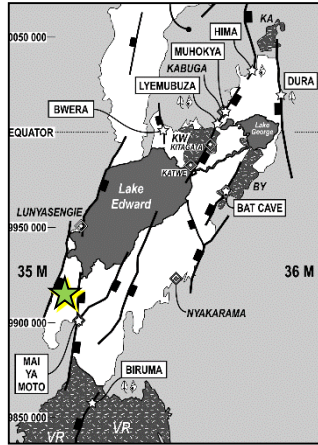
- V2, drilled respectively through its light brown very crumble and carbonates in vugs porosity layers avoiding the visible rootlets, branches or plant tubes, gave a typical Carbonatites signature with very good correlation coefficient  $R^2 > 0.90$  with FP#3. No Marine limestones criteria matching. These basic findings are consistent with this research objectives showing that there is involvement of Carbonatites emerging from depth to the subsurface through groundwaters;
- V20, drilled through the carbonates porosity filled textures avoiding the black stained lining in white vugs, gave a typical Carbonatites signature with very good correlation coefficient  $R^2 > 0.90$  with FP#3. No Marine limestones criteria matching. These basic findings are consistent with this research objectives showing that there is involvement of Carbonatites emerging from depth to the subsurface through groundwaters;
- V19, drilled through the carbonates porosity filled textures avoiding the black stained lining in white vugs, the V19 ICP-MS results revealed a Marine limestones spectral signatures interesting facts. No correlation with FP#3 has been scientifically established while a matching has been found with the Marine Limestones Balz paper criteria. This result demonstrates the first evidence of underneath Marine limestone deposit involvement for the origin of the carbonates in this Travertine outcrop;
- V21 and V22, have been drilled as above through the carbonates porosity filled textures avoiding the black stained lining in white vugs, these samples ICP-MS results revealed a kind of weird spectral signatures different from typical Carbonatites or Marine limestones. No to Moderate correlation with FP#3 and No to moderately matching with Balz paper criteria. These results demonstrate that a kind of hybrid source of carbonates does exist within the Rift basin. This hybrid source seems to be a mixture of Carbonatites and Marine limestones sources.

The figures below show all the 2014 field samples analysed by ICP-MS in 2018. These Figures highlight for each sample analysed that little is known about:

- Sample location in the map region
- Sample field photo and description
- Sample geologic environment
- Sample thin section and petrography comments
- The results of ICP-MS, which show planned correlation comparisons revealing either the Carbonatites, marine limestones or mixture involvement in their respective spectral signatures.



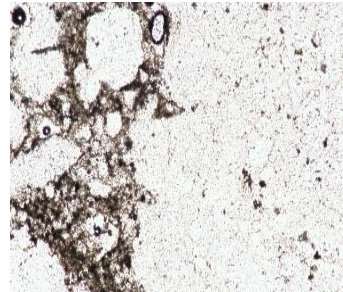




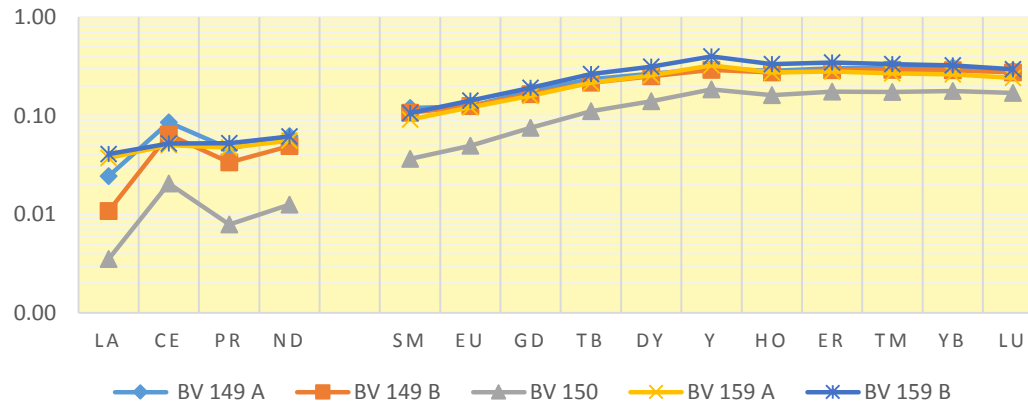
**Mai Ya Moto**  
**Southern Lake Edward,**  
**Block V, DRC**  
**Sample V 149**

**Samples V149:**

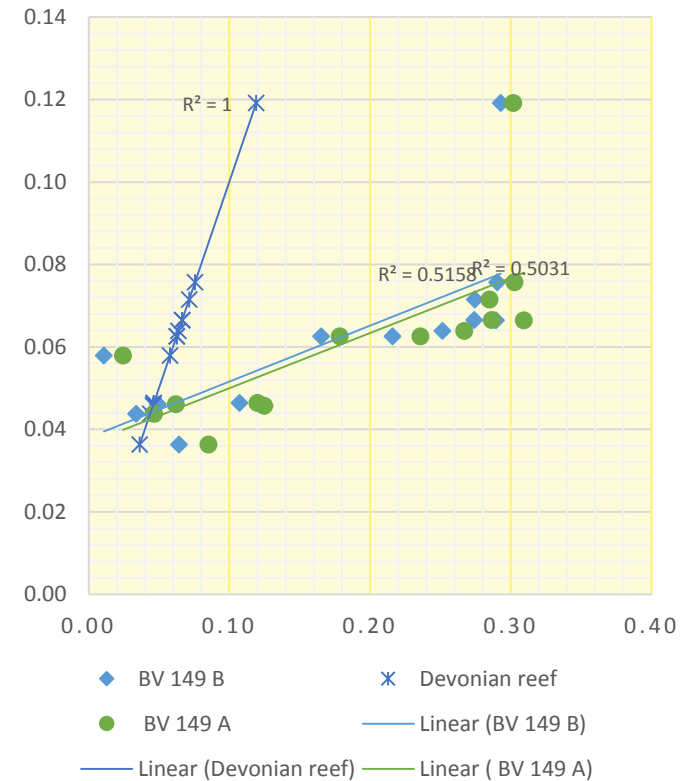
Light Brown very crumble limestone with vugs porosity and visible rootlets branches and plant tubes; Single block. Light brown fibrous Travertine with Breccia gap and cavities.

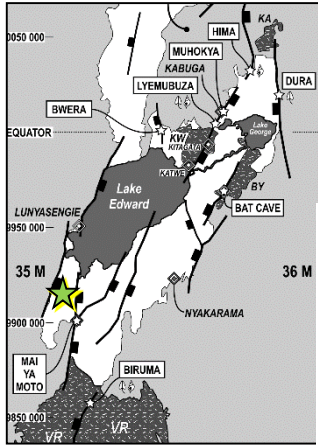


**ICP-MS 2018: HYBRID SIGNATURES**



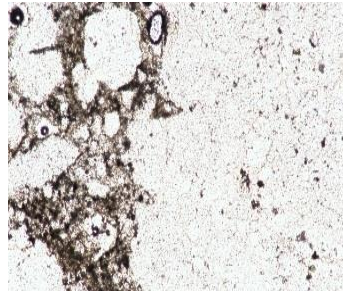
**HYBRID SAMPLES CORRELATION WITH DEVONIAN REEF**



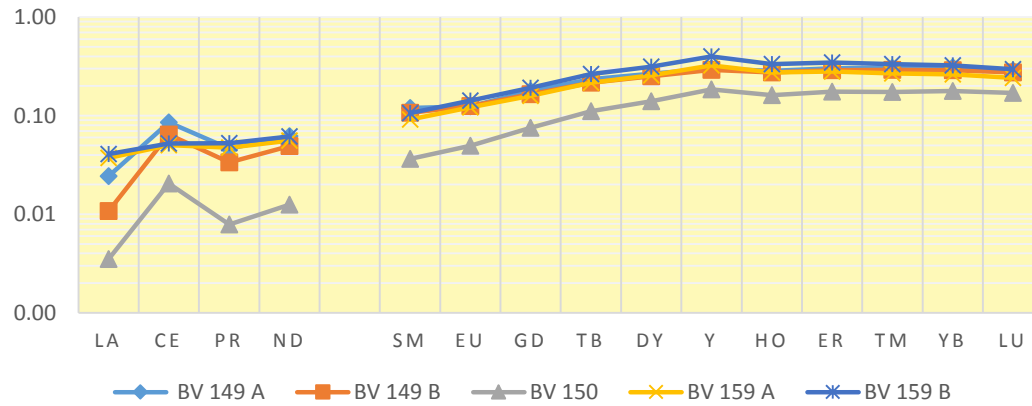


**Mai Ya Moto**  
**Southern Lake Edward,**  
**Block V, DRC**  
**Sample V 149**

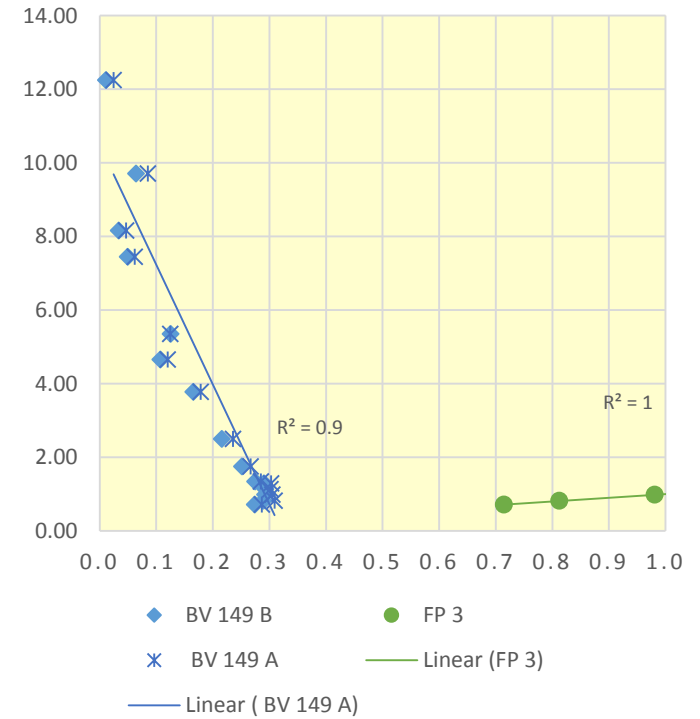
**Samples V149:**  
 Light Brown very crumble limestone with vugs porosity and visible rootlets branches and plant tubes; Single block. Light brown fibrous Travertine with Breccia gap and cavities.

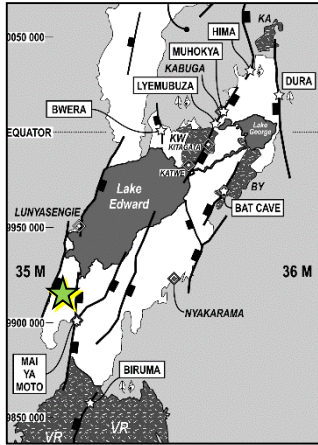


**ICP-MS 2018: HYBRID SIGNATURES**



**HYBRID SAMPLES CORRELATION WITH FORT PORTAL**

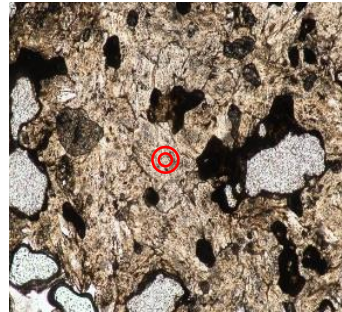




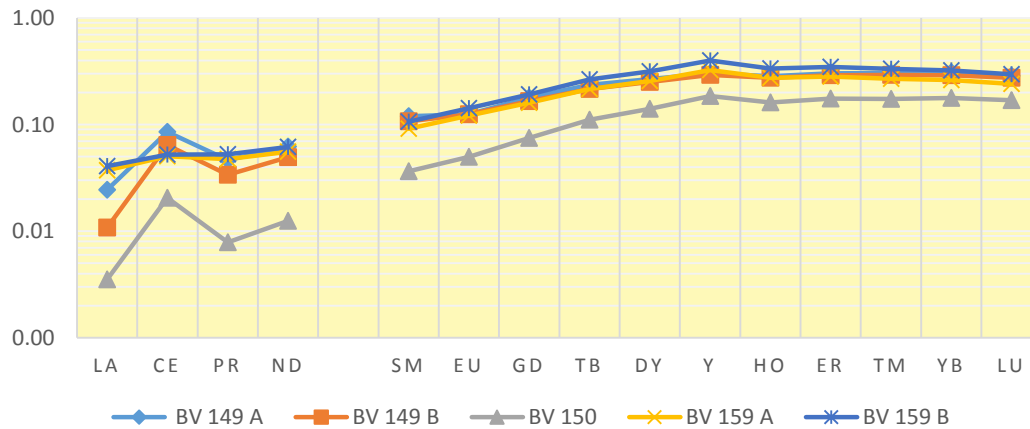
**Mai Ya Moto**  
**Southern Lake Edward,**  
**Block V, DRC**  
**Sample V 150**

**Samples V150:**

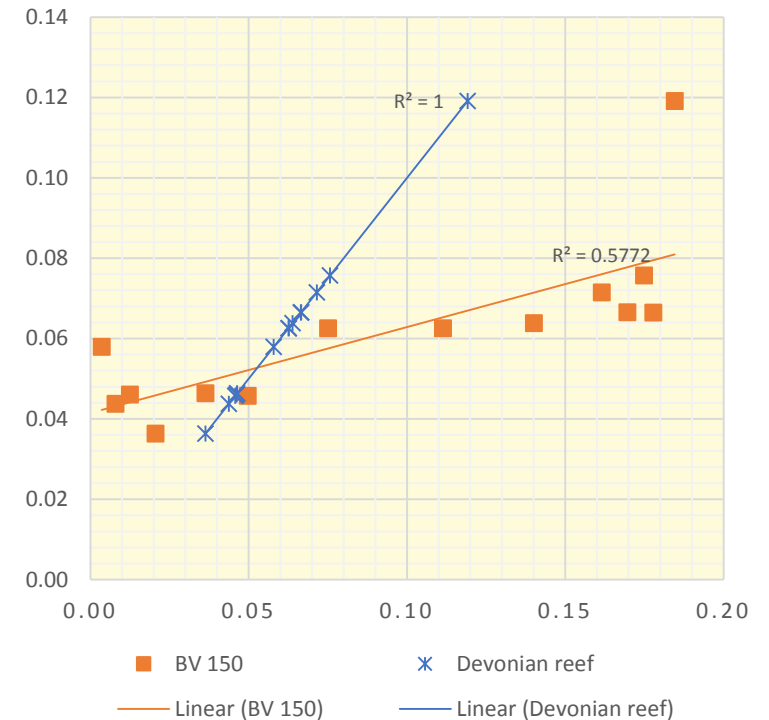
Light Brown very crumble limestone with vugs porosity and visible rootlets branches and plant tubes. Microbially laminated white Travertine with fibrous layers.

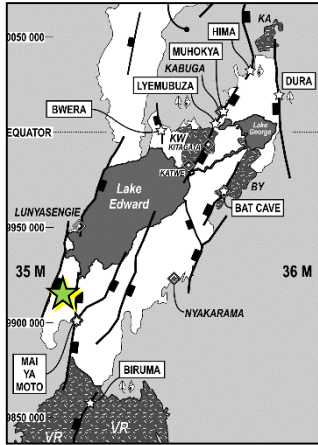


**ICP-MS 2018: HYBRID SIGNATURES**



**HYBRID SAMPLES CORRELATION WITH DEVONIAN REEF**

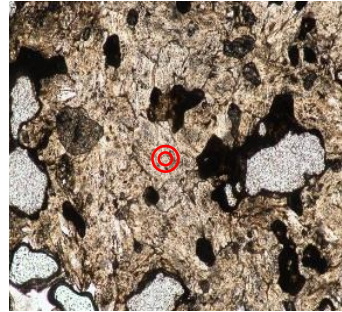




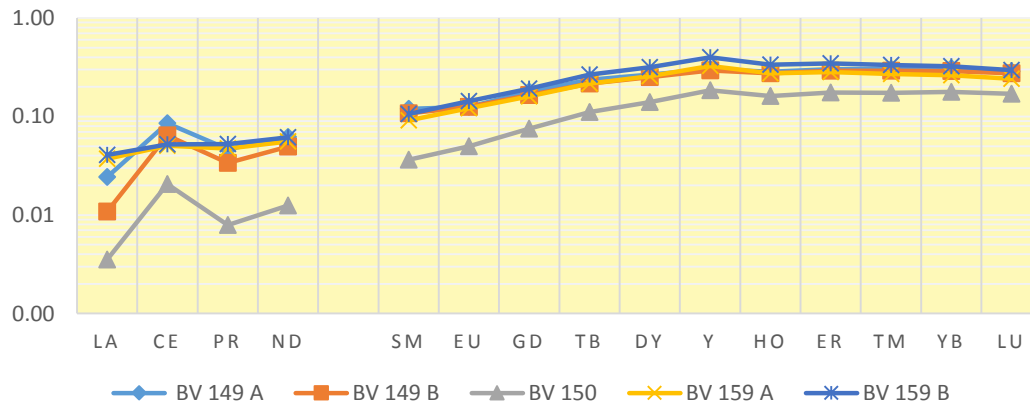
**Mai Ya Moto**  
**Southern Lake Edward,**  
**Block V, DRC**  
**Sample V 150**

**Samples V150:**

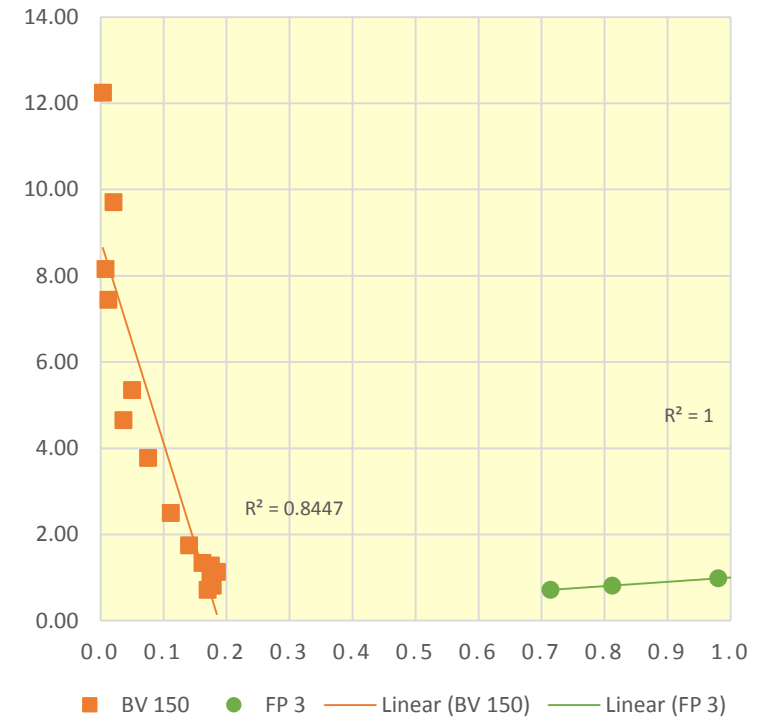
Light Brown very crumble limestone with vugs porosity and visible rootlets branches and plant tubes. Microbially laminated white Travertine with fibrous layers.

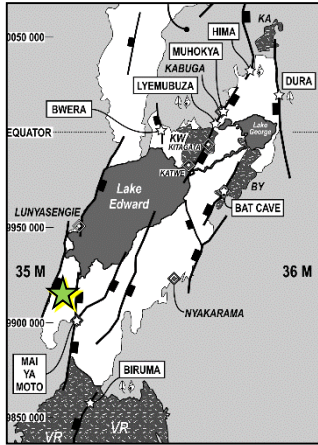


**ICP-MS 2018: HYBRID SIGNATURES**



**HYBRID SAMPLES CORRELATION WITH FORT PORTAL**

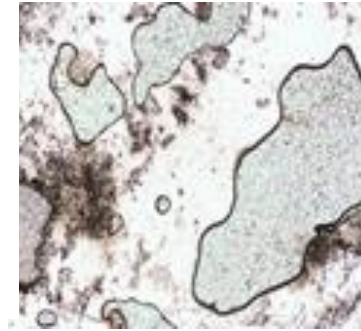




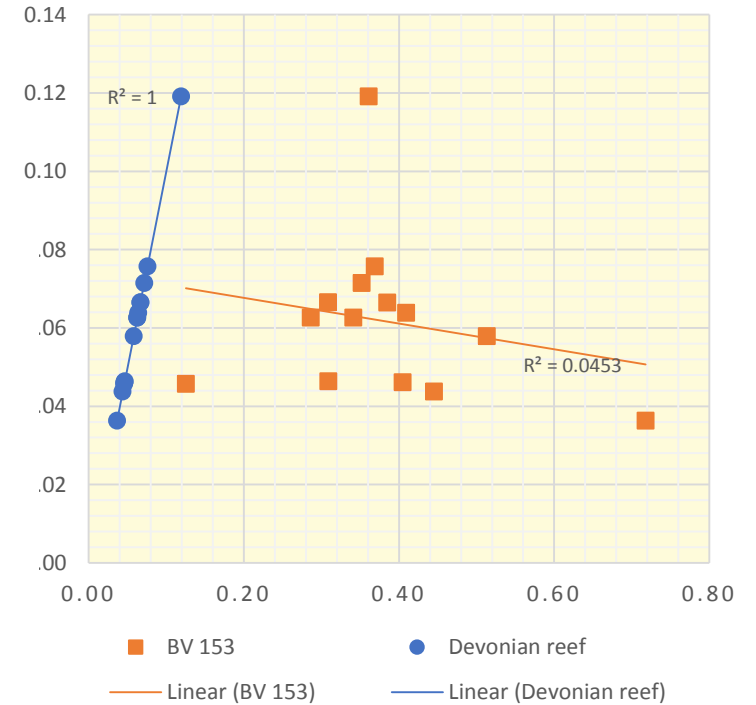
**Mai Ya Moto**  
**Southern Lake Edward,**  
**Block V, DRC**  
**Sample V 153**

**Samples V153:**

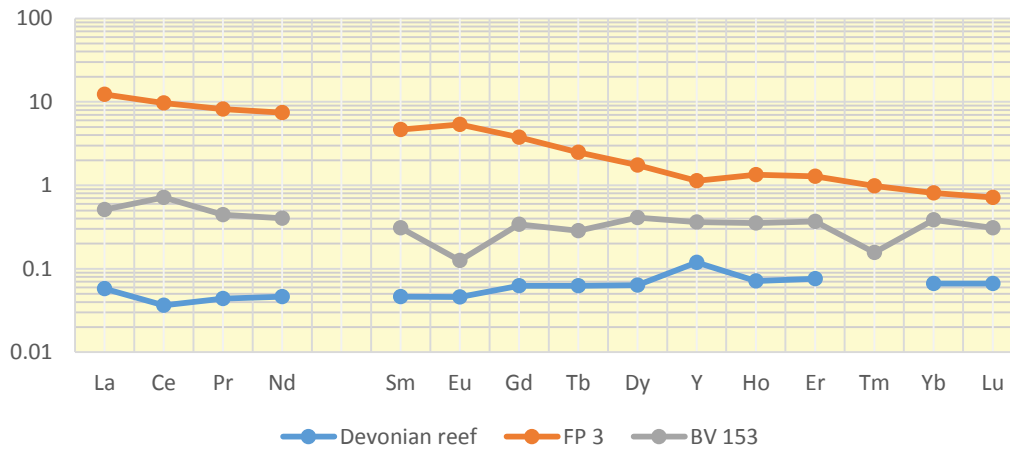
Light Brown very crumble limestone with vugs porosity and visible rootlets branches and plant tubes; Travertine with chimney structure that provides ventilation for hot flue gases or smoke from underground processes, then cooled at surface in ambient temperature.

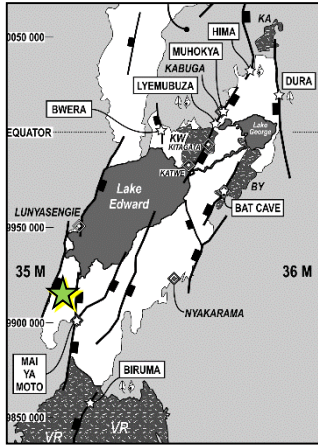


**HYBRID BV 153 SAMPLE**  
**CORRELATION WITH DEVONIAN**  
**REEF**



**REE BV 153 HYBRID SIGNATURE**

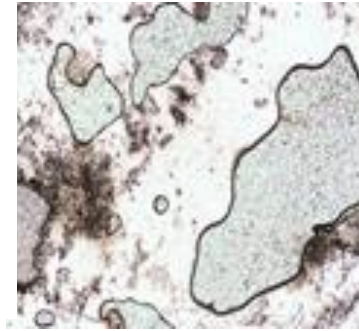




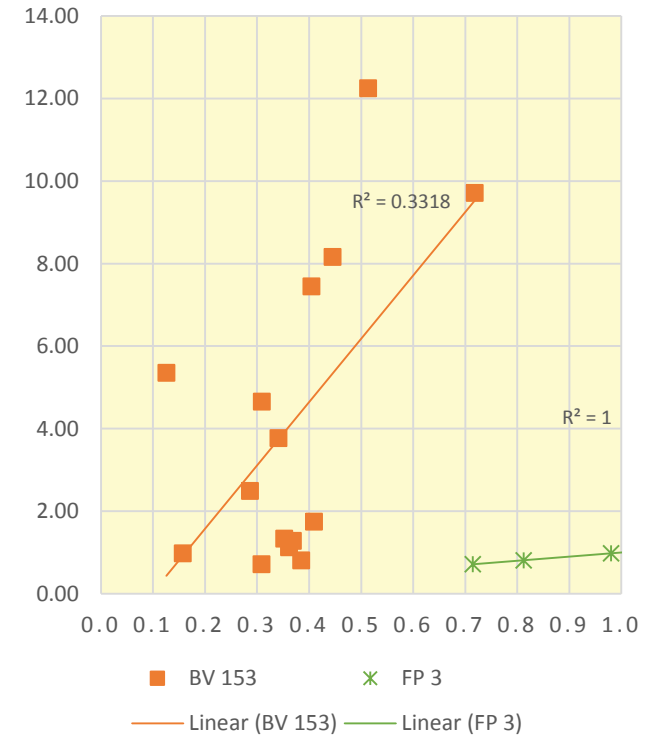
**Mai Ya Moto**  
**Southern Lake Edward,**  
**Block V, DRC**  
**Sample V 153**

**Samples V153:**

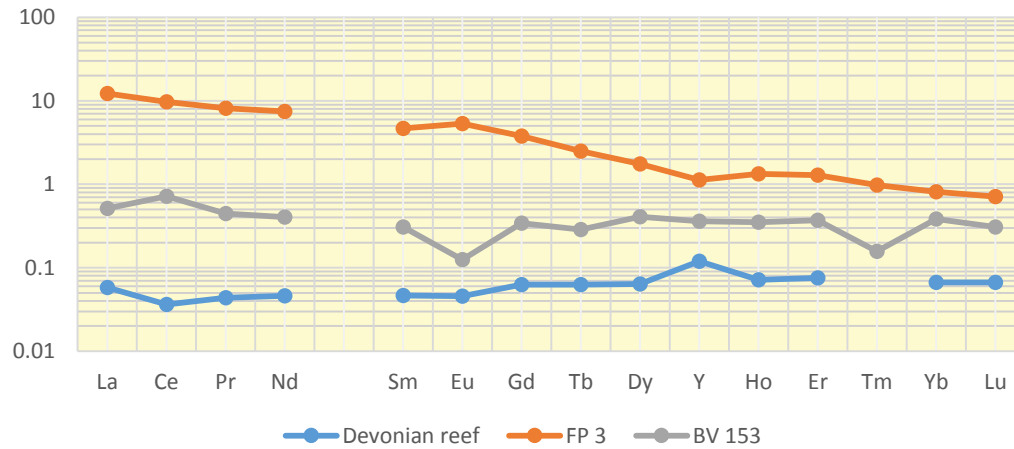
Light Brown very crumble limestone with vugs porosity and visible rootlets branches and plant tubes; Travertine with chimney structure that provides ventilation for hot flue gases or smoke from underground processes, then cooled at surface in ambient temperature.

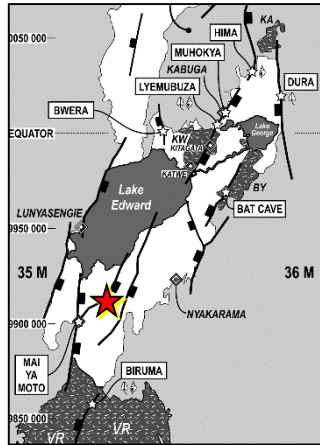


**HYBRID SAMPLES CORRELATION WITH FORT PORTAL**



**REE BV 153 HYBRID SIGNATURE**





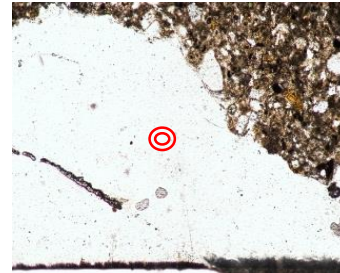
**Mabenga**  
**Southern Lake Edward,**  
**Block V, DRC**  
**Sample V 344**

**Samples V344:**

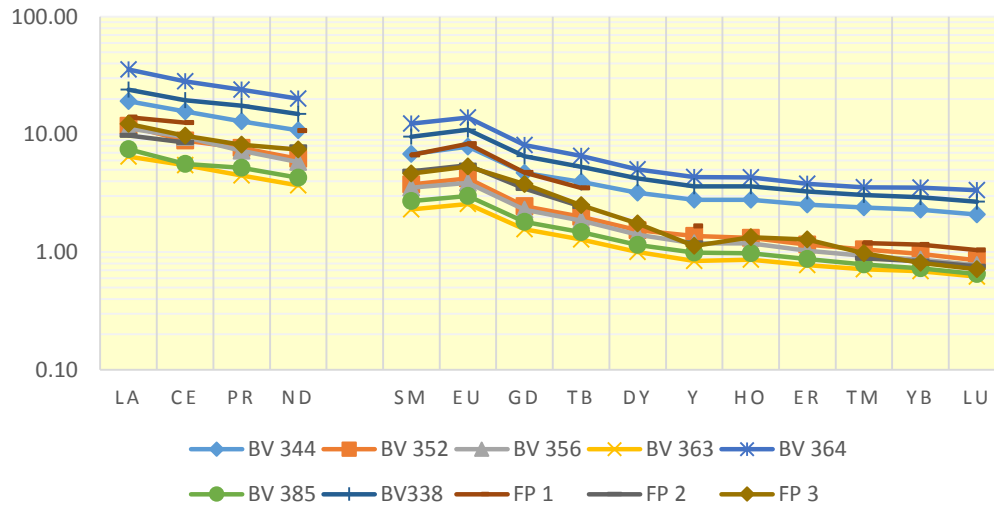
Travertine with inputs of plants and tree rootlets. Presence of white salt crusts and small chimneys with maximal temperatures of 90 °C.

**Gamma ray values:**

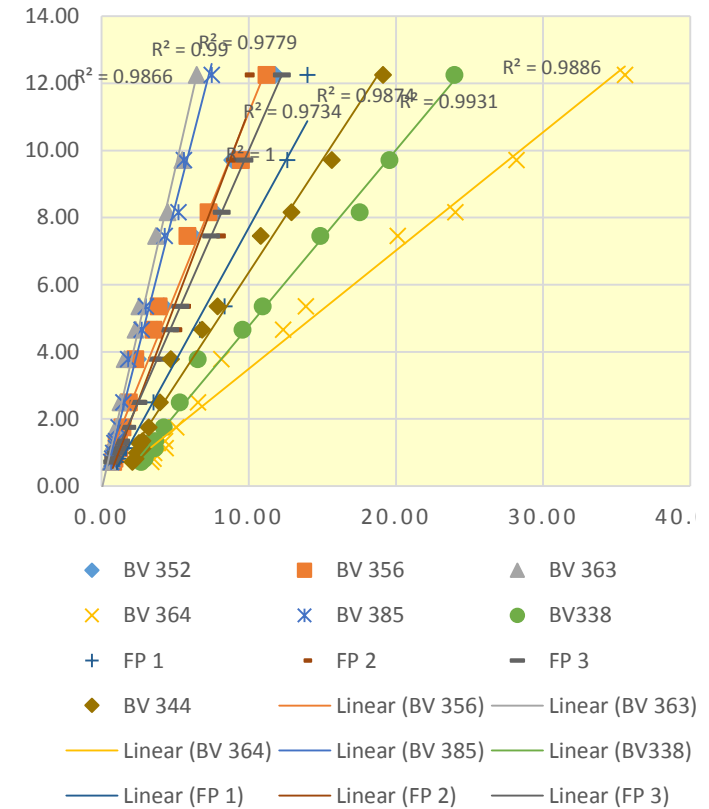
K= 1.0 % U= 200.9 ppm Th = 25.1 ppm (assay # 2268)



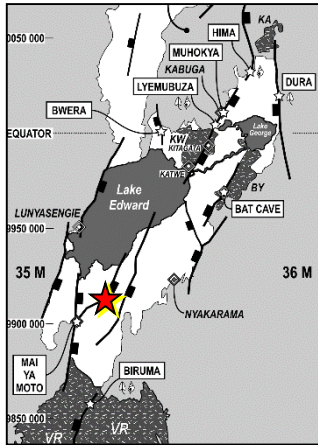
**BLOCK V CARBONATITES & FORT PORTAL LAVAS**



**BLOCK V CARBONATITES CORRELATION FORT PORTAL**







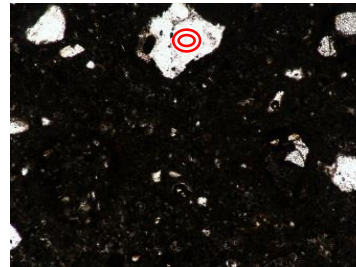
**Mabenga**  
**Southern Lake Edward,**  
**Block V, DRC**  
**Sample V 352 & V356**

**Samples V352 & 356:**

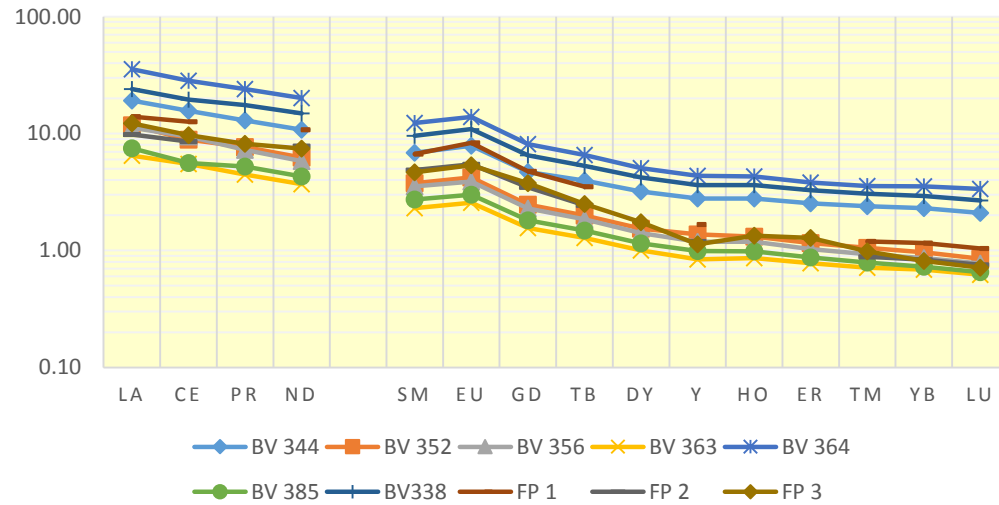
Travertine with inputs of plants and tree rootlets. Presence of white salt crusts and small chimneys with maximal temperatures of 90 °C.

**Gamma ray values:**

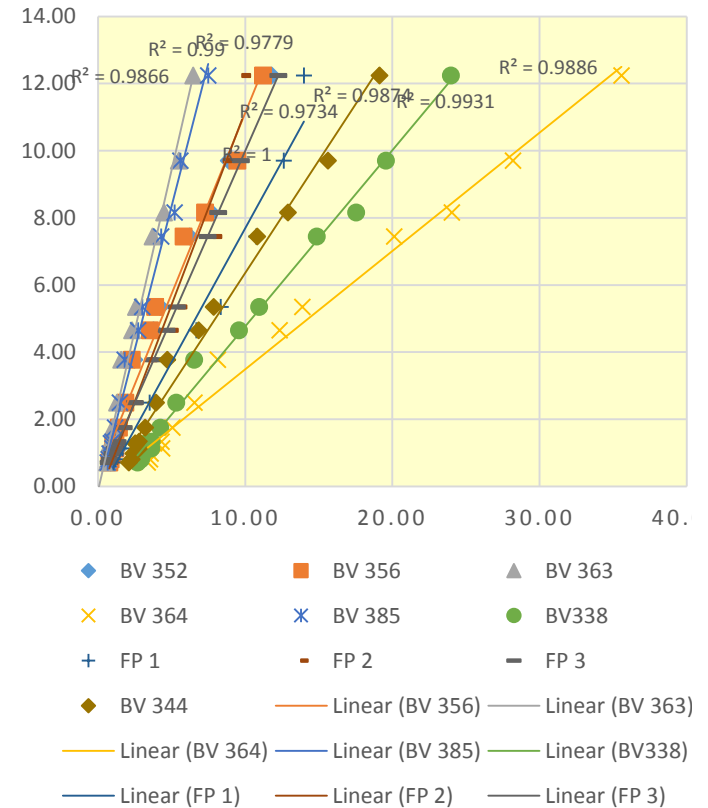
K= 1.0 % U= 200.9 ppm Th = 25.1 ppm (assay # 2268)

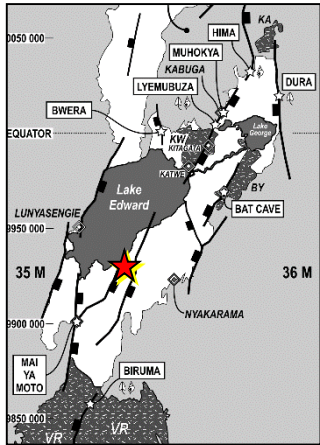


**BLOCK V CARBONATITES & FORT PORTAL**  
**LAVAS**



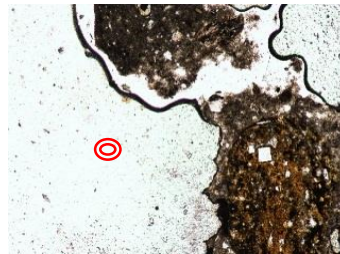
**BLOCK V CARBONATITES**  
**CORRELATION FORT PORTAL**



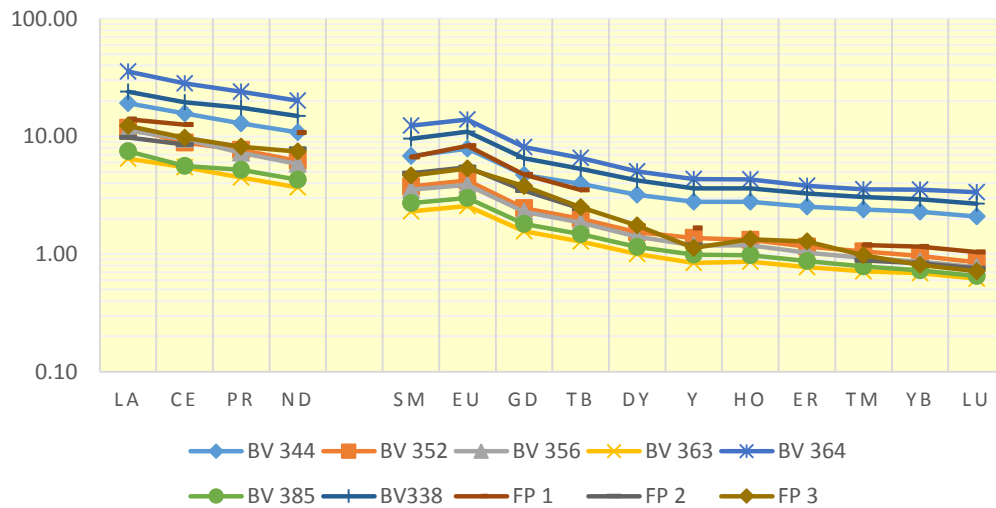


**Vitshumbi fault scarp  
South Eastern Lake  
Edward, Block V, DRC  
Sample V 363 & 364**

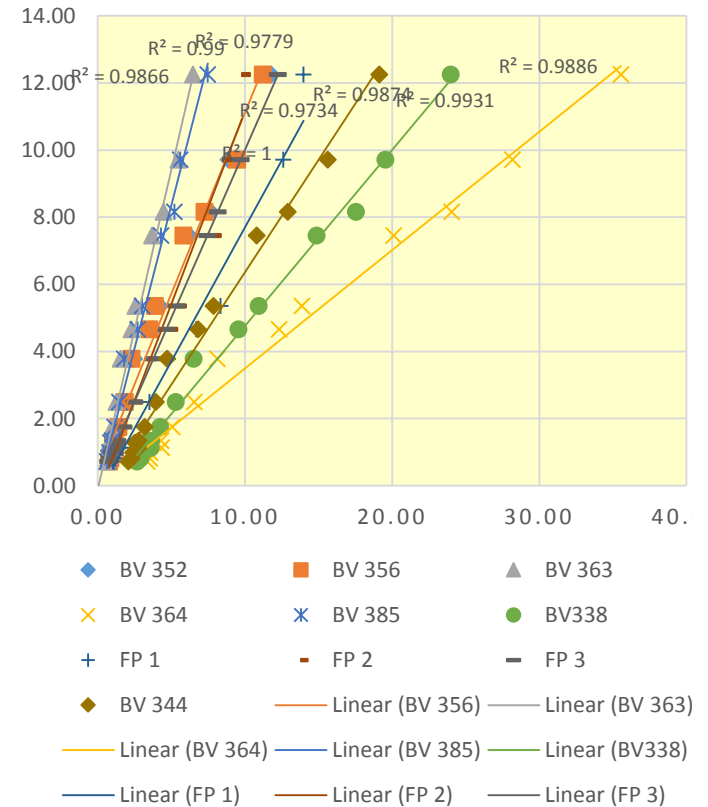
**Samples V363 & 364:**  
Vertical zoned Travertine including gas holes around rootlets cavities.

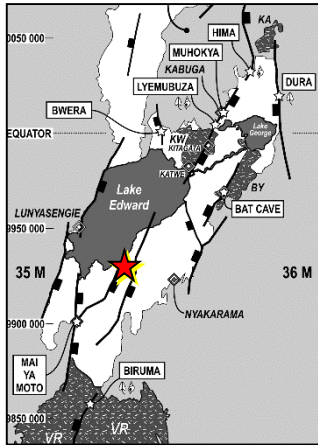


**BLOCK V CARBONATITES & FORT PORTAL  
LAVAS**



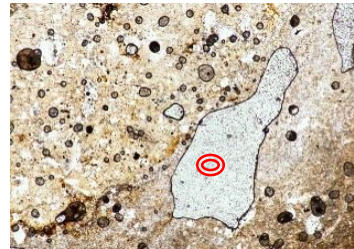
**BLOCK V CARBONATITES  
CORRELATION FORT PORTAL**



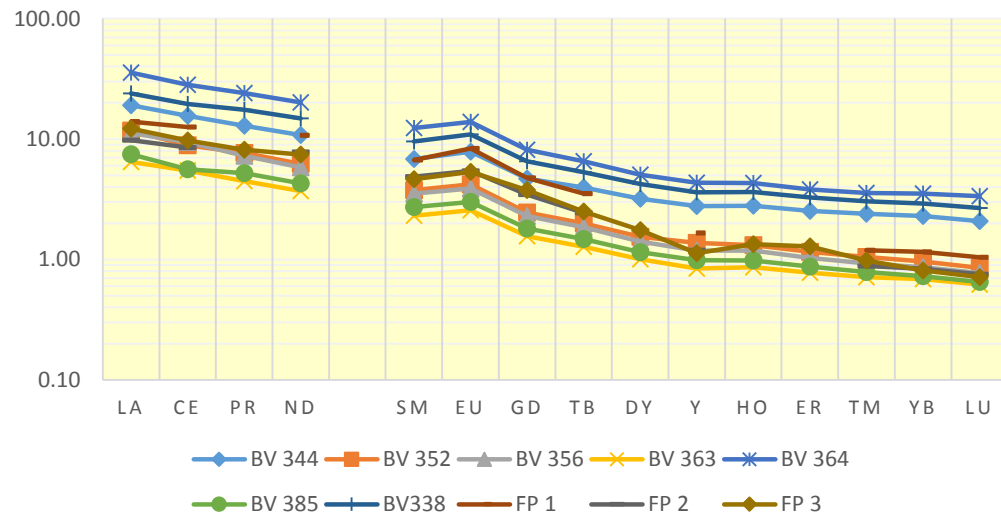


**Vitshumbi fault scarp**  
**South Eastern Lake**  
**Edward, Block V, DRC**  
**Sample V 385**

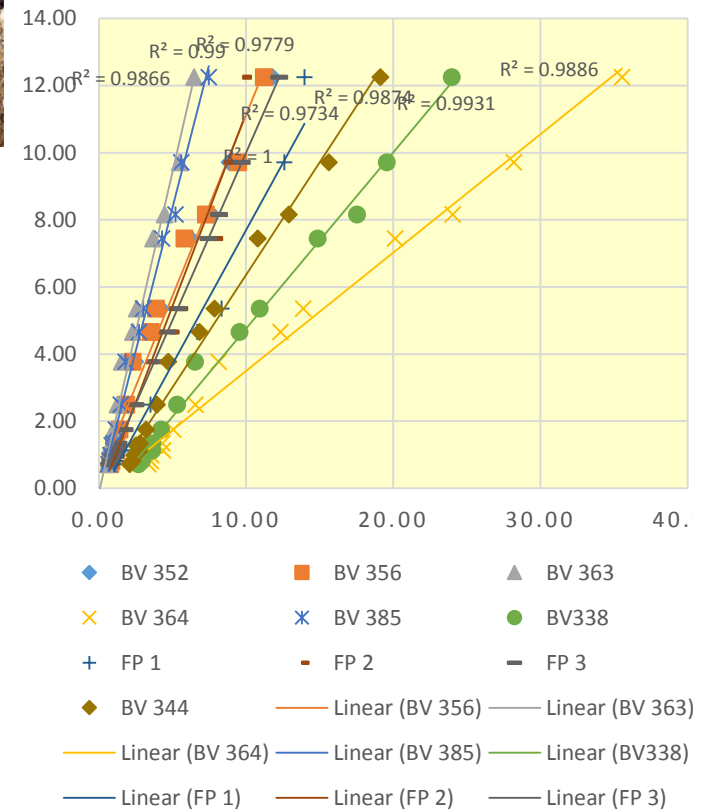
**Samples V385:**  
 Vertical zoned Travertine including gas holes around rootlets cavities.

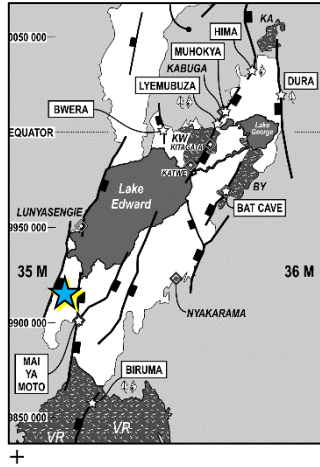


**BLOCK V CARBONATITES & FORT PORTAL**  
**LAVAS**



**BLOCK V CARBONATITES**  
**CORRELATION FORT PORTAL**

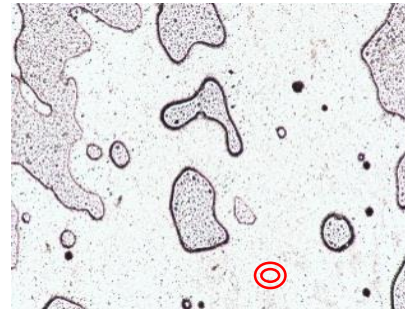




**Katanda Gorge**  
**Southern Lake Edward,**  
**Block V, DRC**  
**Sample V 161**

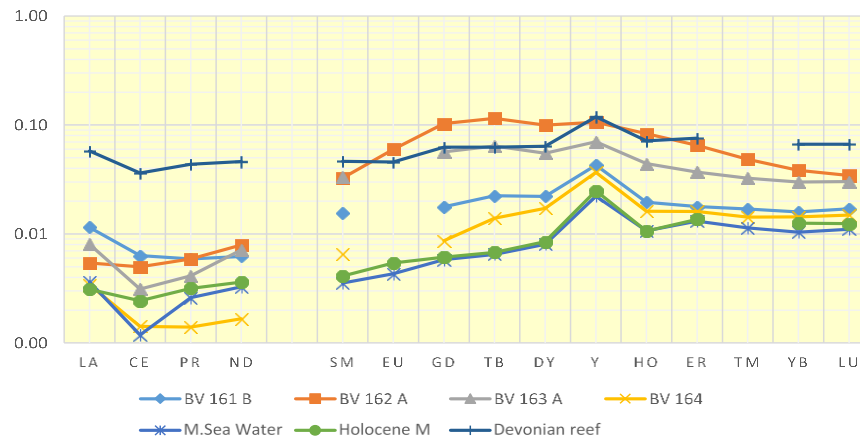
**Samples V161:**

Hematite stained Travertine crumbled.

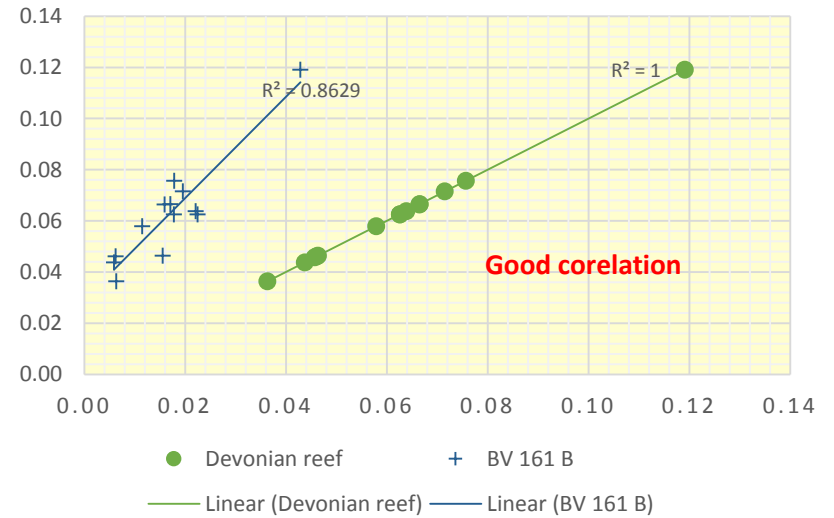


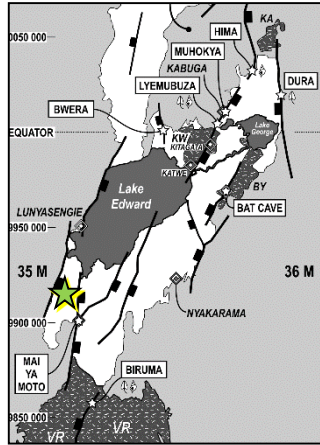
		BV 161 B	
>1.1	La/La*	2.154878	YES
<0.8	Ce/Ce*	1.185219	NO
>1.1	Gd/Gd*	0.778326	NO
<< 1	Prn/Ybn	0.371749	YES
>40	Y/Ho	2.191354	NO

**BLOCK V (2018) & KNOWN MARINE LIMESTONE**



**ICP-MS 2018 : CORRELATION WITH KNOWN MARINE LIMESTONES**

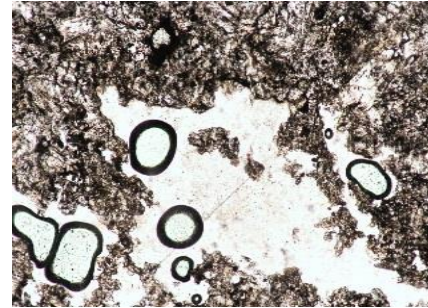




**Katanda Gorge**  
**Southern Lake Edward,**  
**Block V, DRC**  
**Sample V 162**

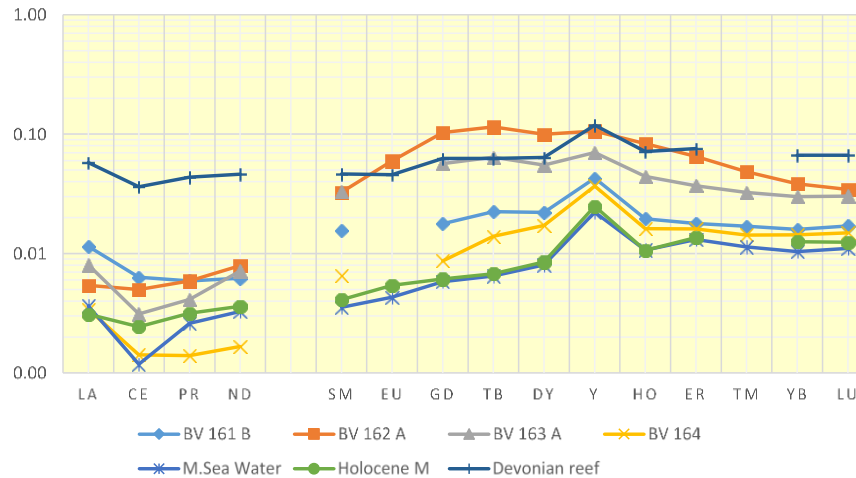
**Samples V162:**

Hematite stained Travertine crumbled interbedded with some clastic facies.

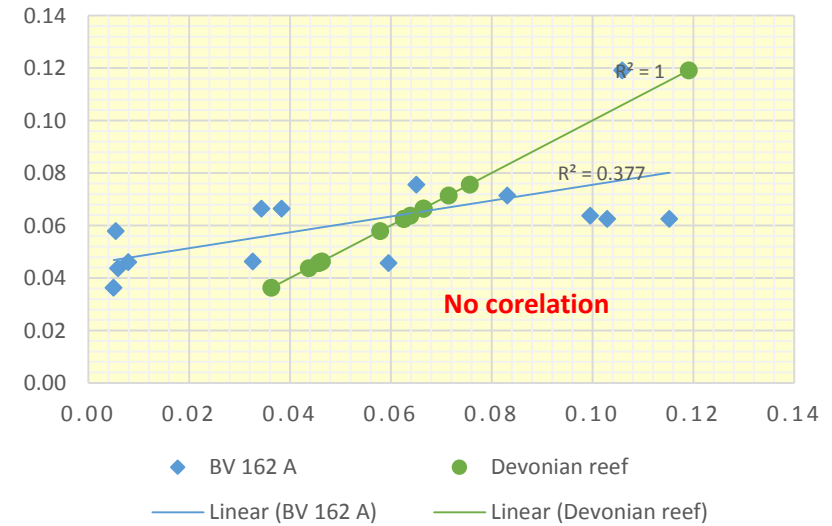


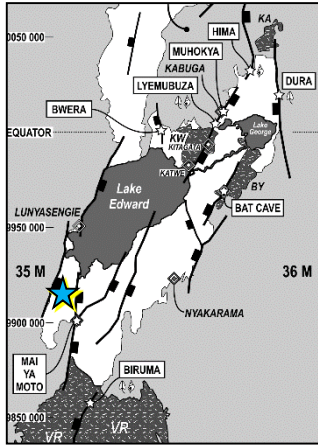
		BV 162	
>1.1	La/La*	1.660919	YES
<0.8	Ce/Ce*	1.529005	NO
>1.1	Gd/Gd*	0.771417	NO
<< 1	Prn/Ybn	0.154034	YES
>40	Y/Ho	1.274174	NO

**BLOCK V (2018) & KNOWN MARINE LIMESTONE**



**ICP-MS 2018 : CORELATION WITH KNOWN MARINE LIMESTONES**

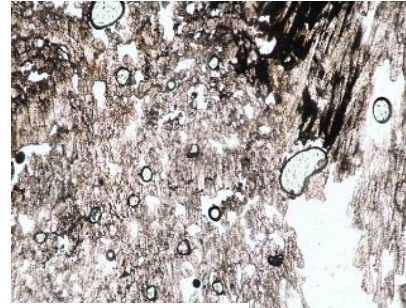




**Katanda Gorge**  
**Southern Lake Edward,**  
**Block V, DRC**  
**Sample V 163**

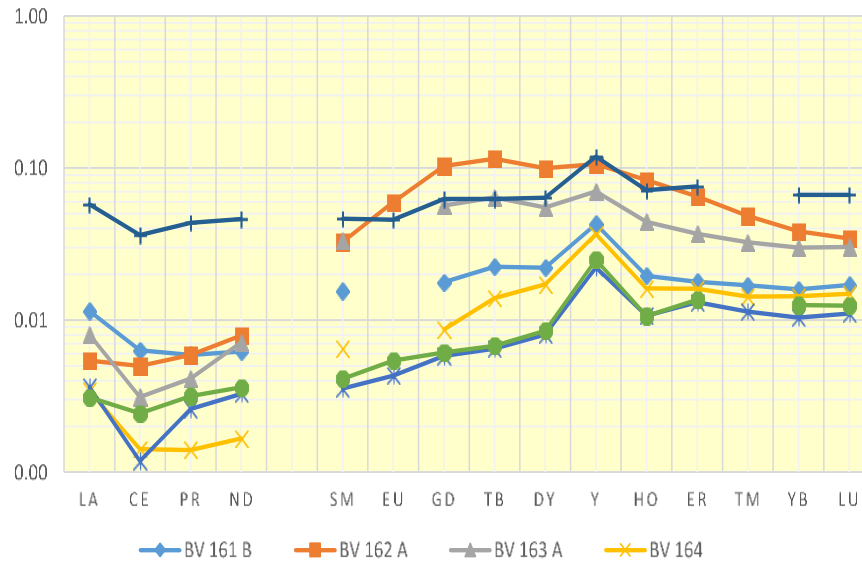
**Samples V163:**

Hematite stained Travertine crumbled.

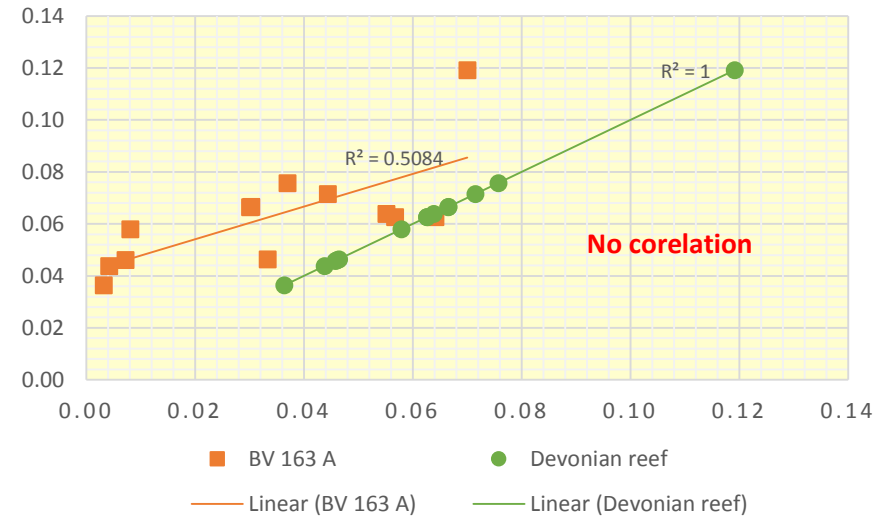


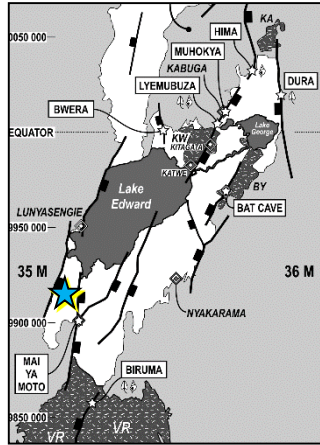
		BV 163	
>1.1	La/La*	5.823986	YES
<0.8	Ce/Ce*	2.257441	NO
>1.1	Gd/Gd*	0.761166	NO
<< 1	Prn/Ybn	0.137344	YES
>40	Y/Ho	1.57862	NO

**BLOCK V (2018) & KNOWN MARINE LIMESTONE**



**ICP-MS 2018 : CORRELATION WITH KNOWN MARINE LIMESTONES**



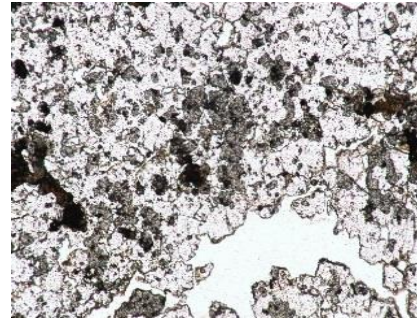


**Katanda Gorge**  
**Southern Lake Edward,**  
**Block V, DRC**  
**Sample V 164**

**Samples V164:**

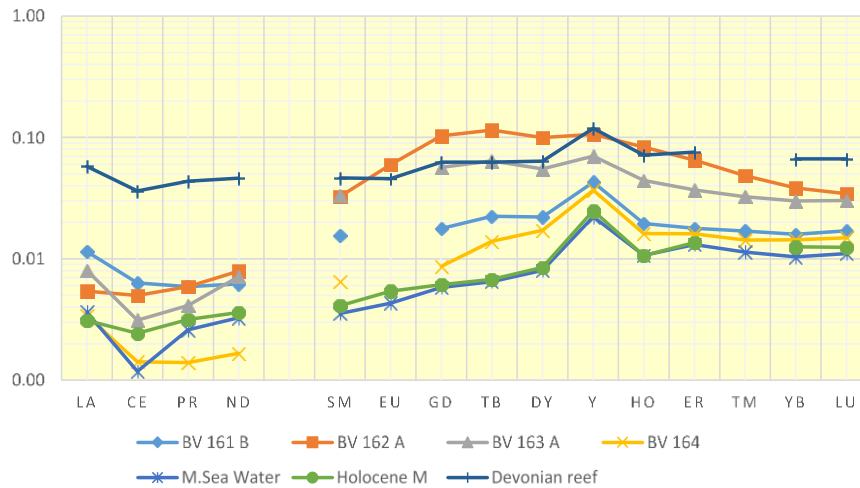
Hematite stained Travertine crumbled.

*( due to security and logistic conditions, the restricted time on the field didn't allow more field description)*

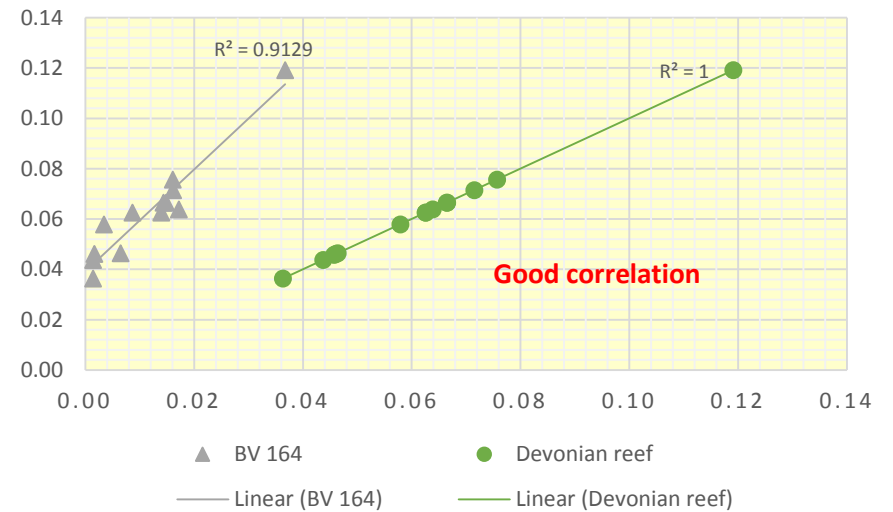


		BV 164	
>1.1	La/La*	3.464977	YES
<0.8	Ce/Ce*	1.438689	NO
>1.1	Gd/Gd*	0.765242	NO
<< 1	Prn/Ybn	0.097544	YES
>40	Y/Ho	2.275306	NO

**BLOCK V (2018) & KNOWN MARINE LIMESTONE**



**ICP-MS 2018 : CORELATION WITH KNOWN MARINE LIMESTONES**



From these results here above it is clear that the 2018 ICP-MS provides some more evidence of geochemistry origin for different Carbonates outcropping in the DR Congo side of Albert Graben, EARS. They have demonstrated that:

- BV344, BV 352, BV 356, BV 363, BV 364, BV 385, drilled respectively through their light carbonates minerals avoiding the visible rootlets, branches or plant tubes, gave a typical Carbonatites signature with very good correlation coefficient  $R^2 > 0.90$  with FP#3. ( Figures VII.35 and VII.36) No Marine limestones criteria matching. These basic findings are consistent with this research objectives showing that there is involvement of Carbonatites emerging from depth to the subsurface through groundwaters;
- BV150, BV 161, and BV 164, drilled through the carbonates porosity filled textures avoiding the black stained lining in white vugs, these samples ICP-MS results revealed a Marine limestones spectral signatures interesting facts. (Figures VII.44 and VII.45) No correlation with FP#3 has been scientifically established while a matching has been found with the Marine Limestones Balz paper criteria. This result demonstrates another further evidence of underneath Marine limestone deposit involvement for the origin of the carbonates in this Travertine outcrop;
- BV 149, BV 153, BV 162, and BV 163, have been drilled as above through the carbonates porosity filled textures avoiding the black stained lining in white vugs, these samples ICP-MS results revealed a kind of weird spectral signatures different from typical Carbonatites or Marine limestones. No to Moderate correlation with FP#3 and No to moderately matching with Balz paper criteria. (Figures VI. 44 and VI.45) These results demonstrate that a kind of hybrid source of carbonates does exist within the Rift basin. This hybrid source seems to be a mixture of Carbonatites and Marine limestones sources.

The ICP-MS results obtained for each sample analysed in the present Msc research study revealed 3 sources of Bicarbonates in the EARS Travertines which have been grouped per field locations as below:

**Definite presence of Marine Limestones at depth at:**

**Mai ya Moto hot springs** (Bloc V, DRC)  
**Katanda gorge** (Bloc V, DRC)  
**Lyemubuza quarry** (EA4A, Uganda)  
**Muhokya** (EA4A, Uganda)  
**Okumu** (EA1, Uganda)

**Definite presence of Carbonatites at depth at:**

**Biruma quarry** (Bloc V, DRC)  
**Mai ya Moto springs** (Bloc V, DRC)  
**Mabenga springs** (Bloc V, DRC)  
**Vitshumbi fault scarp** (Bloc V, DRC)  
**Bat cave** (EA4B, Uganda)  
**Bwera** (EA4A, Uganda)  
**Hima** (EA4A, Uganda)

**Definite presence of hybrid signature**

**At depth at:**

**Bwera, Dura and Muhokiya (Uganda)**  
**Mai ya Moto, Katanda and Biruma (DR CONGO)**



Consequently to this above field location sorting, all of this allowed to update the Travertines occurrence map in the Albertine Graben as illustrated in the Figure VII.1 below:

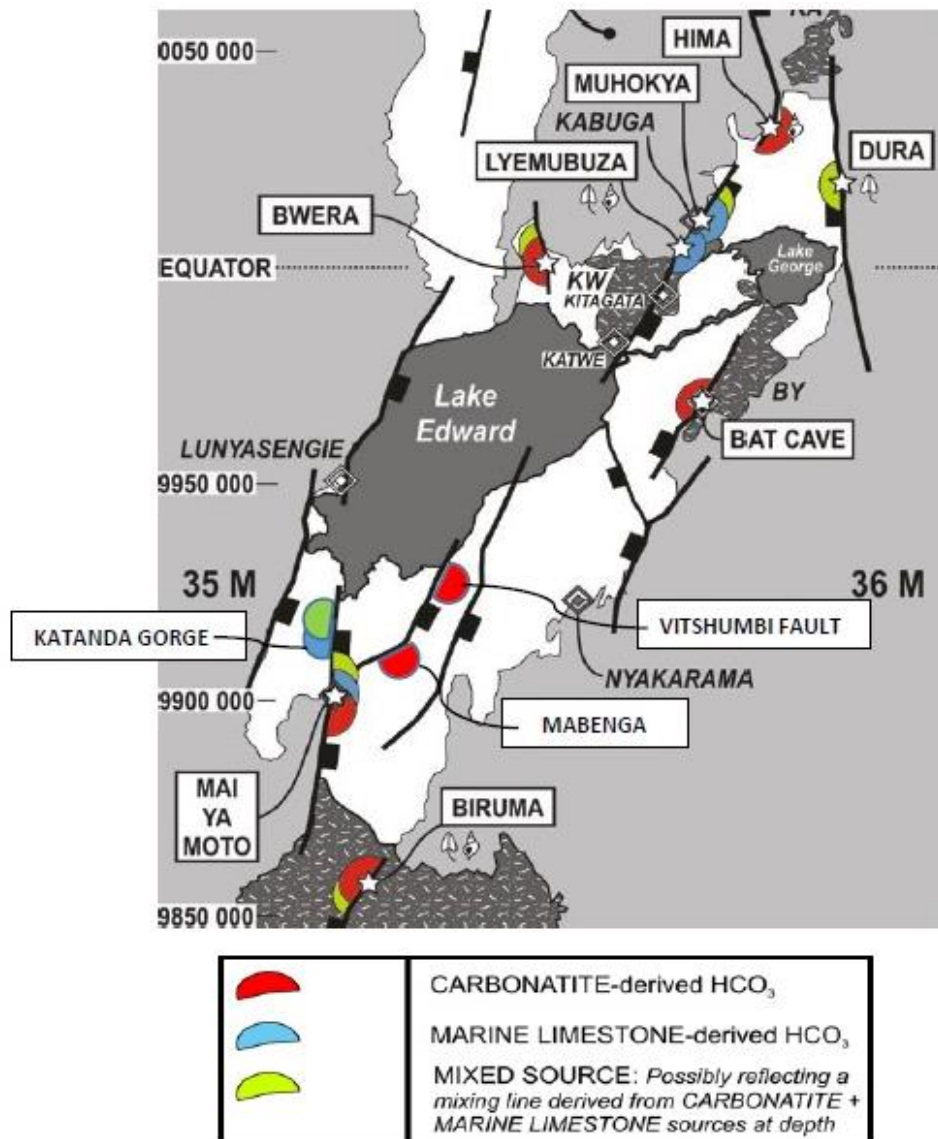


Figure VII. 1: Travertine ICP-MS results Map of Albertine Rift basin

Combining all the results discussions and interpretations with some geologic correlations and considerations allow to the assay of overlapping different analysis results and obtain the helpful general framework of the geologic theory, field evidences, microscopy facts, and geochemical laboratory results for answering the query about the geochemical origins of Travertines in the Eastern Africa Rift System and confirm this Msc Research study hypothesis.

The Figure VII.2 below illustrate a correlation chart assay trying to compare the Travertine ICP-MS results with the Carbon and Oxygen stable isotopes results. It allow to have a general view of the ratio between Travertines from Carbonatites sources marked in red and those from Marine limestones marked in blue.

Travertines in the center of the graph represent the intermediate geochemistry source.

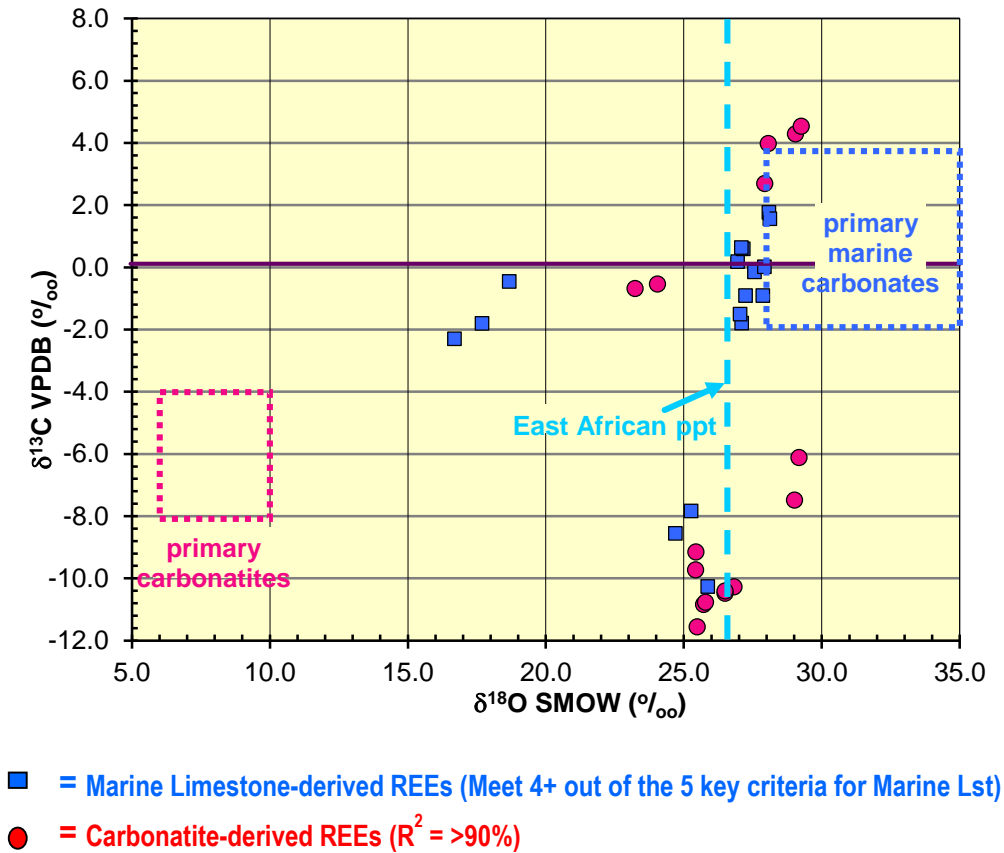


Figure VII. 2: Travertine ICP-MS results Vs Carbon and Oxygen stable isotopes results.

The figure VII.2 above, show the relative abundance discrimination of Carbonatites and Marines limestones based on their respective values of Oxygen (SNOW) in x axis, and Carbon (PDB) in y axis.

We can interpret from this above Chart that no apparent correlation seems to be between REE carbonatite signature and Marine limestone isotopic composition. This make them enough far away results to be considered like the two end-members of the EARS Travertines geochemical origin. This figure suggests also that no apparent correlation seems to be between REE marine limestones signature and Carbonatites isotopic composition.

Most of REE signature seems to be derived from carbonate at depth, but the typical Travertine isotopic signature is acquired during surface fractionation processes in the hot spring pool.

Most of the REE signature derived from marine limestones at depth, but the Travertines isotopic signature is progressively reduced during geothermal waters fractionation processes upraising them at the surface.

The chart in the above figure allow also the hybrid isotopic signature to be considered like intermediate source between the two Carbonatites and marines limestones end-members of the geochemical origins of EARS Travertines.

## Chapter 7 Conclusion

*The field investigations and descriptions for Travertines samples collection, their microscopy observations and petrographic descriptions merged with all geochemistry results provided the scientific facts and geological evidences used to interpret and document this chapter.*

*All the above Travertines results have been respectively discussed in detail regarding their:*

- Location map in the field;*
- Sample photo in the field;*
- Field description (sample and outcrop environment);*
- Sample thin section photo in microscopic sizes;*
- ICP-MS spectral signatures charts and marine limestones Balz's criteria check boxes;*

*The conclusive thoughts and venues summarized in the next Chapter titled Conclusion, are based on geologic evidences and scientific facts discussed in details throughout all the previous Chapters.*

*They provided a high level of confidence to give the geologic answer of the geochemical origin of the Travertines samples found in outcrops throughout the Eastern Africa Rift System, then help to write down this Msc research study conclusion and give a range of strong recommendations for further improvements in the actual knowledge of the entire rift and its implications for the Oil exploration industry.*

## CHAPTER 8: CONCLUSIONS

This MSc research study has demonstrated the success of the methodology in achieving its objectives. The methodology began with a literature review to document a proper field campaign for sample collections and documentation. After field considerations and macroscopic observations, a detailed microscopy was necessary to determine the appropriate carbonate textures, structures and/or fabrics to run the geochemical analysis using carbon, oxygen and strontium isotopes ratios. The use of GC-GCMS, both Ce and La anomalies ICP-MS combined with Y/Ho ratios helped to find out the most plausible origin of the bicarbonates contained in the EARS travertines samples found in outcrops around faulting lined hot springs in the basin boundaries.

The detailed review of previous literature revealed that there are no Travertines outcrops signalled in the whole classical siliclastic rift fill sediment deposited in the EARS. These old studies indicate most of the oldest geologic units lying within sediments are close to the rift shoulders while the youngest are comprised of sediments laying in the middle basin fill closer to the present-day sediment filling. Moreover, these publications document that all the EARS geologic units have no clear bounding surfaces defined to be correlated laterally with enough degree of certainty and confidence. According to earlier literature, the EARS is mostly dominated by both fluvial-alluvial distributary fan packages and lacustrine depositional environment. The described lacustrine deposits are selectively located within the centre basin fill sediments while the observed alluvial-fluvial fan packages are mainly encountered and located closer to the rift shoulders. However, no literature has mentioned the existence and field location of any Travertines outcrops in the EARS.

The evidence of Travertines spring outcrops discovered in the EARS siliclastic basin, was the main reason for undertaking detailed field trips in the region. The above-mentioned literature review provided a good tool for planning several site visits to find, describe and collect the famous Travertines outcrops in the EARS. The gamma ray values recorded in some of the EARS cliffs in DRC recommended using the Th/U ratios as both good indicators of sedimentary processes and a tool for the recognition of their geochemical facies. They suggested also separately using the Th/K log sharpness to define the Cretaceous/Permian boundary and the Th/U log sharpness as an excellent indicator of transgression/regression contrasting the marine upper cretaceous rocks and the non-marine to transitional rocks of the lower cretaceous. The macroscopic field observations demonstrated the famous EARS Travertines observed in hot spring outcrops have been formed in clear, warm, near surface, shallow marine waters in palaeo environments such as deltas and/or estuaries where organic filling is caused by the precipitation of calcium carbonate from lake or ocean water accumulation of shell, coral, algal, and faecal debris within their visible structures, textures and/or fabrics.

The microscopic observations of the EARS Travertines structures, textures and or fabrics have revealed their originate calcium carbonate from various precipitation processes in a variety of temperatures, palaeo environments, deposit conditions and palaeo climates.

The petrography work done in this Msc research study has compared the EARS travertines thin section microscopic observations with the main petrographic specifications of referenced Fort Portal, Mandawa Basin and Devonian Reef. It is observed in the microscopic size that the Mandawa carbonates sediments displayed in the microscope with enough petrographic similarities to EARS Travertines samples P12, LE 24, LE 26, LE 28, V 19 found with marine limestones spectral signature within their related structures, textures and/or fabrics.

The C/O isotopes ratio experiments run through this study were convenient to define the palaeo temperatures at the time of deposition. Once combined with IRMS results on EARS Travertines samples, they suggest the three Travertines follow palaeo environments:

- Primary marine limestones in Lyemubuzza, Muhokiya, Duma, Hira localities in Uganda where carbon dioxide outgassing evaporation removes C and O isotopes;
- Primary carbonatite lavas in Mayi ya Moto and Biruma localities in DRC;
- Hybrid results mixing both above palaeo environments in Bat Cave, Okumu and Bwera localities in Uganda where strong carbon plants soil zone a CO<sub>2</sub> contribution.

In others terms, these above palaeo environment temperature of EARS carbonates C/O ratios reveal three (3) main groups made of cold marine limestones (eg. Tufa, Travertines), hot Carbonatites (eg. Travertines) and clearly a kind of intermediate mixed group considered like the hybrid one.

The strontium isotope ratios of selected EARS Travertines samples showed a very high range of strontium isotope ratios from 0.7068069 to 0.7482648. Sr Isotope Ratios within the seawater carbonate range may be Late Neoproterozoic, Late Permian or Late Jurassic in age.

However, only two values LE 41 and LE 42 (a, b) correspond with marine limestones dating from Jurassic to Permian. These samples are from Bwera and Dura, at the northern end of Lake Edward.

The GC / GCMS analysis results indicate that the pre-peak oil apparently generated from a marine shale source rock has migrated into the very porous EARS Travertines Lyemubuzza outcrops. This is interpreted as the source rock type that would typically generate oils with the relict biomarker distributions seen in the EARS Travertines samples being from MARINE SHALES source. This is the scientific evidence the GC/GCMS analysis run by Dominion Ltd in 2011 proved the relict oil preserved in the Travertines cavities at Lyemubuzza and the same one leaking to the surface on Lake Edward are from the same originate marine shale source rock.

The specific study of hydrothermal chemistry in the EARS helped to better understand the potential impact hydrothermal emissions have on the chemistry of the crossing geologic formations, and how this chemistry differs between the varied geologic units crossed through, during the uprising process to flush the geothermal waters out to the surface at hot springs pools. Hydrothermal fluid formed as circulating groundwaters are modified through interactions with heat and the earth's crust. These kinds of fluids may emanate back into underground water affected by geothermal gradient from the volcanic region of Nyragongo and Nyamulagira, the closest volcanoes to Biruma Travertines outcrops in the south east of the Albertine Graben.

The hydrothermal fluids encountered in the EARS are subdivided into two categories: the high-temperature or focused flow, and the low-temperature or diffuse flow.

The high-temperature fluids, generally > 100–150°C, have been described in the field as focused jets of water that have precipitated from the hydrothermal fluids themselves due to the mixing of hydrothermal fluids with carbonatite lavas. The low-temperature fluids, generally < 75°C have been observed in the field as the flows of water that have precipitated from the hydrothermal fluids themselves when they encountered some possible cold marine limestones.

The use of ICP-MS as per Balz Kamber's (2004) procedures for successful quantification of REE concentrations in EARS Travertines samples by ICP-MS. Balz Kamber (2004) suggested the best procedures to reliably determine REE abundances in carbonate waters with REE high concentrations with more or less accurate result confidence.

The MUQ (Queensland alluvial sediment average representing a compilation of the sedimentary composition of 25 Queensland rivers (Kamber et al., 2005b)) normalized results obtained from experiments done on diluted natural rock standard correlate favourably with previously published results on fresh water and Devonian reefs spectral signatures. (Lawrence and Kamber, 2006)

The differences in the REE pattern of the respective carbonates textures, structures and /or fabrics as analysed by ICP-MS, are explained by differences in soil-type, lithology or different weather patterns and are likely the result of differing deposit conditions (resulting in a lowering of pH).

The REE concentrations in EARS palaeo deposits from geothermal water flux have been discussed in terms of their carbonate sourcing and the major solute chemistry employed to model the REE speciation according to Balz Kamber procedures.

These procedures tested also the robustness of the relative REE anomalies calculated to MUQ by normalising with data interpretation provided by Kamber et al (2004).

The choice of normalising REE concentrations to MUQ has a greater improvement in the final interpretation of the obtained results. The most important calculated anomalies are more specifically the Ce anomaly (0.727) which is normally (~0.93) if calculated from Pr and Nd.

Whilst the magnitude of the La, Ce and Gd anomalies vary according to the choice of the normaliser, the other REE concentrations themselves keep the same pattern. The biggest deviations are found when comparing MUQ-normalised anomalies with those calculated using PAAS normalisation, probably due to slightly inaccurate PAAS Pr values, see (Kamber et al., 2005a) for a full discussion.

The key point to retain from the EARS Travertines ICP-MS results is that the anomalies are real, and not the result of inappropriate normalisation. However, we still observe variability in REE anomalies when PAAS normalising. Therefore, if the ICP-MS experiment consistently uses the same normalising MUQ-normalised anomalies values for all samples, the relative differences in the REE anomalies indicate that these anomalies have the potential to serve as provenance tracers.

In order to assess the geochemical origin of the carbonate REE fingerprint in the EARS Travertines, an extensive REE dataset of concentration values from Fort Portal Carbonatites lavas, Devonian reef marine limestones normalized from South East Queensland Carbonates were developed using an ICP-MS technique capable of directly quantifying all 15 naturally occurring heavy and light detectable REE.

This study demonstrates a remarkable variability in REE abundance within the EARS Travertines samples from a relatively huge region. This suggests that REE have the potential to be used as a source of geochemical fingerprint.

Furthermore, the results have proven that certain typical 'marine' REE features appear to develop in essentially carbonate layers beneath the Cenozoic basin, prior to entering the surface outlet boiling springs. According to (Kamber and Webb, 2001; (Van Kranendonk et al., 2003), 2004; Nothdurft et al., 2004) the geochemical origin of the marine dissolved REE abundance has attracted renewed attention as hydrogenous sediments (e.g. cherts, iron oxide, carbonate) appear to preserve marine REE features as far back as 3.71 Ga.

Combining all the above literature review, field geology, microscopy observations and geochemical analysis (Stables C and O isotopes, Sr isotopic ratios, CG/CGMS, ICP-MS) from the EARS study area, the following conclusions can be deduced:

This project succeeds at answering the geologic question to determine the origin of the Travertine limestones in the Albertine Graben in EARS by mainly analysing their respective stable isotopic and elemental geochemistry. This answer is that there is enough scientific evidence of three (3) geochemical sources of bicarbonate precipitating in the EARS Travertines.

The first of these geochemical sources is the igneous Carbonatites lavas or intrusions, either present at depth as buried carbonatite lavas, or as intrusives within the rift. Rare carbonatite lavas are indeed present at the surface at a single locality in the Albertine rift to the east of the Ruwenzori Mountains, between Lakes Albert and Edward. However, this result greatly increases the geographical extent of carbonatite within the rift than previously thought.

The second geochemical source is a marine limestone, which suggests that it is part of a pre-Tertiary rift unit; likely to be either a failed Karoo-Mesozoic rift package, or part of the 'basement' Proterozoic (possibly Neoproterozoic 'Schisto-Calcaire'). This is more intriguing, as the current EARS contains no marine sediments and it is still essentially a rift in progress. If any limestones were to occur, they would eventually be freshwater lacustrine units because there is no sea story in the region.

However, no fresh water lacustrine spectral signature has been found in the EARS REE plots which rather indicate the presence of a marine limestone source for bicarbonate at depth.

The third geochemical source does exist and seems to be a 'half-way house' mixture between these two previous geochemical sources.

Figure VIII.1 below illustrates the predictive cross-section (not to scale) describing the hypothetical configuration of the Bloc V DRC with the potential hydrothermal fluids up movement through both Eastern and Western bounding faults:

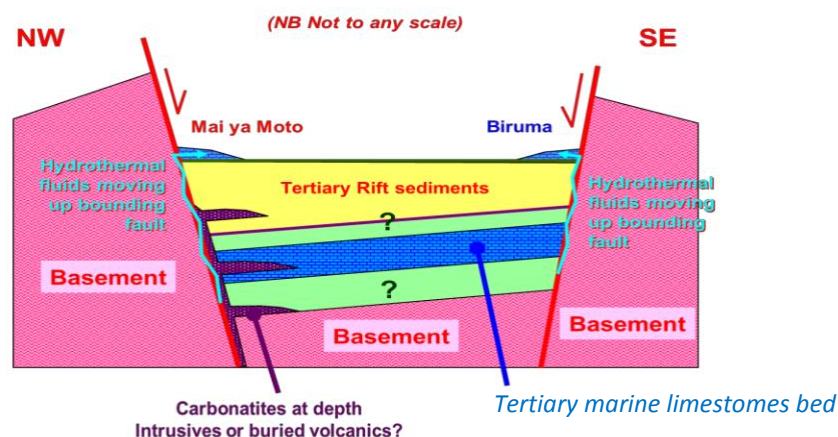


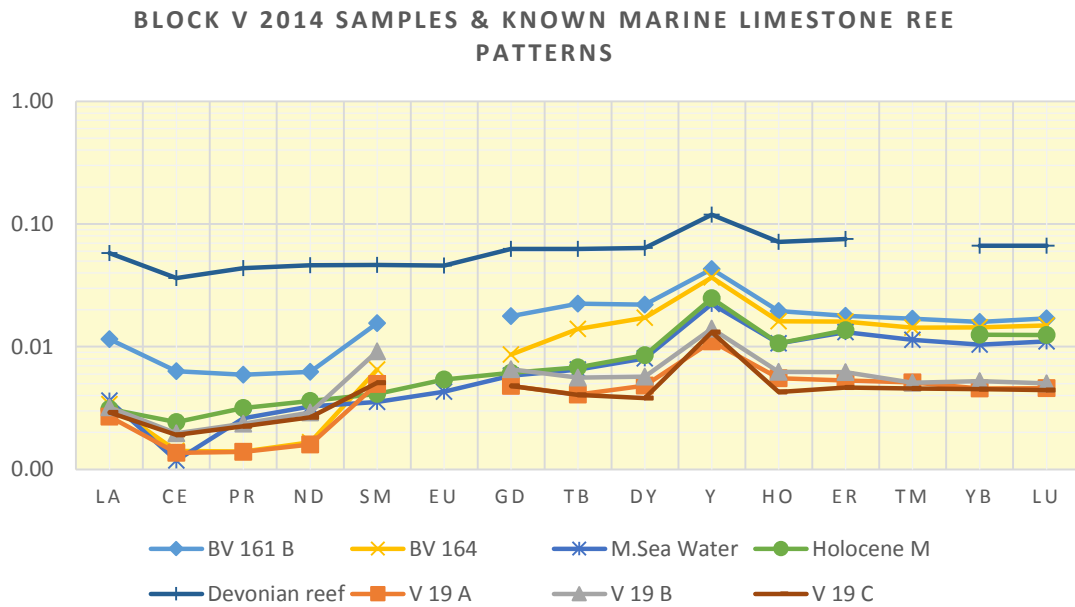
Figure VIII.1: Schematic hypothetical cross section of Bloc V, DRC. (Nicholas, 2013)

In summary, the curiosity created by the unexpected Travertine's occurrences found within the classical siliclastic EARS sediment fill type, has pushed this present research study to moving successfully trace back their geological and geochemistry origins according to their spatial extension in the regional level. In order to reach each of this study objectives (detailed in the Introduction Chapter one), the literature review (presented in the Literature Review Chapter two) allowed reviewing the existing documentation related to any Travertine's previous publications. The appropriate methodologies for field sample collection, petrography and geochemical analysis to undertake have been detailed step by step (in the methodology Chapter three). The EARS field investigation details (summarized in Field Trips Chapter four) allowed to macroscopically describe document and collect the Travertines samples for geochemistry analysis purposes.

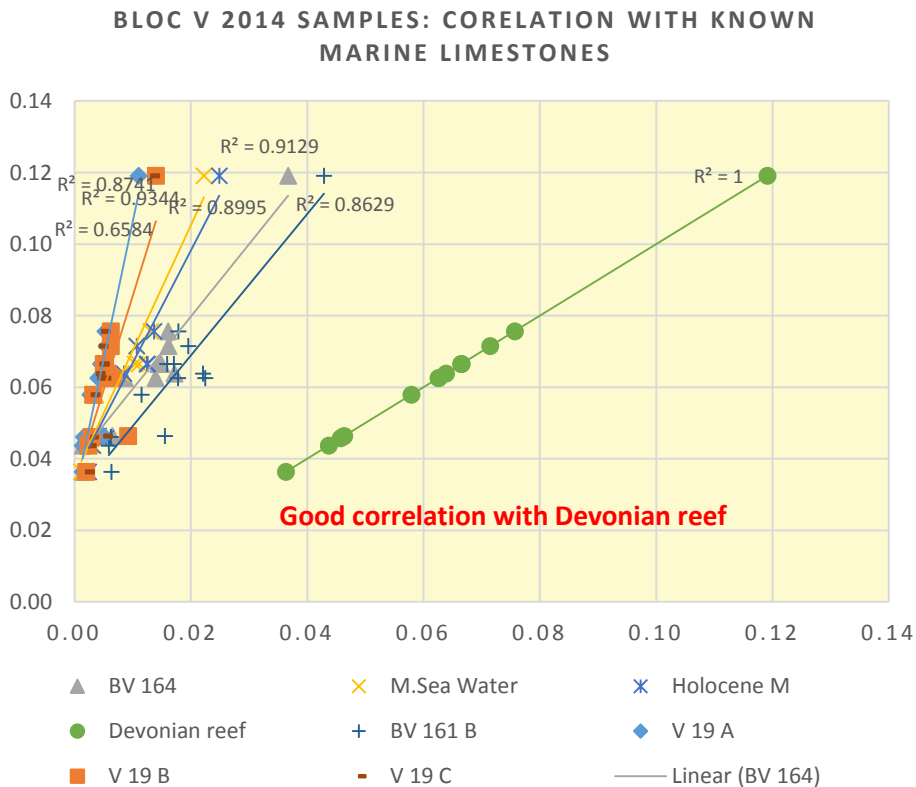
In order to follow the intra- and inter- sites geochemistry variability REE+Y results, a detailed microscopic samples observation have been undertaken on all the collected Travertine's petrography. These sample's respective micro textures, structures and /or fabrics have been detailed (in Geochemical analysis Chapter five) prior to drill through them. These residual powders obtained for each sample drilling, have been fully dissolved and digested in HNO<sub>3</sub> then run through the ICP-MS geochemical process. All the results obtained have been presented (in Results Chapter Six) and their related discussions mainly based on various additional contributions varying from recent publications to our own interpretation have been placed in evidence (in Discussion Chapter Seven).



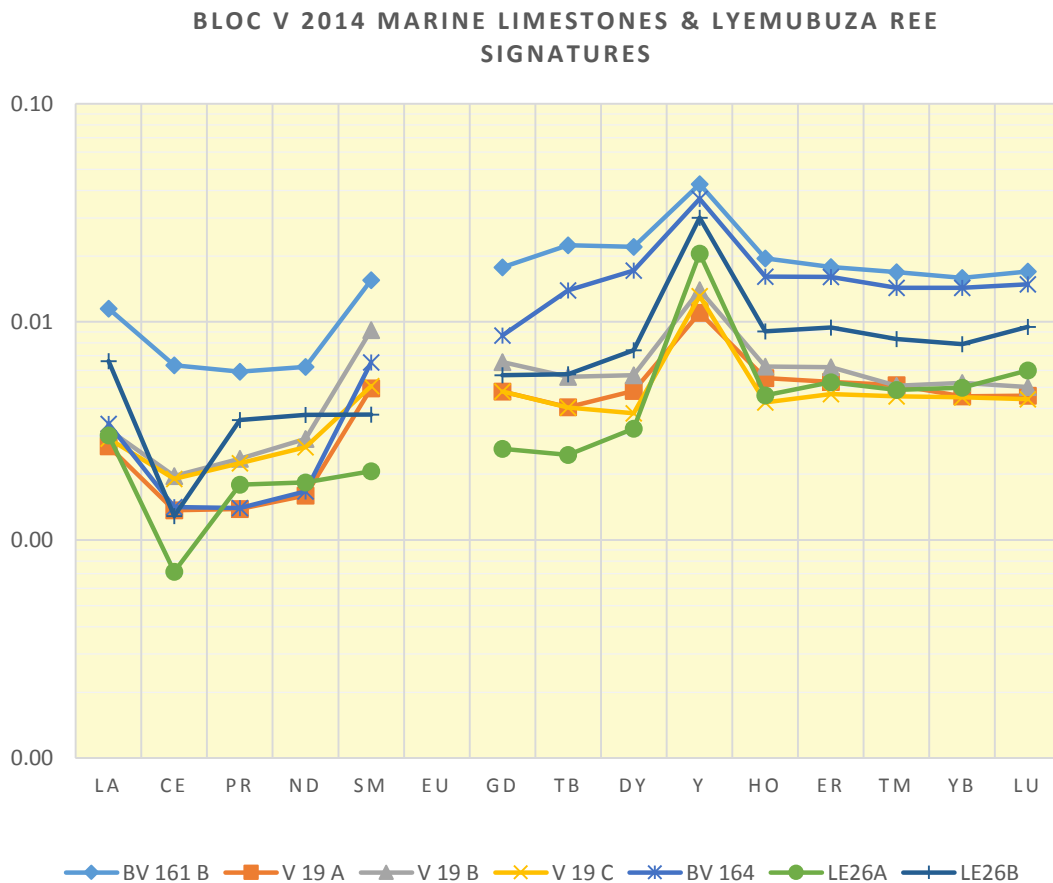
In conclusion from all above sets of recorded information, and consequently to the fruitful discussion here above, it is absolutely evident that there is no more doubt about the definite presence of marine limestone REE clear signatures + increase of Yttrium (within the Bloc V) as the figure below points the same pattern it:



This evident presence is also pointed out in the following graph below indicating that these Bloc V Travertine's samples found with Marine limestone REE signatures are greatly correlating with the Devonian reef with a correlation coefficient above  $R^2 \geq 75\%$ .



The presence of these carbonates sourcing the deposit of Marine Travertines in Mayi ya Moto hot springs and Katanda gorge (DRC) and Lyemubuza Quarry (Uganda) with matching REE+Y patterns with low Cerium and high Yttrium concentrations confirms the geological hypothesis that a potential pre-tertiary marine limestone bedrock could exist beneath the Cenozoic EARS basins through which, geothermal waters are passing and obtaining their spectral signature observed and interpreted from the ICP-MS results here compared in the figures below:



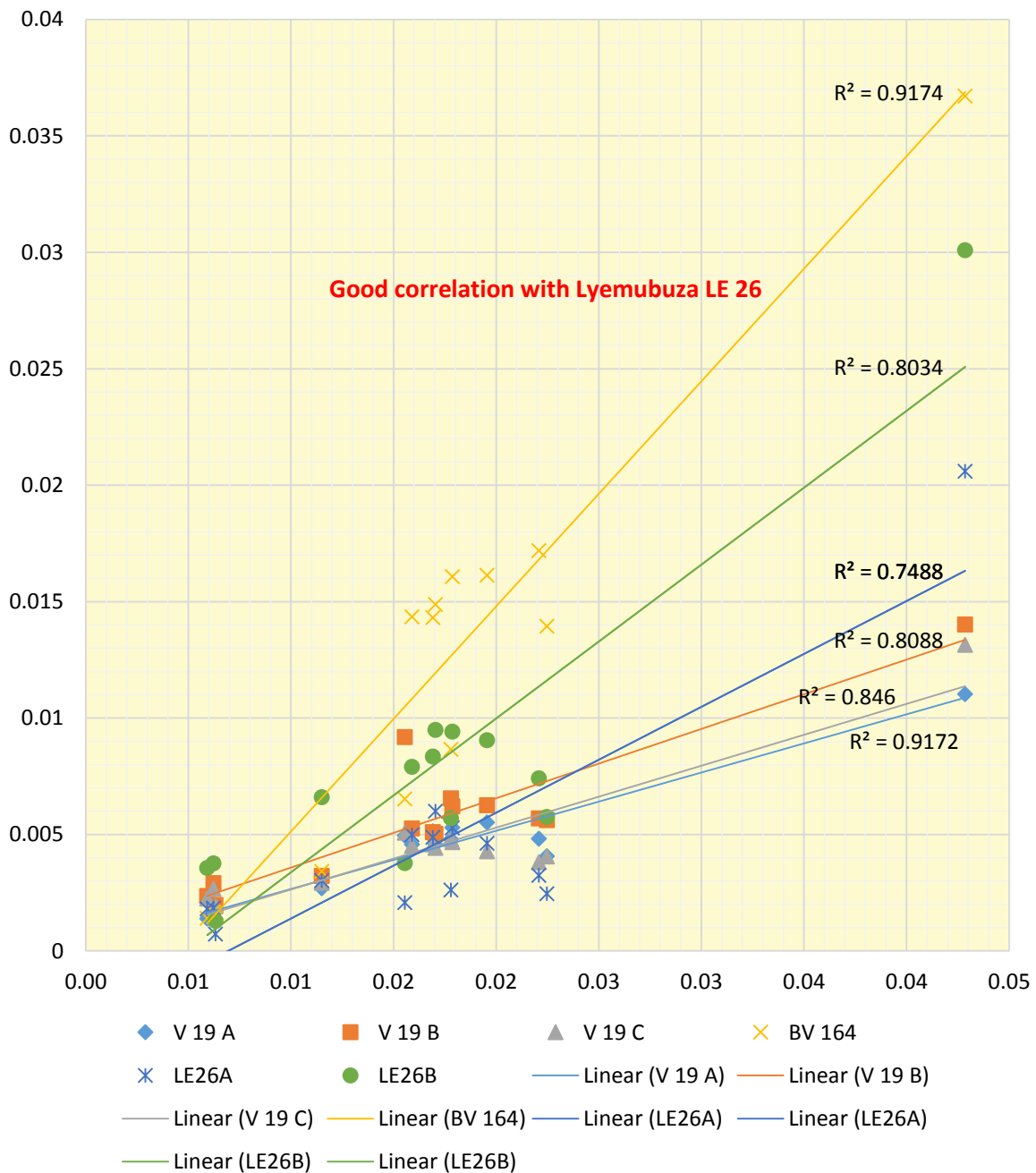
This potential pre-tertiary marine bedrock evidence has been possible through geochemistry results on carbonates structures, textures or fabrics from EARS Travertines samples V 19, BV 161 and BV 164 respectively in Mayi ya Moto hot Springs and Katanda Gorge along the western bounding fault (DRC side of the basin) and sample LE 26 found with living oil relics in Lyemubuza quarry along the eastern bounding fault (Ugandan side of the basin).

However, further field investigations are recommended to deepen these marine limestones' involvement. More samples should be collected in the basin margins and more geochemical analysis are needed not only to confirm these findings but also to define their spatial extension within the EARS basin. Exploration drillings in the linear axis (SW-NE) between Mayi ya Moto and Lyemubuza (where Oil relic have been found in cavities) would be better to confirm more evidences of pre-tertiary carbonate bedrock in cuttings.

The correlation coefficients of all MUQ normalized values have clearly discriminated the Marine limestone source of bicarbonate and excluded the possible correlation with either the Permian Karoo ( Cenomian limestones) or the west Congo Schisto-Calcaire (Neoproterozoic stromatolites). The figures Vi.42,VI.43 and VI.44 in pages 156,157 and 158 detail more about this no correlation discrimination with a coefficient  $R^2 \ll 75\%$ .

Evidently, the correlation coefficient between Bloc V (V19, BV 161 and BV 164) and Lyemubuza Travertines (LE 26) as shown in the figure below, reveals a good correlation above  $R^2 \geq 75\%$ .but also to define their spatial extension within the EARS basin.

**BLOC V 2914 MARINE LIMESTONES CORRELATION WITH LYEMUBUZA SAMPLE**



The map in Figure VIII.2 below, which illustrates the actual locations of the EARS Travertine samples in the Albertine Graben according to their respective geochemical origin, has updated the Introduction Map in Figure I.1 in page15, published in 2013 by Dr Chris Nicholas. (Nicholas, 2013). The Marine limestones considered of cold geochemical origin are marked from the Map legend in blue, while the Carbonatites considered of hot geochemical origin are in red and the hybrid geochemical origin or mixed geochemistry in green light.

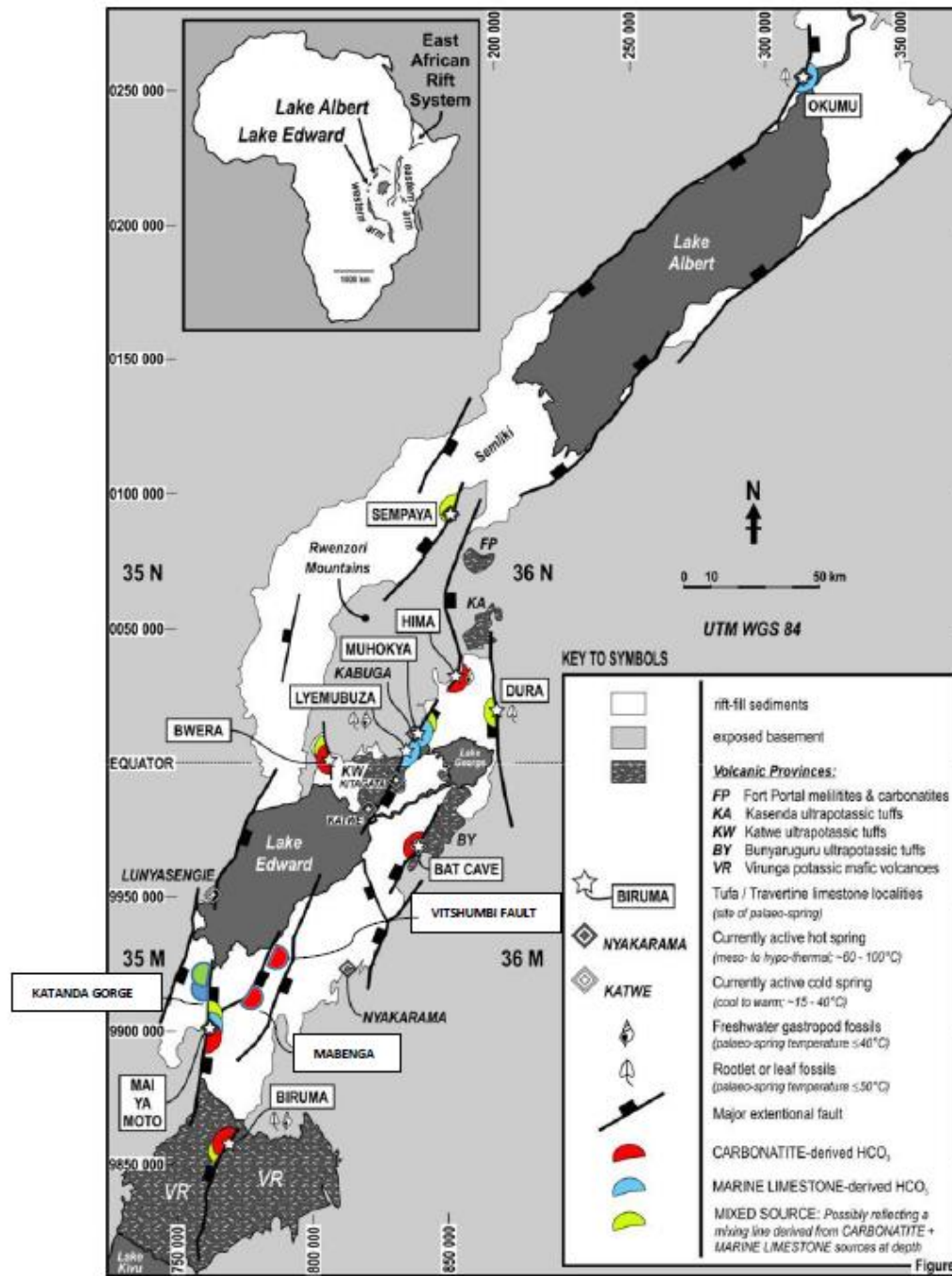


Figure VIII.2 Updated Map of Travertine geochemical origin localisation in the Albertine Graben (Kezir, Nicholas, 2020)

## RECOMMENDATIONS FOR PETROLEUM EXPLORATION IN THE LAKE EDWARD BASIN

Thus, the marine limestones must have been deposited in an older sedimentary basin that lies buried beneath the present Albertine Rift. The presence of such an older basin greatly multiplies the petroleum exploration opportunities in this region, with the possibility of potential oil source rocks, reservoirs and traps below the Albertine Rift. It also raises the possibility that marine shale source rocks are present beneath EARS basins, generating oil to migrate into it, thus delivering a higher quality light sweet crude than waxier, lacustrine sources.

This part of the rift is currently undergoing active petroleum exploration and the presence of either extensive igneous intrusives (Carbonatites “hot” origin), or Cretaceous pre-rift sediments (marine limestones “cold” origin) would have a huge impact on exploration (for very different reasons).

The “hot” origin of Travertine Carbonatites is helping the Oil exploration industry to derisk technically and financially their exploration operations by avoiding the surroundings of Carbonatites signatures locations in the basin because of the risk of high thermal gradient level supposed to have burned all the Oil prone out of the Oil window to the gas prone side.

The only previously known example of carbonatite at the surface is at Fort Portal, east of the Ruwenzori Mountains; the presence of several examples of Carbonatites at depth clearly has important implications for petroleum exploration:

- a. Avoid these ‘hot spots’ as any pre- carbonatite emplacement petroleum will be over-matured;
- b. Alert that they may be encountered on seismic surveys both onshore and offshore along major rift faults.

However, the “cold” origin of Travertine marine limestones is helping the Oil exploration to focus on a new opportunity to think and explore for the Oil potential of a probable Cenozoic basin under the siliclastic rift sediments in the Eastern Africa Rift System. This is something which will be very enthusiastic topic needing to be dug deeply beyond this present MSc. Research project from which the obtained results may be a good scientific article to publish.

As no known Marine Limestones are supposed to be present in the Tertiary Rift, the carbonate REE+Y signature must probably come from a limestone unit in the pre-rift section considering the following new knowledges:

- The REE normalized values correlates neither with Karoo-Mesozoic nor with Late Neoproterozoic ‘Schisto-Calcaire’. The fact is clearly that it is definitively a marine limestone evident source of bicarbonate which raises the possibility of a deeper, ‘pre-tertiary rift’ petroleum play system.
- Given the asymmetry of the Lake Edward basin, this marine limestone unit may have a greater relict thickness on the western side of the basin – note on the maps that the presence of a marine limestone was always recorded in samples lying on a western bounding fault in the sub-basins.

## REFERENCES

- BABECHUK, M. G., KAMBER, B. S., GREIG, A., CANIL, D. & KODOLÁNYI, J. 2010. The behaviour of tungsten during mantle melting revisited with implications for planetary differentiation time scales. *Geochimica et Cosmochimica Acta*, 74, 1448-1470.
- BAUER, F., GLASMACHER, U., RING, U., SCHUMANN, A. & NAGUDI, B. 2010. Thermal and exhumation history of the central Rwenzori Mountains, Western Rift of the East African Rift system, Uganda. *International Journal of Earth Sciences*, 99, 1575-1597.
- BELLANCA, A., MASETTI, D. & NERI, R. 1997. Rare earth elements in limestone/marlstone couplets from the Albian-Cenomanian Cismon section (Venetian region, northern Italy): assessing REE sensitivity to environmental changes. *Chemical geology*, 141, 141-152.
- BELLON, H. & POUCKET, A. 1980. Datations K-Ar de quelques laves du Rift-Ouest de l'Afrique Centrale; implications sur l'évolution magmatique et structurale. *Geologische Rundschau*, 69, 49-62.
- BEUNING, K. R. & RUSSELL, J. M. 2004. Vegetation and sedimentation in the Lake Edward Basin, Uganda–Congo during the late Pleistocene and early Holocene. *Journal of Paleolimnology*, 32, 1-18.
- BOVEN, A., PASTEELS, P., PUNZALAN, L., YAMBA, T. & MUSISI, J. 1998. Quaternary perpotassic magmatism in Uganda (Toro-Ankole Volcanic Province): age assessment and significance for magmatic evolution along the East African Rift. *Journal of African Earth Sciences*, 26, 463-476.
- BURKE, W., DENISON, R., HETHERINGTON, E., KOEPNICK, R., NELSON, H. & OTTO, J. 1982. Variation of seawater  $87\text{Sr}/86\text{Sr}$  throughout Phanerozoic time. *Geology*, 10, 516-519.
- BYAKAGABA, A. 1997. Report on the Geological mapping of the Lakes Edward-George Basin. *Report of the Department of Petroleum Exploration and Production*, 1-55.
- CHOROWICZ, J. 1990. Dynamics of the different basin-types in the East African Rift. *Journal of African Earth Sciences (and the Middle East)*, 10, 271-282.
- CHOROWICZ, J. 2005. The east African rift system. *Journal of African Earth Sciences*, 43, 379-410.
- CORKERON, M., WEBB, G. E., MOULDS, J. & GREY, K. 2012. Discriminating stromatolite formation modes using rare earth element geochemistry: Trapping and binding versus in situ precipitation of stromatolites from the Neoproterozoic Bitter Springs Formation, Northern Territory, Australia. *Precambrian Research*, 212, 194-206.
- CRAIG, H. 1953. The geochemistry of the stable carbon isotopes. *Geochimica et Cosmochimica Acta*, 3, 53-92.
- CROSSLEY, R. 1984. Controls of sedimentation in the Malawi rift valley, central Africa. *Sedimentary Geology*, 40, 33-50.
- DOORNKAMP, J. & TEMPLE, P. 1966. Surface, drainage and tectonic instability in part of southern Uganda. *The Geographical Journal*, 132, 238-252.
- EBINGER, C. 1989. Tectonic development of the western branch of the East African rift system. *Geological Society of America Bulletin*, 101, 885-903.
- EBY, G. N., LLOYD, F. E. & WOOLLEY, A. R. 2009. Geochemistry and petrogenesis of the Fort Portal, Uganda, extrusive carbonatite. *Lithos*, 113, 785-800.
- EGGINS, S., WOODHEAD, J., KINSLEY, L., MORTIMER, G., SYLVESTER, P., MCCULLOCH, M., HERGT, J. & HANDLER, M. 1997. A simple method for the precise determination of  $\geq 40$  trace elements in geological samples by ICPMS using enriched isotope internal standardisation. *Chemical Geology*, 134, 311-326.

- FROSTICK, L. & REID, I. 1990. Structural control of sedimentation patterns and implication for the economic potential of the East African Rift basins. *Journal of African Earth Sciences (and the Middle East)*, 10, 307-318.
- HAYS, P. D. & GROSSMAN, E. L. 1991. Oxygen isotopes in meteoric calcite cements as indicators of continental paleoclimate. *Geology*, 19, 441-444.
- HEPWORTH, J. & MACDONALD, R. 1966. Orogenic belts of the northern Uganda basement. *Nature*, 210, 726.
- HILL, R. 2007. MAKING THIN SECTIONS BY HAND.
- KAMBER, B. S., WEBB, G. E. & GALLAGHER, M. 2014. The rare earth element signal in Archaean microbial carbonate: information on ocean redox and biogenicity. *Journal of the Geological Society*, 171, 745-763.
- KAMPUNZU, A., BONHOMME, M. & KANIKA, M. 1998. Geochronology of volcanic rocks and evolution of the Cenozoic Western Branch of the East African Rift System. *Journal of African Earth Sciences*, 26, 441-461.
- KARP, T., SCHOLZ, C. A. & MCGLUE, M. M. 2012. Structure and stratigraphy of the Lake Albert Rift, East Africa: Observations from seismic reflection and gravity data.
- KOEHN, D., AANYU, K., HAINES, S. & SACHAU, T. 2008. Rift nucleation, rift propagation and the creation of basement micro-plates within active rifts. *Tectonophysics*, 458, 105-116.
- LÆRDAL, T., TALBOT, M. R. & RUSSELL, J. M. 2002. Late Quaternary Sedimentation and Climate in the Lakes Edward and George Area, Uganda—Congo. *The East African Great Lakes: Limnology, Palaeolimnology and Biodiversity*. Springer.
- LAMBIASE, J. & BOSWORTH, W. 1995. Structural controls on sedimentation in continental rifts. *Geological Society, London, Special Publications*, 80, 117-144.
- LE FOURNIER, J., CHOROWICZ, J., THOUIN, C., BALZER, F., CHENET, P.-Y., HENRIET, J.-P., MASSON, D., MONDEGUER, A., ROSENDAHL, B. & SPY-ANDERSON, F.-L. 1985. Le bassin du lac Tanganyika: évolution tectonique et sédimentaire. *Comptes rendus de l'Académie des sciences. Série 2, Mécanique, Physique, Chimie, Sciences de l'univers, Sciences de la Terre*, 301, 1053-1058.
- LYNCH-STIEGLITZ, J., STOCKER, T. F., BROECKER, W. S. & FAIRBANKS, R. G. 1995. The influence of air-sea exchange on the isotopic composition of oceanic carbon: Observations and modeling. *Global Biogeochemical Cycles*, 9, 653-665.
- MASTANDREA, A., BARCA, D., GUIDO, A., TOSTI, F. & RUSSO, F. 2010. Rare earth element signatures in the Messinian pre-evaporitic Calcare di Base formation (Northern Calabria, Italy): evidence of normal seawater deposition. *Carbonates and Evaporites*, 25, 133-143.
- MCCABE, R. 2015. Inorganic Geochemistry of the South Eastern Tanzanian Sedimentary Basins.
- MUSISI, J. 1991. *The neogene geology of the Lake George–Edward basin, Uganda*. PhD thesis.
- NERBRÅTEN, K. B. 2014. *Petrology and sedimentary provenance of Mesozoic and Cenozoic sequences in the Mandawa basin*.
- NICHOLAS, C. J. 2009. Summary technical evaluation of Exploration Area 4B, Ugandan Lake Edward.
- NICHOLAS, C. J. 2017. Atlas of Fluvial, Deltaic, and Marginal Lacustrine Depositional Environments in Continental Rift Settings of the equatorial Tropics. *Avalonia Geosciences*, 190.
- NICHOLAS, C. J., NEWTH, I. R., ABEINOMUGISHA, D., TUMUSHABE, W. M. & TWINOMUJUNI, L. 2016. Geology and stratigraphy of the south-eastern Lake Edward basin (Petroleum Exploration Area 4B), Albertine Rift Valley, Uganda. *Journal of Maps*, 12, 237-248.
- PAVLOVA, A. & PAPAZOVA, D. 2003. Oil-spill identification by gas chromatography-mass spectrometry. *Journal of chromatographic science*, 41, 271-273.

- PICKFORD, M., SENUT, B. & HADOTO, D. P. M. 1993. *Geology and Palaeobiology of the Albertine Rift Valley, Uganda-Zaire: Geology, Cifeg.*
- PLATZ, T., FOLEY, S. F. & ANDRÉ, L. 2004. Low-pressure fractionation of the Nyiragongo volcanic rocks, Virunga Province, DR Congo. *Journal of Volcanology and Geothermal research*, 136, 269-295.
- RING, U. 2008. Extreme uplift of the Rwenzori Mountains in the East African Rift, Uganda: Structural framework and possible role of glaciations. *Tectonics*, 27.
- ROSENTHAL, A., FOLEY, S., PEARSON, D. G., NOWELL, G. M. & TAPPE, S. 2009. Petrogenesis of strongly alkaline primitive volcanic rocks at the propagating tip of the western branch of the East African Rift. *Earth and Planetary Science Letters*, 284, 236-248.
- RUBONDO, E. 2005. The hydrocarbon potential of the Albertine Graben, Uganda., 22.
- RUSSELL, J. M. & JOHNSON, T. C. 2005. A high-resolution geochemical record from Lake Edward, Uganda Congo and the timing and causes of tropical African drought during the late Holocene. *Quaternary Science Reviews*, 24, 1375-1389.
- RUSSELL, J. M., JOHNSON, T. C., KELTS, K. R., LÆRDAL, T. & TALBOT, M. R. 2003. An 11 000-year lithostratigraphic and paleohydrologic record from equatorial Africa: Lake Edward, Uganda–Congo. *Palaeogeography, Palaeoclimatology, Palaeoecology*, 193, 25-49.
- SOCO 2010. Partner Technical Meeting Report. 69.
- STOPPA, F. & SCHIAZZA, M. 2013. An overview of monogenetic carbonatitic magmatism from Uganda, Italy, China and Spain: volcanologic and geochemical features. *Journal of South American Earth Sciences*, 41, 140-159.
- TIERCELIN, J.-J., SOREGHAN, M., COHEN, A. S., LEZZAR, K.-E. & BOUROULLEC, J.-L. 1992. Sedimentation in large rift lakes: example from the Middle Pleistocene— Modern deposits of the Tanganyika Trough, East African Rift System. *Bulletin des Centres de Recherches Exploration-Production Elf-Aquitaine*, 16, 83-111.
- TUMUSHABE, W. M. 2012. *Sedimentary Response to Coupled East Africa Climate Change and Active Rifting in the Lake Edward Basin, Albertine Rift, Uganda.* Trinity College Dublin.
- UPCOTT, N., MUKASA, R., EBINGER, C. & KARNER, G. 1996. Along-axis segmentation and isostasy in the Western rift, East Africa. *Journal of Geophysical Research: Solid Earth*, 101, 3247-3268.
- VEIZER, J., GODDERIS, Y. & FRANÇOIS, L. M. 2000. Evidence for decoupling of atmospheric CO<sub>2</sub> and global climate during the Phanerozoic eon. *Nature*, 408, 698.
- VERSELT, J. & ROSENDAHL, B. 1989. Relationships between pre-rift structure and rift architecture in Lakes Tanganyika and Malawi, East Africa. *Nature*, 337, 354.
- VINER, A. & SMITH, I. 1973. Geographical, historical and physical aspects of Lake George. *Proceedings of the Royal Society of London B: Biological Sciences*, 184, 235-270.
- WALLNER, H. & SCHMELING, H. 2010. Rift induced delamination of mantle lithosphere and crustal uplift: a new mechanism for explaining Rwenzori Mountains' extreme elevation? *International Journal of Earth Sciences*, 99, 1511-1524.
- WIERZBOWSKI, H. Strontium isotope composition of sedimentary rocks and its application to chemostratigraphy and palaeoenvironmental reconstructions. *Annales Universitatis Mariae Curie-Sklodowska*, 2013. De Gruyter Open Sp. z oo, 23.
- WOLF, R. E. 2005. What is ICP-MS? and more importantly, what can it do. *US Geological Survey*, 7.



## **Appendix 1: Samples preparation lab notes**

Museum Building, TCD

9<sup>th</sup> July 2016

**SAMPLES PROPOSED FOR THE FIRST BATCH OF 2016 ICP-MS ANALYSIS.**

The Tufa / Travertines samples shipped to TCD for lab analysis have been collected during fields works in ten (10) palaeo-spring sites in the Albertine Graben, East African Rift system where no previous literatures have mentioned their presence so far. However, successive field works and some of exploration drillings have reported their presence in the Albertine Basin.

The ICP-MS method and instrument which rapidly become established as a preferred way for the analysis of trace elements in geological samples aims to find out the detailed geochemical origin of these “weird” limestones which are not theoretically supposed to outcrop or to meet a drilling there. The hypothetic origins could be Carbonatites lavas (hot origin) lacustrine (palaeo-lake) or fluvial (palaeo river) (cold) origin.

**Sixteen (16) Tufas / Travertines samples** drilled exactly from the same drilling sites in 2013 and prepared for their re-analysis now in 2016, have already been analyzed in 2013 by the ICP-MS by Mike Babechuk with the help of Jean Dwyer.

✚ Samples found with Marine limestones REE signatures or isotopic fingerprints had satisfied the following 5 key criteria:

- *High ratio of Y/Ho*
- *Light REE depletion*
- *High Sr*
- *High ratio U/Th*
- *Ce anomalies*
- *La anomalies*

✚ Samples found with Carbonatites limestones REE signatures or isotopic fingerprints had satisfied the following criteria:

- *Light and heavy REE enriched*
- *High Li, Rb, Cs, and Ti concentration*
- *Perfect matching correlation with Fort Portal Carbonatites (universally recognized in the literature with Carbonatites fingerprint) with a correlation coefficient above or equal to 0.95.*

The Procokin PCK limestone sample has been collected in a quarry in the western side of DR Congo where literature universally recognized the presence of stromatolites fossils which suggest a shallow water depositional environment or origin.

The laboratory analysis of the **four (4) PCK limestone samples** in 2016 aims to confirm by ICP-MS method and instrument the marine limestone origin of this stromatolites neighboring sample which will later be used as matching correlation tool or comparator for or with any other marine limestone REE signature or isotopic fingerprint sample from East

African Rift System exactly as it was done in 2013 for the Fort Portal Carbonatites. All the samples re-drilled for the second time in 2016 has been labelled with the same label of 2013 and added with slash two /2 to make the difference and to show that they have been drilled for the second time in 2016.

The ICP-MS analysis which will be run by Cora Mc Kenna and Sylvain M.Kezir in September 2016 will double-check the 2013 results reproducing ability using different way and different people involved in.

So, a total of 20 powder samples (weight about 8 to 10 mg each) has been prepared for the first batch of 2016 lab analysis as below:

<b>Carbonatites</b>		<b>Correlation coefficient with Fort Portal lavas</b>	<b>Marine limestones</b>		<b>Comments On Kamber (2014) Criterias</b>
1	V2b/2	$R^2 = 0.9$	1	P12b/2	Satisfy all 5 criteria
2	V20a/2	$R^2 = 0.95$	2	LE24a/2	Satisfy all 5 criteria
3	V20b/2	$R^2 = 0.95$	3	LE24b/2	Satisfy all 5 criteria
4	V22a/2	$R^2 = 0.95$	4	LE26a/2	Satisfy all 5 criteria
5	LE44a/2	$R^2 = 0.95$	5	LE26b/2	Satisfy all 5 criteria
6	LE44b/2	$R^2 = 0.95$	6	LE28a/2	Satisfy all 5 criteria
7	LE41a/2	$R^2 = 0.9$	7	LE28d/2	Satisfy all 5 criteria
8	LE41b/2	$R^2 = 0.9$	8	V19a/2	Satisfy 4 of 5 criteria
			9	PCK a/1	Grey texture
			10	PCK b/1	Replica of Grey texture
			11	PCK c/1	Light texture
			12	PCK d/1	Replica of Light texture

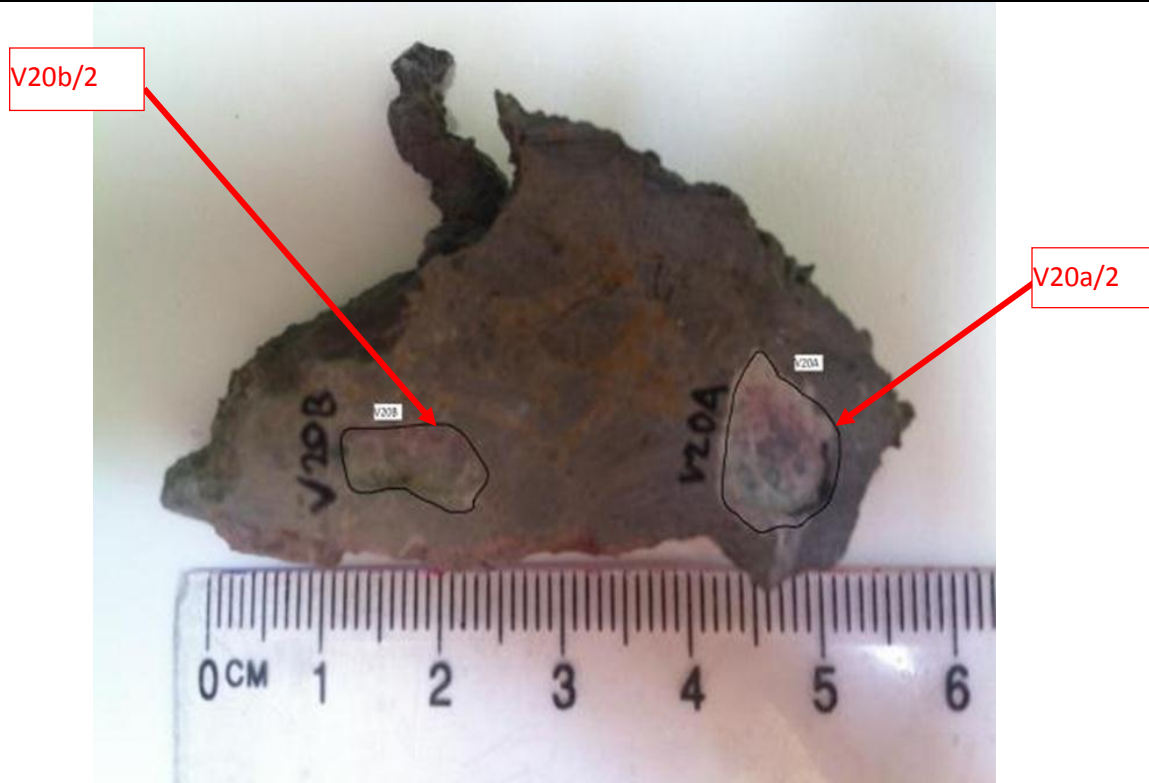
**SAMPLES DESCRIPTIONS AND DRILLING OPERATIONS SUMMARY.**

Sample ID	Sample description	Weight tube	Weight Sample	Drilling bit size	Powder colour	Remarks
01/09/2016 V2b/2	- No visible fabrics or crystal phases; - Very crumbly texture	0.906 g	8.514 mg	Small	Dark brown	

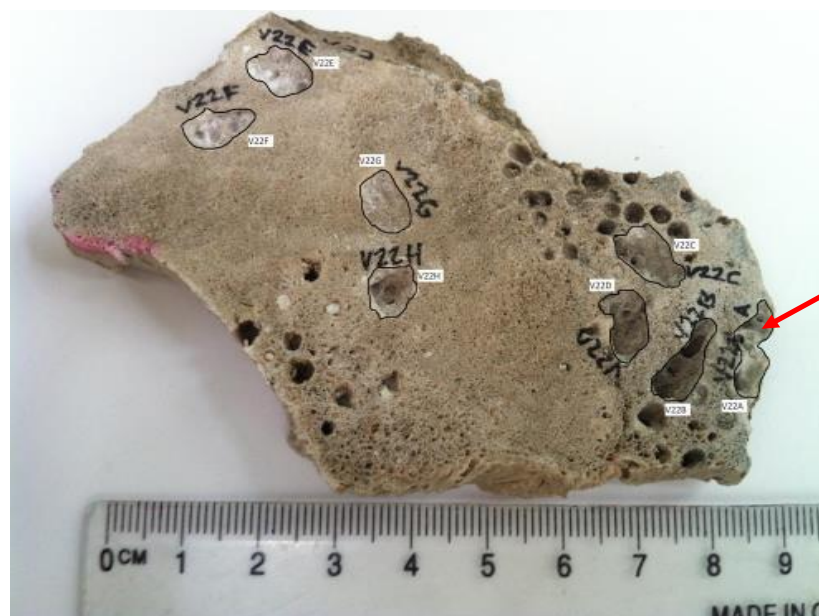
V2b/2



Sample ID 01/09/2016	Sample description	Weight tube	Weight Sample	Drilling bit size	Powder colour	Remarks
V20a/2	<ul style="list-style-type: none"> <li>- Dark grey crystal surrounded by a lighter matrix containing orange /rusty flecks</li> <li>- The matrix is in lands and too friable to drill</li> </ul>	0.909 g	9.518 mg	medium	Dark grey	One sample and one replica of the dark grey crystal avoiding as possible the matrix have been drilled
V20b/2	Replica of V20a/2	0.912 g	8.520 mg	Medium	Grey	Replica drilled from different site of the same slice face

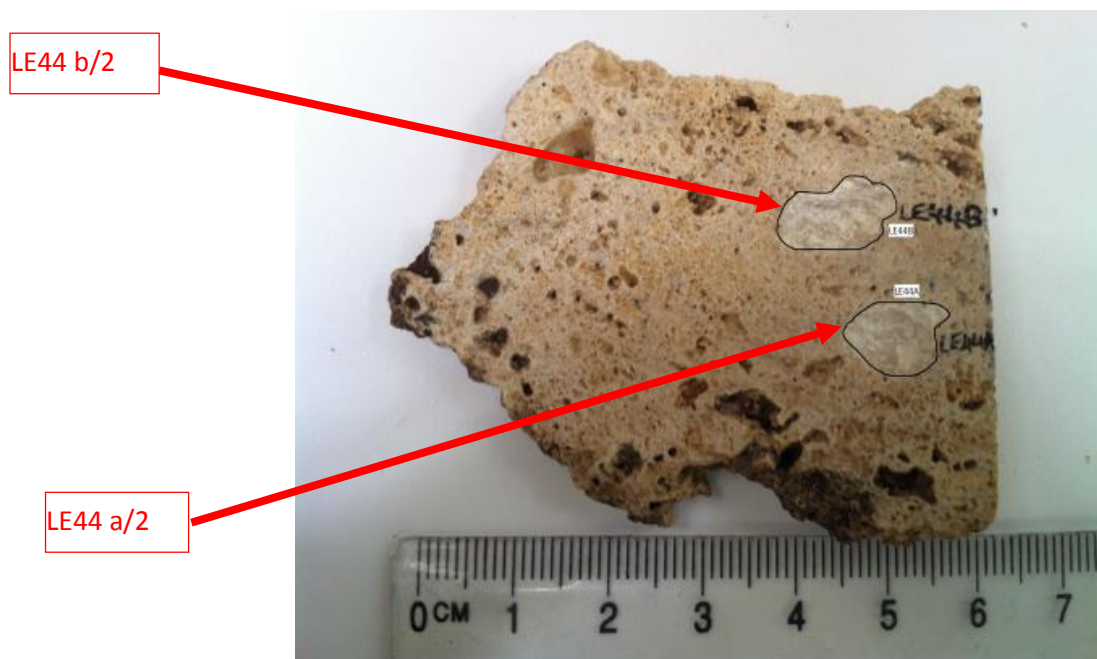


Sample ID 30/08/2016	Sample description	Weight tube	Weight Sample	Drilling bit size	Powder colour	Remarks
V22a/2	<ul style="list-style-type: none"> <li>- 4 crystals fabrics were identified, a portion of the sample contained large pores (up to 5mm in diameter) and the large pore appeared lined with a light coloured calcite;</li> <li>- Some portions of the sample near the edges had smaller more uniform pores in a darker coloured calcite with very few pores;</li> <li>- These areas were concentrated in the centre of the sample.</li> </ul>	0.910 g	10.521 mg	Small	white	15 samples were drilled with replicas for the purpose of having enough material to run ICP-MS.

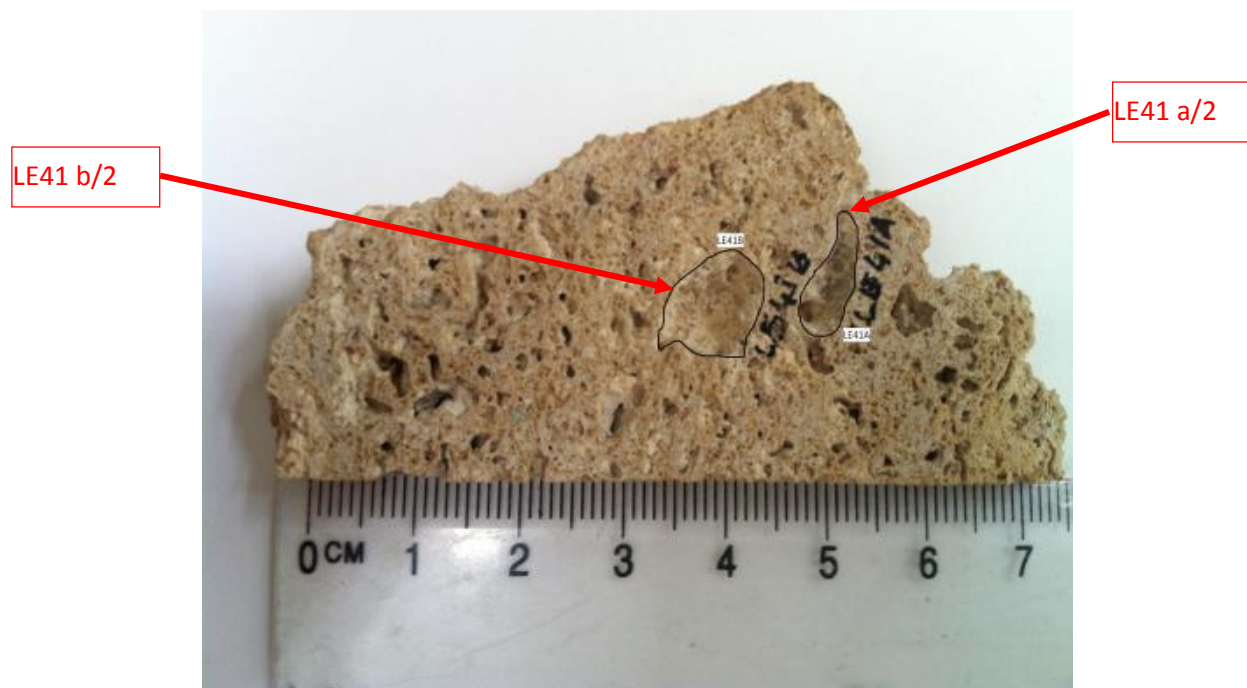


V22a/2

Sample ID	Sample description	Weight tube	Weight Sample	Drilling bit size	Powder colour	Remarks
01/09/2016 <b>LE44a/2</b>	<ul style="list-style-type: none"> <li>- No visible fabrics/textures differences;</li> <li>- Moderately porous fine-medium crystalline carbonate.</li> </ul>	0.911 g	7.518 mg	medium	White	Some black flecks in the white powder may have come from weathered surface of the sample while tapping out the powder from the sample.
<b>LE44b/2</b>	Replica of LE44a/2	0.910 g	9.523 mg	Medium	White	Replica drilled from different site of the same slice face. Black flecks still present.



Sample ID	Sample description	Weight tube	Weight Sample	Drilling bit size	Powder colour	Remarks
01/09/2016 <b>LE41a/2</b>	<ul style="list-style-type: none"> <li>- 2 (two) colours of carbonates crystals were visible: A milky cream colour and light brown colour.</li> <li>- Although the two are too finely interspersed for separate sampling.</li> </ul>	0.909 g	9.518 mg	medium	Milky cream	One sample and one replica were drilled from an area enough representative of the whole sample.
<b>LE41b/2</b>	Replica of LE41a/2	0.913 g	10.522 mg	Medium	Milky cream to Light brown	Replica drilled from different site of the same slice face. Black flecks still present.

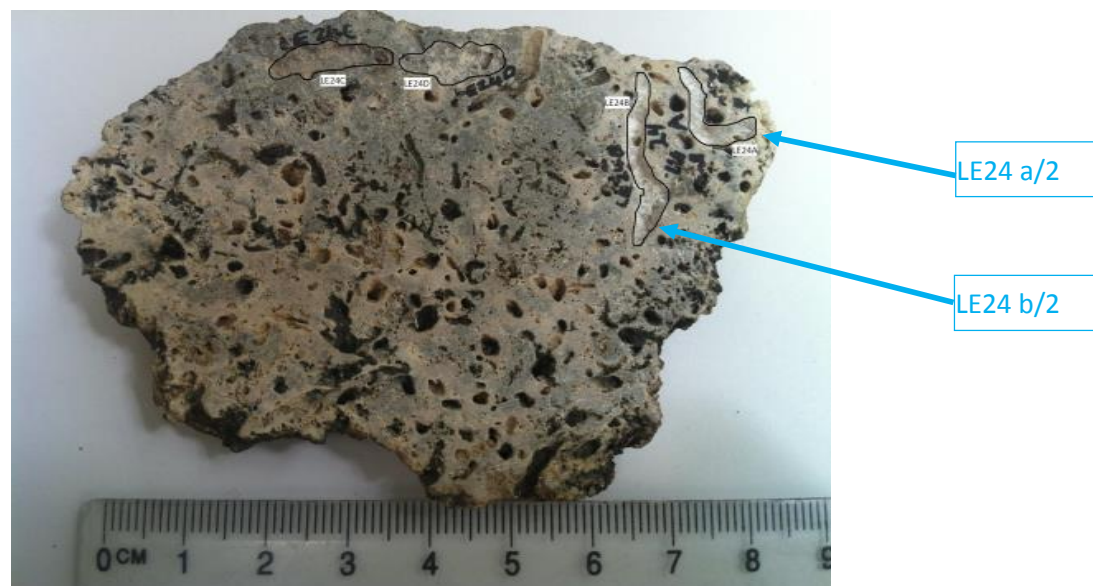




Sample ID	Sample description	Weight tube	Weight Sample	Drilling bit size	Powder colour	Remarks
02/09/2016						
P12b/2	<ul style="list-style-type: none"> <li>- Crumbly, porous light brown carbonate;</li> <li>- Deposits around the pores look more crystalline than surrounding carbonates. However, they are smaller than the drill bit tip.</li> </ul>	0.905 g	8.515 mg	Small, then well cleaned medium	Light brown	The sample was much harder than expected, it was crystalline and not crumbly (as previously described) beneath the surface. Presence of some small black flecks.



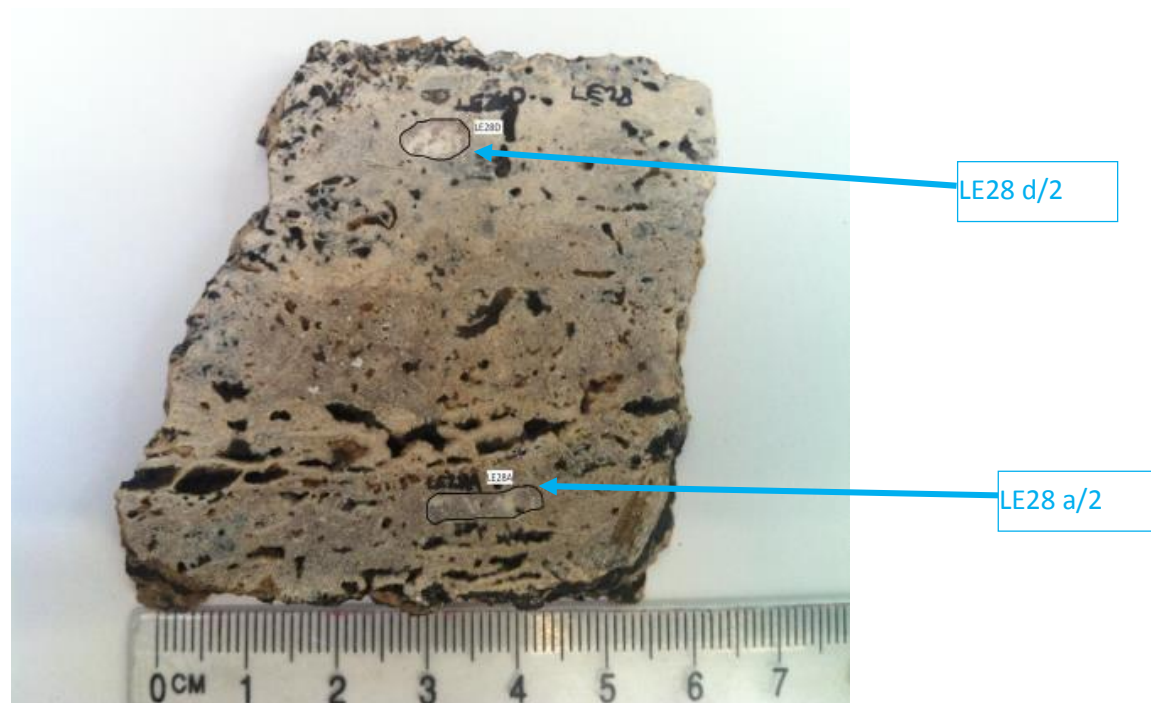
Sample ID 02/09/2016	Sample description	Weight tube	Weight Sample	Drilling bit size	Powder colour	Remarks
LE24a/2	<ul style="list-style-type: none"> <li>- Porous sample with a black lining in the cavities;</li> <li>- Two distinct colours of Carbonates: Grey and Creamy.</li> <li>- Although, individual crystals are not regularly visible and are very fine when they are.</li> <li>- The two Carbonates can be drilled separately.</li> </ul> <p>However the boundaries between the two are quite gradational/diffuse</p>	0.910 g	8.319 mg	medium	Creamy	<p>Care was taken to avoid the cavities lined in black. However, they cannot be accurately avoided in 3 dimensions.</p> <p>Black flecks visible in the powder appear to confirm this contamination.</p>
LE24b/2	Replica of LE24a/2	0.911 g	9.520 mg	Medium	Creamy without black flecks avoided while drilling	Replica drilled from different site of the same slice face



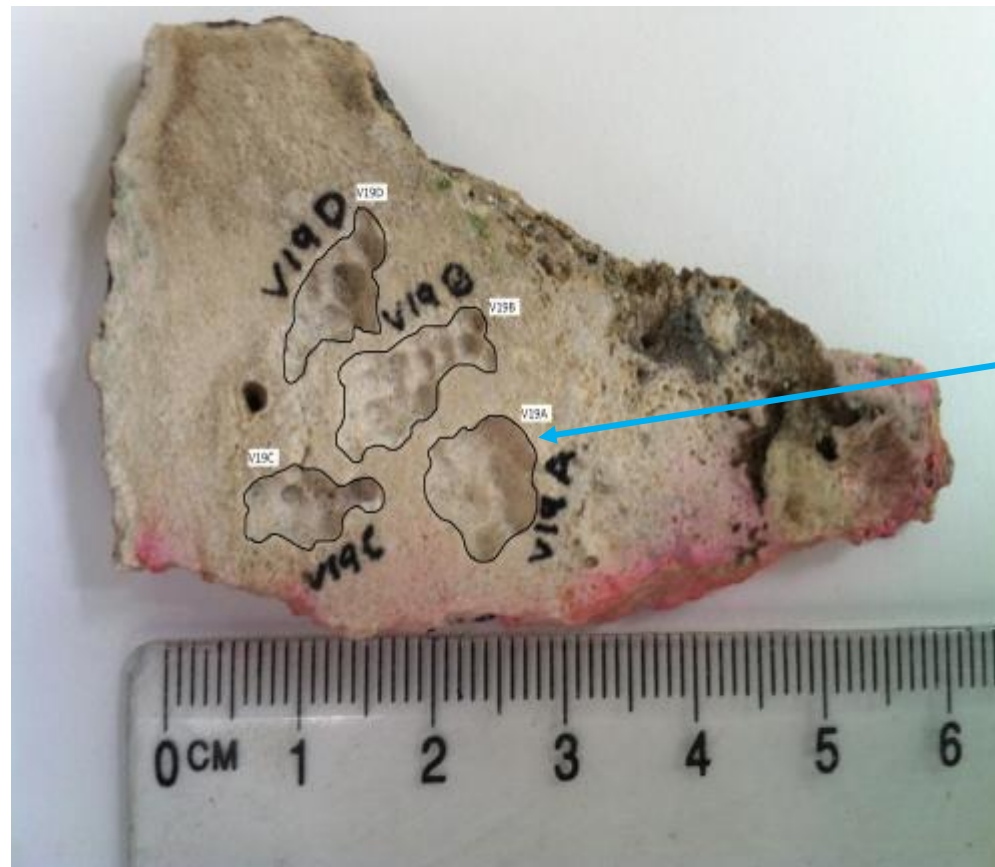
Sample ID 02/09/2016	Sample description	Weight tube	Weight Sample	Drilling bit size	Powder colour	Remarks
LE26a/2	<ul style="list-style-type: none"> <li>- No visible fabric or crystal phase apart from the dark cavity lining.</li> <li>- Drilled samples on a large Patch</li> </ul>	0.996 g	10.004 mg	medium	Dark brown	One sample and one replica were drilled. Exhaustion of tube stock. No time to wait new stock. Change in the tube size.
LE26b/2	Replica of LE26a/2	0.997 g	11.006 mg	Medium	Dark brown	Replica drilled from different site of the same slice face



Sample ID 02/09/2016	Sample description	Weight tube	Weight Sample	Drilling bit size	Powder colour	Remarks
LE28a/2	The sample is layered with creamy and pink brown layers and cavities lined in black which were avoided while drilling.	0.911 g	9.520 mg	medium	creamy	Drilled texture: <i>pink brown</i> layer.
LE28d/2	Replica of LE28c/2	0.910 g	7.918 mg	Medium	Creamy with black flecks	Drilled texture: <i>cream</i> layer. Replica drilled from different site of the same slice face

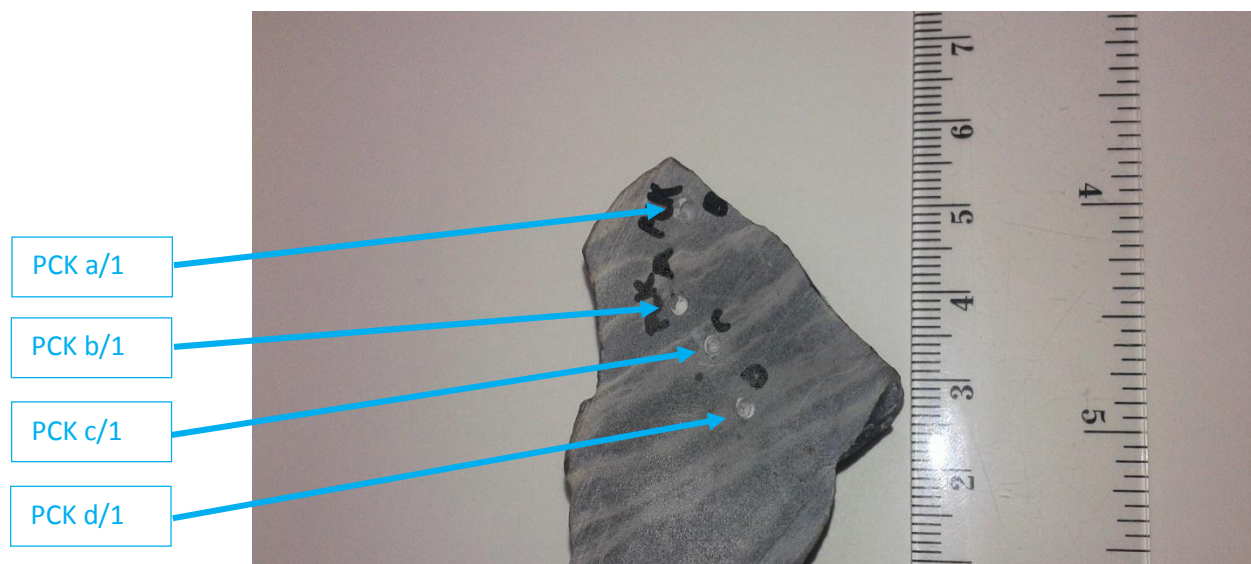


Sample ID	Sample description	Weight tube	Weight Sample	Drilling bit size	Powder colour	Remarks
02/09/2016						
V19a/2	<p>Two textures are visible:</p> <ul style="list-style-type: none"> <li>• A more porous darker portion;</li> <li>• A lighter coloured less porous portion.</li> </ul>	0.920 g	8.752 mg	medium	white	Drilled texture: lighter less porous texture



V19 a/2

Sample ID 02/09/2016	Sample description	Weight tube	Weight Sample	Drilling bit size	Powder color	Remarks
PCK a/1	2 crystal phases are visible: - <b>Grey crystal phase</b> , the most common; - Light /white phase with most euhedral and irregular crystals.	0.913 g	9.458 mg	medium	white	Drilled samples will be probably containing all the 2 phases; however will be mostly one kind and will hopefully maintain "geochemical difference". Hard to drill, very small Black flecks.
PCK b/1	Replica of PCK a/1	0.912 g	10.345 mg	Medium	White	Replica drilled from different site of the same slice face
PCK c/1	<b>Light /white phase</b> with most euhedral and irregular crystals	0.913 g	13.246 mg	Medium	White	Hard to drill, very small black flecks.
PCK d/1	Replica of PCK c/1	0.914 g	12.653 mg	Medium	White	Replica drilled from different site of the same slice face



2<sup>nd</sup> batch of Limestones samples for REE ICP-MS

Objective:

Being more confident during the analyse of the 1<sup>st</sup> batch of limestones samples (collected during the Albertine Graben field trips from 2007 to 2010 and analysed in 2013) by the ICP-MS method ability to reproduce identical results whenever the time or whatever the team involved to run it, the next batch (2<sup>nd</sup> one) of limestones samples (collected during 2014's field trip) would be ideally analysed and interpreted in June 2017 before the next and last field trip planned in July 2017.

The main objective of this actual (2<sup>nd</sup> batch samples) 2017 REE- ICP/MS analyse is to give the best geochemical understanding of the bicarbonate double origin in the limestones outcropping in the western branch of the East African Rift System "before" to re-visit the field for more samples collection helping to fill any gap in the geochemical understanding of the historical way of bicarbonate dissolving in the outcropping limestones.

Method:

The results confidence got after the REE ICP-MS analyse of the 1<sup>st</sup> batch of limestones samples imposed to reduce the number of analyses per sample during the analysis of the 2<sup>nd</sup> batch.

Indeed, for the 1<sup>st</sup> batch of limestone samples, the necessity to drill through any visible texture/structure/fabric in each limestone sample collected from 2007 to 2014, was due to the geochemical need to see how the REE-Y trends are varying through all carbonate textures/structures/fabric present in one single sample in order to confirm the method results reproducing ability in the same sample.

However, as this reproducing ability is confirmed, there is no more need to drill any visible texture in a single sample. In order to get only the origin of the bicarbonate (Carbonatites lavas or marine limestone), each limestone sample will be drilled through any white/ lightest single texture/structure/fabric which represents the most carbonate fabric. Avoid to drill through any black or dark texture/structure/fabric.

Samples considered as references:

The Fort Portal Carbonatites lavas have got from the existing literature a known REE-Y Spectral signature which characterizes the "hot" origin of bicarbonates in the outcropping limestones. All the East African Rift Carbonatites lavas could be easily correlated with Fort portal as they are close located and have approximately the same age. So, the Fort Portal Carbonatites are the best reference so far to correlate all the East African possible Carbonatites spectral signatures in the future.

Unfortunately, no marine limestones so far could be considered as the best reference in term of close location and age dating for any East African Rift marine limestone characterizing the "cold" origin of their bicarbonate:

- The Procokin (PCK) limestone sample analysed in 2016 by REE-Y ICP-MS met the marine limestone criterias but gave a very different trend of Spectral signature from these collected in Albertine Graben from 2007 to 2010 and analysed twice in 2013 and 2016 during the results reproducing ability check experiment. This could be explained by the facts that the PCK sample doesn't

have the same location than the Albertine Rift limestones. Either they're all from a marine source, they didn't followed the same geochemical process to be precipitated. Also, the PCK sample doesn't have the same age with the Albertine Rift marine limestones. The different trend of the PCK spectral signature suggests different age while the criteria indicates marine limestone same origin.

- The Mandawa (MDW) basin in the Southern coastal Tanzania is closer to the Albertine Rift than the PCK quarry located in the western DRC. MDW limestones have been found in outcrop and samples properly collected and analysed by REE ICP-MS in October 2010 by Wellington Hudson (PhD, Trinity College). The results trend is likely marine limestone spectral signature with a suggested ages from Jurassic, Early to late Cretaceous.

### Samples analysed by ICP-MS in June 2018

N°	Sample Field ID	Area	X	Y	Field descriptions
1	V149	Katanda	761765	9900632	Mai ya Moto hot springs and limestones
2	V150	Katanda	761980	9900850	Tufa limestone on roadside
3	V153	Katanda	762300	9901850	?Hot springs
4	V159	X3-L688			Terrace with black shinning stuffs above Mai moto
5	V161b	X2-L690			Terrace with black shinning stuffs above Mai moto
6	V162a	X2-L690			Terrace with black shinning stuffs above Mai moto
7	V163b	X2-L690			Terrace with black shinning stuffs above Mai moto
8	V164	X2-L690			Terrace with black shinning stuffs above Mai moto
9	V338	Vitshumbi	761012	9915285	Samples collected from a cliff of 21.5m height @ 50cm interval.  BV- G 10
10	V344	Vitshumbi	761012	9915285	
11	V352	Vitshumbi	761012	9915285	
12	V356	Vitshumbi	761012	9915285	
13	V363	Vitshumbi	761012	9915285	
14	V364	Vitshumbi	761012	9915285	
15	V385	Vitshumbi	761012	9915285	
16	MDW 42	Kiturika fm			Early cretaceous Reef limestones
17	MDW 43	Kiturika fm			Early cretaceous Peloids limestones
18	MDW 74	Kiturika fm			Early cretaceous Coral
19	MDW 125	Lower Mitole			Late Jurassic Oolithic limestones
20	MDW162	Mtumbei fm			Middle Jurassic Reef limestones
21	MDW 276	Mtumbei fm			Middle Jurassic light grey bioclast and ooids lst
22	MDW 277	Mtumbei fm			Middle Jurassic light green ooids + Qtz lst.

#### **Supervisor's instructions:**

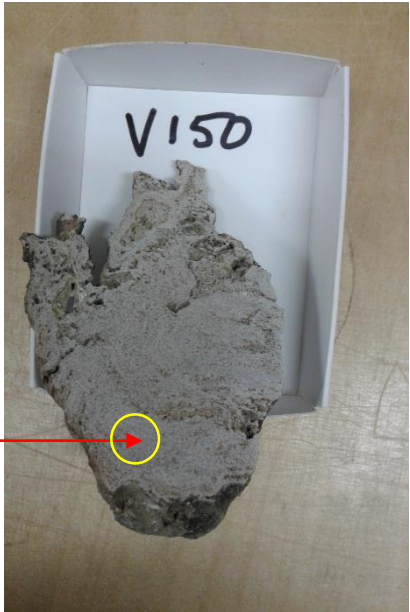
- Use petrographic observations of the above samples as background for drilling
- Drill trough the best Carbonates texture/structure/fabrics evidences in each sample
- Avoid any weathered layers, black stains, or confusing texture/structure/fabrics
- Respect the lab quality-quantity requirements for the results efficiency (see Cora)





Sample drilled accordingly to Supervisor instruction  
Powder well conserved accordingly to lab requirements

Sample drilled accordingly to Supervisor instruction  
Powder well conserved accordingly to lab requirements





Sample drilled accordingly to Supervisor instruction  
Powder well conserved accordingly to lab requirements



Sample drilled accordingly to Supervisor instruction  
Powder well conserved accordingly to lab requirements



Sample drilled accordingly to Supervisor instruction  
Powder well conserved accordingly to lab requirements

Sample drilled accordingly to Supervisor instruction  
Powder well conserved accordingly to lab requirements





Sample drilled accordingly to Supervisor instruction  
Powder well conserved accordingly to lab requirements



Sample drilled accordingly to Supervisor instruction  
Powder well conserved accordingly to lab requirements



Sample drilled accordingly to Supervisor instruction  
Powder well conserved accordingly to lab requirements



Sample drilled accordingly to Supervisor instruction  
Powder well conserved accordingly to lab requirements



Sample drilled accordingly to Supervisor instruction  
Powder well conserved accordingly to lab requirements



Sample drilled accordingly to Supervisor instruction  
Powder well conserved accordingly to lab requirements



Sample drilled accordingly to Supervisor instruction  
Powder well conserved accordingly to lab requirements



Sample drilled accordingly to Supervisor instruction  
Powder well conserved accordingly to lab requirements



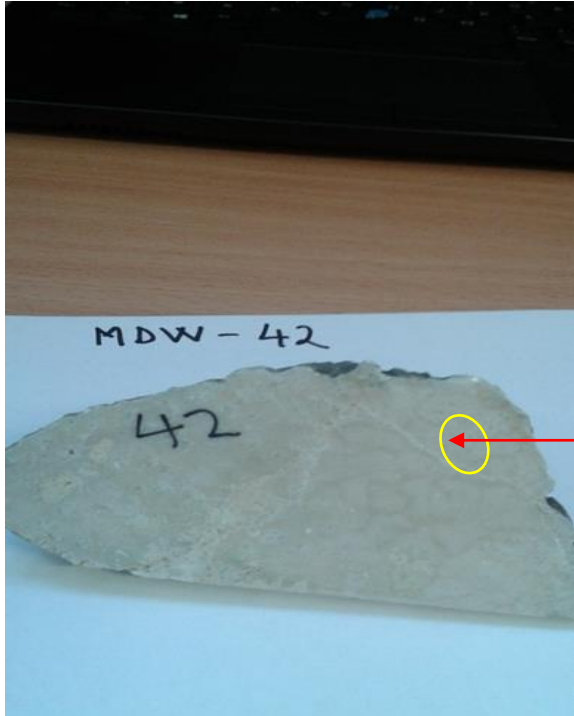


Sample drilled accordingly to Supervisor instruction  
Powder well conserved accordingly to lab requirements



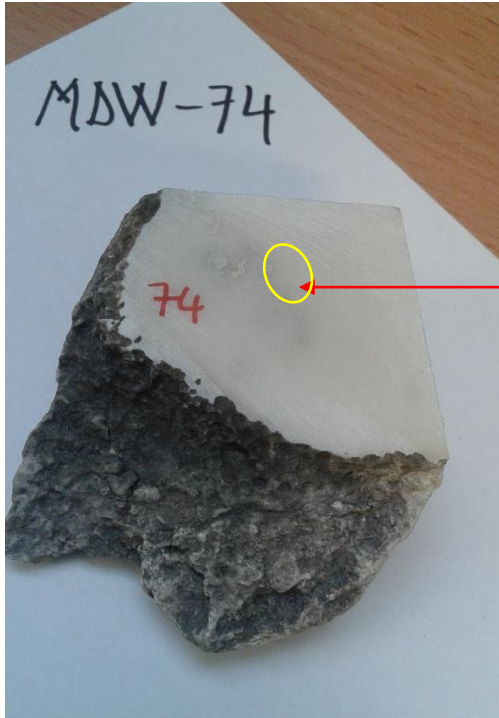
Sample drilled accordingly to Supervisor instruction  
Powder well conserved accordingly to lab requirements





Sample drilled accordingly to Supervisor instruction  
Powder well conserved accordingly to lab requirements

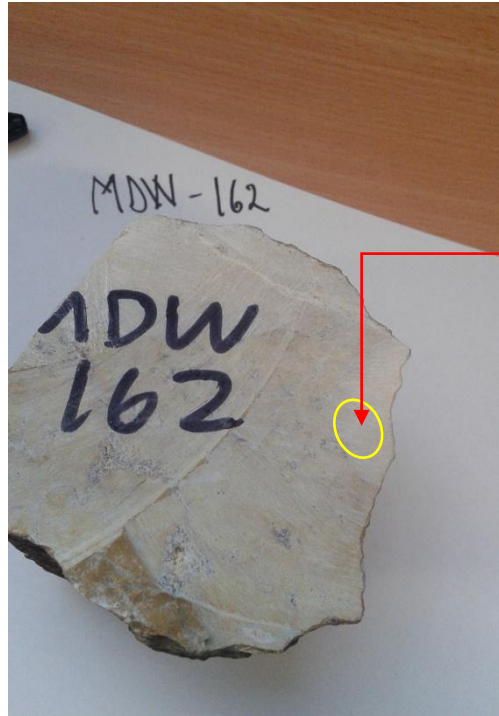




Sample drilled accordingly to Supervisor instruction  
Powder well conserved accordingly to lab requirements



Sample drilled accordingly to Supervisor instruction  
Powder well conserved accordingly to lab requirements



Sample drilled accordingly to Supervisor instruction  
Powder well conserved accordingly to lab requirements



Sample drilled accordingly to Supervisor instruction  
Powder well conserved accordingly to lab requirements



Sample drilled accordingly to Supervisor instruction  
Powder well conserved accordingly to lab requirements

name: Sylvain Mangoni project: batch no 2 date: 02/05/2018

Sample ID	Lab ID	Empty Tube (g)	Tube + 1.5ml 5% HNO3 (g)	Weigh Paper (mg)	Mass of sample (mg)	Mass Sample (g)	Weigh Paper (After Sample) (mg)	Tube + acid + sample (g)
SMK IS B	SMK IS B							
Procedural Blank 2	SMK Blank 2	1.0251	2.5322	46.324	8.000	0.0080	46.26	2.5318
Procedural Blank 3	SMK Blank 3	1.0198	2.5567	50.478	8.000	0.0080	50.49	2.5567
Limestone BCS 393	SMK LSTD 2	0.9961	2.4045	49.925	7.965	0.0080	50.50	2.4079
Limestone JLS-1	SMK JLS 1	1.0079	2.5288	44.903	7.902	0.0079	45.34	2.5330
Dolomite BCS 368	SMK DMR 1	0.9962	2.5163	57.321	9.798	0.0098	57.34	2.5255
MDW 74 A	SMK 021	1.0185	2.5433	50.579	6.997	0.0070	51.08	2.5452
MDW74 B	SMK 022	1.008	2.5253	51.665	7.429	0.0074	52.69	2.5262
MDW 74 C	SMK 023	1.0292	2.5404	38.847	6.282	0.0063	39.33	2.5421
MDW 125 A	SMK 024	1.0373	2.5517	39.717	9.098	0.0091	39.71	2.5596
MDW 125 B	SMK 025	1.0193	2.5344	39.827	7.581	0.0076	40.32	2.5391
MDW 276 A	SMK 026	1.0192	2.5358	56.028	7.789	0.0078	56.58	2.5391
MDW 276B	SMK 027	1.0293	2.5465	58.216	7.980	0.0080	58.22	2.5398
MDW 277	SMK 028	0.9966	2.2554	39.946	9.097	0.0091	39.98	2.5525
MDW 162 A	SMK 029	1.0221	2.5191	39.681	8.619	0.0086	40.56	2.5320
MDW 162B	SMK 030	1.0191	2.5492	39.462	11.456	0.0115	40.45	2.5227
MDW 43	SMK 031	1.0293	2.5583	43.083	9.294	0.0093	44.58	2.5532
MDW 42 A	SMK 032	1.0373	2.5532	43.323	5.994	0.0060	44.02	2.5621
BV 344	SMK 033	1.0329	2.5523	42.128	10.767	0.0108	42.33	2.5560
BV 352	SMK 034	1.0289	2.5463	41.343	8.856	0.0089	41.94	2.5622
BV 356	SMK 035	1.0219	2.5502	42.268	10.750	0.0108	42.81	2.5520
MDW 42 B	SMK 036	1.0371	2.5513	37.342	11.330	0.0113	37.48	2.5578

BV 364	SMK 037	1.0322	2.5498	46.721	7.930	0.0079	46.78	2.5593
BV 385	SMK 038	1.0223	2.5405	47.656	10.096	0.0101	47.78	2.5571
BV 149 A	SMK 039	1.0322	2.5476	54.667	7.039	0.0070	54.69	2.5493
BV 363	SMK 040	1.0247	2.5486	59.465	8.300	0.0083	59.46	2.5531
BV 149 B	SMK 041	1.0374	2.5484	59.867	9.917	0.0099	59.97	2.5566
BV 150	SMK 042	1.0322	2.5613	58.743	8.507	0.0085	58.95	2.5664
BV 153	SMK 043	1.0289	2.5416	59.601	8.706	0.0087	59.74	2.5480
BV 338	SMK 044	0.9966	2.5253	60.366	8.617	0.0086	60.45	2.5334
BV 159 A	SMK 045	1.0289	2.5544	44.259	10.479	0.0105	44.67	2.5613
BV 159 B	SMK 046	1.0373	2.5502	46.320	10.791	0.0108	46.56	2.5576
BV 161 B	SMK 047	1.0184	2.5483	57.081	11.125	0.0111	57.24	2.5560
BV 162 A	SMK 048	1.0393	2.5635	44.662	10.298	0.0103	44.69	2.5713
BV 163 A	SMK 049	1.0294	2.553	43.875	9.854	0.0099	43.96	2.5600
BV 164	SMK 050	1.0193	2.5005	45.800	8.530	0.0085	45.83	2.5069
SMK IS C	SMK IS C							

white - fill in
green - fixed calcs

## **Appendix 2 : ICP-MS Results Tables**

**2007-2010 Field works: Travertines samples results obtained by the ICP-MS 2013 Experiment**

	ppb	V2A	V2A	V2B	V19A	V19A	V19A	V19B	V19C	V19D	V20A
La		199.9501	205.2632	133.3059	99.64422	150.6873	87.41905	104.3309	94.85417	140.9222	10643.84
Ce		351.6072	359.0498	213.7606	85.02589	98.3204	97.12464	139.7895	135.5724	203.7521	15734.55
Pr		42.16585	44.80458	25.75071	10.65297	12.37874	11.72978	19.91068	19.01688	32.17197	1675.517
Nd		155.2363	158.8085	89.10466	52.20575	53.80405	52.61852	95.55807	87.56833	142.341	5253.763
Sm		29.81596	29.70705	14.73693	32.94166	39.22575	34.0704	63.1377	34.92836	55.55133	877.0401
Gd		26.00549	25.04321	10.0951	29.09465	30.37674	30.47925	41.63514	30.53021	42.92982	672.9751
Tb		3.059212	3.149175	1.344655	3.902009	4.378444	4.025846	5.552049	4.009274	5.673344	91.36803
Dy		15.24285	15.7029	7.22501	27.82158	29.61542	28.38052	33.50993	22.42983	38.7763	458.1363
Y		113.8247	121.6527	63.85561	451.7733	661.417	350.9032	446.2395	418.2968	511.6283	1800.525
Ho		3.071848	3.190915	1.549314	6.537065	6.935108	6.731718	7.620653	5.210771	8.090806	81.78915
Er		7.081965	8.585806	4.125496	17.81907	18.46056	17.84956	20.89055	15.71339	20.55745	213.8294
Tm		0.921339	1.023871	0.672814	2.484238	2.605084	2.617191	2.59899	2.326124	2.768509	31.17804
Yb		5.221316	5.784631	4.217063	14.50067	14.33109	14.83114	17.08097	14.65864	16.32676	205.0678
Lu		0.659482	0.811154	0.60934	2.206648	2.417504	2.245177	2.460903	2.165773	2.280742	29.07088
	MUQ	V2A	V2A	V2B	V19A	V19A	V19A	V19B	V19C	V19D	V20A
La	32510	0.00615	0.006314	0.0041	0.003065	0.004635	0.002689	0.003209	0.002918	0.004335	0.327402
Ce	71090	0.004946	0.005051	0.003007	0.001196	0.001383	0.001366	0.001966	0.001907	0.002866	0.221333
Pr	8460	0.004984	0.005296	0.003044	0.001259	0.001463	0.001386	0.002354	0.002248	0.003803	0.198052
Nd	32910	0.004717	0.004826	0.002708	0.001586	0.001635	0.001599	0.002904	0.002661	0.004325	0.15964
Sm	6880	0.004334	0.004318	0.002142	0.004788	0.005701	0.004952	0.009177	0.005077	0.008074	0.127477
Gd	6360	0.004089	0.003938	0.001587	0.004575	0.004776	0.004792	0.006546	0.0048	0.00675	0.105814
Tb	990	0.00309	0.003181	0.001358	0.003941	0.004423	0.004067	0.005608	0.00405	0.005731	0.092291
Dy	5890	0.002588	0.002666	0.001227	0.004724	0.005028	0.004818	0.005689	0.003808	0.006583	0.077782
Y	31850	0.003574	0.00382	0.002005	0.014184	0.020767	0.011017	0.014011	0.013133	0.016064	0.056531
Ho	1220	0.002518	0.002616	0.00127	0.005358	0.005685	0.005518	0.006246	0.004271	0.006632	0.06704
Er	3370	0.002101	0.002548	0.001224	0.005288	0.005478	0.005297	0.006199	0.004663	0.0061	0.063451
Tm	510	0.001807	0.002008	0.001319	0.004871	0.005108	0.005132	0.005096	0.004561	0.005428	0.061133
Yb	3250	0.001607	0.00178	0.001298	0.004462	0.00441	0.004563	0.005256	0.00451	0.005024	0.063098
Lu	490	0.001346	0.001655	0.001244	0.004503	0.004934	0.004582	0.005022	0.00442	0.004655	0.059328
	ppb	V20B	V21A	V21A	V21B	V22A	V22B	V22C	V22D	V22E	V22F
La		14185.2	712.273	699.6443	396.6492	4099.455	1103.198	413.8515	1032.56	168.8862	129.0359



Ce		25421.05	1697.035	1662.928	943.8481	9519.382	3594.647	1556.216	3236.047	683.2962	568.8726
Pr		2560.361	193.0548	192.7117	107.0222	823.4895	225.394	84.34469	206.4269	35.20515	22.51037
Nd		8709.86	823.9725	813.4504	443.7006	2895.007	818.3797	328.3413	770.2204	138.3396	88.32151
Sm		1563.174	265.064	269.6611	148.8356	486.4496	158.6087	91.95915	153.2306	40.8409	32.17411
Gd		1214.438	511.5588	513.6503	278.7251	340.3917	91.77841	59.63234	83.45047	29.50919	31.0496
Tb		160.4293	88.0588	88.5061	47.29053	44.347	11.83335	6.443131	10.0314	3.983675	4.198801
Dy		780.1142	522.939	505.2738	277.248	221.8342	59.43712	30.4639	46.51887	19.21987	21.8377
Y		2989.628	3569.666	3582.377	1957.937	1210.054	520.5079	334.7962	517.6278	307.1092	341.4442
Ho		135.0681	104.1986	102.5893	55.70823	40.97336	11.50446	6.133336	9.223445	3.470626	4.335542
Er		334.9313	266.763	266.6615	142.28	101.5155	29.76953	16.7924	25.47915	9.573451	11.35229
Tm		48.26288	34.79452	35.95574	18.85502	14.29745	4.259307	2.660388	3.855092	1.286439	1.553524
Yb		301.6627	201.8633	202.5283	109.5866	85.02826	25.28603	18.4739	24.55243	8.50056	9.299934
Lu		43.32317	28.23824	28.94557	15.47436	12.08704	3.688308	2.917776	3.588966	1.282174	1.204398
	<b>MUQ</b>	<b>V20B</b>	<b>V21A</b>	<b>V21A</b>	<b>V21B</b>	<b>V22A</b>	<b>V22B</b>	<b>V22C</b>	<b>V22D</b>	<b>V22E</b>	<b>V22F</b>
La	32510	0.436333	0.021909	0.021521	0.012201	0.126098	0.033934	0.01273	0.031761	0.005195	0.003969
Ce	71090	0.35759	0.023872	0.023392	0.013277	0.133906	0.050565	0.021891	0.04552	0.009612	0.008002
Pr	8460	0.302643	0.02282	0.022779	0.01265	0.097339	0.026642	0.00997	0.0244	0.004161	0.002661
Nd	32910	0.264657	0.025037	0.024717	0.013482	0.087967	0.024867	0.009977	0.023404	0.004204	0.002684
Sm	6880	0.227205	0.038527	0.039195	0.021633	0.070705	0.023054	0.013366	0.022272	0.005936	0.004676
Gd	6360	0.190949	0.080434	0.080763	0.043825	0.053521	0.014431	0.009376	0.013121	0.00464	0.004882
Tb	990	0.16205	0.088948	0.0894	0.047768	0.044795	0.011953	0.006508	0.010133	0.004024	0.004241
Dy	5890	0.132447	0.088784	0.085785	0.047071	0.037663	0.010091	0.005172	0.007898	0.003263	0.003708
Y	31850	0.093866	0.112077	0.112477	0.061474	0.037992	0.016342	0.010512	0.016252	0.009642	0.01072
Ho	1220	0.110712	0.085409	0.08409	0.045662	0.033585	0.00943	0.005027	0.00756	0.002845	0.003554
Er	3370	0.099386	0.079158	0.079128	0.04222	0.030123	0.008834	0.004983	0.007561	0.002841	0.003369
Tm	510	0.094633	0.068225	0.070501	0.036971	0.028034	0.008352	0.005216	0.007559	0.002522	0.003046
Yb	3250	0.092819	0.062112	0.062316	0.033719	0.026163	0.00778	0.005684	0.007555	0.002616	0.002862
Lu	490	0.088415	0.057629	0.059073	0.03158	0.024667	0.007527	0.005955	0.007324	0.002617	0.002458
	<b>ppb</b>	<b>V22G</b>	<b>V22H</b>	<b>P12A</b>	<b>P12B</b>	<b>LE24A</b>	<b>LE24B</b>	<b>LE24C</b>	<b>LE24D</b>	<b>LE26A</b>	<b>LE26B</b>
La		117.392	216.0105	2167.09	2029.377	1042.287	438.514	269.4935	132.1388	97.88369	214.6054
Ce		481.5143	1175.271	3594.861	2644.704	297.3215	133.553	247.648	135.4144	50.82687	91.50231
Pr		19.31949	35.30733	496.8179	452.8864	89.48443	28.92648	28.545	15.75259	15.18296	30.06095

Nd		84.38802	130.6892	2013.917	1745.219	396.381	133.9366	111.5104	59.06835	60.40458	123.4174
Sm		30.85784	48.59279	384.3884	327.2836	72.60106	25.20869	23.58911	11.15856	14.20824	25.88511
Gd		24.71482	48.89867	437.8467	351.444	147.897	80.00905	47.03425	19.8956	16.61448	36.25812
Tb		2.804386	7.276705	70.13979	54.73034	20.41159	11.72009	6.938539	3.16882	2.429906	5.692518
Dy		13.10911	31.13047	491.0079	377.7735	141.2702	86.47117	56.14521	25.46508	19.08796	43.64721
Y		357.2993	395.9129	5728.19	4231.744	1630.249	1124.699	931.3594	509.3773	655.8235	958.3634
Ho		2.51633	5.875525	130.6869	96.66989	37.08142	23.7953	17.23531	8.269785	5.624103	11.03188
Er		6.802767	14.74952	433.4099	297.4275	111.8711	67.64439	52.77571	25.76731	17.78938	31.73575
Tm		1.064532	2.215279	64.70834	43.10357	15.11544	9.077764	7.165181	3.505534	2.482704	4.256531
Yb		6.875204	15.04475	398.1464	262.681	89.20682	53.72979	42.38417	21.25619	16.21336	25.65673
Lu		1.121446	2.518959	60.33363	39.96341	15.58615	9.103461	7.757396	3.827187	2.935213	4.650298
	<b>MUQ</b>	<b>V22G</b>	<b>V22H</b>	<b>P12A</b>	<b>P12B</b>	<b>LE24A</b>	<b>LE24B</b>	<b>LE24C</b>	<b>LE24D</b>	<b>LE26A</b>	<b>LE26B</b>
La	32510	0.003611	0.006644	0.066659	0.062423	0.032061	0.013489	0.00829	0.004065	0.003011	0.006601
Ce	71090	0.006773	0.016532	0.050568	0.037202	0.004182	0.001879	0.003484	0.001905	0.000715	0.001287
Pr	8460	0.002284	0.004173	0.058726	0.053533	0.010577	0.003419	0.003374	0.001862	0.001795	0.003553
Nd	32910	0.002564	0.003971	0.061195	0.05303	0.012044	0.00407	0.003388	0.001795	0.001835	0.00375
Sm	6880	0.004485	0.007063	0.05587	0.04757	0.010552	0.003664	0.003429	0.001622	0.002065	0.003762
Gd	6360	0.003886	0.007688	0.068844	0.055258	0.023254	0.01258	0.007395	0.003128	0.002612	0.005701
Tb	990	0.002833	0.00735	0.070848	0.055283	0.020618	0.011838	0.007009	0.003201	0.002454	0.00575
Dy	5890	0.002226	0.005285	0.083363	0.064138	0.023985	0.014681	0.009532	0.004323	0.003241	0.00741
Y	31850	0.011218	0.012431	0.179849	0.132865	0.051185	0.035312	0.029242	0.015993	0.020591	0.03009
Ho	1220	0.002063	0.004816	0.10712	0.079238	0.030395	0.019504	0.014127	0.006779	0.00461	0.009043
Er	3370	0.002019	0.004377	0.128608	0.088257	0.033196	0.020073	0.01566	0.007646	0.005279	0.009417
Tm	510	0.002087	0.004344	0.126879	0.084517	0.029638	0.0178	0.014049	0.006874	0.004868	0.008346
Yb	3250	0.002115	0.004629	0.122507	0.080825	0.027448	0.016532	0.013041	0.00654	0.004989	0.007894
Lu	490	0.002289	0.005141	0.12313	0.081558	0.031808	0.018578	0.015831	0.007811	0.00599	0.00949
	<b>ppb</b>	<b>LE27A</b>	<b>LE27B</b>	<b>LE28A</b>	<b>LE28B</b>	<b>LE28C</b>	<b>LE28D</b>	<b>LE32A</b>	<b>LE32B</b>	<b>LE32C</b>	<b>LE32D</b>
La		6351.464	23835.61	82.24817	278.0228	50.74439	93.9399	6076.536	16809.3	5356.619	4441.579
Ce		5515.583	33287.38	35.14719	163.9083	62.55929	76.37994	14865.53	*	12816.63	11499.91
Pr		959.4462	3984.488	12.91078	46.34273	9.013477	16.35604	1458.818	3916.117	1480.873	1246.02
Nd		3437.245	13779.03	52.8306	164.4387	33.55761	58.98192	5865.9	14755.89	6259.755	5228.115
Sm		550.7019	2144.552	9.50594	29.26509	6.796352	11.91887	1700.787	3357.133	1811.707	1559.607

Gd		553.9223	1866.873	13.00591	29.6337	8.033465	15.61177	2815.659	3943.266	2831.572	2510.649
Tb		81.28811	264.5246	2.297671	4.885708	1.514085	2.603287	483.2861	601.5753	480.2789	430.5847
Dy		518.4445	1520.685	16.72013	32.05666	11.46062	18.48793	3173.966	3638.042	3117.662	2915.834
Y		4807.563	11737.04	304.8989	442.5796	371.1597	389.9112	30448.35	*	31452.73	30093.95
Ho		120.7872	333.4857	5.229524	8.987425	3.883309	5.335123	759.1098	854.4365	755.3507	711.6104
Er		347.1573	916.7331	17.22676	27.36456	14.71579	17.62931	2259.765	2555.082	2307.188	2189.441
Tm		49.83461	127.1526	2.544856	4.320554	2.464802	2.820819	328.8425	376.7705	347.4808	330.813
Yb		301.5185	765.2787	16.27476	25.34957	15.45057	19.04999	2082.714	2382.461	2190.511	2116.251
Lu		43.82354	112.9508	2.379555	4.094086	2.542166	2.836512	357.3331	422.9293	395.1442	376.1889
	<b>MUQ</b>	<b>LE27A</b>	<b>LE27B</b>	<b>LE28A</b>	<b>LE28B</b>	<b>LE28C</b>	<b>LE28D</b>	<b>LE32A</b>	<b>LE32B</b>	<b>LE32C</b>	<b>LE32D</b>
La	32510	0.19537	0.733178	0.00253	0.008552	0.001561	0.00289	0.186913	0.51705	0.164768	0.136622
Ce	71090	0.077586	0.468243	0.000494	0.002306	0.00088	0.001074	0.209109	*	0.180287	0.161765
Pr	8460	0.11341	0.47098	0.001526	0.005478	0.001065	0.001933	0.172437	0.462898	0.175044	0.147284
Nd	32910	0.104444	0.418688	0.001605	0.004997	0.00102	0.001792	0.178241	0.448371	0.190208	0.158861
Sm	6880	0.080044	0.311708	0.001382	0.004254	0.000988	0.001732	0.247207	0.487955	0.26333	0.226687
Gd	6360	0.087095	0.293534	0.002045	0.004659	0.001263	0.002455	0.442714	0.62001	0.445216	0.394756
Tb	990	0.082109	0.267197	0.002321	0.004935	0.001529	0.00263	0.488168	0.607652	0.48513	0.434934
Dy	5890	0.088021	0.258181	0.002839	0.005443	0.001946	0.003139	0.538874	0.617664	0.529314	0.495048
Y	31850	0.150944	0.36851	0.009573	0.013896	0.011653	0.012242	0.955992	*	0.987527	0.944865
Ho	1220	0.099006	0.273349	0.004286	0.007367	0.003183	0.004373	0.622221	0.700358	0.61914	0.583287
Er	3370	0.103014	0.272028	0.005112	0.00812	0.004367	0.005231	0.670553	0.758185	0.684625	0.649686
Tm	510	0.097715	0.249319	0.00499	0.008472	0.004833	0.005531	0.644789	0.738766	0.681335	0.648653
Yb	3250	0.092775	0.23547	0.005008	0.0078	0.004754	0.005862	0.640835	0.733065	0.674003	0.651154
Lu	490	0.089436	0.230512	0.004856	0.008355	0.005188	0.005789	0.729251	0.863121	0.806417	0.767733
	<b>ppb</b>	<b>LE32E</b>	<b>LE32F</b>	<b>LE37A</b>	<b>LE37B</b>	<b>LE38A</b>	<b>LE38B</b>	<b>LE41A</b>	<b>LE41B</b>	<b>LE42A</b>	<b>LE42B</b>
La		6116.652	6435.41	18636.77	41607.05	43548.97	97236.54	958.4531	1844.765	977.815	1140.12
Ce		17950.37	16338.17	32971.29	70077.88	*	168041.9	1737.101	3351.368	1631.759	1973.748
Pr		1632.923	1670.609	3322.877	5974.386	7619.252	8846.702	164.0832	329.9259	178.9129	211.0226
Nd		6631.197	6690.313	10871.24	19410.58	24929.53	28614.15	553.4254	1105.671	601.1938	694.2109
Sm		1652.766	1698.691	1408.216	2481.606	3189.255	3665.443	81.88093	157.1	83.89447	98.0512
Gd		2117.884	2494.841	856.6686	1477.174	1949.033	2144.948	54.80583	106.7644	55.34537	64.80149
Tb		337.5046	417.9429	101.8886	171.8369	232.1214	249.8993	7.672973	13.80094	6.893728	8.039725

Dy		2041.187	2722.071	459.1262	754.3759	1043.1	1084.319	35.70604	65.4915	30.40134	36.82773
Y		16925.44	26798.08	2081.298	3162.46	4692.575	4443.927	240.6644	359.1923	206.0185	206.8756
Ho		458.8679	657.5855	77.25407	121.4204	174.2283	174.4784	6.601662	11.84898	5.629232	6.423365
Er		1292.607	1979.867	177.0549	275.3026	394.4399	389.9945	16.80468	30.69669	14.77757	15.91692
Tm		181.9866	293.254	22.50851	35.03818	51.77739	49.59052	2.575572	4.47076	2.344939	2.377014
Yb		1119.075	1837.957	131.4095	194.3761	297.2072	270.9112	14.6663	25.69766	12.77215	14.77464
Lu		192.0323	323.7433	18.1881	26.34753	40.37461	36.49252	2.219722	3.899193	2.042076	2.111293
	<b>MUQ</b>	<b>LE32E</b>	<b>LE32F</b>	<b>LE37A</b>	<b>LE37B</b>	<b>LE38A</b>	<b>LE38B</b>	<b>LE41A</b>	<b>LE41B</b>	<b>LE42A</b>	<b>LE42B</b>
La	32510	0.188147	0.197952	0.573263	1.279823	1.339556	2.990973	0.029482	0.056745	0.030077	0.03507
Ce	71090	0.252502	0.229824	0.463797	0.985763	*	2.363791	0.024435	0.047143	0.022953	0.027764
Pr	8460	0.193017	0.197471	0.392775	0.706192	0.900621	1.045709	0.019395	0.038998	0.021148	0.024944
Nd	32910	0.201495	0.203291	0.330332	0.589808	0.757506	0.869467	0.016816	0.033597	0.018268	0.021094
Sm	6880	0.240228	0.246903	0.204683	0.360699	0.463555	0.532768	0.011901	0.022834	0.012194	0.014252
Gd	6360	0.333001	0.392271	0.134696	0.23226	0.306452	0.337256	0.008617	0.016787	0.008702	0.010189
Tb	990	0.340914	0.422165	0.102918	0.173573	0.234466	0.252424	0.00775	0.01394	0.006963	0.008121
Dy	5890	0.346551	0.462151	0.07795	0.128077	0.177097	0.184095	0.006062	0.011119	0.005162	0.006253
Y	31850	0.531411	0.841384	0.065347	0.099292	0.147334	0.139527	0.007556	0.011278	0.006468	0.006495
Ho	1220	0.376121	0.539005	0.063323	0.099525	0.14281	0.143015	0.005411	0.009712	0.004614	0.005265
Er	3370	0.383563	0.587498	0.052539	0.081692	0.117044	0.115725	0.004987	0.009109	0.004385	0.004723
Tm	510	0.356836	0.575008	0.044134	0.068702	0.101524	0.097236	0.00505	0.008766	0.004598	0.004661
Yb	3250	0.344331	0.565525	0.040434	0.059808	0.091448	0.083357	0.004513	0.007907	0.00393	0.004546
Lu	490	0.391903	0.660701	0.037119	0.05377	0.082397	0.074475	0.00453	0.007958	0.004168	0.004309
	<b>ppb</b>	<b>LE42C</b>	<b>LE42D</b>	<b>LE42E</b>	<b>LE42F</b>	<b>LE42G</b>	<b>LE42H</b>	<b>LE42I</b>	<b>LE42J</b>	<b>LE44A</b>	<b>LE44B</b>
La		155.3588	211.6713	824.4166	892.7311	148.3533	201.4321	63.55093	49.45939	76.7662	52.8725
Ce		294.2449	367.9756	1455.84	1691.191	280.4893	377.8635	105.3039	83.40076	125.5427	102.4533
Pr		26.61657	37.63918	141.9585	166.4948	25.96657	35.1339	11.6424	9.41596	14.96193	10.31803
Nd		91.9328	123.7713	477.997	560.8917	85.85461	119.9662	40.23213	32.65993	48.96881	32.51104
Sm		14.37981	18.89813	72.10125	87.03561	15.50659	17.14074	7.157597	7.750896	8.509481	5.404087
Gd		8.780098	12.1206	52.5059	60.7801	8.80177	11.74228	4.596066	4.094044	5.856876	3.361825
Tb		1.160466	1.673868	6.876559	8.395098	1.072411	1.402627	0.68622	0.584265	0.748726	0.435928
Dy		5.966414	7.062149	35.8762	42.08304	5.357945	7.401093	3.271195	3.536209	3.599987	2.272966
Y		50.21269	62.89558	261.61	286.5142	54.28185	63.29994	36.89933	42.36883	32.6667	21.81886

Ho		1.196406	1.483016	7.275962	8.511413	1.073568	1.635458	0.82517	0.691325	0.926362	0.610373
Er		3.195134	3.618218	19.8824	22.86938	2.898702	3.949154	2.142766	1.841253	1.991589	1.800528
Tm		0.454106	0.489135	3.126772	3.294261	0.417021	0.581886	0.304877	0.202453	0.359437	0.252643
Yb		3.099815	3.082795	19.95993	21.33987	2.739724	3.559133	1.694092	1.307025	1.723429	1.397868
Lu		0.38724	0.438274	2.985499	3.09818	0.431301	0.543984	0.272908	0.272908	0.318625	0.20023
	<b>MUQ</b>	<b>LE42C</b>	<b>LE42D</b>	<b>LE42E</b>	<b>LE42F</b>	<b>LE42G</b>	<b>LE42H</b>	<b>LE42I</b>	<b>LE42J</b>	<b>LE44A</b>	<b>LE44B</b>
La	32510	0.004779	0.006511	0.025359	0.02746	0.004563	0.006196	0.001955	0.001521	0.002361	0.001626
Ce	71090	0.004139	0.005176	0.020479	0.023789	0.003946	0.005315	0.001481	0.001173	0.001766	0.001441
Pr	8460	0.003146	0.004449	0.01678	0.01968	0.003069	0.004153	0.001376	0.001113	0.001769	0.00122
Nd	32910	0.002793	0.003761	0.014524	0.017043	0.002609	0.003645	0.001222	0.000992	0.001488	0.000988
Sm	6880	0.00209	0.002747	0.01048	0.012651	0.002254	0.002491	0.00104	0.001127	0.001237	0.000785
Gd	6360	0.001381	0.001906	0.008256	0.009557	0.001384	0.001846	0.000723	0.000644	0.000921	0.000529
Tb	990	0.001172	0.001691	0.006946	0.00848	0.001083	0.001417	0.000693	0.00059	0.000756	0.00044
Dy	5890	0.001013	0.001199	0.006091	0.007145	0.00091	0.001257	0.000555	0.0006	0.000611	0.000386
Y	31850	0.001577	0.001975	0.008214	0.008996	0.001704	0.001987	0.001159	0.00133	0.001026	0.000685
Ho	1220	0.000981	0.001216	0.005964	0.006977	0.00088	0.001341	0.000676	0.000567	0.000759	0.0005
Er	3370	0.000948	0.001074	0.0059	0.006786	0.00086	0.001172	0.000636	0.000546	0.000591	0.000534
Tm	510	0.00089	0.000959	0.006131	0.006459	0.000818	0.001141	0.000598	0.000397	0.000705	0.000495
Yb	3250	0.000954	0.000949	0.006142	0.006566	0.000843	0.001095	0.000521	0.000402	0.00053	0.00043
Lu	490	0.00079	0.000894	0.006093	0.006323	0.00088	0.00111	0.000557	0.000557	0.00065	0.000409
	<b>ppb</b>	<b>SEMPA</b>	<b>SEMP B</b>	<b>SEMP C</b>	<b>SEMP D</b>	<b>FP #1</b>	<b>FP #2</b>	<b>FP #3</b>	<b>ppb</b>	<b>Neo. Stroms</b>	<b>Cenom Lst</b>
La		139.6259	287.3266	152.7857	312.8726	454500	318500	398000		5970	6490
Ce		308.4762	671.3686	364.3443	821.7321	896500	606100	690000		8540	6970
Pr		31.8839	67.03131	37.07521	107.5204			69000		1060	970
Nd		126.5569	267.1093	147.8366	472.6629	354000	257600	245000		3530	3990
Sm		28.96897	61.23731	34.61996	105.3005	46000	33500	32000		550	790
Gd		31.68512	65.55687	36.86235	101.8932	30200	22000	24000		470	830
Tb		5.150497	11.13068	6.382101	15.17451					60	120
Dy		32.26325	69.27499	37.28253	85.38841			10300		330	750
Y		1244.018	872.1245	674.6628	859.0509	53000	38000	36000		1770	
Ho		7.467053	16.01281	8.722975	17.14336			1630		70	200
Er		23.71041	47.51117	26.39717	47.27499			4320		180	540

Tm		3.407051	7.532899	3.98353	7.23992	610	450	500		30	90
Yb		23.74783	47.84925	27.28967	45.22595	3760	2720	2640		140	480
Lu		3.573556	7.524985	4.101395	6.851154	510	370	350		20	80
	<b>MUQ</b>	<b>SEMPA</b>	<b>SEMP B</b>	<b>SEMP C</b>	<b>SEMP D</b>	<b>FP #1</b>	<b>FP #2</b>	<b>FP #3</b>	<b>MUQ</b>	<b>Neo. Stroms</b>	<b>Cenom. Lst</b>
La	32510	0.004295	0.008838	0.0047	0.009624	13.980314	9.79699	12.2424		0.183635804	0.199631
Ce	71090	0.004339	0.009444	0.005125	0.011559	12.610775	8.52581	9.70601		0.120129413	0.098045
Pr	8460	0.003769	0.007923	0.004382	0.012709			8.15603		0.125295508	0.114657
Nd	32910	0.003846	0.008116	0.004492	0.014362	10.756609	7.82741	7.44455		0.10726223	0.12124
Sm	6880	0.004211	0.008901	0.005032	0.015305	6.6860465	4.86919	4.65116		0.07994186	0.114826
Gd	6360	0.004982	0.010308	0.005796	0.016021	4.7484277	3.45912	3.77358		0.073899371	0.130503
Tb	990	0.005203	0.011243	0.006447	0.015328	3.5151515	2.43434	2.49495		0.060606061	0.121212
Dy	5890	0.005478	0.011761	0.00633	0.014497			1.74873		0.056027165	0.127334
Y	31850	0.039059	0.027382	0.021183	0.026972	1.6640502	1.19309	1.1303		0.055572998	
Ho	1220	0.006121	0.013125	0.00715	0.014052			1.33607		0.057377049	0.163934
Er	3370	0.007036	0.014098	0.007833	0.014028			1.2819		0.053412463	0.160237
Tm	510	0.00668	0.01477	0.007811	0.014196	1.1960784	0.88235	0.98039		0.058823529	0.176471
Yb	3250	0.007307	0.014723	0.008397	0.013916	1.1569231	0.83692	0.81231		0.043076923	0.147692
Lu	490	0.007293	0.015357	0.00837	0.013982	1.0408163	0.7551	0.71429		0.040816327	0.163265
		<b>ppb</b>	<b>V2b/2</b>	<b>V22a/2</b>	<b>LE44a/2</b>	<b>LE44b/2</b>	<b>LE41a/2</b>	<b>LE41b/2</b>	<b>P12b/2</b>	<b>LE24a/2</b>	<b>LE24b/2</b>
La			195.7	2614	396.8	131.7	2857	3047	2328	1693	610.7
Ce			308	7183	572.1	229.9	5201	5323	2363	618	204.9
Pr			36.46	521.7	96.48	28.25	518.2	543.4	530.7	136.5	40.35
Nd			131.7	1850	380	96.65	1760	1804	2166	637.7	191.3
Sm			21.37	315.6	89.03	15.09	249.8	265.2	418.7	114.2	35.44
Eu			2.982	40.39	19.29	3.669	65.21	64.52	103.5	37.59	13.74
Tb			2.356	29.64	22.11	1.438	21.98	22	75.95	34.25	16.28
Gd			16.96	222.5	124.2	12.37	180.7	181.3	489.8	248.3	114.2
Dy			12.24	155.4	147.7	7.493	108	103.9	534.4	240.6	124.5
Y			113.072	1276.754	1580.262	51.28363	679.6646	593.6026	6288.787	2698.247	1656.768
Ho			2.241	30.88	36.01	1.637	19.19	19.77	138.7	64.04	33.71
Er			6.16	78.01	115.2	3.855	48.82	49.24	431.4	183.1	100.9
Tm			0.856	11.38	17.21	0.418	6.853	7.003	63.23	25.5	13.14

Yb		5.392	73.72	115	2.566	39.96	38.22	377.6	147.3	76.4
Lu		0.862	9.968	20.54	0.444	5.969	6.079	57.73	26.47	13.34
	<b>MuQ</b>	<b>V2b/2</b>	<b>V22a/2</b>	<b>LE44a/2</b>	<b>LE44b/2</b>	<b>LE41a/2</b>	<b>LE41b/2</b>	<b>P12b/2</b>	<b>LE24a/2</b>	<b>LE24b/2</b>
La	32510	0.00602	0.08041	0.01221	0.00405	0.08788	0.09373	0.07161	0.05208	0.01878
Ce	71090	0.00433	0.10104	0.00805	0.00323	0.07316	0.07488	0.03324	0.00869	0.00288
Pr	8460	0.00431	0.06167	0.01140	0.00334	0.06125	0.06423	0.06273	0.01613	0.00477
Nd	32910	0.00400	0.05621	0.01155	0.00294	0.05348	0.05482	0.06582	0.01938	0.00581
Sm	6880	0.00311	0.04587	0.01294	0.00219	0.03631	0.03855	0.06086	0.01660	0.00515
Eu	1570	0.00190	0.02573	0.01229	0.00234	0.04154	0.04110	0.06592	0.02394	0.00875
Gd	6360	0.00267	0.03498	0.01953	0.00194	0.02841	0.02851	0.07701	0.03904	0.01796
Tb	990	0.00238	0.02994	0.02233	0.00145	0.02220	0.02222	0.07672	0.03460	0.01644
Dy	5890	0.00208	0.02638	0.02508	0.00127	0.01834	0.01764	0.09073	0.04085	0.02114
Y	31850	0.00355	0.04009	0.04961	0.00161	0.02134	0.01864	0.19746	0.08471	0.05203
Ho	1220	0.00184	0.02531	0.02952	0.00134	0.01573	0.01620	0.11369	0.05249	0.02763
Er	3370	0.00183	0.02315	0.03418	0.00114	0.01449	0.01461	0.12801	0.05433	0.02994
Tm	510	0.00168	0.02231	0.03375	0.00082	0.01344	0.01373	0.12398	0.05000	0.02576
Yb	3250	0.00166	0.02268	0.03538	0.00079	0.01230	0.01176	0.11618	0.04532	0.02351
Lu	490	0.00176	0.02034	0.04192	0.00091	0.01218	0.01241	0.11782	0.05402	0.02722

**2007-2010 Field works: Travertines samples results by ICP-MS 2016 Experiment (Results Reproducibility of the Method )**

	<b>ppb</b>	<b>LE26a/2</b>	<b>LE26b/2</b>	<b>LE28a/2</b>	<b>LE28d/2</b>	<b>V19a/2</b>	<b>PCK a/1</b>	<b>PCK b/1</b>	<b>PCK c/1</b>	<b>PCK d/1</b>
La		169.9	599.5	94.32	192.3	270.6	2745	2801	3478	3227
Ce		163.6	158.1	47.02	96.08	326.1	4849	4993	6225	5732
Pr		29.74	83.63	15.04	28.45	41.71	546.9	568.3	721.9	656.1
Nd		118.4	330.3	61.33	120.9	172.4	1892	1990	2540	2270
Sm		23.47	63.89	12.6	22.39	82.98	305.1	338.3	441.8	387
Eu		5.985	21.61	4.409	5.613	4.781	56.98	62.49	84.02	72.79
Tb		4.07	12.73	3.188	5.439	9.298	36.26	40.18	54.93	47.02
Gd		29.71	87.75	18.28	31.08	72.98	249	279.5	381	321
Dy		26.82	82.03	22.72	40.92	58.02	193.1	219.7	301.2	251.5
Y		922.4897	1342.21	465.0734	740.3612	867.3339	1098.509	1228.574	1641.364	1382.347
Ho		7.575	19.24	7.071	11.79	13.14	37.5	43.07	58.2	48.62
Er		25.79	55.3	23.02	39.15	35.35	94.1	107.7	144.9	122.8
Tm		3.378	7.184	3.468	5.785	4.96	13.14	14.93	19	15.78
Yb		20.2	39.48	23.9	36.51	29.17	76.22	87.97	106.3	90.89
Lu		3.711	7.321	3.693	5.822	4.261	10.53	12.36	14.89	12.81
	<b>MuQ</b>	<b>LE26a/2</b>	<b>LE26b/2</b>	<b>LE28a/2</b>	<b>LE28d/2</b>	<b>V19a/2</b>	<b>PCK a/1</b>	<b>PCK b/1</b>	<b>PCK c/1</b>	<b>PCK d/1</b>
La	32510	0.00523	0.01844	0.00290	0.00592	0.00832	0.08444	0.08616	0.10698	0.09926
Ce	71090	0.00230	0.00222	0.00066	0.00135	0.00459	0.06821	0.07023	0.08757	0.08063
Pr	8460	0.00352	0.00989	0.00178	0.00336	0.00493	0.06465	0.06717	0.08533	0.07755
Nd	32910	0.00360	0.01004	0.00186	0.00367	0.00524	0.05749	0.06047	0.07718	0.06898
Sm	6880	0.00341	0.00929	0.00183	0.00325	0.01206	0.04435	0.04917	0.06422	0.05625
Eu	1570	0.00381	0.01376	0.00281	0.00358	0.00305	0.03629	0.03980	0.05352	0.04636
Gd	6360	0.00467	0.01380	0.00287	0.00489	0.01147	0.03915	0.04395	0.05991	0.05047
Tb	990	0.00411	0.01286	0.00322	0.00549	0.00939	0.03663	0.04059	0.05548	0.04749
Dy	5890	0.00455	0.01393	0.00386	0.00695	0.00985	0.03278	0.03730	0.05114	0.04270
Y	31850	0.02896	0.04214	0.01460	0.02325	0.02723	0.03451	0.03859	0.05152	0.04339



Ho	1220	0.00621	0.01577	0.00580	0.00966	0.01077	0.03074	0.03530	0.04770	0.03985
Er	3370	0.00765	0.01641	0.00683	0.01162	0.01049	0.02792	0.03196	0.04300	0.03644
Tm	510	0.00662	0.01409	0.00680	0.01134	0.00973	0.02576	0.02927	0.03725	0.03094
Yb	3250	0.00622	0.01215	0.00735	0.01123	0.00898	0.02345	0.02707	0.03271	0.02797
Lu	490	0.00757	0.01494	0.00754	0.01188	0.00870	0.02149	0.02522	0.03039	0.02614

**2014 Field works: Travertines samples results obtained by the 2018 ICP-MS Experiment**

	ppb	MDW 74 A	MDW74 B	MDW 74 C	MDW 125 A	MDW 125 B	MDW 276 A	MDW 276B	MDW 277	MDW 162 A	MDW 162B
La		734	888	936	32550	34340	6337	7255	13860	312	90
Ce		1092	1215	1276	60180	55470	10820	12690	26810	474	120
Pr		123	137	146	7188	7602	1424	1699	3553	59	15
Nd		453	505	527	28940	30510	5670	6855	14070	232	61
Sm		82	90	91	6028	6318	1162	1392	2844	45	10
Eu		22	24	26	1306	1393	289	334	657	10	2
Tb		13	13	14	901	958	199	218	380	8	2
Gd		83	90	93	6060	6448	1321	1455	2587	50	14
Dy		75	85	86	5104	5484	1248	1270	2076	49	14
Y		614	681	691	36080	38140	12350	10400	11980	556	233
Ho		16	18	18	1040	1109	274	267	403	11	4
Er		46	50	50	2620	2801	742	698	1009	36	13
Tm		6	7	7	344	368	102	93	137	5	2
Yb		37	42	41	1917	2082	578	534	794	33	12
Lu		5	6	6	259	282	83	75	111	5	2

	<b>MUQ</b>	<b>MDW 74 A</b>	<b>MDW74 B</b>	<b>MDW 74 C</b>	<b>MDW 125 A</b>	<b>MDW 125 B</b>	<b>MDW 276 A</b>	<b>MDW 276B</b>	<b>MDW 277</b>	<b>MDW 162 A</b>	<b>MDW 162B</b>
La	32510	0.0225623	0.0273024	0.0288	1.00123039	1.05629037	0.19492464	0.2231621	0.42633	0.00958167	0.002767
Ce	71090	0.0153608	0.017091	0.017949	0.84653256	0.78027852	0.15220143	0.17850612	0.377128	0.00667042	0.001691
Pr	8460	0.0145508	0.0162293	0.017305	0.84964539	0.89858156	0.16832151	0.20082742	0.419976	0.006974	0.001717
Nd	32910	0.013777	0.0153388	0.016022	0.87936797	0.92707384	0.17228806	0.20829535	0.42753	0.00704345	0.001845
Sm	6880	0.0118663	0.0130538	0.013266	0.87616279	0.91831395	0.16889535	0.20232558	0.413372	0.00655959	0.001516
Eu	1570	0.0140573	0.0151338	0.016268	0.83184713	0.88726115	0.18401274	0.21261146	0.418535	0.00630828	0.001355
Gd	6360	0.0130818	0.0141887	0.014557	0.95283019	1.01383648	0.2077044	0.22877358	0.406761	0.00790252	0.002263
Tb	990	0.0128283	0.0135354	0.014212	0.90989899	0.96717172	0.20131313	0.22020202	0.383939	0.00777071	0.002056
Dy	5890	0.0126689	0.0143905	0.014608	0.86655348	0.93106961	0.21188455	0.21561969	0.352462	0.00824448	0.002419
Y	31850	0.0192873	0.0213721	0.021705	1.13281005	1.19748823	0.3877551	0.32653061	0.376138	0.01745369	0.007316
Ho	1220	0.0131721	0.015082	0.015016	0.85245902	0.90901639	0.22467213	0.21860656	0.330492	0.00940164	0.003029
Er	3370	0.0136172	0.0146884	0.014777	0.77744807	0.83115727	0.22008902	0.20718101	0.299407	0.01081009	0.003772
Tm	510	0.0120765	0.0129824	0.013465	0.67352941	0.72215686	0.19921569	0.18245098	0.268824	0.01007059	0.003857
Yb	3250	0.0113138	0.0130031	0.012529	0.58984615	0.64061538	0.17775385	0.16415385	0.244215	0.01024308	0.0038
Lu	490	0.011098	0.0113878	0.012539	0.52918367	0.57571429	0.1695102	0.15361224	0.226735	0.0108898	0.004424

	<b>ppb</b>	<b>MDW 43</b>	<b>MDW 42 A</b>	<b>BV 344</b>	<b>BV 352</b>	<b>BV 356</b>	<b>MDW 42 B</b>	<b>BV 364</b>	<b>BV 385</b>	<b>BV 149 A</b>	<b>BV 363</b>
La		2824	360	621800	383200	364400	324	1156000	243100	792	2102000
Ce		5190	490	1111000	631200	672900	436	2004000	397800	6059	3898000
Pr		608	55	109200	64900	61480	49	203400	44080	393	378600
Nd		2309	194	355600	204700	191500	175	662100	141200	2042	1215000
Sm		429	36	46980	25890	24240	29	84840	18720	825	158700
Eu		93	9	12350	6626	6088	8	21790	4719	196	40330
Tb		51	6	3910	1977	1832	4	6488	1463	233	12650
Gd		367	38	29910	15660	14580	32	51750	11490	1135	99300
Dy		271	34	18820	9057	8303	29	29800	6791	1572	59060

Y		2479	316	88670	43630	37840	265	138600	31450	9607	267700
Ho		55	8	3401	1607	1445	6	5255	1196	348	10540
Er		140	23	8551	3897	3469	19	12830	2936	1020	26170
Tm		19	3	1223	536	474	3	1817	402	156	3642
Yb		108	20	7461	3134	2800	16	11480	2365	1005	22370
Lu		15	3	1023	418	379	2	1649	319	140	3037
	<b>MUQ</b>	<b>MDW 43</b>	<b>MDW 42 A</b>	<b>BV 344</b>	<b>BV 352</b>	<b>BV 356</b>	<b>MDW 42 B</b>	<b>BV 364</b>	<b>BV 385</b>	<b>BV 149 A</b>	<b>BV 363</b>
La	32510	0.086866	0.01108	19.12642	11.78714	11.20886	0.009969	35.55829	7.477699	0.024371	6.465703
Ce	71090	0.073006	0.006886	15.62808	8.878886	9.465466	0.006136	28.18962	5.595724	0.08523	5.48319
Pr	8460	0.071868	0.006504	12.9078	7.671395	7.267139	0.005752	24.04255	5.210402	0.046466	4.475177
Nd	32910	0.070161	0.005898	10.80523	6.219994	5.8189	0.005314	20.11851	4.290489	0.062048	3.691887
Sm	6880	0.062369	0.005263	6.828488	3.763081	3.523256	0.004158	12.3314	2.72093	0.119855	2.306686
Eu	1570	0.05914	0.005937	7.866242	4.220382	3.877707	0.00512	13.87898	3.005732	0.124777	2.56879
Gd	6360	0.057736	0.006019	4.70283	2.462264	2.292453	0.004987	8.136792	1.806604	0.178459	1.561321
Tb	990	0.051182	0.005724	3.949495	1.99697	1.850505	0.004317	6.553535	1.477778	0.235657	1.277778
Dy	5890	0.045993	0.005735	3.195246	1.537691	1.409677	0.004983	5.059423	1.152971	0.266893	1.002716
Y	31850	0.077834	0.009925	2.783987	1.369859	1.188069	0.008333	4.351648	0.987441	0.301633	0.840502
Ho	1220	0.044705	0.006375	2.787705	1.317213	1.184426	0.005308	4.307377	0.980328	0.284836	0.863934
Er	3370	0.041484	0.006855	2.537389	1.15638	1.029377	0.00554	3.807122	0.871217	0.302671	0.776558
Tm	510	0.037314	0.006445	2.398039	1.051765	0.930196	0.005233	3.562745	0.787255	0.304902	0.714118
Yb	3250	0.033231	0.006163	2.295692	0.964308	0.861538	0.004886	3.532308	0.727692	0.309231	0.688308
Lu	490	0.03151	0.005941	2.087755	0.852653	0.773673	0.004594	3.365306	0.650816	0.286531	0.619796

	ppb	<b>BV 149 B</b>	<b>BV 150</b>	<b>BV 153</b>	<b>BV 338</b>	<b>BV 159 A</b>	<b>BV 159 B</b>	<b>BV 161 B</b>	<b>BV 162 A</b>	<b>BV 163 A</b>	<b>BV 164</b>
La		351	114	16680	779500	1213	1323	374	176	262	111
Ce		4573	1460	51040	1390000	3587	3706	450	355	222	101
Pr		285	67	3764	148400	400	444	50	50	35	12
Nd		1623	412	13310	489100	1831	2029	205	261	234	55
Sm		739	250	2125	65800	628	732	107	225	229	45
Eu		197	78	197	17170	191	224	*	94	*	*

Tb		214	110	284	5251	214	263	22	114	63	14
Gd		1051	477	2169	41500	1016	1218	113	655	361	55
Dy		1481	825	2411	24890	1514	1857	130	586	325	101
Y		9325	5879	11500	115100	10340	12730	1365	3373	2230	1169
Ho		335	197	429	4427	335	409	24	101	54	20
Er		979	589	1243	11030	949	1167	60	219	124	54
Tm		149	89	80	1555	138	170	9	25	17	7
Yb		941	578	1251	9482	851	1049	52	125	98	47
Lu		134	83	151	1310	118	145	8	17	15	7
	<b>MUQ</b>	<b>BV 149 B</b>	<b>BV 150</b>	<b>BV 153</b>	<b>BV 338</b>	<b>BV 159 A</b>	<b>BV 159 B</b>	<b>BV 161 B</b>	<b>BV 162 A</b>	<b>BV 163 A</b>	<b>BV 164</b>
La	32510	0.0108	0.003516	0.513073	23.97724	0.037312	0.040695	0.011501	0.005426	0.008053	0.003408
Ce	71090	0.064327	0.020537	0.717963	19.55268	0.050457	0.052131	0.006326	0.004995	0.003121	0.001415
Pr	8460	0.0337	0.007882	0.444917	17.54137	0.047317	0.05247	0.005913	0.005905	0.004124	0.0014
Nd	32910	0.049316	0.012504	0.404436	14.86174	0.055637	0.061653	0.006223	0.00794	0.007122	0.001669
Sm	6880	0.10734	0.036366	0.308866	9.563953	0.091206	0.106323	0.015552	0.032645	0.033256	0.006516
Eu	1570	0.125159	0.049707	0.12535	10.93631	0.121656	0.142675	*	0.059573	*	*
Gd	6360	0.165252	0.075063	0.341038	6.525157	0.159748	0.191509	0.017799	0.10294	0.056698	0.008654
Tb	990	0.21596	0.111313	0.286364	5.30404	0.216061	0.265253	0.022475	0.115253	0.064081	0.013939
Dy	5890	0.251443	0.140119	0.409338	4.225806	0.257046	0.31528	0.022088	0.099542	0.055127	0.017182
Y	31850	0.292779	0.184584	0.361068	3.613815	0.324647	0.399686	0.042857	0.105903	0.070016	0.036703
Ho	1220	0.274344	0.161475	0.351721	3.628689	0.274262	0.334918	0.019557	0.083115	0.044352	0.016131
Er	3370	0.290386	0.174896	0.368843	3.272997	0.281632	0.346291	0.017864	0.065074	0.036914	0.016062
Tm	510	0.291961	0.174431	0.157059	3.04902	0.269608	0.332745	0.016924	0.04849	0.03249	0.014312
Yb	3250	0.289508	0.177785	0.384923	2.917538	0.261846	0.322769	0.015905	0.038338	0.030028	0.014348
Lu	490	0.273878	0.169633	0.308367	2.673469	0.241224	0.295918	0.017047	0.034327	0.030245	0.014871


**Note:**

\*for diverse technical reasons, the ICP-MS equipment didn't detect some few elements signature in some samples.

### **Appendix 3 : Travertines investigation Field Notes**

*Special acknowledgement :*

*The field notes from the 2007-2009 Travertines investigation campaigns in Uganda and 2014 in DRC are personal notes and scketchs drawn by Dr Christopher Nicholas.*

<p>025 @ 827 709 9994 238</p>	<p>Western wall of Kyemango crater (Baboon cliff) Another excellent viewpoint stop. To the NNE of here you can see into the wall of the crater west of Kyamatumu hill. Apparent extensional faults are present on both flanks, and possibly in back wall - tectonic? or more likely to be extensional collapse as floor of crater subsides post eruption:  Kyamatumu  View looking NNE at when wide crater ~2.5km away.  026 830930 9992 854 LE18 bottle of black scum</p>  <p>Continued driving, and from eastern flank of Lake Kitagoma saw oily scum floating round lake margin on SW side where hot springs are marked. Fought our way down and sampled a black algal scum floating on the lake shore. Frothyest bubbles. oil seep up spring conduit?</p>		<p>Drove on towards Kaseso to look for exposed border fault.  027 @ 167967 0005261 @ 1007 n. (161950)</p> <p>Tried getting a track west into the Rwenzori border fault. Failed once. Second one here ended in a 1st Quarry. Collected two grab samples, one of which appears to have bitumen residue lining the cavities. Collected both as LE19 and LE20 (bitumen) or is it some sort of black mineral grains? Bucketing down with rain.  NB. the 1sts at 027 are 92m above the current level of Lake George, which is not far away from here. Uplift of 1sts along Rwenzori border fault?</p>	
---------------------------------------	-------------------------------------------------------------------------------------------------------------------------------------------------------------------------------------------------------------------------------------------------------------------------------------------------------------------------------------------------------------------------------------------------------------------------------------------------------------------------------------------------------------------------------------------------------------------------------------------------------------------------------------------------------------------------------------------------------------------------------------------------------------------------------------------------------------------------------------------------------------------------------------------------------------	--	-------------------------------------------------------------------------------------------------------------------------------------------------------------------------------------------------------------------------------------------------------------------------------------------------------------------------------------------------------------------------------------------------------------------------------------------------------------------------------------------------------------------------------------------------------------------------------------------------------------------------------------------------------------	--



TUES 11/21 THE QUESTION OF THE BORDER LIMESTONES

D28a  
833417  
0000617  
@ 974m  
The GIS  
position  
is at  
advance  
to the  
stream  
bed  
028b  
is ~200m  
NW of  
28a at  
behind  
of the  
stream

left cars at end of track just North  
of Kasere / Congo border road junction.  
A series of 3 valleys incise the low hills  
along the Kivu-Mtn front.  
We have walked up the base of the middle  
one to top.

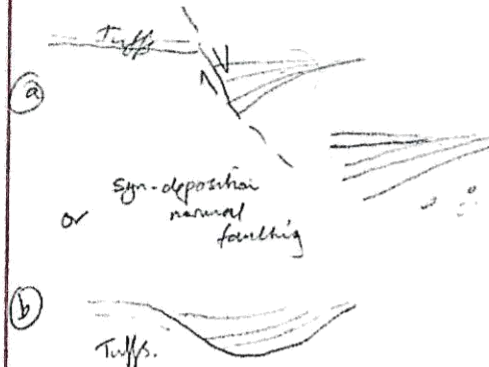
Here there are dark yellowish orange  
ms coarse Qtz sands, gels and pebbly  
sands ~ 10m thick measurably overlain  
with extreme regularity by Kabwe tuffs  
~ 2m thick.

No evidence of continuous 1st bands  
here, but top of the sands has formed  
a caliche. (in situ)

Fairly impressive cliffs here - uplift or  
rotational uplift on top of normal fault  
block?

Dry waterfall here testifies to incision of  
channel.

Traced down about 2m from old river  
floor too. - Recent base level fall?



Tuffs fill erosional gully?  
View from road back at our valley -  
the tuffs on the side far or thicker  
against a fault active during Kabwe  
epoch?? or just an erosional valley?

029 @  
995m  
167934  
0005144

Actually in the 1st quarry we visited  
yesterday in the rain - allowed access and  
it is now clear that there is a black  
organic-rich fill to the primary porosity in  
the tufa limestone.

It compares with the finger nail but we  
are undecided about the oily/bituminous  
smell.

Samples for petrographic study: LE21, 22, 23  
24, 25  
Zx bags LE26 for geochemistry



This place is called LYEMUBUZA

The black organic-rich deposit appears to fill vuggy cavities in the tufa. In terms of the original depositional environment, were these algal organic-rich beds within the 1st forming pools - i.e. from distinct beds?

In the fresh cliff exposure the presence seems to be cavity fill only and there are no 'shale' beds or laminae. Also there are exposures where the 'black' vug fill cross-cuts the tufa in cross-section very irregularly i.e. it is a later migration not an original in situ feature conclusion - reflect hydrocarbons.

030 @ 1134m 831712 0002091 Kitearingo

Quarry in gneissic basement close to border fault

Why are the 1sts on the footwall of the border fault here? See above

The 1st at the surface that the locals have led us to is actually fine texture ash with calcite developed in it so that it fries.

031 171989 0011737 @ 949m

Rae back N. towards Kasee. Stopped just on N side of Muhokya.

Only ~100m NW of the taruae road they are quite quarrying 1st in a stream bed.

Here the 1st is 'cleaner', there is less porosity (and surely less effective porosity). There is evidence of bitumen fill in the tufa cavities, but it is far less well developed and clearly in more porous patches.

conclusion - bitumen present, but less porosity in 1st has blocked much of its migration.

LE27 for geochem: had bituminous smell when freshly broken

LE28 } for petrography. ran  
LE29 } thinning

032 @ 989m 171394 0011611

MUHOKYA village KABUGA Hot springs - follow path up to S. of Live hills at 031





Unit 2 has same effective porosity as there are same later calcite cement fingers in the cavities.

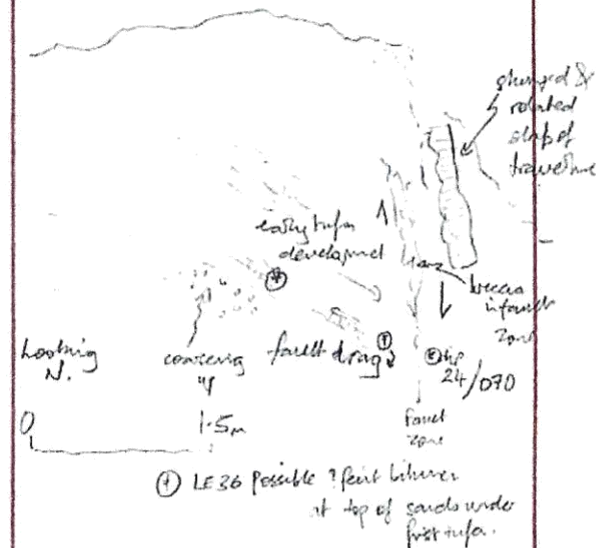
However the cavities (which are rare) in the tuffaceous unit ③ are 'clean' i.e. no fluid has subsequently passed through them.

Overall, the presence of poorly sorted sands mixed in with the tufa here suggests more clastic debris was being influenced down the active border fault scarp during hot spring 1st deposition.

The border fault this side seems to be sealing.

- LE 32 - Unit 2
- LE 33 - Unit 3
- LE 34 - Unit 4
- LE 35 - Unit 5

Another 10m W. the scarp at the same level shows easterly dipping Ms. friable Qtz sands and grits, poorly sorted in a matrix soft matrix pale grey/buff, passing up into sands with early tufa 1st development.



035 Drove back to thia, to the cement wastes mine on the N River bank, just downstream.

0031483 Here they pulled several samples from the one strike in the adit far up and poured hot water on them. Half stayed normal, but half heated up, went white (spotted with bitumen in vuggy cavities) and became extremely hot.

@967m Sodium or potassium salts?

The porosity in the 1st is much tighter

than the vugs previously on this  
Kumera, border fault.  
sampled ?bituminous Na or K carb  
and vuggy carb.

LE 37 - Lsts

LE 38 - Lsts

LE 39 - Na/K? partly burnt?

LE 40 - Na/K? protic

THURS

13th

ROAD TO BWERA/CONGO BORDER

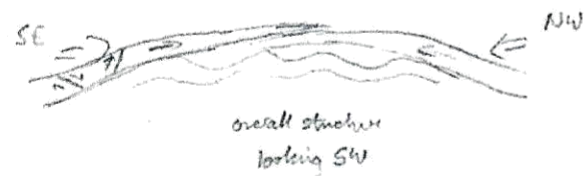
Drove road to junction between Kasese  
and Bwera tarmac roads at Kikorango  
crater.

Took the road to Bwera at the Congo  
border.

Almost immediately that the road starts  
to climb, there is an excellent road  
section exposed for about 250m on the  
SW cutting of the road, actually  
crossing the equator walking through  
the section!

Took a series of panoramic photos  
of the section, but what follows are  
key points along its length.

THE  
EQUATOR  
ROAD  
SECTION



Hill they go or whether it is a superficial covering only.

If into hill, must be a 1st thickness of ~50m

At the base there are conglan pebbles which suggests they are developed on old fluvial scots.

Must be a bounding fault trending NW-SE, against which the hot springs have developed.



② LE41 - tufa at base.

No biomass present, but there are some excellent examples of paleo stalactites collected a couple as LE42.

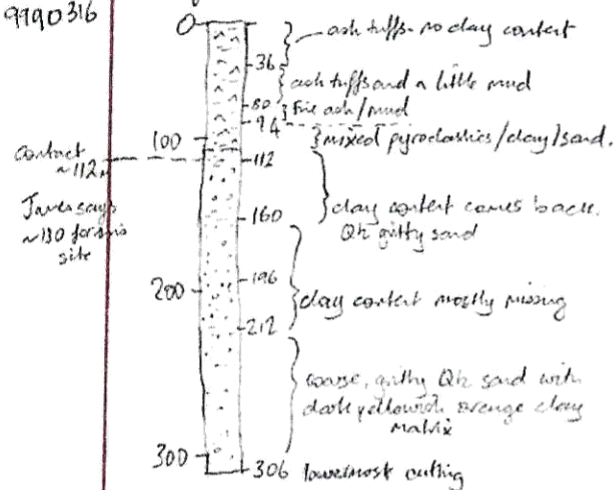
044 @  
823 077  
9986612

[310m deep cased hole #1]

Drove back to meet the Geothermal Drilling team from Ministry of Energy - drilling shallow holes in and around <sup>native</sup> <sub>clearings</sub>

045 @  
822 374  
9990316

Next hole they have just finished drilling. We were able to look at the cuttings



Still close to the mountain front - fluvial fans delivering immature scots from s end of Ruwenzori.

So, no source rocks under here as likely as not.



049@  
176156  
9971630

Quickly stopped at a nice quarry in the west of a crater. Total mess of boulders/blocks and some steeping normal faults

050@  
177790  
9966892

Narrowing wedge of volcanics - here there is an excellent view of folded basement to the SSW (see map).  
turned back.

Turned down the track to JACANA LODGE, to head for the 'BAT CAVE'.

Looked and walked in through forest for ~15-20min

later led to low-roofed cave apparently with tufo in its walls, but a roof of tufts.

Took a piece of the tufo. LE44

Walked on up hill to some pools - these seem to be springs emanating here and the river flows down and has ponded the cave (which is more of an underground river system with potholes through the tufo caves)

Spring river flows to 264° (almost due W). Spring must be along a geological junction - border fault? Water runs up along

Spring @  
051  
171976  
9969576

Junction between impermeable basement and Sintered sands on top?

Potholes through tufo just N of river  
Ravine @ 171883, 9969620 (052)

Downstream entrance to bat cave (which studies) @ 171930, 9969684 (053)



055 Campsite at end of track @ 171607 9968758.

1st bar. fine suggy, caustic, friable and no bitumen.

NB If the volcanics are older than the tuff, then the eastern tuffs are older than those at Muloaya  
i.e. because fault moved post-eastern boundary fault



<p>27/11/2010          locality 002          @          833417          0000617          Elevation 977m</p> <p>Local name          Biruma</p>	<p><u>Biruma quarry</u>          Limestone quarry operated by          artisanal diggers extracting          limestones block, crushed and          sold for construction purposes</p> <p>②: light brown, very crumble          lot + vugs porosity +          visible rootlets branches          and plant tubes</p>	
<p>03/12/2010          locality          006          @          313104          252027          Elevation:          670m</p>	<p><u>Mayi ya Moto</u>          Hot Springs: boiling water          Black stained lining liquid          flowing along the parallel          direction of the road          Goma - Vitshumbi</p> <p>→ Black stain in white          vugs spreaded travertines</p>	

Mayi ya Nato

(\*)  $V_{19}$ : Possible relict, degraded oil coating cavities in a hot spring Travertines limestone

Looks more "soily" but enough work at look

→ Due to safety issue, no time to examine in details

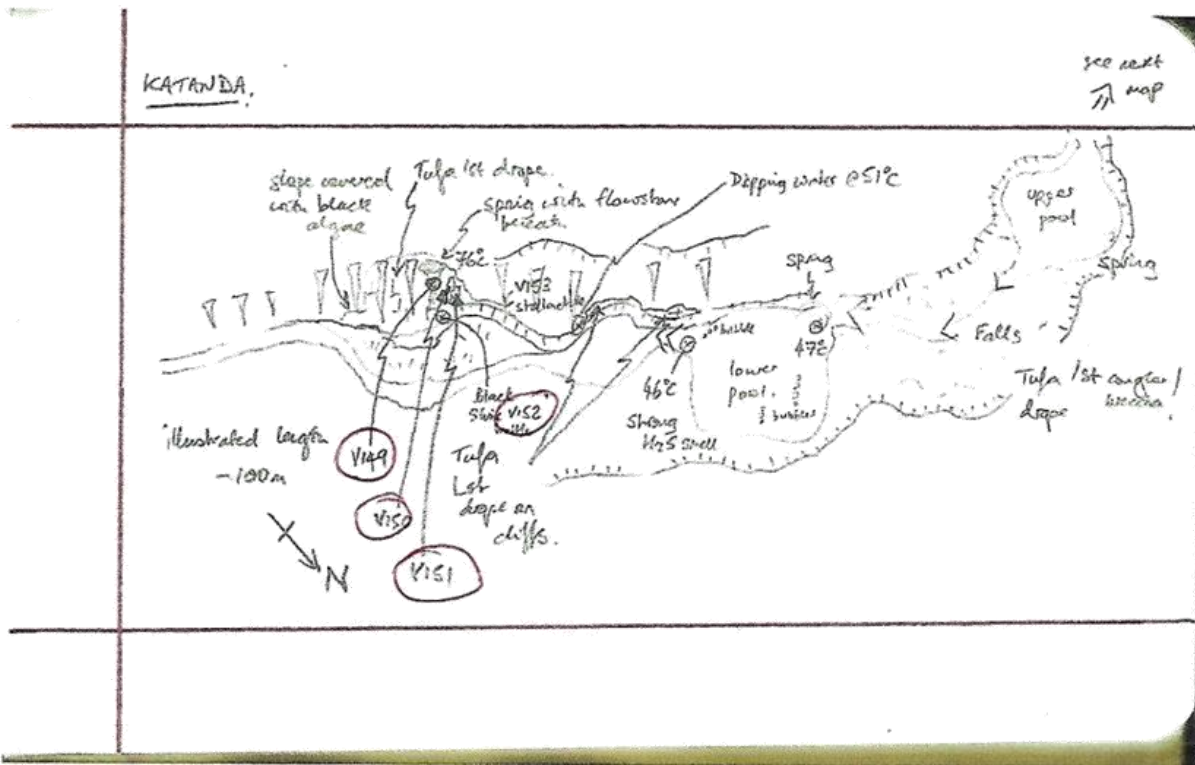
(\*)  $V_{20}$ : Travertine samples identical with  $V_{19}$  but collected in the same line downstream the

(\*)  $V_{21}$ : liquid flow

Travertines samples collected further downstream of  $V_{20}$ .



Tarvertines investigation campaign 2014



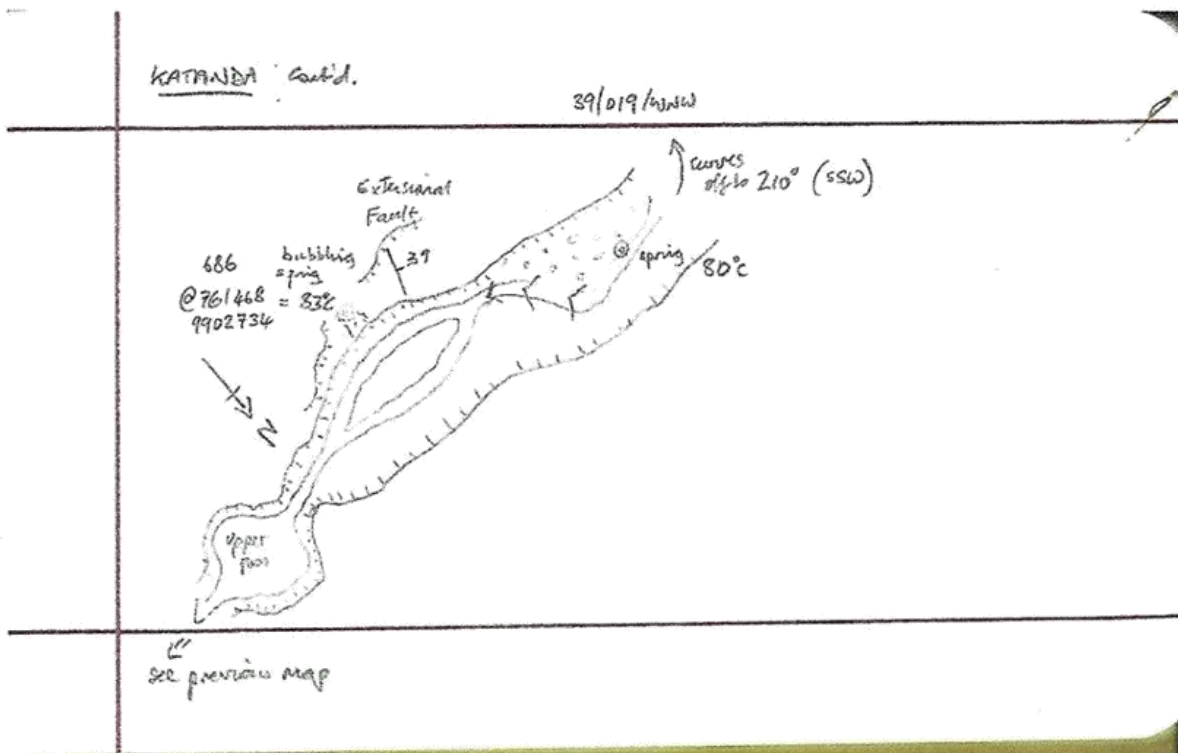
MAI YA MOTO: AREA 2  
 Here a incised valley trending 325° (NW) at first glance from the helicopter appeared to have a solid oil seep.  
 Now here on the ground it is a linear hot spring locality with algae growing up the steep sides.  
 A network of limestone Venus shells through the rift. Fall side here, and this is tufa 1st drape on the steep valley sides.  
 The stream flows back on itself further to the NW and it supports it is following the steeply dipping and curving basement edge, rather than a 'linear' rift fault.  
 see over for map.  
 SW NE  
 faulting? from faulting  
 Plants

TUES 15th

6850  
71474  
1902714

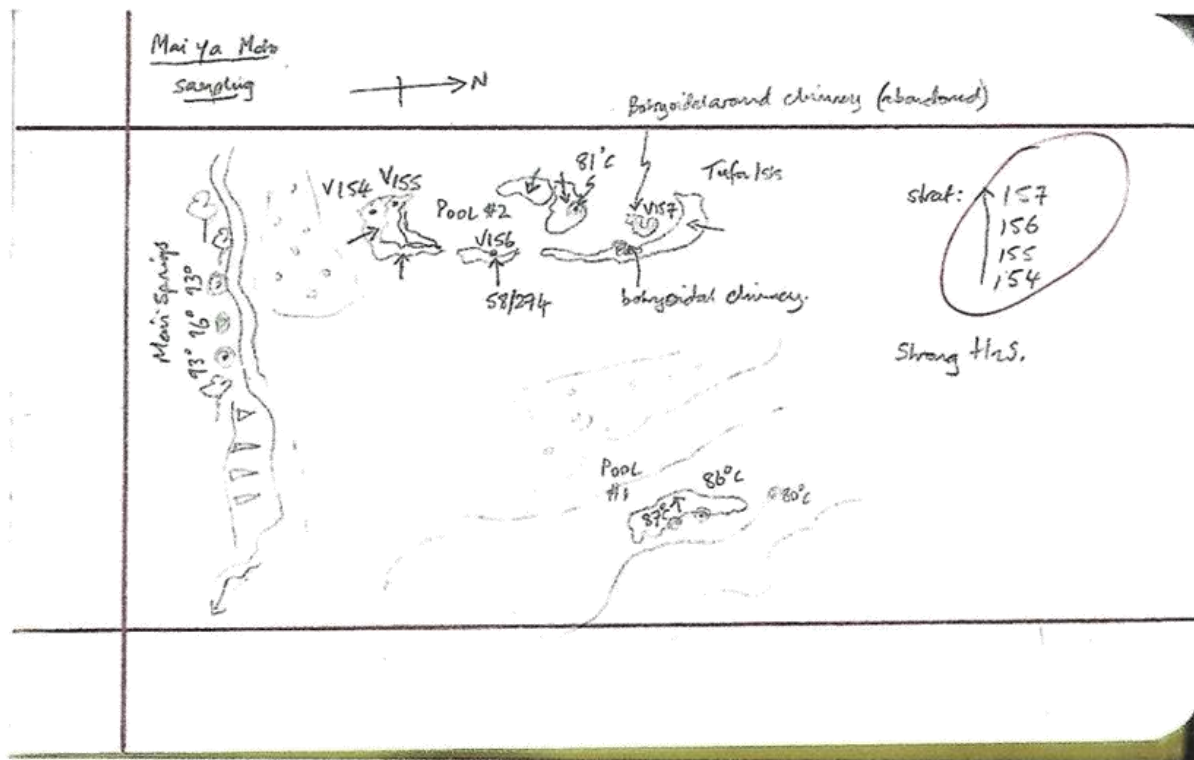
local name  
KATANDA

031 Moved on to Mai ya Moto:  
 K U Th #2263  
 S.9.5043 262.1 3  $\frac{1}{2}$  ft  $\frac{1}{4}$  ft  
 Just below one of the main active  
 bubbling vents on southern margin.  
 Vent temp: 93°C  
 Next vent to SSW, at 96°C  
 and the next is 93°C  
 • New patches of dipping tufa lot:  
 2 distinct beds  
 12.7 mending  
 0.9 66.8 KUTh  
 12.7 mending  
 0.9 66.8 KUTh  
 cavity top  
 fibrous layers  
 fibrous layers  
 V155  
 V154a  
 V154b  
 V154c  
 V154d  
 V154e  
 V154f  
 V154g  
 V154h  
 V154i  
 V154j  
 V154k  
 V154l  
 V154m  
 V154n  
 V154o  
 V154p  
 V154q  
 V154r  
 V154s  
 V154t  
 V154u  
 V154v  
 V154w  
 V154x  
 V154y  
 V154z





<p>687 @ 761774 9900764</p>	<p>Moved north to west of roadside at x1. Small pool of 4 bubbling vents: main one 84.7°C 2nd 75.2°C 3rd 82.2°C 75.0°C 69.8°C</p> <p>No tufa lots as such, just white salt crusts. Small chimney on its own @ 90°C</p> <p>Flow on to here - no access to X2 far roadside. Here a boiling spring is present on the eastern river bank - max temp 90°C (87, 88, 89)</p> <p>Mostly white salt crusts, but here just found some tufa 1st, with imprints of plant and tree rocklets, big the 'piss-hole': coming out at 82°C.</p> <p>V158 } vertical zoned pits. V159 } V160 } - includes zoning around large cavity.</p>
<p>688 @ 763142 9902342 Strong H<sub>2</sub>S swell</p>	<p>Moved north to west of roadside at x1. Small pool of 4 bubbling vents: main one 84.7°C 2nd 75.2°C 3rd 82.2°C 75.0°C 69.8°C</p> <p>No tufa lots as such, just white salt crusts. Small chimney on its own @ 90°C</p> <p>Flow on to here - no access to X2 far roadside. Here a boiling spring is present on the eastern river bank - max temp 90°C (87, 88, 89)</p> <p>Mostly white salt crusts, but here just found some tufa 1st, with imprints of plant and tree rocklets, big the 'piss-hole': coming out at 82°C.</p> <p>V158 } vertical zoned pits. V159 } V160 } - includes zoning around large cavity.</p>



<p>WED 16th</p> <p>670 @ 761 634 9901649</p>	<p>Return to Mai Ya Moto: Area 2. After traveling through thick bush, missed base at 'X2'. Moderate-smelling smell of M.S. No. white oil. Small cause on hillside seems to be main hot spring, at base of outcrop. Above it, however, is a sloping drape of older tufa led. Futcher-slope up slope 82°C 86°C 88°C 75°C abandoned spring Dipping Slope of tufa led Small spring on top main Spring 76°C 82°C Soil mud 83°C 87°C 5m looking 270° Polar-spring 2 (direct) Polar-spring (blue) active ? A measure of uplift Rate as forecast</p>
------------------------------------------------------	------------------------------------------------------------------------------------------------------------------------------------------------------------------------------------------------------------------------------------------------------------------------------------------------------------------------------------------------------------------------------------------------------------------------------------------------------------------------------------------------------------------------------------------------------------------------------------------------------------------------------------------------------

<p>K U Th # 2265</p> <p>1.0 200.9 25.1</p> <p>689 763580 9903605</p>	<p>Moved on to former X5. Here, bubbling springs on west bank of Futshara River - bubbling along a length of ~400m in a series of pools at the main river. Here at one of the main pools 71.5°C</p>
------------------------------------------------------------------------------	-------------------------------------------------------------------------------------------------------------------------------------------------------------------------------------------------------------



	<p>A5 for sketch on last page - have just realised there are a series of relict tufa patches up hill from the current one; A measure of footwall uplift? (or! subsidence on a W border fault)</p> <p>collect each: Highest @ 691 761804 9901639 @ 995m. #4</p> <p>Tufa Terrace @ 985m slightly south of active spring #3</p> <p>Tufa Terrace @ 976m, directly above outcrop of active spring. #2</p> <p>Tufa Terrace currently forming tufa @ 972m. at spring mouth. #1</p> <p>K U Th at site in current spring 3-6 410-8 1118 #2266.</p> <p>1/4 3092 57-2 #2267 a little further (N-S) down stream.</p>
	<p>V162 a+b</p> <p>V163 a+b</p> <p>V161 12 trestle + 15 sample in bag.</p> <p>V144</p>

	<p>692 Base of section @ 766111 9908410 @ 937m</p>
<p>K U Th #2268 Another ~5m. downstream 2-5 210-3 44-1</p>	<p>The U and Th values appear to decrease downstream away from the main stream - scavenged by the cyanobacteria!! (- Increasing oxygenation downstream)</p> <p>did low aerial film over the hot springs and then moved on to X7. Ruindi is 17km away - ? Ruindi District Large over cliff here on west bank of Rutshuru River; BVy-6.</p>





NAME: *W. ...*  
 DATE: *2/12/84*  
 SHEET: *2 of 3*

LOCATION & STRATIGRAPHIC SECTION:  
*20 km W of ...*

*East of ...*

*BY-10*



CUMULATIVE THICKNESS (m)	UNIT THICKNESS (m)	GRAPHIC LITHOLOGY	GRAIN SIZE											TRENDS & SURFACES	COLOUR	SPECTRAL GAMMA LOG				ASSAY #	DESCRIPTION	FACIES
			M	st	vf	f	m	c	vc	gr	pb	cb	ASSAY TIME (sec):			K (%)	U (ppm)	Th (ppm)				
11.3																			2474	light reddish brown, fine to coarse sandy mud, fine to coarse, ...		
11.4																			2475	light brown, ...		
11.5																			2476	light brown, ...		
11.6																			2477	light brown, ...		
11.7																			2478	light brown, ...		
11.8																			2479	light brown, ...		
11.9																			2480	light brown, ...		
12.0																			2481	light brown, ...		
12.1																			2482	light brown, ...		
12.2																			2483	light brown, ...		
12.3																			2484	light brown, ...		
12.4																			2485	light brown, ...		
12.5																			2486	light brown, ...		
12.6																			2487	light brown, ...		
12.7																			2488	light brown, ...		
12.8																			2489	light brown, ...		
12.9																			2490	light brown, ...		
13.0																			2491	light brown, ...		
13.1																			2492	light brown, ...		
13.2																			2493	light brown, ...		
13.3																			2494	light brown, ...		
13.4																			2495	light brown, ...		
13.5																			2496	light brown, ...		
13.6																			2497	light brown, ...		
13.7																			2498	light brown, ...		
13.8																			2499	light brown, ...		
13.9																			2500	light brown, ...		
14.0																			2501	light brown, ...		
14.1																			2502	light brown, ...		
14.2																			2503	light brown, ...		
14.3																			2504	light brown, ...		
14.4																			2505	light brown, ...		
14.5																			2506	light brown, ...		
14.6																			2507	light brown, ...		
14.7																			2508	light brown, ...		
14.8																			2509	light brown, ...		
14.9																			2510	light brown, ...		
15.0																			2511	light brown, ...		
15.1																			2512	light brown, ...		
15.2																			2513	light brown, ...		
15.3																			2514	light brown, ...		
15.4																			2515	light brown, ...		
15.5																			2516	light brown, ...		
15.6																			2517	light brown, ...		
15.7																			2518	light brown, ...		
15.8																			2519	light brown, ...		
15.9																			2520	light brown, ...		
16.0																			2521	light brown, ...		

